

Some pages of this thesis may have been removed for copyright restrictions.

If you have discovered material in AURA which is unlawful e.g. breaches copyright, (either yours or that of a third party) or any other law, including but not limited to those relating to patent, trademark, confidentiality, data protection, obscenity, defamation, libel, then please read our [Takedown Policy](#) and [contact the service](#) immediately

**GROUND CRACKING AND FROST HEAVING ASSOCIATED WITH
CHILLED GAS PIPELINE OPERATIONS IN BRITAIN.**

DENIS PATRICK GREENE
Doctor of Philosophy

ASTON UNIVERSITY
April 1992

This copy of the thesis has been supplied on condition that anyone who consults it is understood to recognise that its copyright rests with its author and that no quotation from the thesis and no information derived from it may be published without the author's prior, written consent.

**TO MY PARENTS
PADDY AND BRIDE**

**TO MY BROTHERS AND SISTERS
COLETTE, MAURA, DONAL & PADRIAG**

**TO MY RELATIONS
especially NANA & BELLA**

TO TIM LEAHY (deceased)

ACKNOWLEDGEMENTS

I wish to thank my supervisor Dr Roger Kettle (Head of Department) for his constant enthusiasm, support, technical advice and discussions during this study, also to thank Roger and Terri for their friendship during both my undergraduate and postgraduate periods at Aston.

Aston Departmental Staff including John Purkiss, John Elgy and Neil Short for their helpful discussions and suggestions. To the technical staff, especially Mike Lyons who was greatly involved with the laboratory work in this project and Ron Neale for his assistance with instrumentation systems. To Bill, Bill, Cal and Pete who constructed the small-scale model and the all of the technical staff involved including Colin, John, Rob, Dave, Trevor. To Nigel Foot for use of his computer. To the secretarial staff, Joy, Joan and Audrey.

The author expresses his gratitude to the British Gas Corporation for funding this project, for the use of their facilities and for the helpful assistance provided by both the Engineering Research Station, Newcastle-upon-Tyne and British Gas North West, Transmission Department. Special thanks are given to Eric Middleton (Senior Engineer) and Grahame Archer (Principal Engineer) at the Engineering Research Station, who acted as External Supervisors to this project, for their continual support, guidance and friendship during this investigation. The author is indebted to Alan Makinson (Assistant Regional Gas Transmission Engineer, North West Gas) for permission to allow a large-scale test to be undertaken within the North West Region, and supporting the project with engineering and technical staff:- Peter Tipping, Mark Williams and Ken Hinkson of Northern Unit, Mike O'Hare and Neil Hitchmough of Southern Unit, Nigel Basquill and Jim McDonald of C&I, John Blackburn of Scientific Services. The large-scale test was co-ordinated at regular Pre-heating meetings under the chairmanship of Alan Makinson with many of the above mentioned present and their input allowed the project to run smoothly. The author is indebted to N.A. Wilkinson and J. Gurdlestone of British Gas South Eastern for supplying soil samples from Tatsfield A.G.I.

To the friends who have helped, Cormac O'Hare, Mark Scanlon, Tim Leahy, Mike Wood, Darryn Evans, Paul Edmunds, Colin Sudlow, Pat Dunne, Mark Hughes, Paul Adamson and Yin.

To Massud and George of Aston Material Services Ltd for employments over the last two years.

To Barry and Kelly at the Sacks of Potatoes for the employment over the last two and half years and their friendship.

Finally to my parents and family for their support and encouragement.

THESIS SUMMARY.

Aston University.

Ground Cracking and Frost Heaving Associated with Chilled Gas Pipeline Operations in Britain.

Denis Patrick Greene.

PhD.

1992.

This thesis investigates the soil-pipeline interactions associated with the operation of large-diameter chilled gas pipelines in Britain, these are frost/pipe heave and ground cracking. The investigation was biased towards the definition of the mechanism of ground cracking and the parameters which influence its generation and subsequent development, especially its interaction with frost heave.

The study involved a literature review, questionnaire, large-scale test and small-scale laboratory model experiments. The literature review concentrated on soil-pipeline interactions and frost action, with frost/pipe heave often reported but ground cracking was seldom reported. A questionnaire was circulated within British Gas to gain further information on these interactions. The replies indicated that if frost/pipe heave was reported, ground cracking was also likely to be observed. These soil-pipeline interactions were recorded along 19% of pipelines in the survey and were more likely along the larger diameter, higher flow pipelines.

A large-scale trial along a 900 mm pipeline was undertaken to assess the soil thermal, hydraulic and stress regimes, together with pipe and ground movements. Results indicated that cracking occurred intermittently along the pipeline during periods of rapid frost/pipe heave and ground movement and, that frozen annulus growth produced a ground surface profile that was approximated by a normal probability distribution curve. This curve indicates maximum tensile strain directly over the pipe centre. Finally a small-scale laboratory model was operated to further define the ground cracking mechanism. Ground cracking was observed at small upward ground surface movement, and with continued movement the ground crack increased in width and depth. At the end of the experiments internal soil failure planes slanting upwards and away from the frozen annulus were noted. The suggested mechanism for ground cracking involved frozen annulus growth producing tensile strain in the overlying unfrozen soil, which when sufficient produced a crack.

Key words:- Pipelines, Frost Heave, Ground Cracking, Small-Scale Laboratory Model, Instrumentation.

TABLE OF CONTENTS

DEDICATION.....	2
ACKNOWLEDGEMENTS.....	3
THESIS SUMMARY.....	4
TABLE OF CONTENTS.....	5
LIST OF FIGURES	11
LIST OF TABLES	18
LIST OF PLATES	20
LIST OF SYMBOLS	22
CHAPTER 1 INTRODUCTION	25
CHAPTER 2 BACKGROUND TO LOW TEMPERATURE OPERATION.....	28
2.1 Introduction	28
2.2 The British Gas Corporation National Transmission System.....	28
2.2.1 Development of the National Transmission System.....	28
2.2.2 The National Transmission System.	29
2.2.3 Design of Pipelines.....	29
2.3 Blackrod Above Ground Installation.....	32
2.3.1 Station Requirements.....	32
2.3.2 Station Description.	32
2.3.3 Pre-Heating and Pressure Reduction.....	35
CHAPTER 3 FROST ACTION IN SOIL.....	37
3.1 Soil Classification.	37
3.2 Ground Thermal Conditions.	37
3.2.1 Ground Surface Energy Balance.....	37
3.2.2 Thermal Properties of Soils.	38
3.2.2.1 Heat Transfer.....	38
3.2.2.2 Thermal Conductivity.....	39
3.2.2.3 Heat Capacity and Latent Heat.....	41
3.2.2.4 Thermal Diffusivity.....	43
3.2.3 Ground Thermal Regime.	44
3.2.3.1 Ground Temperature Profile.....	44
3.3 Principles of Soil Freezing.....	46
3.3.1 Ice Segregation.....	46
3.3.2 Thermodynamics of Soil Freezing.....	49
3.3.3 Soil Water Movement and Unfrozen Water Content.	51
3.3.3.1 Soil Water Movement in Unfrozen Soils.....	51
3.3.3.2 Unfrozen Water Content.	53
3.3.3.3 Soil Water Movement in Frozen Soils.....	56
3.3.4 Pressures Generated During Soil Freezing.	58
3.3.4.1 Suction Pressures.....	58
3.3.4.2 Frost Heave Pressures.....	58
3.3.5 Heat Extraction Rate.....	59

3.3.6	Theories of Frost Heave.....	60
3.3.6.1	Capillary Theory.....	60
3.3.6.2	Hydrodynamic Theory.....	62
3.3.6.3	Secondary Heave Theory.....	64
3.3.6.4	Mechanistic Theory of Frost Heaving (Segregation Potential Concept).....	66
3.3.7	Classification of Frost Susceptible Soils.....	68
3.4	Mechanics of Frozen Ground.....	71
3.4.1	Thermal Contraction of Frozen Ground.....	73
3.4.1.1	The Basic Laws Temperature Cracking of Frozen Ground.....	73
3.4.1.2	Contraction Crack Theories of Frozen Soils.....	75
3.5	Thawing of Frozen Soils.....	76
3.5.1	Thaw Settlement.....	77
3.5.2	Thaw Consolidation.....	78
3.6	Freeze-Thaw Cycles.....	79
3.6.1	Natural Phenomena Involving Frost Action.....	80
3.6.1.1	Growing Stones.....	80
3.7	Summary.....	82
CHAPTER 4 SOIL-PIPELINE INTERACTION.....		83
4.1	Introduction.....	83
4.2	Pipeline Design.....	83
4.2.1	Route Selection.....	84
4.2.2	Pipe Design.....	84
4.2.3	Geotechnical Design.....	85
4.2.4	Post-Construction and Monitoring.....	86
4.3	Soil-Pipeline Interactions.....	86
4.3.1	Definition of Soil-Pipeline Interaction.....	86
4.3.2	Vertical Pipeline and Soil Movements.....	87
4.3.2.1	Vertical Pipe Movements.....	87
4.3.2.2	Vertical Pipeline Movement Due to Floatation.....	90
4.3.2.3	Vertical Ground Movements Due to Tunnelling.....	91
4.3.2.4	Other Pipe Movements.....	92
4.4	Frost Action and its Influence on Structures.....	93
4.4.1	Introduction.....	93
4.4.2	Frost Action on Structures.....	93
4.4.3	Frost Action on Pipes.....	96
4.4.4	Warm Oil and Gas Pipelines In Permafrost Regions.....	97
4.4.5	Soil-Pipeline Temperature Profiles.....	98
4.5	Chilled Gas Pipeline Operation.....	99
4.5.1	Introduction.....	99
4.5.2	Chilled Gas Pipeline Operation in Temperate Climates.....	100
4.5.2.1	Britain.....	100
4.5.2.2	North America.....	102
4.5.3	Arctic and Northern Pipelines.....	105
4.5.4	Caen Test Facility.....	112
4.5.4.1	Description of Test Facility.....	113
4.5.4.2	Instrumentation.....	115
4.5.4.3	Observations and Results.....	115
4.5.4.4	New Experimental Design.....	124
4.6	Small-Scale Laboratory Models of Pipelines.....	125
4.6.1	Chilled Pipe Operation.....	125
4.6.2	Controlling Frost Heave Around Chilled Pipelines.....	126
4.6.3	Freezing Air Temperatures on Pipe Stresses.....	127

4.6.4	Thaw Settlement Tests Using a Centrifuge.....	128
4.6.5	Uplift Pipe Tests.....	129
4.7	Summary.....	130
CHAPTER 5 SCOPE.....		131
5.1	Soil-Pipeline Interactions.....	131
5.1.1	Ground / Pipe Heave.....	132
5.1.2	Ground Cracking.....	133
5.2	Objectives.....	134
5.2.1	Soil-Pipeline Interactions.....	134
5.3	Methodology.....	134
5.3.1	Questionnaire.....	135
5.3.2	Full-Scale Test.....	135
5.3.3	Small-Scale Laboratory Model Test.....	135
5.3.4	Soil Testing.....	136
CHAPTER 6 QUESTIONNAIRE.....		137
6.1	Subject Areas for Investigation.....	137
6.2	Design of a Questionnaire.....	137
6.2.1	Definition of the Objectives.....	137
6.2.1.1	Chilled Gas Pipeline Operation and Associated Interactions.....	137
6.2.1.2	Influence of Pipeline Operating Conditions and Soil Properties.....	138
6.2.2	Selection of Data Collection Method.....	139
6.2.3	Respondents and Their Limitations.....	140
6.2.4	General Layout of the Questionnaire.....	140
6.2.5	Expert Assistance.....	141
6.2.6	Sending the Questionnaire.....	141
6.3	Results.....	141
6.3.1	Replies to the Questionnaire.....	141
6.3.2	Occurrence of Soil-Pipeline Interactions.....	142
6.3.3	Influence of Pipeline Diameter on Frost Heave and Ground Cracking.....	146
6.3.4	Influence of Soil Type on Frost Heave and Ground Cracking.....	150
6.3.5	Periods of Observable Frost Heave and Ground Cracking.....	150
6.4	Main Conclusions.....	154
CHAPTER 7 LARGE-SCALE STUDY PROGRAMME.....		155
7.1	Introduction.....	155
7.2	Objectives.....	155
7.3	Site Selection.....	156
7.3.1	Selection of a Pressure Reduction Station.....	156
7.3.2	Selection of Downstream Sites For Instrumentation.....	156
7.3.2.1	Severe Cracking (Site C).....	157
7.3.2.2	Moderate Cracking (Site A).....	157
7.3.2.3	No Cracking (Site B).....	158
7.4	Instrumentation of Sites A, B and C.....	158
7.4.1	Thermal Instrumentation.....	160
7.4.2	Hydrological Instrumentation.....	161
7.4.3	Soil Stress Instrumentation.....	165
7.4.4	Pipe Movement Instrumentation.....	167
7.4.5	Pipe Strain Instrumentation.....	168
7.4.6	Blackrod PRS Operating Characteristics.....	170
7.4.7	Ambient Conditions.....	170

7.4.8	Automatic Data Acquisition System.....	170
7.4.8.1	Data Logging.....	171
7.4.8.2	Data Interpretation.....	172
7.5	Instrumentation of Pressure Reduction Station.....	172
7.5.1	Pipe Heave/Ground Surface Movement.....	173
7.5.2	Pipe Bending Stress.....	173
7.6	Reading Intervals.....	176
7.7	Results.....	177
7.7.1	Blackrod PRS Operating Conditions.....	177
7.7.2	Ambient Conditions at Blackrod PRS During the Trial.....	178
7.7.3	Downstream Sites.....	180
7.7.3.1	Soil Classification.....	182
7.7.3.2	Thermal Regime.....	182
7.7.3.3	Hydraulic Regime.....	185
7.7.3.4	Soil Stress Regime.....	186
7.7.3.5	Pipeline Movements and Strains.....	186
7.7.3.6	Ground Cracking.....	192
7.7.4	Pressure Reduction Station Monitoring.....	203
7.7.4.1	Pipe Movement.....	203
7.7.4.2	Ground Movements.....	203
7.8	Summary.....	210
CHAPTER 8 SMALL-SCALE LABORATORY MODEL.....		211
8.1	Introduction.....	211
8.2	Objectives.....	211
8.3	Model Design.....	211
8.3.1	Introduction.....	211
8.3.2	Model Selection.....	212
8.3.3	Model Construction.....	213
8.4	Instrumentation.....	216
8.4.1	Thermal Instrumentation.....	216
8.4.2	Hydrological Instrumentation.....	218
8.4.3	Soil Stress Instrumentation.....	218
8.4.4	Pipe and Ground Movement Instrumentation.....	218
8.4.5	Operation of the Frost Heave Tank.....	220
8.4.6	Monitoring System.....	221
8.5	Results.....	222
8.5.1	Experimental Validation.....	222
8.5.1.1	Ground Surface Cracking.....	222
8.5.1.2	Ground Surface Movement.....	224
8.5.2	Tatsfield Test Run.....	225
8.5.2.1	Introduction.....	225
8.5.2.2	Soil Classification.....	225
8.5.2.3	Pipe Operating Characteristics.....	226
8.5.2.4	Soil Temperatures.....	226
8.5.2.5	Soil Water Potentials.....	228
8.5.2.6	Ground Cracking.....	233
8.5.2.7	Pipe Movement.....	239
8.5.2.8	Ground Surface Movement.....	241
8.5.3	Blackrod Test.....	244
8.5.3.1	Introduction.....	244
8.5.3.2	Soil Classification.....	244
8.5.3.3	Operating Characteristics.....	244
8.5.3.4	Soil Temperature.....	245
8.5.3.5	Soil Water Potentials.....	247
8.5.3.6	Ground Cracking.....	251

8.5.3.7	Pipe Movement.....	259
8.5.3.8	Ground Surface Movement.....	259
8.6	Summary.....	262
CHAPTER 9 DISCUSSION.....		263
9.1	Introduction.....	263
9.2	Summation of Questionnaire Results.....	263
9.2.1	Introduction.....	263
9.2.2	Extent of SPIs.....	263
9.2.3	SPI and Pipe Diameter.....	264
9.2.4	SPI and Soil Type.....	264
9.2.5	Ground Cracking and Frost Heave.....	265
9.2.6	Problems Associated with Chilled Gas Pipe Operation.....	267
9.3	Large-Scale Test Site.....	267
9.3.1	Introduction.....	267
9.3.2	Blackrod PRS Operating Conditions and Ambient Conditions.....	269
9.3.3	Sites A, B and C.....	269
9.3.3.1	Soil Thermal, Hydraulic and Stress Regimes.....	270
9.3.3.2	Pipe Movement.....	270
9.3.3.3	Pipe Floatation.....	273
9.3.3.4	Ground Cracking.....	274
9.3.4	Blackrod PRS.....	275
9.3.4.1	Pipe Movement.....	275
9.3.4.2	Ground Movement.....	276
9.3.4.3	Ground Cracking.....	278
9.3.5	Ground Cracking and Frost Heave at the Large-Scale Test.....	280
9.4	Small-Scale Laboratory Model.....	281
9.4.1	Soil Thermal, Hydraulic and Stress Regimes.....	281
9.4.2	Pipe Movement.....	282
9.4.3	Ground Movement.....	282
9.4.4	Ground Cracking.....	284
9.4.5	The Influence of the Pipe Flange Plates on Ground Cracking.....	287
9.4.6	Ground Cracking and Frost Heave.....	287
9.5	Relationship Between Ground Cracking and Frost/Pipe Heave.....	288
9.6	Summary.....	290
CHAPTER 10 CONCLUSIONS.....		291
10.1	Introduction.....	291
10.2	Aims of the Thesis.....	291
10.3	Summary of Study Programme.....	292
10.3.1	Introduction.....	292
10.3.2	Previous Studies.....	292
10.3.3	Questionnaire.....	292
10.3.4	Large-Scale Study Programme.....	293
10.3.5	Small-Scale Laboratory Model.....	294
10.4	Ground Cracking Above Chilled Large Diameter Gas Pipelines.....	295
10.5	Engineering Considerations.....	297
10.5.1	In-Service Pipelines.....	297
10.5.2	Planned Pipelines.....	298
10.6	Recommendations for Future Work.....	298
REFERENCES.....		301
APPENDIX A PROBLEMS ENCOUNTERED AT LARGE-SCALE TEST.....		320
APPENDIX B QUESTIONNAIRE RESULTS.....		324

APPENDIX C	TEMPERATURE AND WATER POTENTIAL RESULTS FOR SITES A AND B.	341
APPENDIX D	WATER POTENTIAL COMPUTER PROGRAM	352
APPENDIX E	GROUND SURFACE MOVEMENTS WITHIN BLACKROD PRS	354
APPENDIX F	GROUND SURFACE MOVEMENTS IN SMALL-SCALE LAB TEST.....	361

LIST OF FIGURES

FIGURE 2.1	The First National Transmission System (after Copp, 1967).....	30
FIGURE 2.2	The British Gas Corporation National Gas Transmission System (after Francis, 1984)	31
FIGURE 2.3	Schematic Drawing of that Part of the North West Gas Transmission System which includes Blackrod Above Ground Installation (A.G.I)	33
FIGURE 2.4	Schematic Drawing of Blackrod Above Ground Installation (AGI).....	34
FIGURE 3.1	Daily Ground Surface Energy Balance (after Lunardini, 1981).	38
FIGURE 3.2	Ground Temperature Profiles Calculated from Equation 3.13.....	45
FIGURE 3.3	Diagram Illustrating the Zero Curtain Effect that the Latent Heat of Soil Freezing can have on a Ground Temperature Profile within a Soil Mass (after Harlan and Nixon, 1978).....	45
FIGURE 3.4	Diagrams Illustrating the Formation of Ice within differing Soils.	47
FIGURE 3.5	Schematic Illustration of Frost Heaving (after Anderson <i>et al</i> , 1984b).....	48
FIGURE 3.6	A Diagram Illustrating the Formation of Ice Lenses Under Constant Air and Ground Temperatures.....	49
FIGURE 3.7	The Relationship between Water Content and Suction for a Sand and a Loam Soil (Moisture Characteristic Curves), (after Marshall and Holmes, 1988).	51
FIGURE 3.8a	Graph of Hydraulic Conductivity against Degree of Saturation for Selected Soils from Ingersoll and Berg (1985).....	52
FIGURE 3.8b	Graph of Soil Water Potential against Water Content for Selected Soils from Ingersoll and Berg (1985).	53
FIGURE 3.9	Diagrammatic View of the Co-existence of Ice, Unfrozen Water and Air in Equilibrium within an Unsaturated Frozen Soil Matrix.	54
FIGURE 3.10	Illustration of Unfrozen Water Content against Temperature Curves for Three Different Soil Types, from Anderson <i>et al</i> . (1978).	55
FIGURE 3.11	Diagrammatic Illustration of Secondary (Continued) Heave.....	57
FIGURE 3.12	Diagrammatic Illustration of the Heave Rate against Net Heat Extraction Rate under Constant Cold and Warm Side Boundaries (after Konrad, 1987a).....	60
FIGURE 3.13	Diagrammatic Illustration of the Idealised Capillary Theory Showing the Pore Radius (r_p) for Ice Propagation.....	61
FIGURE 3.14	Diagrammatic Illustration of the Hydrodynamic Model (after Smith, 1985b).....	63
FIGURE 3.15	Schematic Diagram of the Frozen Fringe involved in the Secondary Heave Model.	64
FIGURE 3.16	Main Features and Dimensions of the TRRL Frost Heave Cabinet (after Roe and Webster, 1984).....	70
FIGURE 3.17	Idealized Illustration of the Creep of Frozen Soils under a Constant Loading Insufficient to cause Instantaneous Failure (Johnston, 1981).....	73

FIGURE 3.18	Stress at Ground Surface near an Isolated Crack (after Lachenbruch, 1962).	76
FIGURE 3.19	Typical Response of a Frozen Soil Undergoing Thaw Settlement (after Nixon and Ladanyi, 1978).	77
FIGURE 3.20	Generalized Thaw-Settlement Curve (after Watson <i>et al.</i> , 1973).	78
FIGURE 3.21a	The Frost-Pull Mechanism (after Lunardini, 1981).....	81
FIGURE 3.21b	The Frost-Push Mechanism (after Lunardini, 1981).....	81
FIGURE 4.1	Classic Soil Failure Pattern resulting from the Uplift of Small Diameter Pipes.....	88
FIGURE 4.2	Simplified Vertical Load-Displacement Response of the Buried Pipe.	89
FIGURE 4.3	Illustration of the Failure Surface Observed by Matyas and Davis (1983b).	90
FIGURE 4.4	Buoyancy Forces Acting on a Pipe.	90
FIGURE 4.5	Normal Probability Curve of Settlement Across an Advancing Tunnel.	91
FIGURE 4.6	Shallow Wedge Failure Mechanism Resulting from Lateral Pipe Displacement (after Audibert and Nyman, 1975).	92
FIGURE 4.7	Deep Punching Failure Mechanism Resulting from Lateral Pipe Displacement (after Audibert and Nyman, 1975).	93
FIGURE 4.8	Basal and Tangential Adfreeze Forces on a Pile and Pad Footing Foundations within Frozen Ground.	94
FIGURE 4.9	LNG Tank In-Ground Failure Modes (after Goto <i>et al.</i> , 1988).	95
FIGURE 4.10	Graph Showing Pipe Lift, Ambient Ground Temperature and Pipe Temperature during the Pre-heating Season (Nov to May) at Orrell PRS (after Archer <i>et al.</i> , 1984).....	101
FIGURE 4.11	Diagrammatic Illustration of the Hydraulic Regime around a Chilled Gas Pipeline incorporating Moisture Movements for Ground Surface Evaporation.	101
FIGURE 4.12	Plans Showing Pipe Movement Stations and Lignosol Injection Area (after Kempner, 1968)	103
FIGURE 4.13	Pipe Movements at Station No.3 (adapted from Kempner, 1968).	104
FIGURE 4.14	Grout Injection using a Single or Double Pipe Technique (after Yie, 1969a).	105
FIGURE 4.15	Pipeline Subject to Differential Frost Heave Forces.	106
FIGURE 4.16	Diagrammatic View of the Six Test Sections at the Calgary Test Facility (after Carlson <i>et al.</i> , 1981).....	107
FIGURE 4.17	Pipe Heave and Depth of Frost Penetration Below Bottom for Non-Insulated and Insulated Sections (after Carlson, 1984).	108
FIGURE 4.18	Frost Penetration around Deep Burial Section (after Slusarchuk <i>et al.</i> , 1978).....	109
FIGURE 4.19	Illustration of Frost Heave Test Plates used at Calgary Test Facility (after Nixon, 1982).....	110
FIGURE 4.20a	Longitudinal Section Through the Caen Test Chamber (after Kettle, 1984).....	114
FIGURE 4.20b	Cross Section Through the Caen Test Chamber (after Kettle, 1984).	114
FIGURE 4.21	Progression and Recession of the Frost Front beneath the Pipe (after Dallimore and Crawford, 1984).....	115

FIGURE 4.22a	Deformation of the Pipe during the Third Freeze Cycle (after Geotechnical Science Laboratories, 1988a).....	116
FIGURE 4.22b	Pipe Bending Stress during the First Freeze Cycle (after Geotechnical Science Laboratories, 1988a).....	116
FIGURE 4.23	Vertical Pipe Profile at the Start of Each Freeze Cycle (after Geotechnical Science Laboratories, 1989).....	117
FIGURE 4.24	Soil Pressures at the B-B Section Below the Pipe in the Silt Section during the Third Freeze Cycle (after Geotechnical Science Laboratories, 1988a).....	118
FIGURE 4.25	Soil Strain 25 cm Perpendicular to the Pipe Axis at Section B-B during the Third Freeze Cycle (after Geotechnical Science Laboratories, 1988a).....	119
FIGURE 4.26	Ground Surface Heave along Section B-B during the Third Freeze Cycle (after Geotechnical Science Laboratories, 1986b).....	120
FIGURE 4.27	Net Ground Surface Heave on Day 503 of the Fourth Freeze Cycle (after Geotechnical Science Laboratories, 1989).....	120
FIGURE 4.28	Plan View of Soil Surface Cracking during the Second Freeze Cycle (after Geotechnical Science Laboratories, 1985).....	121
FIGURE 4.29	Ground Surface Fissures, Day 30 Second Thaw Cycle (after Geotechnical Science Laboratories, 1986b).....	122
FIGURE 4.30	Ice Lensing around the Caen Pipeline (after Van Vliet-Lanoe and Dupas, 1991).....	124
FIGURE 4.31	Cross-Section of Model Tank used by Svec (1980).....	126
FIGURE 4.32.	Cross-Section of Model Tank used by Vermeulen <i>et al.</i> (1981).	127
FIGURE 4.33	Cross-Section of Model Tank used by Edil and Bahmanyar (1983).	128
FIGURE 4.34	Centrifuge Model for Pipe Thaw Settlement (after Vinson and Palmer, 1988).	129
FIGURE 4.35	Physical Small-Scale Model used by Trautmann <i>et al.</i> (1985) for Pipe Pull-Out Tests.....	130
FIGURE 5.1	Diagram Showing the Frozen Soil Annulus that forms around Chilled Gas Pipelines.....	131
FIGURE 5.2	Diagram Showing Ice Lenses within the Frozen Soil Annulus Surrounding a Chilled Gas Pipeline.	132
FIGURE 5.3	Diagram Showing the Ground Cracking that has been Observed Downstream of Blackrod PRS	133
FIGURE 6.1	Illustration of the Number of Pipelines that have been Operated Below 0°C and those where Soil-pipeline Interactions have occurred on a Regional Basis.....	143
FIGURE 6.2	Illustration of the Range of Pipeline Diameters Operated by each Region.....	143
FIGURE 6.3	Illustration of the Locations where Ground Cracking and Frost Heave occur when considered Independently.	144
FIGURE 6.4	Illustration of the Locations where Ground Cracking, Frost Heave and both Frost Heave and Ground Cracking occur.....	145
FIGURE 6.5	Bar Chart Illustrating the Diameters of the Pipelines that have Operated below 0°C in Relation to the known Soil-pipeline Interactions.....	146
FIGURE 6.6	Bar Chart Illustrating Soil Types in Relation to Frost Heave and Ground Cracking.....	150

FIGURE 6.7	Bar Chart Illustrating the Number of Pipelines with Frost Heave or Ground Cracking Soil-Pipe Interactions during each Month.....	154
FIGURE 7.1	Diagrammatic View of the Excavation.....	158
FIGURE 7.2	Layout of Platinum Resistance Thermocouples at Site C.....	160
FIGURE 7.3	Layout of the Thermocouple-Psychrometers at Site C.....	163
FIGURE 7.4	Thermocouple-Psychrometer (after Briscoe, 1984).....	163
FIGURE 7.5	Output from a Typical Wescor Thermocouple-Psychrometer (after Briscoe, 1984).....	164
FIGURE 7.6	Layout of Soil Pressure Transducers at Site C.	166
FIGURE 7.7	Schematic Layout of Pipe Heave Rods at Site C.	167
FIGURE 7.8	Pipe Heave Rod.	168
FIGURE 7.9	Layout Of Strain Gauges at Site C.	168
FIGURE 7.10	Vibrating Wire Strain Gauge Arrangement.....	169
FIGURE 7.11a	Data Flow Diagram for Data Collection from Blackrod Instrumentation.....	171
FIGURE 7.11b	Data Flow Diagram for Data Interpretation at Aston University.....	171
FIGURE 7.12	Diagrammatic Layout of Blackrod PRS Showing the Positions of the Pipe Heave Rods.....	174
FIGURE 7.13	Typical Pipe Heave Arrangement during the Study	175
FIGURE 7.14	Average Weekly Operating Conditions during the Monitoring Period at Blackrod PRS.	179
FIGURE 7.15	Average Weekly Ambient Air and Ground (at pipe depth) Temperatures.	180
FIGURE 7.16	Average Weekly Inlet Pipe and Ambient Ground (at pipe depth) Temperatures.	180
FIGURE 7.17	Weekly Rainfall during the Trial Period (3/2/88 to 7/3/90).	181
FIGURE 7.18	Average Weekly Temperature Profile at 90° to the Vertical at Site C.	183
FIGURE 7.19	Average Weekly Temperature Profile at 60° to the Vertical at Site C.	183
FIGURE 7.20	Average Weekly Temperature Profile at 45° to the Vertical at Site C.	184
FIGURE 7.21	Average Weekly Temperature Profile at 30° to the Vertical at Site C.	184
FIGURE 7.22	Average Weekly Temperature Profile at 0° to the Vertical at Site C.	185
FIGURE 7.23	Depth to Water Table at Sites A, B and C.....	185
FIGURE 7.24	Results from Thermocouple-Psychrometers at Site C.	187
FIGURE 7.25	Pipe Movement at the Three Pipe Heave Station at Site C.	188
FIGURE 7.26	Average Weekly Station Outlet Temperature, Average Weekly Pipe Temperature and Average Pipe Movement during Monitoring at Site C.	188
FIGURE 7.27	Average Pipe Movement and Water Table Movement during Monitoring at Site C.	189
FIGURE 7.28	Vibrating Wire Strain Gauge Readings for Gauges at 0° (No2), 90° (No3) and 270° (No1) at Site C.	190
FIGURE 7.29	Pipe Movement at the Three Pipe Heave Stations at Site A.	190
FIGURE 7.30	Station Outlet Temperature and Average Pipe Movement at Site A during the Monitoring Period.....	191

FIGURE 7.31	Pipe Movement at Site B Pipe Heave Station for New and Old TBM's.....	191
FIGURE 7.32	Average Pipe Movement at Sites A, B and C.....	192
FIGURE 7.33	Illustration of Maximum Observed Ground Cracking during 1987/88 Pre-heating Season (Week 5 (11/3/88)) between MP18 and MP21.....	194
FIGURE 7.34	Illustration of Maximum Observed Ground Cracking during 1988/89 Pre-heating Season (Week 55 (23/2/89)) between MP18 and MP21.....	195
FIGURE 7.35	Illustration of Maximum Observed Ground Cracking during 1989/90 Pre- heating Season (Week 106 (14/2/90)) between MP18 and MP21.....	196
FIGURE 7.36	Illustration of the Cavity at MP19+37.5 m.....	202
FIGURE 7.37	Pipe Heave and Pipe Temperature against Time for Sites C' and D' within Blackrod PRS.	203
FIGURE 7.38	Horizontal Temperature Profile from the Pipe within Blackrod PRS.....	204
FIGURE 7.39a	Ground Surface Profile Across the Pipeline at Site C' within Blackrod PRS from 26/1/89 to 23/2/89 (Week 51 to 55).	205
FIGURE 7.39b	Ground Surface Profile Across the Pipeline at Site C' within Blackrod PRS from 23/2/89 to 30/6/89 (Week 55 to 73).....	205
FIGURE 7.39c	Ground Surface Profile Across the Pipeline at Site C' within Blackrod PRS from 9/11/89 to 14/2/90 (Week 92 to 106).....	205
FIGURE 7.40	Plan View of Ground Cracking Perpendicular to the Ground Surface Profile Apparatus at Site C' within Blackrod PRS from 9/2/89 to 16/3/89 (Week 53 to 58).....	206
FIGURE 7.41a	Ground Surface Profile Across the Pipeline at Site D' within Blackrod PRS from 26/1/89 to 23/2/89 (Week 51 to 55).....	208
FIGURE 7.41b	Ground Surface Profile Across the Pipeline at Site D' within Blackrod PRS from 23/2/89 to 28/7/89 (Week 55 to 77).	208
FIGURE 7.41c	Ground Surface Profile Across the Pipeline at Site D' within Blackrod PRS from 9/11/89 to 14/2/90 (Week 92 to 106).....	208
FIGURE 7.42	Plan View of Ground Cracking Perpendicular to the Ground Surface Profile Apparatus at Site D' within Blackrod PRS from 9/2/89 to 16/3/89 (Week 53 to 58).....	209
FIGURE 8.1	Plan View of the Frost Heave Tank.....	214
FIGURE 8.2	Section through the Frost Heave Tank.	215
FIGURE 8.3	Schematic View of the Small-Scale Laboratory Model.....	215
FIGURE 8.4	Diagram of the Temperature Control System for the Pipe.....	216
FIGURE 8.5	Diagram Showing the System for Maintaining the 'Artificial' Water Table.....	217
FIGURE 8.6	Diagram Showing the Positions of the Copper/Constantan Thermocouples.....	217
FIGURE 8.7	Diagram Showing the Positions of the Thermocouple-Psychrometers.....	218
FIGURE 8.8	Plan View of the Ground Heave and Cracking Instrumentation.....	219
FIGURE 8.9	Diagram Showing the Position of the Linear Voltage Displacement Transducers.	219
FIGURE 8.10	Data Flow Diagram for the Small-Scale Model Tests.....	221
FIGURE 8.11	Plan View of the Soil Surface during the Final Validation Test Showing the Width of Ground Cracking after Four Days.	223

FIGURE 8.12	Ground Surface Profile Perpendicular to the Line of the Pipe at the Centre (Section B-B) of the Small-Scale Model.....	224
FIGURE 8.13	Pipe Temperature during the Tatsfield Small-Scale Test.	226
FIGURE 8.14	Vertical Temperature Profile above Pipe Crown.	227
FIGURE 8.15	Temperature Profile at 45° to the Vertical above the Pipe.	227
FIGURE 8.16	Horizontal Temperature Profile from the Pipe.....	227
FIGURE 8.17	Temperature Profile at 45° to the Vertical below the Pipe.....	228
FIGURE 8.18	Vertical Temperature Profile below Pipe.	228
FIGURE 8.19a	Soil Water Potential Profile Vertically above Pipe Crown.	229
FIGURE 8.19b	Soil Temperatures at the Positions where Soil Water Potential was Measured Vertically above Pipe Crown.....	229
FIGURE 8.20a	Soil Water Potential Profile at 45° to the Vertical above the Pipe.....	230
FIGURE 8.20b	Soil Temperatures at the Positions where Soil Water Potential was Measured at 45° to the Vertical above the Pipe.....	230
FIGURE 8.21a	Soil Water Potential Profile Horizontally from the Pipe.....	231
FIGURE 8.21b	Soil Temperatures at the Positions where Soil Water Potential was Measured Horizontally from the Pipe.....	231
FIGURE 8.22	Water Added to Model during the Tatsfield Test to Maintain a Constant Water Table Level.....	232
FIGURE 8.23	Average of Width of Cracking Across the Soil Surface at the Locations of the Dial Gauges and LVDT's in Relation to Pipe Temperature.....	233
FIGURE 8.24	Plan View of the Soil Surface during the Tatsfield Test Showing the Width of Ground Cracking after 48 hours.	234
FIGURE 8.25	Plan View of the Soil Surface during the Tatsfield Test Showing the Width of Ground Cracking after 96 hours.	235
FIGURE 8.26	Plan View of the Soil Surface during the Tatsfield Test Showing the Width of Ground Cracking after 240 hours.....	236
FIGURE 8.27	Plan View of the Soil Surface during the Tatsfield Test Showing the Width of Ground Cracking after 312 hours.....	237
FIGURE 8.28	Plan View of the Soil Surface during the Tatsfield Test Showing the Width of Ground Cracking after 384 hours.....	238
FIGURE 8.29	Vertical Pipe Movement in Relation to Pipe Temperature.....	241
FIGURE 8.30	Mean Ground Surface Profile Across the Line of the Two Sets of Dial Gauges from 0 to 54 hours.....	242
FIGURE 8.31	Mean Ground Surface Profile Across the Line of the Two Sets of Dial Gauges from 54 to 240 hours.....	242
FIGURE 8.32	Mean Ground Surface Profile Across the Line of the Two Sets of Dial Gauges from 240 to 384 hours.	242
FIGURE 8.33	Pipe and Ground Surface Movement over Pipe Centre against Pipe Temperature.....	243
FIGURE 8.34	Pipe Temperature during the Blackrod Small-Scale Test.....	245
FIGURE 8.35	Vertical Temperature Profile above Pipe Crown.	246
FIGURE 8.36	Temperature Profile at 45° to the Vertical above the Pipe.	246
FIGURE 8.37	Horizontal Temperature Profile from the Pipe.....	246
FIGURE 8.38	Temperature Profile at 45° to the Vertical below the Pipe.....	247
FIGURE 8.39	Vertical Temperature Profile below Pipe.	247
FIGURE 8.40a	Soil Water Potentials Vertically above the Pipe Crown.....	248
FIGURE 8.40b	Soil Temperature at the Positions of Soil Water Potential Measurement Vertically above the Pipe Crown.....	248

FIGURE 8.41a	Soil Water Potentials at 45° to the Vertical above the Pipe.....	249
FIGURE 8.41b	Soil Temperature at the Positions of Soil Water Potential Measurement at 45° to the Vertical above the Pipe.....	249
FIGURE 8.42a	Soil Water Potentials Horizontal to the Pipe Centre.....	250
FIGURE 8.42b	Soil Temperature at the Positions of Soil Water Potential Measurement Horizontal to the Pipe Centre.....	250
FIGURE 8.43	Water Added to Model during the Blackrod Test to Maintain a Constant Water Table Level.....	251
FIGURE 8.44	Average of the Total Width of Cracking Across the Soil Surface at the Locations of the Dial Gauges and LVDT's in Relation to Pipe Temperature.....	252
FIGURE 8.45	Plan View of the Soil Surface during the Blackrod Test Showing the Width of Ground Cracking after 18 hours.....	253
FIGURE 8.46	Plan View of the Soil Surface during the Blackrod Test Showing the Width of Ground Cracking after 66 hours.....	254
FIGURE 8.47	Plan View of the Soil Surface during the Blackrod Test Showing the Width of Ground Cracking after 144 hours.....	255
FIGURE 8.48	Plan View of the Soil Surface during the Blackrod Test Showing the Width of Ground Cracking after 204 hours.....	256
FIGURE 8.49	Illustration of the Soil Failure Planes shown in Plate 8.14.....	257
FIGURE 8.50	Illustration of the Soil Failure Planes shown in Plate 8.15.....	258
FIGURE 8.51	Vertical Pipe Movement in Relation to Pipe Temperature.....	259
FIGURE 8.52	Pipe and Ground Surface Movement over Pipe Centre against Pipe Temperature.....	260
FIGURE 8.53	Mean Ground Surface Profile Across the Line of the Two Sets of Dial Gauges from 0 to 36 hours.....	261
FIGURE 8.54	Mean Ground Surface Profile Across the Line of the Two Sets of Dial Gauges from 36 to 126 hours.....	261
FIGURE 8.55	Mean Ground Surface Profile Across the Line of the Two Sets of Dial Gauges from 126 to 217 hours.....	262
FIGURE 9.1	Average Pipe Movement at Sites A and C, and Outlet Pipe Temperature for the 1987/88 Pre-heating Season.....	272
FIGURE 9.2	Average Pipe Movement at Sites A, B and C, and Outlet Pipe Temperature for the 1988/89 Pre-heating Season.....	272
FIGURE 9.3	Average Pipe Movement at Sites A, B and C, and Outlet Pipe Temperature for the 1989/90 Pre-heating Season.....	272
FIGURE 9.4	Pipe Heave and Ground Movement Directly above the Pipe Centreline at Site C' (datum 6/1/89).....	279
FIGURE 9.5	Pipe Heave and Ground Movement Directly above the Pipe Centreline at Site D' (datum 6/1/89).....	279
FIGURE 9.6	Plan View of Cracking during the Tatsfield Experiment Showing Crack Growth with Time.....	285
FIGURE 9.7	Plan View of Cracking during the Blackrod Experiment Showing Crack Growth with Time.....	286

LIST OF TABLES

TABLE 3.1	Thermal Properties of Soil Constituents (after Williams and Smith, 1989).....	40
TABLE 3.2	Variations in Thermal Conductivity with Temperature for Typical Soil Constituents (after Farouki, 1986).....	40
TABLE 3.3	Average Values of Thermal Contraction for Clays and Sands (after Grechischev, 1973).....	74
TABLE 4.1	Pipe Heave and Frost Penetration for Non-Insulated Section in mid-1977 and at the end of 1980.....	109
TABLE 4.2	Physical Characteristics of the Soils at the Caen Test Facility.....	113
TABLE 4.3	Operating Cycles at Caen Test Facility (after Geotechnical Science Laboratories, 1989).....	113
TABLE 6.1	List of Variables under Consideration in the Data Collection Programme.....	138
TABLE 6.2	Details of Numbers of Replies and Dates Received.....	142
TABLE 6.3	Tables Showing the Relationship between the Likelihood of Ground Cracking and Frost Heave occurring Along the same Pipeline.....	145
TABLE 6.4	Ranges of Ground Crack Widths and Frost Heave (Pipe Heave).....	146
TABLE 6.5	Tables Showing the Relationship between Observed Frost Heave and Pipeline Diameter.	147
TABLE 6.6	Tables Showing the Relationship between Observed Ground Cracking and Pipeline Diameter.	148
TABLE 6.7	Tables Showing the Relationship between Occurrences of both Ground Cracking and Frost Heave with Pipeline Diameter.....	149
TABLE 6.8	Frequency Tables Showing the Relationship between Frost Heave and Soil Type.....	151
TABLE 6.9	Frequency Tables Showing the Relationship between Ground Cracking and Soil Type.	152
TABLE 6.10	Frequency Tables Showing the Relationship between Frost Heave and Ground Cracking with Soil Type.....	153
TABLE 7.1	Observations of Cracking along the Blackrod to Engine Lane Pipeline during the Pre-Heating Season 1983-84.....	157
TABLE 7.2	Position of the Platinum Resistance Thermocouples at Site C.....	160
TABLE 7.3	Position of Thermocouple-Psychrometers at Site C.	163
TABLE 7.4	Position of Soil Pressure Transducers at Site C.....	166
TABLE 7.5	Reading Intervals of Instruments at Sites A,B and C Downstream of PRS.....	176
TABLE 7.6	Reading Intervals of Pipeline Operating Characteristics, Ambient Conditions and Soil Temperature Profile taken in PRS.....	176
TABLE 7.7	Reading Intervals of Pipe and Ground Movement in the PRS.....	176
TABLE 7.8	Outlet Temperature Setpoints for Blackrod PRS during the Trial.....	177
TABLE 7.9	Soil Properties at Sites A, B and C	182
TABLE 7.10	Installation Dates for Downstream Data Loggers.....	182

TABLE 8.1	Reading Intervals of the Instrumentation during the Small-Scale Model Experiments.	221
TABLE 8.2	Soil Properties for Tatsfield Soil.....	225
TABLE 8.3	Soil Properties for Blackrod Soil.....	244
TABLE 9.1	Summary of Pipelines Where Frost Heave and Ground Cracking have been Observed.....	266
TABLE 9.2	Output Showing Sample Co-efficient of Determination (r^2) for Assumed Maximum Deflection (w_{max}) and Inflection Point (i) at Site C' during the Pre-heating Season 1988/89.....	277
TABLE 9.3	Output Showing Sample Co-efficient of Determination (r^2) for Assumed Maximum Deflection (w_{max}) and Inflection Point (i) at Site D' during the Pre-heating Season 1988/89.....	277
TABLE 9.4	Output Showing r^2 for Assumed Maximum Deflection (w_{max}) and Inflection Point (i) At Selected Intervals during the Tatsfield Experiment.....	283
TABLE 9.5	Output Showing r^2 for Assumed Maximum Deflection (w_{max}) and Inflection Point (i) At Selected Intervals during the Blackrod Experiment.	284

LIST OF PLATES

PLATE 7.1	Excavation at Site C.....	159
PLATE 7.2	300 x 300 mm grid Marked on Trench Wall at Site C.....	159
PLATE 7.3	Installation of PRTs at Site C.....	162
PLATE 7.4	Installation of Thermocouple-Psychrometers at Site C.....	162
PLATE 7.5	Installation of Soil Pressure Transducers at Site C.....	166
PLATE 7.6	Installation of the Vibrating Wire Strain Gauges at Site C.	169
PLATE 7.7	Pipe Heave/Ground Surface Profile Arrangement at Site C'.....	175
PLATE 7.8	Typical Ground Cracks between MP18 and MP19 on 16/2/89 (Week 54).....	197
PLATE 7.9	Typical Ground Cracks between MP18 and MP19 on 16/2/89 (Week 54).....	197
PLATE 7.10	Typical Ground Cracks between MP18 and MP19 on 23/2/89 (Week 55).....	198
PLATE 7.11	Typical Ground Cracks between MP18 and MP19 on 23/2/89 (Week 55).....	198
PLATE 7.12	Typical Ground Cracks between MP19 and MP20 on 16/2/89 (Week 54).....	199
PLATE 7.13	Cross Section Through a Ground Crack between MP19 and MP20 on 23/2/89 (Week 55).	200
PLATE 7.14	Depression Across the Pipeline between MP19+50 m and MP20.....	200
PLATE 7.15	Cavity at MP19+37.5 m on 11/8/89 (Week 79).....	201
PLATE 7.16	Cavity at MP19+37.5 m on 11/8/89 (Week 79).....	201
PLATE 7.17	Ground Cracks at Site C' within Blackrod PRS on 16/2/89 (Week 54).....	207
PLATE 8.1	Photograph Showing the Extent of Ground Cracking after Four Days of the Final Validation Test.....	223
PLATE 8.2	Photograph Showing the Shape of the Frozen Annulus above the Pipe and the Ground Crack Above the Annulus at the end of the Final Validation Test.	224
PLATE 8.3	Photograph Showing the Extent of Ground Cracking after 48 hours during the Tatsfield Test.....	234
PLATE 8.4	Photograph Showing the Extent of Ground Cracking after 96 hours during the Tatsfield Test.....	235
PLATE 8.5	Photograph Showing the Extent of Ground Cracking after 240 hours during the Tatsfield Test.....	236
PLATE 8.6	Photograph Showing the Extent of Ground Cracking after 312 hours during the Tatsfield Test.....	237
PLATE 8.7	Photograph Showing the Extent of Ground Cracking after 384 hours during the Tatsfield Test.....	238
PLATE 8.8	Side View of Perspex Frost Heave Tank Showing the Internal Soil Failure Plane during the Tatsfield at 396 hours.....	240
PLATE 8.9	Plan View of the Excavation of the Unfrozen Soil Overlying the Frozen Annulus during the Tatsfield Test at 396 hours.....	240
PLATE 8.10	Photograph Showing the Extent of Ground Cracking after 18 hours during the Blackrod Test.....	253
PLATE 8.11	Photograph Showing the Extent of Ground Cracking after 66 hours during the Blackrod Test.....	254

PLATE 8.12	Photograph Showing the Extent of Ground Cracking after 144 hours during the Blackrod Test.	255
PLATE 8.13	Photograph Showing the Extent of Ground Cracking after 204 hours during the Blackrod Test.	256
PLATE 8.14	Photograph of the Soil Failure Pattern 200 mm from the Side of the Tank Closest to the Normal Camera Position.....	257
PLATE 8.15	Photograph of the Soil Failure Pattern 200 mm from the Side of the Tank Furthest from the Normal Camera Position.....	258
PLATE 9.1	Ground Surface Depression Over the Pipeline on the Exit from Tatsfield PRS.	268

SUMMARY OF SYMBOLS

a_s	=	Area of pipe material
A	=	Cross-sectional area
A_0	=	Thaw settlement parameter
A_p	=	Relative Settlement
A_s	=	Amplitude of the temperature sine wave
C	=	Volumetric heat capacity
C_{ap}	=	Apparent volumetric heat capacity
C_s, C_p, C_w, C_i, C_a	=	Volumetric heat capacity, soil, soil particles, water, ice and air respectively
C_f, C_u	=	Volumetric heat capacity, frozen soil and unfrozen soil respectively
c	=	Specific heat capacity
c_{ap}	=	Apparent specific heat capacity
c_s, c_p, c_w, c_i, c_u	=	Specific heat capacity, soil, soil particles, water, ice and unfrozen water respectively
c_v	=	Coefficient of consolidation
C_p	=	Specific heat of gas at constant pressure
dP	=	Pressure change on the system
dT	=	Change in temperature
dx	=	Width of sample
D	=	Nominal outside diameter
e	=	Strain, Voids ratio
E	=	Young's modulus
F_F	=	Interface friction force
F_H	=	Frost heave pressure
F_L	=	Longitudinal force
F_r	=	Resistance force
$\text{grad } T$	=	Temperature gradient across frozen fringe (at onset of final lens)
H	=	Total heave
H_u	=	Hydrostatic force
i	=	Point of inflexion
ISR	=	Ice segregation ratio
J	=	Joule-Thompson effect
k	=	Hydraulic conductivity
k_f	=	Frozen hydraulic conductivity
L_s	=	Volumetric latent heat of fusion of the soil system
l_w	=	Mass latent heat of fusion of water
m_v	=	Co-efficient of volume compressibility
m_1, m_2	=	Characteristic soil parameters
n	=	Soil porosity
P	=	Pressure, Pressure potential, Pipe design pressure
P_{ad}	=	Tangential adfreeze bond

P_b	= Basal heave pressure
P_f	= Pressure at frost front
P_i	= Ice pressure
P_{ov}	= Overburden pressure
P_w	= Water pressure
P_u	= Pipe uplift force
p	= Period of oscillation
Q_G	= Conduction of heat through the ground
Q_H	= Convection at the ground surface
Q_{LE}	= Latent heat involved in evaporation, snow melting etc.
Q_N	= Net exchange of radiation between the ground surface and atmosphere
q	= Mass flow rate
q_x	= Energy flow in the x-direction
$r_{i w}$	= Radius of the ice/water interface
r_p	= Pore radius
R	= Thaw consolidation ratio
R_L	= Radius to L
R_p	= Outside pipe radius
S	= Soil specific area
SP_o	= Segregation potential (at onset of final lens)
SP_{ov}	= Segregation Potential at steady-state conditions at overburden P_{ov}
SP_s	= Segregation Potential at steady-state conditions at zero overburden
ΔT	= Temperature change
T	= Temperature, Equilibrium temperature, Pipe wall thickness
T'	= Temperature of melting ice at atmospheric pressure
T_1, T_2	= Gas temperature at x_1 and x_2
T_g	= Ground temperature
T_L	= Temperature at L
T_m	= Mean air temperature in the time interval under consideration
T_o	= Uniform horizontal tension before failure
T_p	= Pipe temperature
T_y, T_z	= Component of tension, perpendicular to crack after fracture and parallel to crack after failure respectively
t	= Time
u	= Neutral stress
U, U_r	= Heat transfer co-efficients
V	= Specific volume
V_i	= Specific volume of ice
V_o	= Water influx in frozen fringe (at onset of final lens)
V_s	= Settlement volume
V_w	= Specific volume of water
w	= Water content of the soil, Total water content

W_h	=	Vertical ground heave
$W_{h \max}$	=	Maximum vertical ground heave
W_i, W_u	=	Water content, frozen and unfrozen water respectively
w_s	=	Vertical settlement
$w_{s \max}$	=	Maximum vertical settlement
W	=	Effective weight of overburden soil mass
W_f, W_T	=	Weight of frozen soil, tank
W_p	=	Weight of pipe and contents
x_1, x_2	=	Downstream distances
X	=	Distance between x_1 and x_2 , Frost penetration depth
X_p, X_w, X_i, X_a	=	Volume fraction, soil particles, water, ice and air respectively
ΔX	=	Change in frost penetration depth
y	=	Perpendicular distance from tunnel centre-line
Z	=	Gravitational potential
z	=	Depth
α	=	Thermal diffusivity, Stefans constant, Co-efficient of thermal expansion
γ_d	=	Dry density of the soil
δ_f	=	Displacement at soil failure
ϵ	=	Dimensionless factor taking into account the unfrozen water content
λ	=	Thermal conductivity
ν	=	Poisson's ratio
Π	=	Osmotic Potential
ρ_i, ρ_w	=	Density, ice and water
σ_H	=	Hoop stress.
$\sigma_{i w}$	=	Surface tension along the curved water/ice interface
σ_L	=	Longitudinal stress
σ'	=	Effective stress, Effective pressure
τ	=	Effective shearing resistance of overburden soil mass
ϕ	=	Total Potential
χ	=	Stress partition factor
ω	=	Angular frequency ($= 2\pi / P$)
$\frac{dx}{dt}$	=	Rate of advance of the frost front

CHAPTER 1 INTRODUCTION

In Britain, natural gas is transported from onshore terminals such as St. Fergus in Scotland via the National Transmission Pipeline Network. This consists of an array of large-diameter pipelines, operating at high pressures and mass flow rates and controlled from a National Grid Control operated in response to demand requirements (Francis, 1981). This network of pipelines supplies demand centres, at which gas is taken from the National Transmission Network into the Regional Transmission Network at Pressure Reduction Stations. As a result of pressure reduction there is an associated temperature drop (Archer *et al.*, 1984) and if this pressure drop is sufficiently large then the outlet pipe temperature will be sub-zero. Downstream of the Pressure Reduction Station the gas temperature rises by heat transfer with the surrounding soil. Eventually, in the absence of a nearby downstream Pressure Reduction Station, the gas temperature will rise to the ambient ground temperature. It has been British Gas Corporation policy to *PRE-HEAT* the gas prior to pressure reduction so as to maintain a minimum outlet temperature of +5°C, but this is very costly and Archer *et al.* (1984) estimated savings of £10 million per annum could be made by reducing the amount of pre-heat applied.

In 1981 an internal study programme was initiated, within the British Gas Corporation, in order to assess the minimum acceptable gas temperature after pressure reduction (Archer *et al.*, 1984). This study investigated the mechanical integrity of the system, methods of improving pre-heater efficiency and the downstream gas temperature profile. Frost heave, which was known to produce pipe heave (Slusarchuk *et al.*, 1978) was monitored during sub-zero operations, and this occurred in a frozen soil annulus that formed around the pipe. More importantly to this thesis an unforeseen soil-pipeline interaction, ground cracking, was observed directly over and parallel to the pipe. These cracks were noted intermittently along that part of the downstream pipeline where the gas temperature had not recovered to 0°C (Archer *et al.*, 1984). These cracks had depths up to 600 mm with maximum ground surface widths of 150 mm, and Archer *et al.* (1984) suggested that they were a consequence of soil desiccation above the frozen annulus that produced a soil shrinkage crack. Similar cracking above large-diameter gas pipelines has been reported by Williams (1987), but very little information was available.

The remit of this study programme was to further investigate and define these two troublesome consequences, pipe heave and ground cracking, so that their effects could be incorporated into any future operational methodologies for chilled gas pipelines. Frost action has been the focus of many studies and it was known to produce two disruptive influences, frost heave and thaw settlement (Anderson *et al.*, 1984, Johnson *et al.*, 1984,

Crory *et al.*, 1984), both of which are considered to affect the safe operation of pipelines, especially in Arctic Regions (Williams, 1986). Frost heave leads to pipe uplift, which can affect pipeline integrity especially at locations of pipe restraint (Archer *et al.*, 1984) and at the interfaces between soils of different frost susceptibility (Nyman and Lara, 1986). Recently a large-scale indoor test facility at Caen, France has been operating a pipeline under long-term freeze-thaw cycles with freezing air temperatures (Geotechnical Science Laboratories, 1992), and much valuable data have been gathered on the fundamental nature of frost heave and its affect on chilled gas pipeline operation. However, ground cracking, particularly in temperate regions, has been rarely reported (Archer *et al.*, 1984, Williams, 1987). Through this study it was envisaged that this mechanism could be defined and further information collected on those parameters that influence the process of ground cracking. Such a definition is necessary prior to the advancement of any predictive methodologies or mitigative methodologies *ie.* techniques for reducing the severity of ground cracking.

This investigation was carried out in four distinct stages, the first involved a comprehensive literature review of the complex processes of frost heave and thaw settlement and, subsequently, their interaction with pipelines and other structures. During the second phase a questionnaire was carefully designed and sent to all the British Gas Corporation Regions to assess the full extent of the both chilled gas pipeline operation and the extent of these soil-pipeline interactions. Both these stages had a direct input to the design of a large-scale test that was carried out at Blackrod Pressure Reduction Station, which was one of the sites examined in the earlier study by Archer *et al.* (1984). The large-scale test was instrumented in two parts, initially the soil thermal, hydraulic and stress regimes around the pipe were monitored at three downstream sites, together with pipe movement and strain. These three sites were selected on their previous susceptibility to ground cracking. Subsequently Blackrod Pressure Reduction Station was instrumented to assess the effect of the growth of the frozen annulus on pipe heave and ground surface movement. Monitoring took place over three Pre-heating Seasons (Feb 1988 to Mar 1990) and two trials were undertaken (31/1/89 to 23/2/89, and 5/2/90 to 16/2/90) during which the outlet temperature was lowered to -5°C. The findings of these three stages were input, as design parameters, for a small-scale laboratory controlled model in which ground cracking was reproduced and monitored in carefully controlled conditions in two experiments on soils known to be crack susceptible.

This thesis presents the results from each stage of the study which, as the study progressed, led to the increased definition of the ground cracking mechanism, together with the provision of information on the parameters which affect both frost/pipe heave and ground

cracking. The large-scale test indicated that ground cracking occurred at times of rapid pipe heave, and this was further examined in the laboratory model. During the expansion of the pipe/frozen annulus composite the ground surface was noted to move upwards with the maximum directly over the pipe centre. The small-scale model successfully reproduced ground cracking showing the value of such tests when the parameters under consideration are correctly incorporated into the design. Again cracking was noted after upward ground surface movements. This led to the development of the mechanism of ground cracking in response to upward ground movement. Mitigative solutions and pre-installation measures are discussed, and finally suggested techniques for pipeline operation avoiding excessive ground cracking and frost heave are put forward.

CHAPTER 2 BACKGROUND TO LOW TEMPERATURE OPERATION

2.1 Introduction

Natural gas has been utilized as a fuel for over one hundred and fifty years in certain areas of the U.S.A. (Katz *et al.*, 1959). However the availability and utilization of the material increased dramatically after World War Two, when it was technically feasible to supply gas through 750 mm (30 inch) diameter pipelines operating at pressures up to 6.9 MN/m² (69 bar). These large diameter pipelines together with associated compressors can supply domestic and commercial users located at vast distances from the gas fields. This resulted in the progressive modification and expansion of Coal Gas (Town Gas) mains distribution systems to cope with Natural Gas.

In the last thirty years vast deposits of natural gas have been discovered in the Netherlands, Algeria, Canada, Siberia, Pakistan and of course in the North Sea. This has led to massive increases in natural gas transmission lines, together with increased demand and again modification to the distribution systems already in place. Natural gas is also liquefied to produce Liquefied Natural Gas (LNG) which is exported in specially constructed tankers typically to countries, such as Japan, which have no natural gas reserves.

This chapter describes the National Gas Transmission System within the British Isles as this is the system under consideration for sub-zero temperature operations. Information is also provided on the role of pre-heating and pressure reduction in relation to low temperature operation as this provides the technical background to some of the decisions taken by the British Gas Corporation to alter the outlet temperature during the course of the field study.

2.2 The British Gas Corporation National Transmission System.

2.2.1 Development of the National Transmission System.

" Town Gas " which was produced from the destructive distillation of coal, had been utilized as a fuel for nearly two centuries. Originally this was supplied at low pressures however, as demand increased so did the distribution system which resulted in medium pressure mains and finally high pressure mains (Copp, 1967). Until the Gas Act of 1949 the industry was made up of many regionalised gas companies, however these were all nationalized forming the British Gas Corporation as it is now known.

In the mid 1960's LNG at -162 °C was imported from Algeria and stored in specially constructed cryogenic tanks at Canvey Island. This gas was allowed to expand by heating and subsequently passed along the first National Transmission line, running 560 km from Canvey Island to Leeds, as illustrated in Figure 2.1. This 450 mm (18 inch) diameter steel

line passes through the Midlands and has off-takes to several large cities along the route. Gas flow is induced by the 600 times volume expansion produced by the warming from -162 °C to ambient ground temperature (Copp, 1967).

Natural gas was discovered in the Southern Basin of the North Sea in the late 1960's, and subsequently lead to the planning, design and construction of a national transmission system in the early 1970's. In 1977 natural gas from Northern Basin of the North Sea entered an expanded National Transmission System at St Fergus in Scotland. More recently Morecambe Bay has come on-line and further vast reserves are known to occur in the North Sea and off the Dorset coast.

2.2.2 The National Transmission System.

This is a comprehensive network of large diameter steel pipelines receiving natural gas from the North Sea, Morecombe Bay, and in the future, off the Dorset coast, and which are used to supply each of the twelve Regions (Figure 2.2). Within each Region gas is distributed to large centres of population via high pressure pipelines, from which the gas pressure is reduced for distribution to local districts through medium pressure mains and finally to the consumers via low pressure pipelines.

Design and management of the system is very complex as the correct amount of gas at a specified pressure must be delivered to each Region at a minimum cost. (Francis, 1981). Managing the system involves efficient utilization of the following:-

1. Weather forecasts to predict gas demand,
2. Compressors to optimize overall fuel usage,
3. Block valves to optimize the movement of gas and the mixing of gases of different origin to obtain a specified calorific value,
4. Line packing near Regional off-takes to satisfy the diurnal peaks in demand,
5. Peak shaving which is the ability to supply Winter peak demands from strategic storage ie. LNG tanks, salt cavities and B.G.C. owned gas fields,
6. Maintenance, whereby sections of the system are closed for routine or emergency repairs.

2.2.3 Design of Pipelines.

The design of the pipe characteristics, Pressure Reduction Stations and pipeline routing are derived from the Recommendations on Transmission and Distribution Practice from the Institute of Gas Engineers, IGE/TD/1 which is referred to as the technical directive on Steel Pipelines for High Pressure Gas Transmission (IGE, 1970). Amendments to IGE/TD/1 have been discussed in detail by Knowles *et al.* (1977).

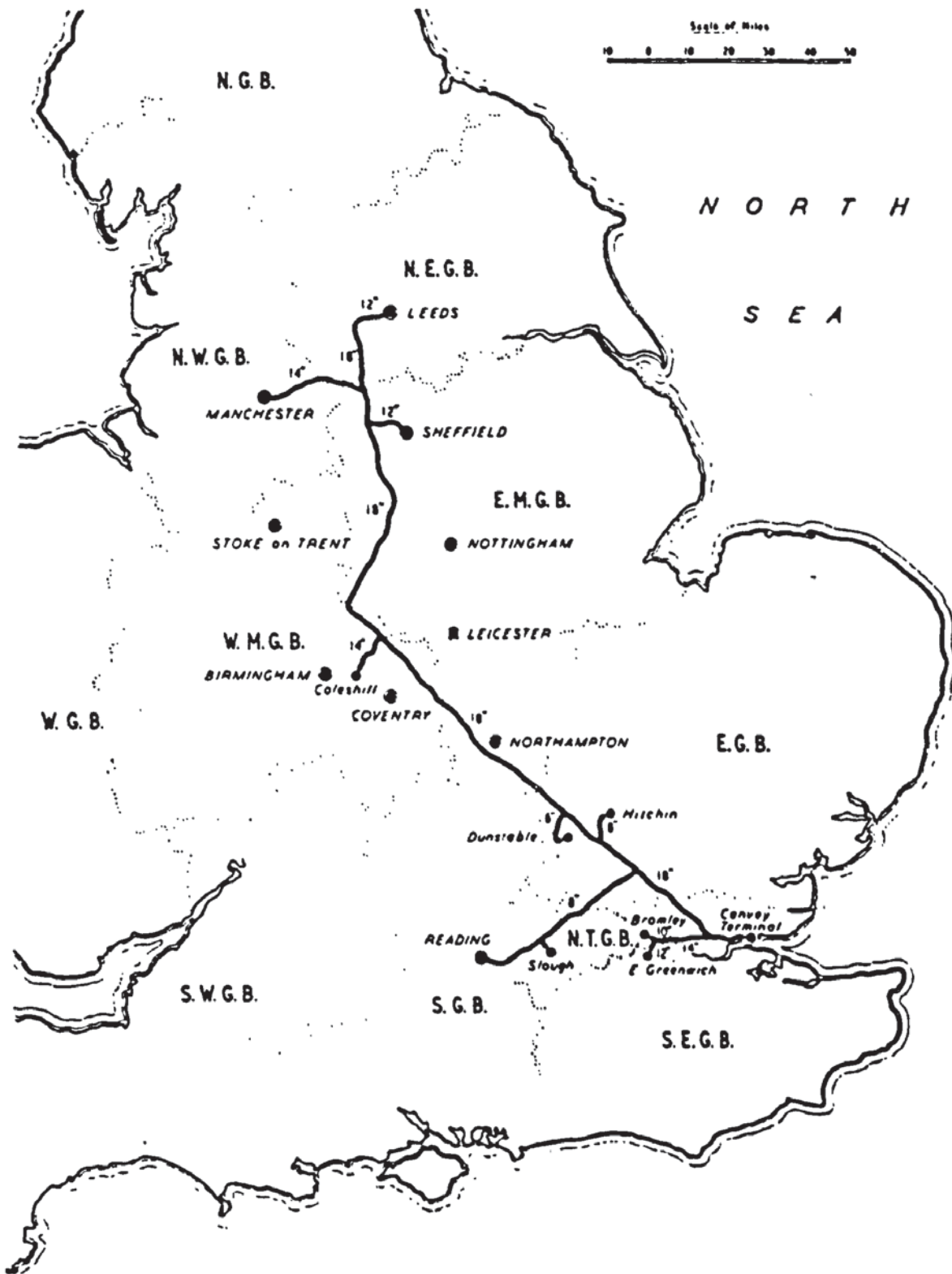


FIGURE 2.1 The First National Transmission System (after Copp, 1967)



Aston University

Illustration removed for copyright restrictions

FIGURE 2.2 The British Gas Corporation National Gas Transmission System (after Francis, 1984).

Once the requirements have been established for gas flow and pressure the pipeline material and thickness is selected, but additional allowances must also be made for both accidental damage by contractors' plant and thickness for stability for known defects. Route analysis is governed by safety considerations allowing for proximity to dwellings, population density and road crossings. The population density element is taken into account by using the rolling circle principle (Knowles *et al.*, 1977). Environmental awareness has grown over the last forty years and has recently resulted in an EEC Directive on the Environmental Impact Assessment of Certain Public and Private Projects (Clark, 1988). Therefore a formal Environmental Impact Assessment must be submitted to the local planning authority for approval prior to construction.

2.3 Blackrod Above Ground Installation.

2.3.1 Station Requirements.

Blackrod is the Pressure Reduction Station at the terminal point of a 900 mm nominal diameter pipeline in the North Western Region of British Gas. The layout of the system is shown in Figure 2.3 with gas supplied to Blackrod through Salmesbury. On leaving Blackrod it is routed to either Shevington, via a 600 mm x 9.5 mm X52 SAW pipe, or Partington, via a 900 mm x 12.7 mm X60 SAW pipe, both of these pipelines operating at 3.2 MNm^{-2} (32 bar). Furthermore these two lines are within the Regional Transmission System (Archer *et al.*, 1984) and, although Blackrod station is part of the National Transmission System, it is operated and maintained by the North Western Region to satisfy the design requirements of their system, namely:-

1. Gas supplies to the North Western Region under outlet pressure and volumetric controls,
2. Regional Grid Control with gas metering requirements,
3. Upstream line-packing,
4. Future gas storage in pipe array systems,
5. Emergency supply route to Partington.

Line-packing is no longer feasible for technical reasons, but the emergency supply route has been utilized as described by Francis (1984), however its use has been negated with construction of the 1050 mm (42 inch) nominal diameter line between Lupton and Partington (Figure 2.2), which has opened up the Morecambe Bay development.

2.3.2 Station Description.

A schematic diagram of the installation is shown in Figure 2.4 . When gas is supplied via Salmesbury under normal operating conditions it passes through the station and undergoes the following operations:-

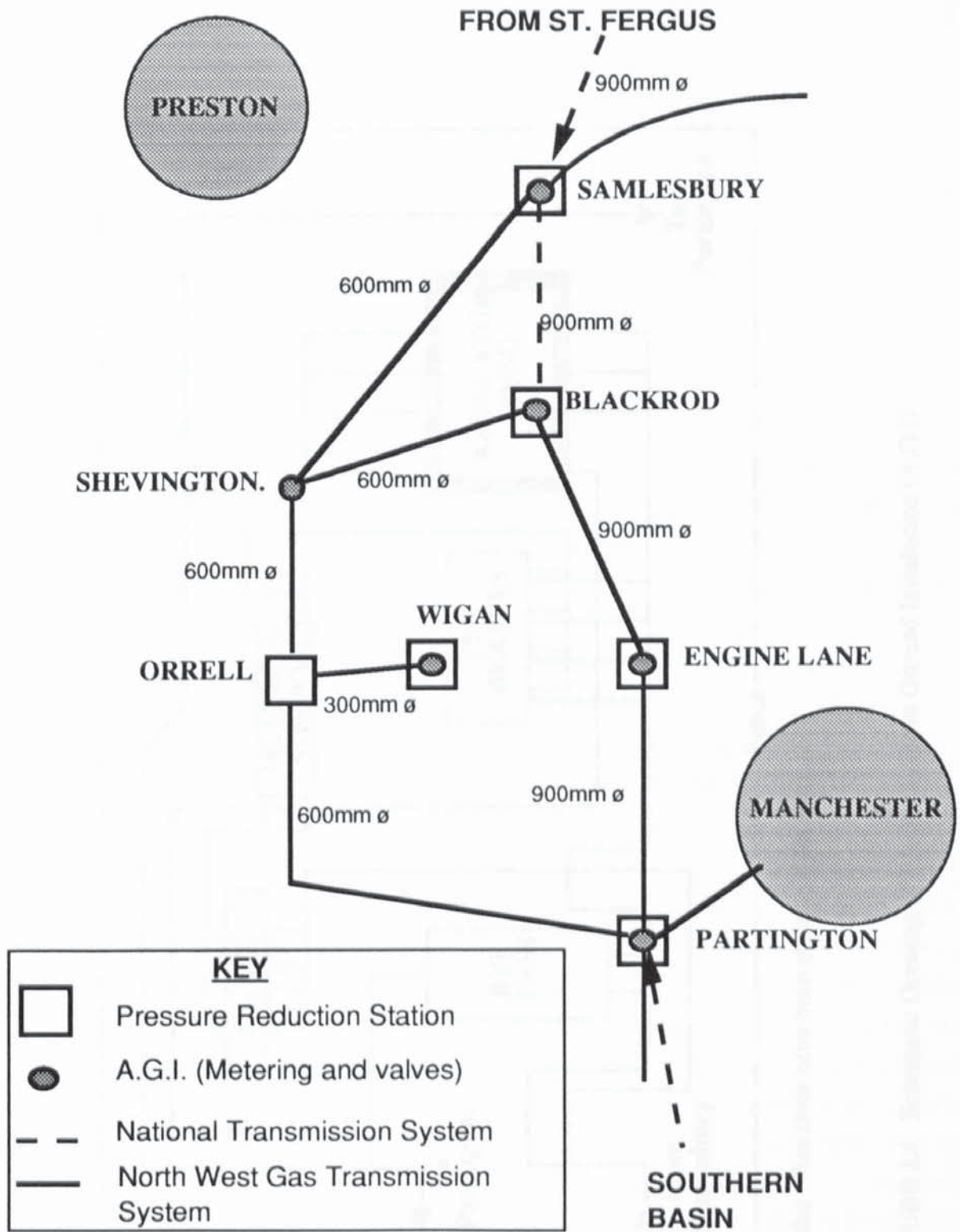
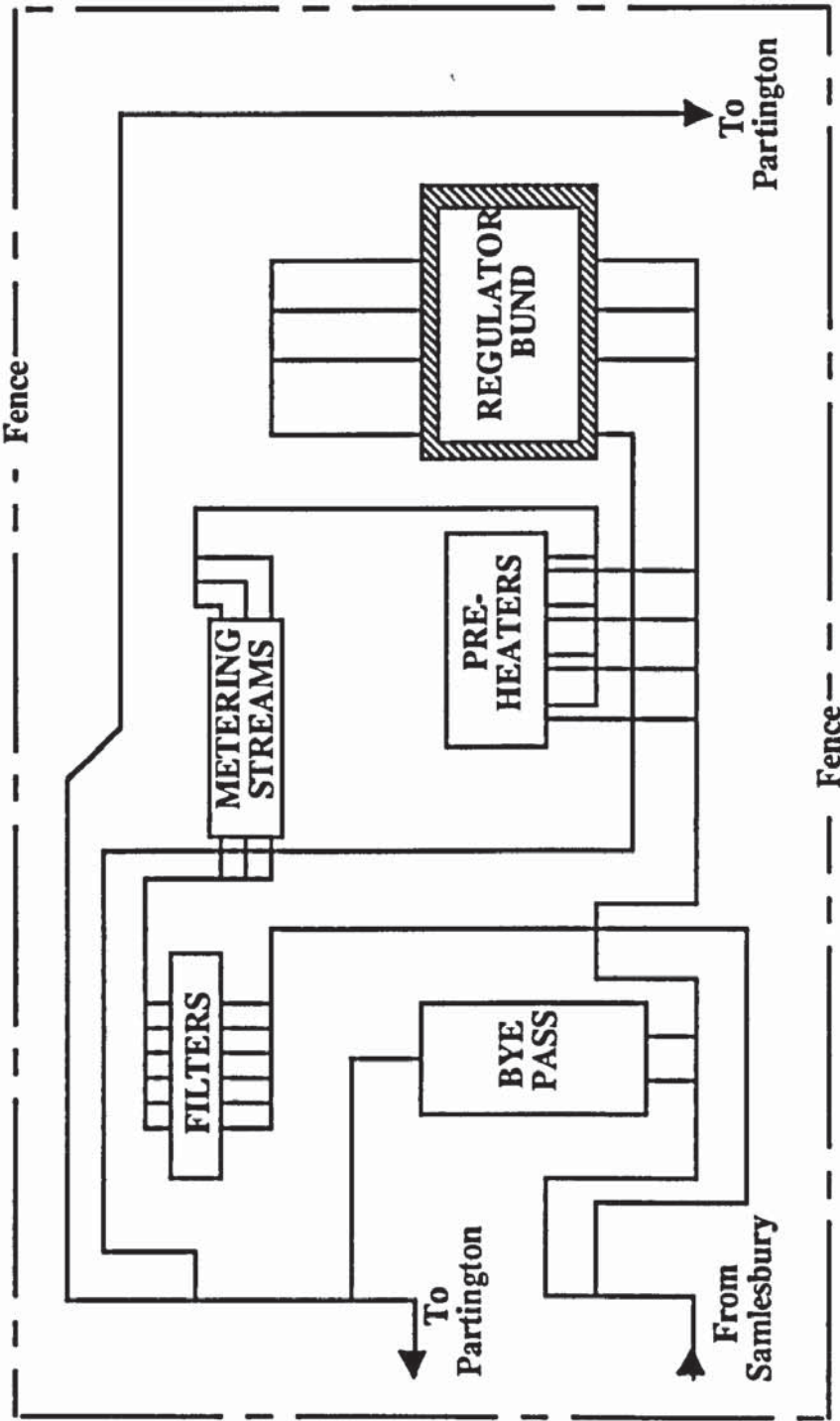


FIGURE 2.3 Schematic Drawing of That Part of the North West Gas Transmission System Which Includes Blackrod Above Ground Installation (A.G.I).



Note: The valves have been omitted for clarity.

FIGURE 2.4 Schematic Drawing of Blackrod Above Ground Installation (A.G.I)

1. Gas filtration,
2. Gas metering,
3. Pre-heating,
4. Pressure reduction,
5. Volumetric regulation.

In emergencies the station has a remote controlled by-pass system to allow diversion of gas supplies to Partington. The above sequence of operations is typical of many of the Pressure Reduction Stations in the National Transmission System.

2.3.3 Pre-Heating and Pressure Reduction

Pre-heat is applied to gas flowing at high pressures prior to pressure reduction in order to maintain an outlet temperature above 0°C. The need for and amount of pre-heating is dependent upon the inlet temperature, hydrocarbon and water dewpoint temperatures and the amount of pressure reduction anticipated (Huskens and Rick, 1980). During pressure reduction such as at Blackrod from 6.9 MNm⁻² (69 bar) to 3.2 MNm⁻² (32 bar) there is a drop in gas temperature resulting from the adiabatic expansion of natural gas through pressure reduction valves which is known as the Joule-Thomson effect (Katz *et al.*, 1959). If the temperature reduction is sufficient then two distinct problems may occur.

First, hydrocarbon and or water condensates may form if the gas temperature drops below either of the dewpoint temperatures. The formation of one or both of these condensates is likely to result in damage to filters, pressure reduction valves, and lead to the partial blockage of pipelines resulting in a reduction of the gas transportation capacity of the system. Gas hydrates, which are formed from hydrocarbon and water condensates, pose a greater risk to the systems' security than condensates alone as they are solids (Cooper, 1976). Both hydrocarbon and water dewpoints are controlled by treatment at the reception terminals, therefore eliminating condensates and hydrates from the National Grid System. Typically the water dewpoint temperature within natural gas from the St. Fergus reception terminal in Scotland is -10°C at 6.9 MNm⁻² (69 bar), and decreases as the pressure decreases (Archer *et al.*, 1984). The hydrocarbon dewpoint temperature is governed by a retrograde reaction, during pressure reduction from high pressures there is an increase in the dewpoint temperature to a maximum at about 3 MNm⁻² (30 bar), after which further pressure reduction produces the expected decrease in dewpoint temperature (Cooper, 1976). Therefore, at first stage pressure reductions such as Blackrod, hydrocarbon condensates are more likely after pressure reduction. Natural gas from St. Fergus supplied through Blackrod has a dewpoint temperature of - 20°C at 6.9 MNm⁻² (69 bar) so this does not present a problem to safe operation. Natural gas supplied from the Bacton reception terminal has a maximum dewpoint temperature of 0°C at 2.7 MNm⁻² (27 bar) and this could lead to

problems during low temperature operation but, as the gas flows downstream, it will heat up and so the condensates will vaporize due to the retrograde reaction (Archer *et al.*, 1984).

Secondly, and more importantly to this project, gas temperatures below 0°C will result in heat flow from the soil to the cooler pipeline. This will lead to soil freezing and, under unfavourable conditions of water supply, soil type, overburden pressure and temperature gradient will result in the expansive formation of ice lenses (Anderson *et al.*, 1984). The volume changes accompanying soil freezing around a chilled pipeline can lead to breakages in pipes, together with damage to structural foundations and concrete roads (Katz *et al.*, 1959).

" It has therefore been the British Gas Corporation policy to pre-heat gas prior to pressure reductions in excess of 1.4 MNm⁻² (14 bar) to maintain a minimum outlet temperature of +5°C" Archer *et al.* (1984). This is expensive as typically at Blackrod the pre-heaters use 0.125% of through flow to effect the heating required. Archer *et al.* (1984) estimated a Corporation saving of £10 million per annum if pre-heat were reduced from +5°C to a safe sub-zero temperature, according to the criteria set out in his paper.

This chapter details the background to the efficient and safe operation of the National Transmission Network. It also demonstrates the cost benefits that can be attained by operating the Network at sub-zero temperatures. However with respect to this study two troublesome soil-pipelines interactions which are ground cracking and frost/pipe heave, both of which are associated with the growth and recession of the frozen soil annulus around the pipe were identified.

Prior to a comprehensive review of these soil-pipeline interactions it is necessary to understand fully the complex interrelationships involved in the frost action processes of frost heave and thaw settlement. Similarly a summary of soil-pipeline interactions in the absence of frost action has to be considered before the introduction of a frozen annulus so as to assess novel aspects of the soil-pipeline interactions involved in chilled gas pipeline operation. Therefore the following chapter provides a full literature review of frost action from fundamentals and then by a chapter devoted to soil-structure interaction. In the soil-structure interaction chapter an introduction to and comments on the effect of frost action especially with respect to chilled gas pipeline operation are presented.

CHAPTER 3 FROST ACTION IN SOIL

This chapter is an overview of the frost action process in soils, but emphasis is placed on frost action under natural conditions. Frost action under artificially imposed conditions is very similar to the process under natural conditions except that the boundary conditions are different. Prior to the discussion of frost action it is necessary to assess the following soil properties; thermal, hydraulic, and stress. Once ample consideration has been given to these properties, their interaction in frost action will be discussed in terms of frost heaving and thaw settlement.

3.1 Soil Classification.

Soil classification is dependent on the discipline which is making the examination, eg. in agriculture the soil is referred to as a dynamic and living system in which biological processes are continually occurring (Farouki, 1986). In this study soil is considered in geotechnical terms, namely as "a matrix of grains and particles which are dependent on the deposition process, previous loading history and soil pore content, these can be filled with water, air or a mixture" (Wilun and Starzewski, 1975).

3.2 Ground Thermal Conditions.

3.2.1 Ground Surface Energy Balance.

The energy reaching the Earth's surface from the Sun has an affect on the ground surface temperature. This zone of temperature variation extends to a depth of between 5 and 25 m annually, while the diurnal variations extend to a depth of 1 m (Sellars, 1972). From the principle of the conservation of energy, a simple equation can be constructed to describe the surface energy balance.

$$Q_N = Q_H + Q_G + Q_{LE} \quad (3.1)$$

- Q_N = net exchange of radiation between the ground surface and atmosphere,
- Q_H = convection at the ground surface,
- Q_G = conduction of heat through the ground,
- Q_{LE} = latent heat involved in evaporation, snow melting etc.

This equation is illustrated in Figure 3.1 for the daily ground surface energy balance (Lunardini, 1981).

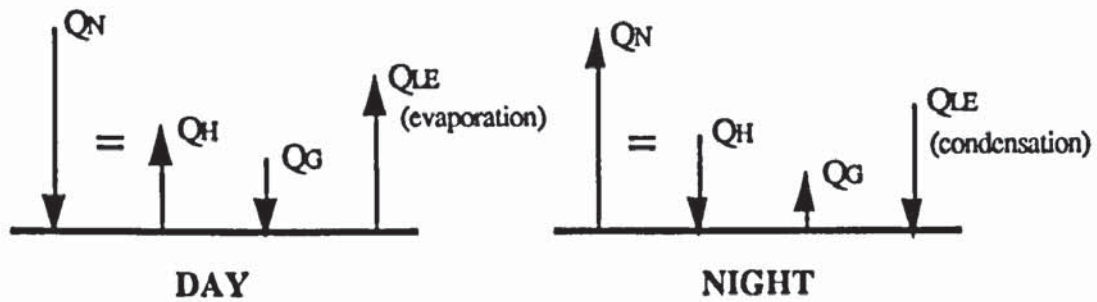


FIGURE 3.1 Daily Ground Surface Energy Balance (after Lunardini, 1981).

In the short term the net exchange in radiation may be positive or negative resulting in summer warming or winter cooling of the soil subject to temperature variations. In the long term, this can be a year, decade or longer, the net radiation exchange will balance unless there is an on-going climatic change. Local variations in vegetation, slope orientation, snow cover, micro-climate and both surface and sub-surface drainage can modify each of the energy transfer mechanisms shown in Figure 3.1. This can produce ground surface temperature variations between areas that are in close proximity (Harlan and Nixon, 1978).

3.2.2 Thermal Properties of Soils.

3.2.2.1 Heat Transfer.

Heat transfer occurs by the processes of conduction, radiation and the mass heat flow process of convection. Within soils under normal field conditions only conduction and convection are significant.

Conduction is the principal mechanism of heat transfer in both frozen and unfrozen soils, and encompasses all the soil constituents, soil particles, water, ice, water vapour and air. It is simply the transmission of heat by the passage of kinetic energy from one atom to another by vibration. Conduction can be described by a Fourier Law Equation, and for one-dimensional heat flow can be written as follows:-

$$q_x = -\lambda A \frac{dT}{dx} \quad (3.2)$$

q_x	=	energy flow in the x-direction	(W)
λ	=	thermal conductivity	(W m ⁻¹ K ⁻¹)
A	=	cross-sectional area	(m ²)
dT	=	change in temperature, across dx	(K)
dx	=	width of sample	(m)

Convection is the transmission of heat by the mass movement of heated particles (Harlan and Nixon, 1978). When a temperature gradient is applied across a soil sample there is a resultant increase in soil water density with decreasing temperature. The net result is that the less dense (higher temperature) water rises through the sample, and hence heat transfer occurs due to the mixing of these water currents. However at temperatures between 0 and 4°C there is an analogous expansion of water, therefore a reversal of normal convection flow can be expected in this region (Yen.Y.C, 1990). Other convection sources include ground water flow, suction to a freezing front and water redistribution during thawing.

For an engineering assessment of the thermal regime within a soil the thermal conductivity must be defined under steady state conditions. Furthermore it is necessary to define the heat capacity, latent heat and thermal diffusivity under transient thermal conditions.

3.2.2.2 Thermal Conductivity.

This is the measure of the heat flow in unit time through a unit cross-sectional area of soil under a temperature gradient in the direction of heat flow (Farouki, 1986). Thermal conductivity of a soil is dependent on the following:-

1. Soil mineralogy,
2. Soil density, particle and pore size distributions,
3. Soil moisture content,
4. Soil temperature,
5. Unfrozen water content and ice content for frozen soils.

Table 3.1 (Williams and Smith, 1989) shows the influence that soil mineralogy has on thermal conductivity, typically quartz has a thermal conductivity three times that of clay minerals. Increasing the dry density results in closer packing of the soil particles and therefore an increased particle contact area and so creating increased heat transmission. The thermal conductivity of a soil will increase with increasing moisture content, at constant dry density, up to saturation because the air is being replaced by water which has a higher thermal conductivity. Beyond initial saturation, further increases in total moisture leads to an increase in the voids ratio and a consequent reduction in soil contact area, therefore thermal conductivity will fall. Ice has a thermal conductivity four times that of water at 0° C, so that frozen soils generally have higher thermal conductivities than in their unfrozen state. It can be seen from Table 3.2 that the thermal conductivity of soil constituents are also temperature dependent but, over the temperature range of interest in this study programme, this property can be regarded as constant.

Estimation of thermal conductivity can either be made by physical measurements or empirical calculations. Laboratory measurements under steady-state or transient temperature conditions using the Guard Hot Plate (Johansen, 1980) and Thermal Probe (Riseborough *et al.*, 1983 and VanLoon *et al.*, 1988) respectively are the most commonly used methods. Slusarchuk and Watson (1975) and Goodrich (1986) have reported *insitu* measurements using the thermal probe.

Soil Constituents	Density (kg m^{-3})	Thermal Conductivity ($\text{W m}^{-3} \text{K}^{-1}$)	Volumetric Heat Capacity ($\text{MJ m}^{-3} \text{K}^{-1}$)	Thermal Diffusivity ($\times 10^{-6} \text{m}^2 \text{s}^{-1}$)
Quartz	2660	8.80	2.128	4.14
Clay	2650	2.92	2.385	1.22
Organic	1300	0.25	2.496	0.10
Water (0°C)	1000	0.56	4.180	0.13
Ice (0°C)	917	2.24	1.926	1.16
Air	1.2	0.025	0.0012	20.63

TABLE 3.1 Thermal Properties of Soil Constituents (after Williams and Smith, 1989)

Temperature (0°C)	Ice ($\text{W m}^{-3} \text{K}^{-1}$)	Water ($\text{W m}^{-3} \text{K}^{-1}$)	Quartz ($\text{W m}^{-3} \text{K}^{-1}$)
30		0.613	7.28
20		0.597	7.58
10		0.579	7.86
0	2.26	0.560	8.16
-10	2.32		8.50
-20	2.40		8.84
-30	2.48		9.18

TABLE 3.2 Variations in Thermal Conductivity with Temperature for Typical Soil Constituents (after Farouki, 1986)

Farouki (1986) describes the many empirical techniques available for estimation of thermal conductivity, of which the Kersten equations have been the most popular. Sanger (1968) produced a monogram from Kersten's equations for use in freeze-wall design. However Kersten's equations were known to give errors at low and high quartz contents and, additionally, they did not allow for the unfrozen water content in silts and clays (Johansen and Frivik, 1980 and Farouki 1986). Consequently Johansen and Frivik (1980) developed Kersten's equations to allow for both quartz and unfrozen water contents (Williams, 1989). Jesseberger (1980) used Kersten's equations as a first estimate and Johansen's equations as an exact solution for the estimation of thermal conductivity in freeze-wall design, but Jesseberger (1980) stated that under certain circumstances the use of empirical or graphical methods is unsuitable and so laboratory techniques are to be used for these circumstances.

3.2.2.3 Heat Capacity and Latent Heat.

Under steady-state conditions the temperature dependent thermal conductivity of the material is the only quantity that needs to be defined, but under transient temperature conditions the amount of heat flow through the material must also be determined. Heat flow is dependent on the heat capacity of a substance which is defined as the heat required to raise a given material by 1° C. It can either be defined in relation to mass or volume, these terms are known as specific heat capacity and volumetric heat capacity respectively (Harlan and Nixon, 1978).

For a composite material such as soil, the volumetric heat capacity is described as the summation of the appropriate value for each constituent as given below:-

$$C_s = C_p X_p + C_w X_w + C_i X_i + C_a X_a \quad (3.3)$$

C	=	Volumetric Heat Capacity (MJ m ⁻³ K ⁻¹),
X	=	Volume Fraction,
s,p,w,i,a	=	Soil, soil particles, water, ice and air.

Table 3.1 shows that the effects of the air volumetric heat capacity are negligible so can be ignored:-

$$C_s = C_p X_p + C_w X_w + C_i X_i \quad (3.4)$$

A similar equation involving mass fractions applies to the specific heat capacity of a soil.

At the phase change between water and ice there is a significant change in the total energy content (enthalpy) of a soil-water system (Smith and Riseborough, 1985). This occurs due to the large amount of heat liberated (334 kJ kg⁻¹) upon freezing of the soil water at constant temperature, and is known as the latent heat of fusion of water (Lunardini, 1981). This quantity can be calculated from:-

$$L_s = \gamma_d w l_w \quad (3.5)$$

L _s	=	Volumetric latent heat of fusion of the soil system (MJ m ⁻³),
γ _d	=	Dry density of the soil (kg m ⁻³),
w	=	Water content of the soil (m ³ m ⁻³),
l _w	=	Mass latent heat of fusion of water (MJ kg ⁻¹).

This quantity is dominant with respect to volumetric heat capacity of a moist soil at temperatures close to 0° C. In clays and silts freezing of the soil water occurs over a range

of temperatures below 0° C (Section 3.3.1.3) but, for sands, gravels and peats, the soil water freezes very close to 0° C. To allow for the latent heat effects taking place over a range of sub-zero temperatures in fine grained soils an apparent specific heat capacity can be calculated (Hoeskstra, 1969, Harlan and Nixon, 1978, Anderson and Morgenstern, 1973).

$$c_{ap} = c_s + \frac{1}{\Delta T} \int_{T_1}^{T_2} l_w \frac{\partial w_u}{\partial T} dT \quad (3.6)$$

- c_{ap} = Apparent specific heat capacity (MJ kg⁻¹ K⁻¹),
 c_s = Specific heat capacity of the soil (MJ kg⁻¹ K⁻¹),
 T = Temperature of the soil (K),
 ΔT = Temperature change = $T_2 - T_1$ (K),
 w_u = Unfrozen water content of the soil (m³ m⁻³).

The first term in equation 3.6 is referred to as the sensible heat process, the second term allows for the latent heat effects between temperatures T_1 and T_2 .

The most popular laboratory method for the determination of heat capacity is the Adiabatic Calorimeter and its use has been described by Johansen and Frivik (1980). Numerical and graphical techniques for the estimation of heat capacities for engineering methodologies have been presented by Lunardini (1981) and Farouki (1982). Sanger (1968) derived the following widely used equations for volumetric heat capacity based on Kersten's work:-

$$C_s = \gamma_d (c_p + c_i w_i + c_u w_u) \quad (3.7)$$

- C = Volumetric Heat Capacity (MJ m⁻³ K⁻¹),
 c = Specific Heat Capacity (MJ kg⁻¹ K⁻¹),
 w = Water content (m³ m⁻³),
 γ_d = Dry density (kg m⁻³),
 s,p,i,u = Soil, soil particles, ice and unfrozen water.

for frozen soils:-

$$C_f = \gamma_d (c_p + c_i w) \quad (3.8)$$

for unfrozen soils:-

$$C_u = \gamma_d (c_p + c_u w) \quad (3.9)$$

- C_f = Volumetric heat capacity for a frozen soil (MJ m⁻³ K⁻¹),
 C_u = Volumetric heat capacity for an unfrozen soil (MJ m⁻³ K⁻¹).

To use either the above equations or the graphical method described by Lunardini, it is necessary to establish both the soil water content and dry density. Lunardini (1981) recommends that the actual physical properties are obtained where possible when describing heat capacity. In civil engineering applications for freeze-wall design these equations, in conjunction with the latent heat equation (Equation 3.5), have been used very successfully (Sanger, 1969 and Lunardini, 1980).

3.2.2.4 Thermal Diffusivity.

Thermal diffusivity is a measure of the rate of change of temperature of a material and is applicable to transient temperature conditions. It is defined as the rise in temperature of a unit volume in response to a given quantity of heat, and is proportional to the thermal conductivity and inversely proportional to the volumetric heat capacity (Harlan and Nixon, 1978).

$$\alpha = \frac{\lambda}{C} \quad (3.10)$$

α	=	Thermal diffusivity	$(\text{m}^2 \text{s}^{-1}),$
λ	=	Thermal conductivity	$(\text{W m}^{-3} \text{K}^{-1}),$
C	=	Volumetric heat capacity	$(\text{MJ m}^{-3} \text{K}^{-1}).$

This term is used in transient heat flow equations for such purposes as engineering applications. This is the unidirectional heat transfer equation that assumes no phase change takes place:-

$$\frac{\partial T}{\partial t} = \alpha \frac{\partial^2 T}{\partial z^2} \quad (3.11)$$

t	=	Time	$(\text{s}),$
z	=	Depth	$(\text{m}),$
T	=	Temperature	$(^\circ\text{C}).$

The higher the value of thermal diffusivity the more rapidly a soil will exhibit temperature change, and so the values shown in Table 3.1 indicate that quartz will more readily undergo temperature change, under similar conditions, than either clays or peats. At temperatures close to 0°C , the latent heat effects produce a very large increase in the apparent volumetric heat capacity in relation to the thermal conductivity. This occurs especially in moist fine grained soils and results in the apparent thermal diffusivity decreasing by up to two orders of magnitude (Williams and Smith, 1989). Many numerical techniques have been used to allow for the latent heat of fusion (Lunardini, 1981).

3.2.3 Ground Thermal Regime.

This study is targeted at the soil-pipeline interactions associated with the operation of large diameter chilled gas pipelines at shallow depths (to a maximum depth of 5 metres). The ground temperature regime within the depth of burial of the pipeline is primarily influenced by the pipeline operating conditions in conjunction with the solar radiation and the ambient air temperatures (Horten *et al.*, 1983 and Lunardini, 1981).

3.2.3.1 Ground Temperature Profile.

Ground temperatures are determined from air temperatures, soil thermal properties (Section 3.2.2) and the heat flow from the interior of the Earth. Heat flow from the interior of the Earth is negligible in comparison to the other two parameters. Temperature records show that air temperature oscillate diurnally and annually and that this oscillation can be approximated to a sine wave by the following equation (Horton *et al.*, 1983):-

$$T_g = T_m + A_s \sin(\omega t) \quad (3.12)$$

- T_g = Ground temperature ($^{\circ}\text{C}$),
- T_m = Mean air temperature in the time interval under consideration ($^{\circ}\text{C}$),
- A_s = Amplitude of the temperature sine wave ($^{\circ}\text{C}$),
- ω = Angular frequency, ($= 2\pi / p$), (s^{-1}),
- p = Period of oscillation (s),
- t = Time (s).

Due to changing solar radiation and air temperatures on both diurnal and annual time scales a temperature wave propagates downwards through the soil mass. The amplitude of the assumed sine wave attenuates with depth until a constant point is reached as is illustrated in Figure 3.2 . This can be described by the following equation:-

$$T_g(z,t) = T_m + A_s \exp\left(-z \sqrt{\frac{\pi}{\alpha p}}\right) \sin\left(\frac{2\pi t}{p} - z \sqrt{\frac{\pi}{\alpha p}}\right) \quad (3.13)$$

- z = Depth (m),
- α = Thermal diffusivity ($\text{m}^2 \text{s}^{-1}$)

This equation assumes that heat transfer is by conduction, heat flow is uni-directional, soil and thermal properties are constant during temperature change and with time (Bahmanyar, 1982). Typically heat given out by microbiological interactions, ground cover resulting

from vegetation or snow cover, non homogeneous soil properties lead to deviations from this ideal equation.

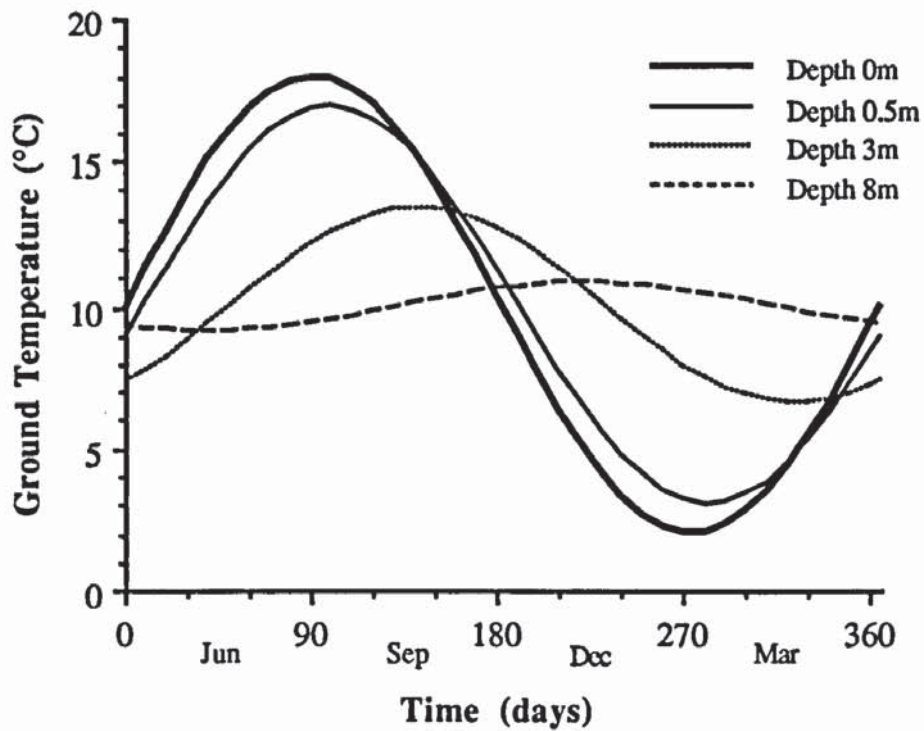


FIGURE 3.2 Ground Temperature Profiles Calculated from Equation 3.13 Assuming $\alpha = 1.22 \times 10^{-6} \text{ m}^2 \text{ s}^{-1}$ (typically for clays), $T_m = 10^\circ \text{ C}$ and $A_s = 8^\circ \text{ C}$.

The latent heat evolved during soil freezing produces a phenomena referred to as the " zero curtain effect " (Williams and Smith, 1989), this produces a plateau on the sine curve during the freezing process (Figure 3.3). This effect is due to the latent heat released upon freezing balancing the decrease in specific heat of all the soil constituents.

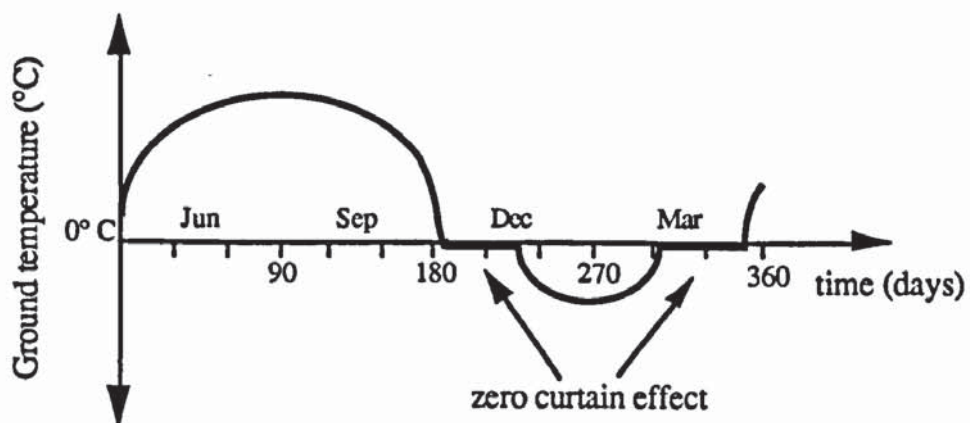


FIGURE 3.3 Diagram Illustrating the Zero Curtain Effect that the Latent Heat of Soil Freezing can have on a Ground Temperature Profile within a Soil Mass (after Harlan and Nixon, 1978).

3.3 Principles of Soil Freezing.

Soil freezing was first subject to detailed investigation by Taber (1917,1929,1930), and further experimentation and numerical modelling has since built upon and modified his original conclusions (Anderson *et al.*, 1984a). In his experiments Taber (1929, 1930) froze soil specimens from the top downwards, allowing an adequate supply of water at the base of the sample. He demonstrated that the heave of the soil specimen was greater than could be accounted for by the 9% expansion of water to ice within the soil mass. This was also demonstrated by soaking the sample in benzene or nitrobenzene which, unlike water, contracts upon freezing, during these freezing tests segregated layers of solid benzene appeared and the sample heaved (Taber, 1930). Ice segregation was also shown (Taber, 1929) to be related to the particle size distribution, pore size, availability of soil water and to the rate of cooling. Indeed his experiments demonstrated the significance of the soil particle surface and interfacial energies on both frost heave and ice segregation (Anderson *et al.*, 1984b).

Extensive research into frost action has been carried out since the initial studies by Taber (1929, 1930) mainly in connection with road, building and pipeline design. This has resulted in many laboratory testing programmes and currently, with the use of computers, numerical techniques have been developed using the basic principles of coupled mass-heat transfer (Williams and Smith, 1989).

The soil freezing process can pose severe problems to many civil engineering structures, due to the potentially troublesome consequences of:-

1. Frost heave and,
2. Thaw settlement.

O'Neill and Miller (1985) stated that frost heave alone has led to world-wide damages to civil engineering structures worth billions of dollars per annum and the engineering consequences of thaw settlement in permafrost areas is thought to pose a greater problem.

3.3.1 Ice Segregation.

Under natural freezing conditions, the zero isotherm penetrates into the ground. The resulting frozen soil may simply be a strong matrix of soil particles held together by ice or, under conditions favouring frost heave, segregated ice lenses may form. Fine grained clays may give rise to a reticulate ice lens structure, which is polygonal in the direction of heat flow, and has interconnecting horizontal ice lenses (Figure 3.4).

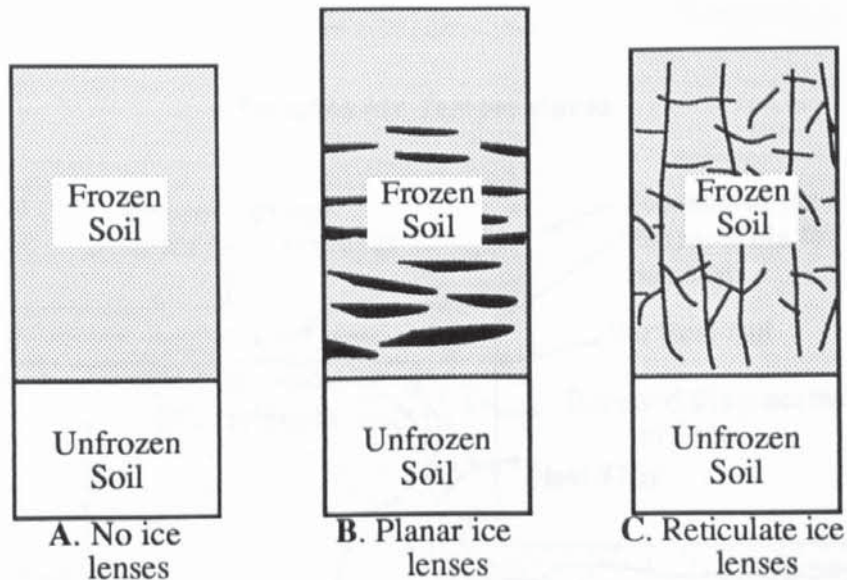


FIGURE 3.4 Diagrams Illustrating the Formation of Ice within Differing Soils.

Frost heave is the upward displacement of a surface resulting from ice segregation, and this occurs only if the following three conditions are satisfied:-

1. The soil is frost susceptible,
2. An adequate supply of water is present to supply ice lensing, and
3. Freezing ground temperatures are present.

It follows that if one of the above conditions is excluded then the risk frost heave will be significantly reduced. Anderson *et al.* (1984b) illustrated the ice segregation and frost heave processes in Figure 3.5.

Figure 3.5 illustrates a number of conditions that occur during soil freezing:-

1. Heat and soil water flux gradients are not independent,
2. Heat and soil water flow are perpendicular to the ground surface,
3. Ice lenses are planar and form perpendicular to both the heat and soil water flux,
4. Water for ice segregation is drawn from a close supply, in this case the water table, and
5. Ice lenses form slightly behind the 0°C isotherm.

The upward surface displacement (frost heave) is approximately equal to the summation of the thickness of the individual ice lenses, only if soil consolidation does not take place. When the water table is closer to the ground surface, it is more readily accessible and the total amount of frost heave will be larger (Anderson *et al.*, 1984b).

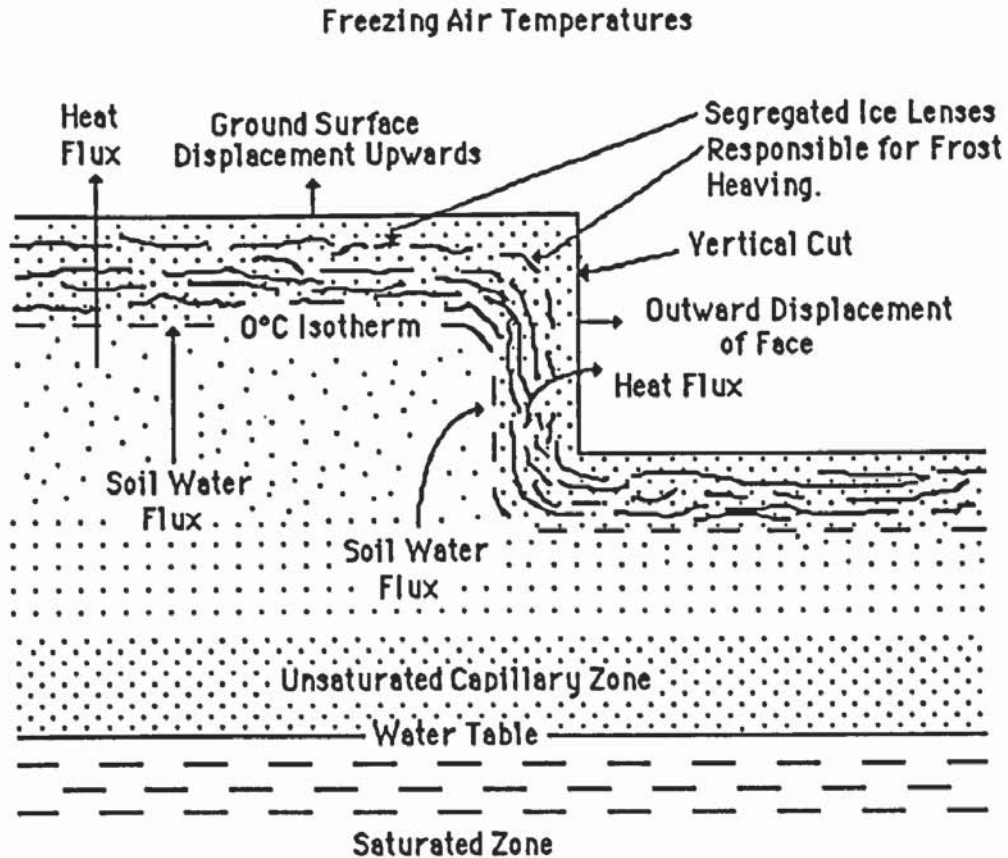


FIGURE 3.5 Schematic Illustration of Frost Heaving (after Anderson *et al*, 1984b).

At constant freezing air temperatures a 0°C isotherm will penetrate into a soil mass, the rate of penetration decreases exponentially with time (Lunardini, 1981). Under conditions favourable for frost heaving, segregated ice lenses form and grow at localities where there is a balance between the thermal and moisture migration gradients. This occurs slightly behind the descending 0°C isotherm. The balance is a result of the equilibrium of the coupled mass-heat flow at the base of the growing ice lens. At equilibrium the rate of latent heat dissipation through the frozen soil (along the thermal gradient) is just sufficient to change the state of all the moisture arriving at the base of the ice lens (along the moisture gradient) to ice. The ice lens will continue to enlarge until this balance is disturbed and, as the 0°C isotherm subsequently descends, a new balance will occur leading to the formation of a new ice lens (Figure 3.6). As the rate of penetration of the 0°C isotherm slows, the coupled heat-moisture flow will be in balance for longer, producing larger ice lenses. If freezing under constant conditions were to continue then a final ice lens would form and enlarge indefinitely.

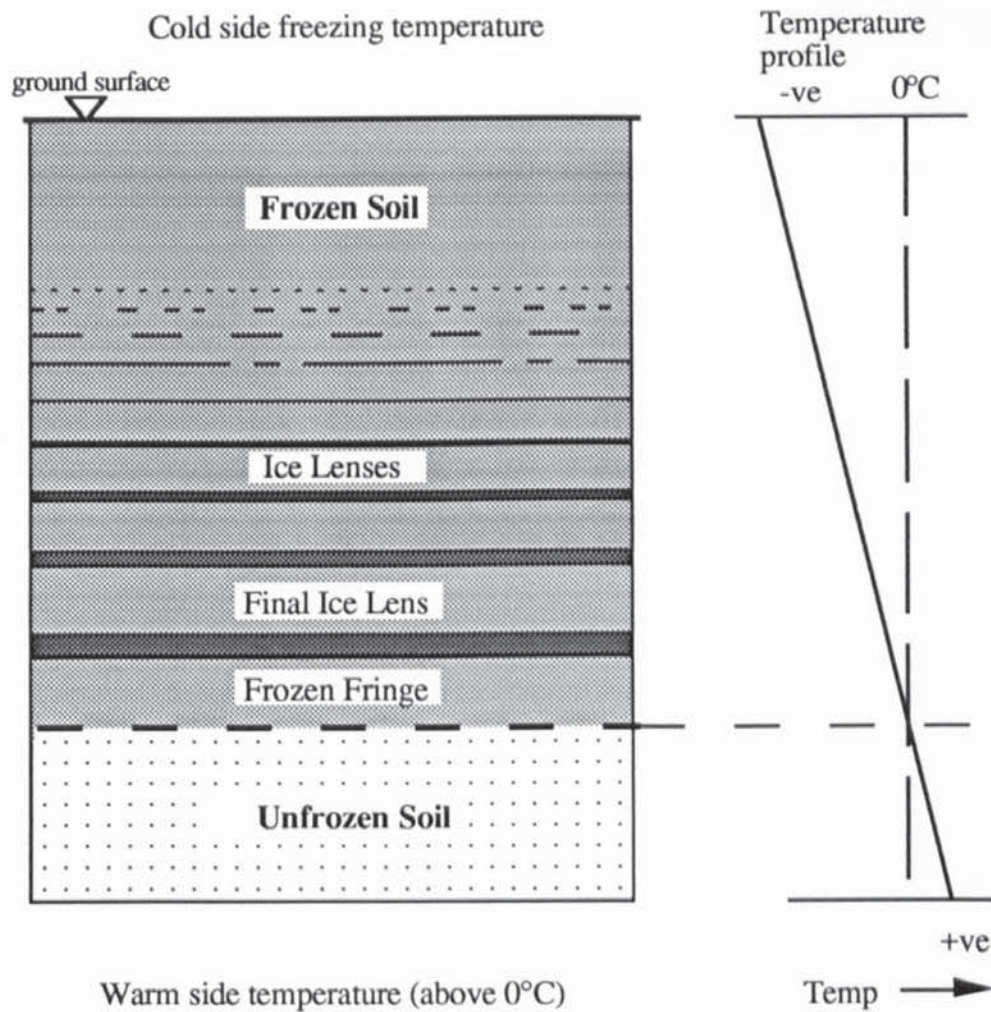


FIGURE 3.6 A Diagram Illustrating the Formation of Ice Lenses under Constant Air and Ground Temperatures.

3.3.2 Thermodynamics of Soil Freezing.

The form of the Clausius-Clapeyron shown in Equation 3.14 describes the fundamental relationship between temperature and pressure of the pore water (unfrozen and frozen) in frozen soils.

$$\frac{dT}{dP} = \frac{(V_i - V_w)T'}{l_w} \quad (3.14)$$

- dT = Temperature below melting point of ice (K), = $(T - T')$,
- T = Equilibrium temperature (K),
- T' = Temperature of melting ice at atmospheric pressure (K),
- dP = Pressure change on the system (kN m^{-2}),
- P = Pressure (kN m^{-2}),
- V = Specific volume ($\text{m}^3 \text{kg}^{-1}$),
- l_w = Mass latent heat of fusion of water (kJ kg^{-1}).

This equation describes the freezing point depression due to application of overburden pressures. However, the change in pressure must be taken equally by both the liquid and solid water phases. For ice segregation to occur the ice pressures must exceed both the soil strength and overburden pressure but, in reality, the water pressure becomes more negative indicating an increasing suction force. Therefore Equation 3.14. cannot successfully describe the pressure-temperature relations during ice segregation. From basic Gibbs Free Energy considerations (Williams, 1982) it can be shown that the freezing temperature can be related to unfrozen water pressure by Equation 3.15

$$dT = -dP_w \frac{T' V_w}{l_w} \quad (3.15)$$

Equation 3.15 describes the increasing negative pressures in the unfrozen soil water resulting from decreasing temperatures assuming that the ice pressure is atmospheric. Therefore to successfully define the pressure-temperature regime in a freezing soil Equations 3.14 and 3.15 are combined to give the form of the Clausius-Clapeyron equation (Equation 3.16) that is associated with ice segregation.

$$T - T' = \frac{(dP_w V_w - dP_i V_i) T'}{l_w} \quad (3.16)$$

- P_i = Ice pressure (kN m^{-2}),
- P_w = Water pressure (kN m^{-2}),
- V_i = Specific volume of ice ($\text{m}^3 \text{kg}^{-1}$),
- V_w = Specific volume of water ($\text{m}^3 \text{kg}^{-1}$),
- T = Equilibrium temperature (K),
- T' = Temperature of melting ice at atmospheric pressure (K),
- l_w = Mass latent heat of fusion of water (kJ kg^{-1}).

Equation 3.16 can be used to explain the effects of overburden pressure (Equation 3.14) and temperature (Equation 3.15) on the matric potential (suction) of the unfrozen water. It also successfully describes the presence of unfrozen water in frozen soils as a result of the pressure difference ($P_i - P_w$) that exists between the unfrozen water and ice in the frozen soil.

These equations apply only under equilibrium or steady-state conditions, that is where there is no change in temperature or pressure on the system with time. Under natural conditions it is unlikely that equilibrium would occur, but Perfect *et al.* (1989) have stated that this does not invalidate their use because the moisture, stress and temperature movements are all to a lower energy status (equilibrium).

3.3.3 Soil Water Movement and Unfrozen Water Content.

3.3.3.1 Soil Water Movement in Unfrozen Soils.

Soil water is acted upon by a number of forces, which include, gravity, osmosis, surface adsorption and capillary effects. The sum of these forces is known as the Total Potential and is defined by the following equation:-

$$\phi = P + \Pi + Z \quad (3.17)$$

- ϕ = Total Potential (m),
- P = Pressure Potential (m),
- Π = Osmotic Potential (m),
- Z = Gravitational Potential (m).

Soil water flows from a high potential to a lower potential, so as to exist at its lowest energy state (Hillel, 1971).

Individual soils have a unique soil moisture characteristic curve that relates the soil moisture content to the soil suction. Typical curves for loam and sand are shown in Figure 3.7 (Marshall and Holmes, 1988). In Figure 3.7 the effects of osmosis are ignored and the Matric Suction is the term applied to the pressure potential when it is negative (suction). Matric potential occurs due to the interactions of capillarity and adsorption.

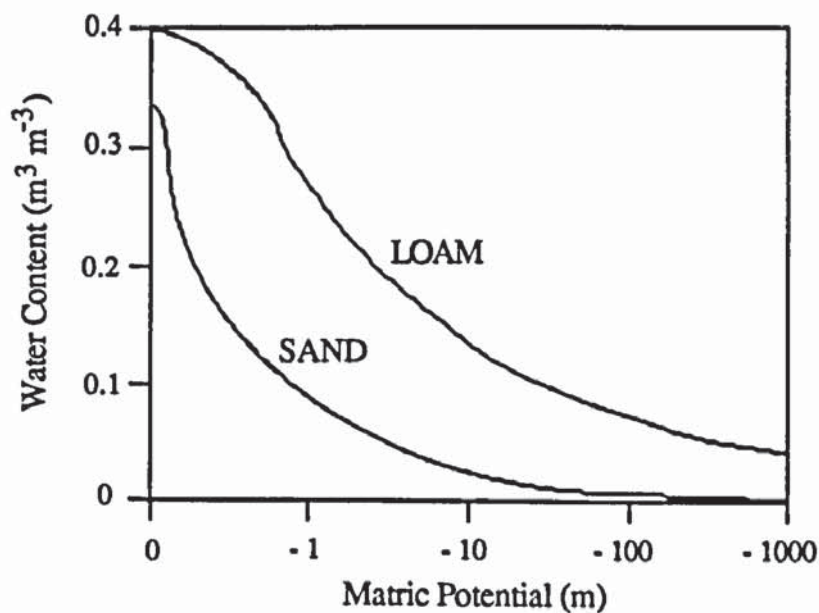


FIGURE 3.7 The Relationship between Water Content and Suction for a Sand and a Loam Soil (Moisture Characteristic Curves), (after Marshall and Holmes, 1988).

Capillarity exerts a greater influence on the frost heave process than adsorption, which is the attraction of the slightly polarized water molecules to the soil particle surfaces due to its chemical characteristics. This phenomenon is most marked in clayey soils due to the nature of their specific mineralogy (Marshall and Holmes, 1988). Capillary action results from the surface tension mobilized at the interface between soil water and air within the soil pores. The forces developed increase within decreasing pore size and this can be related to the simple theory of capillary rise (Marshall and Holmes, 1988). Under the influence of capillarity and adsorption, soil water will move upwards from a water table under a matric potential gradient. Equilibrium with gravitational potential will occur if sufficient time is allowed under static conditions (Hillel, 1971).

The rate of movement of water through a soil mass is governed by its hydraulic conductivity, which is dependent on pore size, porosity and degree of saturation (Marshall and Holmes, 1988). At saturation all the soil pores and voids are full and therefore soil water flow is at a maximum. However, from capillary theory, the application of a suction gradient causes the larger pores to empty first. As the suction increases smaller and smaller soil pores evacuate. In gravels and sands with large diameter pores, the hydraulic conductivity will fall by orders of magnitude under relatively small suctions. Clays on the other hand retain pore water until much higher suctions are applied (Figures 3.8a and 3.8b).

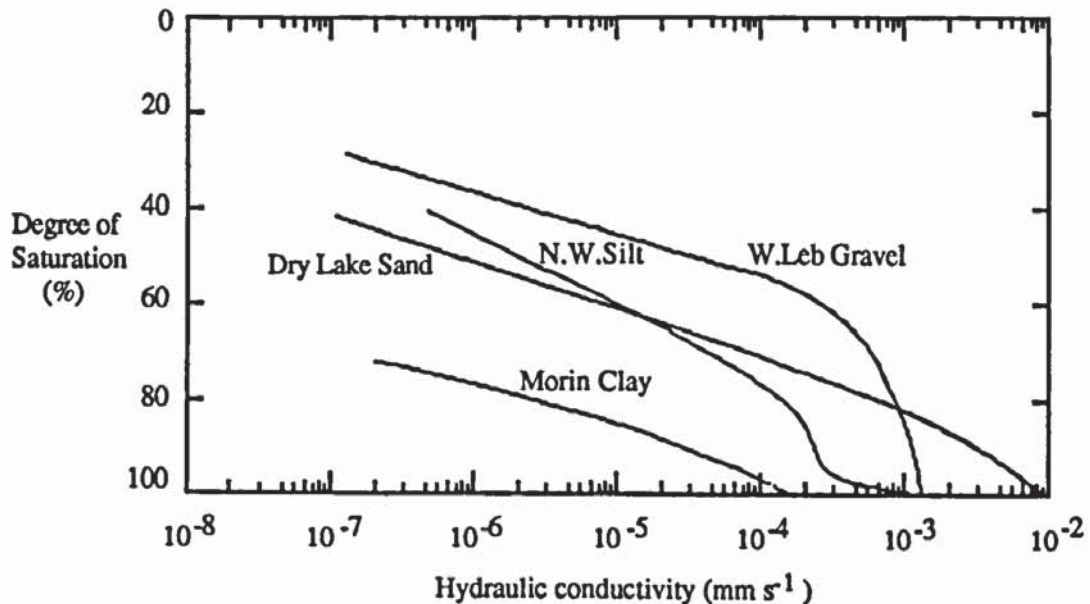


FIGURE 3.8a Graph of Hydraulic Conductivity against Degree of Saturation for Selected Soils adapted from Ingersol and Berg (1985).

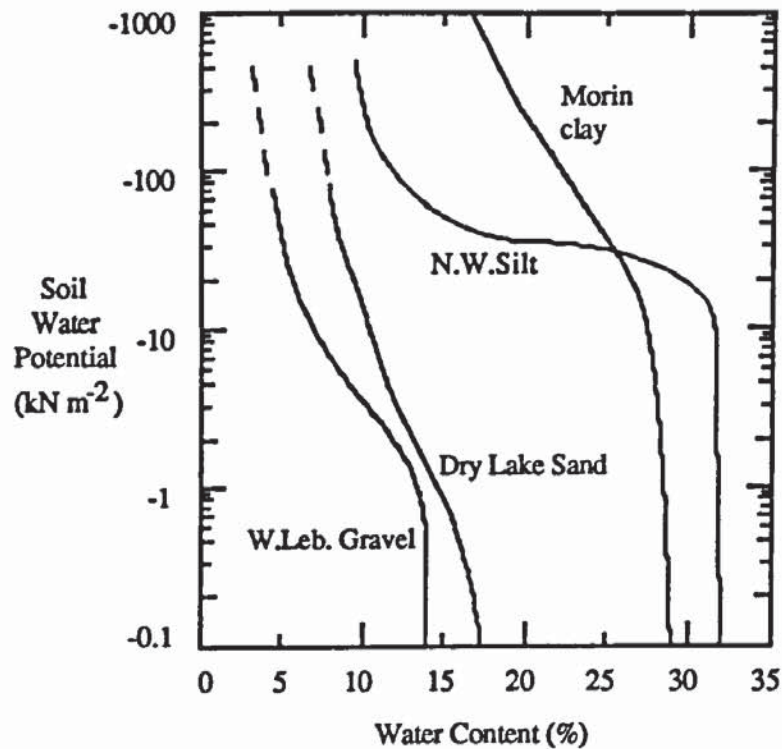


FIGURE 3.8b Graph of Soil Water Potential against Water Content for Selected Soils from Ingersol and Berg (1985).

This section demonstrates that the amount of water arriving at the 0°C isotherm is dependent on the following:-

1. Suction force developed behind the 0°C isotherm,
2. The hydraulic conductivity of the soil,
3. Soil porosity and pore size distribution, and
4. Distance of the 0°C isotherm from the water table (matric potential).

3.3.3.2 Unfrozen Water Content.

At temperatures below 0°C, ice, water and air co-exist in equilibrium in moist unsaturated frozen soils (Figure 3.9). The presence of unfrozen water can be explained in terms of matric and osmotic potentials, and is dependent on the temperature and pressure on the system (Xiaoui *et al.*, 1987). Total water content of a frozen soil is given by:-

$$w = w_i + w_u \quad (3.18)$$

- w = Total water content (%),
 w_i = Frozen water content (%),
 w_u = Unfrozen water content (%).

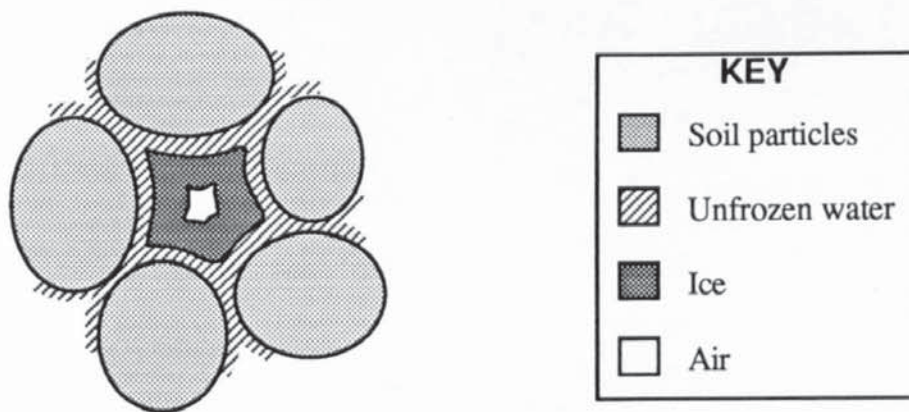


FIGURE 3.9 Diagrammatic View of the Co-existence of Ice, Unfrozen Water and Air in Equilibrium within an Unsaturated Frozen Soil Matrix.

Matric potential is the summation of the capillarity and adsorption potentials and this results in unfrozen water being held in a thin film around soil particles (Johnston, 1981). As freezing continues the amount of unfrozen water held by capillarity decreases until it is all held by adsorption. The amount of unfrozen water in a soil is dependent on the following (Lunardini, 1981 and Kay and Perfect, 1988):-

1. Soil temperature,
2. Soil specific area,
3. Salt concentration of the soil water,
4. Chemical characteristics of the soil particle surface,
5. Pressure on the soil (ie. on the unfrozen water-ice interface),
6. Mineralogical composition of the soil particles.

Clays have both a high soil specific area, and strong chemical interactions between the soil particles and polarized water molecules. In contrast, sands have a relatively small soil specific area and few if any chemical interactions exist between the soil and water (Marshall and Holmes, 1988). Therefore, under equivalent temperature and pressure conditions, the matric potential leads to much greater unfrozen water contents in fine grained soils (clays) as compared those in coarser grained soils. The overriding relationship is between unfrozen water content and soil specific area and is illustrated in Figure 3.10. This also demonstrates the limited effect of the total water content on the unfrozen water content for if the total water content is increased, the ice content will increase while the unfrozen water content is relatively unaltered (Anderson *et al.*, 1978).

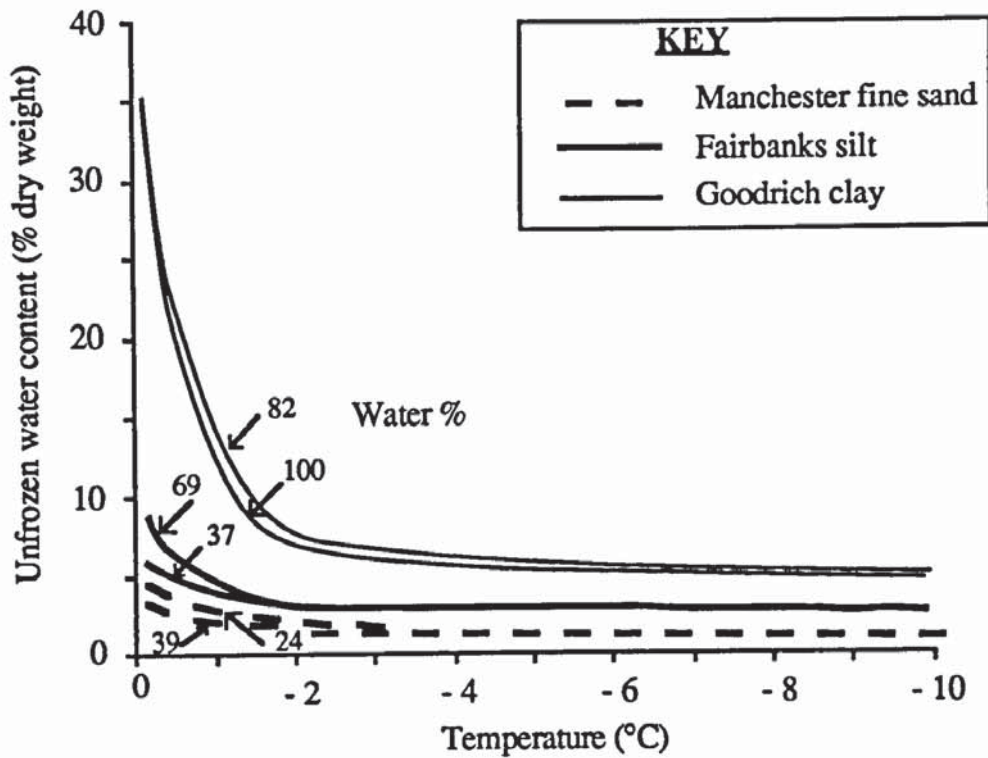


FIGURE 3.10 Illustration of Unfrozen Water Content against Temperature Curves for Three Different Soil Types, from Anderson *et al.* (1978).

Anderson and Morgenstern (1973) demonstrated that the unfrozen water content of a soil could be approximated by the following power law:-

$$w_u = m_1 T^{m_2} \quad (3.18)$$

T = Temperature below 0°C (°C),
 m_1, m_2 = characteristic soil parameters.

and from analysis of a number of experiments on different soils types the following regression equation was derived (Anderson and Morgenstern, 1973):-

$$\ln w_u = 0.2618 + 0.5519 \ln S - 1.449 S^{-0.264} \ln T \quad (3.19)$$

S = Soil specific area ($m^2 g^{-1}$)

Osmotic potential can affect the unfrozen water content when there are solutes present in the soil water. Solutes are known to depress the freezing point of soil water and, at constant temperature, increased salinity results in increased unfrozen water content (Xiaozu *et al.*, 1987). During progressive freezing the solutes are excluded from the growing ice lattice,

leading to an increasingly concentrated unfrozen water film around the soil particles and this change in the energy status of the system, between the ice and unfrozen water, results in increased unfrozen water contents (Kay and Perfect, 1988). Anderson and Tice (1989) and Xiaozu *et al.* (1987) have provided experimental information on the effects of salinity on a range of soils.

The application of pressure to a frozen soil results in an increased unfrozen water content. This is related to the basic thermodynamic Clausius-Clapeyron Equation (Equation 3.16) that links the pressure of the ice and unfrozen water with temperature. The pressure on the ice is increased and this causes ice to melt for the equilibrium to be re-established.

The physical occurrence of unfrozen water affects the hydraulic, stress and thermal regimes associated with soil freezing. Within a frozen soil an increase in unfrozen water content at constant temperature will produce a consequent increase in suction forces, therefore affecting the hydraulic gradient to the frost front. The unfrozen water is a critical parameter in determining the rate of creep of frozen soil, and so is related to the shear strength of the frozen soil (Sayles, 1988). The liberation of the latent heat of fusion takes place over a temperature range dependent on the unfrozen water content, and so the estimation thermal properties of a frozen soil, which are essential to geotechnical engineering design, are complex (Kay and Perfect, 1988). The unfrozen water content is the critical parameter for engineering purposes at temperatures close to 0°C. Indeed Ogata *et al.* (1983) have demonstrated the adverse affect on the compressive and creep properties due to the presence of salt in a frozen soil.

3.3.3.3 Soil Water Movement in Frozen Soils.

Moisture movement and redistribution are known to take place within frozen soils (Burt and Williams, 1976 and Xiaozu *et al.*, 1987). The presence of unfrozen water provides a route for moisture movement so that frozen soils have a hydraulic conductivity. Moisture flow in a frozen soil occurs in the thin liquid films around the soil grains and by regelation of the ice lenses. The hydraulic conductivity is primarily dependent on the unfrozen water content, and this is a function of temperature, soil particle distribution and soil particle specific area (Burt and Williams, 1976). As an example Smith (1985) has reported hydraulic conductivities in silty-clays in the range of 10^{-12} m s⁻¹ at temperatures of -1°C. He also observed that there is a rapid rise in hydraulic conductivity above -1°C but below this point it tends to stabilize. These values were calculated from simple Darcian flow theory. If ice segregation occurs there is a regelation movement of the ice along the temperature gradient, and this is responsible for water movement (Wood and Williams, 1985a). Water arrival at an ice lens results in increased water pressure and disturbs the water-ice equilibrium

(Clausius-Clapeyron equation), which is re-established by the freezing the unfrozen water. This exerts an increased pressure on the ice-water interface on the cold side of the lens, the ice melts in order to preserve equilibrium. In soils susceptible to ice segregation, water flow occurs by a series (regelation) - parallel (thin liquid film flow) process (Perfect *et al.*, 1989).

The temperature-pressure equilibrium of the ice-water interface indicates that for a decrease in temperature, the differential pressure ($P_i - P_w$) between the two phases will increase. Generally, this differential pressure increases with distance from the freezing front and, if the ice pressure is considered atmospheric, increasingly negative water pressures will be generated. Therefore, within a frozen soil, a temperature gradient can induce a hydraulic gradient, that in turn is the driving force for water migration. However these large suction forces are counterbalanced by the very low hydraulic conductivity of the frozen soil.

Ohari and Yammamoto (1985) demonstrated under precise laboratory conditions that a number of ice lenses could grow simultaneously behind the freezing front. Williams and Smith (1989) added that ice lenses were the areas for further ice accumulation because it is the hydraulic conductivity of the unfrozen water films not the ice layers that were the limiting factor in moisture migration. The hydraulic conductivity on the cold side of the ice lens is less than the warm side, thus some flow is accumulated by the ice lens (Figure 3.11).

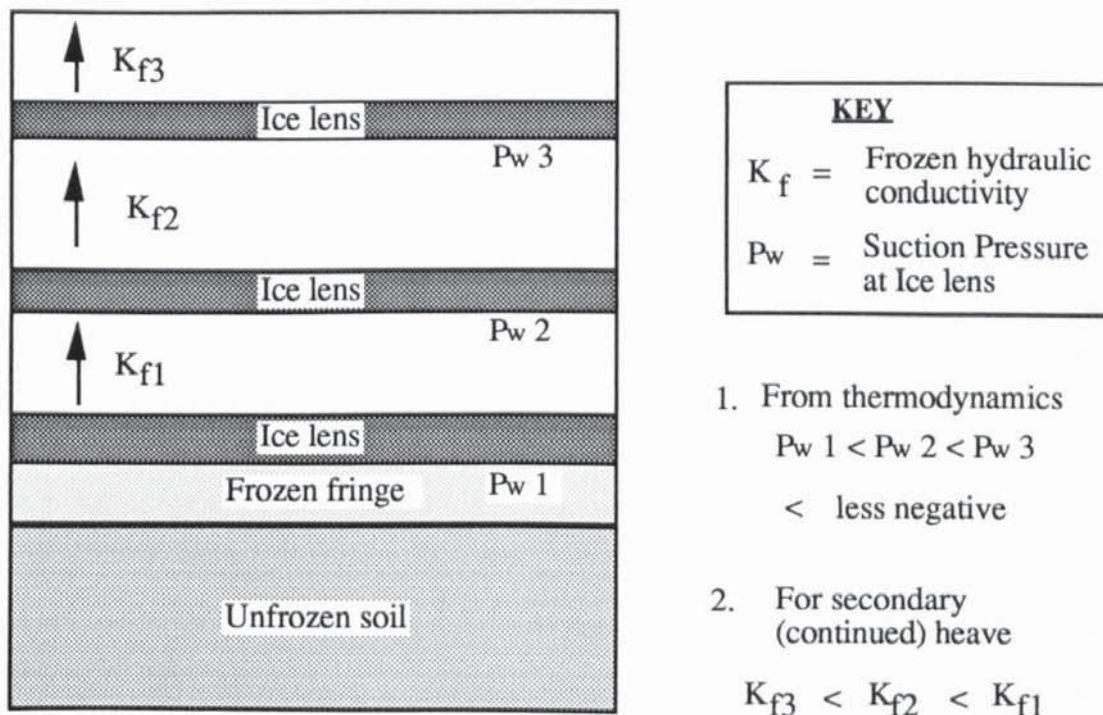


FIGURE 3.11 Diagrammatic Illustration of Secondary (Continued) Heave.

This simultaneous growth of ice lenses is termed Secondary Heaving (not to be confused with Miller's concept of secondary heave) and ice lens growth at the freezing front is termed Primary Heave (Williams and Smith, 1989). However, Smith (1985) refers to Continued and Initial heave respectively. Continued heave has been observed under field conditions by Mackay (1979), Smith (1985) and at a large-scale test facility at Caen (Smith and Patterson, 1989).

3.3.4 Pressures Generated During Soil Freezing.

Two basic pressures are generated during the freezing process, these take place in the water and the ice phases and are inter-related according to the temperature dependent Clausius-Clapeyron equation (Equation 3.16) as discussed in Section 3.3.2.

3.3.4.1 Suction Pressures.

Suction (negative) pressure is the matric potential in the unfrozen water behind the zero isotherm. Its effect on the unfrozen soil is to redistribute soil water towards the zero isotherm for ice lens enlargement in frost susceptible soils. However, this is dependent on the hydraulic, stress and temperature regimes of the surrounding soil. The influence of suction on water movement is primarily dependent on the hydraulic conductivity of the soil, because the large pressure gradients generated by the high suctions can be negated in soils with low hydraulic conductivities.

In clayey soils with little overburden pressure, these relatively large negative pressures can cause desiccation of the soil mass slightly in front of the zero isotherm leading to the reticulate nature of ice lenses in fine grained soils (Chamberlain and Gow, 1979). Small blocks of soil are desiccated producing small polygonal shrinkage cracks in the direction of heat flow and interconnecting fissures at right angles to the heat flow (Figure 3.4). These blocks of soil become over-consolidated leading to a permanent change in soil structure. In larger grained soils desiccation is unlikely because of their relative incompressibility in comparison to clays.

3.3.4.2 Frost Heave Pressures.

The pressures generated by an enlarging ice lens are responsible for frost heave pressures at the ground surface under natural freezing conditions. However, before an ice lens can form the ice pressure at the point of the temporary thermodynamic balance, where ice lens formation takes place, must be large enough to overcome the internal resistance of the surrounding frozen soil.

These pressures developed in the ice lens are highly temperature dependent and are maximal when the negative water pressure approaches atmospheric (zero). This occurs when the applied overburden pressure is sufficient to stop water inflow to the growing ice lens as defined by the Clausius-Clapeyron Equation (Equation 3.16). This will result in no water for ice accumulation, therefore the frost heave process is effectively halted. However the transfer of the microscopic ice lens pressures to macroscopic frost heave pressures is dependent on the properties of the frozen soil. Frozen soils are liable to creep and this tendency increases dramatically as the temperature approaches 0°C, as it is a function of unfrozen water content and soil grain size. Therefore the ice pressure difference between two adjacent ice lenses may be altered by the mechanical behaviour of the frozen soil separating them. Williams and Wood (1985a) demonstrated, using a specially constructed frost heave cell, that the magnitude of the internal stresses generated at temperatures close to 0°C were in good agreement with the Clausius-Clapeyron Equation. They also reported that substantial pressure gradients occurred across the sample and inferred that these resulted from the creep and stress relaxation (rheological properties) of the frozen soil matrix (Woods and Williams, 1985b). Therefore, the heaving pressure is related to the theoretical temperature-dependent, maximum pressure as modified by the temperature-dependent rheological properties of the frozen soil matrix. However, Perfect *et al.* (1989), notes that problems relating the macroscopic frost heave pressures to the microscopic pressures occurring in the ice lens have still to be overcome.

Overburden pressures on frozen soil are counteracted by the ice lens pressure (this roughly equates to the frost heave pressure), continued growth of the ice lens can result in very high frost heave pressures being generated if sufficient overburden is present. At temperatures close to 0°C a saturated frozen soil has a high rate of creep (Sayles, 1988) and this reduces the potential frost heave pressure. If Continued heave takes place at lower temperatures, then considerable frost heave pressure could be generated and these will be less likely to be modified by the creep properties of the soil. This could result in very large heaving pressures under very little displacements and would be presumably largest in finer grained soils such as clays. This is of special concern to the long-term soil-structure interactions, associated with prolonged frost heave, associated with chilled gas pipeline and cold storage tanks as identified by Williams and Smith (1989).

3.3.5 Heat Extraction Rate.

Loch (1979) and Konrad (1984) reported that the heave rate for a given soil was strongly dependent on the rate of heat extraction. Konrad (1987a) provided a diagrammatic illustration of the heave rate against net heat extraction rate for a fully saturated soil and splits the heave into segregational and "in situ" components (Figure 3.12).

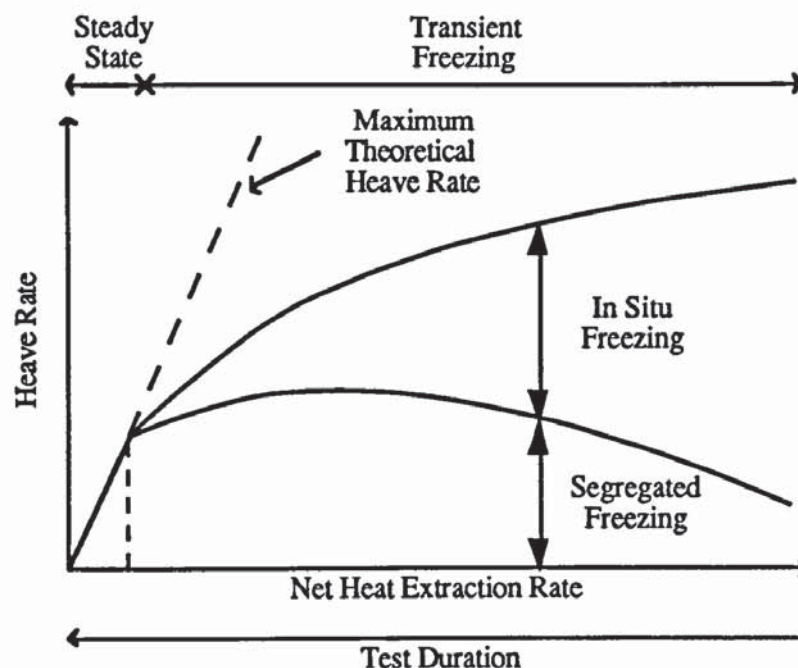


FIGURE 3.12 Diagrammatic Illustration of the Heave Rate against Net Heat Extraction Rate under Constant Cold and Warm Side Boundaries (after Konrad, 1987a).

In Figure 3.12 the theoretical maximum rate of heave is calculated from the assumption that all the water influx to the sample under test accumulates at a single growing ice lens. The diagram also indicates that, the net heat extraction rate decreases with increasing test duration. The graph also shows that at high rates of heat extraction the frost heave is primarily a result of *in situ* freezing however, as this extraction rate decreases, segregational freezing becomes the prominent mechanism of frost heave. Segregational heave is a function of heat extraction rates, and is maximal over a range of heat extraction rates (Loch, 1979).

3.3.6 Theories of Frost Heave.

This section summarizes some of the most popular theories at the present time. Frost heave is essentially a transport mechanism including water, heat, solutes and charge flow in relation to a solid matrix (Perfect *et al.*, 1989) and, from the preceding discussions, it is obvious that these theories only address a small range of the interactions that have been observed.

3.3.6.1 Capillary Theory.

This is analogous to capillary theory in unfrozen soils, but the interfacial energy involved is between the ice and water within the soil pores. The ice and water pressures can be related

to the pore geometry and ice/water interfacial energies by Equation 3.20, a full derivation is provided by Everett (1961).

$$P_i - P_w = \frac{2\sigma_{i w}}{r_{i w}} \quad (3.20)$$

$\sigma_{i w}$ = Surface tension along the curved water/ice interface (kN mm^{-2})

$r_{i w}$ = Radius of the ice/water interface (mm).

The basic assumptions within this model are:-

1. Soil is saturated,
2. Soils are ideal granular materials,
3. Adsorption and osmotic potentials are neglected,
4. Ice pressures are constant,
5. Ice lenses grow at the zero isotherm,
6. Angle of contact at ice/water interface is zero.

When Equation 3.20 is combined with the Clausius-Clapeyron Equation the limiting radius of the ice/water interface can be calculated and is shown to be temperature dependent (Equation 3.21).

$$r_{i w} = \frac{2\sigma_{i w} V_w T'}{l_w (T - T')} \quad (3.21)$$

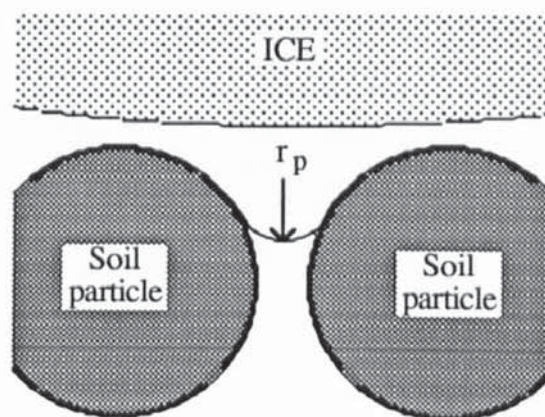


FIGURE 3.13 Diagrammatic Illustration of the Idealized Capillary Theory Showing the Pore Radius (r_p) for Ice Propagation.

Figure 3.13 illustrates the formation of an ice lens in a soil, and is dependent on the magnitude of the pore radius (r_p) to ice-water interface radius ($r_{i w}$). Ice will penetrate

through a soil with a descending frost front when r_p is greater than r_{iw} . When r_{iw} is greater than r_p ice cannot propagate through the pore, the temperature drops causing a drop in r_{iw} and, from Equation 3.20, a hydraulic gradient is formed providing water for ice lens growth. Eventually, as a result of local thermal and hydraulic imbalances at the ice lens r_{iw} falls below r_p and ice propagates downwards until favourable conditions for ice lens growth.

3.3.6.2 Hydrodynamic Theory.

Harlan (1973) proposed a model that interrelates heat and moisture flows in the partially frozen soil behind the frost front via the application of coupled flow equations. He assumed that the unfrozen liquid flow around the soil particles, from the warm to the cold side temperatures in partially frozen soil, could be described by Darcian flow. The model is therefore based on an analogy with moisture flow in unsaturated unfrozen soil. The existence of this partially frozen zone and its moisture flow characteristics have been investigated by others (Kay and Perfect, 1988), and Miller (1978) termed this region the 'Frozen Fringe'. In this model the ice lens is considered to be immobile and under atmospheric pressure. However, ice lens formation has a profound affect on moisture flows.

In the hydrodynamic theory, the heat and moisture flow equations (3.22 and 3.23) are combined to form Equation 3.24. However, convection is neglected in the heat flow equation and an Apparent Volumetric Heat Capacity (C_{ap}) term is used in the final coupled flow equation.

$$\text{Heat flow:-} \quad \frac{\partial}{\partial z} \left(\lambda \frac{\partial T}{\partial z} \right) + l_w \rho_i \frac{\partial w_i}{\partial t} = C_s \frac{\partial T}{\partial t} \quad (3.22)$$

$$\text{Water flow:-} \quad \frac{\partial}{\partial z} \left(k \frac{\partial P_w}{\partial z} \right) = \frac{\partial w_u}{\partial t} + \frac{\rho_i}{\rho_w} \frac{\partial w_i}{\partial t} \quad (3.23)$$

$$\text{Coupled flow:-} \quad \frac{\partial}{\partial z} \left(\lambda \frac{\partial T}{\partial z} \right) + l_w \rho_w \frac{\partial}{\partial z} \left(k \frac{\partial P_w}{\partial z} \right) = C_{ap} \frac{\partial T}{\partial t} \quad (3.24)$$

- k = Hydraulic conductivity ($m \ s^{-1}$),
- ρ_i = Density of ice ($kg \ m^{-3}$),
- ρ_w = Density of water ($kg \ m^{-3}$).

Frost heaving can be modelled by solving the coupled flow equation together with a form of the Clausius-Clapeyron equation and applying a net heat flow concept at the frost front (Smith, 1985b).

The hydrodynamic theory assumes that, within the frozen fringe, the hydraulic conductivity decreases very rapidly as was subsequently established by experimental observations. At a position behind the frost front there will be a divergence of water flux (Figure 3.14), occurring where the rate of decrease of hydraulic conductivity is maximal with respect to temperature change (this will also correspond to where the rate of change of unfrozen water content with time is maximal). At this position water will accumulate and an ice lens will form. As growth continues the thermal and hydraulic gradients will alter and eventually favourable conditions will exist lower down for a new ice lens to form and grow. Under steady cold and warm side temperatures, initially the rate of advance of the frost front will be rapid, however, as it slows down the ice lens growth will be larger and the spacing between consecutive lenses will decrease (Konrad and Morgenstern, 1980) and is illustrated in Figure 3.6.

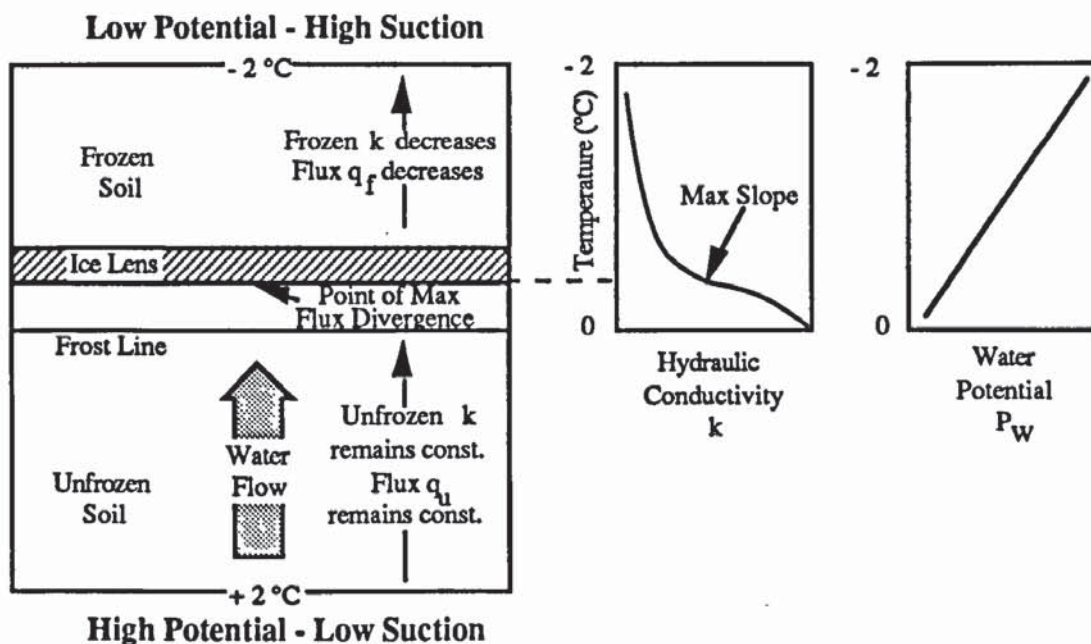


FIGURE 3.14 Diagrammatic Illustration of the Hydrodynamic Model (after Smith, 1985b).

This model does not adequately account for overburden pressures but is suited to soil science studies of the redistribution of moisture in frozen soils. Konrad and Morgenstern (1980) advanced the Segregation Potential Concept, which is a generalized hydrodynamic model with input parameters that are realistically obtainable and they have demonstrated its use in engineering applications (Konrad and Morgenstern, 1984).

3.3.6.3 Secondary Heave Theory.

Capillary theory underestimates the heaving pressures generated during freezing and, as a result, Miller (1978) put forward his Secondary Heave Model. Miller (1972) envisaged that heaving could occur by the following three processes:-

1. Primary heave - ice lens formation at the frost line, steady conditions,
2. Secondary heave - ice lens formation behind the frozen fringe, unsteady conditions,
3. Tertiary heave - water redistribution within frozen soil.

Primary heaving is unlikely to occur in nature and is described by Capillary theory. In Secondary Heave an ice lens forms and grows behind a partially frozen zone known as the frozen fringe (Figure 3.15) and differs from the hydrodynamic model in that ice lens is considered mobile. From thermodynamic considerations this would allow for much higher frost heave pressures that have been observed during freezing and so can take into account overburden pressures. The rate of Secondary Heave depends on the rate of water flow through the frozen fringe. An increase in the temperature gradient reduces the width of the frozen fringe and consequently its resistance to moisture flow. Therefore heave rate increases with increasing temperature gradient and decreasing fringe thickness.

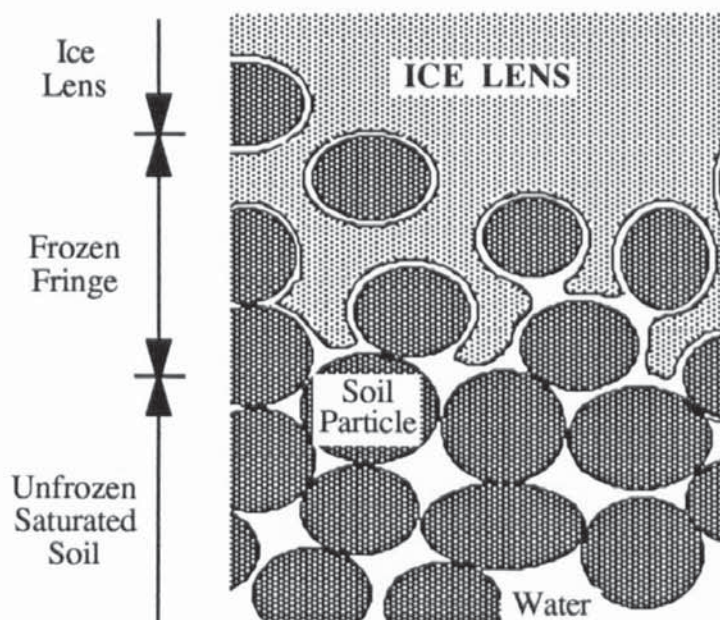


FIGURE 3.15 Schematic Diagram of the Frozen Fringe involved in the Secondary Heave Model.

The theory is based upon moisture flow through the fringe being sustained by a regelation process involving the properties of ice and soil particles within a saturated, frozen soil matrix. Miller (1980) discusses the two regelation gradients of:-

1. Ice regelation - from warm to cold side temperatures,
2. Thermally induced soil particle regelation - from cold to warm side temperatures, this flux increases dramatically at temperatures very close to 0°C.

The ice in the frozen fringe is considered both continuous and connected to the base of the growing ice lens (Figure 3.15) and this concept is also known as the Rigid Ice Model. It is also assumed that the ice velocity is uniform and equal to the rate of heave. The regelation movements of the ice and soil particles are in opposite directions, the ice velocity is uniform and the soil particle velocity increases with increasing temperature. Thus in the vicinity of the frozen fringe there is a net regelation movement of the soil particles towards the frost front but further, within the frozen soil, the net movement is with the ice towards the cold end. At a level behind the warm side of the frozen fringe there will be a divergence of the net movements of these soil particles resulting in zero effective stress, and so the ice can push apart the soil particles and accumulate as an ice lens. As freezing continues causing the frozen fringe to increase in length, the stress conditions will alter until favourable conditions exist for ice lens formation at a lower level, so that Secondary Heave predicts the rhythmic nature of ice lensing and the position of new ice lenses.

To describe the stress regime necessary for ice lens initiation Miller (1978) used Classical Effective Stress Theory to link the overburden pressure to the loads carried by the particles and the pore fluid (Equation 3.25),

$$P_{ov} = \sigma' + u \quad (3.25)$$

- P_{ov} = Overburden pressure (kN m⁻²),
 σ' = effective stress (kN m⁻²),
 u = neutral stress (kN m⁻²).

and applied the formula, developed by Bishop and Blight (1963) for partially saturated soils, to partially frozen saturated soils with ice and water as the pore fluids.

$$P_{ov} = \sigma' + \left[\chi P_w + (1 - \chi) P_i \right] \quad (3.26)$$

- χ = Stress partition factor.

The stress partition factor varies between unity when the pores are fully occupied by water and zero when fully occupied by ice. For ice lens formation the neutral stress must be maximal and equal to the overburden pressure, however the effective stress must be minimal and zero. In reality the ice pressure must be larger than the overburden pressure to allow for the rheological properties of the frozen soil.

The stress partition concept is combined with the heat and mass flow concepts embedded in the hydrodynamic theory to produce the Secondary Heave Model. Williams and Smith (1989) suggest that this is the most rigorous model developed to date, but is only applicable to fine grained soils or soils with a substantial amount of fines and does not take into account adsorption or the effects of osmosis. O'Neill and Miller (1985) and Piper *et al.* (1988) have demonstrated its usefulness during computer simulations based on this concept.

3.3.6.4 Mechanistic Theory of Frost Heaving (Segregation Potential Concept).

In this theory, developed by Konrad and Morgenstern (1980), the mass transport of water only takes place in the frozen fringe and unfrozen soil, and so the coupling of heat and mass transfer is restricted to these domains. The suction forces, developed according to the Clausius-Clapeyron Equation at the ice-water interface at the base of the ice lens, are considered as the driving force for heaving but, as these suctions are influenced by the permeability characteristics of the frozen fringe, the suction at the frost front is significantly less negative. Under this potential water is transported through the frozen fringe, with decreasing permeability as the ice lens is approached, so that this can be viewed as an impeded flow mechanism. The theory provides that, during initial freezing, the rate of penetration of the frost front is very high so that water accumulation does not produce visible ice lenses but merely leads to ice enrichment. However, with a reduction in the rate of advancement of the frost front, sufficient time elapses for water to move through the frozen fringe to enrich a growing ice lens. There is also an associated increase in the length of the frozen fringe so that the ice lenses increase in both size and spacing.

This theory was originally developed for the freezing of soils under steady state conditions, and assumed that:-

1. Clausius-Clapeyron equation holds at the base of the warmest ice lens, but not in the frozen fringe,
2. Incompressibility of the soil skeleton,
3. Unfrozen soil is fully saturated,
4. Zero overburden pressure,

5. Darcy's law holds in the frozen fringe and that water flow across it is continuous and accumulates only at the base of the ice lens,
6. The frozen fringe is characterized by an overall permeability, and
7. Ice lens initiation occurs at a segregation freezing temperature.

Konrad and Morgenstern (1981) showed from theoretical considerations that the freezing characteristics of a soil under constant boundary conditions are a unique function of the average suction and temperature across the frozen fringe at the onset of the final ice lens that could be satisfied by Equation 3.27 in which the constant of proportionality was called the Segregation Potential (SP). The development of the theoretical basis for this theory was vindicated by experimental laboratory results (Konrad and Morgenstern, 1981).

$$V_o = SP_o \text{ grad}T \quad (3.27)$$

- V_o = Water influx to the frozen fringe (at onset of final lens) (mm s^{-1}),
 SP_o = Segregation potential (at onset of final lens) ($\text{mm}^2 \text{ s}^{-1} \text{ }^\circ\text{C}^{-1}$),
 $\text{grad } T$ = Temperature gradient across frozen fringe (at onset of final lens) ($^\circ\text{C mm}^{-1}$).

It was shown that the water influx could be determined from the inflow to the soil sample and that the temperature gradient could be approximated by the gradient across the frozen soil. These quantities are therefore easily quantifiable from a simple unidirectional frost heave test, but SP_o is known to be dependent on the suction at the frost front and a suitable freezing test to determine its magnitude has been described by Konrad (1987b).

Further work led to modifications (Konrad and Morgenstern, 1982a) for the effects of transient freezing by the development of a unique, *characteristic* frost heave surface involving Segregation Potential, suction at the frost front and the rate of cooling of the frozen fringe for a specific soil. However, Van Gassen and Sego (1989) question the validity of this *characteristic* frost heave surface for they state that this surface is not unique for a given soil.

Finally, the effects of overburden pressure were investigated with respect to both transient and steady state heat flow conditions. Segregation Potential was found to be dependent on the suction at the frost front, applied overburden pressure and intake flux of water (Konrad and Morgenstern, 1982b). They have suggested a simplified engineering theory, which assumes that in the field the rate advancement of the freezing front is slow in comparison to that in laboratory frost heave tests, so these engineering problems can be regarded as close to steady state heat flow conditions. In laboratory freezing tests the warm side temperature

is kept close to 0°C thereby producing zero suction conditions at the frost front, thus an upper bound solution to frost heave will be predicted. Consequently the Segregation Potential is simply related to the overburden pressure by Equation 3.28.

$$SP_{ov} = SP_s e^{-b P_{ov}} \quad (3.28)$$

- SP_s = Segregation Potential at steady-state conditions at zero overburden ($\text{mm}^2 \text{s}^{-1} \text{ } ^\circ\text{C}^{-1}$),
 SP_{ov} = Segregation Potential at steady-state conditions at overburden P_{ov} ($\text{mm}^2 \text{s}^{-1} \text{ } ^\circ\text{C}^{-1}$),
 b = Constant for the soil (kN mm^{-2}),
 P_{ov} = Overburden pressure (kN mm^{-2}).

Equation 3.28 is substituted into Equation 3.27 (putting SP_o equal to SP_{ov}) to calculate the water influx over a known time period. The total frost heave can be calculated from the summation of the water influx over the total time period (segregated frost heave) and the volume expansion of the 'in situ' water upon freezing (Equation 3.29).

$$H = 1.09 SP_o \text{ grad}T \text{ dt} + 0.09 n \epsilon \text{ dx} \quad (3.29)$$

- H = Total heave (mm),
 n = Soil porosity ($\text{m}^3 \text{ m}^{-3}$),
 ϵ = Dimensionless factor taking into account the unfrozen water content,
 dx = Movement of frost front during time interval dt (mm).

Konrad and Morgenstern (1982b) note that water expulsion during frost heave can occur under high overburden pressures however, by putting the suction pressure at the frost front equal to zero, they ignore this effect. Nixon (1987) has suggested a method to incorporate this effect into a modified Segregation Potential theory.

3.3.7 Classification of Frost Susceptible Soils.

It is generally accepted that under normal, annual freeze-thaw cycles, silts are the most frost susceptible, clays are somewhat intermediate in their behaviour and gravels are non-frost susceptible soils. However under longer freezing periods, such as those induced by artificial ground freezing methods (eg. LNG storage tanks, chilled gas pipelines etc.), frost susceptibility extends to dirty gravels and silty clays. From a simplistic viewpoint, frost susceptibility can be regarded as dependent on the suction force at frost front and the permeability of unfrozen soil, since these largely control the flow of water to the freezing front. The suction force being inversely proportional to pore size and permeability being directly proportional to pore size.

Silt is classified as frost susceptible due to its medium pore size and permeability, thus the permeability allows water to migrate to the freezing front under the suction gradient. Clays on the other hand develop much higher suctions due to the smaller pore size however, their very low permeability inhibits water migration to a freezing front. Thus thick ice lenses are unlikely to form at the frost front, and so they are not classified as highly frost susceptible. Sands and gravels with their relatively large pore sizes have very high permeabilities but only limited suction forces and are generally classified as non-frost susceptible (Anderson *et al.*, 1984b).

For engineering purposes, large numbers of tests, criteria and methods of characterising soils have been developed to predict the likelihood of heave and its magnitude (Chamberlain, 1981). This highlights the difficulty of the problems in classifying the frost susceptibility of soils. Casagrande (1931) was the first to apply a criterion in 1931, which stated that "under natural freezing conditions and with sufficient water supply one should expect considerable ice segregation in non-uniform soils containing more than 3% of grains smaller than 0.02 mm, and in very uniform soils containing more than 10% of grains smaller than 0.02 mm". Modifications based on these principles form the basis of many frost susceptibility criteria some fifty years on (Chamberlain *et al.*, 1984). This gradation classification is now supplemented by unidirectional freezing tests under laboratory conditions. Chamberlain (1981) and Chamberlain *et al.* (1984) have reviewed most of the tests and identified three levels of sophistication:-

- Level 1 Based on particle size distribution, eg. Casagrande's criterion,
- Level 2 Based on particle size distribution and supplemented with data such as Atterberg limits, permeability etc,
- Level 3 Specialized laboratory freezing tests.

In the U.K. the Level 3 approach is followed which involves use of the TRRL Frost Heave Test (Roe and Webster, 1984), where nine cylindrical specimens 102 mm in diameter and 152 mm high are placed in a frost heave cabinet (Figure 3.16). The specimens rest on porous ceramic discs within copper carriers, with the discs in contact with water. A freezing gradient is induced through the specimen as the ambient air temperature above the specimens is set at $-17^{\circ}\text{C} \pm 1^{\circ}\text{C}$, with the water temperature kept between 3 and 4.5°C . The sides of the specimen are wrapped with waxed paper, and the intervening space filled with coarse dry sand (5 to 2.36 mm fraction) for lateral insulation. Push rods bearing on caps placed on top of the specimens enable the heave to be measured. Heave and water intake are monitored every 24 hours, and thermocouples monitor the boundary and internal temperatures of the specimen. Heave should not exceed 9 mm in a freezing period of 96 hours if the sample is

to be classified as non-frost susceptible (Roe and Webster, 1984). This test has now been adopted by the British Standards Institution (1989) for the determination of frost susceptibility for aggregates that would otherwise be used in an unbound form in road bases and sub bases at depths where frost penetration is likely.

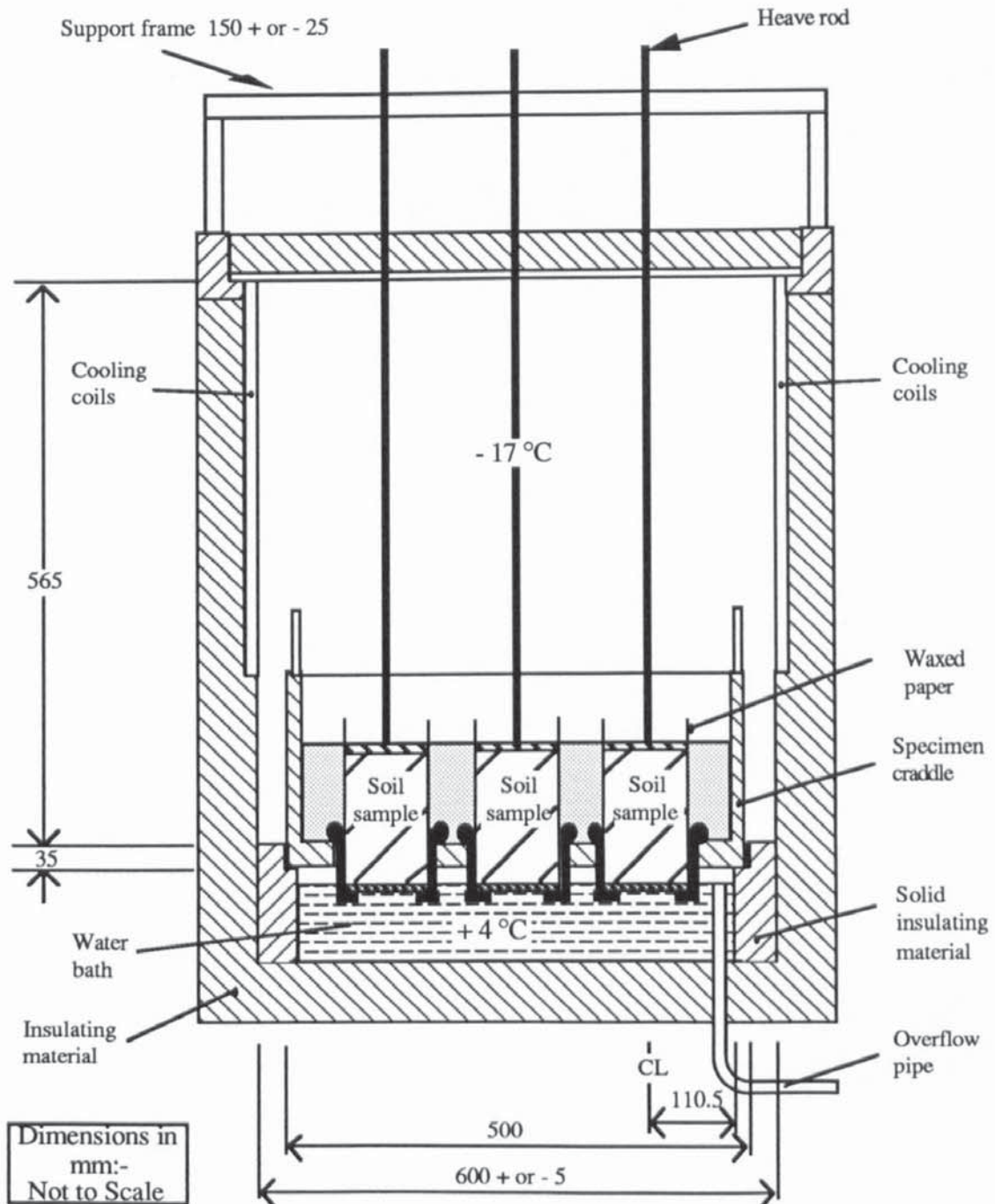


FIGURE 3.16 Main Features and Dimensions of the TRRL Frost Heave Cabinet (after Roe and Webster, 1984).

The US Army Corps of Engineers have used a frost heave cabinet test to investigate the frost susceptibility of unbound highway materials and subgrade soils. This test is used to classify materials regarded as borderline by a gradation test and has been in use for over thirty years (Chamberlain, 1981). The test is similar in principle to the TRRL frost heave test except that the cold side temperature is varied to maintain the rate of advance of the frost front at about 1.3 mm per day. An overburden pressure of 3.5 kPa is applied to each of the four specimens to simulate pavement depth. The samples are initially saturated and, during the twelve days of the freezing cycle, are allowed free access to water. There are no prescribed limits but categories of frost susceptibility have been developed. Recently Chamberlain (1988) has developed a more detailed, but faster test which involves two full freeze-thaw cycles. Each freeze-thaw cycle lasts for 48 hours, a constant rate of frost or thaw penetration is not used however, the cold and warm side temperatures are varied in a step-wise function. This new test can investigate a greater range of potential frost action problems, these are a single freezing period, repeated freeze-thaw cycles and thawing behaviour (from a terminal CBR Test).

3.4 Mechanics of Frozen Ground.

The mechanical properties of frozen soil have primarily been investigated through laboratory experimentation, involving creep, constant rate of deformation and relaxation tests. The results obtained from these tests have been used to describe three main engineering functions:-

1. The strength and creep parameters of frozen soils in Permafrost Regions which are to be loaded by possible structures, and where the soil temperatures can fall to -15°C .
2. The strength and creep parameters for soils to be frozen as an aid to construction works (Artificial Ground Freezing),
3. The development and validation of numerical models for the prediction of strength and creep parameters of frozen soils.

Indeed much of the work carried out over the past forty years into this subject has been summarized by Andersland *et al.* (1978), Ladanyi (1981), Johnston, (1981) and more recently by Sayles (1988). Williams and Smith (1989) have discussed the mechanical properties on a more fundamental basis, involving thermodynamics of the water-ice interface which is particularly important at temperatures close to 0°C .

A frozen soil is usually regarded as a composite of soil particles, ice, unfrozen water and air, although salts may also be present (Johnston, 1981), and so its response to any loading regime is a function of the combined interactions of all these materials. The mechanical properties of the soil particle derive from the ice-particle bond, together with the frictional resistance and cohesion between the particles. The ice provides resistance to stresses mainly under short-term loadings, as it leads to creep, through a regelation process, even under low stresses. The unfrozen water has little direct effect on strength, however it allows the movement of soil water from areas of high stress to low stress and, therefore contributes to the creep properties of frozen soils. Although air has no effect on strength, it can account for the compressibility of frozen soils at temperatures close to 0°C (Sayles, 1988).

The strength of frozen ground can be considered under two interrelated conditions, instantaneous (short term) and long term loading. Under short term loading the stress-strain response can be idealized as elastic, with an abrupt failure point at high loadings. This failure mode is of a similar magnitude to that of pure ice. It is therefore evident that failure occurs in the ice matrix and any residual strength is a function of the inter-particle reactions of friction and cohesion.

When the loading is insufficient to produce instantaneous failure but it is maintained over a relatively long period, then the frozen soil will deform slowly and it has been suggested (Johnston, 1978) that, for engineering purposes, its strain-time dependent characteristics are similar to the classic creep curve (Figure 3.17). After the initial elastic strain, the rate of strain decreases in the Primary creep zone (I) until a constant rate is observed in the secondary creep range (II). If the loading is sufficient the rate of strain will begin to accelerate denoting plastic failure in the tertiary creep zone (III). Sayles (1988) argues that some researchers have found that only an apparent secondary creep zone exists and it is a function of the shape of the curve at the point of inflection (Point D in Figure 3.17) between decelerating and accelerating strain rates. Initially the load is taken by the ice however, under loading cases not exceeding the instantaneous strength, the ice will creep allowing the movement of unfrozen water (and ice) from high to low stress. At the same time the soil particles become more closely packed and there is a resultant increase in their frictional and cohesive strength. If this increase in strength exceeds the loss due to ice creep, a long-term failure will not occur, otherwise eventually failure will result.

With decreasing temperature, there is an increase in both instantaneous and long term frozen soil strength, however the rate of strain decreases, and this can be attributed to the increased ice strength (Williams and Smith, 1989) and reduction in the unfrozen water content. In general, at equal total water contents, coarse grained soils have higher strengths and undergo less creep than fine grained soils. This is important at temperatures close to 0°C where there can be significant amounts of unfrozen water. It has also been recognized that

the form of ice influences the mechanical properties, as soils with ice held predominantly within the pores is stronger than soils with the ice in lenses or reticulate veins. In summary, the mechanical properties are dependent on temperature, applied stress, soil composition, water content, unfrozen water content, ice content, ice distribution, and time.

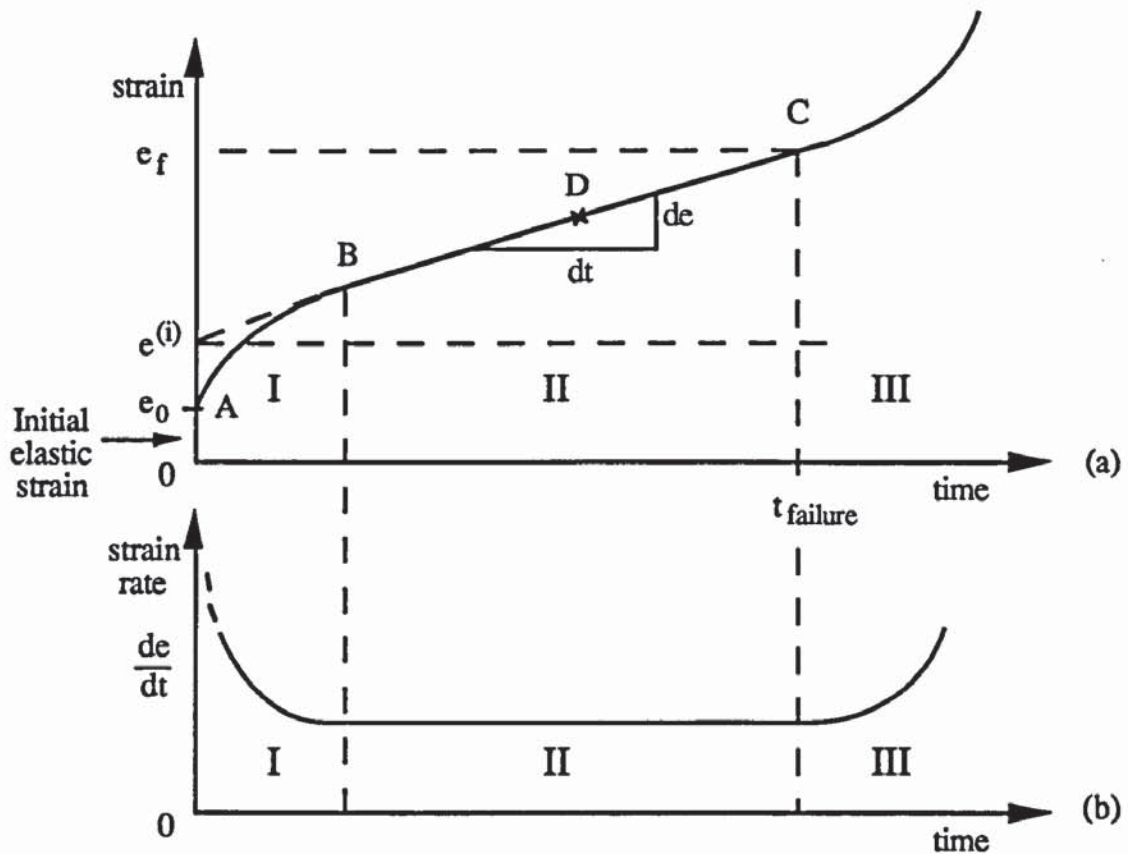


FIGURE 3.17 Idealized Illustration of the Creep of Frozen Soils under a Constant Loading Insufficient to cause Instantaneous Failure (Johnston, 1981).

3.4.1 Thermal Contraction of Frozen Ground.

This has been investigated by many authors (Lachenbruch, 1962, Grechischev, 1973, Mackay, 1974, Zhaojun, 1985, Andersland and Al-Moussawi, 1988).

3.4.1.1 The Basic Laws Temperature Cracking of Frozen Ground.

Frozen soils behave like many other materials (eg. steel, concrete etc.) as they change volume in response to a change in temperature, neglecting changes in the unfrozen water content. Frozen soils have large coefficients of thermal expansion, typical values are given in Table 4.3.

Soil Type	Co-efficient of Thermal Expansion (per °C)
Clay	0.002
Sand	0.00002 to 0.00005

TABLE 3.3 Average Values of Thermal Contraction for Clays and Sands (after Grechischev, 1973)

The magnitude of this coefficient of thermal expansion is temperature dependent, with the coefficient decreasing with decreasing temperature. The thermal deformation has been related to the total moisture content of the frozen soil and generally, for soils at their natural moisture contents, the relationships can be summarized as follows:-

1. Clays - coefficient of thermal expansion increases with a decrease in moisture content,
2. Sands - coefficient of thermal expansion increases with increasing moisture content,
3. Clay/sand mixture - decreasing the clay content (with a corresponding increase in sand content) results in the coefficient of thermal expansion increasing exponentially.

In nature, fluctuations in air temperature are relatively small, and so these do not over stress the frozen soil mass as the induced stresses can be alleviated by creep. It is thought by Grechischev (1973), that ground cracking is initiated by secondary short-term temperature fluctuations, ie. those that occur over a few days (thermal shock). The higher the frequency of these secondary temperature fluctuations, the greater the individual temperature fluctuation must be to initiate crack formation. Zhaojun (1985) also noted that crack initiation can occur with rapidly falling temperatures, such as the rapid temperature drop in autumn in Northern China. When a "primary crack" occurs, it relieves the thermal stress at right angles to the line of the crack but it has little effect on the thermal stress parallel to the line of the crack. Consequently a "secondary crack" may subsequently occur at right angles to the primary crack, the occurrence of which is dependent on the amplitude of the temperature fluctuation. The result of this is that the frozen ground is divided into irregular blocks known simply as "polygons". The effective diameter of these polygons is also dependent on the amplitude of the secondary temperature fluctuation (Lachenbruch, 1962 and Mackay, 1974) or the rate of temperature drop (Zhaojun, 1985). The smaller the amplitude or temperature drop, the larger the the effective diameter of the polygon.

3.4.1.2 Contraction Crack Theories of Frozen Soils.

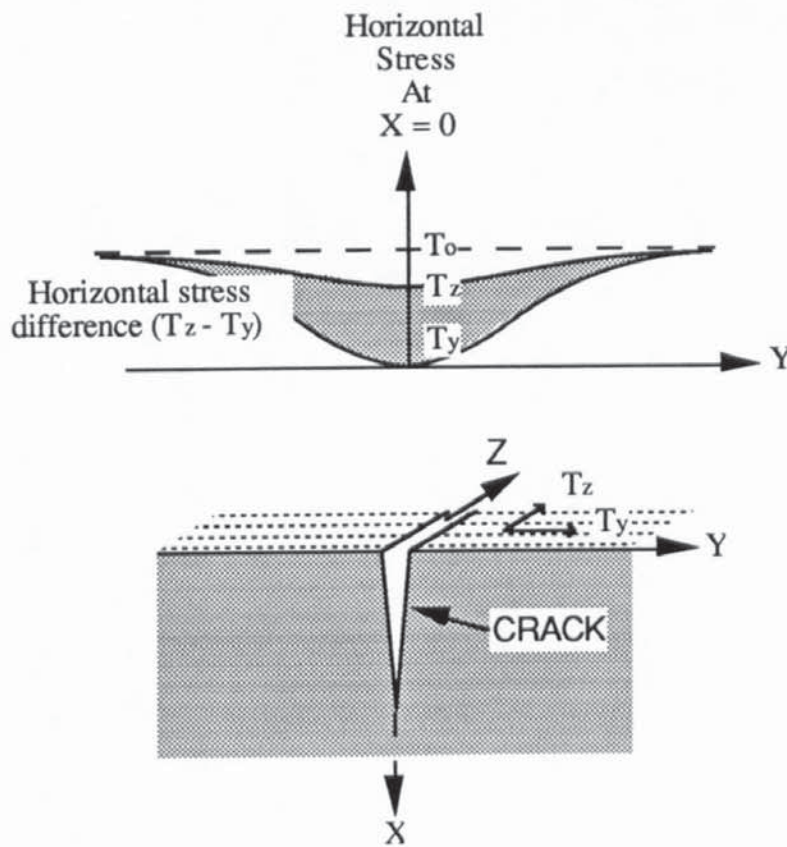
Contraction cracks are produced by thermal contraction stresses which occur in frozen ground subjected to a further fall in temperature. The theories suggested by Lachenbruch (1962), Zhaojun (1985), Andersland and Al-Moussawi (1988) are very briefly outlined in this section.

Lachenbruch (1962) was the first author to quantitatively discuss thermal contraction of frozen ground. He was concerned with the origin of ice-wedge polygons, which are many-sided ground features found in Arctic Regions and have diameters typically between 10 and 20 metres. Under each side is a wedge of ice which can extend to a depth of 3 to 10 metres, the width diminishing with depth. Lachenbruch (1962) put forward an idealized model, determined from a theoretical approach, and based on a temperature-stress relationship which assumes a visco-elastic response from the frozen soil. This is expressed as a non-linear relationship involving distortional strain and distortional stress. When the tensile stress at the soil surface is sufficient, a crack will form and propagate into the soil mass until it enters a zone of compressive stress where its progress is halted. This is described by The Modified Griffith Theory (Irwin, 1958), which has previously been applied to the brittle fracture of metals. At right angles to the crack, a zone of stress relief will form after cracking (Figure 3.18) and the subsequent stress distribution is described using Muskhelishvili's Method of Complex Stress Functions (Lachenbruch, 1961). This demonstrates that the deeper the crack propagates, the wider the zone of stress relief and, consequently, the horizontal spacing of the cracks is increased.

Zhaojun (1985) analyzed tensile frost cracks in a more simplified context, by deriving a relationship involving the tensile and shearing strength of the frozen soil together with thermal gradient across the frozen soil. This relationship assumes that there is a linear temperature profile and that the coefficient of thermal expansion is constant. Stefan's equation is used to predict the depth of freezing from the thermal properties of latent heat of fusion and thermal conductivity (Zhaojun, 1985). It also allows the input of geotechnical properties, such as moisture content and dry density. Therefore, by incorporating thermodynamic and geotechnical parameters into an elastic model, the depth and spacing of these cracks can be predicted.

Andersland and Al-Moussawi (1988) have investigated contraction cracking at landfill sites in the USA, where crack development can lead to water ingress possibly leading to leachate generation and, subsequently the escape of associated gases. They state that cracking will occur during rapid temperature drops and so assume that the frozen soil behaves elastically.

Very basic elastic equations involving Young's Modulus, Poisson's Ratio, strain and stress were put forward to define the behaviour of this frozen soil.



T_0 = Uniform horizontal tension before fracture.
 T_z = Component of tension parallel to crack after fracture.
 T_y = Component of tension perpendicular to crack after fracture.

FIGURE 3.18 Stress at Ground Surface near an Isolated Crack (after Lachenbruch, 1962).

3.5 Thawing of Frozen Soils.

In permafrost areas thawing of frozen ground poses a far greater threat to the integrity of structures than frost heave (Johnston, 1981). However, thaw settlement behaviour is partially dependent on the process of freezing which can alter the internal structure of the soil mass by forming ice lenses or reticulate ice veins, thereby increasing the total water content and by local consolidation of the soil matrix. The thawing of frozen soils is therefore related to its thermal, stress and hydraulic history.

During thawing, soil water will be released and, if this exceeds the capacity of the soil matrix, water will accumulate at the thawing front. If water drains away freely the soil

Watson *et al.* (1973) describe a practical method for the calculation of thaw settlement from representative soil samples. A sample is placed in a lubricated chamber and allowed to thaw at room temperature under constant pressure. After thawing is completed, additional loading stages are undertaken while the vertical deformation of the sample is regularly monitored. From a plot of relative settlement against applied pressure (Figure 3.20), the Thaw Settlement Parameter (A_0) and volume compressibility (m_v) of the sample can be determined. These parameters allow the prediction of thaw settlement under field conditions and can account for any subsequent loading conditions. Watson *et al.* (1973) also note that there is a general relationship between increasing frozen bulk density and decreasing thaw settlement.

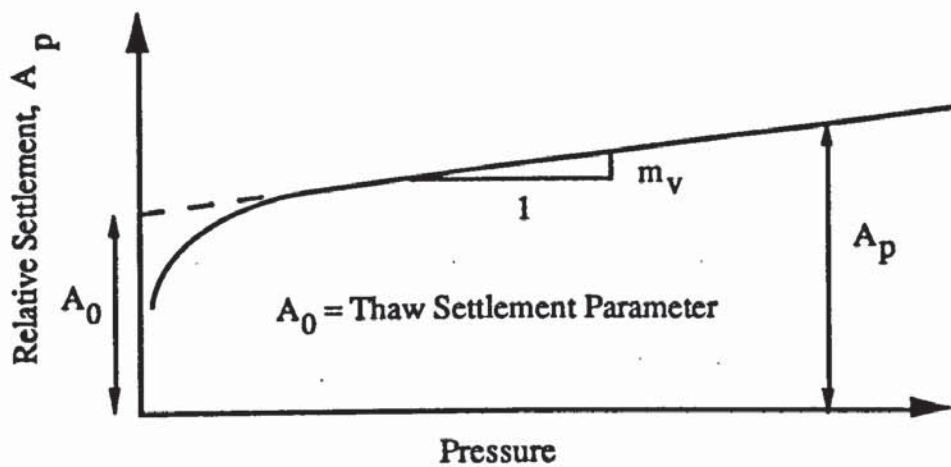


FIGURE 3.20 Generalized Thaw-Settlement Curve (after Watson *et al.*, 1973).

3.5.2 Thaw Consolidation.

This is an analysis of the settlement of ice rich soils, in which drainage is impeded by either the low permeability of the unfrozen soil behind the thawing front or the velocity of advancement of the thawing front. This is of importance as it provides information linking the rate of thawing and the rate of consolidation, so that the stability of the soil during thawing can be ascertained.

Morgenstern and Nixon (1971) formulated a solution to the problem in terms of linear, one-dimensional thaw consolidation, in which thawing proceeds downwards from the ground surface. The theory assumes that the soil is fully saturated, the water surface coincides with a free draining ground surface and the effective stress at the thawing plane is zero. This solution involves coupling the classical theories of heat conduction and soil consolidation. This is achieved by combining Stefan's solution to the problem of the rate of advance of a

thawing front with the coefficient of consolidation by the empirical Thaw Consolidation Ratio, R,

$$R = \frac{\alpha}{2\sqrt{c_v}} \quad (3.30)$$

- R = Thaw consolidation ratio,
 α = Constant from Stefan's equation ($\text{mm s}^{-1/2}$),
 c_v = Coefficient of consolidation ($\text{mm}^2 \text{s}^{-1}$).

This empirical parameter is a measure of the ratio between water generation at the thawing front and rate of movement of water away from the thawing front, and can be used to estimate the excess pore water pressures generated. When the thaw consolidation ratio exceeds unity it is likely that excess pore water pressures will be generated at the thaw front.

Morgenstern and Nixon (1971) have also provided a mathematical formulation for the average degree of consolidation that occurs at time t, under self weight and applied loading. It is assumed that the average degree of consolidation is equal to the ratio between thaw consolidation at time t and the total thaw consolidation that would occur if thawing ceased at time t. This theory has been verified by comparing laboratory and in situ tests, and has also been developed to provide solutions for non-linear consolidation and layered soil profiles (Nixon and Ladanyi, 1978). The concept of residual stress which is the initial effective stress at thawing front, has been investigated in connection with thaw consolidation. The higher the residual stress the lower will be resultant settlement since lower pore water pressures are generated and this also provides for a higher undrained shear strength (Nixon and Morgenstern, 1973).

3.6 Freeze-Thaw Cycles.

The effects of soil freezing and thawing have been described individually in the previous sections. These combined effects can lead to changes in both the physical structure and engineering properties of soil. Johnson *et al.* (1984) have summarized the process under three conditions:-

1. Silts frozen under maximal conditions for frost heave and subsequently subject to rapid thawing. This results in an underconsolidated soil with a residual stress equal to zero, producing a very low initial shear strength and modulus of deformation (stress divided by strain),

2. Clays, which during freezing generate large suction forces, leading to overconsolidation and shrinkage cracks in the soil directly in-front of the frost line. Due to overconsolidation the soil has a substantial shear strength,
3. Sands that exhibit frost heave due to the expansion of ice, upon thawing the soil particles fully consolidate under the normal overburden conditions. Therefore the soil has strength and deformation properties similar to those prior to freezing.

Chamberlain (1981) notes that very few observations have been reported on the effect of freeze thaw cycles on frost heave. However he reported that under laboratory testing, the total frost heave of a frozen till had quadrupled, much of this occurred in the second freeze cycle and was also dependent on the applied surcharge on the sample. Clays were observed to have increased their total frost heave by up to a factor of eight at low surcharges, again most of this occurred in the second freeze cycle. A silty sand was reported (Chamberlain, 1981) to have decreased its total heave. For clays Chamberlain and Gow (1979) demonstrated that freezing a clay soil would increase its vertical permeability due to shrinkage cracking. This would obviously affect its frost heave potential in a laboratory test however, in the field, an undisturbed layer of clay may exist between the frost front and the water table, thus the frost heave potential would be only slightly affected. Chamberlain (1988) compared laboratory freeze-thaw tests to field freezing conditions for a variety of soils and found that during the first cycle the average and laboratory heave rates were related, though the field heave was an order of magnitude lower than observed in the laboratory. During the second freeze-thaw cycle, this relationship was less evident. Chamberlain (1981) also pointed out that repeated freeze thaw cycles have been shown to decrease the thaw-CBR values of clays.

3.6.1 Natural Phenomena Involving Frost Action.

Growing stones and ice wedge cracking are manifestations of freezing and thawing and are of interest to chilled pipeline operation, and formed part of the initial study programme. Ice wedge cracking is discussed in Section 3.4.1.

3.6.1.1 Growing Stones.

In moderately cold climates 'growing' stones are a familiar feature. They are stones that have moved up through the ground until they eventually protrude through the ground surface and can ultimately form a feature known as patterned ground (Lunardini, 1981). This is part of a process called vertical sorting, which can also involve the movement of

'fines' (fine grained soil particles) ahead of the freezing front (Corte, 1961). Two theories (Lunardini, 1981) have been put forward to explain the phenomenon of 'growing' stones.

Frost Pull-Mechanism, whereby freezing around the top of a stone results in the 'fines' around the stone gripping it due to frost expansion. With continuing frost heave development in the soil, the stone is moved up with the rest of the frozen soil mass (Figure 3.21a). This results in a cavity forming under the stone. During thawing from the ground surface downwards, the 'fines' tend to settle around the stone. Eventually the cavity will fill with saturated fines as the thawing front further descends. The result is that the stone cannot settle to its original position (Lunardini, 1981).

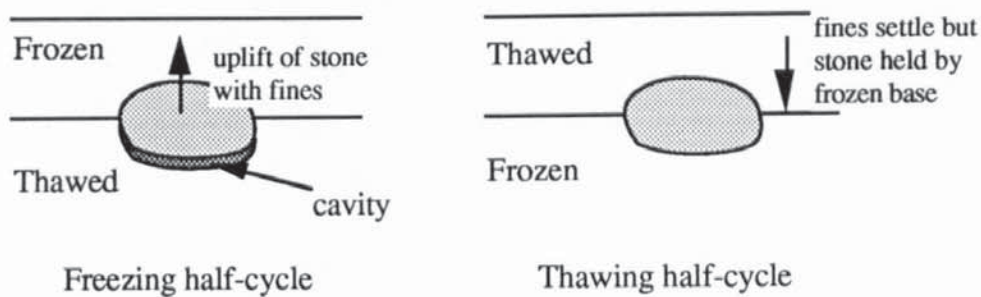


FIGURE 3.21a The Frost-Pull Mechanism (after Lunardini, 1981)

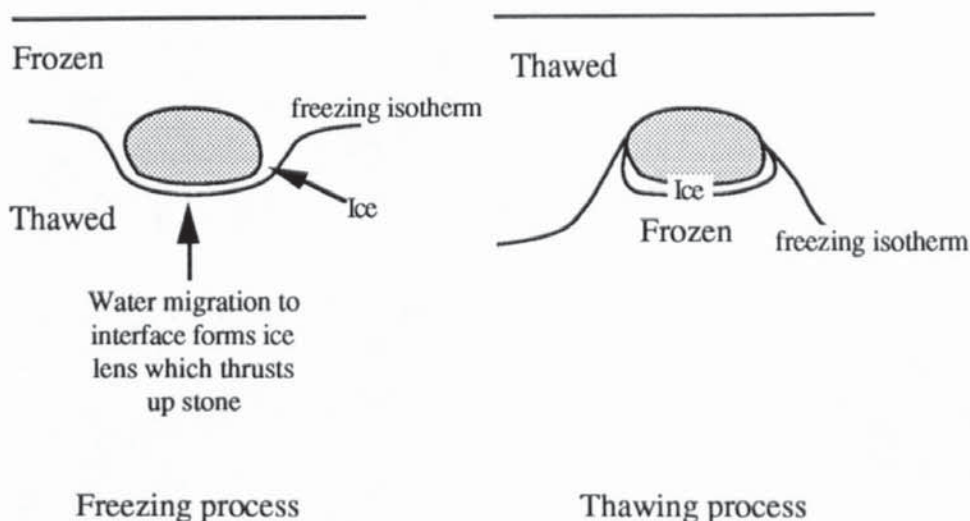


FIGURE 3.21b The Frost-Push Mechanism (after Lunardini, 1981)

Frost Push Mechanism, whereby the thermal conductivity of the stone is much greater than that of its surrounding soil mass. Thus, when the freezing front descends to the top of a stone, the whole stone will reach 0°C faster than the surrounding soil. The result is the formation of an ice lens below and to the sides of the stone (Figure 3.21b). Water migration

to the frozen front (ice lens) results in the stone being pushed upwards by the enlarging ice lens. Later when thawing begins the ice lens will thaw at a slower rate than the surrounding soil mass even though the stone will reach the thawing temperature more rapidly than the surrounding soil mass. This is a result of the latent heat of ice. As thawing continues the 'fines' settle around the stone and eventually the ice lens totally melts. The stone may settle slightly as some of the meltwater is expelled, however under the stone is a saturated cavity into which 'fines' will flow. These 'fines' will stop the stone from returning to its original position (Lunardini, 1981).

3.7 Summary.

Chilled gas pipeline operations can lead initially to frost heave and subsequently to thaw settlement within the outer extent of the frozen annulus. Chilled gas pipeline operation in the Pre-heating Seasons takes place annually and therefore the surrounding soil mass is subjected to freeze-thaw cycles. This chapter provides a discussion on the thermal properties of soil which determine the size and shape of the frozen annulus *ie.* the soil mass under consideration. Subsequently frost heave is defined in basic thermodynamic terms involving the soil thermal, hydraulic and stress regimes. The complex nature of frost heave is highlighted in the limitations of both the mathematical theories that have been developed and in the multitude of laboratory tests in use for the classification of frost susceptibility. However thaw settlement is a more clearly defined subject area and its prediction is dependent on laboratory testing. A further complication to the prediction of frost heave is the effect that previous freeze-thaw cycles impart on the soil structure, thereby altering the frost susceptibility from one year to the next. The uncertainty in the prediction of the soil-pipeline interactions involving frost heave and thaw settlement around a chilled gas pipelines is further compounded by the variability of soil classification, hydraulic conditions, thermal interactions, depth of pipe burial, etc, along its length.

The next chapter provides overviews on pipeline design and soil-pipeline interactions without the influence of frost action. Subsequently the influence of frost action is introduced first with respect to civil engineering structures and then with chilled gas pipeline operation, which under British, USA and Arctic conditions are all expanded upon in terms of the soil-pipeline interactions of frost heave and ground cracking, especially in terms of engineering predictive and mitigative procedures. Importantly, consideration is given to the Caen project (Geotechnical Science Laboratories, 1991) which addresses the soil-pipeline interactions from a fundamental viewpoint and therefore highlights the deficiencies in the knowledge base of chilled gas pipeline operation.

CHAPTER 4 SOIL-PIPELINE INTERACTION

4.1 Introduction.

Utility and oil companies have made massive investments in transporting oil and gas by pipeline. Consequently, there have been extensive investigations into both pipeline failure and the associated soil-pipeline interactions that pose problems to smaller diameter pipelines. Most of these research efforts have been *in house* and so have regarded by the companies as commercially sensitive.

This study project examines the effect of the pipe on the surrounding soil and not the effects of the ground on the integrity of the pipe. However it must be noted that this is an interaction problem, so that the operating conditions of the pipe may influence the ground conditions in such a way as to detrimentally affect the pipeline performance.

In this chapter the problem of soil-pipeline interactions are initially addressed without the influence of sub-zero temperatures, subsequently the discussion is extended to consider the influence of sub-zero temperatures on the integrity of the pipeline structures. Chilled gas pipeline operation is expanded upon in terms of previous studies, including full-scale tests. A section is also included which reports previous small-scale physical models with respect to sub-zero temperatures and pipe movement.

4.2 Pipeline Design.

The function of a pipeline is to deliver safely and efficiently a fluid to its destination. Many liquids are transported including oil, gas, water, sewerage, crushed coal and liquefied waste by-products, and so pipeline design must account for the potential hazards resulting from breakage. Therefore the maintenance of the mechanical integrity of a gas pipeline is more important than a water or sewerage line for example. The operation of pipelines in the gas industry is split into two categories, National Transmission and Local Distribution pipelines, each are operated under different conditions and are subjected to individual design procedures. This section provides an general overview of the complex processes of pipeline design, however further information is available in codes such as the ASI/ASME Code for Pressure Piping, B31.8 (1986) and IGE/TD/1.Ed 2 (1977). The discussion provided on the geotechnical design aspects (Section 4.3.2) is equally applicable to all underground conduits. The overall design procedure for the Transmission pipelines within the British Gas network is reviewed in Chapter 2.

4.2.1 Route Selection.

Prior to the actual detailed design an environmental impact assessment (EIA), including an outline design, is submitted to the appointed legislative body for approval of the scheme (Clarke, 1988 and ASME, 1986). The submitted EIA should put forward a route that is the least environmentally destructive. Design should also cover pipeline route selection to reduce to a minimum the number of dwellings (person) in close proximity (Knowles *et al.*, 1977 and ASME, 1986). The route selection can be substantially affected by adverse terrain and geotechnical conditions.

4.2.2 Pipe Design.

The design pressures and mass flows are reflected during the design procedure on the positioning and specification of the associated compressor and Pressure Reduction Stations. These operating conditions also provide the input characteristics in determining the pipe specifications for material type, diameter and wall thickness (Wilbur, 1963, Peng, 1978a, Ahmed *et al.*, 1981). Pipe thickness is derived from Barlow's formula (Wilbur, 1963):-

$$T = \frac{P D}{2 \sigma_H} \quad (4.1)$$

- T = Pipe wall thickness (mm),
- P = Pipe design pressure (kN mm⁻²),
- D = Nominal outside diameter (mm),
- σ_H = Hoop stress (kN mm⁻²).

A factor of safety can be applied to Equation 4.1 to cover the expected construction loads, types of pipe connections, in-service loadings due to traffic or geotechnical interactions, maintenance, repair and replacement costs (ASME, 1986). The longitudinal stress in a restrained pipeline is given by:-

$$\sigma_L = E \alpha \Delta T - \sigma_H(\nu - 0.5) \quad (4.2)$$

- σ_L = Longitudinal stress = F_L / a_s , (kN mm⁻²),
- F_L = Longitudinal force (kN),
- a_s = Area of pipe material (mm²),
- E = Young's Modulus of pipe material (kN mm⁻²),
- α = Co-efficient of thermal expansion of pipe material (°C⁻¹),
- ΔT = Temperature change (°C),
- ν = Poisson's ratio.

Equation 4.2 incorporates the thermal co-efficient of expansion in the first term, and allows for the hoop stress in the second term. The hoop stress produces a resultant shrinkage in the longitudinal direction as defined by Poisson's ratio, however the internal gas pressure also produces a longitudinal pressure equal to half the hoop stress (Wilbur, 1963, Peng, 1978a). For safe operation the hoop and longitudinal stresses must be less than specified minimum yield strength (SMYS) of the pipe selected, this SMYS is often corrected to allow for a factor of safety.

Once the pipe specifications have been decided upon, then a protection system is designed for both external and internal corrosion (for steel pipes that are normally used in large-diameter transmission pipelines), using the techniques such as pipe surface coatings, cathodic protection, sacrificial anodes etc.

4.2.3 Geotechnical Design.

Peng (1978a, 1978b) and Luscher *et al.*, (1979) note that soil-pipeline interaction is a major concept in pipeline design since it encompasses all the relative soil pipe movements. Essentially a pipe is laid at the 'tie-in' temperature and if the operating temperature is substantially different then large longitudinal stresses are generated. In a long section of straight steel pipe these stresses are resisted by the soil friction at the pipe surface and if the pipe is in compression they may also be restrained by thrust blocks or anchors at the points direction changes. Anchors or thrust blocks are used to reduce the potential for excessive bending stresses. Excessive bending stresses coupled with the hoop stress either produce pipe failure or necessitate a gas pressure decrease to reduce the combined stress to less than the SMYS.

Loading regimes can be imposed on a pipeline during construction and operation, if these are significant, then the pipe must be designed to withstand them. Typical loadings are from vehicular traffic, and the pipeline may be strengthened at these locations by using a thicker pipe wall or placing the pipe within a sleeve. Vehicular loadings are important since uneven soil pressures may be transferred to the pipe producing bending stresses. During a pipeline's design life it may be subject to the following relative ground movements:-

1. Excavations (including tunnels and mining subsidence),
2. Boundaries between frost and non-frost susceptible soils,
3. Boundaries between thaw and non-thaw stable soils,
4. Land slides,
5. Earthquake slip planes,
6. Rising water table (pipeline floatation).

Each of these situations where necessary should be incorporated in both the pipe design and risk assessment procedures during pipeline operation. The proper modelling of such soil-pipeline systems and the prediction of bending stresses needs an accurate estimation of the soil subgrade response to pipe movement in the vertical uplift, vertical foundation, horizontal and longitudinal directions.

4.2.4 Post-Construction and Monitoring.

Ideally after pipe-laying has been completed the land within the construction easement should be returned, as close as possible, to its pre-construction state. Wilkins (1988) discusses the British Gas Corporation methodology both to land re-instatement and post-construction liaisons with the landowners.

With a large capital investments in large-diameter pipelines, a comprehensive monitoring and risk assessment programme is undertaken to maintain the integrity of the pipeline and its associated installations (ASME, 1986).

4.3 Soil-Pipeline Interactions.

Soil-pipeline interactions are not solely the result of chilled gas pipeline operation for they are commonly observed under normal loading conditions. These interactions are a result of imposed loadings on the pipe or ground surface, excavations close to the pipeline, mass soil movements (earthquakes, landslides, etc), thermal strains, pipeline floatation etc. In this section soil-pipeline interactions are introduced without the effects of sub-zero temperatures, but its effects are discussed later (4.4, 4.5 and 4.6).

4.3.1 Definition of Soil-Pipeline Interaction.

Soil-pipeline interactions by definition describe the process by which loads are transferred between the soil mass and the pipe and, under the imposed loading, this continues until the deformations of both the soil and pipe are at a (dynamic) equilibrium. This load transfer does not therefore produce a single reaction but a set of very complex interactions associated with the mechanical properties of both the soil and pipe.

This definition needs to be extended to include the responses produced by heat transfer between the pipeline and soil when the pipeline is being operated significantly above or below ambient ground temperature. Under these conditions heat transfer can indirectly influence the soil deformation characteristics and moisture movements close to the pipe. Typically, during low temperature operation, the frozen soil annulus acts to change the interaction from a two layered to a multi-layered system. In this study both heat transfer and

moisture movement greatly influence and compound the uncertainty of predicting potential soil-pipeline interactions.

4.3.2 Vertical Pipeline and Soil Movements.

Most studies involving relative pipe movement are, out of necessity, biased towards investigating the integrity of the pipeline. The soil mass deformations resulting from relative pipe movements are usually of secondary importance, however a simple investigation of the ground surface deformations can indicate the nature of the soil-pipeline interactions.

4.3.2.1 Vertical Pipe Movements.

Vertical pipe displacements are of concern at the boundaries between areas where the pipe is held rigidly (fixed) and areas where settlement or uplift occurs. Across such a zone bending stresses are developed within the pipe and, depending on the pipe characteristics, failure may ensue.

Casson (1984) reported tests undertaken as part of the Pipe Loading Underground Project at the British Gas Engineering Research Station that involved the upward displacement of small diameter mains (100 to 200 mm in dia). The study investigated the effects of settlement loading on pipes at different depths in differing soil types. During settlement the pipe behaves as a structural beam supporting a wedge of overlying backfill and, if this loading is excessive, failure may result. The tests involved lifting lengths of abandoned main at depths between 0.5 and 1.5 metres using two hydraulic rams at each end of a 2.5 to 3.2 m pipe, thus simulating settlement loading. In the tests maximum pipe displacements occur at the edge of the trench (Figure 4.1). However, in practice maximum pipe displacement occurs at the midspan. Casson (1984) notes that the experimental results are applicable since the same classic soil failure pattern (Figure 4.1) has been observed in the experiments and in practice. A soil failure plot (for test site No.4) indicated that this failure pattern is dependent on parameters such as soil type, soil strength and proximity to overburden loads (Casson, 1984). It was noted that the angle of the diagonal internal soil crack was related to soil strength and soil type, 40-55° and 35° to the vertical for cohesive and non-cohesive soils respectively (Casson, 1984).

In this test the pipe cannot be considered as 'Rigid' since its cross-sectional area is not constant. Casson (1984) suggests that the diagonal crack is a 'limiting crack' and its shape may be dependent on a least energy shape (log spiral), man-made layering above pipe, or changes in the direction of the stresses during crack growth. These changes occur after the formation of the limiting crack and result in horizontal tensile stresses being generated in the soil block above the pipe. If vertical failure occurs, two wedges will form and, due to the resultant weight redistribution compressive stresses will develop between the crack apex and

the soil surface. Consequently during further pipe lifting, the crack will deviate away from the ground surface until it runs parallel to it (Figure 4.1). The shape of this wedge was observed both during the trial and at the location of the failure of a 600 mm main (Howe, 1982) from differential settlement.

Ground settlement around a rigid pipe has been the subject of many analytical studies and these have been summarized by Matyas and Davis (1983a) and Trautmann *et al.* (1985). These studies have produced semi-empirical models to define the force-displacement characteristics during a pipe loading test in relation to pipe diameter, depth of burial, soil

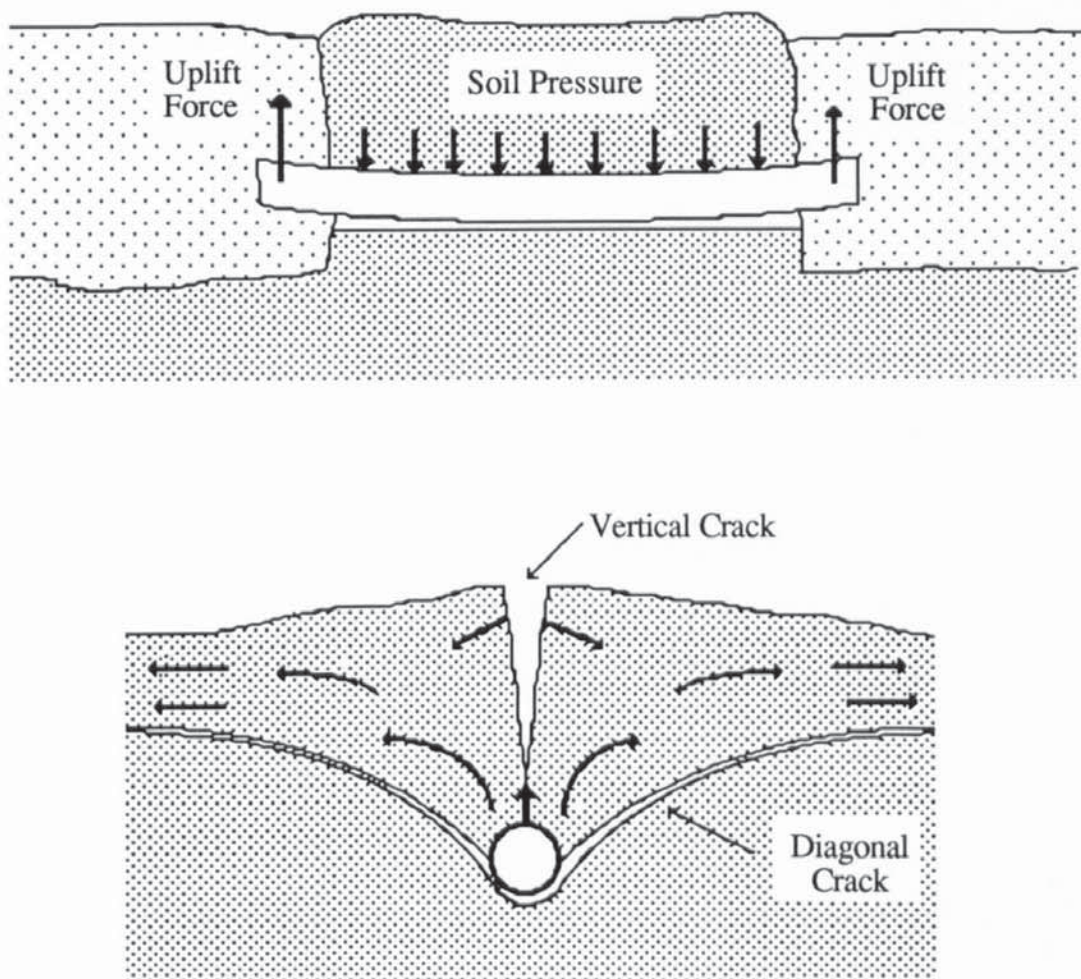


FIGURE 4.1 Classic Soil Failure Pattern resulting from the Uplift of Small Diameter Pipes.

type and density. Most of the models in use in the USA and Canada are derived from work carried out by Spangler in the 1940's (Matyas and Davis, 1983a). These models assume that the loading is due to the weight of the backfill and the internal angle of friction of this

backfill. Trautmann *et al.* (1985) report the use of these models in designing pipelines for the maximum loading expected during earthquakes. However, Matyas and Davis (1983a and 1983b) describe their use for designing underground service pipes that are hung from slabs supported by piles in poor ground. These models can also be applied to any general situation where excessive soil loading takes place at transitions and slip planes (earthquakes, frost heave, mining subsidence, slope failure etc).

Matyas and Davis (1983b) and Trautmann *et al.* (1985) undertook laboratory tests (Section 4.6.5) on small diameter rigid steel pipes, 48 mm and 102 mm O.D., to develop enhanced procedures for pipeline design. Basic measurements of soil loading and pipe displacement were taken at various pipe depths and soil densities in sandy soils. Trautmann *et al.* (1985) found increased depth of burial resulted in increased maximum soil loading and also that increased sand density produced higher maximum soil loadings. Matyas and Davis (1983b) results are in general agreement with those of Trautmann *et al.* (1985). Both tests indicated that maximum soil loading takes place at upward vertical pipe displacements between $0.005H$ to $0.015H$ (H is depth of burial to pipe centre), indicating that soil failure occurs at small displacements. After the maximum soil load had been observed the load tended to either decrease slightly or remain constant (Figure 4.2) again dependent on soil and test conditions. Matyas and Davis (1983b) noted failure surfaces during the tests and, typically for the test with a depth to diameter ratio of 8.75, the failure surfaces consisted of two diagonal surfaces radiating from the side of the pipe. These failure surfaces were observed at approximately four times the net pipe movement at the maximum soil load, and in the reported test the failure surfaces tended towards the vertical and halted within the soil mass (Figure 4.3).

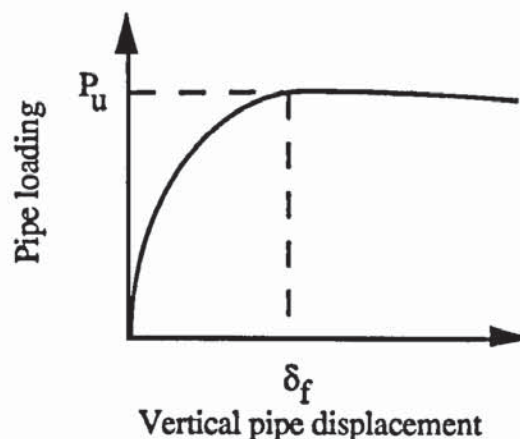


FIGURE 4.2 Simplified Vertical Load-Displacement Response of the Buried Pipe.

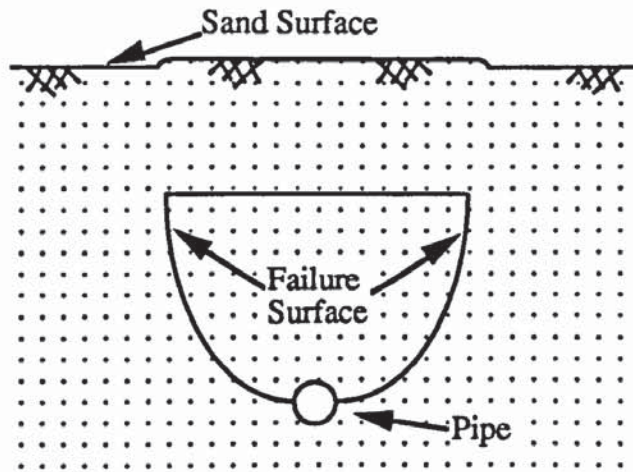


FIGURE 4.3 Illustration of the Failure Surface Observed by Matyas and Davis (1983b).

4.3.2.2 Vertical Pipeline Movement Due to Floatation.

Large-diameter steel gas pipelines are buoyant when in water, thus when the water table rises to the pipe level an upward force will be exerted. The estimation of buoyancy can be considered as a function of a floatation force and a resisting force (Bonar and Ghazzaly, 1973). When the water table is above the pipe crown the hydrostatic uplift force is simply described by Archimedes' law (Johnson *et al.*, 1984). The resistance to floatation is provided by the overburden weight and shearing resistance of the soil (Figure 4.4).

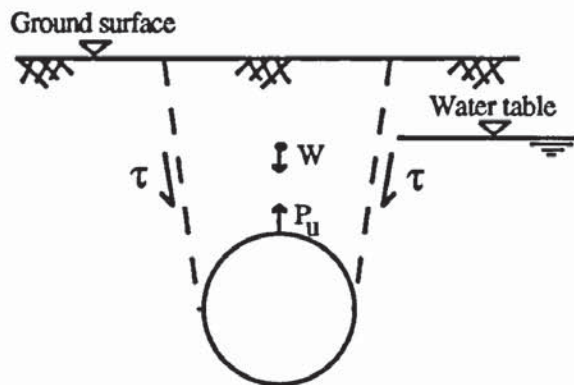


FIGURE 4.4 Buoyancy Forces Acting on a Pipe.

At pipe floatation the uplift force must equal or exceed the resistance force (Equation 4.3)

$$\text{Uplift force } (P_u) = \text{Resistance force } (F_r)$$

$$H_u - W_p = W + 2\tau \quad (4.3)$$

- H_u = Hydrostatic force,
 W_p = Weight of pipe and contents,
 W = Effective weight of overburden soil mass,
 τ = Effective shearing resistance of overburden soil mass.

4.3.2.3 Vertical Ground Movements Due to Tunnelling.

During tunnel excavation a ground settlement trough will form perpendicular to the direction of tunnelling. O'Reilly and New (1982), Attewell and Woodman (1982) and Howe (1982) report that the settlement trough especially in clays can be described by a normal probability curve, assuming no soil consolidation above the pipe. The normal probability curve shows that settlement 'W' at any distance 'y' from the tunnel centre-line is given by:-

$$w_s = w_{s \max} \exp \left(\frac{-y^2}{2(i^2)} \right) \quad (4.4)$$

- w_s = vertical settlement (mm),
 $w_{s \max}$ = maximum vertical settlement (mm),
 y = perpendicular distance from the tunnel centre-line (mm),
 i = distance to point of inflexion, ie. $w_s = 0.606 w_{s \max}$, (mm).

Figure 4.5 illustrates the normal probability curve described by Equation 4.4.

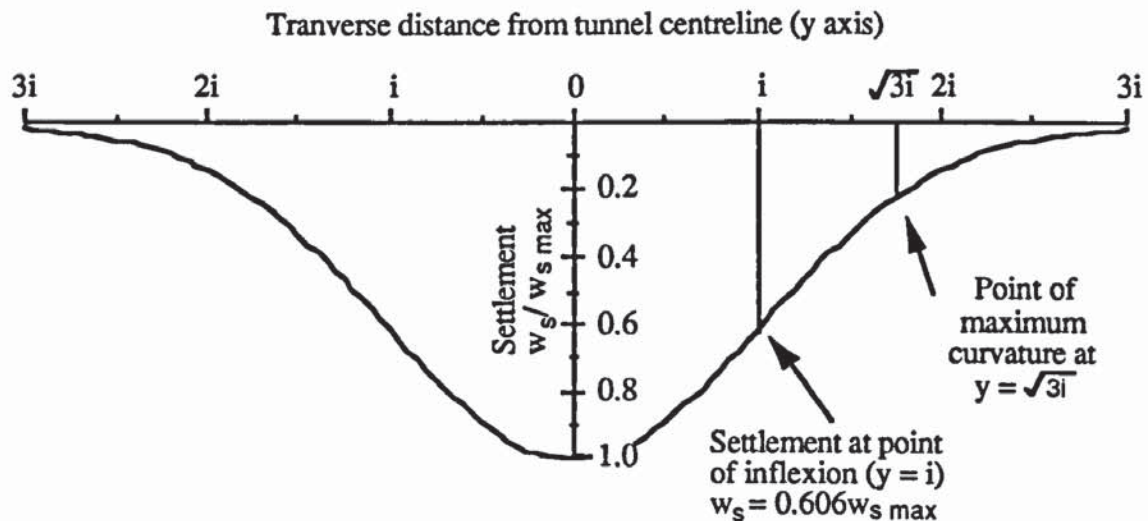


FIGURE 4.5 Normal Probability Curve of Settlement Across an Advancing Tunnel.

Mathematically the inflection point can be related to the settlement volume by Equation 4.5 which is derived from Equation 4.4.

$$V_s = \sqrt{2\pi} i w_{s \max} \approx 2.5 i w_{s \max} \quad (4.5)$$

V_s = Settlement volume (mm^2).

The shape and size of settlements are influenced by soil type, depth to tunnel and amount of over-dig during tunnel construction.

4.3.2.4 Other Pipe Movements.

Lateral pipeline movements are very important for the design and damage/risk assessment in a number of situations such as across faults and close to excavations. Audibert and Nyman (1977) and Trautmann and O'Rourke (1985) review the previous analytical models and laboratory testing programmes associated with lateral pipe displacements resulting from mass soil movements. Audibert and Nyman (1975) undertook a testing programme to investigate soil restraint during the lateral displacement of a buried pipeline. The pipe diameters were 25, 60 and 114 mm, and were buried at various depths in a sand, the sand density and therefore its internal angle of friction were also altered. Trautmann and O'Rourke (1985) undertook a similar testing regime with diameters of 102 and 324 mm, again with different sand densities and depths of burial but with variable pipe surface roughness. Audibert and Nyman (1975) noted the failure modes for their tests, and at shallow depths tensile cracks developed above the pipe (Figure 4.6), at greater depths a simple contained zone of failure in front of the moving pipe was observed (Figure 4.7).

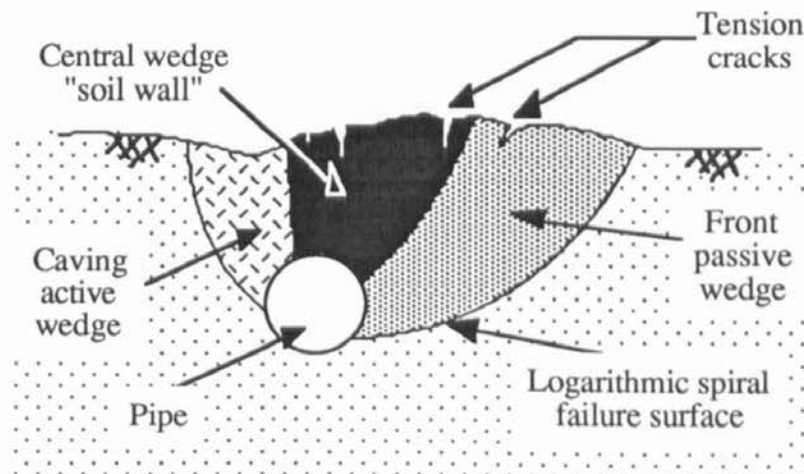


FIGURE 4.6 Shallow Wedge Failure Mechanism Resulting from Lateral Pipe Displacement (after Audibert and Nyman, 1975).

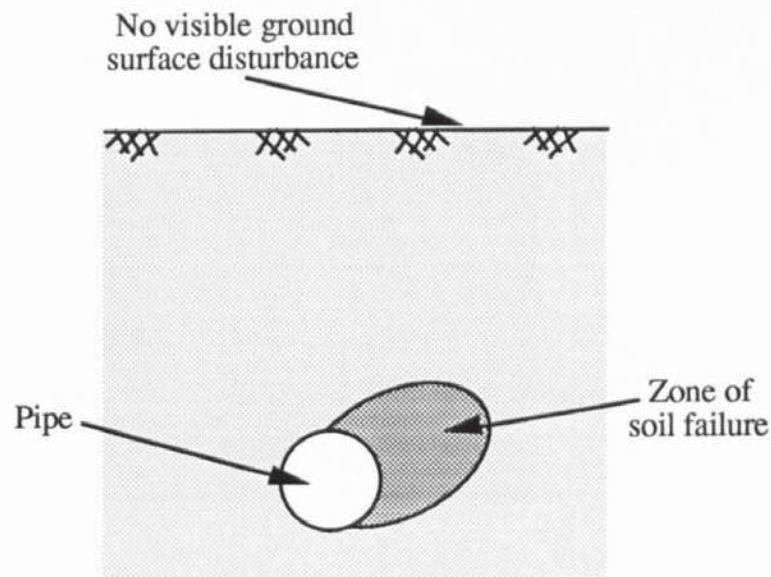


FIGURE 4.7 Deep Punching Failure Mechanism Resulting from Lateral Pipe Displacement (after Audibert and Nyman, 1975).

The longitudinal displacement of a pipeline and is commonly caused by temperature and pressure induced strains (Peng, 1978a and 1978b, Ahmed and McMickle, 1981, Luscher *et al.*, 1979). The tendency of the pipe to longitudinally contract or expand is resisted by the longitudinal soil-skin friction which is a function of the shear strength of the surrounding soil and the roughness of the coating on the pipe. Hunter (1983) reports that for cast iron mains as the soil temperature falls tensile forces are developed in the pipe, however below 0°C thermal contraction of frozen ground is greater than that of the pipe and compressive stresses are induced.

4.4 Frost Action and its Influence on Structures.

4.4.1 Introduction.

Frost action is detrimental to any structure if left uncontrolled or ignored, this section discusses the implications of frost action in general civil engineering. Emphasis is placed on pipes, gas industry tests and soil-structure interactions of relevance to chilled gas pipeline operation.

4.4.2 Frost Action on Structures.

Pavements and Ice Rinks

During natural freezing improper design of pavements structures can lead to failure due to excessive differential heave or thaw weakening of the sub-grade (Johnson *et al.*, 1984). This is a particular problem in colder climates however, design criteria exist in the United

Kingdom to reduce the risk to a minimum (Roe and Webster, 1984). The operation of ice rinks has been shown to be vulnerable to excessive differential frost heave displacement (Chapuis, 1988, Leonoff and Lo, 1981). Frost heave can continue for many years under these conditions and the most effective remedial solution is to excavate the frost susceptible foundation material and replace with a non-frost susceptible gravel or sand (Chapuis, 1988). If necessary insulating layers and/or heating systems can be combined with sub-grade replacement to provide a comprehensive solution.

Foundations and Piles

Frost heaving can affect foundations by two soil-structure interactions, basal heave and tangential adfreeze (Figure 4.8).

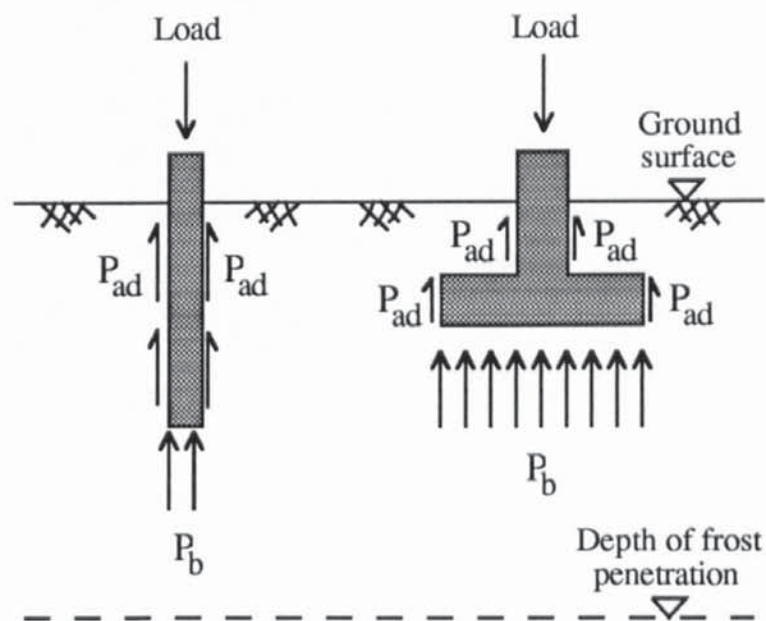


FIGURE 4.8 Basal and Tangential Adfreeze Forces on a Pile and Pad Footing Foundations within Frozen Ground.

Basal heave pressures (P_b) are simply the vertical frost heave pressures acting on the underside of the foundation. Johnston (1981) notes that there is limited information on basal heave pressures and that an indication of these can be ascertained from a knowledge of frost heave pressures (Section 3.3.4). Domaschuk (1981) collated the literature from a number of investigations and found that the basal heave pressure varied between 200 to 3000 kN m⁻² and that the results were influenced by the testing regime rather than soil type. After the frozen soil freezes to the side of the foundation the soil may expand vertically as a result of ice lens formation. This bond strength is related to surface characteristics of the foundation and is referred as the tangential adfreeze bond (P_{ad}). Again Domaschuk (1981) reports maximum adfreeze stress as between 45 and 2750 kN m⁻², and that these results are more

affected by the test methodology than by the soil factors. The values of these stresses are dependent on the soil type, foundation loading, soil temperature profiles, rate of advancement of the frost front, duration of freezing temperatures, foundation material and coating etc (Johnston, 1981). Thus prediction of these forces requires a knowledge of the soil thermal, moisture and stress regimes over the period of sub-zero temperatures and the foundation materials.

LNG Tanks

LNG tanks contain liquid natural gas at -163°C and thus the surrounding ground will freeze, however the amount of frozen soil depends on design considerations. Goto *et al.* (1988) have investigated the shear strength of the soil around a LNG tank in relation to tank heave. Two soil failure modes were put forward (Goto *et al.*, 1988), shear failure at or close to the unfrozen/frozen interface or localized edge failure near to the ground surface again at the unfrozen/frozen interface (Figure 4.9). A simple pull-out test indicated that shear failure occurs not at the unfrozen/frozen interface but in front, in the unfrozen soil, thus the shear strength of the unfrozen soil is a governing factor in the resistance to LNG tank heave. It was put forward that the suction forces generated to maintain thermodynamic equilibrium imparted strength to the unfrozen soil close to the interface (Goto *et al.*, 1988).

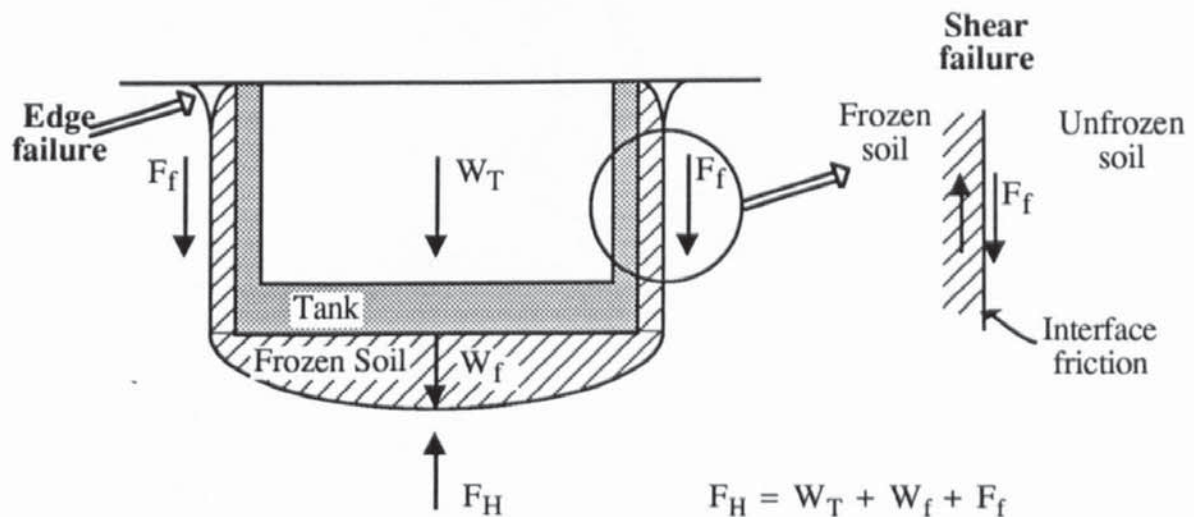


FIGURE 4.9 LNG Tank In-Ground Failure Modes (after Goto *et al.*, 1988).

Takagi and Tanaka (1980) and Kinoshita *et al.* (1982) undertook small-scale tests on in-ground model LNG tanks operating at approximately -25°C in a basin of homogeneous soil. Both these investigations were concerned with the heaving pressures that can be exerted on the tank wall during operation, the thermal and moisture regimes were also monitored. Takagi and Tanaka (1980) demonstrated that the frozen earth pressure on the tank wall reached a maximum after 20 hours and then decreased slowly. In contrast the predicted

pressures increased with time. This difference is accounted for as a result of the cracking at the ground surface which acted to reduce the frozen earth pressures. The ground surface was shown to move upwards and away from the tank as time progressed, measurements within the soil also indicated horizontal displacement. The observed ground cracks appeared at the same time as upward tank displacement started. These cracks at the end of the test were up to 20 mm in width and extended radially from the tank wall, cracking was mainly within the frozen soil with cracks extending into the unfrozen soil (Takagi and Tanaka, 1980). Kinoshita *et al.* (1982) undertook a similar trial and concluded that the frozen earth pressure acting on the tank wall initially rises rapidly but levelled at approximately the same time as ground cracking was reported. At the end of the trial these radial ground cracks were reported to be between 0.5 and 1.0 m in length, 5 to 10 mm wide and 100 to 300 mm deep. Moisture tension measurements in front of the frost front were maximal close to the frost front and decreased rapidly away from the frost front. Vertical soil displacement was a maximum at about 250 mm from the tank wall indicating that the tank exerts an influence on the soil close to it (Kinoshita *et al.*,1982).

4.4.3 Frost Action on Pipes.

The effect of frost penetration from the ground surface under freezing air temperatures has been investigated due to the increased likelihood of pipe failure during the Winter months (Yie, 1968b, Smith, 1976, Bahmanyar, 1982 and Hunter 1985). These investigations cover small diameter pipelines, carrying either gas (Yie, 1968b, Hunter 1985) or water (Smith, 1976 and Bahmanyar, 1982) and so, during the periods of low temperatures, the pipe fluids exhibited a resultant temperature drop thereby inducing thermal strains into the pipe.

Monie and Clark (1974) report a test on a 225 mm (9") cast iron water main, the results showed that as the freezing front descended towards the pipe there was an associated increase in the load on the pipe which was attributed to the expansion of the soil water upon freezing. This increased load can result in the failure of a pipe if combined with other conditions such as live loads, corrosion, relative soil movements. This trial was flawed (Smith, 1976) since the load cells were located directly on top of concrete piers and attached to the underside of the pipe, and so the measured stresses were not those that would be found under a pipe resting on a continuous foundation. Smith (1976) in a continuation of Monie and Clark's test used a pipe split in the longitudinal direction (at 90° and 270° to the vertical), with load cells placed vertically within the split pipe and similarly noted an increase in load on the pipe during sub-zero air temperatures. Bahmanyar (1982) suggested that this test gave an indication of the effects of a descending isotherm, however it did not fully simulate the pipe bending stresses since the pipe was split.

Bahmanyar (1982) undertook a statistical analysis of pipe failure, a field study and operated a laboratory model filled with a silty-sand, again this bore out the above conclusions. Increased loading was hypothesized to be related to the expulsion of water at the freezing front producing a redistribution of the soil moisture and a change in the soil structure thereby altering the soil load bearing characteristics. The laboratory model indicated that the induced load was related to rate of advancement of the freezing front and the ease of access to water. The small-scale model is further discussed in Section 4.6.3.

Hunter (1983) reported tests where three 100 mm ductile iron mains had forced sub-zero air temperatures applied to the ground surface within a canopy. Only minimal bending stresses were reported as the frost front descended to pipe level within a homogeneous soil type. However where the pipe crossed a granular fill zone significant bending stresses were measured and it was suggested that they occurred from moisture redistribution to the freezing front, that in turn produced a relative expansion or contraction of the backfill material compared to the gravel.

This section illustrates that the imposition of frost action to a small-diameter pipe can produce significant changes in pipe loading and bending stresses. The tests draw different conclusion from varying test results, however these suggest that a clear understanding of the frost action process is necessary for understanding the imposed pipe stresses.

4.4.4 Warm Oil and Gas Pipelines In Permafrost Regions.

Oil pipelines often have to be operated at above ambient ground temperatures since crude oil can have a high viscosity which precludes high rates of flow under economic pumping energy inputs. Therefore the oil is heated prior to transportation to decrease the viscosity. An economic "trade-off" between crude oil temperature and energy requirements for pumping determines the oil temperature, other factors such as pipe material, soil conditions will also influence crude oil temperature. Hot oil pipelines pose a significant problems when they pass through Permafrost Regions since thawing of frozen ground will take place. Over the design life of the pipeline a thaw bulb will form and grow and settlements may result. Differential settlements can occur in zones of discontinuous permafrost that can produce a loss of integrity of the pipeline. The formation of the thaw bulb can alter the precarious thermal balance within the ground altering the moisture movements affecting both the pipeline integrity and the local terrain (Harris, 1986, Williams, 1986). The rate of growth of the thaw bulb with time and the ice content of the soil within the bulb determines the settlement of the pipeline. Lachenbruch (1970) and Wheeler (1978) developed 2D techniques to predict the size of the thaw bulb incorporating the latent heat effects.

Trans Alaskan Pipeline (TAPS)

In Alaska a 1.22 m diameter pipeline was constructed for commission in 1977 to transport crude oil 1290 km from Prudhoe Bay on the North coast to Valdez on the South coast. This pipeline transports crude oil at temperatures between 60 and 65°C and passes through permafrost areas for over 70% of its length (Harris, 1986, Williams, 1986).

Norman Wells Pipeline

In 1985 the 869 km Norman Wells Pipeline was brought into commission. This is a 324 mm diameter pipe passing through discontinuous permafrost and is buried along its full length. Its design differs from the TAPS project in that some degradation of the surrounding permafrost is anticipated, the pipe is designed as a structural member to withstand the resultant differential settlements and it is situated on previous right-of-ways where feasible (Nixon *et al.*, 1984). This crude oil can flow freely at temperatures slightly below 0°C and the opportunity was taken to minimize the energy exchange by setting the inflow temperature to -2°C and allowing the pipeline temperature profile to follow that of the ambient ground temperature. Therefore the pipeline can operate at sub-zero or above zero temperatures and differential pipe movements due to thaw settlement and frost heave were included in the design procedure.

4.4.5 Soil-Pipeline Temperature Profiles.

The Schorre Equation (Equation 4.6) has been used, and modified, by many authors for applications involving the prediction of the temperature profile along gas pipelines (Schorre, 1954, Vinson and Burgar, 1964, Haynes, 1974, Firoozabadi, 1977 and Archer *et al.*, 1984).

$$\text{Log}_{10} \left[\frac{(T_1 + Jx_1) - (T_g + J/a)}{(T_2 + Jx_2) - (T_g + J/a)} \right] = \frac{aX}{2303} \quad (4.6)$$

- T_1, T_2 = Gas temperature at point x_1 and x_2 (°C),
- T_g = Ground temperature (°C),
- x_1, x_2 = Distance downstream (m),
- X = Distance between x_1 and x_2 (m),
- J = Joule - Thompson Effect (°C m⁻¹),
- a = $(2 \pi R_p U) / (q C_p)$,
- R_p = Outside pipe radius (m),
- U = Heat transfer co-efficient (W m⁻²°C⁻¹),
- q = Mass flow rate (kg s⁻¹),
- C_p = Specific heat of gas at constant pressure (kJ kg⁻¹ °C⁻¹)

This equation can be simplified by assuming that x_1 is at the station outlet (Firoozabadi, 1977 and Archer *et al.*, 1984). The accuracy of the the Schorre equation is dependent on the estimates of the heat transfer co-efficient (U) which is analogous to the thermal conductivity of the surrounding soil mass. The thermal conductivity (Section 3.2.2) has been shown to be dependent on soil type, soil moisture content and temperature, and so it will vary along the length of the pipeline. This value can be measured directly from soil samples or by monitoring the temperature profile along pipeline and by back analysis deriving an overall heat transfer co-efficient (Archer *et al.*, 1984). King (1977) and Lunardini (1981) used classical heat transfer theory to develop a similar equation for heat flow from a pipe.

The prediction of the zero isotherm around a chilled pipeline is very difficult since, again, local soil types and moisture contents must be known. Archer *et al.* (1984) used a simple equation based on the radial temperature profile from a cylinder (Equation 4.7) and provided an approximate solution under British Gas operating conditions.

$$R_p = R_L e^{U_r(T_p - T_L)} \quad (4.7)$$

- R_L = Radius to isotherm (m),
- U_r = Heat transfer co-efficient ($^{\circ}\text{C}^{-1}$),
- T_p, T_L = Temperature of pipe and isotherm at R_L ($^{\circ}\text{C}$).

4.5 Chilled Gas Pipeline Operation.

4.5.1 Introduction.

The economics, security of supplies and physical barriers to Natural Gas transportation have on the whole dictated the use of large diameter steel pipelines in preference to haulage. Therefore the concept of gas pipelines operating at sub-zero temperatures has evolved from the necessity to transport large quantities of Natural Gas from inaccessible locations to demand centres. Sub-zero operation can take place either on route to or within the Transmission System. Katz and King (1973) have discussed the merits of LNG, Dense Phase and Chilled Mode gas transportation in connection with large diameter pipelines to carry gas from Arctic fields to the Southern Canadian Transmission System. Both the necessity to maintain the integrity of the permafrost and economics indicated that chilled operation was most suitable. Normally chilled gas pipeline operation is a manifestation of reducing the amount of pre-heat applied at upstream Pressure Reduction Stations within a Transmission System (Archer *et al.*, 1984, Kempner, 1968).

4.5.2 Chilled Gas Pipeline Operation in Temperate Climates.

At Pressure Reduction Stations (PRS's) there is a considerable economic saving to be made if the amount of pre-heating prior to pressure reduction is minimized (Section 2.3.3). In Britain it has been British Gas policy to operate the outlet temperature at +5°C, thus a study was initiated to assess the lowest safe outlet temperature (Archer *et al.*, 1984). Study programmes in the USA have recognised the potential savings and have investigated methodologies of reducing the troublesome soil-pipe interaction associated with frost heaving (Kempner, 1968, Yie, 1968a, 1968b, 1969a, 1969b, Browning, 1970, Ahmad, 1978).

4.5.2.1 Britain

Archer *et al.* (1984) undertook a full-scale trial involving assessment of the mechanical integrity of the system as a whole, improving pre-heater efficiency, predicting temperature distributions along the pipe and investigating soil-pipeline interactions. Two troublesome soil-pipeline interactions were reported in the system under trial, namely frost heave and ground cracking.

Frost heave can express itself as pipe heave and/or ground surface displacement, and the pipelines were monitored at the points of restraint within the PRS's using strain gauges and pipe heave rods. At Orrell PRS pipe displacement was monitored regularly and the restraint on the pipe was minimized by releasing the pipe from above-ground mountings and mechanical fixings. Pipe bending stresses were calculated from pipe displacement data using a FEM computer program, and were found to be less than 20 Nmm⁻² (20 MPa) which did not adversely impair the integrity of the pipe. A maximum pipe uplift of over 85 mm was reported in April of 1984 and had steadily risen to this level since November in response to ground and pipe temperature drops (Figure 4.10). Ground heave was a concern at road crossings but, since these are typically sleeved or buried at greater depths than normal, it was suggested that it would not present a major problem (Archer *et al.*, 1984).

Ground cracking was reported intermittently along that part of the pipeline within the distance necessary for the gas temperature to rise above 0°C. The cracks consisted of a vertical crack penetrating from the ground surface to its apex slightly above the pipe. At the locations of ground cracking it was reported that no pipe or ground heave was observed (Archer *et al.*, 1984). It was suggested (Archer *et al.*, 1984) that the cracks formed due to moisture migrations to the frost front and to the ground surface for evaporation during warm spells. This would ultimately produce a desiccated zone between the frozen soil annulus and the ground surface (Figure 4.11), where a soil shrinkage crack would develop

and enlarge. These ground cracks were observed to be more prevalent in clayey soils which by their general nature are susceptible to soil shrinkage cracking (Reeve *et al.*, 1980).

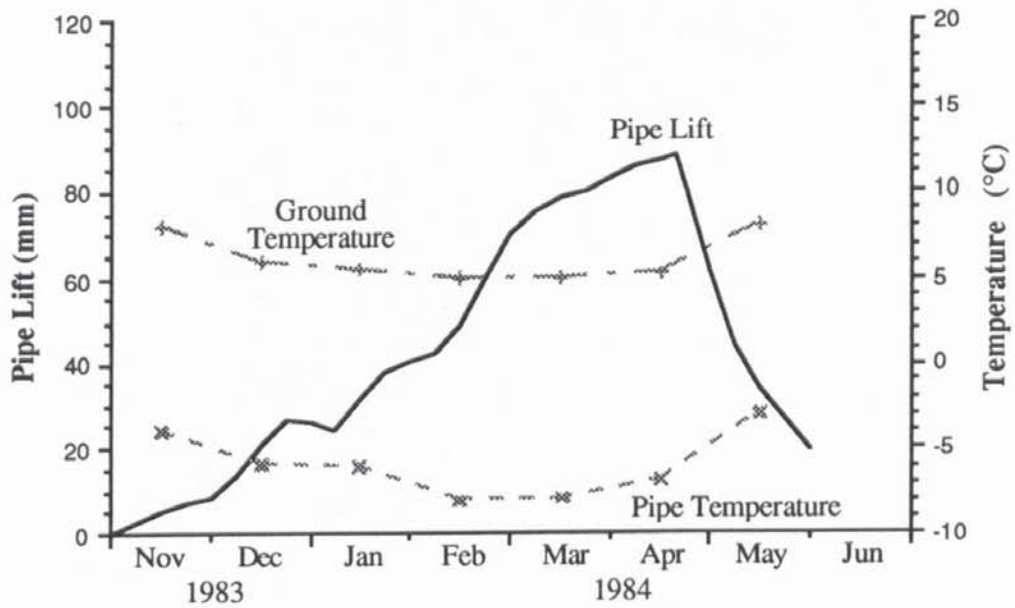


FIGURE 4.10 Graph Showing Pipe Lift, Ambient Ground Temperature and Pipe Temperature during the Pre-heating Season (Nov to May) at Orrell PRS (after Archer *et al.*, 1984).

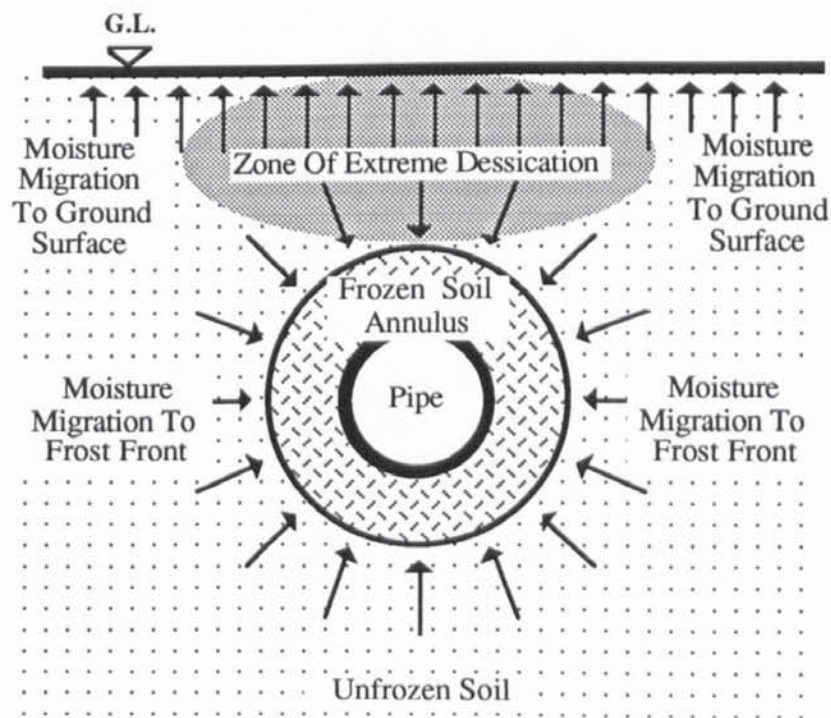


FIGURE 4.11 Diagrammatic Illustration of the Hydraulic Regime around a Chilled Gas Pipeline incorporating Moisture Movements for Ground Surface Evaporation.

The cost saving for the trial involving the operation of two Pressure Reduction Stations during the Pre-heating Seasons 1982-1983 and 1983-1984 amounted to about £550,000, of which a vast majority came from the much higher flow Blackrod Station. Therefore the cost savings were very significant and particularly appropriate to large diameter, high flow National Transmission Pressure Reduction Stations (Archer *et al.*, 1984).

4.5.2.2 North America.

Research into chilled gas pipeline operation has been carried out since the 1960's, for many purposes. The initial work concentrated on problems due to the encasement of distribution mains with frozen soil. This was a result of either operating the mains at sub-zero temperatures or the penetration of the zero temperature isotherm into the ground to below the pipe. Yie (1969a) noted that pipe stresses induced by frost heave downstream of a PRS were known to result in excessive pipe bending stresses and even failure. Four organisations have been identified involved in assessing potential problems, and investigating mitigative solutions:-

1. Michigan Consolidated Gas Company, Detroit, Michigan (Kempner, 1968),
2. Consumers Power Company, Jackson, Michigan (Browning, 1970),
3. Institute of Gas Technology, Chicago, Illinois (Yie, 1968a, 1968b, 1969a and 1969b),
- 4 Northern and Central Gas Corporation Ltd, Ontario, Canada (H.Ahmad, 1978).

These all identified ground/pipe heave as the main problem and showed grouting to be a very useful mitigative solution. Browning (1970) also suggested improving the drainage characteristics of poor draining soils by installing land drains as a positive solution.

Kempner (1968) described a practical and effective method of controlling the ground distress, caused by the operation of chilled gas pipelines, other than expensive pre-heating of the gas prior to pressure reduction. In the 1958/59 Pre-heating Season four different installations showed adverse effects due to the operation at sub-zero temperatures in the distribution system operated by the Michigan Consolidated Gas Company, in Detroit, Michigan (Kempner, 1968). There were also fifteen other installations operated under similar conditions that did not experience any problems. As a result of these problems a study programme was initiated (Kempner, 1968), paying particular interest to the main problem which was the damage caused by ground heave and not the encasement of the pipe by frozen ground.

The study (Kempner, 1968) involved two main areas of activity:-

1. Field measurement programme:- this was undertaken to study the formation of the frozen annulus around the pipe and the extent of ground heaving. This involved the measurement of the temperature regime around the pipe, the strain in the pipe and the heave of the pipe. These measurements were undertaken at seven locations within the distribution system. In addition soil samples were taken to determine the particle size distribution and moisture content of the soils at each location.
2. Soil additive programme:- this investigated methods to reduce or eliminate ground heaving. Two types of additives were considered:-
 - i. additives to reduce the freezing point of the soil, eg. calcium chloride and sodium chloride injection,
 - ii. additives to reduce the permeability, eg. emulsified asphalt, cut-back asphalt and Lignosol (a wood derivative).

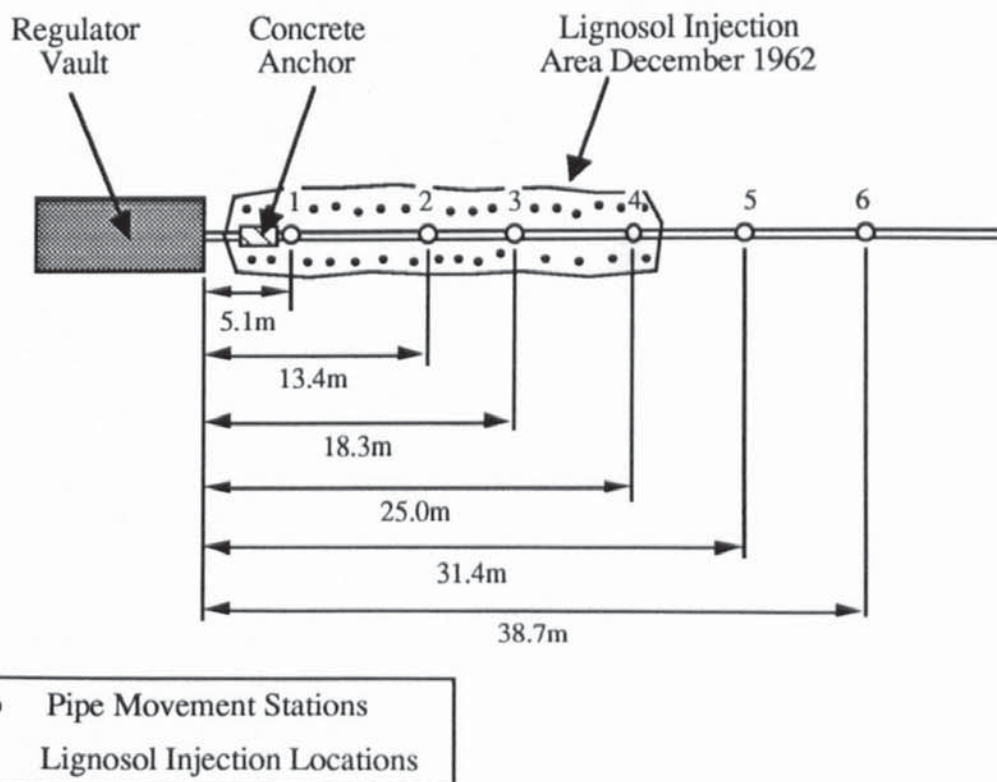


FIGURE 4.12 Plans Showing Pipe Movement Stations and Lignosol Injection Area (after Kempner, 1968)

Freezing point-depression tests indicated that neither of the additives for reducing the freezing point had any permanency, this was due to the leaching of the salts by the

movement of the soil water. Permeability and capillary tests indicated Lignosol was the most effective additive at reducing permeability. Thus, in late 1962, Lignosol was injected around a gas main (Figure 4.12) at one of the locations which had previously been chosen for pipe heave monitoring. During the first winter, pipe and ground heave remained the same as in previous year, this was thought to be due to the fact that the Lignosol had not dispersed completely around the pipe. However when the ground thawed in the next summer, dispersion was able to take place, this was demonstrated by the reduction in pipe heave in the following six years (Figure 4.13). Up to 1968 when this paper was published (Kempner, 1968), five other locations had been treated with Lignosol and showed positive results both from the cost savings (ie. not having to run pre-heaters) and reductions in the ground and pipe heave. A similar successful trial (Ahmad, 1978) was carried out by the Northern and Central Gas Corporation Ltd, Ontario, Canada. In this trial Lignosol was again used to control both pipe and ground heave.

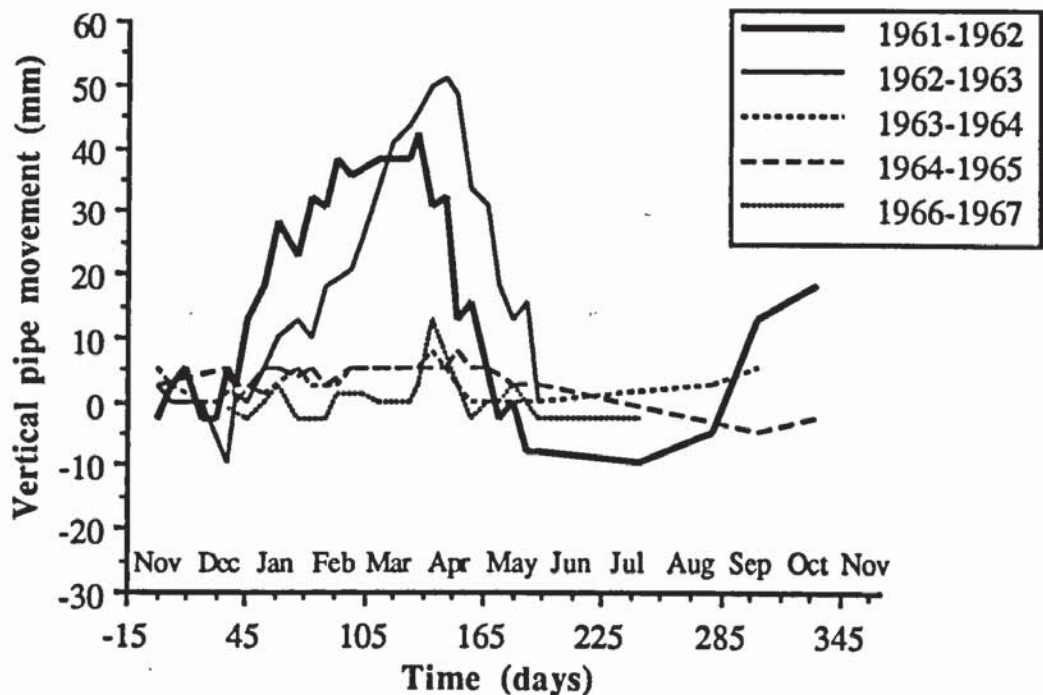


FIGURE 4.13 Pipe Movements at Station No.3 (adapted from Kempner, 1968).

During 1968-1969 a test program was undertaken by Yie (1968a, 1968b, 1969a, 1969b) at the Institute of Gas technology, Chicago, Illinois funded by the American Gas Association. The objective was to find a mitigative solution to the breakage of cast iron mains which occurred more frequently during the winter months. This has been attributed to the zero-isotherm penetrating below the pipe in response to freezing air temperatures. The cast-iron main breakage was due to soil/pipe interaction as a result of either pipe heave or thaw

settlement of the surrounding ground, both giving rise to differential movements. The project considered grouting as a solution, initially identifying ten grouting processes (Yie, 1968a). The Polymer grouting process was selected for further study after an extensive literature survey. This process involved the injection of two free-flowing monomers into the soil, polymerisation into hard or rubbery solids subsequently occurring in the soil pores. Lignosol, which has been used by both Kempner (1968) and Ahmad (1978), was rejected due to problems with its grouting properties (viscosity, permanency, etc). The two polymer grouts used were a Phenol grout and a Siroc grout (similar to AM-9 which is a widely used one-shot chemical grout).

Four sites were selected and the results showed that both grouts were effective in stabilizing the soil around the pipe, and considerably reduced water migration to zones where ice lensing would cause pipe heave (Figure 4.14). To assess the grouting effectiveness a vibration technique was used. This involved dropping a standard mass on the ground before and after grouting and measuring the pipe vibration from a riser linked to a chart recorder. Soil-pipeline interaction conditions were adequately reflected by the vibration characteristics of the pipe, with the accuracy improving when the mass was dropped closer to the riser (Yie, 1969b).

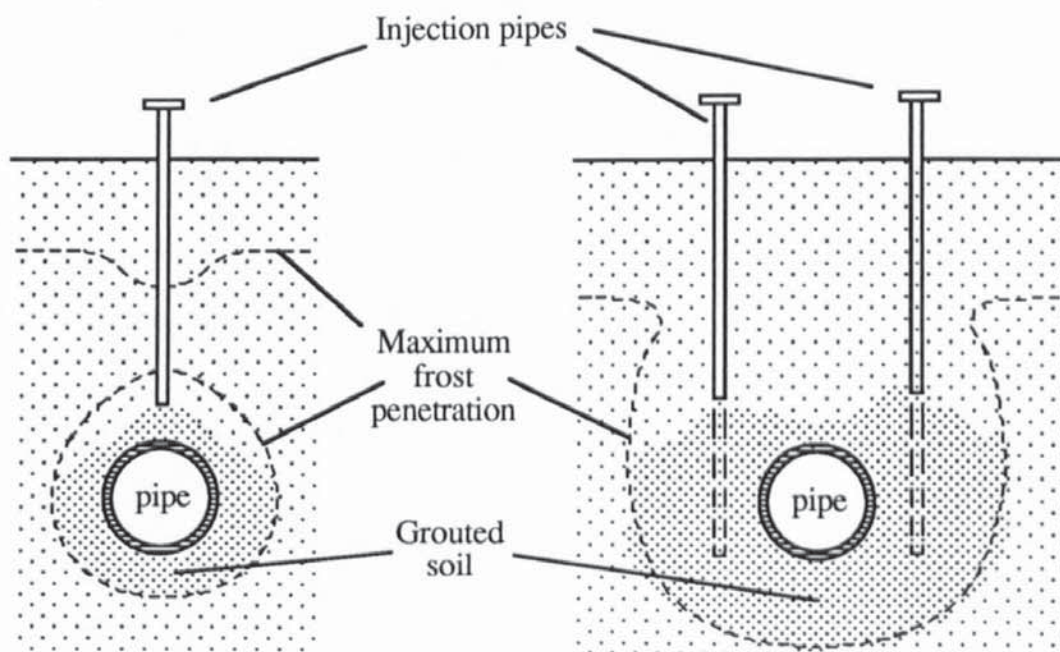


FIGURE 4.14 Grout Injection Using a Single or Double Pipe Technique (after Yie, 1969a).

4.5.3. Arctic and Northern Pipelines.

Davison *et al.* (1979), Jahns and Heuer (1983) report on potential mitigative solutions for frost heave and permafrost protection in Arctic climates. Since interest in Northern pipelines

started in the early 1970's large-scale research facilities have been constructed and operated to assess the potential problems associated with transporting very large volumes of chilled natural gas from Arctic Regions, to southern consumers many hundreds of miles away. Problems are a result of the "permanent" frozen annulus around the pipeline which, if conditions are favourable for frost heaving, would lead to excessive pipe heave. The structural integrity of the pipeline at the interfaces between frost susceptible and non-frost susceptible soils, such as discontinuous permafrost zones could also be threatened due to differential heaving of the pipe (Figure 4.15).

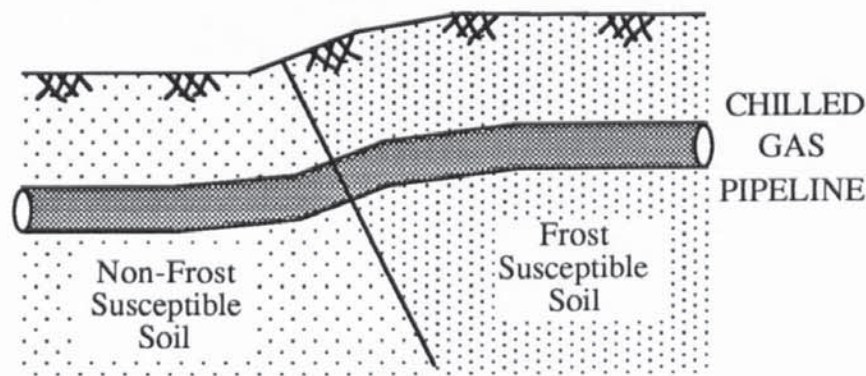


FIGURE 4.15 Pipeline Subject to Differential Frost Heave Forces.

Calgary was one of two frost heave test facilities operated by the Foothills Pipelines and its American partner Northwest Alaskan Pipelines. The other test facility is in Fairbanks, Alaska and very limited information is available on the results obtained (Slusarchuk *et al.*, 1978, Carlson *et al.*, 1981, Carlson, 1984, and Williams, 1986). A further test facility was operated in Inuvik by the above organisations to assess the effect of warm gas pipelines on permanently frozen ground (Hanna *et al.*, 1983, Carlson *et al.*, 1983, Carlson 1984, Williams, 1986). Extensive laboratory testing programmes have been undertaken to compliment the data received from the test facilities. The overall objective of these programmes was to develop an empirical engineering model for frost heave prediction with respect to chilled gas pipeline operation (Slusarchuk *et al.*, 1978, Nixon *et al.*, 1981 and Nixon, 1982).

At the Calgary test facility the upper stratum was a very frost susceptible silt, over 8 m deep, with the water table about 2 m below the ground surface (Slusarchuk *et al.*, 1978). These characteristics coupled with freezing air temperatures in the Winter and chilled gas flowing through the pipeline produced ideal conditions for excessive frost heave displacements. The facility was constructed in the Winter of 1973-74 and initially consisted of four sections of 1.22 m diameter pipe operating at -10°C , the cross-sections are shown in Figure 4.16 (a),(b),(c) and (d). The objective was to assess the mitigative potential of the following on frost heaving:-

1. Increasing the depth of burial of the pipe,
2. Applying restraint to the pipe, and
3. Replacing the soil under the pipe with a non-frost susceptible gravel pad.

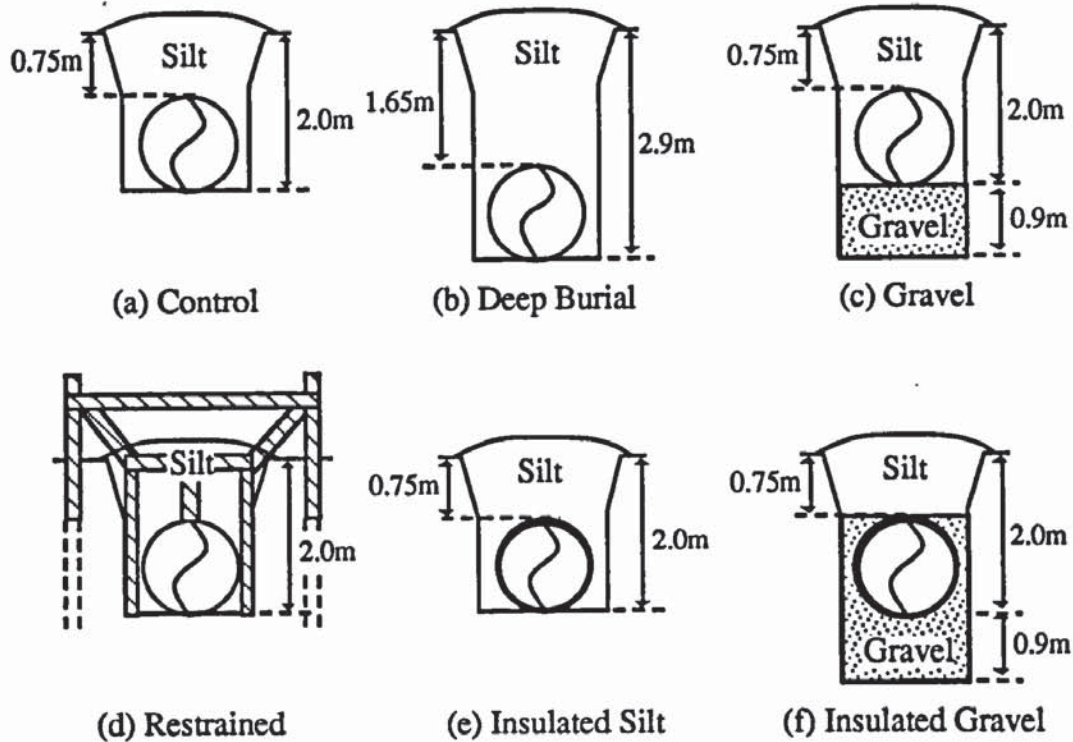


FIGURE 4.16 Diagrammatic View of the Six Test Sections at the Calgary Test Facility (after Carlson *et al.*, 1981).

All the sections (Figure 4.16 (a), (b), (c) and (d)) were backfilled with the material excavated from the trench (Slusarchuk *et al.*, 1978). Measurements of the following were taken in all six sections (Carlson *et al.*, 1981, Carlson, 1984):-

1. Temperature profile around pipe - vertical thermistor arrays,
2. Pore water pressure - pneumatic piezometers,
3. Ground heave - heave gauges,
4. Pipe movement - pipe heave rods,
5. Ambient air and ground temperatures - thermistors and thermistor strings,
6. Rainfall - rainfall gauges.

Figure 4.17 shows the development of pipe heave and frost front penetration below the pipe in the non-insulated sections until the end of 1980. The values at the end of 1980 are given in Table 4.1. Figure 4.17 illustrates the mitigative potential of deep burial, restraint and gravel bed sections (Slusarchuk *et al.*, 1978, Carlson, 1984) and the effects of the

subsequent imposition of a 1.5 m high soil berm. It should be noted that, in the gravel section, the pipe heave reached a limiting value in 1979/80, with the subsequent responses being directly related to seasonal temperature fluctuations.

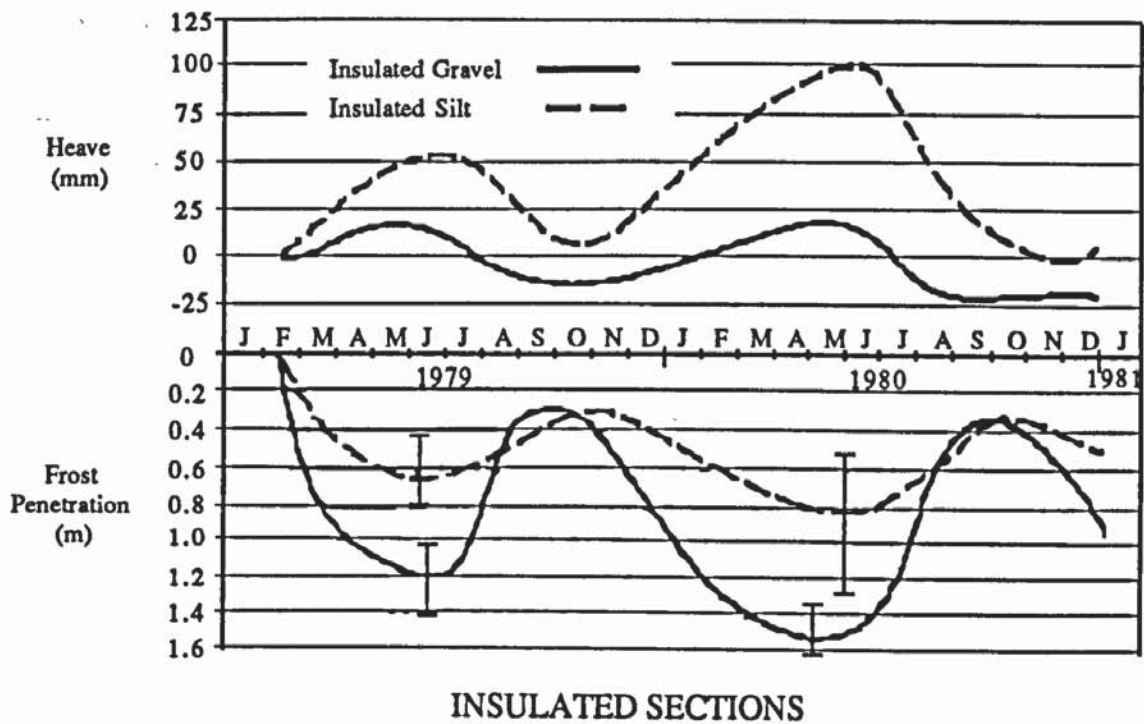
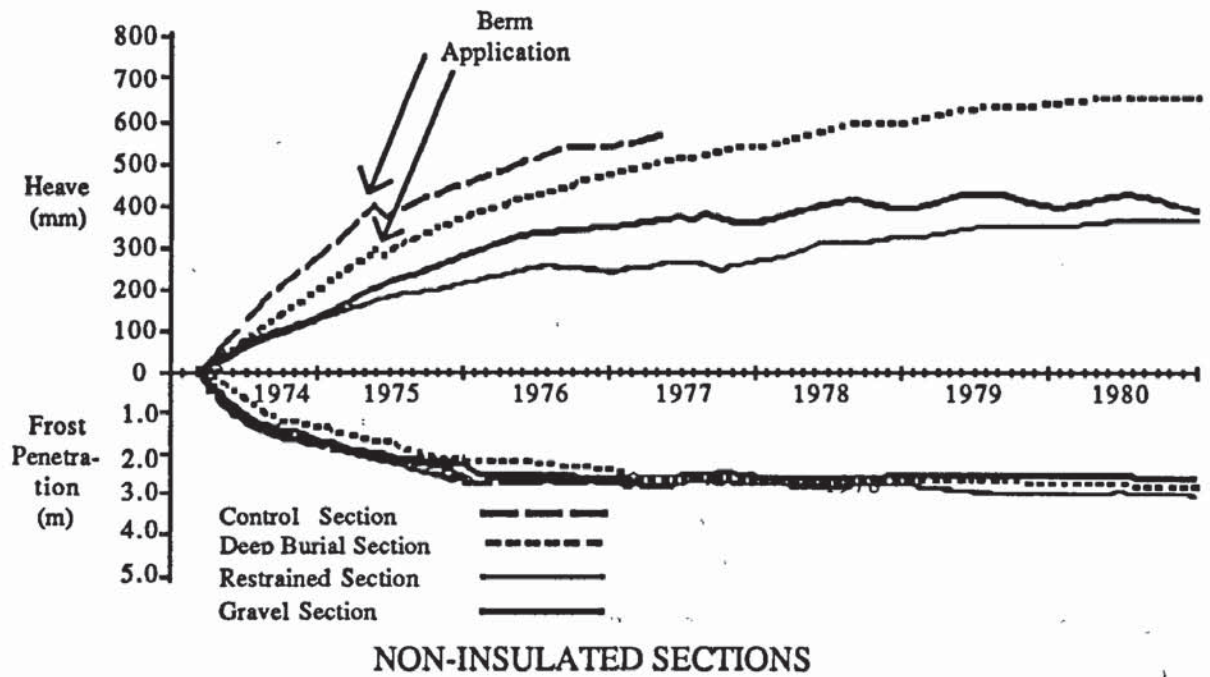


FIGURE 4.17 Pipe Heave and Depth of Frost Penetration Below Bottom for Non-Insulated and Insulated Sections (after Carlson, 1984).

Section	Pipe Heave (m)		Frost Penetration Below Pipe (m)	
	1980-end	1977-mid	1980-end	1977-mid
Control	-----	0.60	2.7	2.7
Deep Burial	0.69	0.54	2.7	2.7
Restraint	0.43	0.39	2.7	2.7
Gravel Bed	0.40	0.27	2.7	2.7

TABLE 4.1 Pipe Heave and Frost Penetration for Non-Insulated Sections at the end of 1980 and in mid-1977.

In 1977 two more sections were installed so that the pipes were insulated with 16 mm of polyurethane and the operating temperature was maintained at -10°C . The first insulated section was backfilled with the excavated silt and in the other section the pipe was surrounded in imported gravel fill with silt merely used as backfill above the pipe (Figure 4.16 (e) and (f)). The pipe heave and frost penetration shown in Figure 4.17, for the insulated sections are very different to those for the non-insulated sections, being significantly less than were measured in the non-insulated sections after similar operating times. Pipe heave and frost penetration were negated in the summer months, showing that these quantities fluctuated in response to annual temperature fluctuations. Insulating the pipe sections is a very effective method in reducing both pipe heave and frost penetration, particularly when the section is backfilled with gravel (Carlson, 1984).

The movement of a frost bulb around the deep burial non-insulated section is shown in Figure 4.18. This illustrates the initial rapid growth and the effect of sub-zero ambient air temperatures in the Winter on the shape of the frost bulb.

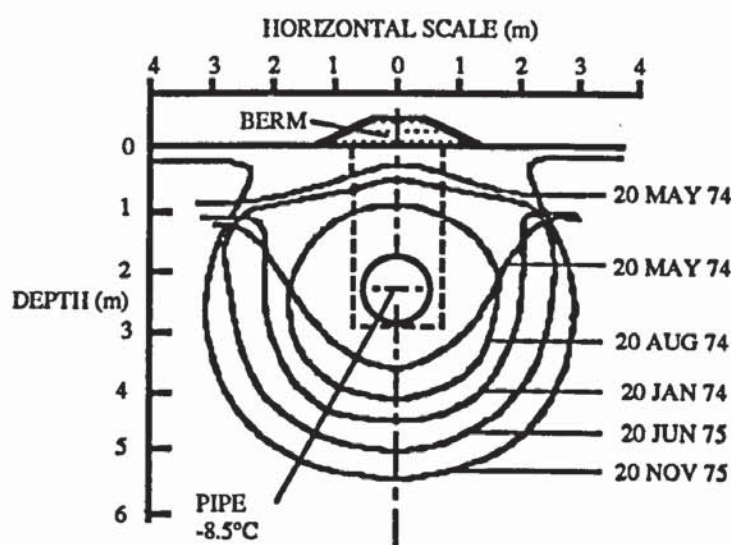


FIGURE 4.18 Frost Penetration around Deep Burial Section (after Slusarchuk *et al.*, 1978).

Extensive laboratory testing programmes were undertaken to supplement data received from the large-scale field test. The laboratory testing programme was mainly centred on the unidirectional freezing of small soil samples (approx 100 mm in diameter and 100 mm in height) under controlled conditions (Carlson *et al.*, 1981). This involved varying cold and warm side temperatures, applied pressure, access to water etc. When comparing the parameters of heat flux, time and soil volume with respect to the small-scale laboratory tests and the large-scale field test, it is obvious that difficulties would emerge in modelling (Nixon *et al.*, 1981). Thus a cold plate (Nixon *et al.*, 1981, and Nixon, 1982) 0.76 m in diameter was developed, allowing these parameters to be more closely modelled. These cold plates were placed *in situ* (Figure 4.19), thus allowing a better representation of the soil and ground-water conditions to which a section of pipeline would be subject. An *in situ* cold plate is particularly useful in areas which are difficult to model in the laboratory such as silty gravels, loose sands, low water table, etc (Nixon *et al.*, 1981). A frost bulb forms under the plate, and frost heave may occur depending on the *in situ* soil conditions. The cold plate installation allows plate heave, temperature profile under and total vertical stress on the plate to be measured with time.

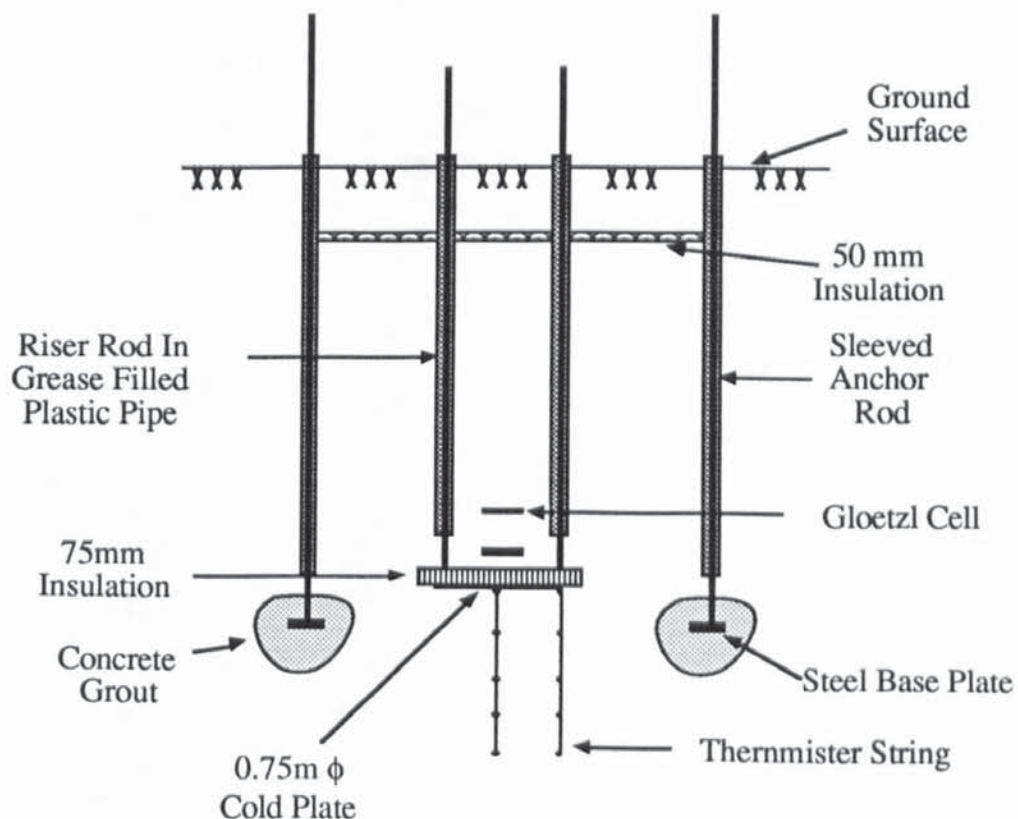


FIGURE 4.19 Illustration of Frost Heave Test Plates used at Calgary Test Facility (after Nixon, 1982).

An ice-segregation theory was developed to predict frost heave from the initial results at the test site and involved plotting graphs of pipe heave against frost front penetration depth. The critical parameter is the ice-segregation ratio (ISR), which is the ratio of pipe heave to frost front penetration depth, and it is dependent on the pressure at the frost front and the frost penetration rate (Carlson *et al.*, 1981). The incremental ice-segregation ratio is calculated as a series of incremental heaves from Equation (4.8)

$$\text{HEAVE} = \sum \Delta H = \sum \left[\Delta \text{ISR} (X, P_f) \right] \Delta X \quad (4.8)$$

- ISR = Ice-segregation ratio,
- X = Frost penetration depth (m),
- P_f = Pressure at frost front (kN m⁻²).

Carlson *et al.* (1981) reported that further testing was underway, but its application has not since been reported. The results from the laboratory tests were later input in to the Segregation Potential Method of frost heave prediction (Section 3.3.6.4) to predict frost heave of the non-insulated test sections at Calgary test facility. Good agreement has been found between these predictions of heave and the observed heave (Konrad and Morgenstern, 1984). However Nixon (1986) and, Carlson and Nixon (1988) have advocated the use of their 2-D thermal simulator which incorporates a Modified Segregation Potential Theory to improve the prediction of frost heave of the non-insulated test sections.

In the early 1980's the test sections underwent considerable thawing resulting from ice blockages in the pipes. During 1982 a Canadian Governmental Agency took an interest in the project and undertook more detailed studies on the sections (Burgess, 1985) and finally in March 1986 the site was dismantled (Williams, 1986, Carlson and Nixon, 1988). During the dismantling stage the opportunity was taken to log the frost bulb around the deep burial and insulated silt section (Carlson and Nixon, 1988). They found that the ice lensing in the deep burial section was more pronounced than in the insulated silt section and that the orientation of the ice lenses tended to be influenced more by stratigraphic features than the direction of the thermal gradient towards the chilled pipe.

Williams (1986) criticized the nature of the test facility since its primary function was to demonstrate the positive mitigative effect that the application of overburden pressure on pipe heave. He also suggests that the sections were laid without due concern for the previous stress and freezing history of the soil at the site. Since the soil conditions were not carefully selected the results yielded could not be analyzed from a fundamental viewpoint.

The Fairbanks frost heave test facility has been described by Hale (1979), Beheshti (1980), Carlson (1984), again operating 1.22 m diameter pipe sections at between -10 and -13°C at 4.8 Nmm⁻² (4.8 MPa). Ten pipe sections are buried in various ditch configurations to measure the effects of rapid freezing, gravel backfill and pipe insulation, a single section was buried across a transition zone between a frost susceptible and non-frost susceptible soil, and a further section in frozen ground to quantify secondary heave effects (Beheshti, 1980). This test was much more carefully and extensively monitored than the Calgary site and, included heat flux transducers, heave rods, radial extensometers, strain gauges and pressure transducers (Beheshti, 1980). The test facility was also operated to validate Hwang's numerical model for 2-D frost heave. As with Calgary very limited information has been published and that this may have been due to the adverse results obtained in respect to pipe heave by the sponsoring organisations (Williams, 1986). In 1982 a joint Canadian-French Study at a large-scale indoor facility at Caen, France was instigated to investigate the fundamental behaviour of the soil around a chilled gas pipeline in Northern climates (Geotechnical Science Laboratories, 1989).

4.5.4 Caen Test Facility.

This represents the most thorough investigation into the soil behaviour at and in close proximity to a frost susceptible/non-frost susceptible soil interface in response to chilled gas pipeline operation. The test facility was previously used by French scientists to investigate the behaviour of pavement structures under frost action. The facility provides a temperature-controlled hall, 8 m wide and 18 m long, which can be filled with soil to a depth of 2 m. The indoor environment provides two main advantages for large-scale testing:-

1. natural variations in hydrological, thermal and soil conditions are largely eliminated, and initial conditions can be selected to suit the environment to be modelled,
2. the protected environment allows more detailed and comprehensive instrumentation than can be achieved in the field.

An understanding of water migration in the unfrozen and frozen soil, and the resultant frost heave pressures are of great importance to the successful operation of chilled Arctic pipelines (Kettle, 1984). Thus the indoor environment can reduce the number of variables such as environmental conditions and soil homogeneity, therefore providing comparative results relating the soil hydraulic, thermal and stress regimes.

4.5.4.1 Description of Test Facility.

An 18 m length of 273 mm diameter steel pipeline was buried in the facility at a depth of 330 mm across a transition between a non-frost susceptible sandy soil and a highly frost susceptible silt (Figure 4.20). The physical characteristics of the soils are described in Table 4.2.

	Caen Silt	Sneek Sand
% by weight		
Clay (< 0.002 mm)	5 - 15	-
Silt (0.075 - 0.002 mm)	85-90	10
Sand (0.075 - 5 mm)	10	80 - 90
Gravel	-	10
Wp	21%	-
Wl	28.5%	-
Ip	7.5	-
Unified Soil Classification	ML	Sw -Sp
Unfrozen Permeability	$1 \times 10^{-9} \text{ ms}^{-1}$	$1 \times 10^{-5} \text{ ms}^{-1}$
Dry Density	$1.8 \times 10^3 \text{ Kg m}^{-3}$	$2.05 \times 10^3 \text{ Kg m}^{-3}$
Dry Density <i>in situ</i>	$1.65-1.7 \times 10^3 \text{ Kg m}^{-3}$	$1.8-1.85 \times 10^3 \text{ Kg m}^{-3}$

TABLE 4.2 Physical Characteristics of the Soils at the Caen Test Facility.

The soils were placed in the pit in 300 mm layers and compacted using a vibrating plate and small roller. The ground water table in the soils was maintained with a basal irrigation system at a level approximately 300 mm below the pipe. Separate refrigeration systems were used to control the air (ground surface) temperature and the temperature of the air circulating through the pipe. A fuller description of the test facility is provided by Burgess *et al.* (1982). Table 4.3 shows the dates of the freeze-thaw cycles to which the test facility has been subjected since its start-up in September 1982.

Event	Date From	Date To	Operating Air/Ground temp (°C)	Conditions Pipe temp (°C)
First freeze	21/9/82	8/6/83	-0.75	-2.0
First thaw	8/6/83	17/10/83	4.0	-2.0
Second freeze	17/10/83	18/9/85	-0.75	-5.0
Second thaw	18/9/85	1/2/86	4.0	ambient
Re-instrumentation	1/2/86	3/3/86	-	-
Third freeze	3/3/86	25/2/87	-0.75	-5.25
Third thaw	25/2/87	25/5/89	4.0	ambient
Shutdown	21/5/87	6/1/88	-	-
Fourth freeze	6/1/88	24/5/89	-0.75	-5.25

TABLE 4.3 Operating Cycles at Caen Test Facility (after Geotechnical Science Laboratories, 1989).

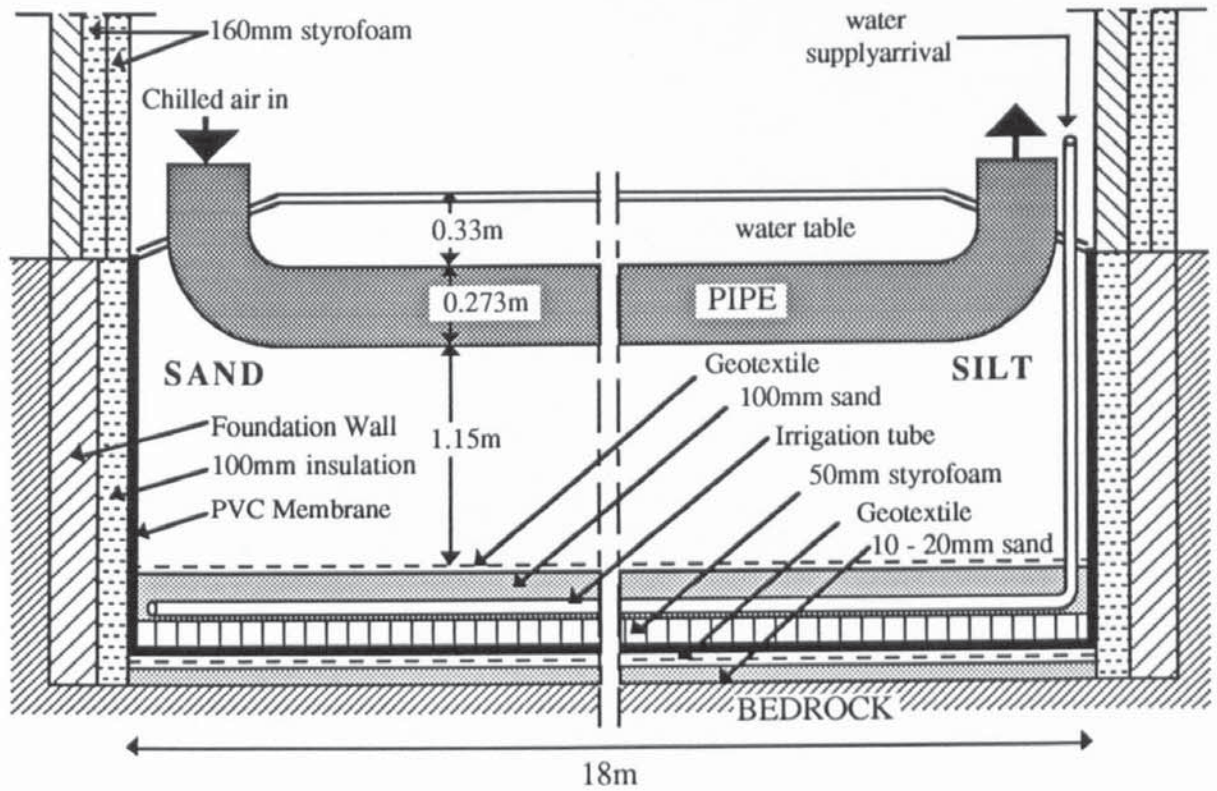


FIGURE 4.20a Longitudinal Section Through the Caen Test Chamber (after Kettle, 1984).

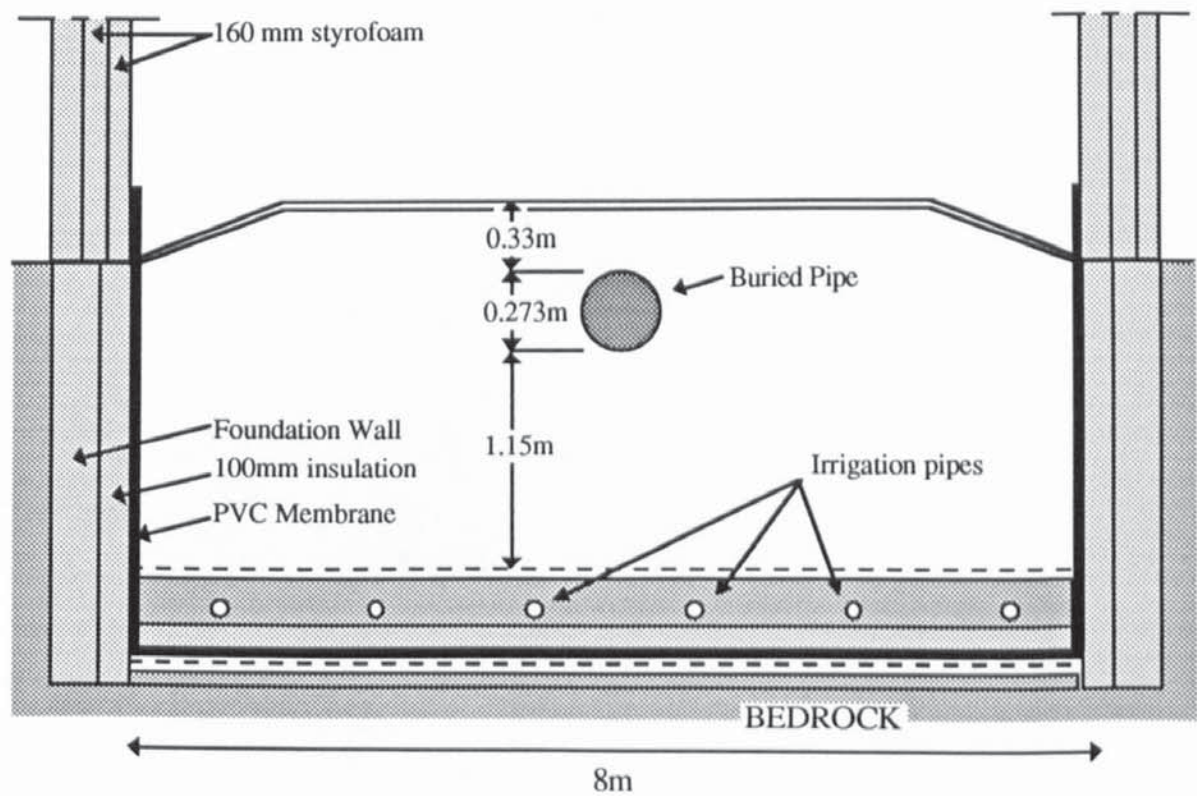


FIGURE 4.20b Cross Section Through the Caen Test Chamber (after Kettle, 1984).

4.5.4.2 Instrumentation.

Instrumentation of the thermal, hydrologic, pipe deformation regimes and soil physical parameters was effected prior to the first freeze-cycle (Geotechnical Science Laboratories, 1983). This included heat flux plates and arrays of thermocouples that were logged by an automatic data acquisition system. This was supplemented by manual measurements of thermistors, water levels, ground surface levels, tensionmeters, glotzl pressure cells, telescopic heave tubes, frost depth tubes, TDR moisture content probes, pipe deflection, pipe curvature and pipe strain. Other, less frequent measurements, included soil density profiling and gravimetric water content determinations (Dallimore and Crawford, 1984). After the second thaw period further magnetic heave devices, Petur pressure cells and thermistor strings were installed (Geotechnical Science Laboratories, 1986b).

4.5.4.3 Observations and Results.

These have been reported in considerable detail in a series of interim reports on the experiment (Geotechnical Science Laboratories, 1982,1983, 1984a, 1985, 1986a, 1986b, 1988a, 1988b, 1989, Dallimore, 1985) and in the proceedings of two seminars held at Caen (Geotechnical Science Laboratories, 1984b, 1991), and so this section only outlines the main results achieved at the test facility.

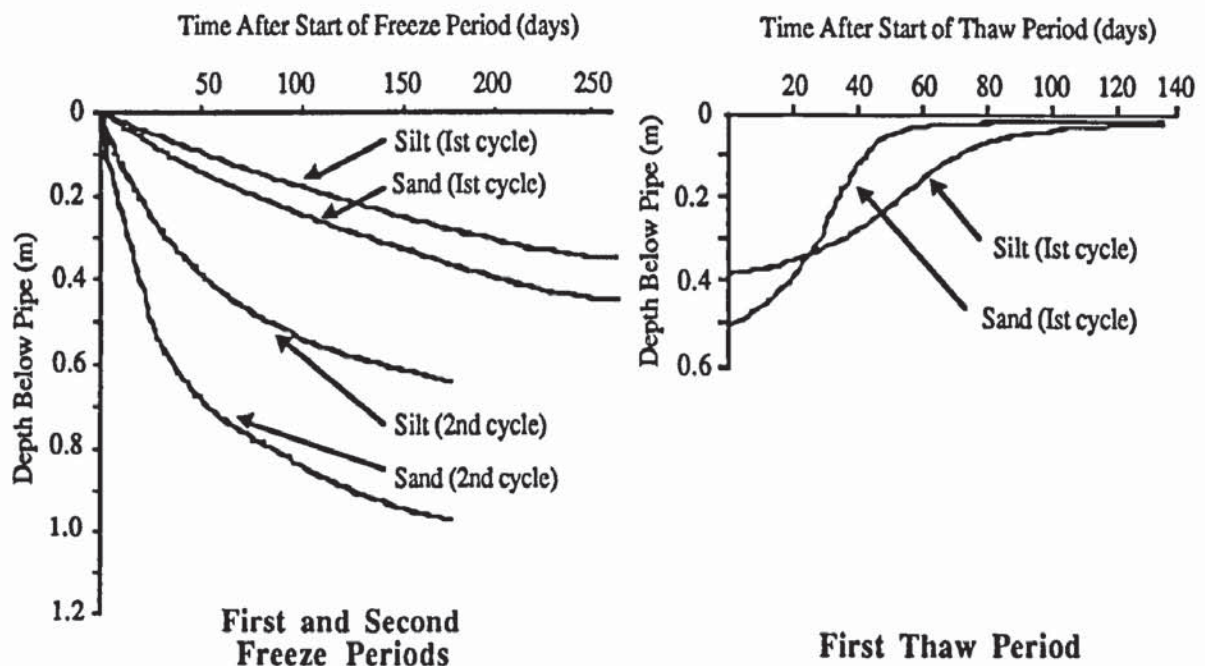


FIGURE 4.21 Progression and Recession of the Frost Front beneath the Pipe (after Dallimore and Crawford, 1984).

Figure 4.21 illustrates that lowering the pipe temperature from -2°C in the first freeze cycle to -5°C in the second freeze cycle, with constant air temperature, results in a quicker progression of the frost front beneath the pipe. Dallimore and Crawford (1984) noted that

during the second freeze period that it took only 60 days for the frost front to penetrate to the same depth in the silt as at the end of the first freeze period after 250 days. The progression and recession of the frost front is faster in the less frost susceptible sand due to its higher thermal conductivity and lower water content.

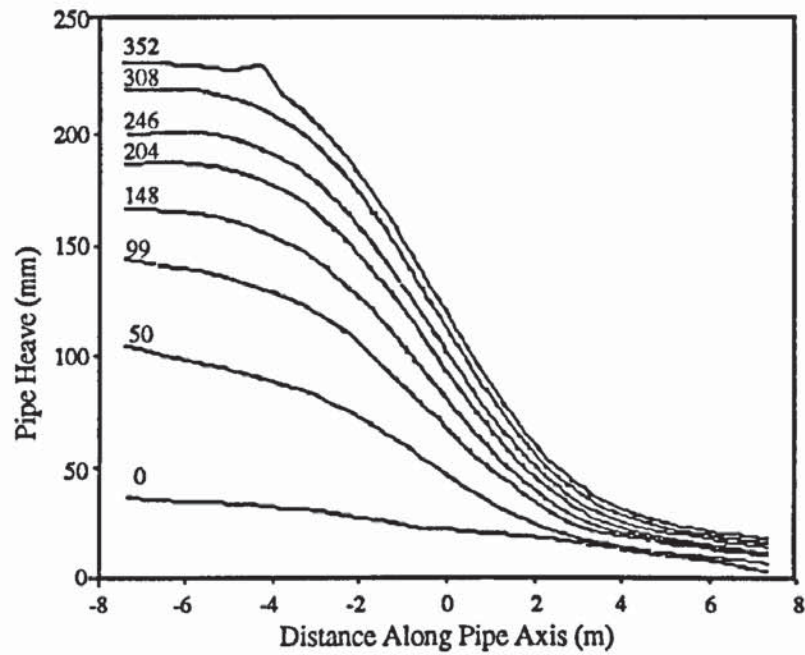


FIGURE 4.22a Deformation of the Pipe during the Third Freeze Cycle (after Geotechnical Science Laboratories, 1988a).

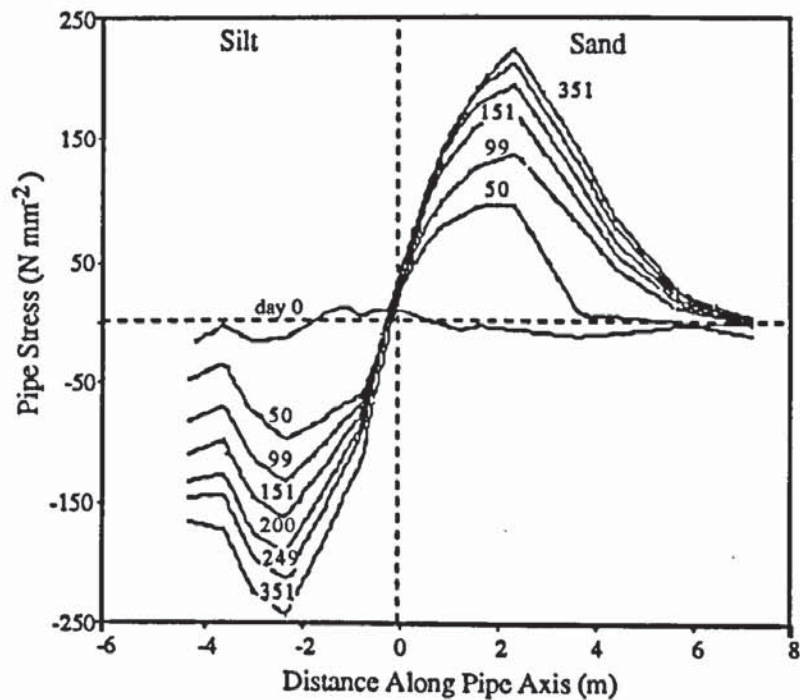


FIGURE 4.22b Pipe Bending Stress during the First Freeze Cycle (after Geotechnical Science Laboratories, 1988a)

Pipe deformation began during the initial weeks of freezing and was due to the differential heave between the silt and the sand. The results of the first freezing period are illustrated in Figures 4.22a and b. The rate of heaving is greatest early in the freeze cycle, when the frost front advancement is quickest, and slows with time. At the end of the thawing period, there was still some residual heave, 20 mm in the silt and 10 mm in the sand. This residual heave increased at the end of the second and third thawing periods respectively and indicated a progressive jacking of the pipe in the silt section (Figure 4.23). During the second freezing period, due to lower gas pipe temperatures there was considerably more pipe deformation and bending stress than in the first freezing period. Analysis was carried out by a number of different methods, of which strain gauges provided the most reliable stress values (Bowes, 1984). In first freezing period the maximum bending stress reached approximately 50% of the yield stress, however in the second period 85% was reached (Geotechnical Science Laboratories, 1985). Thus, if the pipeline had a significant operating pressure, it would be operating beyond its yield stress, and therefore the pressure would have to be dropped. In the design stage, this would necessitate either a more expensive pipe with a thicker wall or the adoption of a special geotechnical design to limit pipe heave (Geotechnical Science Laboratories, 1985, 1986a). Thermal considerations indicate that the amount of net heave during the second, third and fourth freezing periods should be equal after comparable time periods however, at the end furthest from the interface in the silt section, the heave at 99 days increased from 98.8 to 107.7 to 114.0 mm over these three periods. This indicates that the soil was undergoing a structural change (Geotechnical Science Laboratories, 1988b).

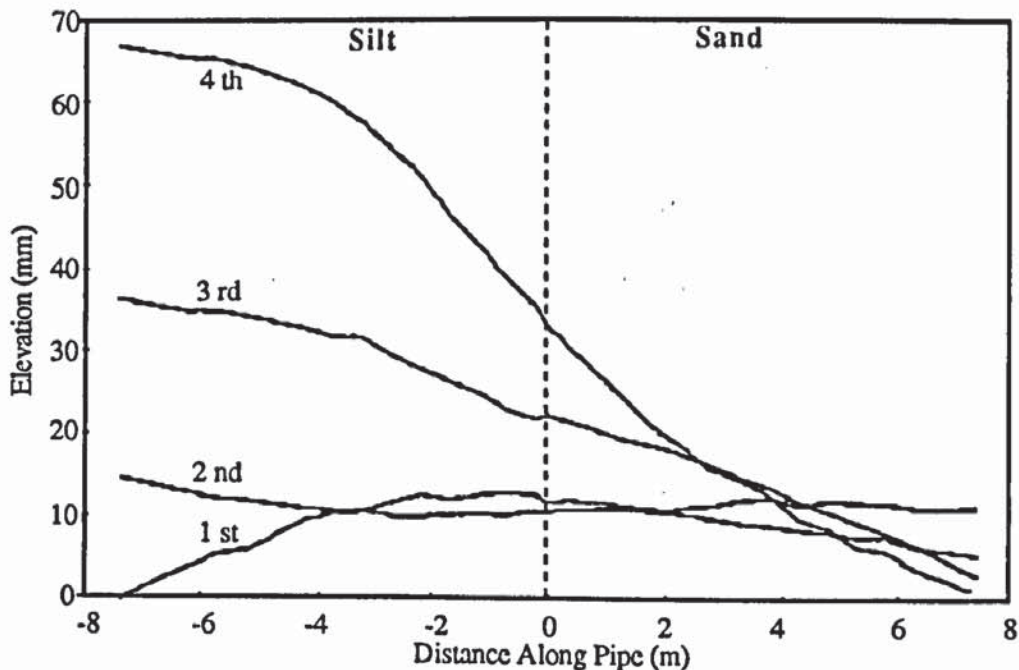


FIGURE 4.23 Vertical Pipe Profile at the Start of Each Freeze Cycle (after Geotechnical Science Laboratories, 1989).

Soil pressure beneath the pipe was initially monitored using Gloetzl cells and in the fourth cycle by much smaller Petur cells. An unexpected result from the three later cycles was that the total stress in the soil below the pipe exhibited minimal increase until the frost front descended to its level when it increased significantly. After the pressure cell was encased in the frozen soil the total stress increased up to a constant level and in the case of the cell at 10 cm below the pipe the total stress later gradually reduced (Figure 4.24). This increase in total pressure implied that it was the frozen annulus, rather than the surrounding unfrozen soil, that provided the reaction to the frost heave force and consequently for pipe uplift. To take this to its natural conclusion the pipe is therefore surrounded by a frozen soil annulus that acts in a manner to crush it (Geotechnical Science Laboratories, 1985). Figure 4.24 also illustrates the effect of the breakdown of the compressor (about day 100) on the total stress within the frozen annulus, there is an associated fall in the total stress which was partially recovered upon the successful repair of the compressor. This shows that the internal pressure is very temperature dependent, and these internal pressures were further investigated in small-scale laboratory tests (Williams and Wood, 1984, 1985b) and have been discussed in terms of thermodynamics and creep properties of frozen soil in Section 3.3.4. In the fourth cycle the Petur cells were installed to monitor the downward, lateral and total soil stresses developed during the test.

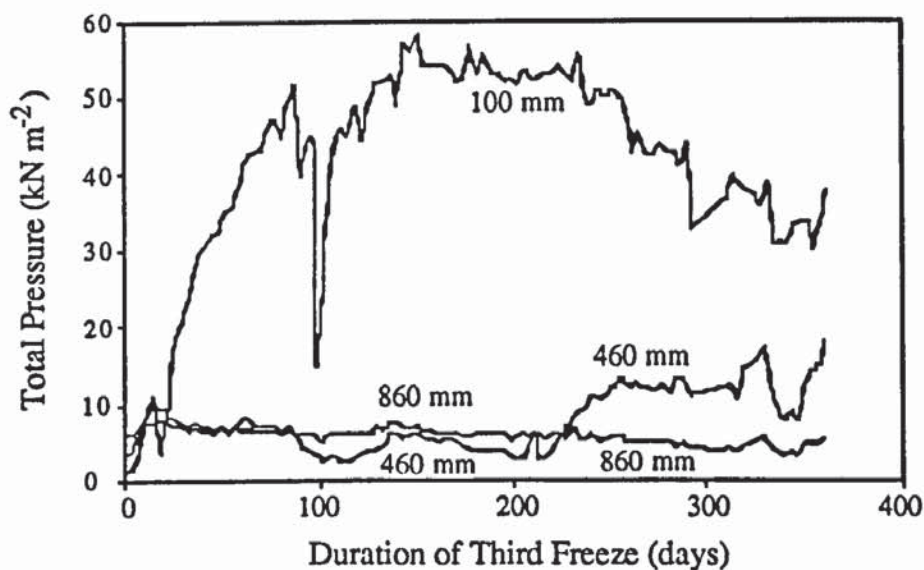


FIGURE 4.24 Soil Pressures at the B-B Section (4.5 m from the Transition) Below the Pipe in the Silt Section during the Third Freeze Cycle (after Geotechnical Science Laboratories, 1988a).

Telescopic heave tubes and magnetic heave devices monitored the relative vertical movement between a number of points within the soil. At Caen they were used to monitor the total frost heave within layers of soil as the freezing progressed downwards (Geotechnical

Science Laboratories, 1989). The amount of heave was expressed as a percentage strain of the initial unfrozen soil layer (Figure 4.25). The strain rate decreases and the total strain increases with time and consequently with depth of frost penetration in the silt section. At the onset of freezing the rate of frost penetration is rapid and the rate of frost heave is high, however as the frost penetration rate slows increasing quantities of water will arrive at the frozen front under generated suction forces. This increased accumulation of water produces greater frost heave and soil strain but lower heave and strain rates within the lower layers. It can be seen from Figure 4.25 that strain increases after the layer is fully frozen and demonstrates that secondary (Continued) heave is a significant process in Caen Silt. It is more evident in the lower layers when the thermal gradient is low (Geotechnical Science Laboratories, 1989).

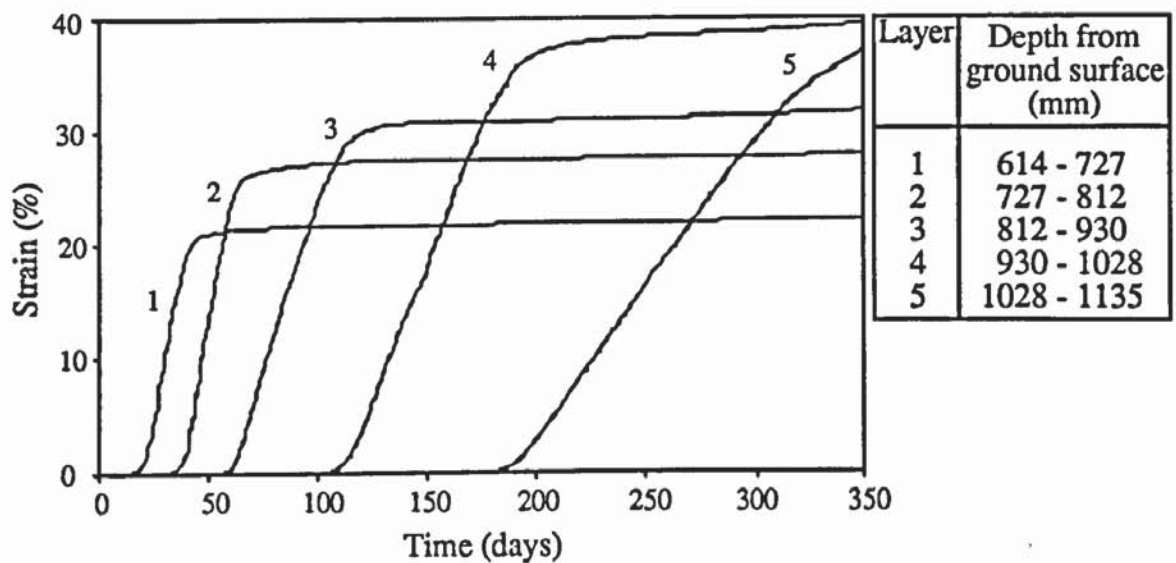


FIGURE 4.25 Soil Strain 25 cm Perpendicular to the Pipe Axis at Section B-B during the Third Freeze Cycle (after Geotechnical Science Laboratories, 1988a)

During the freezing cycles the ground surface heaved in response to both the freezing air and pipe temperatures. Typical ground profile movements, in the third freezing cycle in the silt section, are shown in Figure 4.26. These demonstrate that the pipe operating characteristics had the greatest influence on frost heave with the soil immediately above the pipe exhibiting the highest heave (Geotechnical Science Laboratories, 1986b). Ground heave was more prominent in the frost susceptible silt and this is illustrated in Figure 4.27 which shows the net ground heave on day 503 of the fourth freeze cycle (Geotechnical Science Laboratories, 1989). It is also evident from Figure 4.27 that the pipe-frozen annulus exerts an influence on the frost heave of the soil along the pipe axis and thus the ground surface. Geotechnical Science Laboratories (1989) note that, generally, the heave rate decreased as the freezing period continued.

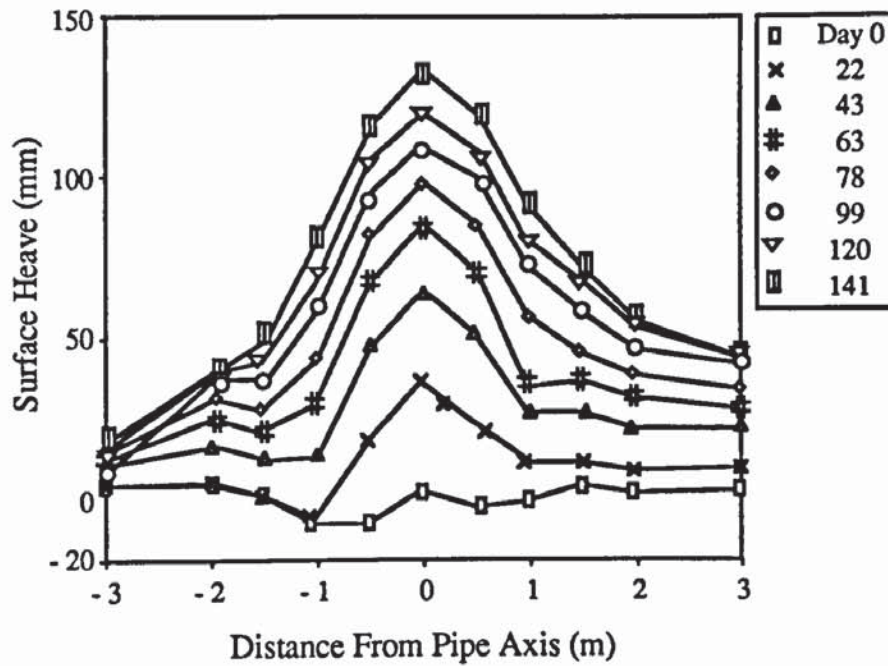


FIGURE 4.26 Ground Surface Heave along Section B-B during the Third Freeze Cycle (after Geotechnical Science Laboratories, 1986b)

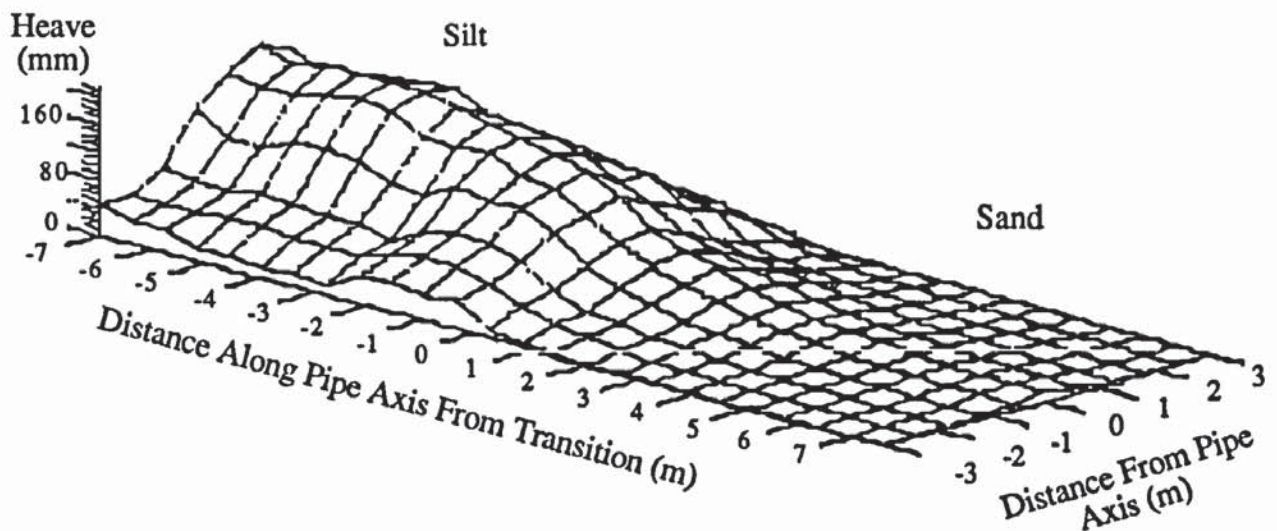


FIGURE 4.27 Net Ground Surface Heave on Day 503 of the Fourth Freeze Cycle (after Geotechnical Science Laboratories, 1989).

Ground cracks were observed during both the freezing (Geotechnical Science Laboratories, 1985) and thawing periods (Geotechnical Science Laboratories, 1986b). The cracks observed in the second freeze cycle were parallel to and on both sides of the pipe (Figure 4.28) and were inclined away from the pipe. The pipe had a residual upward displacement

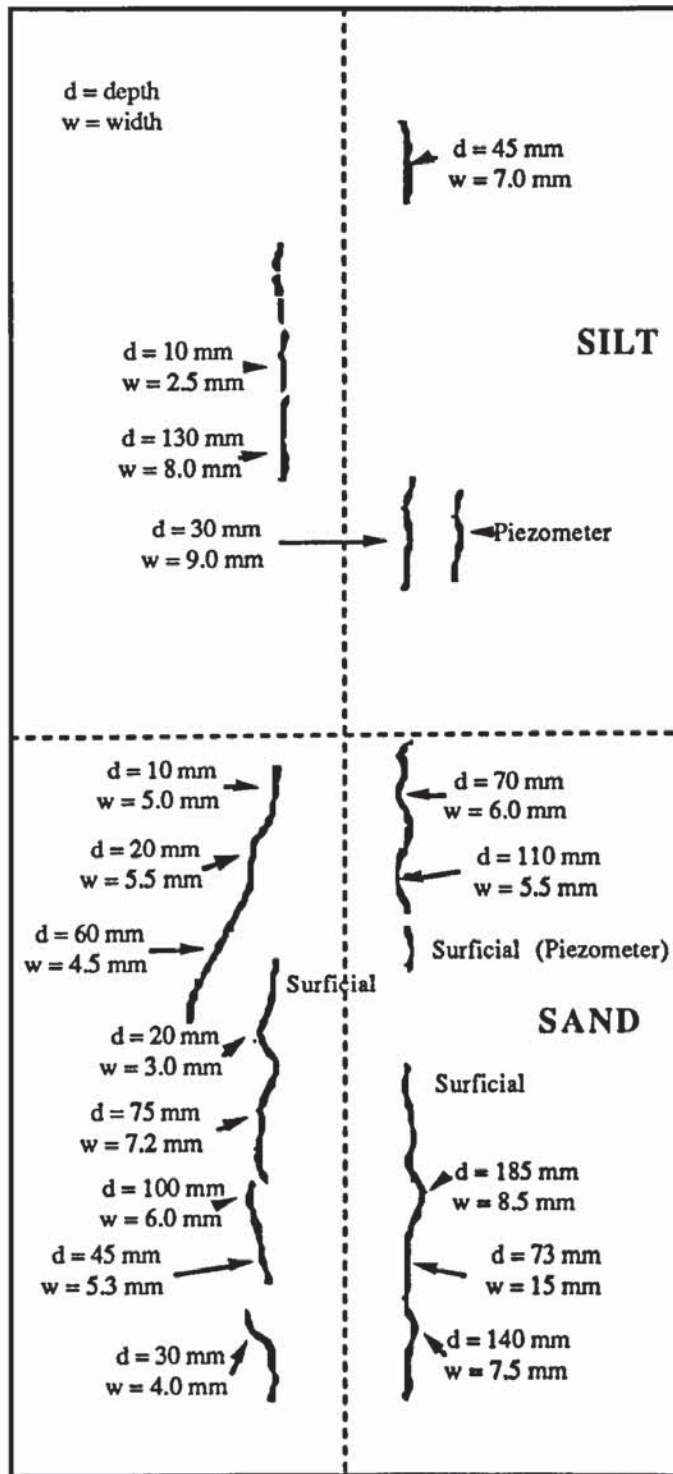


FIGURE 4.28 Plan View of Soil Surface Cracking during the Second Freeze Cycle (after Geotechnical Science Laboratories, 1985).

SURFACE CRACKING DURING
SECOND THAW

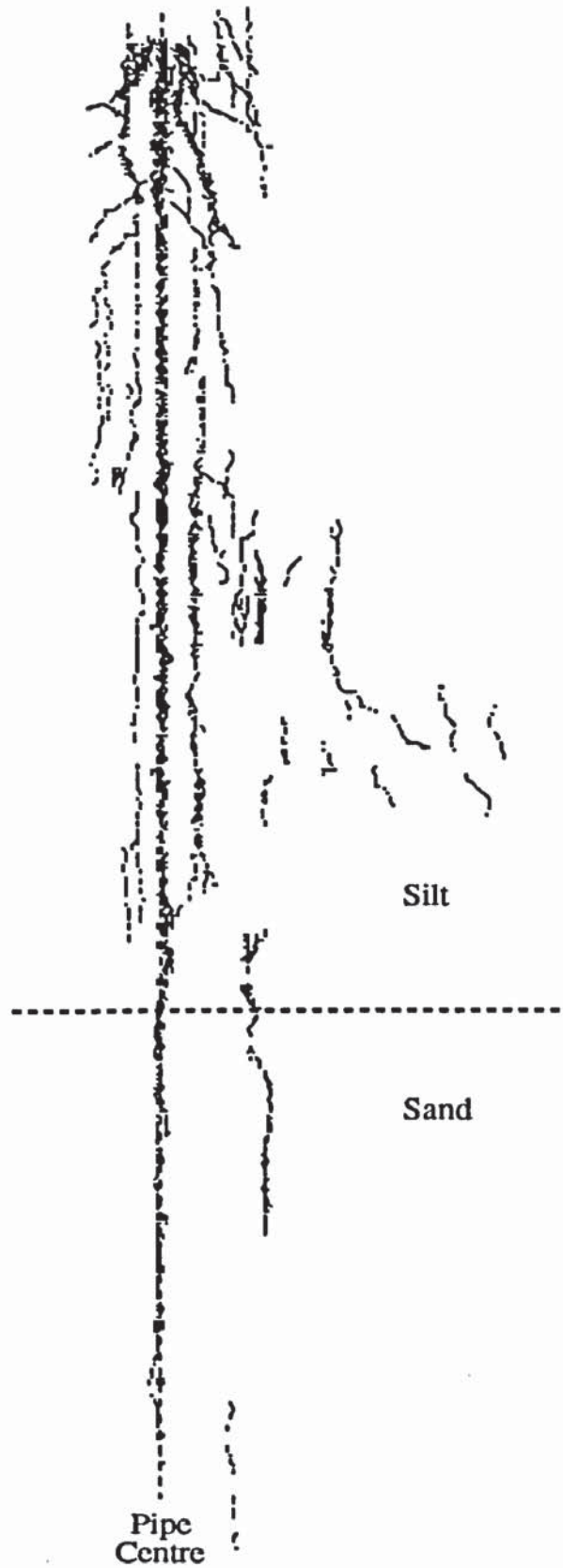


FIGURE 4.29 Ground Surface Fissures, Day 30 Second Thaw Cycle (after Geotechnical Science Laboratories, 1986b).

at the end of each freezing period and, coupled with soil consolidation during thawing, it was suggested that the cracks formed during thawing were a result of the resultant upward displacement of the pipe relative to the surrounding soil (Figure 4.29). Therefore the cracks are more prominent in the silt and enlarged as thawing proceeded since there was a greater residual upward pipe displacement in the silt section (Figure 4.23) (Geotechnical Science Laboratories, 1986b).

Water profiles (Geotechnical Science Laboratories, 1986a) were monitored using Time Domain Reflectometry (TDR) and these showed that the unfrozen water content decreased in front of the descending frost front. It was suggested that this was a result of the partial desiccation of the unfrozen soil due to moisture migration to the freezing front. This zone of desiccation was reported to increase in length as the rate of frost penetration slowed (Geotechnical Science Laboratories, 1986a).

More recently Van Vliet-Lanoe and Dupas (1991) have reported on the change in the soil structure resulting from repeated freeze-thaw cycles at Caen. Upon the excavation of pits in the silt section during the fourth cycle, the ice lens arrangement shown in Figure 4.30 was observed. The ice lenses close to the pipe were circular while those further away were observed to incline towards the pipe.

The ice lens arrangement in Figure 4.30 is not simply a function of the thermal conditions prevailing at the time of observation, but a very complex inter-relationship between (Van Vliet-Lanoe and Dupas, 1991) :-

1. The test operating conditions,
2. Differential consolidation shearings during thaw settlement,
3. Variable thermal gradients during the freezing cycles,
4. Redistribution of hoar ice above the pipe that was formed during the failure of the air circulating system.

The trend of increasing frost heave during the freeze-thaw periods was thought to be related to the changing soil structure (fabric) occurring during each cycle. Van Vliet-Lanoe and Dupas (1991) note that the aggregates formed during freezing are very stable during slow thawing and are strengthened during re-freezing due to the pressures exerted by a growing ice lens. It takes some four to five cycles for the soil structure to be permanently modified and subsequently the ice lenses reform at specific locations due to the formation of fissures which also allow easier water movement along a suction gradient. Thus the frost heave

capability of a soil will increase in response to the alteration of the soil structure by cyclic freezing.

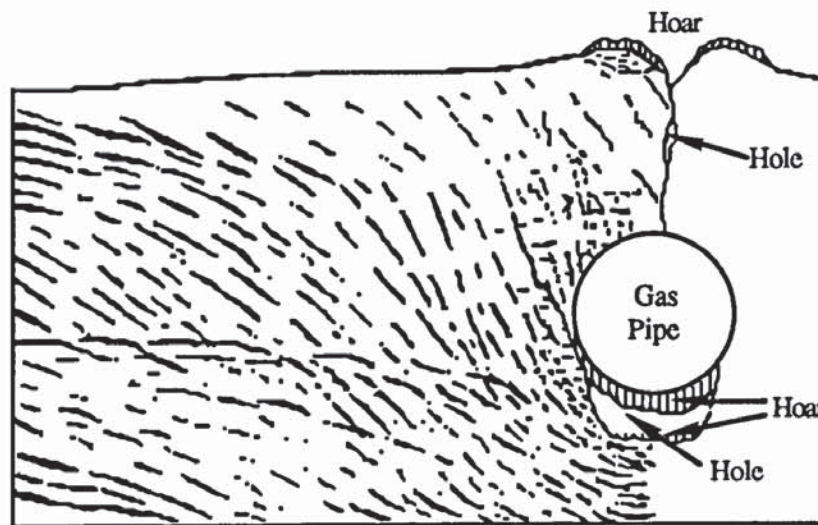


FIGURE 4.30 Ice Lensing around the Caen Pipeline (after Van Vliet-Lanoe and Dupas, 1991).

Mathematical modelling of the experiment has been undertaken in both France (Blanchard and Fremond, 1985) and in Canada (Geotechnical Science Laboratories, 1988b and 1989) with both groups showing success in matching the moisture, thermal and stress fields. The application of the Segregation Potential concept to the prediction of heave had previously been shown to give reliable estimates from 100 to 350 days using consolidated laboratory specimens however, beyond this period, considerable over estimation of heave is likely (Smith *et al.*, 1985). Geotechnical Science Laboratories (1988a) demonstrated that the restraint imposed on the frozen soil by the pipe results in a decrease in the Segregation Potential of the soil with time.

4.5.4.4 New Experimental Design.

During early 1991 the test site was refurbished and new experimental design undertaken. The new experiment has been designed to investigate the effect of a transition zone on differential pipe displacement. The transition zone represents an abrupt demarcation in a discontinuous permafrost area between permafrost and unfrozen soil. Thus the whole test facility has been filled with Caen silt, with half the facility being subject to sub-zero temperatures until the soil was nearly all frozen and the other half being maintained at ambient air temperature. Thus the pipe is 'locked in' in the permafrost side and subject to frost heave pressures on the 'warm side'.

The facility is being operated, as before, with an ambient air temperatures of -0.75°C and a pipe temperature of -5°C . The basic conditions, pipe diameter, depth to water table etc. have not been changed to allow comparison between this new test and previous freeze-thaw cycles. The instrumentation is basically the same as in the previous test, except that more magnetic heave devices have been added and these are located close to thermistor strings. Load cells have been attached to the underside of the pipe to monitor the soil pressures exerted on the pipe and linear voltage displacement transducers have been attached to the pipe to monitor lateral pipe movement. This new test is being supported by both Canadian and French Governmental Agencies in conjunction with a number of oil and gas companies under the guidance of Foothill Pipe Lines (Canada). A smaller length of pipe has also been embedded in the soil and is operating under the same conditions as the main pipe but will, at a later date, be subject to a slow pull-out test. Complete freezing of the permafrost section was completed in August 1991 and the test initiated.

4.6 Small-Scale Laboratory Models of Pipelines.

Physical small-scale studies have been undertaken to investigate soil-pipeline interactions under carefully environmental conditions. Normally a limited number of interactions are of interest in the experiment and therefore a full scaling down of all the soil and pipe characteristics is not necessary.

4.6.1 Chilled Pipe Operation.

Parmuzin *et al.* (1988) describe a physical model to verify their mathematical model to relate pipe heave at any instant during operation to the growth of the frozen annulus below the pipe. The equations presented take into account the soil parameters, pipe characteristics and are based on the pipe, pipe fluid, frozen soil, unfrozen soil masses together with the shear resistance of the overburden soil and that at the unfrozen/frozen interface. The physical model involves a 76 mm pipe of 0.3 mm thickness placed at a depth of 120 mm to its crown in a metal box of dimensions 4.05 x 1.5 x 1.6 m (L x W x H), the pipe could be clamped at either end or allowed free movement. The box was filled with a frost susceptible heavy loam and the water table held between 250 and 280 mm below ground level. Measurements of the soil temperature and pipe displacement were taken and air was circulated at -20 , -30 and -60°C through the pipe. The results were reported for the first 24 hours of operation, and indicated that the rate of freezing directly influenced the rate of frost heave. The pipe displacement was also reported to be a linear function of the increase in the size of the frozen annulus.

The authors (Parmuzin *et al.*, 1988) noted that it would be necessary to investigate the effect of pipe diameter and to operate full-scale tests to further verify their results. The duration and pipe temperature of the tests suggests that little if any ice segregation took place and so it is therefore not surprising that, in a uniform soil under non-variable environmental conditions, there was a direct relationship between frost/pipe heave and growth of the frozen annulus.

4.6.2 Controlling Frost Heave Around Chilled Pipelines.

Svec (1980) and Vermeulen *et al.*, (1981) have operated physical models of a chilled gas pipeline surrounded by frozen soil. The objectives of their studies was to investigate the control of frost heave by using electrical heat cables to thaw the soil under the pipe.

Svec (1980) investigated the negation of ice lenses by using both a layer of insulation under the pipe and heat cables at either side of the insulation (Figure 4.31). The objective was to reduce vertical pipe heave but to permit the development of the less destructive horizontal frost heave. The apparatus consisted of a plexiglass tank 203 x 406 x 305 mm (L x W x H), with a brass pipe (50.8 mm O.D.) passing through it, the arrangement allowed the pipe to heave vertically and insulation at each end of the pipe ensured 2D heat flow. The temperature was measured with 56 thermocouples and two dial gauges monitored pipe displacement. The pipe was operated at sub-zero temperatures and the heat input to control frost heave was monitored. The results illustrated the mitigative potential of heat cables and the reliability of his numerical model.

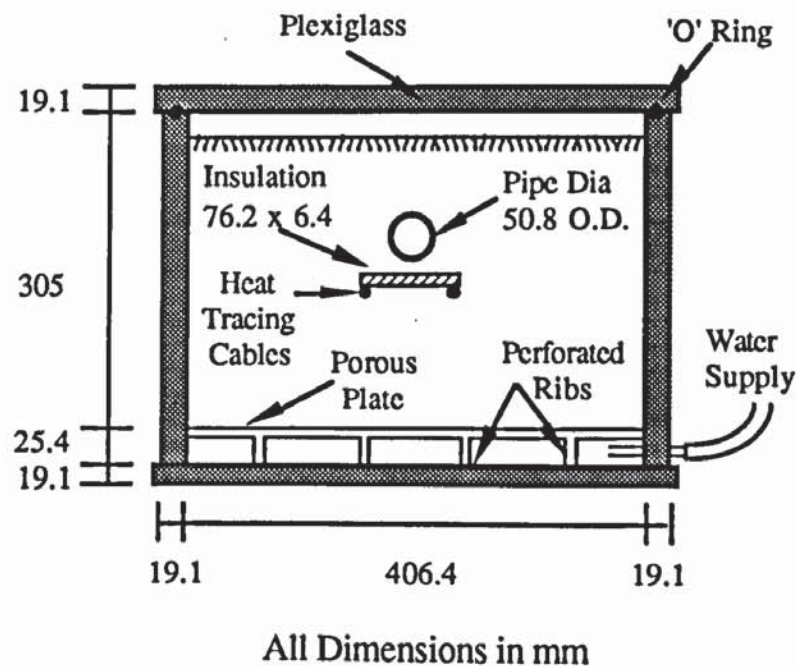


FIGURE 4.31 Cross-Section of Model Tank used by Svec (1980).

Vermeulen *et al.* (1981) constructed a physical model (Figure 4.32) to investigate a mitigative solution to areas where frost heave had become a problem. This simply involved installing electrodes at each side of the pipe and applying a voltage. This produced a melt zone between the two electrodes and in later tests between pairs of electrodes displaced longitudinally along the pipe. The model was scaled to adequately represent the relationship between the physical properties and the electrothermic reactions. The model was 127 x 152 x 127 mm (L x W x H), constructed from PVC (Figure 4.32), and a 2.54 cm diameter plastic pipe (representing a mechanical scale factor of 64) was placed in the soil which was frozen before the heat tests were undertaken. The results indicated the potential of electrothermic scale modelling and provided information on the mitigative potential of permafrost thawing by electrical heating (Vermeulen *et al.*, 1981).

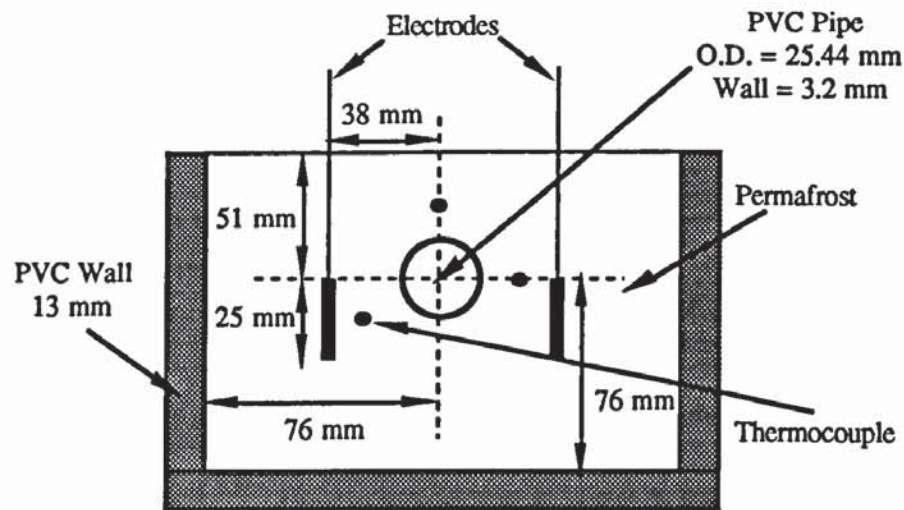


FIGURE 4.32 Cross-Section of Model Tank used by Vermeulen *et al.* (1981).

4.6.3. Freezing Air Temperatures on Pipe Stresses.

Edil and Bahmanyar (1983) have reported on their physical model to further investigate the imposition of a descending freezing front on pipe stresses. The model was constructed from 12.7 mm plexiglass sheets, and the container is 1.83 x 0.61 x 1.22 m (L x W x H) and made up of two sections 0.61 m high (Figure 4.33). The tank was insulated around the sides and on the bottom using 51 mm thick styrofoam boards. The pipe was 54 mm (O.D.) and made of copper and water was pumped through during the test. The pipe had a number of strain gauges attached to it and 8 thermistors were installed in a vertical plane above and below the pipe. The apparatus was placed in a cold room and freezing air temperatures

produced a descending frost front. The results from this test have been described in Section 4.4.3.

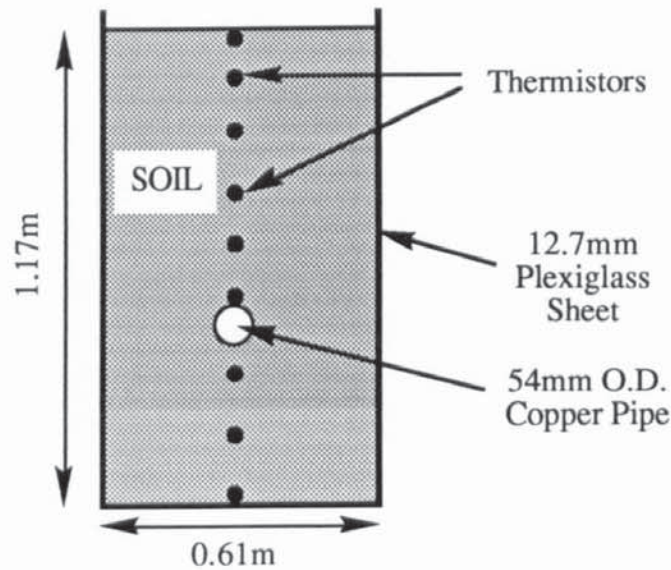


FIGURE 4.33 Cross-Section of Model Tank used by Edil and Bahmanyar (1983).

4.6.4 Thaw Settlement Tests Using a Centrifuge.

Experiments using centrifuges have been used in geotechnical engineering to model soil-structure interactions for over fifteen years. Centrifuges have been used to investigate the soil-pipeline interaction associated with thawing beneath warm oil pipelines buried in shallow offshore areas in Arctic Regions (Vinson and Palmer, 1988). A small-scale test provides scale modeling due to gravity only, however a centrifuge test allows the stress-strain and strength of the soil to be fully scaled in relation to a full-size test. The pipe, pipe thickness, depth of burial etc are directly scaled from expected field conditions. The model is placed in a bucket at the end of a 4 m arm attached to the centre of the centrifuge and is then rotated to produce a radial acceleration equal to the scale of the model conditions in relation to gravitational acceleration. The stress and strains in the model are a scale equivalent to those in practice and the displacements can be scaled to those in practice by using the scaling factor used in model and radial acceleration.

Vinson and Palmer (1988) used a cohesionless sand and a saturated compressible clay to represent the ice-rich permafrost and thawing permafrost. This is an idealization of the soil conditions since it neglects thermal considerations, however the clay will settle with time thus representing thawing behaviour. Conversely sand only exhibits settlement at very high inertial accelerations, and its settlement is not time dependent. The scaled pipe is placed over the clay block, the size of which is dependent on the size of the thawing zone to be modelled

(Figure 4.34). During the tests ground and pipe displacement, pipe strain and pore water pressures in the clay were monitored. Ten tests under various experimental conditions were undertaken, and results indicated that centrifugal testing is a satisfactory method for investigating soil-pipeline interactions associated with thawing soils.

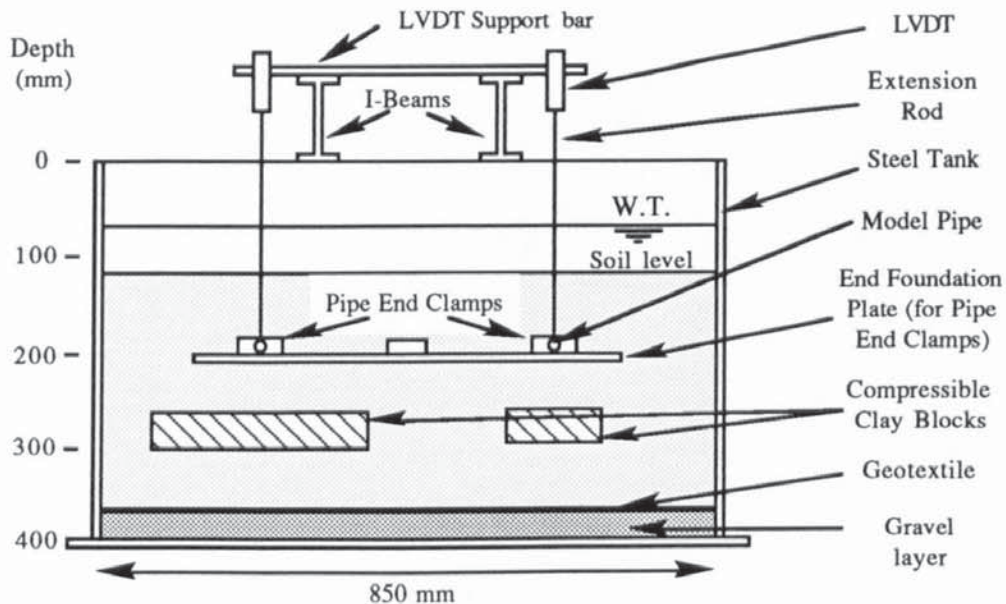


FIGURE 4.34 Centrifuge Model for Pipe Thaw Settlement (after Vinson and Palmer, 1988).

4.6.5 Uplift Pipe Tests.

Laboratory tests have been undertaken to define the load-displacement characteristics of pipes subject to upward vertical displacements under varying depths of burial, soil type and density etc. (Matyas and Davis, 1983b, Trautmann *et al.*, 1985).

Trautmann *et al.* (1985) constructed a model (Figure 4.35) with chamber dimensions 2.29 x 1.22 x 1.52 m (L x W x H). The walls were made of two 20 mm thick layers of plywood and strengthened with 50 x 250 mm struts to reduce side deflections during pipe loading. The inside of the plywood was covered with Formica to reduce side friction and a 12.7 mm thick glass window of dimensions 1.5 x 0.9 m was installed to allow observation of the soil during pipe loading. A steel pipe 102 mm (O.D.) with a wall thickness of 3.2 mm and a length of 1.2 m was jacked up by two rods at either end of the pipe. Sand was placed in 50 mm layers in the chamber by a hopper, with white powder and short dowel bars placed adjacent to the window. The upward average rate of movement was 20 mm/min and continued until displacement was between 50 and 100 mm. From this the force-displacement characteristics of the system were determined. The results of this study have been discussed in Section 4.3.2.1.

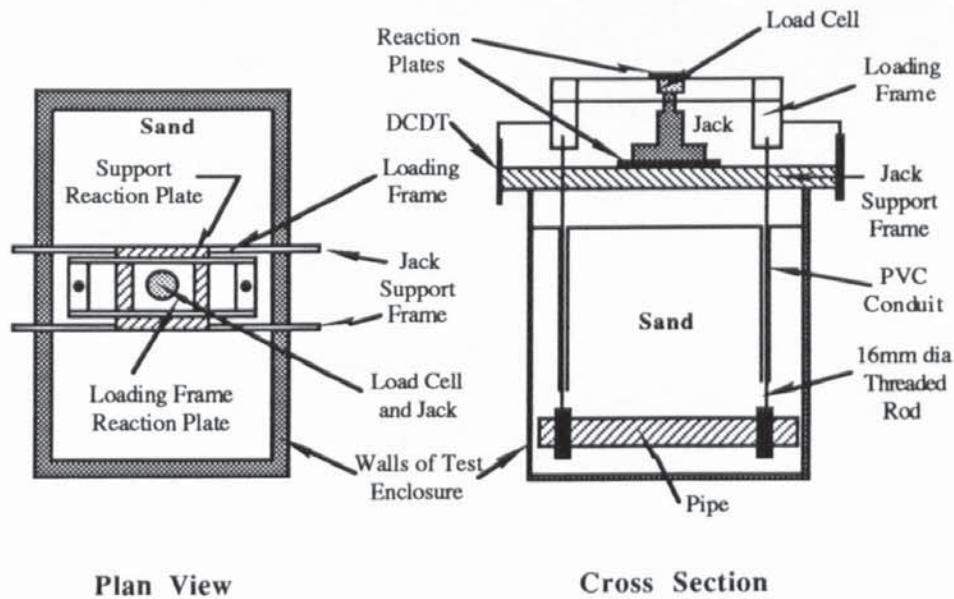


FIGURE 4.35 Physical Small-Scale Model used by Trautmann *et al.* (1985) for Pipe Pull-Out Tests.

4.7 Summary.

Soil-pipeline interactions can produce detrimental effects on safe pipeline operations and these interactions typically involve the relative movement of the pipe in relation to its surround soil mass. Chilled gas pipeline operations have also produced soil-pipeline interactions and this project specifically investigates the effect of frost action on the soil surrounding a pipeline. In this chapter it has been demonstrated that large frost heave pressures have been generated in the presence of sub-zero temperatures which have severely affected the integrity of roads, ice rinks, buildings etc. Subsequently this discussion was extended to cover pipeline operations in both the UK and the USA which highlighted the problems with frost heave and ground cracking. However, grouting around the pipeline has been shown to substantially reduce frost/pipe heave. The experiment at Caen (Section 4.5.4) has approached chilled gas pipeline operation on a fundamental basis, and has provided valuable data on both frost heave and pipe movements. The final section of this chapter has described the various small-scale laboratory models that have been operated to investigate either relative pipe movements or pipeline operations involving frost action.

The soil-pipeline interactions of frost heave and ground cracking have been shown to be problematic *ie.* how they affected the safe operation of a pipeline. Whilst the origins of frost/pipe heave are known, those relating to ground cracking are more uncertain. British Gas have found both interactions to be problematic (Archer *et al.*, 1984), and also their prediction is very complex and uncertain. Therefore this study programme was initiated to assess and define the soil-pipeline interactions of ground cracking and frost/pipe heave.

CHAPTER 5 SCOPE

The study programme has involved two clear stages with, initially, the assessment and, secondly, the definition of the mechanisms of the soil-pipeline interactions associated with the sub-zero temperature operation of large-diameter, high pressure Natural Gas pipelines. There are principally two types of mechanisms, frost heave and ground cracking, of which ground cracking has been of particular interest as its mechanism of formation was uncertain.

5.1 Soil-Pipeline Interactions.

Buried Natural Gas pipelines operating at sub-zero temperatures produce a frozen soil annulus around the pipeline (Figure 5.1). Heat flows from the surrounding soil to the chilled pipe, this heat is initially provided by decreasing the specific heat capacity of the soil, i.e. cooling, and, subsequently by freezing the soil water which liberates the latent heat of fusion (Farouki, 1986 and Lunardini, 1981). The size and rate of growth of the frozen annulus are related to:-

1. Pipeline operating conditions, these include, gas temperature, mass flow rate, gas pressure and pipe wall materials.
2. Soil characteristics, these include, particle size distribution and mineralogy, water content, specific heat capacity, thermal conductivity, ambient ground temperatures, density, permeability and frost heave susceptibility.

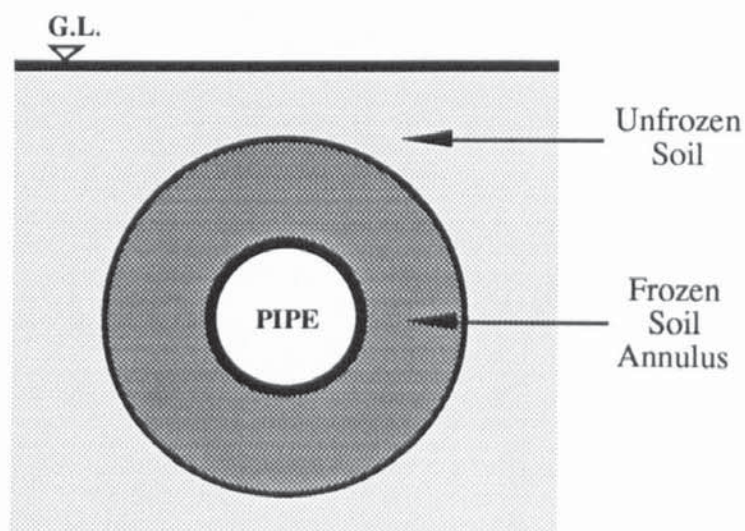


FIGURE 5.1 Diagram Showing the Frozen Soil Annulus that forms around Chilled Gas Pipelines.

As a result of the combination of both the British climate and British Gas operating conditions, the frozen annulus reaches its' maximum size in March or April. When gas flows downstream of the Pressure Reduction Station it gains heat and will, if allowed, reach equilibrium with ambient ground temperature at pipe depth, which in this country will always be above 0°C. The frozen annulus can only form in that part of the pipeline where the gas temperature is below 0°C (Archer *et al.*, 1984), ie. between the Pressure Reduction Station and the equilibrium point.

5.1.1 Ground / Pipe Heave.

The formation and development of ice lenses was detailed in Chapter 3, similarly ice lensing around a chilled gas pipeline is dependent on the soil thermal, hydraulic and stress regimes. If these conditions are favourable ice lenses may develop radially around the pipe in the frozen annulus (Figure 5.2). In Figure 5.2 the frozen soil annulus is shown as circular however, in reality, due to spatially varying thermal gradients, it may be elliptical in shape.

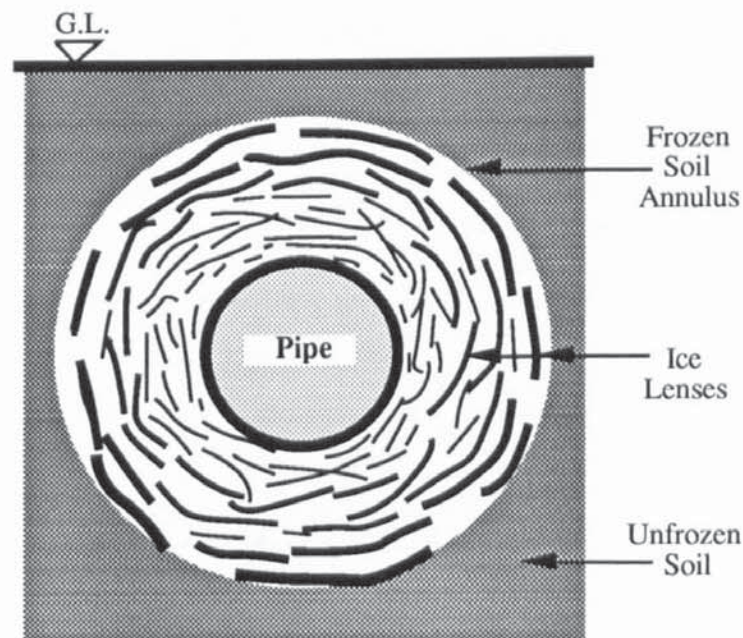


FIGURE 5.2 Diagram Showing Ice Lenses within the Frozen Soil Annulus Surrounding a Chilled Gas Pipeline.

The formation of ice lenses may lead to the formation of several detrimental soil-pipeline interactions:-

1. Net upward movement of the ground surface, this results in damage to overlying foundations, roads and structures.
2. Differential pipe movements at the boundary between two soil types of different frost susceptibilities, this can lead to the development of large bending stresses in the pipe, and if undetected may lead to failure (Williams, 1986, Nyman *et al.*, 1986).

3. Differential pipe movements resulting from pipe heave restraint due to overburden pressures, again this may lead to large bending stresses at the boundary between restrained and unrestrained sections therefore potentially leading to failure.

5.1.2 Ground Cracking.

This is a phenomenon that has only recently been reported by Archer *et al.* (1984), Geotechnical Science Laboratories (1986a) and Williams (1987) with respect to the operation of chilled gas pipelines. The crack is wedge-shaped and extends vertically upwards from its apex above the pipe in the overlying soil mass to the ground surface (Figure 5.3). The cracking runs parallel with and is centred directly over the pipeline, it may be a single crack or a multiple of smaller cracks (Sections 4.5.2.1 and 4.5.4.3).

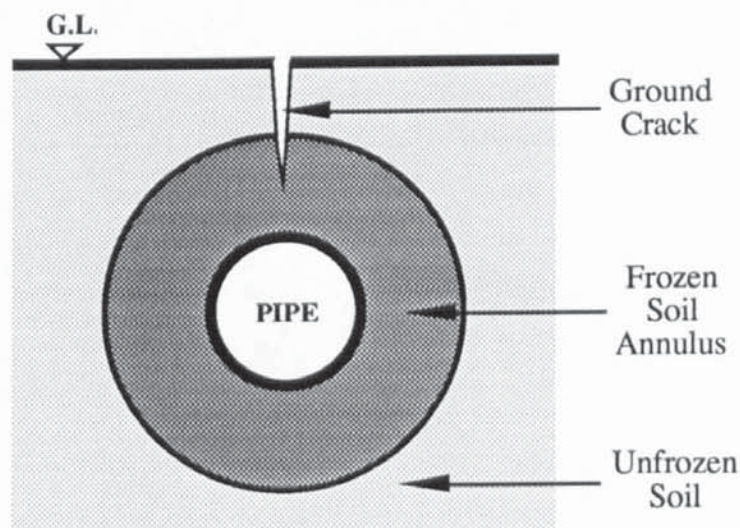


FIGURE 5.3 Diagram Showing the Ground Cracking that has been Observed Downstream of Blackrod Pressure Reduction Station.

Archer *et al.* (1984) reported that cracking occurred intermittently along that length of the Blackrod to Engine Lane pipeline operating at sub-zero temperatures, and a soil shrinkage mechanism was advanced to explain this phenomena (Section 4.5.2.1).

At a large scale test at Caen (Section 4.5.4.3) ground cracking has been noted both in the freezing (Geotechnical Science Laboratories, 1986a) and thawing cycles (Geotechnical Science Laboratories, 1986b), but no general hypothesis has been presented to explain the nature of cracking in the freezing stage. However it was suggested (Geotechnical Science Laboratories, 1986b) that cracking during thawing was related to the thaw consolidation of the soil mass around the pipe (Section 4.5.4.3). These are untested hypotheses about the nature of cracking, as mechanism for this phenomenon has not yet been fully understood (Archer *et al.*, 1984 and Williams, 1987).

In Britain this ground cracking has led to two troublesome consequences. The first affects the integrity of structures, especially pavements passing over the buried pipeline while the second concerns the potential hazard to land management mainly affecting the safety of livestock. In Arctic Regions a further consequence is that an ice wedge may form and develop in the crack. In plan, these ice wedges normally form polygon shapes because of the thermal contraction of frozen ground (Lachenbruch, 1962, Mackay, 1974 and Williams, 1986) and affect both the hydrological and thermal regimes in their vicinity. In the case of those that form in ground cracks it would eventually cause the loss of integrity of the pipeline resulting from changes in the soil conditions around the pipeline.

5.2 Objectives.

This study programme was carried out under a SERC CASE Award, the collaborating organisation was the British Gas Corporation plc., Engineering Research Station in Newcastle-Upon-Tyne. The Corporation had initiated a research programme in 1981 to assess the minimum temperature, after pressure reduction, at which the Pressure Reduction Station and the associated downstream pipelines could be safely operated (Archer *et al.*, 1984). This earlier study trial indicated, first, that the temperature profile of the pipeline downstream of a Pressure Reduction Station could be calculated from the Modified Schorre Equation. Secondly, that two soil pipeline interactions could occur, frost heave that was expected and ground cracking that was unforeseen (Archer *et al.*, 1984).

5.2.1 Soil-Pipeline Interactions.

This study continues from the earlier study (Archer *et al.*, 1984) and is primarily targeted to investigate the soil-pipeline interactions that have been reported. The major objective of this study was to investigate the 'unforeseen' phenomenon of ground cracking. There were two aims first, to define the mechanism by which ground cracking occurred and secondly, to collect data for the development of possible predictive procedures for ground cracking. The subsidiary objective was to investigate methods of mitigating frost heave both in the laboratory and subsequently on site but, due to limits on both time and resources this testing was not undertaken.

5.3 Methodology.

The study programme was specifically designed to investigate the ground cracking mechanism. Therefore the first stage of the study involved a comprehensive literature review to identify previous research and methods of approaching the investigation (Chapters 3 and 4).

5.3.1 Questionnaire.

This was designed and sent, via the British Gas Engineering Research Station, to each Regional Transmission Engineer within the twelve British Gas Regions. The questionnaire was designed both to assess the amount of chilled gas pipeline operation within the Corporation and to provide information on the following factors:-

1. The number of pipelines operated at sub-zero temperatures,
2. The amount of both frost heave and ground cracking observed,
3. The pipeline operating conditions when operating at sub-zero temperatures,
4. The general soil classification of the soil surrounding the pipe especially where frost heave or ground cracking has occurred,
5. The periods during which frost heave and ground cracking are observed.

Upon analyses of the above information it was hoped to correlate both pipeline operating conditions and surrounding soil characteristics with either or both frost heave and ground cracking.

5.3.2 Full-Scale Test.

After close examination of the replies to the questionnaire, Blackrod Pressure Reduction Station was selected to be the site for the full-scale test. This selection was based on two criteria that both ground cracking and frost heave had been previously observed downstream and that the British Gas Region involved, in this case the North Western Region, had both experience with and a positive interest in the operation of chilled gas pipelines.

Three sites were selected downstream of Blackrod for further study based on their varying potential for ground cracking, this information being supplied by the local Engineer. A detailed instrumentation system was designed, this allowed the measurement of the soil hydraulic, thermal and stress regimes around the pipeline together with the pipeline strain and movement. The instrumentation was installed during November and December 1987 and monitored using both automatic data acquisition systems and manual readings each week until March 1990. At the Pressure Reduction Station the site instrumentation and data loggers were used to provide information on the pipeline operating conditions. The information from these sites was collected using portable computers and returned to Aston for analysis on both the Vax Cluster Mainframe and Apple Macintosh Microcomputers.

5.3.3 Small-Scale Laboratory Model Test.

With experience gained from operating the full-scale test site a small-scale model was designed and constructed for operation in a controlled laboratory environment. The site conditions at Blackrod cannot be directly modelled by a small-scale test because the soil hydraulic, stress and thermal regimes are impossible to scale correctly due to their nature.

Therefore the small-scale model was primarily designed to reproduce the soil-pipeline interactions of frost heave and ground cracking observed at Blackrod and other Pressure Reduction Stations and, under controlled conditions, to allow further investigation in to these mechanisms.

5.3.4 Soil Testing.

Soil classification testing was carried out on soil samples collected from the full-scale test at Blackrod Pressure Reduction Station, and were carried out according to the British Standards Institution, Methods of Test for Soils for Civil Engineering Purposes, BS1377 (1975).

CHAPTER 6 QUESTIONNAIRE

This chapter is concerned with the primary stage of the investigation, basically a data collection exercise involving the collation of information on recent chilled gas pipeline operations within the British Gas Network. Of particular interest are the definitions of the scale and extent of both chilled gas pipeline operation and the troublesome soil-pipeline interactions of frost heave and ground cracking. Data was therefore collected to describe the extent of the problems, and then to analytically or descriptively compare the various parameters that have been identified during the literature survey as probably affecting frost heave (pipe heave) and ground cracking.

6.1 Subject Areas for Investigation.

The problem of soil-pipeline interactions has been defined in the earlier chapters and from this three areas for further study were identified early on in this investigation:-

1. Assessment of the amount of experience within the British Gas Corporation of chilled gas pipeline operation and the extent/scale of associated soil-pipeline interactions, so as to assess whether chilled gas pipeline operation poses significant problems.
2. Investigation of relationships of both frost heave and ground cracking with respect to general soil properties and pipeline operating conditions, to identify those factors that would merit further investigation both at the proposed large-scale test site and in the laboratory under controlled conditions.
3. Selection of a site for a large-scale field study.

6.2 Design of a Questionnaire.

In any data collection study the objectives must be clearly stated and the study subsequently reviewed to see if these are obtainable and of use to the instigator (Berdie *et al.*, 1974). The subject areas to be investigated were of great importance in the development of an overall strategy for this research project and therefore initial data collection was deemed necessary.

6.2.1 Definition of the Objectives.

6.2.1.1 Chilled Gas Pipeline Operation and Associated Interactions.

British Gas operates via a regionalized, corporate structure and this presents problems with access to information on pipeline operation and management. It was decided to collate data on chilled gas pipeline operation so as to provide an overview of the total operations and

soil-pipeline interactions. In order to provide descriptive information, the following parameters were assessed:-

1. Number of pipelines operating below 0°C,
2. Number of pipelines along which frost heave was observed/reported,
3. Number of pipelines along which ground cracking was observed/reported,
4. Number of pipelines along which both frost heave and ground cracking were observed/ reported.

6.2.1.2. Influence of Pipeline Operating Conditions and Soil Properties.

This part of the data collection exercise can be termed an analytical or relational type of survey (Oppenheim,1970). It was designed using a Factorial design method whereby the variables are chosen so that they may disentangle a complex set of relationships. The results will allow variables such as soil type to be compared to either or both of the soil-pipeline interactions. The following variables shown in Table 6.1 were identified for further investigation:-

Experimental Variables	Dependent Variables	Controlled Variables	Uncontrolled Variables
Frost heave. Ground cracking.	Soil classification. Depth to water table. Pipe diameter. Outlet temperature. Outlet pressure. Depth of pipe burial. Ambient air temperature. Ambient ground temperature. Periods when experimental variables are observed.		Soil properties:- bulk density, moisture content, strength, atterberg limits, etc. Rainfall. Bias of the respondent and their Region. Respondents appreciation of the soil-pipeline interactions.

TABLE 6.1 List of Variables under Consideration in the Data Collection Programme.

Factorial designs are commonly used in social study research programmes where large groups need to be analysed. For a factorial design to be correctly undertaken an equal and sufficient number of occurrences must be present in each classification group within each variable. However, because of the limited lengths of chilled pipelines and the relatively large number of factorial groups, a full correlation of the variables would be inappropriate as most relationships would be limited to a small number of occurrences. This does not negate its use in this survey since only a descriptive analysis of the the main relationships was to be investigated, namely those between the soil-pipeline interactions and soil type and/or pipeline diameter. The analysis of these results in simple frequency tables usually provides an indication of whether a potential relationship exists but, more complex statistical analysis was not be undertaken, due to the limited number of potential pipelines operating at sub-zero temperatures.

6.2.2. Selection of Data Collection Method.

Four methods were considered:-

1. Literature and record search,
2. Observations,
3. Questionnaire,
4. Interview.

Literature searches are potentially a fruitful source of information but, due to the scale of the task, it would have been non-productive to make an examination in each Region, assuming that access to the records was allowed. Within each Region there are staff with "hands on" experience of pipeline operation who would offer a far better source of information. Observational techniques were discounted early on, due to the scale of such a task. However, it must be noted that the occurrence of frost heave and ground cracking is primarily noted as a result of observation in the field by the local Engineer or his assistants. Interviews were not entirely discounted and it was planned to use them to back up "promising" questionnaire replies. It was not used in the first stage because it was deemed necessary to gain the basic facts without clouding the issue with engineering decisions and personal judgements.

A questionnaire was chosen as it was considered to be the best way of collecting reliable data when the questionnaire is carefully worded in a simple and direct manner. This allowed the collection of data without the views of the respondent or the Region having a substantial impact on the final results. A weakness of such as survey is that a control group could not be used as soil-pipeline interactions can occur without the pipe operating in chilled mode. Pipe movements and visible surface features can result from many events such as nearby

excavations, water table movements etc and so some of the occurrences could be influenced to an unknown extent by these *external* factors.

6.2.3 Respondents and Their Limitations.

Before the questionnaire was written, judgements had to be made on the respondents with respect to their:-

1. Position within the Regional Office,
2. Knowledge of the Regional pipeline network,
3. Knowledge level with respect to soil-pipeline interactions in general,
4. Exposure to Geotechnical Engineering,
5. Access to information on pipeline operating conditions.

The background of the respondents, in this case Transmission Engineers, was investigated to gather information on the above factors. This allowed the questionnaire to be designed so that the individual questions were limited to the likely knowledge base of these respondents. This knowledge base was relatively low in only Geotechnical Engineering, but it was decided that valuable information could be collated using a general classification for soils (ie. clayey, sandy etc).

6.2.4 General Layout of the Questionnaire.

The questionnaire was designed to investigate the selected variables and the knowledge level was based on the expertise of the respondents. The questions were kept short and concise, thereby giving the respondent less room for personal qualification on the selected topics. By keeping the questionnaire short, the respondent was not discouraged from completing the task, and at the same time this allowed the results to be analysed in an efficient manner.

Three sections were included in the questionnaire:-

1. Section A:- Details of the upstream Pressure Reduction Station and its operating conditions together with information on the pipeline such as general depth of burial and surrounding soil classification. A table was also attached in which the average monthly operating conditions of the Pressure Reduction Station were to be entered covering the period in which heave or cracking took place. This section ended with a question about the occurrence of frost heave and ground cracking which subsequently led in to Section B and/or C.

2. Section B:- This was a short section asking for details of frost heave, such as where and when it occurred, estimated pipe lift (this is easier to quantify than frost heave and for the remainder of this chapter will be referred to as frost heave) whether there was any associated ground cracking. This section had to be filled out for all events of frost heave.
3. Section C:- This again was a short section asking for details of ground cracking such as where and when it occurred, and estimated crack width. As with section B it had to be filled out for each case of ground cracking.

It was recognised that there would be a definite spread in the knowledge base of the respondents, therefore some questions would be difficult or impossible to answer. Redundant questions which would allow a check on the validity of an individual questionnaire by cross examination of the respondent were omitted since the respondents were regarded as very reliable.

6.2.5 Expert Assistance.

After completing these steps in the questionnaire design, the draft questionnaire was sent to the British Gas Engineering Research Station where an experienced Engineer carefully criticized the draft and suggested modifications and improvements to make it more appropriate to Transmission Engineers without further sacrificing its usefulness.

6.2.6 Sending the Questionnaire.

Within British Gas there are regular meetings of the Senior Transmission Engineers, with members of each of the twelve Regions in attendance. It was decided the best way to circulate such a questionnaire was to explain the project and its aims at one of these meetings and then ask the individual(s) representing each Region to arrange its completion by the appropriate staff. A covering letter was also included to provide any necessary information, especially stressing its beneficial nature to the overall project.

The final version of the questionnaire can be seen in Appendix B.

6.3 Results.

6.3.1 Replies to the Questionnaire.

The questionnaire was presented in April 1987 to the relevant committee (Section 6.2.6) and early in 1988 a reminder was sent to the recalcitrant Regions urging them to make their replies. Replies were received from ten of the twelve regions on the dates shown in Table 6.2.

REGION	Number of replies	Month of reply
Northern	4	May 1987
South Eastern	1	June 1987
North West	6	July 1987
South West	1	Sept 1987
East Midlands	17	Jan 1988
West Midlands	12	Feb 1988
Eastern	8	Mar 1988
North Thames	14	May 1988
Southern	1	June 1988
Wales (Cymru)	1	July 1988
Scotland	0	-----
North Eastern	0	-----

TABLE 6.2 Details of Numbers of Replies and Dates Received.

Overall the questionnaires were filled in with the required information, although some of the questions proved to be too demanding or time consuming and were very rarely answered. Section A (General Information) was successfully completed by the Regions and this allowed a general overview to be formed, however Table 1 of the questionnaire (Appendix B) was only filled-in fully by some respondents, with the other returns ranging from incomplete to nil. This can be put down to the variations in the knowledge base and also to the number of replies made by the individual Regions. When answered, Sections B and C were filled in carefully, however the depth to the water table was unknown as was to be expected in most cases. Consequently the variables that could reasonably be compared to the soil-pipeline interactions were limited by the volume of answers to soil type, pipe diameter and periods of occurrence, but it was these variables that were of fundamental value to the project. Fuller details of the answers to the questionnaire can be seen in Appendix B.

There was a discrepancy between number of replies and number of pipelines operating in chilled mode and this was due to respondents using the form for a number of pipelines when they all shared the same upstream Pressure Reduction Station and had no observable soil-pipeline interactions.

6.3.2. Occurrence of Soil-Pipeline Interactions.

A total of 83 pipelines had been operated in chilled mode of which only 16 reported observable soil-pipeline interactions. This is illustrated in Figure 6.1 which shows the total operation per Region and the cases of the soil-pipeline interactions. In this figure, where ground heave (pipe heave) and ground cracking occur along the same pipeline, it does not necessarily imply that they occurred at the same location. Figure 6.2 illustrates the various diameters that have experienced sub-zero temperature gas flow.

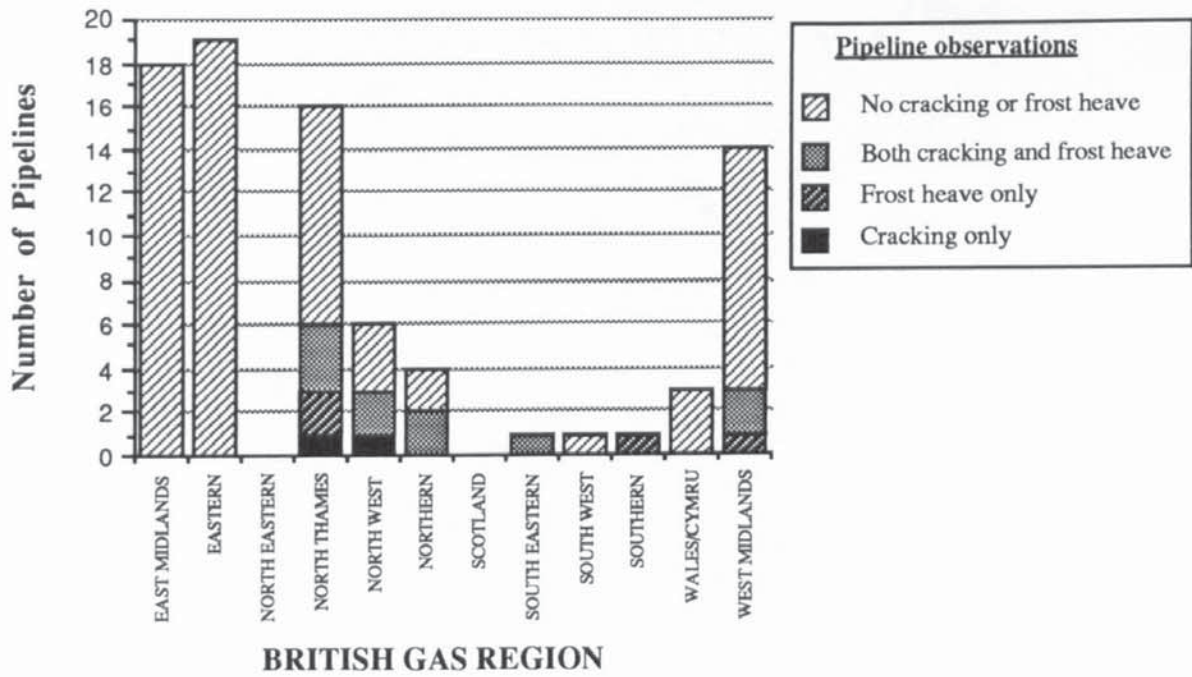


FIGURE 6.1 Illustration of the Number of Pipelines that have been Operated Below 0°C and those where Soil-Pipeline Interactions have Occurred on a Regional Basis.

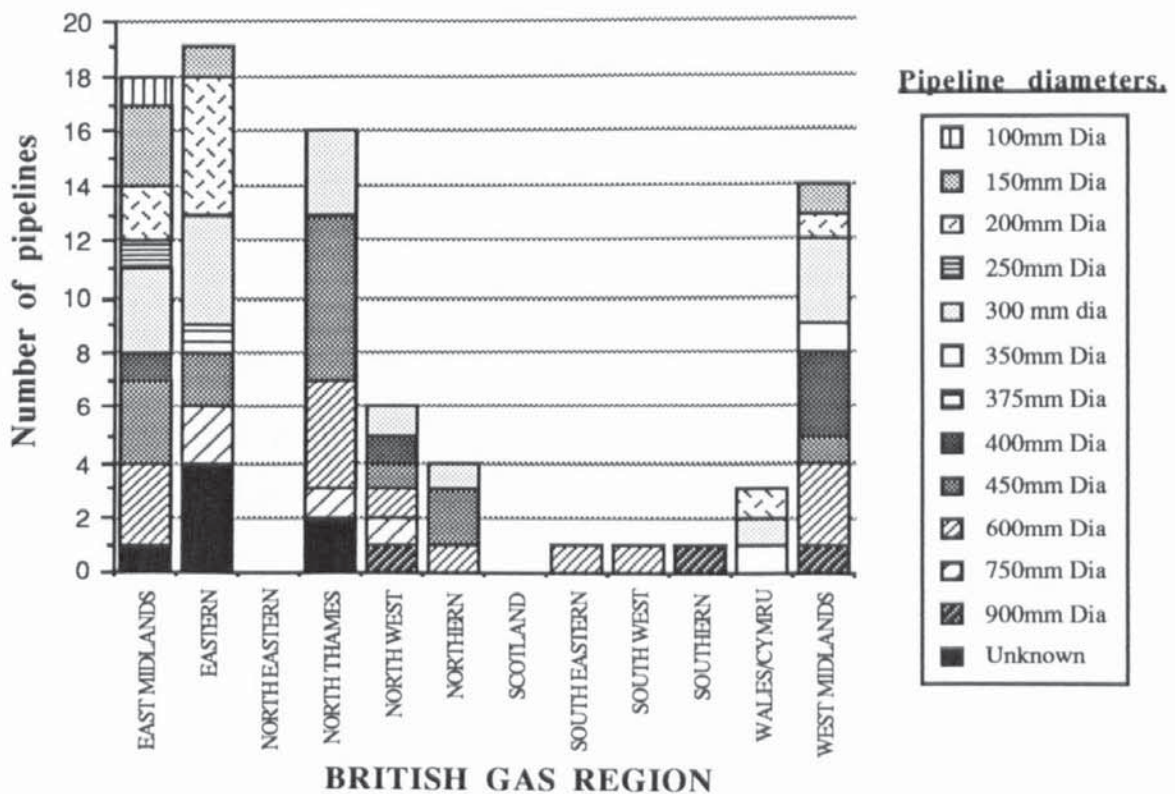


FIGURE 6.2 Illustration of the Range of Pipeline Diameters Operated by Each Individual Region.

In the questionnaire estimates of pipe heave were ascertained as it was easier than ground heave for the Engineer to quantify. When ground cracking and frost heave (pipe heave) are considered separately, it is seen from Figure 6.3 that frost heave is more likely to be observed within a Pressure Reduction Station (PRS), while ground cracking is equally likely to be observed both within or downstream of the PRS. In only one case was frost heave observed both within and downstream of the PRS, similarly with ground cracking, and both cases were reported at Tatsfield AGI (S.E.Gas). Figure 6.4 shows the effect of coupling together pipelines along which frost heave and ground cracking were reported. It can be seen that in seven out of the ten reported cases, that frost heave and ground cracking took place at the same location, mainly within the PRS, however if they occur at different locations then the frost heave was observed within the PRS and ground cracking downstream.

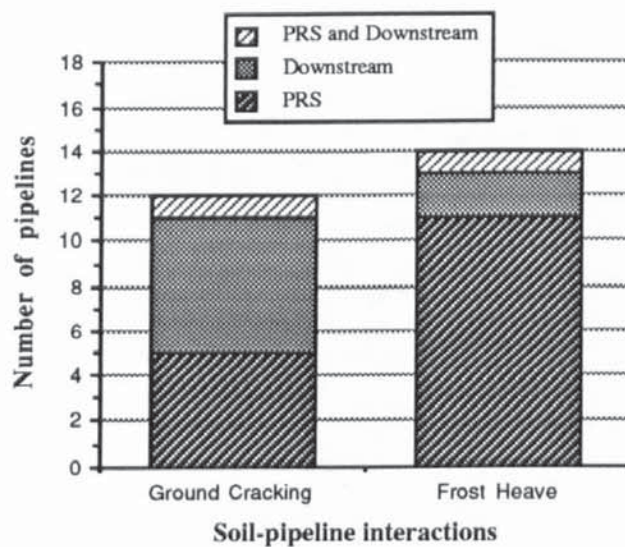


FIGURE 6.3 Illustration of the Locations where Ground Cracking and Frost Heave occur when considered Independently.

The information displayed in Figures 6.3 and 6.4 is summarized in Table 6.3 in the form of observed frequency tables. These tables show that when frost heave occurs there is a 71% likelihood that ground cracking will occur along the same pipeline, and when ground cracking occurs there is an 83% likelihood of frost heave. It also shows that when ground cracking is not observed there is a 6% likelihood of frost heave, and for frost heave to be observed in the absence of cracking there is only a 3% likelihood. These results do not show a relationship between ground cracking and frost heave but indicate that they are influenced by common variables and tend to be observed together, if observed at all.

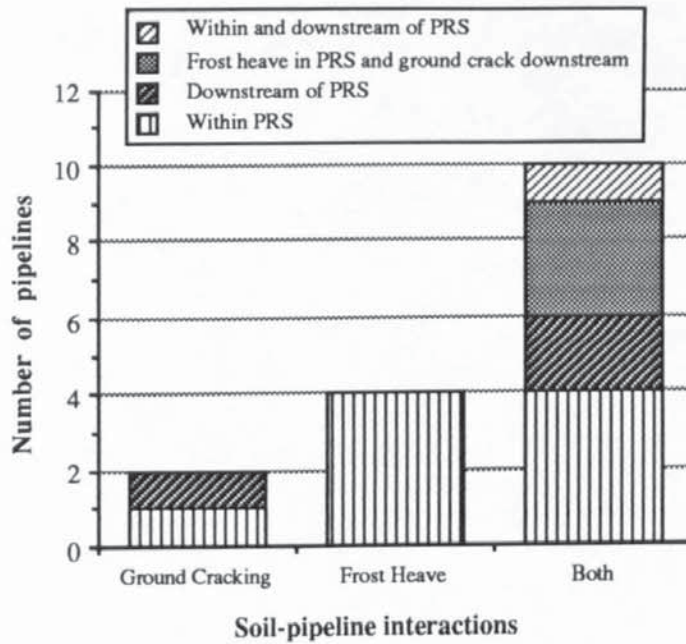


FIGURE 6.4 Illustration of the Locations where Ground Cracking, Frost Heave and both Frost Heave and Ground Cracking occur.

Observed Frequency Table

	Heave	No heave	Totals:
Cracking	10	2	12
No cracking	4	67	71
Totals:	14	69	83

Percents of Row Totals

	Heave	No heave	Totals:
Cracking	83.33%	16.67%	100%
No cracking	5.63%	94.37%	100%
Totals:	16.87%	83.13%	100%

Percents of Column Totals

	Heave	No heave	Totals:
Cracking	71.43%	2.9%	14.46%
No cracking	28.57%	97.1%	85.54%
Totals:	100%	100%	100%

TABLE 6.3 Tables Showing the Relationship between the Likelihood of Ground Cracking and Frost Heave occurring Along the same Pipeline.

Observations indicate that the extent of both frost heave and ground cracking are greatest downstream of the PRS, the ranges are shown in Table 6.4. This could be related to likelihood that the extent of these interactions must be larger downstream of the PRS to be noticed, however it does suggest a relationship between frost heave (pipe heave) and ground cracking.

	GROUND CRACKING			FROST HEAVE (pipe heave)		
	Min Width	Ave Width	Max Width	Min Heave	Ave Heave	Max Heave
PRS	6 mm	12 mm	25 mm	3 mm	45 mm	80 mm
Downstream	40 mm	62 mm	125 mm	26 mm	70 mm	100 mm

TABLE 6.4 Ranges of Ground Crack Widths and Frost Heave (Pipe Heave).

6.3.3 Influence of Pipeline Diameter on Frost Heave and Ground Cracking.

From design considerations large flows and high pressures equate to large, thick walled pipes, at the other extreme low pressure and small flows give rise to small diameter pipelines. Frost heave and ground cracking are more likely to be observed along large-diameter pipelines as is evident from Figure 6.5. Therefore, under normal British Gas operating conditions the frost heave and ground cracking occur more often along large-diameter pipelines, and this is quantified in the observed frequency tables in Tables 6.5, 6.6 and 6.7.

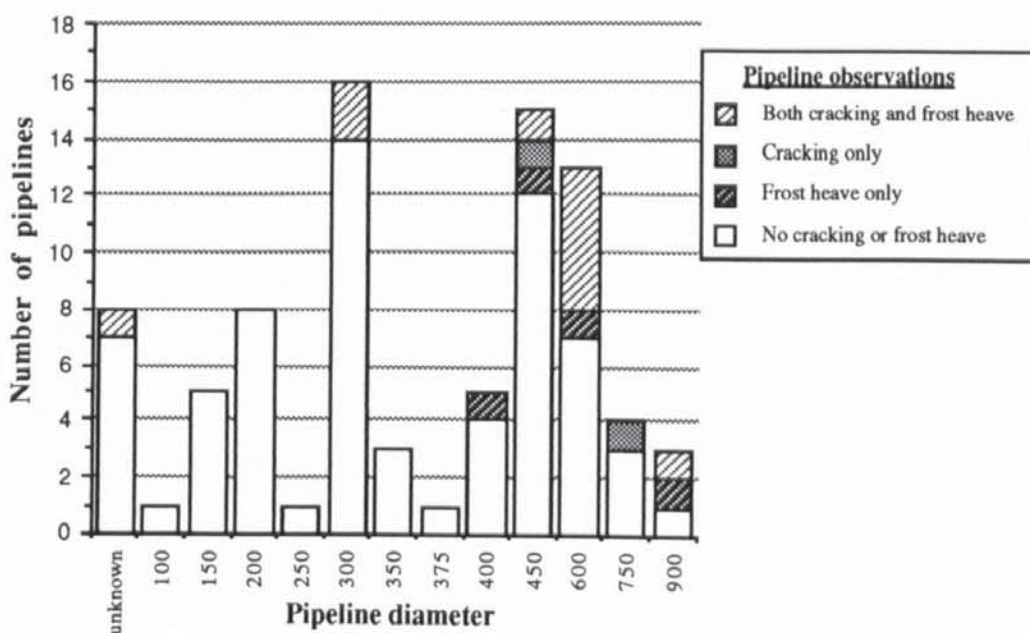


FIGURE 6.5 Bar Chart Illustrating the Diameters of the Pipelines that have Operated below 0°C in Relation to the known Soil-Pipeline Interactions.

Observed Frequency Table

	unknown	100	150	200	250	300	350	375	400	450	600	750	900	Totals:
Heave	1	0	0	0	0	2	0	0	1	2	6	0	2	14
No heave	7	1	5	8	1	14	3	1	4	13	7	4	1	69
Totals:	8	1	5	8	1	16	3	1	5	15	13	4	3	83

Percents of Row Totals

	unknown	100	150	200	250	300	350	375	400	450	600	750	900	Totals:
Heave	7.14%	0%	0%	0%	0%	14.29%	0%	0%	7.14%	14.29%	42.86%	0%	14.29%	100%
No heave	10.14%	1.45%	7.25%	11.59%	1.45%	20.29%	4.35%	1.45%	5.8%	18.84%	10.14%	5.8%	1.45%	100%
Totals:	9.64%	1.2%	6.02%	9.64%	1.2%	19.28%	3.61%	1.2%	6.02%	18.07%	15.66%	4.82%	3.61%	100%

Percents of Column Totals

	unknown	100	150	200	250	300	350	375	400	450	600	750	900	Totals:
Heave	12.5%	0%	0%	0%	0%	12.5%	0%	0%	20%	13.33%	46.15%	0%	66.67%	16.87%
No heave	87.5%	100%	100%	100%	100%	87.5%	100%	100%	80%	86.67%	53.85%	100%	33.33%	83.13%
Totals:	100%	100%	100%	100%	100%	100%	100%	100%	100%	100%	100%	100%	100%	100%

TABLE 6.5 Tables Showing the Relationship between Observed Frost Heave and Pipeline Diameter (mm)

Observed Frequency Table

	unknown	100	150	200	250	300	350	375	400	450	600	750	900	Totals:
Cracking	1	0	0	0	0	2	0	0	0	2	5	1	1	12
No cracking	7	1	5	8	1	14	3	1	5	13	8	3	2	71
Totals:	8	1	5	8	1	16	3	1	5	15	13	4	3	83

Percents of Row Totals

	unknown	100	150	200	250	300	350	375	400	450	600	750	900	Totals:
Cracking	8.33%	0%	0%	0%	0%	16.67%	0%	0%	0%	16.67%	41.67%	8.33%	8.33%	100%
No cracking	9.86%	1.41%	7.04%	11.27%	1.41%	19.72%	4.23%	1.41%	7.04%	18.31%	11.27%	4.23%	2.82%	100%
Totals:	9.64%	1.2%	6.02%	9.64%	1.2%	19.28%	3.61%	1.2%	6.02%	18.07%	15.66%	4.82%	3.61%	100%

Percents of Column Totals

	unknown	100	150	200	250	300	350	375	400	450	600	750	900	Totals:
Cracking	12.5%	0%	0%	0%	0%	12.5%	0%	0%	0%	13.33%	38.46%	25%	33.33%	14.46%
No cracking	87.5%	100%	100%	100%	100%	87.5%	100%	100%	100%	86.67%	61.54%	75%	66.67%	85.54%
Totals:	100%	100%	100%	100%	100%	100%	100%	100%	100%	100%	100%	100%	100%	100%

TABLE 6.6 Tables Showing the Relationship between Observed Ground Cracking and Pipeline Diameter (mm)

Observed Frequency Table

	unknown	100	150	200	250	300	350	375	400	450	600	750	900	Totals:
YES	1	0	0	0	0	2	0	0	0	1	5	0	1	10
NO	7	1	5	8	1	14	3	1	5	14	8	4	2	73
Totals:	8	1	5	8	1	16	3	1	5	15	13	4	3	83

Percents of Row Totals

	unknown	100	150	200	250	300	350	375	400	450	600	750	900	Totals:
YES	10%	0%	0%	0%	0%	20%	0%	0%	0%	10%	50%	0%	10%	100%
NO	9.59%	1.37%	6.85%	10.96%	1.37%	19.18%	4.11%	1.37%	6.85%	19.18%	10.96%	5.48%	2.74%	100%
Totals:	9.64%	1.2%	6.02%	9.64%	1.2%	19.28%	3.61%	1.2%	6.02%	18.07%	15.66%	4.82%	3.61%	100%

Percents of Column Totals

	unknown	100	150	200	250	300	350	375	400	450	600	750	900	Totals:
YES	12.5%	0%	0%	0%	0%	12.5%	0%	0%	0%	6.67%	38.46%	0%	33.33%	12.05%
NO	87.5%	100%	100%	100%	100%	87.5%	100%	100%	100%	93.33%	61.54%	100%	66.67%	87.95%
Totals:	100%	100%	100%	100%	100%	100%	100%	100%	100%	100%	100%	100%	100%	100%

TABLE 6.7 Tables Showing the Relationship between Occurrences of both Observed Ground Cracking and Frost Heave with Pipeline Diameter (mm)

6.3.4. Influence of Soil Type on Frost Heave and Ground Cracking.

Figure 6.6 illustrates that 44 of the 83 pipelines in the survey were laid in clayey soils, and that 11 of the 16 pipelines where observable soil pipeline interactions occurred were buried in clayey soils. The influence of soil type is quantitatively described in the observed frequency tables in Tables 6.8, 6.9 and 6.10. These results are in general agreement with the literature which indicates that frost heave was more likely in silts, clays and silty sands. Chalks are also very frost susceptible, however frost heave was not observed.

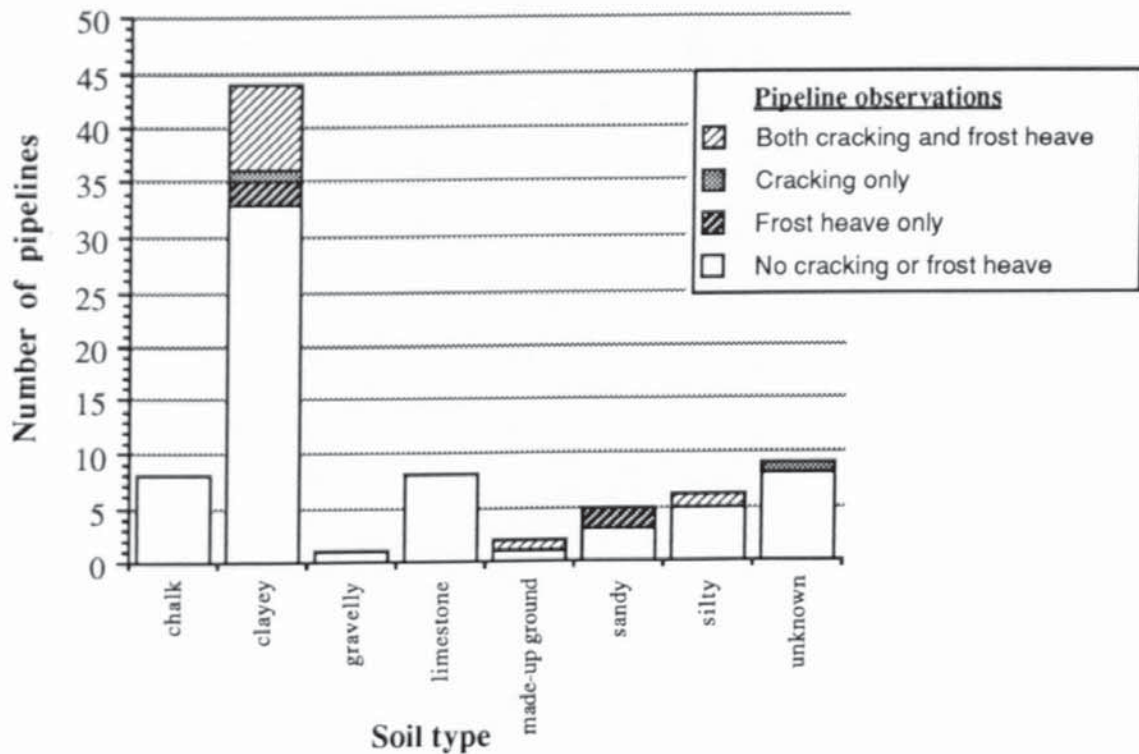


FIGURE 6.6 Bar Chart Illustrating Soil Types in Relation to Frost Heave and Ground Cracking.

6.3.5. Periods of Observable Frost Heave and Ground Cracking.

Figure 6.7 shows the influence of the time of the year on the observation of frost heave and ground cracking. Frost heave and ground cracking were reported along fourteen and twelve pipelines respectively, however not all respondents replied to the time-scale of observations. Thus there is a discrepancy between total frost heave and ground cracking observations with the numbers reported in Figure 6.7. Frost heave occurs mainly from November through to April and this represents the Pre-heating Season, ie. the period when pre-heat is applied prior to pressure reduction. Ground cracking follows a similar pattern, but it continues to be observed until July. This indicates that the soil-pipe interactions are related in part to the operating conditions imposed upon a PRS due to increased flows occurring during the Pre-heating Season.

Observed Frequency Table

	silty	clayey	sandy	gravelly	unknown	limestone	chalk	made-u...	Totals:
Heave	1	10	2	0	0	0	0	1	14
No heave	5	34	3	1	9	8	8	1	69
Totals:	6	44	5	1	9	8	8	2	83

Percents of Row Totals

	silty	clayey	sandy	gravelly	unknown	limestone	chalk	made-u...	Totals:
Heave	7.14%	71.43%	14.29%	0%	0%	0%	0%	7.14%	100%
No heave	7.25%	49.28%	4.35%	1.45%	13.04%	11.59%	11.59%	1.45%	100%
Totals:	7.23%	53.01%	6.02%	1.2%	10.84%	9.64%	9.64%	2.41%	100%

Percents of Column Totals

	silty	clayey	sandy	gravelly	unknown	limestone	chalk	made-u...	Totals:
Heave	16.67%	22.73%	40%	0%	0%	0%	0%	50%	16.87%
No heave	83.33%	77.27%	60%	100%	100%	100%	100%	50%	83.13%
Totals:	100%	100%	100%	100%	100%	100%	100%	100%	100%

TABLE 6.8 Frequency Tables Showing the Relationship between Frost Heave and Soil Type.

Observed Frequency Table

	silty	clayey	sandy	gravelly	unknown limestone	chalk	made-u...	Totals:
Cracking	1	9	0	0	1	0	1	12
No cracking	5	35	5	1	8	8	1	71
	6	44	5	1	9	8	2	83

Percents of Row Totals

	silty	clayey	sandy	gravelly	unknown limestone	chalk	made-u...	Totals:
Cracking	8.33%	75%	0%	0%	8.33%	0%	8.33%	100%
No cracking	7.04%	49.3%	7.04%	1.41%	11.27%	11.27%	1.41%	100%
Totals:	7.23%	53.01%	6.02%	1.2%	10.84%	9.64%	2.41%	100%

Percents of Column Totals

	silty	clayey	sandy	gravelly	unknown limestone	chalk	made-u...	Totals:
Cracking	16.67%	20.45%	0%	0%	11.11%	0%	50%	14.46%
No cracking	83.33%	79.55%	100%	100%	88.89%	100%	50%	85.54%
Totals:	100%	100%	100%	100%	100%	100%	100%	100%

TABLE 6.9 Frequency Tables Showing the Relationship between Ground Cracking and Soil Type.

Observed Frequency Table

	silty	clayey	sandy	gravelly	unknown limestone	chalk	made-u...	
YES	1	8	0	0	0	0	1	10
NO	5	36	5	1	9	8	1	73
Totals:	6	44	5	1	9	8	2	83

Percents of Row Totals

	silty	clayey	sandy	gravelly	unknown limestone	chalk	made-u...	Totals:
YES	10%	80%	0%	0%	0%	0%	10%	100%
NO	6.85%	49.32%	6.85%	1.37%	12.33%	10.96%	1.37%	100%
Totals:	7.23%	53.01%	6.02%	1.2%	10.84%	9.64%	2.41%	100%

Percents of Column Totals

	silty	clayey	sandy	gravelly	unknown limestone	chalk	made-u...	Totals:
YES	16.67%	18.18%	0%	0%	0%	0%	50%	12.05%
NO	83.33%	81.82%	100%	100%	100%	100%	50%	87.95%
Totals:	100%	100%	100%	100%	100%	100%	100%	100%

TABLE 6.10 Tables Showing the Relationship between Both Frost Heave and Ground Cracking with Soil Type.

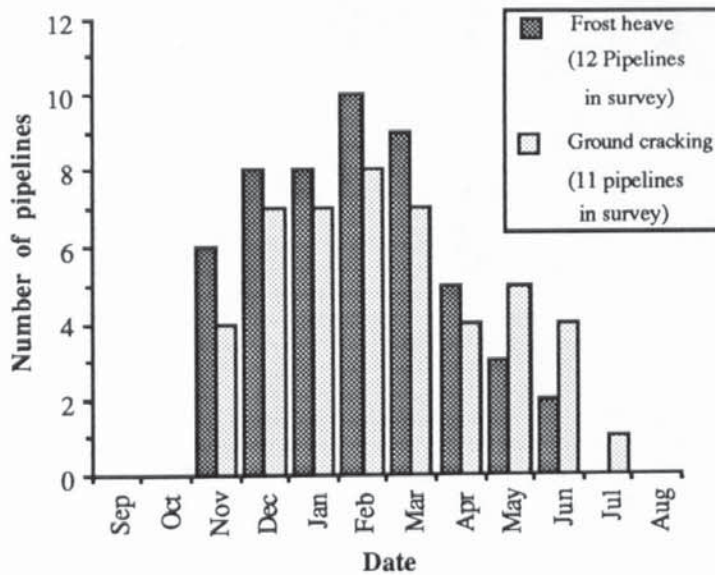


FIGURE 6.7 Bar Chart Illustrating the Number of Pipelines with Frost Heave or Ground Cracking Soil-Pipe Interactions during each Month.

6.4 Main Conclusions.

1. Eighty-three pipelines have been operated in chilled mode, of which only sixteen reported observable soil-pipeline interactions. Along ten of these pipelines both frost heave (pipe heave) and ground cracking were observed, however only six showed both interactions at the same location.
2. The magnitudes of the soil-pipeline interactions are both greater downstream of the PRS.
3. Under British Gas operating conditions both soil-pipeline interactions are more likely to occur along large-diameter pipelines (ie. above 450 mm). Larger pipelines have high mass flow rates and thus gas temperature recovery to 0°C occurs further downstream.
4. The pipelines in this study were predominantly laid in clayey soils, and as expected from the literature frost heave and ground cracking mainly occurred in this soil type. However the small sample size prohibits further interpretation of other soil types, especially very frost susceptible silts.
5. Both soil-pipeline interactions are initially observed in November and total number of observations reaches a maximum in February and steadily decline to zero in June/July. This pattern coincides with the British Gas Pre-heating Season and continues slightly beyond the end of the Season. Frost heave is more predominant early in the Pre-heating Season, with ground cracking being more predominant later in the Season.
6. The above general conclusions suggest a link between ground cracking and frost heave.

CHAPTER 7 LARGE-SCALE STUDY PROGRAMME

7.1 Introduction.

The second phase of the study programme involved monitoring an *operating* Pressure Reduction Station and its associated downstream pipelines. A site was selected and instrumented with the prime aim of identifying the mechanism(s) of ground cracking and subsequently to more thoroughly define the impact of ground cracking on the local environment. Thus, it was hoped to establish an engineering perspective of ground cracking, thereby leading to an appropriate method for the prediction of ground cracking together with a pipeline operating methodology targeted at reducing any ground cracking to acceptable limits.

With a large-scale test there are many uncontrollable variables such as rainfall, ambient air temperatures, water table, soil type and spatial variability along the line, agricultural land usage etc. Selection of the site was partly based on its previous operational history and on its susceptibility to ground cracking. Since the site has out of necessity been operated below 0°C, this will have influenced the frost heave behaviour of the soil within the frozen annulus as a result of the previous freeze/thaw cycles. Consequently previous ground cracking will have had an effect on the stress-strain behaviour of the soil directly above the pipe since soil failure planes (cracks) may exist from one year to the next. However, the operation of a full-scale test allows the *in situ* measurement of ground cracking and practical engineering values to be assigned to the variables under examination.

7.2 Objectives.

Although ground cracking has been observed intermittently along a number of large-diameter pipelines, its mechanism of formation is unknown and has been the subject of a hypothesis put forward by Archer *et al.* (1984). Replies from the questionnaires (Chapter 6) indicated that ground cracking and frost heave have not been the subject of detailed examination within the British Gas Network.

The objectives were to:-

1. Define the extent and problems resulting from ground cracking.
2. Investigate ground cracking in relation to frost heave,
3. Determine the mechanism(s) of ground cracking, and
4. Evolve a predictive procedure for ground cracking.

In order to address the above objectives the following monitoring was undertaken:-

1. Ground cracking and frost/pipe heave under field conditions,
2. Fundamental investigation of the soil thermal, hydrological and stress regimes, especially in the area between the pipe and the ground surface,
3. Pipe operating conditions,
4. Pipe movement, and ground surface movement.

7.3 Site Selection.

7.3.1 Selection of a Pressure Reduction Station.

After consultations with British Gas personnel at both the Engineering Research Station, Newcastle-Upon-Tyne and a number of British Gas Regions, it was decided that British Gas Northwestern would be approached with a view to operating a full-scale facility under controlled test conditions. British Gas Northwestern were selected due to their previous experience (Archer *et al.*, 1984) and because there was a definite commitment from this Region to investigate and define the soil-pipe interactions associated with chilled gas pipeline operation.

British Gas Northwestern (BGNW) agreed to the proposal after a presentation at a regular Pre-heating Meeting in September 1987. Blackrod A.G.I. was again selected for monitoring, since ground cracking had been previously observed. Cracking had been observed intermittently along the line and the size and extent varied from one cracking zone to another.

Site monitoring was effected in two stages:-

1. Investigation of the influence of the formation and growth of a frozen annulus around the pipe on ground cracking at the three downstream sites (A,B and C),
2. Investigation of the relationship between pipe heave and ground surface movement across the line of the pipe within Blackrod PRS.

7.3.2 Selection of Downstream Sites For Instrumentation.

The 900 mm x 12.7 mm pipeline from Blackrod to Engine Lane Pressure Reduction Station was selected in preference to the smaller, lower flow 600 mm x 9.5 mm pipeline to Shevington Pressure Reduction Station. The selection was based primarily on the criteria that more cracking had been observed along the larger pipeline. This pipeline runs for approximately 15 km before entering the next downstream PRS, and ground cracking had

been reported up to 3.1 km downstream of Blackrod PRS, Table 7.1 shows the zones of cracking reported during the 1983-1984 Pre-heating Season.

After discussions with the relevant Engineers and their staff, three sites were selected based upon their susceptibility to ground cracking. All three sites are in areas used for pasture by cattle and therefore instrumentation and its associated cabling had to be laid without disruption to these normal farming activities. The sites were:-

- Site A At chainage 20 m, close to the perimeter of the compound of Blackrod PRS,
- Site B At chainage 200 m, close to Marker Post (M.P.) 1,
- Site C At chainage 2750 m, close to Marker Post (M.P.) 19.

Downstream Chainage (m) (*)	Length of Cracking (m)	Classification of Cracking (#)	Land Usage
000 - 140	140	Moderate	Pasture
380 - 480	100	Slight	Pasture
650 - 860	210	Slight	Pasture
870 - 970	100	Slight	Arable
970 - 1130	160	Severe	Arable
1280 - 1790	510	Slight	Pasture
2100 - 2110	10	Slight	Pasture
2320 - 2470	150	Slight	Pasture
2600 - 2990	390	Severe	Pasture
2990 - 3050	60	Slight	Pasture

Notes. * Chainage 0 m is where the pipeline exits the PRS.

Maximum crack width was 150 mm, British Gas classification scale is based on this maximum.

TABLE 7.1 Observations of Cracking along the Blackrod to Engine Lane Pipeline during Pre-heating Season 1983-84.

7.3.2.1 Severe Cracking (Site C).

This was the most heavily instrumented site, since it is in the area where the most severe cracking had been observed. A wedge-shaped crack with its apex at the crown of the pipe and a maximum width of 150 mm at the ground surface had been previously reported during the months of April, May and June 1984 (Archer *et al.*, 1984). During the rest of the year a slight depression was evident along the line of the pipe. As a result of the severity of cracking, relationships between factors such as pipe temperature, ground temperature regime, soil water potential, etc with respect to ground cracking should be clearer than in an area with only slight cracking.

7.3.2.2 Moderate Cracking (Site A).

This site has been instrumented to provide results and observations which could be compared with those obtained from Site C.



PLATE 7.1 Excavation at Site C.



PLATE 7.2 300 x 300 mm Grid Marked on Trench Wall at Site C.

In the following sections discussion will be limited to Site C, further information on the positioning of the instrumentation at Sites A and B can be found in Appendix C.

7.4.1 Thermal Instrumentation.

The thermal regime was measured using Platinum Resistance Thermocouples (P.R.T's), their layout is shown in Figure 7.2 (Plate 7.3) and the positions are given in Table 7.2.

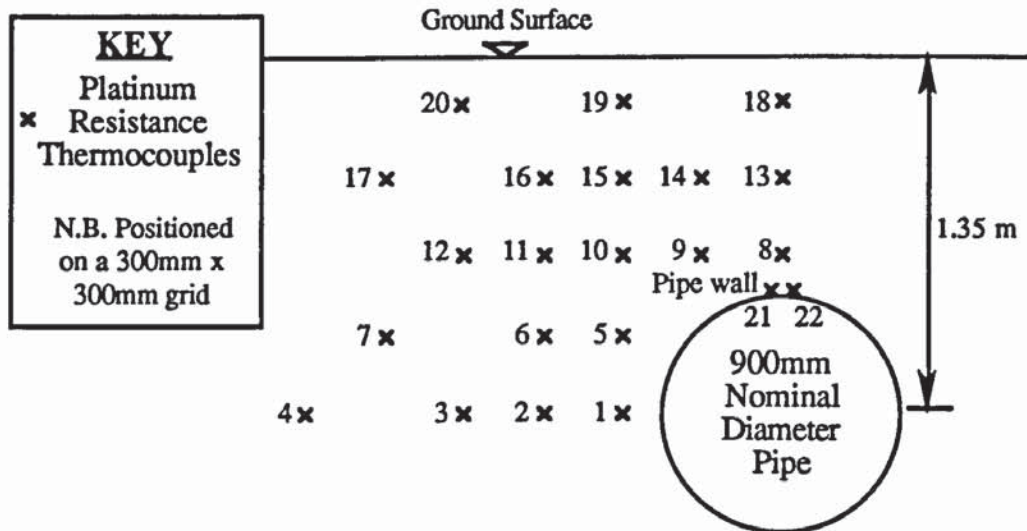


FIGURE 7.2 Layout of Platinum Resistance Thermocouples at Site C.

PRT No.	1	2	3	4	5	6	7	8	9	10	11	12	13	14	15	16	17	18	19	20	21	22
vert. (m)*	0	0	0	0	0.3	0.3	0.3	0.6	0.6	0.6	0.6	0.6	0.9	0.9	0.9	0.9	0.9	1.2	1.2	1.2	0.45	0.45
hor. (m)*	0.6	0.9	1.2	1.8	0.6	0.9	1.5	0	0.3	0.6	0.9	1.2	0	0.3	0.6	0.9	1.5	0	0.6	1.2	0	0

* The origin is taken from the pipe centre.

TABLE 7.2 Positions of the Platinum Resistance Thermocouples at Site C.

A total of 22 PRT's were installed to provide data on the growth and recession of the frozen annulus during and after the Pre-heating Season. Analysis of the results from the previous trial at Blackrod indicated that the frozen annulus could extend to over 600 mm from the pipe wall, thus the grid pattern was designed to encompass this maximum annulus size.

Platinum resistance thermocouples were selected due to their:-

1. Reliability,
2. Robustness,
3. Accuracy ($\pm 0.25^{\circ}\text{C}$, which represents the resolution capability of the data loggers),

4. Linear output over the expected temperature range,
5. Previous British Gas experience had shown their proven reliability over long periods,
6. Automatic data logging facilities were readily available,
7. A suite of computer programs was available to allow the interpretation of data.
8. No cold junction required (a monitor channel with a 100 ohm resistor was used to correct for data logger drift).

The PRT's probe is a 50 mm long x 5 mm diameter stainless steel section with a hole drilled part way through it on its longitudinal axis. The PRT element was connected to four insulated cables and was housed in the element. A sealing compound was injected into the hole to hold the element in place and the connection between the stainless steel section and the cables connecting to the data logger were sealed with heat shrinkable plastic. The PRT's and data loggers were constructed and supplied by British Gas NorthWestern.

7.4.2 Hydrological Instrumentation.

The soil moisture regime was measured by thermocouple-psychrometers, which were installed on a predetermined grid in trench wall "B" (Figure 7.3) *ie.* the opposite wall to where the thermocouples were installed. Plate 7.4 shows the thermocouple-psychrometers at Site A. Again the positioning of the instrumentation was determined by the expected maximum size of the frozen annulus.

Thermocouple-psychrometers directly measure the water potential (soil suction) of the system under observation, for soils the water potential is inferred directly from the vapour pressure of the system (Van Haveren and Brown, 1972). A thermocouple-psychrometer is basically a temperature sensing device, whereby the temperature differential between a junction at ambient and another where free evaporation of water is occurring can be related to the total water potential of the system. The thermocouple-psychrometers were supplied by Wescor (Logan, Utah, USA) and an illustration is given in Figure 7.4.

The wet bulb junction of the thermocouple-psychrometers used in this investigation is a welded junction of chromel and constantan wires each 0.0025 mm diameter. The dry bulb junction (Copper-Constantan) is much larger to allow for the dissipation of heat energy which is generated in response to wet bulb junction cooling. This allows the dry bulb junction to be maintained at the ambient temperature of the surrounding soil and thus the temperature differential between the wet and dry bulb junctions is not affected. A small current is passed across the wet bulb to produce cooling by the Peltier Effect. If an excessive current is used the junction will heat due to the Joule Effect. The current is



PLATE 7.3 Installation of PRT's at Site C.



PLATE 7.4 Installation of Thermocouple-Psychrometers at Site A.

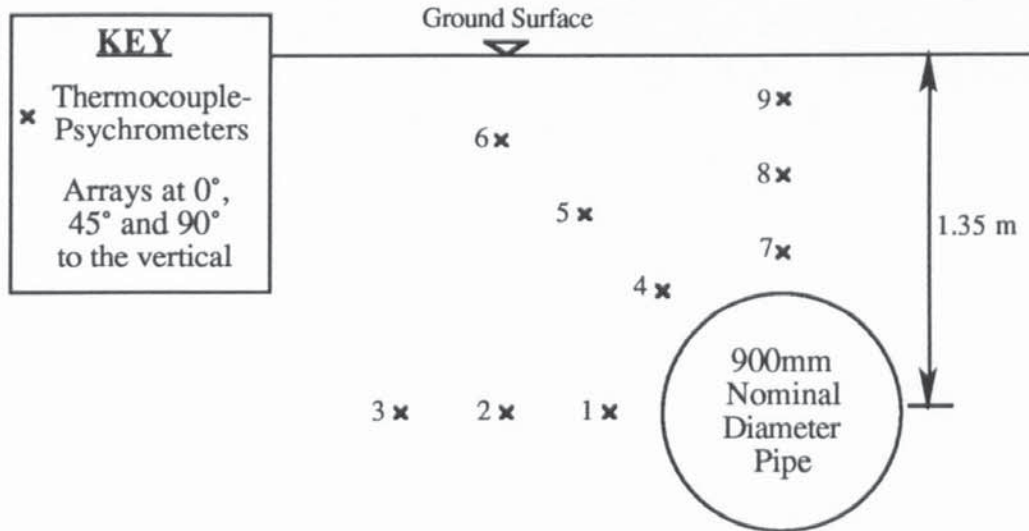


FIGURE 7.3 Layout of the Thermocouple-Psychrometers at Site C.

Ther. Pyc. No.	1	2	3	4	5	6	7	8	9
Vertical (m) *	0	0	0	0.45	0.75	1.05	0.60	0.90	1.20
Horizontal (m) *	0.65	1.05	1.45	0.45	0.75	1.02	0	0	0

* The origin is taken from the pipe centre.

TABLE 7.3 Position of the Thermocouple-Psychrometers at Site C.

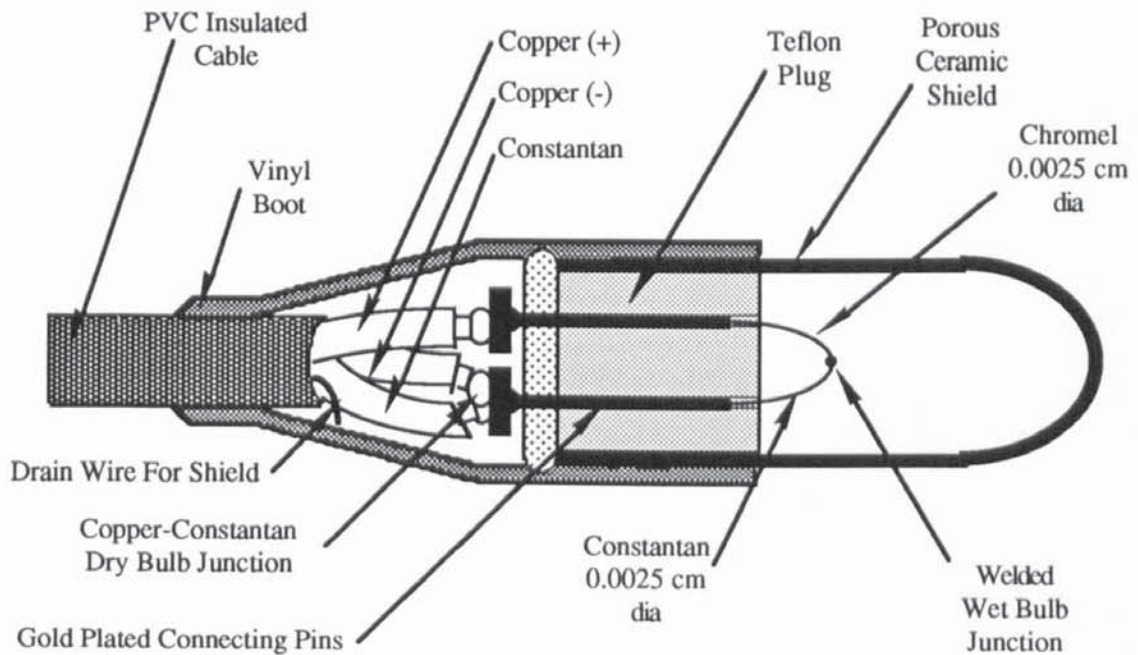


FIGURE 7.4 Thermocouple-Psychrometer (after Briscoe, 1984).

supplied for sufficient time for vapour to condense on the junction, during the application of the current the junction is continuously cooling and this induces a p.d. that is measured as the thermocouple-psychrometer output (points a to b Figure 7.5). This induced p.d. is known as the Seebeck Effect and the copper-constantan junction dissipates the heat generated in response to the cooling of the wet bulb (Van Haveren and Brown, 1972). A typical output from a thermocouple-psychrometer is shown in Figure 7.5. When cooling is stopped the wet bulb junction will immediately heat up and there will be a decrease in p.d. between the two junctions (points b to c Figure 7.5), however the latent heat of the evaporation of water on the wet bulb junction will equal the rate of heat gain at some point (points c to d, Figure 7.5) unless there is zero water potential. The greater the vapour pressure gradient between the wet bulb and the surroundings the greater will be the rate of evaporation and consequently the p.d. between the junction will be higher. Measurement of this plateau (points c to d, Figure 7.5) allows the estimation of the water potential of the surrounding soil (Briscoe, 1984). Once evaporation has completed the p.d. between the junctions will return to pre-cooling state (points d to e Figure 7.5), in this case zero.

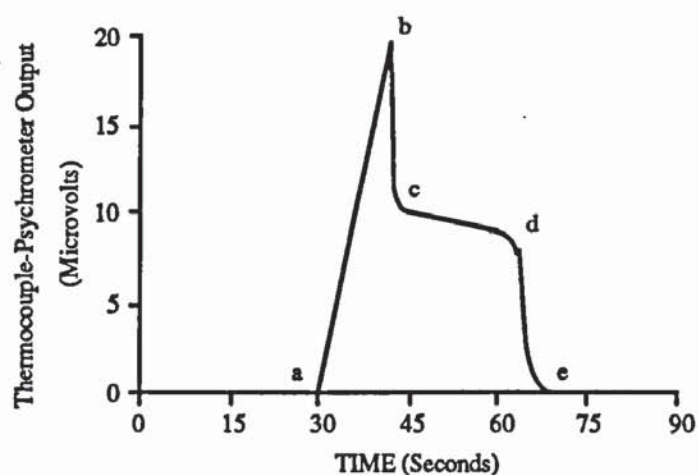


FIGURE 7.5 Output from a Typical Wescor Thermocouple-Psychrometer (after Briscoe, 1984).

The estimation of water potential is dependent on the following variables, microvolt output, equilibrium temperature, Peltier cooling current and the temperature difference between the wet and dry bulbs resulting from thermal gradients (Brown and Bartos, 1982). Merrill and Rawlins (1972) demonstrated that temperature gradients such as those typically found within the upper 0.35 m of the soil horizon can induce large errors in water potential estimation. However, if the thermocouple-psychrometer is placed at right angles to the thermal gradient, these errors can be very considerably reduced.

Brown and Bartos (1982) have developed and verified a mathematical model for the determination of water potential based on its relationship with the above described variables. The computer program based on this model is provided in Appendix D.

Brown and Johnston (1976) report the successful field use of thermocouple-psychrometers for monitoring periods in excess of forty months. Daniel *et al.* (1980) report that thermocouple-psychrometers are the most useful devices for measuring soil suction in relatively dry unsaturated soils. However it was noted that corrosion associated with in acidic or clayey soils caused the rapid deterioration of the 0.0025 mm constantan wire. Clark (1989) reports their success in measuring soil suctions associated with soil freezing in laboratory tests.

Thermocouple-psychrometers were selected since they measure soil suction directly, cover the full range of suctions expected during the trial and have been shown to reliable over long periods. They were gently pushed horizontally into a hole made in the wall of the excavation making sure that good contact was made between the ceramic shield and the soil. The output wires were turned downwards to prevent water travelling along the cable and accumulating at the thermocouple-psychrometer. The wires were subsequently brought to the ground surface through a plastic access tube. The thermocouple-psychrometers used were corrosion protected and measurements were taken weekly using a psychrometer-microvoltmeter (PR-55) supplied by Wescor.

7.4.3 Soil Stress Instrumentation.

The soil stress regime was measured from a vertical array of soil pressure transducers above and slightly offset from the pipe centreline (Figure 7.6, Table 7.4). The soil pressure transducers were installed in a small excavation either upstream or downstream of the main excavation (Plate 7.5). The transducers were placed in an excavation rather than a small access made by an auger since it was hoped to measure the frozen soil stresses during the growth and recession of the frozen annulus in a soil mass that had not previously been subjected to the ground cracking. Only one array of soil pressure cells was installed at each site due to cost considerations. A vertical array was selected to define the actual time that ground cracking occurred and the maximum soil pressure prior to soil failure.

The soil pressure transducers were selected to cover the range of soil pressures expected and that they could be automatically monitored by modifying the data loggers used for PRT measurement. The soil pressure transducers chosen had a 34 mm diameter sensing area, again a larger sensing area would have been better since it gives a better average soil stress but their cost was prohibitive. The range was between 0 and 196 (2) or 0 and 480 (5) KNm⁻² (Kg cm⁻²) and were supplied by Techni Measure (Studley, Warwickshire).

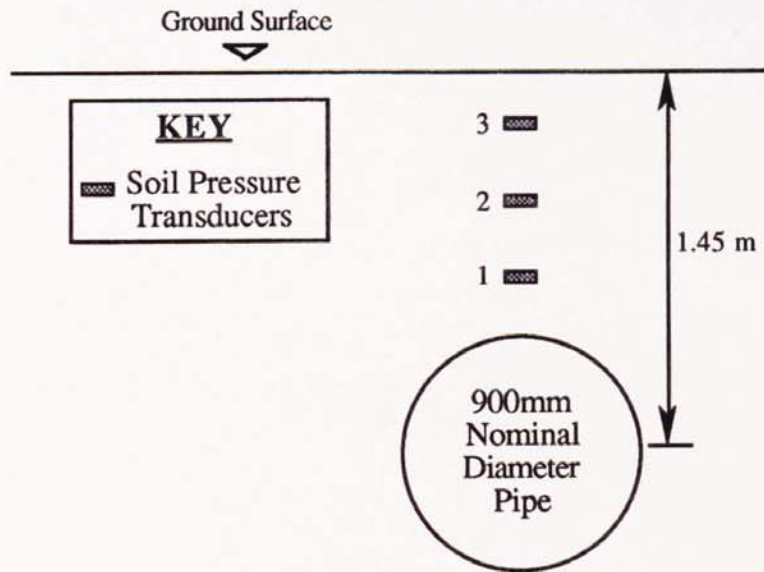


FIGURE 7.6 Layout of Soil Pressure Transducers at Site C.

Soil Pressure No.	1	2	3
Vertical (m) *	0.65	0.95	1.25
Horizontal (m) *	0	0	0

* The origin is taken from the pipe centre.

TABLE 7.4 Position of Soil Pressure Transducers at Site C.



PLATE 7.5 Installation of Soil Pressure Transducers at Site A.

7.4.4 Pipe Movement Instrumentation.

Pipe movement was simply measured from three pipe heave rods attached to the crown of the pipe at 20 m intervals along its line (Figure 7.7). The central rod was installed in the same excavation as the PRT's and the thermocouple-psychrometers. Three pipe heave rods were installed allowing local pipe curvature and average values to be obtained. The tops of the pipe heave rods were levelled weekly using a tilting level, a precise level was not deemed necessary since large movements of up to 80 mm had previously been reported. A T.B.M. was set out close to the pipe heave rods and was regularly checked with respect to a remote T.B.M. The tilting level was also checked weekly.

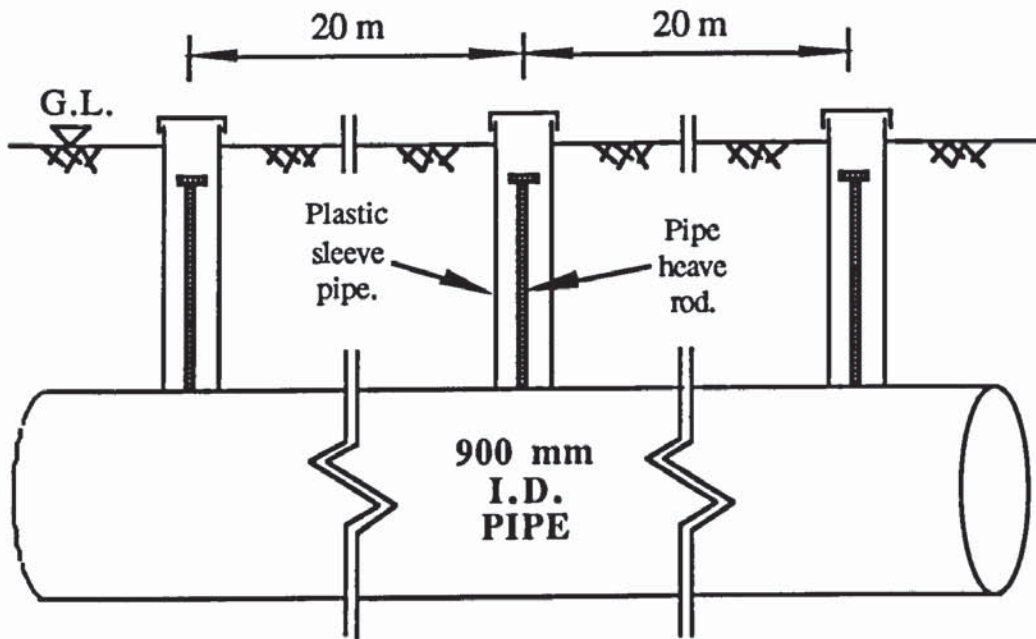


FIGURE 7.7 Schematic Layout of Pipe Heave Rods at Site C.

Since the installation of the pipe heave rod involved cutting through the cold tar around the pipe and attaching a steel object to the pipeline, care was taken to minimize the potential danger of corrosion to the pipeline. The area of cold tar cut out was filled with a low thermal conductivity adhesive supplied by British Gas and two steel blocks 75 mm square, 25 mm thick and with 15 mm diameter holes cut out in their centres were then placed on top. Each pipe heave rod was located in the holes which were subsequently filled with low thermal conductivity adhesive. After this had set the base was covered in a low thermal conductivity putty and the outer plastic case was placed over the pipe heave rod (Figure 7.8).

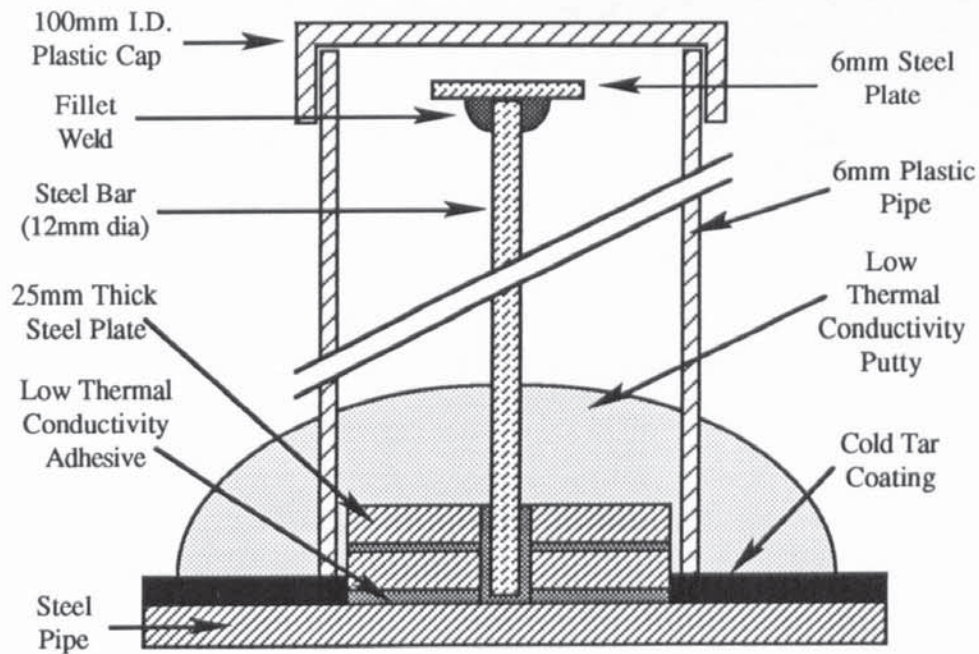


FIGURE 7.8 Pipe Heave Rod.

7.4.5 Pipe Strain Instrumentation.

Strain gauges were attached to the pipe at Site C only (Figure 7.9) to investigate the vertical and lateral pipe strains induced in the pipe during low temperature operation. Osborne (1985) described the installation of vibrating wire strain gauges and the factors affecting the output from such gauges. British Gas have installed many vibrating wire strain gauges as part of the development of risk assessment procedures for pipelines and report that they have been both reliable and durable (Osborne, 1985).

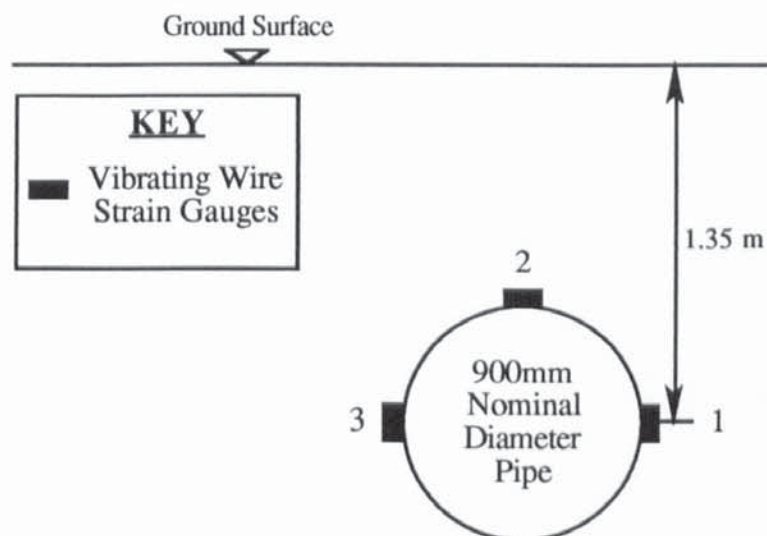


FIGURE 7.9 Layout of Strain Gauges at Site C.

Installation again involved cutting through the protective cold tar coating, and so involved the use of special corrosion inhibiting procedures (Figure 7.10, Plate 7.6).

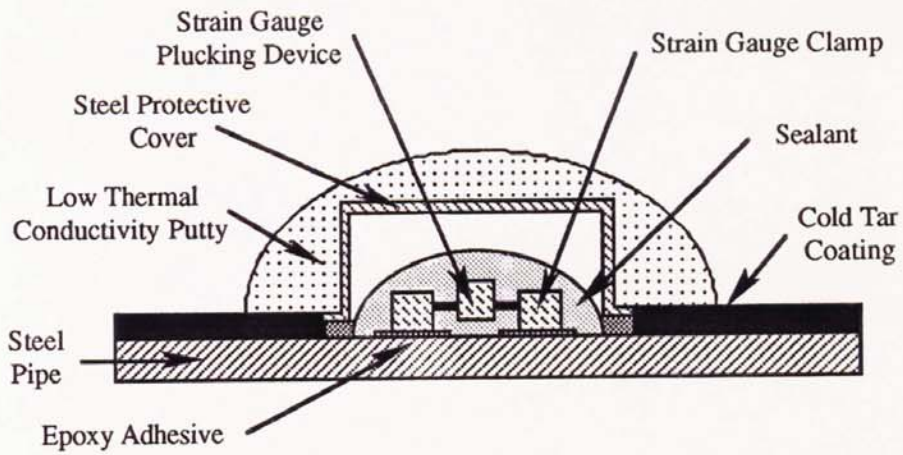


FIGURE 7.10 Vibrating Wire Strain Gauge Arrangement.



PLATE 7.6 Installation of the Vibrating Wire Strain Gauges at Site C.

7.4.6 Blackrod PRS Operating Characteristics.

Pipeline operating conditions are monitored at Pressure Reduction Stations and sent via telemetry to Hinckley Operations Centre. During the earlier study (Archer *et al.*, 1984) monitoring of the Blackrod PRS was undertaken using this instrumentation and PRT's which monitored soil and pipe temperatures. This instrumentation was logged on-site using an automatic data acquisition system. The 18 channel data logger in the station was used to monitor:-

1. Gas temperatures:- station inlet, outlet to Blackrod and outlet to Shevington,
2. Horizontal soil temperatures:- pipe wall, 75, 150, 600 and 900 mm,
3. Ambient temperatures:- air and ground (pipe depth),
4. Gas Pressures:- station inlet, outlet to Blackrod and outlet to Shevington,
5. Gas flow through the station.

The equipment used for pressure and flow measurement is British Gas standard and soil and ambient temperatures were measured with PRT's as described in Section 7.4.1.

7.4.7 Ambient Conditions.

The PRT used to monitor ambient ground temperature was buried at approximately pipe depth (about 1.5 m) and at a sufficient distance from the pipeline or other thermal disturbance to ensure that there would be no influence on the readings. Ambient air temperatures were measured at a height of 1 m above ground level, and the PRT was placed within a small insulated block to reduce the effects of sunlight and wind movements on the output.

Two rainfall gauges were placed in an open area away from obstructions within the Blackrod PRS. These were a siphon rainfall recorder (Casella) as the main recorder and a simple rainfall gauge (Casella) used as a check gauge.

7.4.8 Automatic Data Acquisition System.

This consisted of two distinct systems:-

1. Data logging, and
2. Data conversion and reduction.

Data logging took place at Blackrod PRS and the downstream sites, these data were subsequently transferred to Aston University for analysis.

7.4.8.1 Data Logging.

The data loggers were B10 logger units and were designed by Ketron and constructed under license by British Gas Northwestern. A range of loggers was available, they could monitor between 1 and 24 PRT channels and/or 1 to 8 D.C. voltage channels. The loggers were powered by rechargeable 12volt batteries. The operating characteristics such as interval reading time, start of reading, etc. were set from an lap held Epson PX-8 microcomputer. These data were downloaded from the data logger to the microcomputer where this information was then held in its internal RAM (Figure 7.11a).

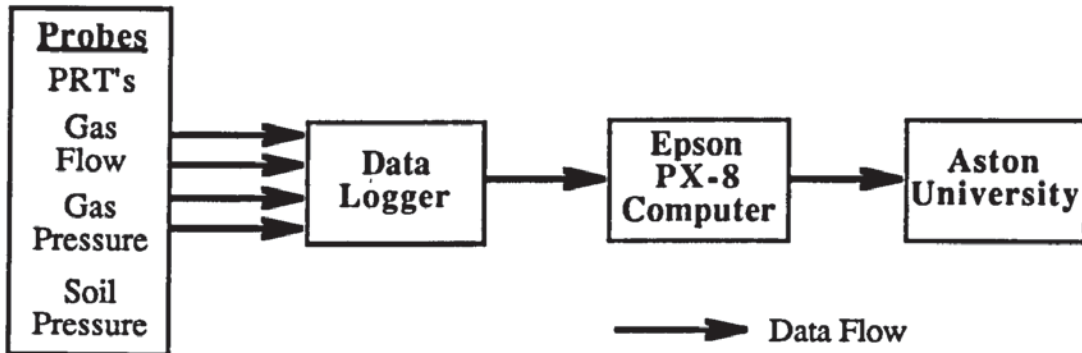


FIGURE 7.11a Data Flow Diagram for Data Collection from Blackrod Instrumentation.

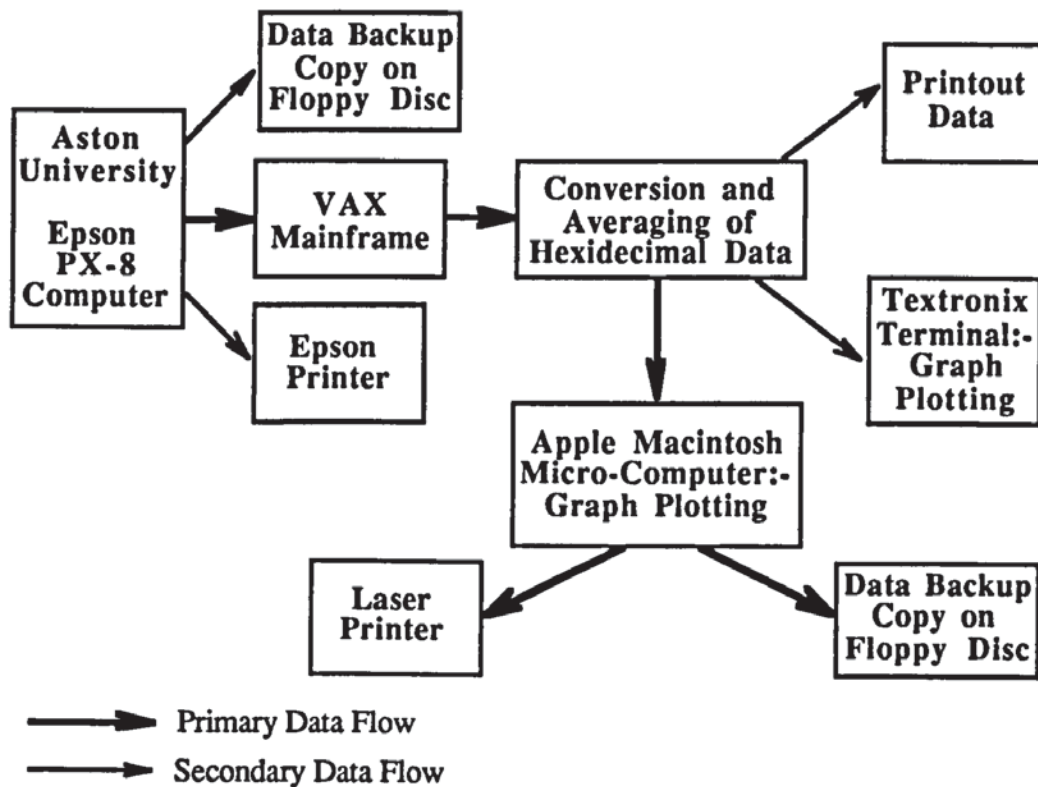


FIGURE 7.11b Data Flow Diagram for Data Interpretation at Aston University.

7.4.8.2 Data Interpretation.

At Aston University the microcomputer's RS232 port was linked to the Vax Cluster mainframe via the Local Area Network. The suite of computer programs for data processing on the Vax were provided by British Gas Engineering Research Station. The file transfer program provided was rewritten and enhanced to make use of the more efficient data transfer facilities available at Aston. The data were transferred in Hexidecimal code, and three programs were then run on the files to:-

1. Hexconvert:- convert data to decimal,
2. Average:- average data on a daily basis,
3. Accumulate:- accumulates data files form individual loggers.

These programs were also modified to run on the Vax Cluster at Aston. These accumulated data files were subsequently transferred to an Apple Macintosh micro-computer for further data reduction in spreadsheets and/or finally printed out using graph plotting packages. Data transfer was effected using a standard file transfer package, in this case KERMIT. All the other data from Blackrod were also analyzed on an Apple Macintosh micro-computer, therefore the final stage allowed direct comparison with these data. Figure 7.11b illustrates data flow during its interpretation at Aston University.

7.5 Instrumentation of Pressure Reduction Station.

The primary objective was to investigate the profile of the ground surface during the formation and recession of the frozen annulus. Initial results indicated that pipe heave even 3 km downstream could reach 50 mm, and so it was probable that ground movements in excess of this could be anticipated. The secure compound of the PRS offered the opportunity to investigate pipe and ground movements without ground surface disturbance from people, cattle or wildlife.

During the earlier study (Archer *et al.* 1984) the structural integrity of the pipeline within the compound area had been monitored by pipe heave rods and strain gauges (British Gas Corporation, 1988). These had shown that significant bending stresses were not introduced into the pipe array as a result of sub-zero temperature operation. In late 1988 the pipe heave rods were refurbished to provide a reliable monitoring system to give the Engineer advance warning of any threats to the integrity of the Blackrod system, and so this refurbished monitoring system was incorporated into this study programme.

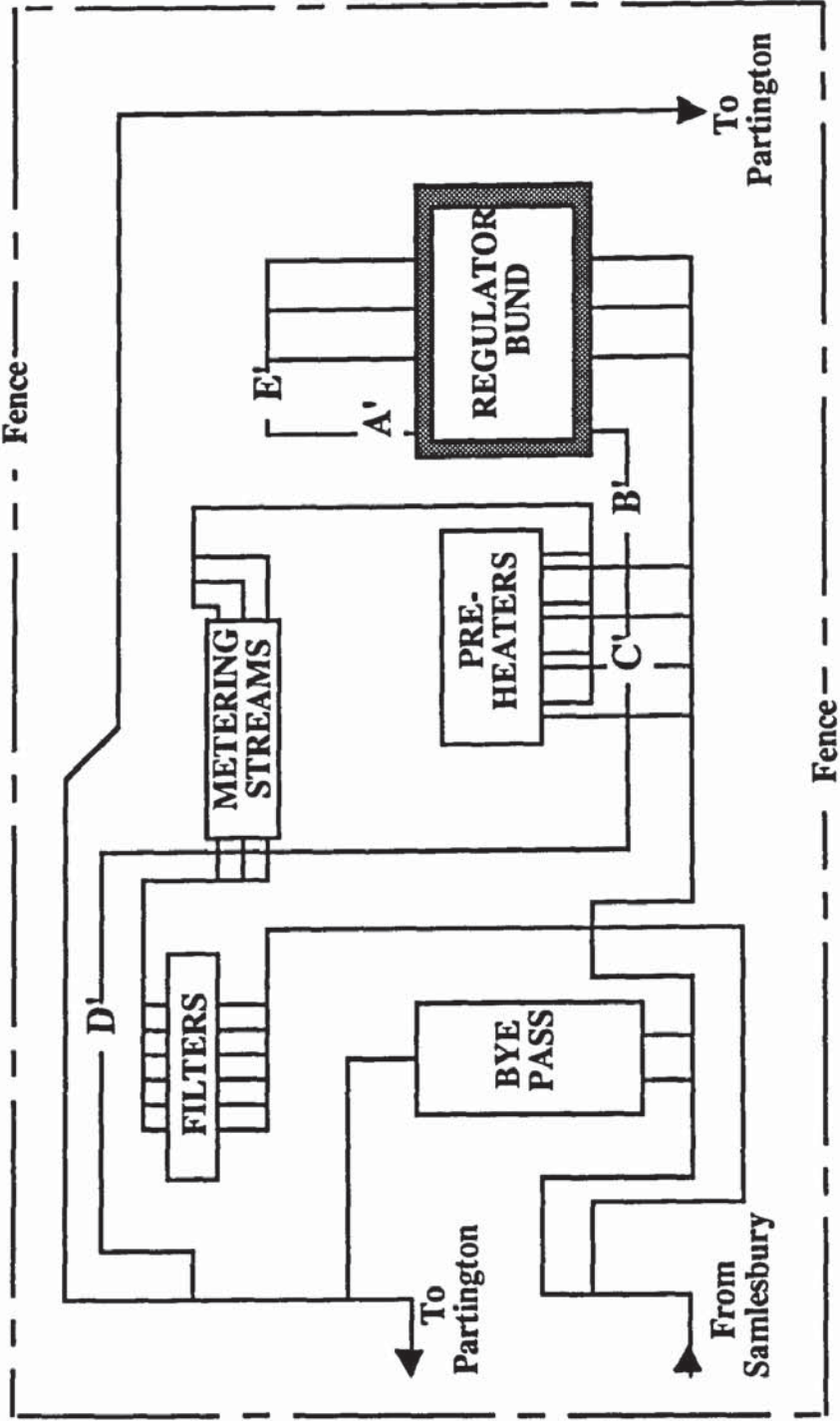
7.5.1 Pipe Heave/Ground Surface Movement.

Pipe movement was originally monitored by five pipe heave rods (Site A', B', C', D' and E') within the PRS (Figure 7.12). Sites C' and D' were selected for further investigation as they had previously shown the largest total pipe heaves (British Gas Corporation, 1988). Pipe heave had formerly been monitored by manual observation of the vertical movement of the pipe heave rod against a ruler attached to the goalpost. In order to reduce the possible effects of frost heave on the goalpost a new pipe heave rod with a large head replaced the old one, thus allowing a levelling staff to be placed directly on it (Figure 7.13, Plate 7.7). The outer casing was previously checked for any residual movement. At the same time, the distances between the top of the pipe heave rod and both the top of the goalpost and outer casing were measured as a further check on the validity of the results.

Ground surface heave perpendicular to the line of the pipe was measured simply by fastening a very taut nylon string between each upright of the goalpost and measuring down to the ground surface with a steel ruler. The ground surface was first stripped of the pea gravel layer to expose the underlying soil, and this exposed surface levelled to an even grade and marker nails driven into this surface. At either side of the pipe centre, nails were placed at 0.1 m intervals for 1 m and then at 0.2 m intervals from 1 to 2 m (Figure 7.13). When readings were taken both ends of the goalpost were levelled to correct for any relative movement of nylon string.

7.5.2 Pipe Bending Stress.

An assessment was undertaken of the pipe network within Blackrod PRS to determine the locations of restraint on the pipe and so verify that the selected pipe heave sites (Sites A', B', C', D' and E') were not subject to excessive restraint. These pipe heave sites were found to be correctly positioned to facilitate the measurement of pipe movement around the regulator bund walls, but Site D' was noted to be close to a location where the pipe passed from being buried to being supported above ground on vertical support members. At each location (Site A' to E') the pipe was buried. The five sites were refurbished as described in Section 7.5.1 to allow direct levelling of the pipe heave rod. Since the goalposts at Sites A', B' and E' had widths of under 2 m, any frost/pipe heave would produce a resultant upward movement of the goalpost, and so levelling was used to provide a reliable datum. Monitoring was undertaken on a weekly basis during periods when little pipe heave was occurring however, during operations at -5°C, this was increased to three times a week.



Note: The valves have been omitted for clarity.

FIGURE 7.12 Diagrammatic Layout of Blackrod showing the Positions of the Pipe Heave Rods.

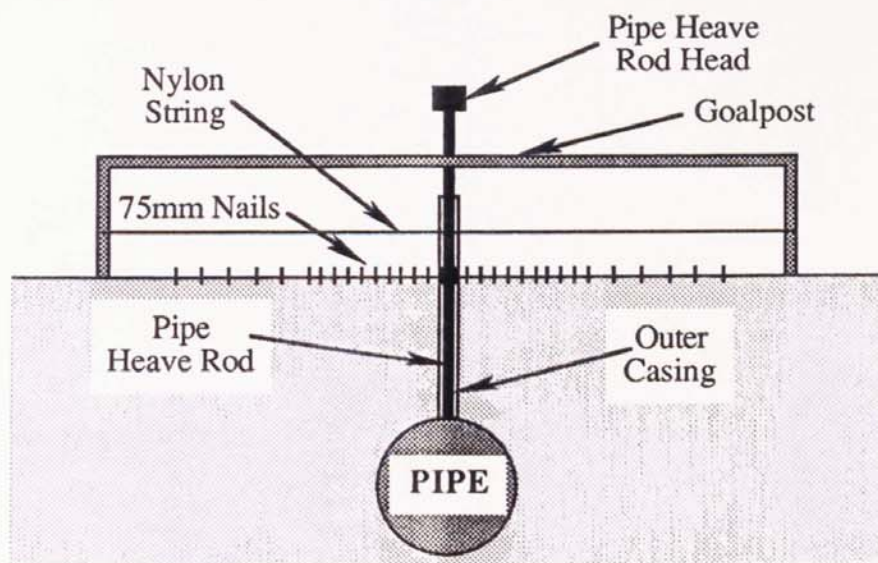


FIGURE 7.13 Typical Pipe Heave Arrangement during the Study.



PLATE 7.7 Pipe Heave/Ground Surface Profile Arrangement at Site C'.

7.6 Reading Intervals.

This section provides information on the reading intervals for the monitoring systems downstream of the PRS at Sites A, B and C (Table 7.5), PRS operating and ambient conditions (Table 7.6) and the pipe/ground heave instrumentation within the PRS (Table 7.7).

Instrument	Reading Interval		
	Site A	Site B	Site C
PRT's (soil)	4 hours	4 hours	4 hours
PRT's (pipe)	4 hours	4 hours	4 hours
Soil Pressure Cells	4 hours	4 hours	4 hours
Thermocouple-psychrometers	weekly	weekly	weekly
Pipe heave rods	weekly	weekly	weekly
Strain gauges	-----	-----	weekly
Water table	weekly	weekly	weekly

TABLE 7.5 Reading Intervals of Instruments at Site A,B and C Downstream of PRS.

Instrument	Reading Interval
PRT's (ambient air)	4 hours
PRT's (ambient ground)	4 hours
PRT's (pipe inlet and outlets)	4 hours
PRT's (horizontal soil)	4 hours
Gas flows (inlet)	4 hours
Gas pressures (inlet and outlet)	4 hours
Rainfall	weekly

TABLE 7.6 Reading Intervals of Pipeline Operating Characteristics, Ambient Conditions and Soil Temperature Profile taken in PRS.

Instrument	Reading Interval				
	Site A'	Site B'	Site C'	Site D'	Site E'
Pipe movement	weekly *	weekly *	weekly *	weekly *	weekly *
Ground movement	-----	-----	weekly *	weekly *	-----

* During trial period (outlet -5°C) readings were taken three times a week.

TABLE 7.7 Reading Intervals of Pipe and Ground Movement in the PRS.

7.7 Results.

The instrumentation was installed with assistance of British Gas Corporation NorthWestern, Transmission Department during the period Nov 1987 to Jan 1988. Regular monitoring of the downstream Sites A,B and C, together with Blackrod PRS operating conditions and ambient conditions were effected from 3rd February 1988 (Week 0) to 7th March 1990 (Week 109). The pipe heave monitoring system within Blackrod PRS, from the earlier British Gas study (Archer *et al.*, 1984), was refurbished in Nov 1988 and regular monitoring of both pipe and ground heave started on 24th Nov 1988 (Week 42) and continued until 7th March 1990 (Week 109).

7.7.1 Blackrod PRS Operating Conditions.

In the earlier study the setpoint temperature was -5°C (Archer *et al.*, 1984) and therefore it was hoped to produce ground cracking under similar operating conditions. Thus -5°C was selected as the setpoint temperature but, due to operational difficulties that arose during the trial, this temperature was only maintained for 34 days out of the total of 763 days. The actual setpoint temperatures and periods of operation for Blackrod PRS are given in Table 7.8.

Outlet Temperature	Start Date	Finish Date	Remarks
-2°C	pre-Dec 1987	24/11/88 (Week 42)	British Gas Engineers confident of ground cracking at this temperature in the Spring. (No significant ground cracking observed)
0°C	24/11/88 (Week 42)	31/1/89 (Week 52)	British Gas Northwest required extra instrumentation to monitor pipe heave within PRS. (Installed Nov 1988)
-5°C	31/1/88 (Week 52)	23/2/89 (Week 55)	First trial.
-2°C	23/2/89 (Week 55)	5/2/89 (Week 105)	Temperature raised since British Gas Northwest were concerned at the frost heave downstream of PRS. The temperature was raised to -2°C , not 0°C to reduce the possibility of thaw settlement.
-5°C	5/2/90 (Week 105)	16/2/90 (Week 106)	Second trial.
-2°C	16/2/90 (week 106)	-----	Operational requirements required an increase in outlet temperature.

Note: Week numbers are approximate and apply to the nearest week.

TABLE 7.8 Outlet Temperature Setpoints for Blackrod PRS during the Trial.

Figure 7.14 illustrates the operating conditions of Blackrod PRS during the monitoring period. However, weekly average values have been used for ease of interpretation, thereby averaging out the daily variations in gas flows, pressure and temperature.

The station outlet setpoint temperature is shown in Figure 7.14a, however the actual station outlet temperature was observed to deviate from this value annually between April and November. This indicated that the maximum temperature drop across the station was insufficient to compensate for the increase in the inlet temperature during this period. Again, during the periods that the station had a setpoint of -5°C there was an insufficient temperature drop, thus an average weekly outlet temperature of -4°C was recorded (Figure 7.14a).

Blackrod PRS operates its downstream pipelines at a nominal outlet pressure of 3.2 MNm^{-2} (465psi) and Figure 7.14b illustrates that this constant outlet pressure was successfully maintained. The flow through the station is shown to cycle on an annual basis (Figure 7.14b) and this is typical of the demand pattern for gas in the UK (Francis, 1984). As a result of the construction of additional pipelines within the British Gas NorthWestern Transmission System, flows through Blackrod PRS were considerably less than in the earlier study (Archer *et al.*, 1984), but local Grid Control supplied a maximum feasible flow through the station during the periods when ground cracking could be anticipated.

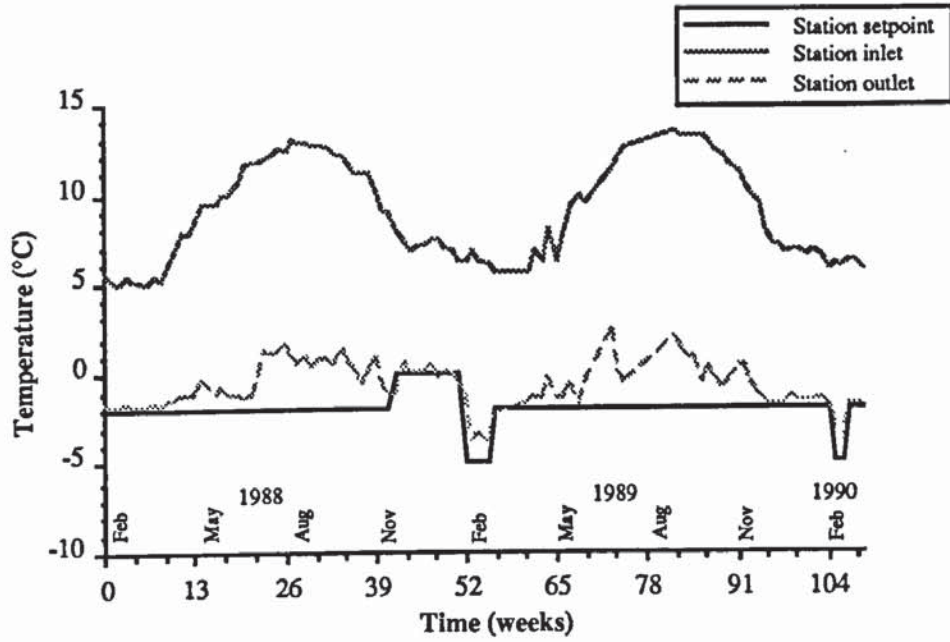
The inlet pressure to Blackrod PRS can be calculated by the addition of the pressure drop across the station (Figure 7.14c) and the outlet pressure (Figure 7.14b). It has an average value of 5.0 MN m^{-2} (725 psi) which is much less than its design value of 6.9 MN m^{-2} (1000 psi) at which it was operated during the earlier study (Archer *et al.*, 1984). This decrease in the potential pressure reduction from 3.7 to 1.8 MN m^{-2} represents, from thermodynamics, a decrease in the potential average temperature drop from 18.5 to 9°C . The actual temperature drop across the station is illustrated in Figure 7.14c and was dependent on inlet pressure, temperature and outlet setpoint temperature.

7.7.2. Ambient Conditions at Blackrod PRS During the Trial.

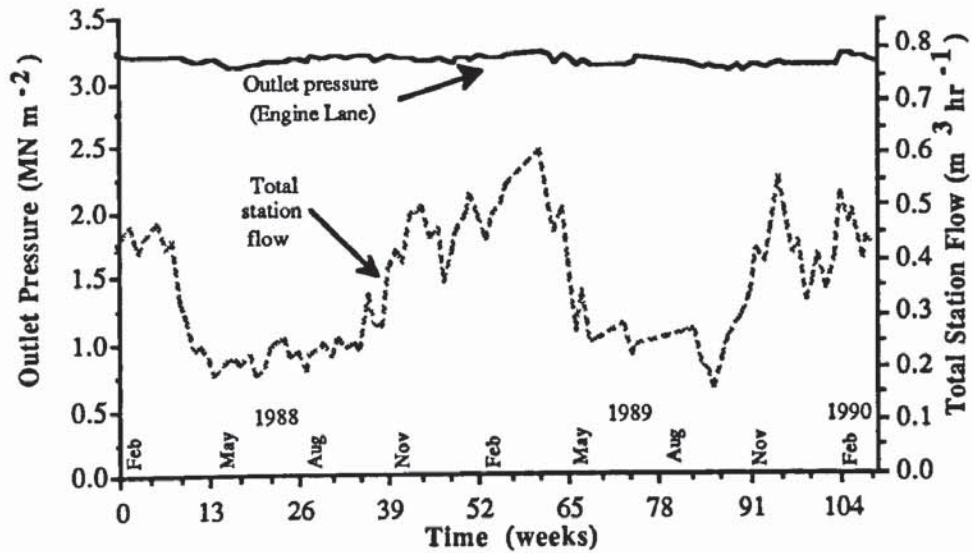
The average weekly air and ground (at pipe depth) ambient temperatures are shown in Figure 7.15. Both the air and ground temperatures follow an approximate sine wave with a period of approximately 1 year. The air temperature oscillates between 2.5 and 17.5°C but, the ground temperature oscillates between 4.5 and 14.5°C and, lags behind the air temperature. These findings are consistent with the discussion in Section 3.2.3.1. It is evident from Figure 7.16 that the inlet temperature at Blackrod PRS is effectively that of the ambient ground temperature throughout the trial period.

Rainfall was monitored from week 14 onwards and a bar chart representation of the weekly rainfall is provided in Figure 7.17.

7.14a



7.14b



7.14c

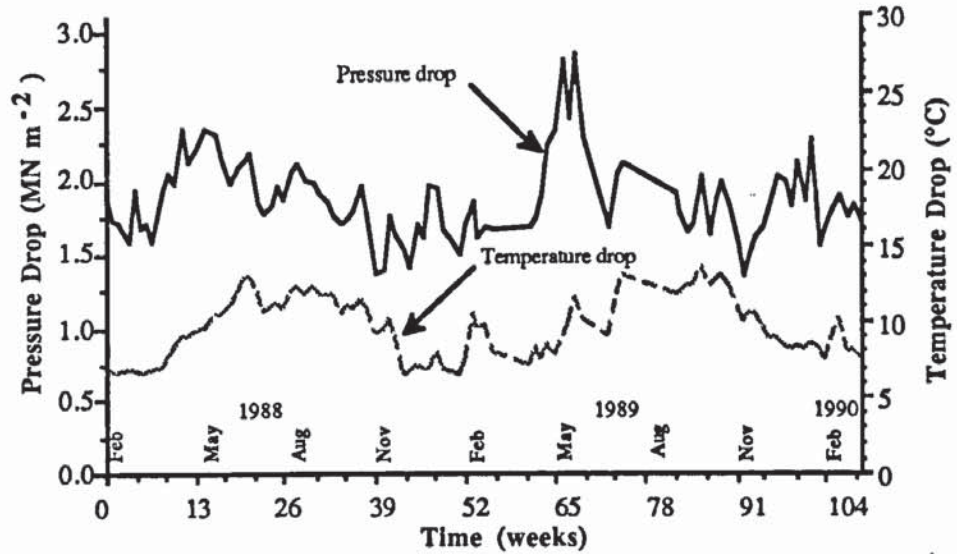


FIGURE 7.14 Average Weekly Operating Conditions during the Monitoring Period at Blackrod PRS.

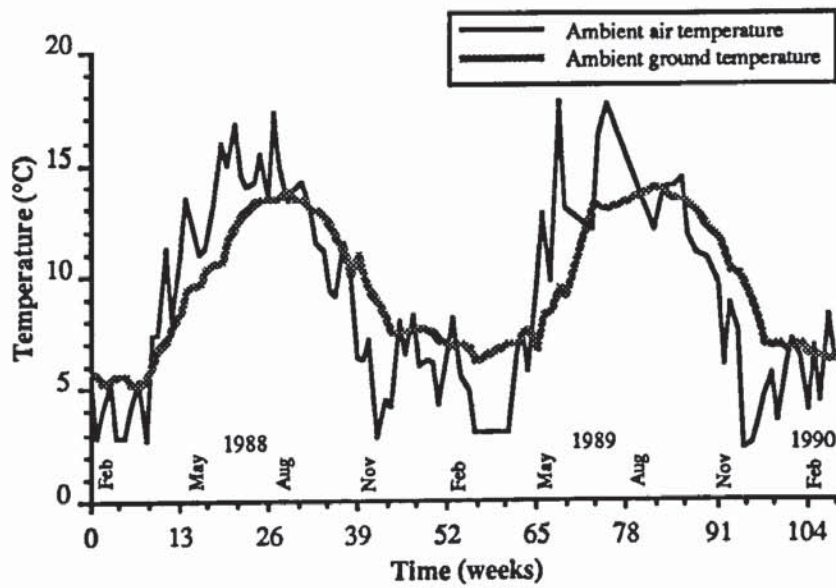


FIGURE 7.15 Average Weekly Ambient Air and Ground (at pipe depth) Temperatures.

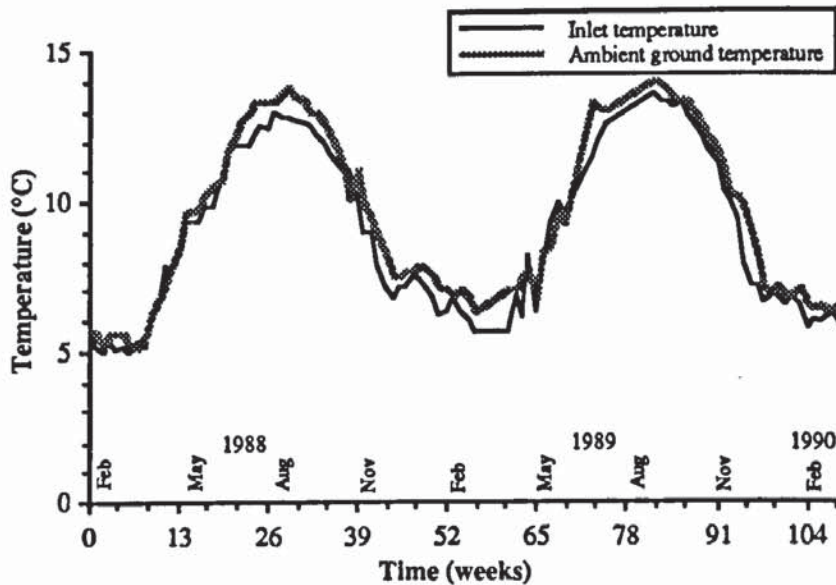


FIGURE 7.16 Average Weekly Inlet Pipe and Ambient Ground (at pipe depth) Temperatures.

7.7.3 Downstream Sites.

Discussion of results in this section is concentrated on Site C since this is the site where ground cracking was observed during the trial and was also the most intensively monitored.

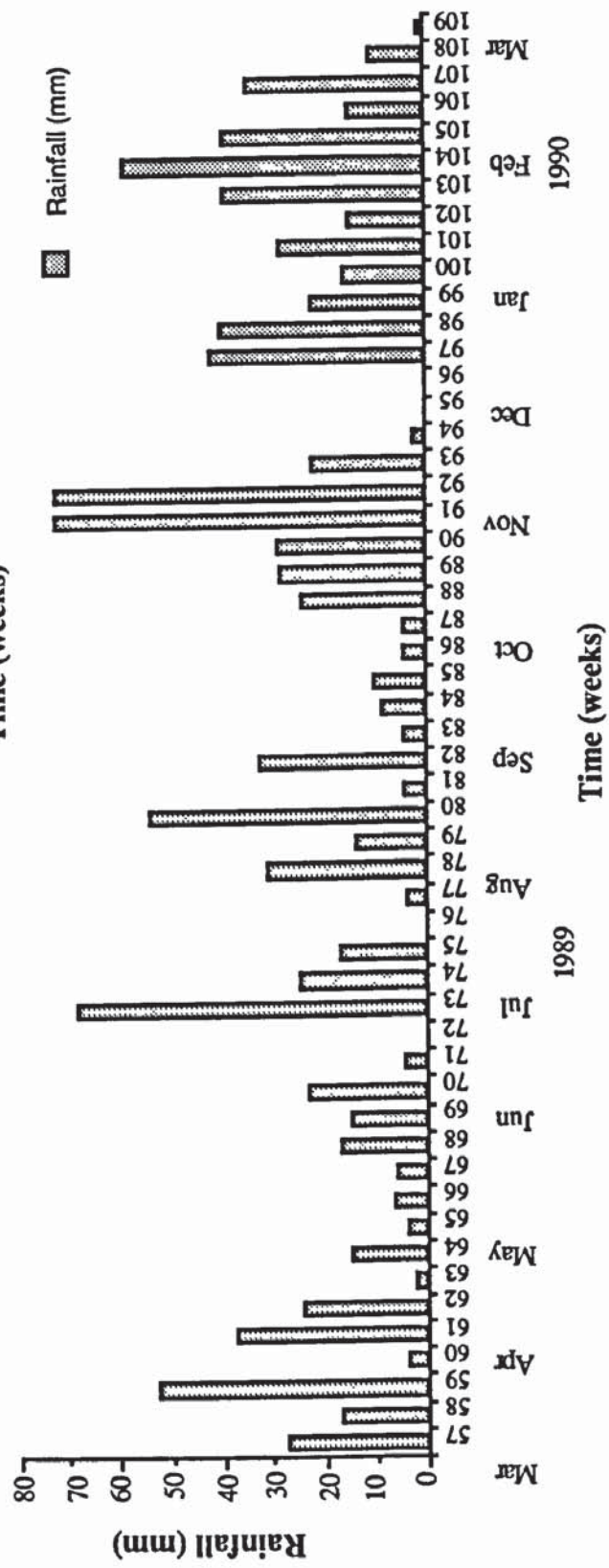
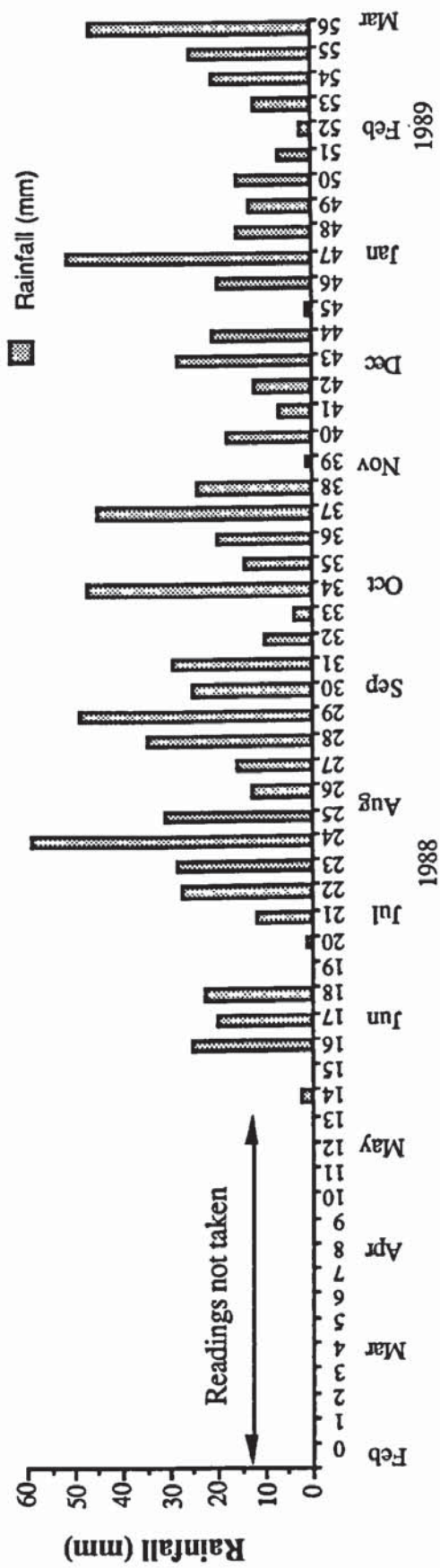


FIGURE 7.17 Weekly Rainfall During the Trial Period (3/2/88 to 7/3/90)

7.7.3.1 Soil Classification.

The soil classifications of the downstream Sites (A, B and C) are provided in Table 7.9

	Site A	Site B	Site C
Gravel Content	17 %	30 %	22 %
Sand Content	6 %	6 %	13 %
Silt Content	50 %	42 %	60 %
Clay Content	27 %	21 %	5 %
Organic Content	-----	-----	15 %
Liquid limit	33 %	36 %	68 %
Plastic limit	15 %	18 %	--- %
Plasticity index	18 %	18 %	NP
Shrinkage limit	10 %	9 %	6 %
Dry density	1890 kg m ⁻³	1930 kg m ⁻³	910 kg m ⁻³

TABLE 7.9 Soil Properties at Sites A, B and C.

7.7.3.2 Thermal Regime.

Data collection was effected by manual readings using a digital hand held temperature indicator (Digitron Model 3204), from 26/7/88 until the relevant data loggers were installed (Table 7.10 summarizes the installation dates of the downstream data loggers). The results from the probes closest to the ground surface are expected to have been affected by daily ambient air conditions.

Data Logger	Site	Function	Date Installed
40	A	24 channel PRT	21/10/88 (Week 37)
41	A	4 channel Soil Stress	Jan 1990 (Week 101)
42	B	24 channel PRT	28/10/88 (Week 38)
43	B	4 channel Soil Stress	Jan 1990 (Week 101)
44	C	24 channel PRT	23/12/88 (Week 46)
45	C	4 channel Soil Stress	Feb 1989 (Week 52)

Note: Week numbers are approximate and apply to the nearest week.

TABLE 7.10 Installation Dates for the Downstream Data Loggers.

The temperature regimes at Site C at 90°, 60°, 45°, 30° and 0° to the vertical above the pipe are shown in Figures 7.18, 7.19, 7.20, 7.21 and 7.22 respectively and the probe numbers refer to Figure 7.2 and the positions given in Table 7.2. The results are provided on a weekly average format using either manual or data logger readings. It is evident that after the data logger (DL44) was installed, only minimal data were collected and this has been attributed to the unreliability of the data logger. A similar pattern emerges for the temperature data loggers at Site A (DL40) and Site B (DL42), and these are given in Appendix C. Figures 7.18-22 illustrate that for Site C, the frozen annulus extended between 150 and 200 mm from the pipe wall during periods of low temperature operation. It is

uncertain whether the frozen annulus was elliptical, with its smallest dimension directly above the pipe crown, or circular in shape.

At Site A there was a much larger frozen annulus which reached a maximum of approximately 400 mm horizontally from the pipe and over 250 mm at 30° to the vertical (Appendix C). The data for Site B shows that the frozen annulus extended over 450 mm horizontally from the pipe wall and over 150 mm vertically upwards from the pipe crown (Appendix C). These two sites indicate that the frozen annulus was elliptical with its smallest dimension from the pipe wall directly above the pipe centre.

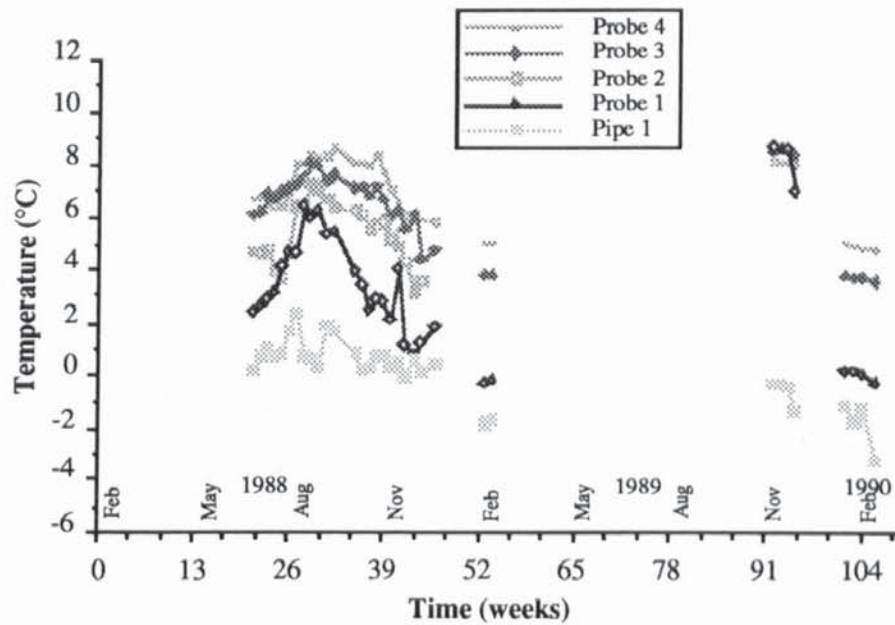


FIGURE 7.18 Average Weekly Temperature Profile at 90° to the Vertical at Site C.

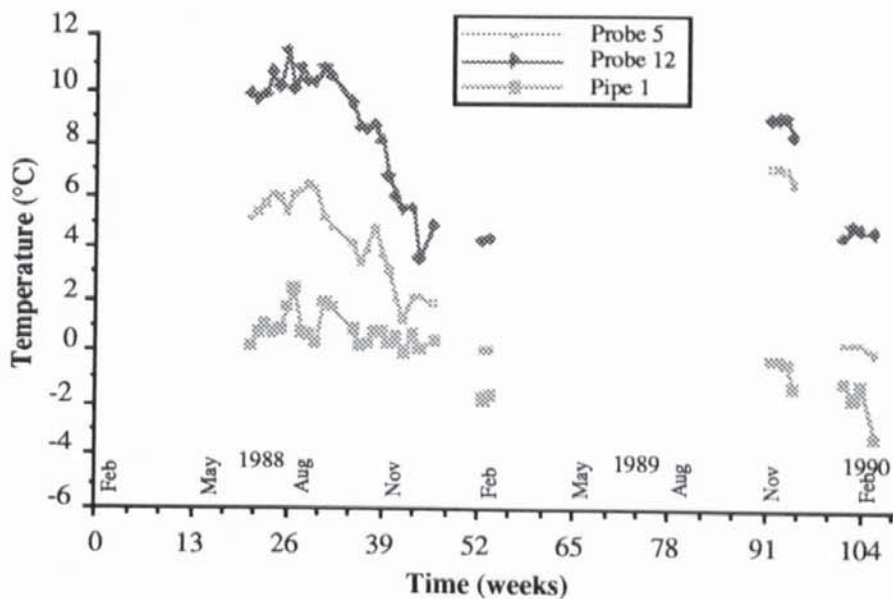


FIGURE 7.19 Average Weekly Temperature Profile at 60° to the Vertical at Site C.

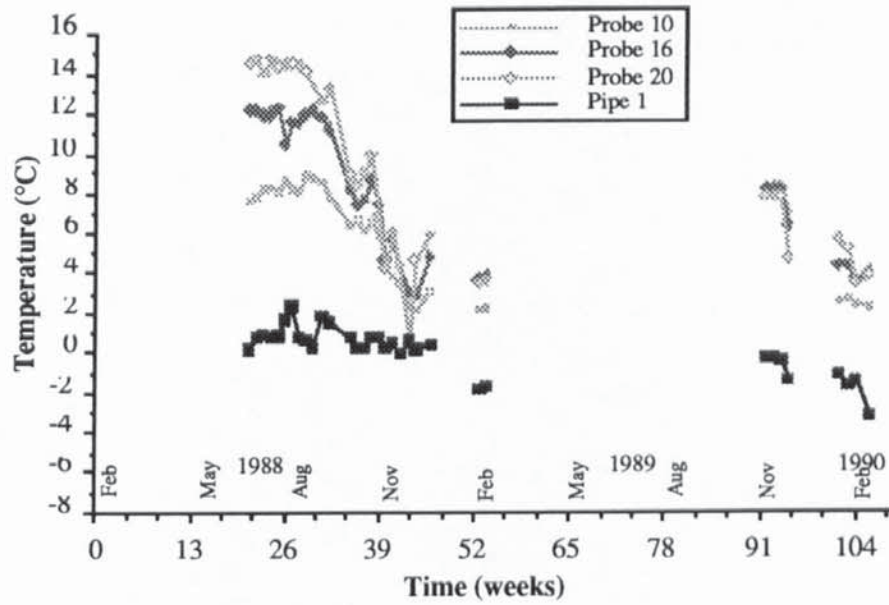


FIGURE 7.20 Average Weekly Temperature Profile at 45° to the Vertical at Site C.

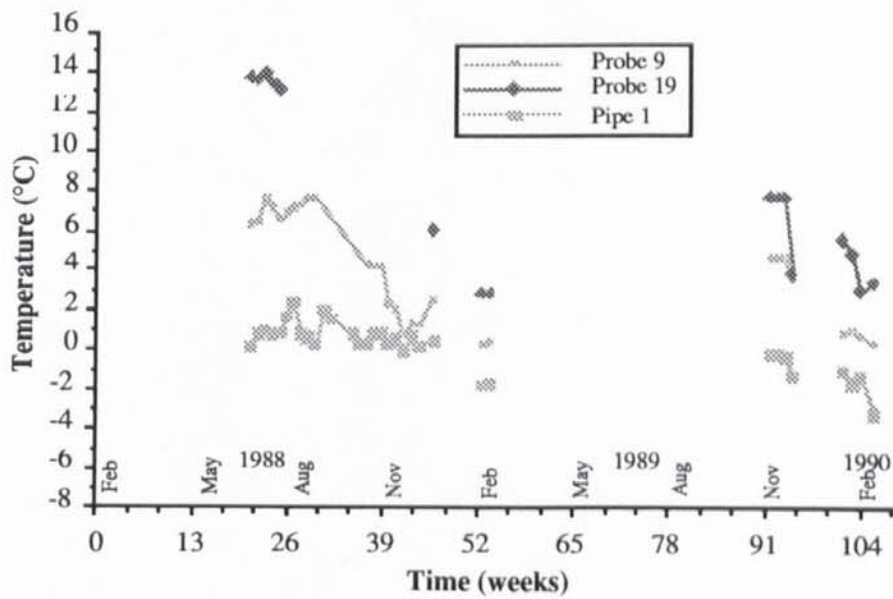


FIGURE 7.21 Average Weekly Temperature Profile at 30° to the Vertical at Site C.

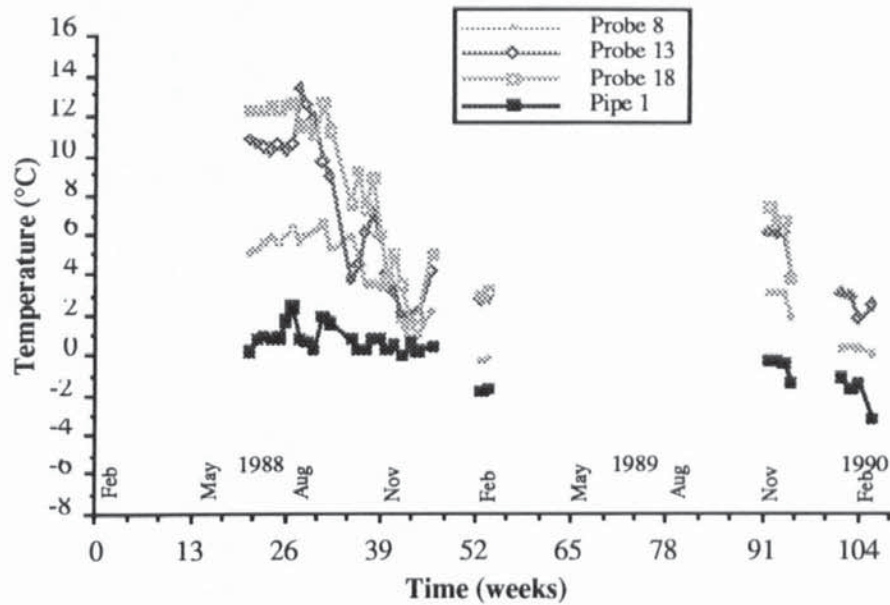


FIGURE 7.22 Average Weekly Temperature Profile at 0° to the Vertical at Site C.

7.7.3.3 Hydraulic Regime.

The water table levels for Sites A, B and C are shown in Figure 7.23 and these were observed from standpipes. At Site A the soil above the pipe was a clay liner overlying a quarry site which had been compacted by mechanical equipment during placement and water was often observed in ground surface depressions. The standpipe at Site A was broken a number of times by farming activities. Site B is in the same area as Site A, but the water table was at pipe invert depth in contrast to Site A, where it was at pipe crown level until the standpipe was broken.

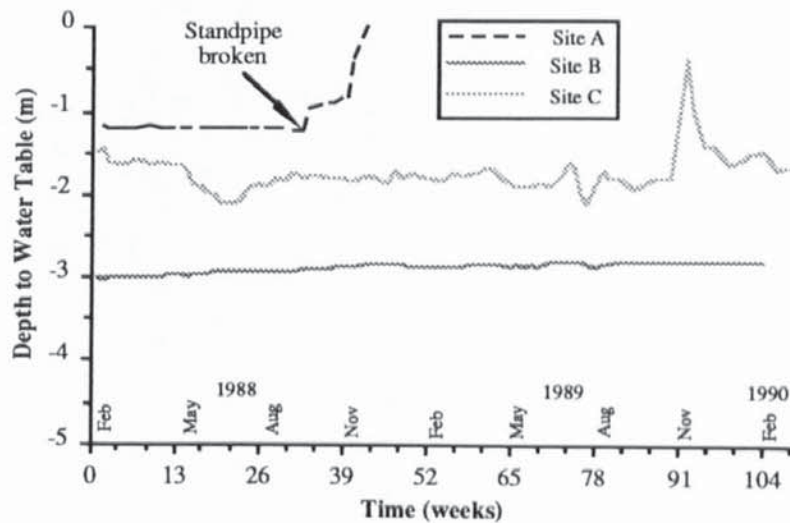


FIGURE 7.23 Depth to Water Table at Sites A, B and C.

At Site C the water table was more prone to fluctuations and there was an anomalous rise during November 1989 (Weeks 91-94). This resulted from the farmer altering the drainage system causing the water to flow directly under Site C, but there was a break in the drainage pipe close to the gas pipeline. Local flooding of this area ensued and this was augmented by the heavy rainfall during this period (Figure 7.17). Subsequently the drainage pipe was repaired and the water table fell to 1.6 m that is 0.2 metres above the pipe invert level.

At Site C the results from the thermocouple-psychrometers are shown Figure 7.24, and, the position of the probes are given in Figure 7.3 and Table 7.3. A positive output indicates that a positive pore water pressure was observed from most probes (Figure 7.24), but the instrument is only capable of measuring a negative pore water pressure. This either indicates that the instruments were affected by chemicals in the soil that produced a corrosive reaction or that positive outputs are observed at zero or positive water potentials. Small positive outputs have been discussed by Brown and Bartos (1982) under saturated conditions. Most of the results indicate positive potentials between 0 and 5 bars, the peaks above this occur at the same time for most of the probes and may be due to errors induced when water entered the microvoltmeter housing box and so unfortunately these data are of little value to the main investigation. The outputs for Sites A and B are given in Appendix C.

7.7.3.4 Soil Stress Regime.

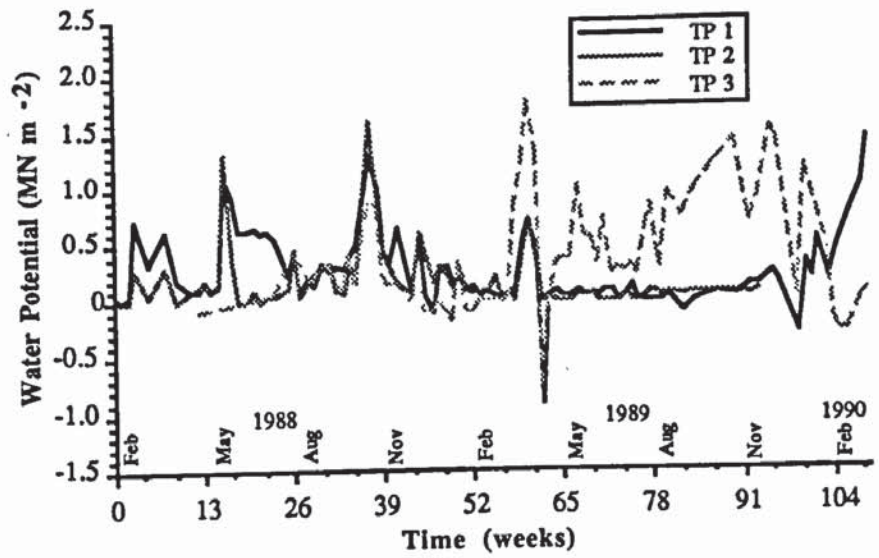
Late installation and improper data logger design resulted in data loss, but initial results in the trial indicated that monitoring of this regime would only provide peripheral information and would not deflect from the objectives of the project, since the soil pressure cells were primarily installed to provide information on when ground cracking was initiated.

7.7.3.5 Pipeline Movements and Strains.

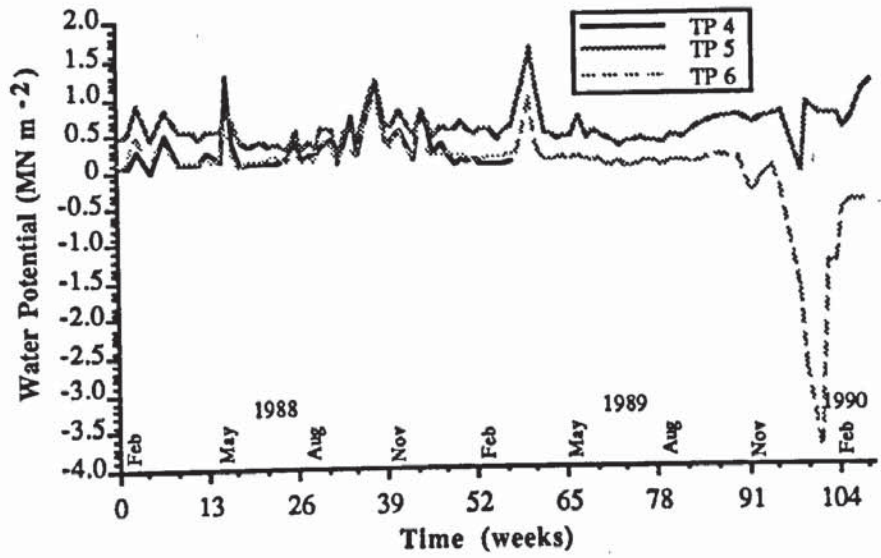
At Site C the pipe movement at each of the three pipe heave stations shows a similar displacement profile with time (Figure 7.25). The total pipe heave during the 1989/90 Pre-heating Season was greater than that observed during the 1988/89 Season and this can be attributed to pipeline operating at -2°C during the two months previous to the trial period (Figure 7.26). Thus substantial heave had taken place prior to the trial period. During the trial periods there was a rapid average pipe heave rate of 1.07 and 1.37 mm/day for the 1988/89 and 1989/90 Pre-heating Seasons respectively. Previous to first and second trial periods the average pipe heave rate was 0 and 0.29 mm/day respectively.

Figure 7.25 shows an anomalous peak in the pipe movement profile at Week 92 (9/11/89) and Figure 7.26 shows a temporary outlet temperature drop below 0°C during Weeks 88 to 90 (12/10/89 to 26/10/89), but data was not available for the actual pipe temperature at Site

7.24a 90° to Vertical



7.24b 45° to Vertical



7.24c 0° to Vertical

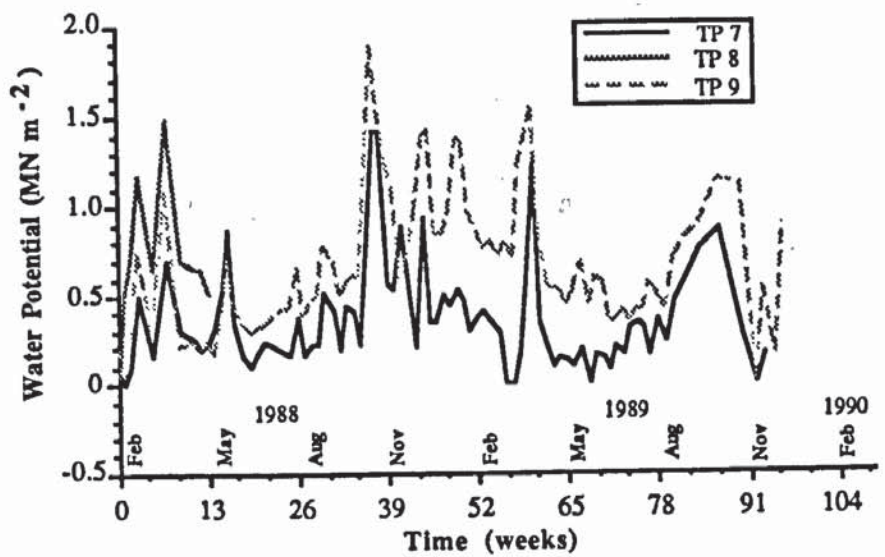


FIGURE 7.24 Results from Thermocouple-Psychrometers at Site C.

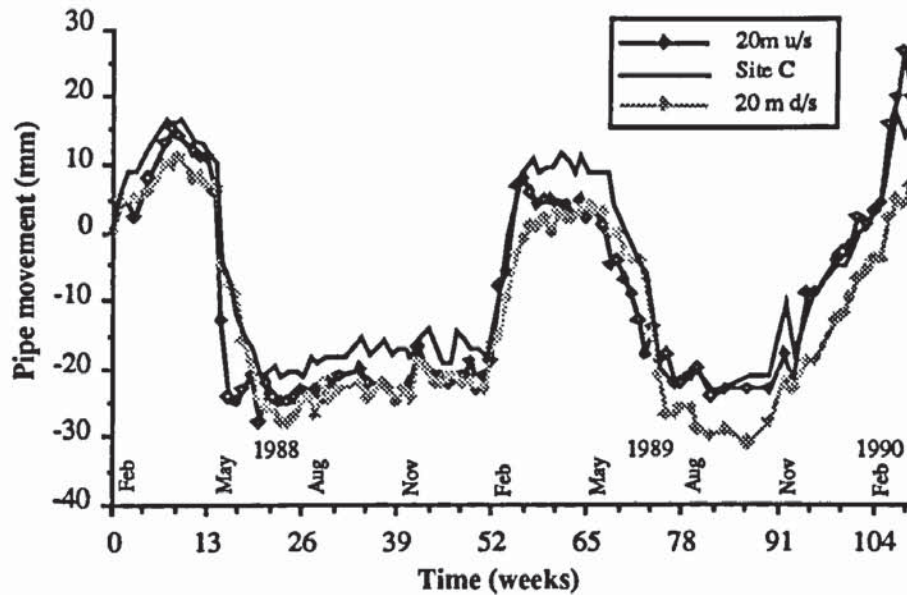


FIGURE 7.25 Pipe Movement at the Three Pipe Heave Stations at Site C.

C. A more probable reason for the anomalous peak is the rise in the water table which started in Week 90 and reached a peak in Week 92 and, subsequently fell to close to its original level. The water level rose from 1.8 m, which is pipe invert level to 0.4 m, therefore the pipe was completely submerged and subject to buoyancy forces as discussed in Section 4.3.2.2. The time periods for water table rise and anomalous pipe movement coincided (Figure 7.27) indicating a relationship between these two variables but, more importantly, this indicates that buoyancy forces did not produce or add to the pipe heave being monitored during the trial periods.

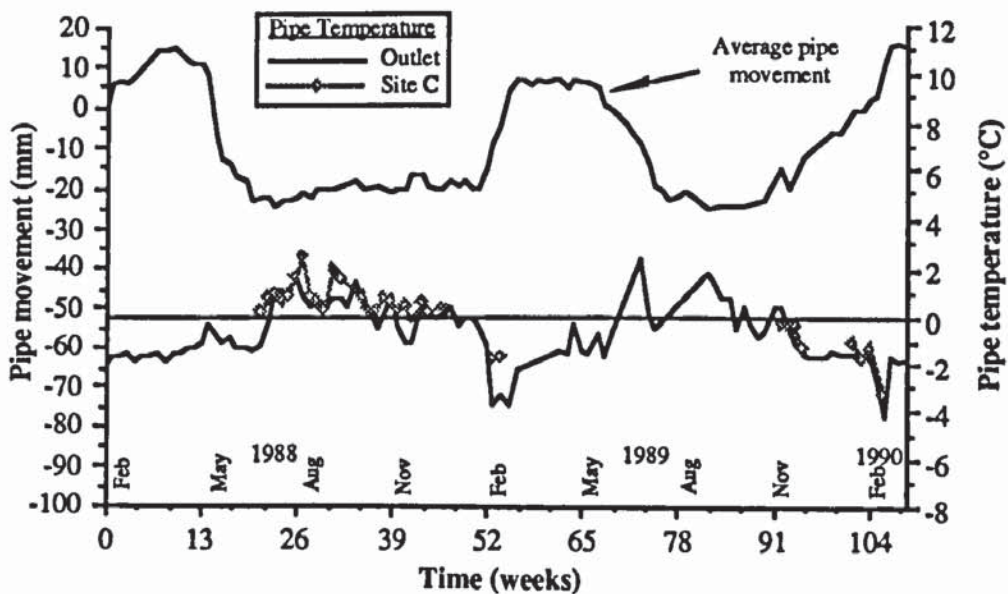


FIGURE 7.26 Average Weekly Station Outlet Temperature, Average Weekly Pipe Temperature and Average Pipe Movement during Monitoring at Site C.

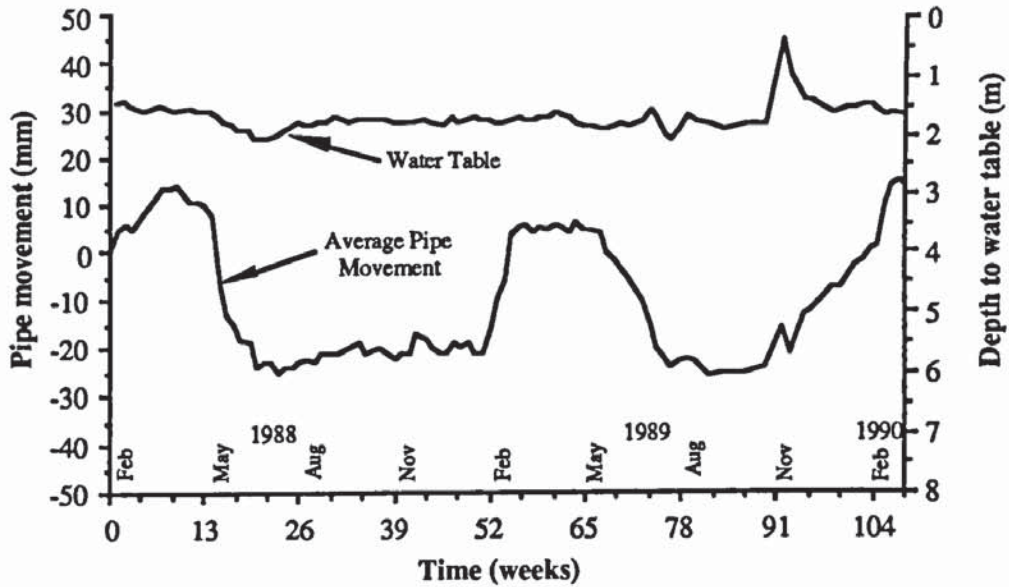


FIGURE 7.27 Average Pipe Movement and Water Table Movement during Monitoring at Site C.

The readings from vibrating wire strain gauge No.2 (Figure 7.28) were the only set that could be monitored throughout the period and, as the gauge was located on top of the pipe, it effectively measured the vertical pipe strain. The vibrating wire strain gauges at Site C show a definite seasonal pattern (Figure 7.28) indicating that the strain became more tensile during the winter periods and more compressive during the summer periods. These strain differences are not absolute since the gauges were installed after the pipe was laid so that the tie-in temperature, pipeline construction and previous in-service strains have not been assessed. Under normal pipeline operating conditions, with pre-heat, the pipe would typically be subject to increasing tensile strains in the winter since it is trying to contract, but soil friction acts in the opposite direction thereby inducing tensile strains (Herbert and Leach, 1990). A similar concept holds for compressive strains induced in the summer (Herbert and Leach, 1990). This is shown in Figure 7.28, however the amplitude of the strain curves No. 1 & 2 was greater than expected and the extra strain may be due to bending strains.

The strains recorded are not significant in comparison to the Yield Strain of approximately 2000 micro strain, assuming a yield stress of 413 Nmm^{-2} for a Grade X60 Steel Pipe (ASME, 1986), Young's Modulus of 210 KN mm^{-2} and elastic behaviour. The step in the curves is a product of the "forced" temperature control of the pipeline. The strain change resulting from the temporary increase in the water table is also clearly seen in November 1989.

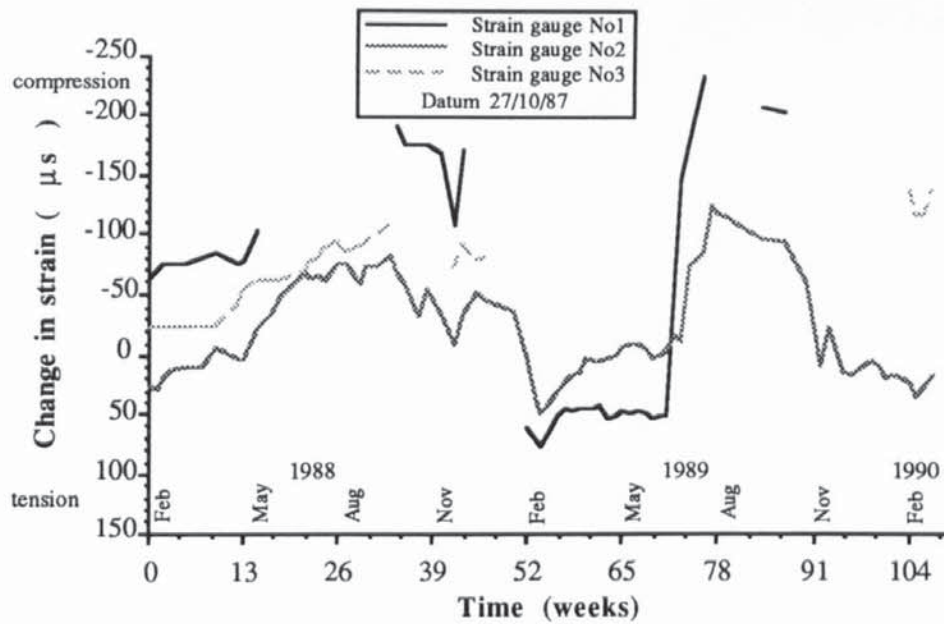


FIGURE 7.28 Vibrating Wire Strain Gauge Readings for Gauges at 0° (No.2), 90° (No.3) and 270° (No.1) at Site C.

All the pipe heave stations at Site A had a similar profile with time (Figure 7.29), but there was a distinct difference in the magnitude of their responses to pipe heave and settlement. Figure 7.30 shows the average pipe movement in relation to the pipe temperature (assuming the station outlet temperature is the same as the pipe temperature). It can be seen that this pipe movement is dependent on the pipe temperature fluctuations and it is clear that when there was a temperature drop below 0°C in Nov 1988 (Weeks 39-42) and Nov 1989 (Weeks 87-90), this resulted in an upward pipe movement. Pipe heave during the 1988/89 Pre-heating Season was less than 1987/88 and 1989/90 since the lowering of the pipe temperature below 0°C was delayed until February (Weeks 52-55) in the 1988/89 Season.

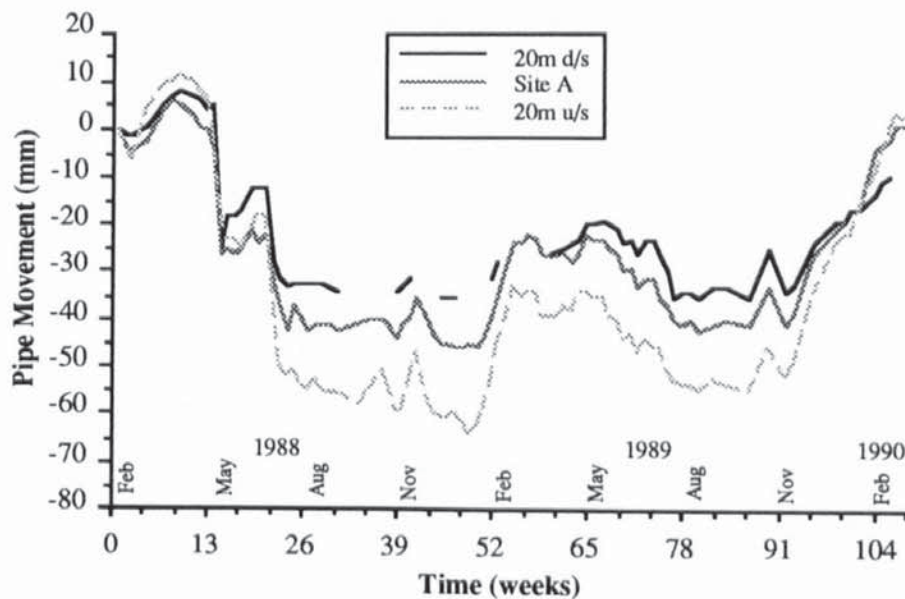


FIGURE 7.29 Pipe Movement at the Three Pipe Heave Stations at Site A.

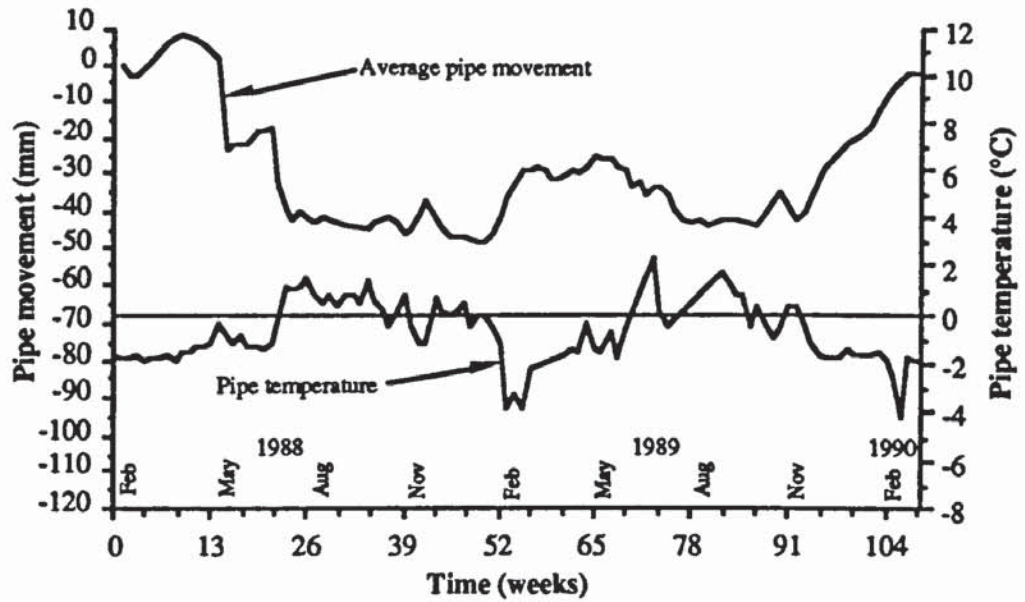


FIGURE 7.30 Station Outlet Temperature and Average Pipe Movement at Site A during the Monitoring Period.

It became evident at Site B that when the TBM and the check TBM were re-levelled, their levels had changed and this led to the installation of a new TBM further from Site B. At Site B the pipe was surrounded with a sand backfill with pipe cover of 150 mm and little pipe movement was expected until the frost front had advanced beyond it. After the new TBM was installed it was found that there was under 10 mm pipe movement (Figure 7.31) and this represented the least pipe movement at any of the three sites (Figure 7.32).

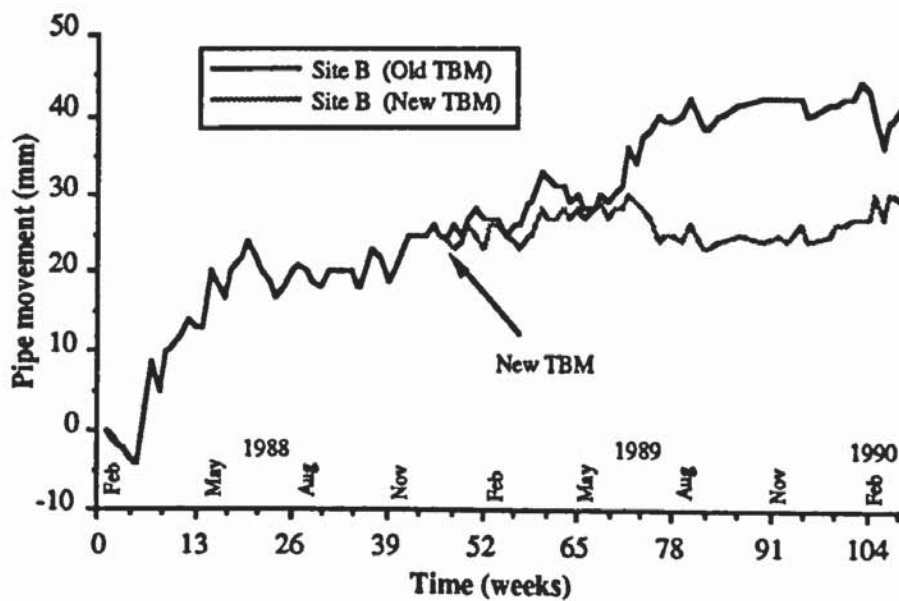


FIGURE 7.31 Pipe Movement at Site B Pipe Heave Station for New and Old TBM's.

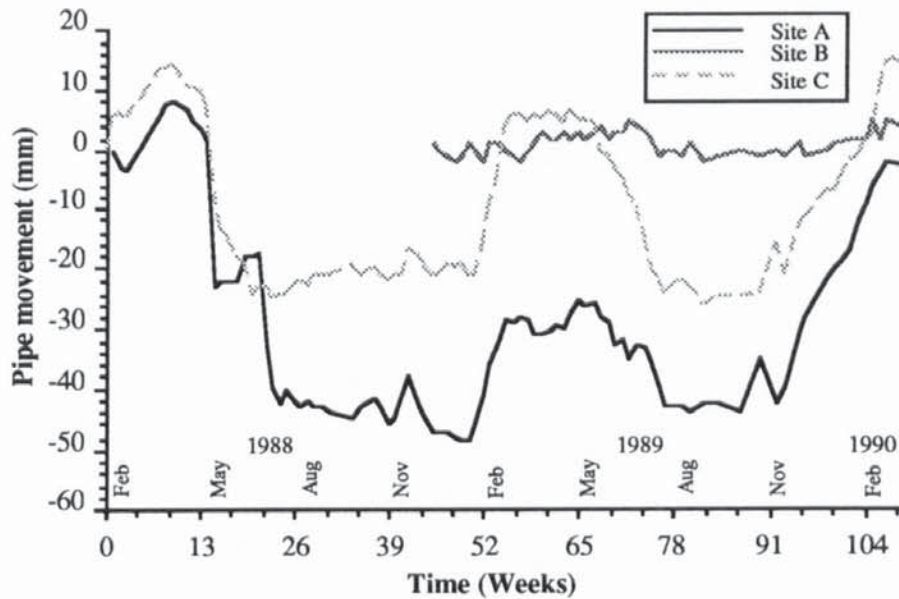


FIGURE 7.32 Average Pipe Movement at Sites A, B and C.

Figure 7.32 shows that the settlement at Site A, between March and July 1988, was significantly greater than that recorded at Site C. The PRS setpoint temperature had been at -2°C since early 1987 and thus, from October onwards, would have produced a frozen soil annulus around the pipe in areas close to the station outlet. The formation of the frozen annulus would have extended downstream with time and it is suggested that pipe heave at Site A, which is at the station outlet, would have been in excess of that taking place at Site C. Consequently the settlement to the pre-frozen annulus level would have been greater at Site A than Site C. This is reinforced by the results from the Pre-heating Season 1988/89 whereby the pipe returned to its previous level after thawing indicating that the subgrade had been conditioned by the freeze-thaw cycles. A similar situation would have occurred in the Pre-heating Season 1989/90 except that the pipe temperature increased above 0°C during November 1989 (Weeks 87-90) thereby negating the pipe heave observed previously at Site A (Figure 7.30).

7.7.3.6 Ground Cracking.

Site C was previously known to be the area most susceptible to ground cracking and so this site was subjected to the closest examination during the trial period. The area under examination was between MP(marker post)18 and MP21 which consisted of three fields used for pasture, and the total distance is 600 metres of which each field is approximately 200 m across.

During the 1987/88 Pre-heating Season ground surface fissures were observed intermittently between MP18 and MP19+50 m. In areas the surface fissures developed into ground cracks and these reached their maximum size on the 11/3/88 (Week 5), however cracking up to 10 mm width and 150 mm deep was only observed intermittently with most cracking limited to surface cracking (Figure 7.33).

The pipeline operating characteristics in the Pre-heating Season 1988/89 provided the greatest ground cracking with widths up to 50 mm and depths of 600 mm (Figure 7.34). Maximum cracking was recorded on 23/2/89 (Week 55) and subsequently these were filled-in using imported topsoil by sub-contractors. Plates 7.8 and 7.9 show cracking between MP18 and MP19 on the 16/2/89 (Week 54) and these cracks have a width of about 5 mm and penetrate up to 100 mm. The larger cracks that were observed on the 23/2/89 (Week 55) are shown in Plates 7.10 and 7.11, these have a width up to 50 mm and depths of up to 600 mm. Plate 7.12 shows the crack extending from MP19+20 m towards MP20 and at this point a trial hole was excavated to show the crack profile (Plate 7.13) revealing that the crack extended to the top of the frozen annulus. Maximum crack size occurred at maximum pipe heave which averaged 26 mm at Site C (Figure 7.32).

During the 1989/90 Pre-heating Season cracking reached a maximum on 14/2/90 (Week 106) , maximum widths of up to 20 mm and depths of 600 mm were recorded between MP19 and MP19+50 m (Figure 7.35). Ground cracks between MP19 and MP20 were recorded in the first 50 m, beyond this point there was a distinct depression across the line of the pipe that continued up to MP20 (Plate 7.14). Excavations to the top of the frozen annulus in this area showed no visible signs of cracking.

On 11th August 1989 (Week 79) trial pits in the area MP19 to MP19+50 m showed that cavities had formed between the ground surface and the pipe top (Plate 7.15 and 7.16). The trial pit shown in Plates 7.15 and 7.16 shows a cavity extending over the pipe at MP19+37.5 m, this had a height of 20 to 30 mm.

Figure 7.36 shows that the cavity was located approximately 400 mm below the ground surface and 350 mm above the pipe crown. Section YY, which is perpendicular to the line of the pipe, shows that the cavity was curved at a distance of over 200 mm from the pipe centreline (Figure 7.36c). However along the line of the pipe the cavity maintained a constant level of 350 mm above the pipe crown. The cavity extended 500 and 300 mm downstream and upstream respectively.

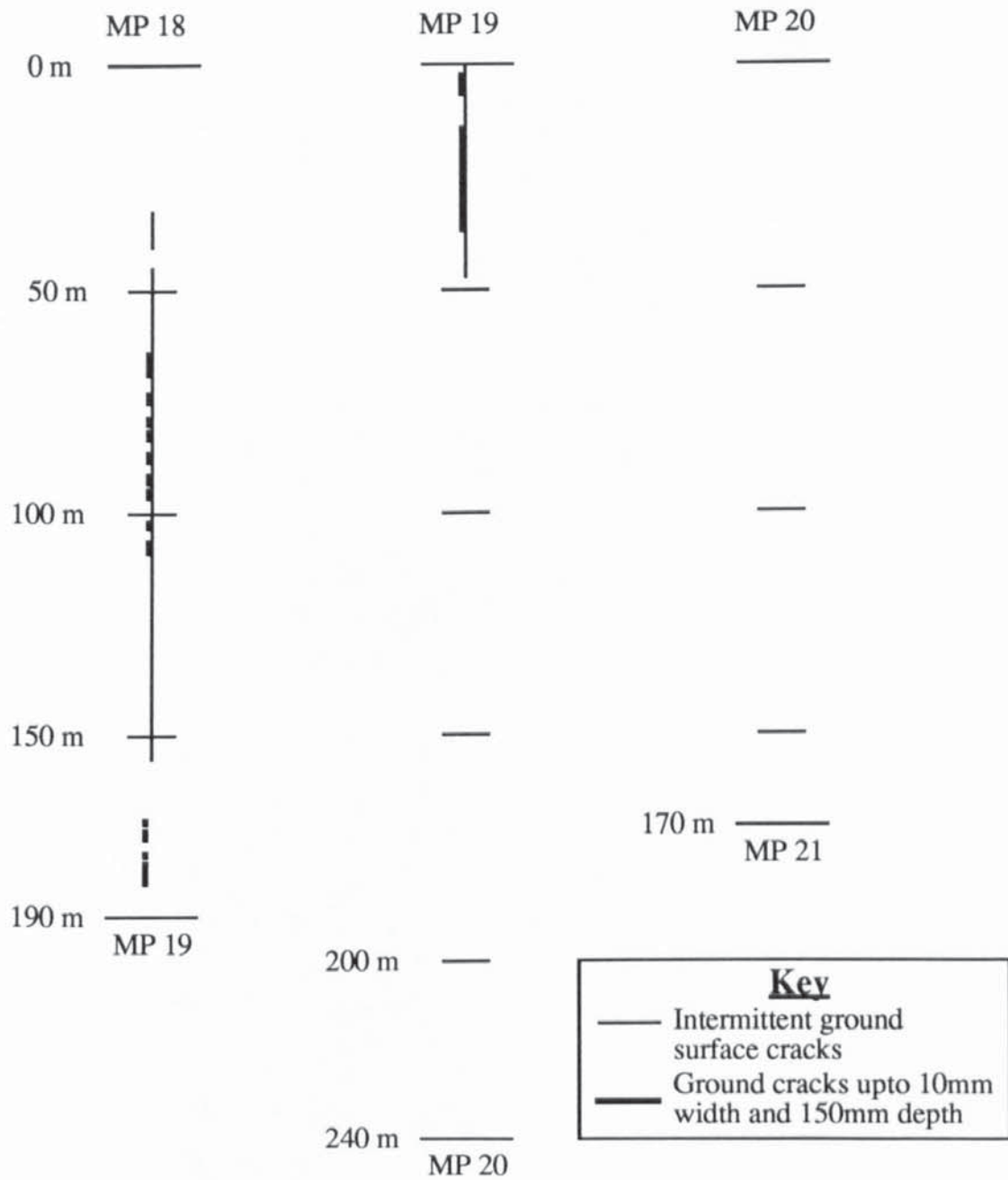


FIGURE 7.33 Illustration of Maximum Observed Ground Cracking during 1987/88 Pre-heating Season (Week 5 (11/3/88)) between MP18 and MP21.

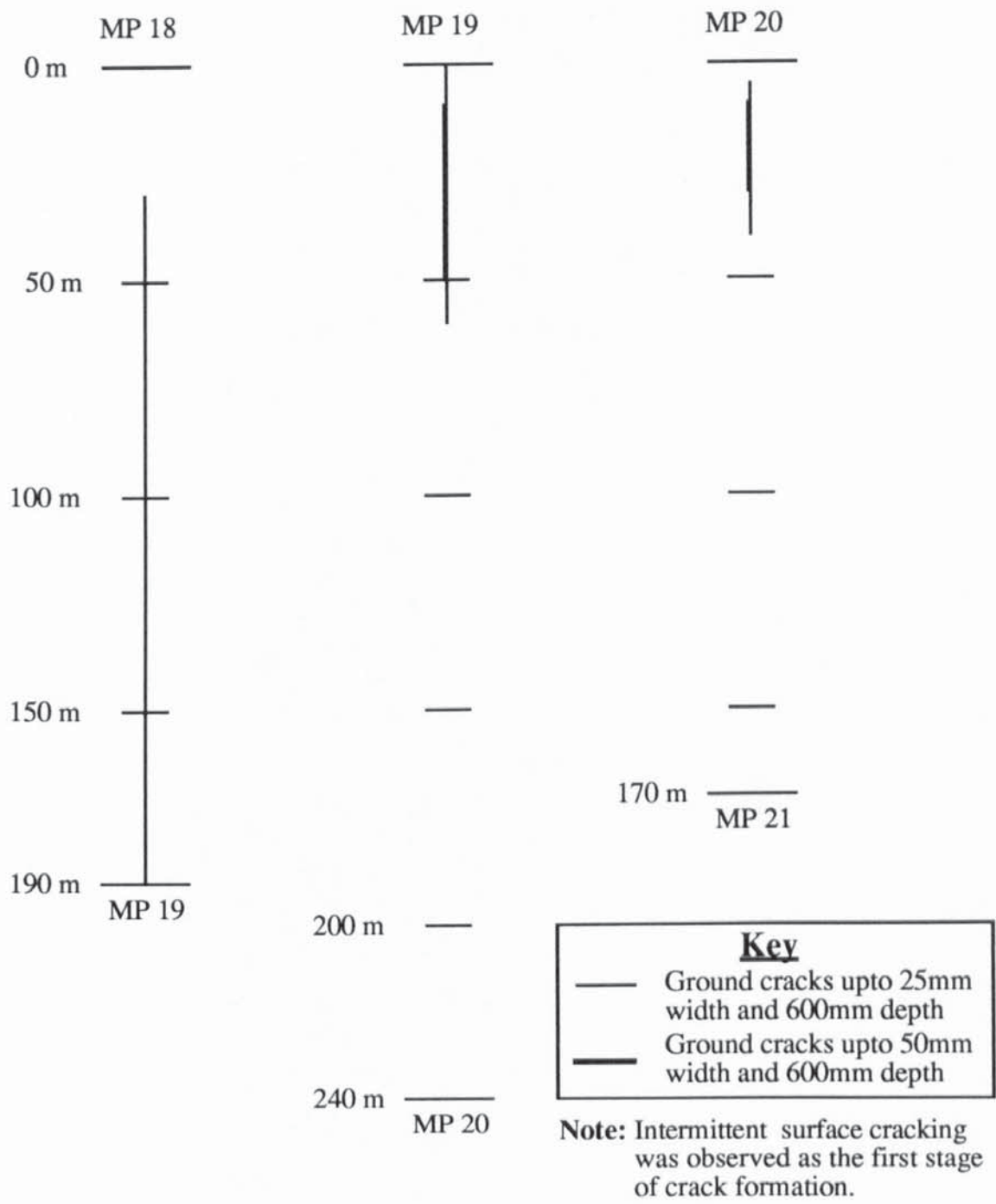


FIGURE 7.34 Illustration of Maximum Observed Ground Cracking during 1988/89 Pre-heating Season (Week 55 (23/2/89)) between MP18 and MP21.

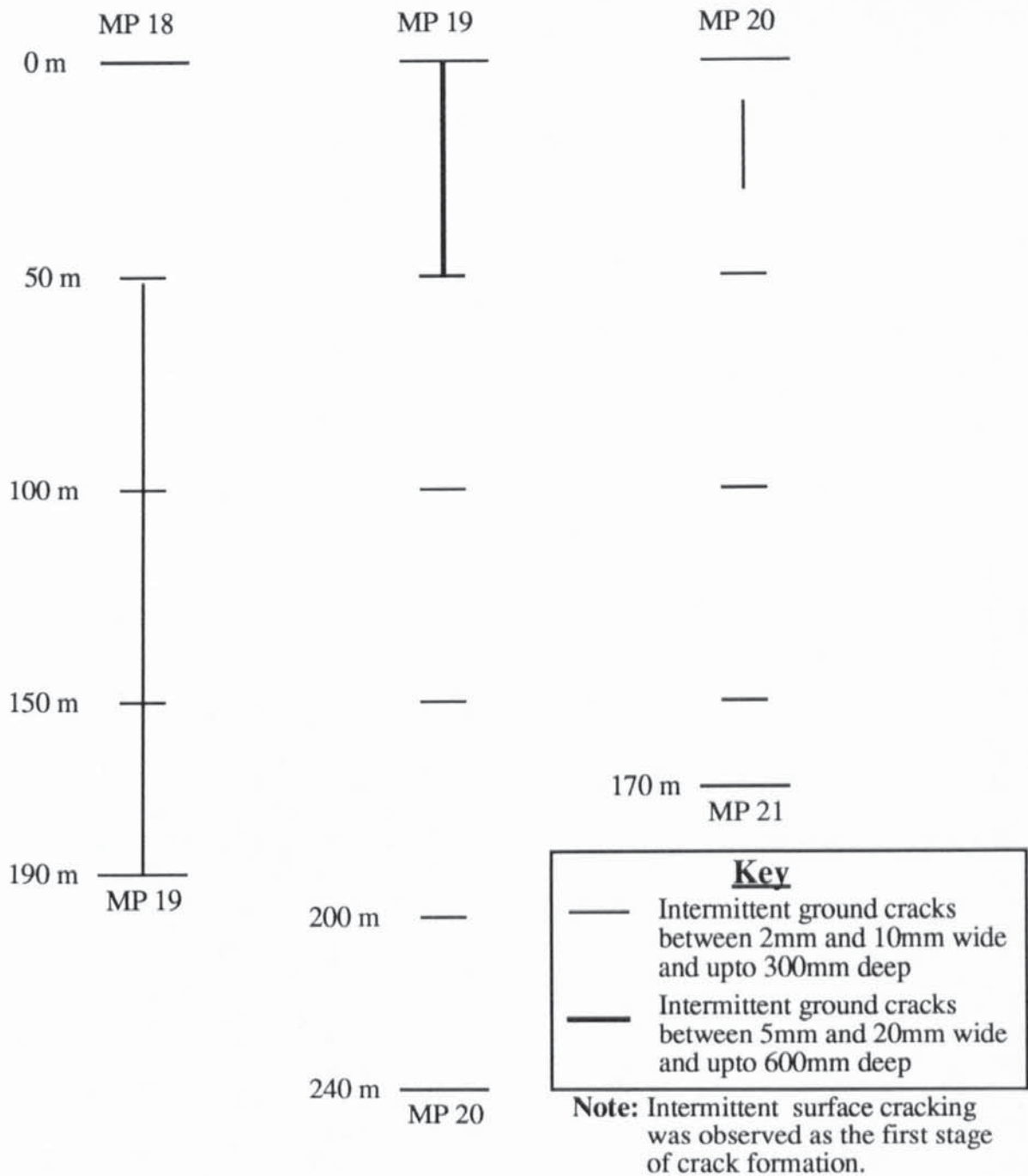


FIGURE 7.35 Illustration of Maximum Observed Ground Cracking during 1989/90 Pre- heating Season (Week 106 (14/2/90)) between MP18 and MP21.



PLATE 7.8 Typical Ground Cracks between MP18 and MP19 on 16/2/89 (Week 54).



PLATE 7.9 Typical Ground Cracks between MP18 and MP19 on 16/2/89 (Week 54).



PLATE 7.10 Typical Ground Cracks between MP18 and MP19 on 23/2/89 (Week 55).



PLATE 7.11 Typical Ground Cracks between MP18 and MP19 on 23/2/89 (Week 55).



PLATE 7.12 Typical Ground Cracks between MP18 and MP19 on 16/2/89 (Week 54).



PLATE 7.13 Cross Section Through a Ground Crack between MP19 and MP20 on 23/2/89 (Week 55).



PLATE 7.14 Depression Across the Pipeline between MP19+50 and MP20.



PLATE 7.15 Cavity at MP19+37.5 m on 11/8/89 (Week 79).



PLATE 7.16 Cavity at MP19+37.5 m on 11/8/89 (Week 79).

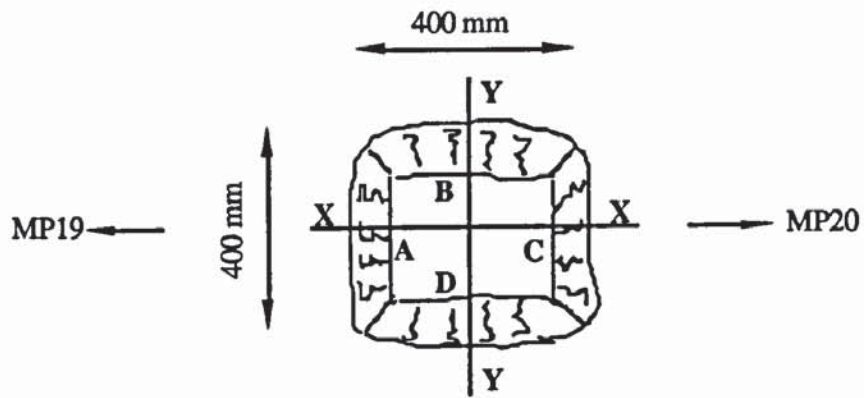


FIGURE 7.36a Plan View of the Trial Pit at MP19+37.5 m

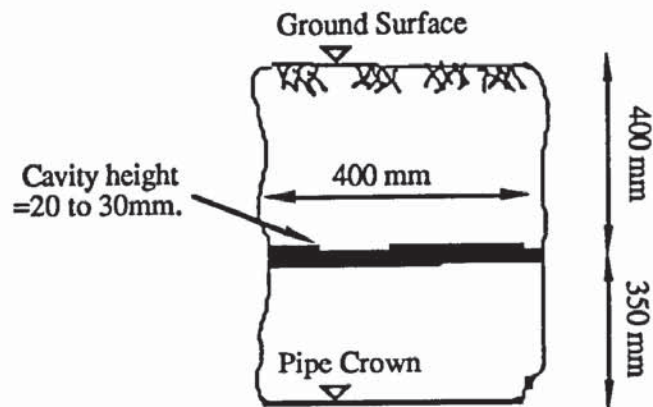


FIGURE 7.36b Typical View of the Faces of the Trial Pit

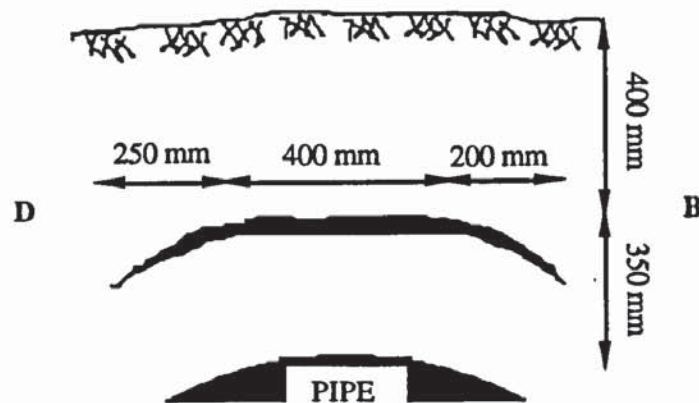


FIGURE 7.36c Section Y-Y

FIGURE 7.36 Illustration of the Cavity at MP19+37.5 m.

7.7.4 Pressure Reduction Station Monitoring.

This was designed specifically to investigate the effect of both pipe movement and the growth of the frozen annulus above the pipe on the ground surface profile perpendicular to the line of the pipe.

7.7.4.1 Pipe Movement.

The vertical movements of the pipe at Sites C' and D' are shown in Figure 7.37 and it is clear that the larger movements were observed at Site D' indicating that, at this point, the pipeline was more susceptible to frost heave displacements. At each location the depth of burial to the crown of the pipe was 600 mm, however, Site C' was located closer to a point of potential restraint than Site D'.

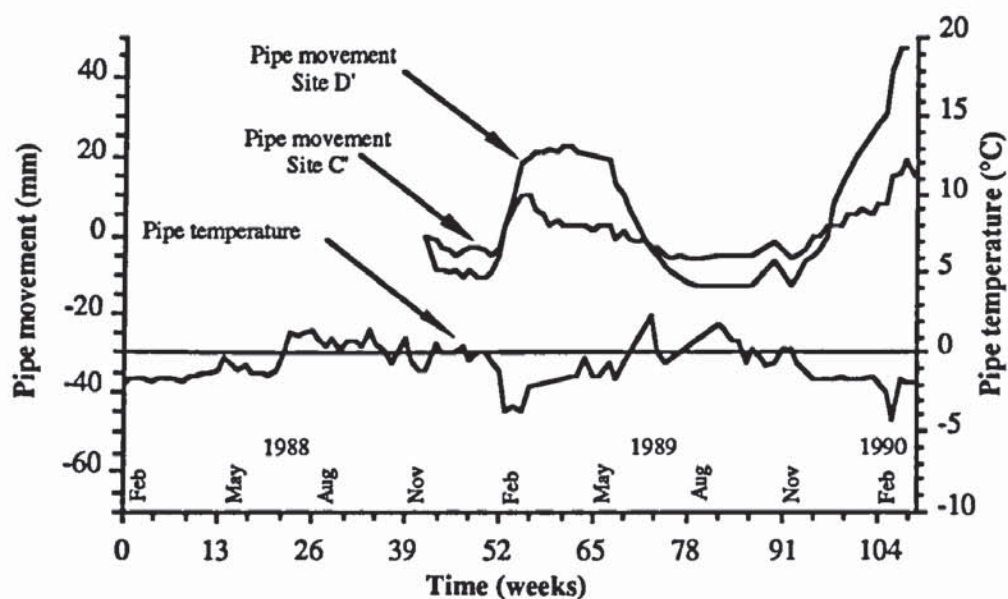


FIGURE 7.37 Pipe Heave and Pipe Temperature against Time for Sites C' and D' within Blackrod PRS.

Figure 7.38 shows that, during those trial periods when the outlet temperature of Blackrod PRS was lowered to -5°C , the frozen annulus grew rapidly. The frozen annulus extended to 300 mm horizontally from the pipe wall at the end of each trial. However, prior to the second trial a smaller frozen annulus had formed and this accounts for the pipe heave occurred prior to this trial (Figure 7.37).

7.7.4.2 Ground Movements.

The ground surface profile for Site C' in the trial periods is shown in Figures 7.39a and c, while Figure 7.39b shows the settlement that accompanied thawing of the frozen annulus after the first trial period. In the first trial the profiles for 9/2/89 (Week 53) and 16/2/89 (Week 54) have the shape approximating to a normal distribution curve, but on the 23/2/89

(Week 55) there is a distinct deviation away from this profile. This profile exhibits two peaks at approximately 0.4 m from the pipe centreline and a depression between these points. The soil mass between these two peaks rose slower than expected and this can be explained in terms of the ground surface cracks that opened during the period 16/2/89 to 23/2/89 (Weeks 54-55). Figure 7.40 shows the formation of ground cracks along the profile and reports only the major cracks after 16/2/89 (Week 54). Until the 16/2/89 (Week 54), the ground cracks had a maximum width of 1 mm and on the 16/2/89 (Plate 7.17) the major cracks were located at approximately 0.4 m from the pipe centreline. During the following week these cracks opened up to 8 and 6 mm (Figure 7.40) and their depths exceeded 50 mm, suggesting that the soil profile was moving unequally around these cracks as pipe heave continued. After the first trial the cracking reduced in size and on 16/3/89 (Week 58) the main cracks were under 1 mm in size (Figure 7.40). Figure 7.39b shows that by 31/3/89 (Week 60) the profile had dropped by a maximum of 20 mm and the two peaks could no longer be observed. By 30/6/89 (Week 73) the profile had settled to approximately its original shape and subsequently did not settle significantly.

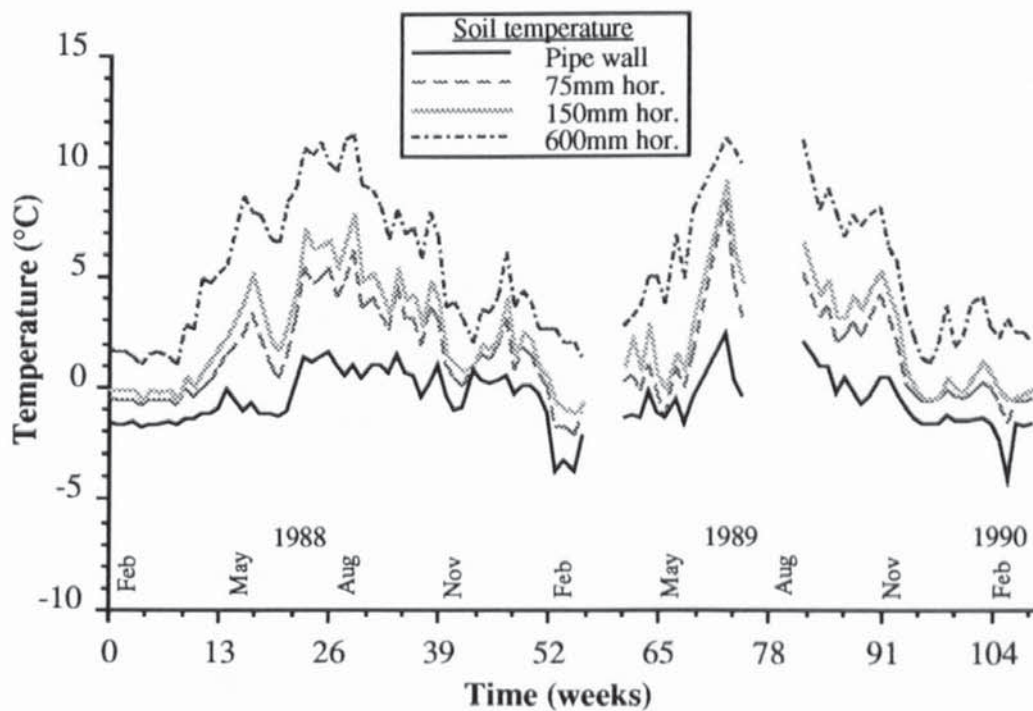


FIGURE 7.38 Horizontal Temperature Profile from the Pipe within Blackrod PRS.

During the 1989/90 Pre-heating Season the pipeline was operated at -2°C prior to the second trial period and significant ground heave was noted. However the upward movement was slower than in the first trial period and it was only after the start of the second trial that the two peaks again formed (Figure 7.39c). During the second trial there was a heavy period of rainfall (Figure 7.17) and no cracking was observed.

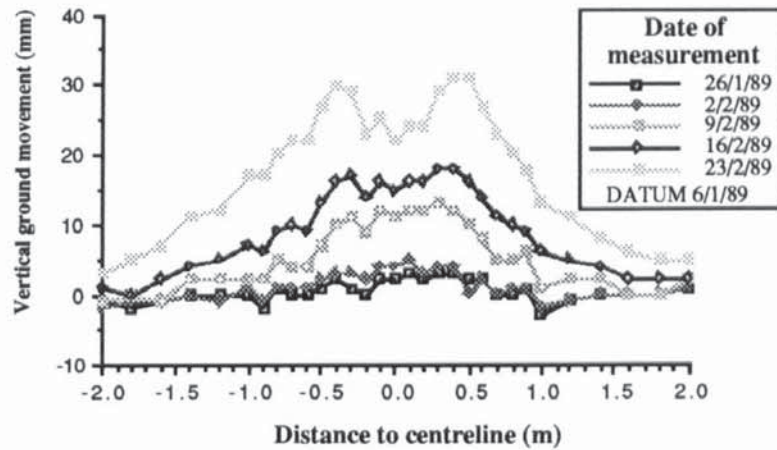


FIGURE 7.39a Ground Surface Profile Across the Pipeline at Site C' within Blackrod PRS from 26/1/89 to 23/2/89 (Week 51 to 55).

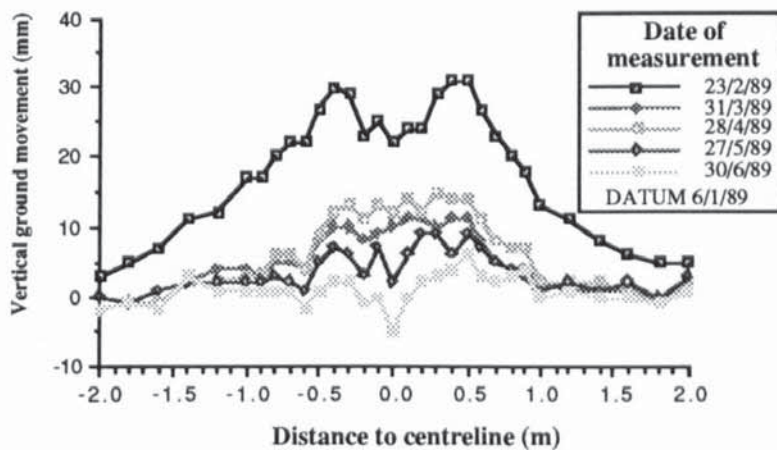


FIGURE 7.39b Ground Surface Profile Across the Pipeline at Site C' within Blackrod PRS from 23/2/89 to 30/6/89 (Week 55 to 73).

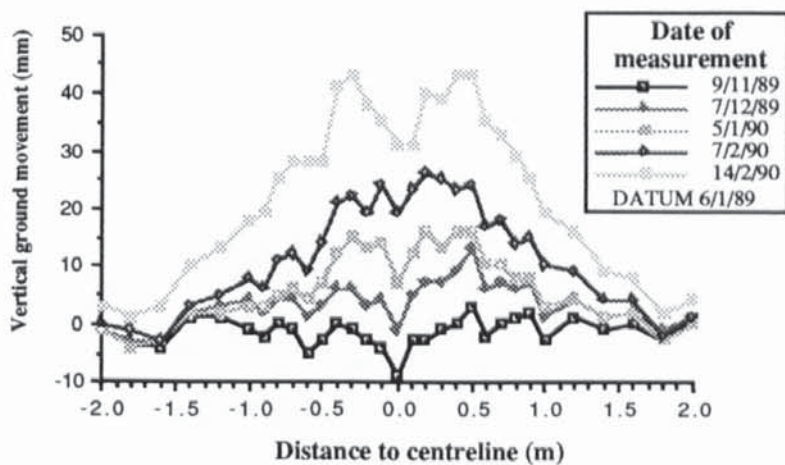
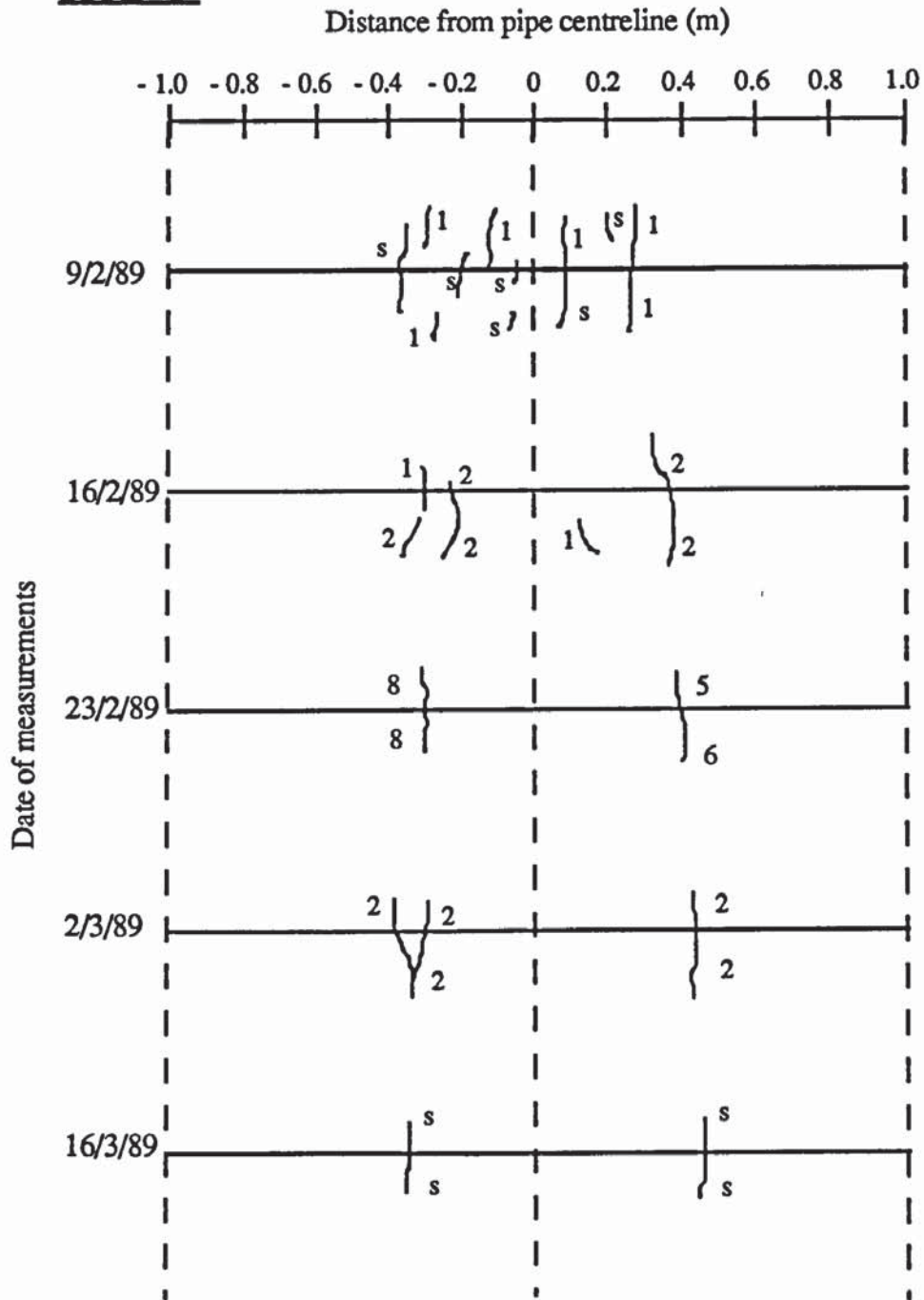


FIGURE 7.39c Ground Surface Profile Across the Pipeline at Site C' within Blackrod PRS from 19/11/89 to 14/2/90 (Week 92 to 106).

SITE C'



Note: Numbers indicate surface crack width in millimetres, s= surficial crack

FIGURE 7.40 Plan View of Ground Cracking Perpendicular to the Ground Surface Profile Apparatus at Site C' within Blackrod PRS from 2/9/89 to 16/3/89 (Week 53 to 58).



PLATE 7.17 Ground Cracks at Site C' within Blackrod PRS on 16/2/89 (Week 54).

During the first trial the ground heave at Site D' reached a maximum of 50 mm (Figure 7.41a) which is 20 mm more than that observed at Site C' (Figure 7.39a). A crack 5 mm wide was observed after 10 days of the trial, subsequently three 1 mm wide cracks were observed between 0.1 m either side of the pipe centreline (Figure 7.42). An inspection of Figure 7.41a reveals that there are no anomalous peaks which at Site C' were indicative of cracking. Again, as with Site C', as thawing proceeded the ground surface profile returned approximately to its original level (Figure 7.41b). Prior to the commencement of the second trial period (Week 105 (5/2/90)) there was over 30 mm of upward ground surface displacement produced by the normal operating outlet temperature of -2°C . When this temperature was lowered to -5°C in the second trial this produced a maximum of 75 mm displacement from the original level at the end of the first trial. However, during this second trial, two peaks formed at 0.2 m from the pipe centreline (Figure 7.41c) when the ground surface profile reached its maximum, but no cracks were observed.

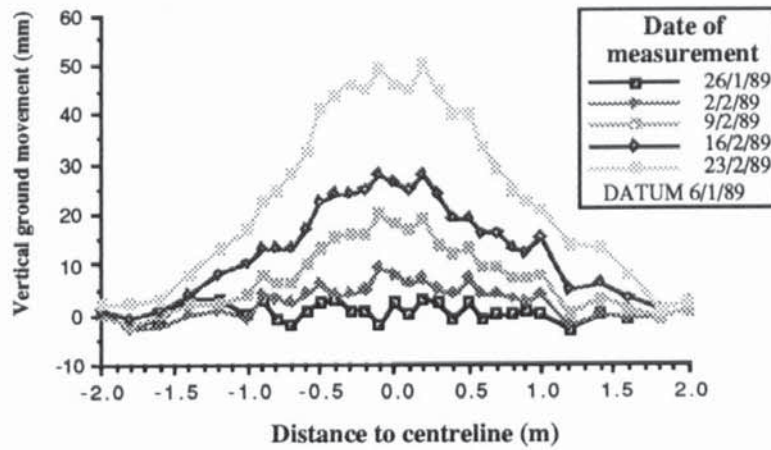


FIGURE 7.41a Ground Surface Profile Across the Pipeline at Site D' within Blackrod PRS from 26/1/89 to 23/2/89 (Week 51 to 55).

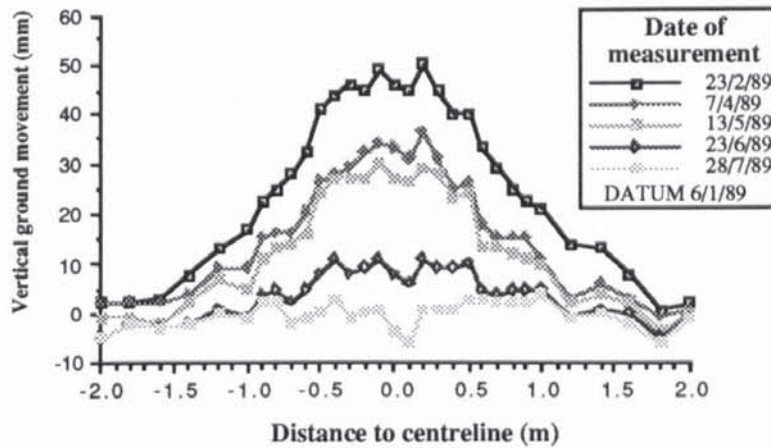


FIGURE 7.41b Ground Surface Profile Across the Pipeline at Site D' within Blackrod PRS from 23/2/89 to 28/7/89 (Week 55 to 77).

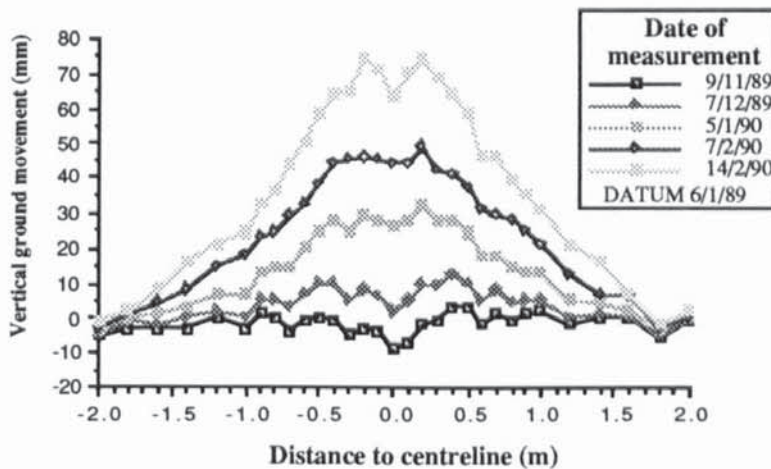


FIGURE 7.41c Ground Surface Profile Across the Pipeline at Site D' within Blackrod PRS from 9/11/89 to 14/2/90 (Week 92 to 106).

7.8 Summary.

Instrumentation of Blackrod to Engine Lane pipeline was undertaken to investigate ground cracking and pipe/frost heave under *in situ* conditions. Monitoring involved assessment of the pipeline operating characteristics, soil thermal, hydraulic and stress regimes around the pipe, together with pipe movement and strain. The pipeline has been subject to sub-zero operating temperatures since 1982 and thus the soil around the pipe had been subjected to freeze/thaw cycles. During a short period in each of the Pre-heating Seasons 1988/89 and 1989/90 the outlet at Blackrod PRS was lowered to -5°C . In each trial period, as the frozen annulus grew, rapid pipe heave was noted but, the amount of heave varied along that part of the pipeline operating below 0°C . Ground cracking was observed in each trial period along with pipe heave and both width and depth of cracking increased as the trial progressed. When the cracks reached a maximum the apex was observed to be within the frozen annulus, and widths of up to 50 mm were recorded at the ground surface. However, ground cracking was only observed between chainage 2600 and 3050 m (Site C) during the trial periods.

Monitoring of the ground surface perpendicular to the line of the pipeline was undertaken within Blackrod PRS. Results showed that ground surface heave exceeded pipe heave at the two points under consideration. Therefore frost heave in the frozen annulus both above and below the pipe produced ground surface displacements. Ground surface heave decreased with increasing distance from the pipe centre and its shape was observed to approximate to a normal probability distribution curve. Slight ground surface cracks were recorded during the 1st trial, but no cracking was reported in the 2nd trial due to heavy rainfall. This large-scale trial indicated that ground cracking was dependent on frost heave that in turn is also dependent on both pipeline operating conditions and soil conditions. Thus a small-scale laboratory model was designed and constructed to investigate the dependence of ground cracking on frost heave under controlled pipe and soil conditions.

CHAPTER 8 SMALL-SCALE LABORATORY MODEL

8.1 Introduction.

Results initially from the questionnaire (Chapter 6) have indicated that along a pipeline that is known to exhibit heave, there is a strong probability that cracking will also appear. This has subsequently been supported by the large-scale trial at Blackrod A.G.I.(Chapter 7) which also indicated a strong relationship between frost heave and ground cracking. The final objective was to study the ground cracking phenomena under laboratory controlled conditions. The model was designed to investigate both the relationship between frost heave and ground cracking, and whether cracking had a similar shape to the classical pattern reported by Casson (1984) during pipe lifting tests.

8.2 Objectives.

The small-scale laboratory model study represents the final stage in defining a mechanism for ground cracking around large-diameter chilled gas pipelines. The objectives were to:-

1. Produce ground cracking under laboratory controlled conditions,
2. Quantitatively describe pipe heave against ground surface movement,
3. Quantitatively describe pipe heave and ground surface movement in relation to crack formation and growth,
4. Investigate the development soil suctions in the soil mass during the growth of the frozen annulus,
5. Investigate the failure planes in the soil mass.

In order to address these objectives, the following monitoring was undertaken:-

1. Vertical pipe and ground surface movement,
2. Fundamental investigation of the soil thermal and hydrological regimes, special attention being directed to the soil mass above the pipe,
3. Ground surface detailing of crack development,
4. Description of failure planes at end of freezing period,
5. Pipe operating characteristics.

8.3 Model Design.

8.3.1 Introduction.

A small-scale model has many limitations since it cannot simultaneously model all the parameters that would be encountered under natural conditions. These parameters include:-

1. Soil conditions; particle size distribution, bulk density, moisture content, depth to water table, ambient ground and air temperatures, overburden stress, etc
2. Pipeline operating conditions; temperature, mass heat flow rate, fluid density, depth of burial, pipe diameter, etc
3. Frost susceptibility parameters; soil thermal, soil stress, soil moisture regimes,
4. Other test conditions; length of freezing period, rate of frost heave, rate of growth of ground cracking, growth of frozen annulus.

A laboratory model is unsuitable for satisfactorily modelling of all the above conditions, and so, during the 1970's, when consideration was given to the operation of large-diameter chilled gas pipelines in Northern Canada, large-scale test facilities were constructed at Calgary, Canada and Fairbanks, Alaska (Carlson, 1984). More recently, a 273 mm diameter chilled gas pipeline has been successfully operated within an environmentally controlled indoor facility at Caen, France (Williams, 1986) to further investigate the soil thermal, stress and hydrological regimes associated with soil freezing (Section 4.5.4). The Caen test has shown that scaled modelled tests can be undertaken when the variables under test are selected and accounted for in the design stage of the facility.

8.3.2 Model Selection.

A small-scale model test allows control of ambient soil temperatures, particle size distribution, moisture content and bulk density at the start of the test. The water table can be maintained at a constant level and the effects of water infiltration from both rainfall and surface runoff are excluded. The soil around the pipe can be placed under uniform conditions, thereby reducing spatial variability in soil properties.

When operating a full-scale test, such as at Blackrod, the downstream pipe temperature distribution is dependent on the previous pipeline operating conditions and the spatial variability in the soil properties along the pipeline. A small-scale laboratory model allows more precise control over the pipe operating temperature and thus the size of the frozen annulus. Consequently the fluid in the pipe does not necessarily need to be that used under actual pipeline operating conditions. A similar pipe material is necessary to achieve a coefficient of heat transfer similar to that at the full-scale site, but the pipe thickness is chosen to match the scaling factor used in the test. The depth of burial of the pipe is assumed to be scaled to that encountered under actual field conditions, but the stress/strain behaviour of the soil mass above the pipe will be altered.

Previous scale models are described in Sections 4.5.4 and 4.6, but the test facility at Caen is regarded as a large-scale test site (Smith *et al.*, 1985). The centrifuge test was regarded as inappropriate since it is primarily a short term settlement test that would be extremely difficult to modify to investigate ground cracking around chilled gas pipelines. The model used by Parmuzin *et al.* (1988) would have been an attractive except that it requires a very

large amount of soil. Therefore the selection of the tank size was based on a scaling factor of 10, which gave a pipe size of 90 mm and a predicted maximum frozen annulus size of 60 mm. The pipe was to be operated so that the pipe heave substantially exceeded that observed under field conditions (Chapter 7) to determine whether internal soil failure planes occurred. Assuming an internal soil failure plane at 45° to the vertical and a maximum depth of burial of two diameters, the zone of influence of the failure planes would be 225 mm from the pipe centre at the ground surface. Therefore the tank's dimensions were 1000 x 600 x 480 mm (L x H x W) and the tank was insulated to maintain constant soil thermal conditions by reducing heat inflow.

The soils used in the model were taken from sites where significant ground cracking had been observed, in this case Blackrod (Site C) and Tatsfield (Appendix B). Thus, the frost heave characteristics (thermal, stress and moisture) of the soils under test were not altered, allowing comparison with actual ground cracking at these sites. The rate of growth of the frozen annulus can be controlled to allow pipe heave to be a resultant of varying amounts of either ice segregation or *insitu* freezing of pore water. Similarly the duration of soil freezing can be controlled, so that the width of the frozen annulus observed in the field is reached after a defined time period has elapsed in the laboratory, thereby ground cracking can be monitored under carefully controlled frost heaving conditions.

8.3.3 Model Construction

The tank which was constructed from perspex sheet was placed on polystyrene sheets and surrounded laterally by an insulated box. Perspex was used for the tank since it offered strength and flexibility, both of which were necessary to allow for the expansive frost heave forces that would be generated during the trials. An insulation box, consisting of 45 mm thick purlboard (insulation) on a backing of 5 mm plywood, was constructed in two halves to form installation around the perspex tank (Figure 8.1). This insulation box could be taken away at any time for inspection of the soil closest to the tank sides. The tank was placed on two layers of 50 mm insulation and space was provided for a pipe to be connected to a header tank from the underside of the perspex tank (Figure 8.2). A hole 100 x 200 mm (W x H), was cut out at each end of the tank to position the steel pipe, the centre of each hole being located at the centre point of the perspex face. A 1.4 m length of 90 mm diameter steel pipe was placed through these holes and was connected to a flow cooler and temperature controller, from which readings could be taken either by a data logger or manually. The general layout of the small-scale model is shown in a schematic diagram (Figure 8.3).

The steel pipe was 90 mm O.D. with a wall thickness of 1 mm and was 1.4 m in length. The pipe was sealed, but outlet/inlet connections were provided at each end. The pipe was connected to two flow coolers, each of which had their own integrated temperature controllers, the second flow cooler was used both as a fine tune controller and a back-up system (Figure 8.4). The flow coolers pumped a water-glycol mixture around the system at

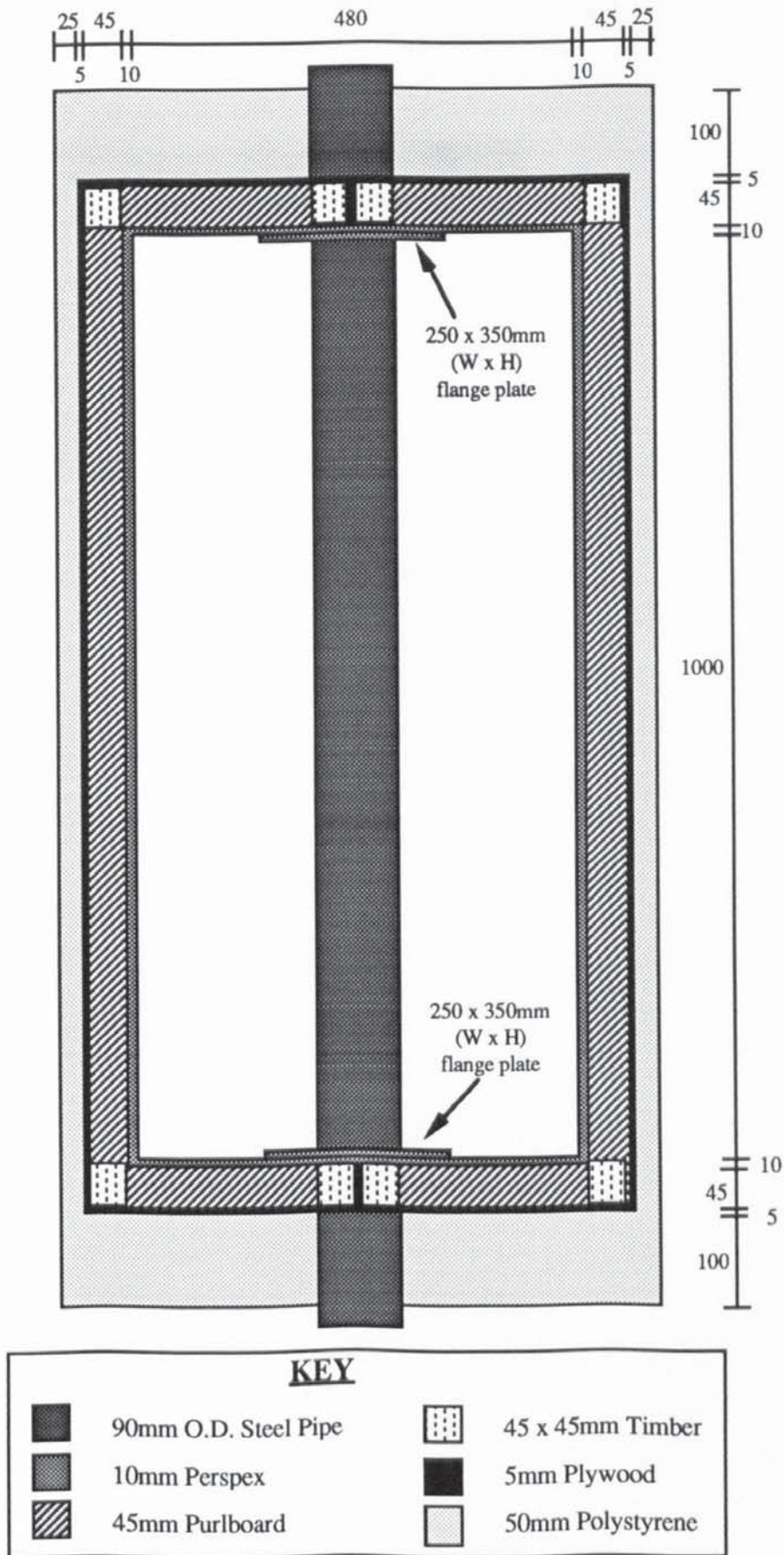


FIGURE 8.1 Plan View of the Frost Heave Tank (dimensions in mm).

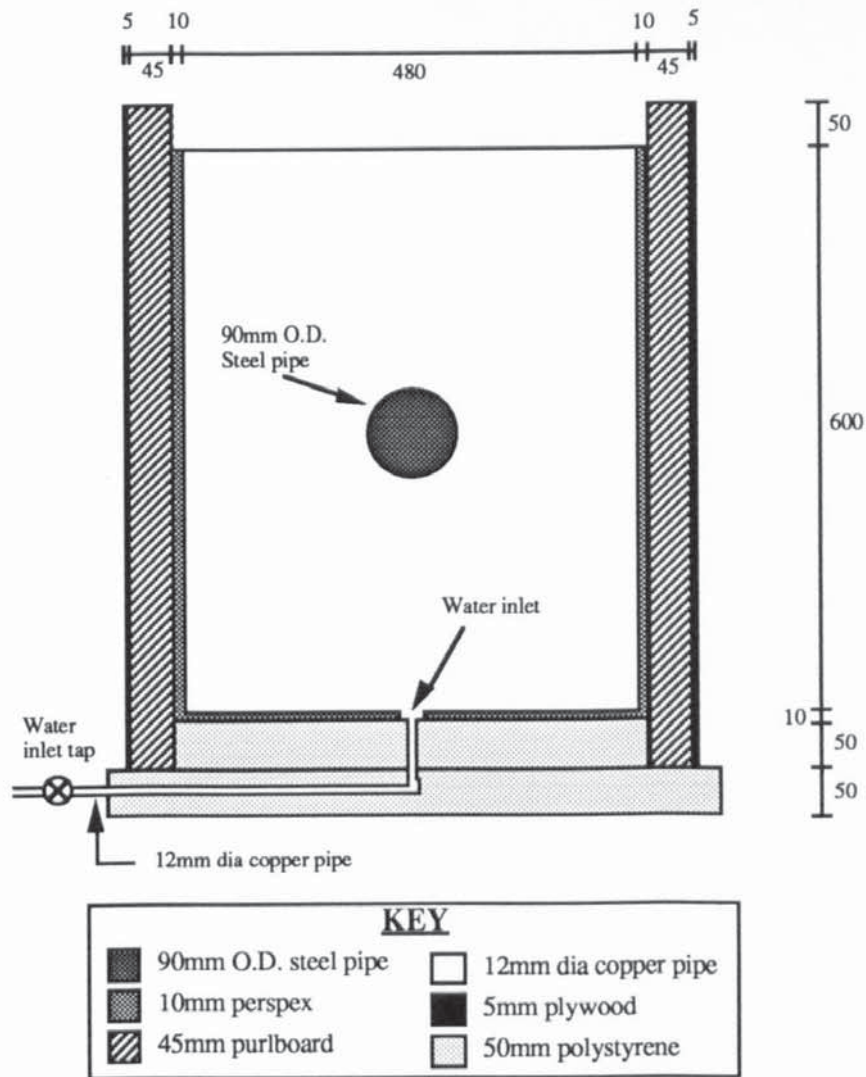


FIGURE 8.2 Section Through the Frost Heave Tank (dimensions in mm).

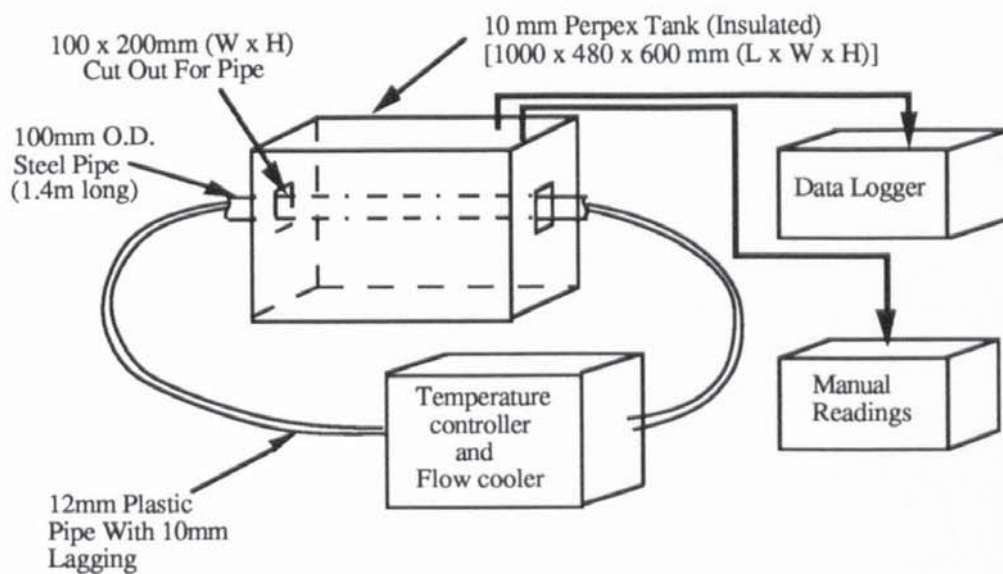


FIGURE 8.3 Schematic View of the Small-Scale Laboratory Model.

a rate of 20 litres per minute. The fluid was transferred from the flow cooler to pipe via 12 mm diameter plastic pipe, insulated with 10 mm thick lagging. The surface of the soil in the perspex tank was covered in heavy gauge aluminium foil, again to reduce heat inflow. The aluminium acted to trapped the cold air in the cracks and at the ground surface, thus direct heat transfer between the ambient air and soil could not take place directly. Two perspex flange plates 250 x 350 mm (W x H) were attached to the pipe and pushed up to the 100 x 200 mm (W x H) holes in the perspex tank, the flange plates were covered in silicon grease in order to form a waterproof seal (Figure 8.1).

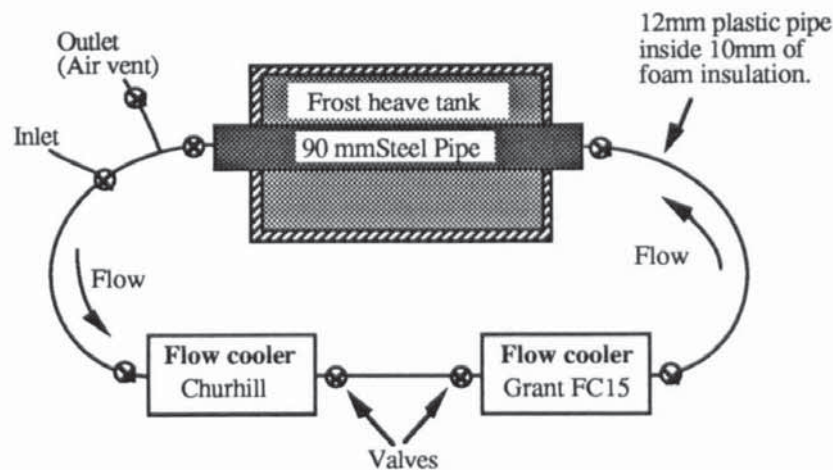


FIGURE 8.4 Diagram of the Temperature Control System for the Pipe.

The height of the water table was controlled by an external header tank (Figure 8.5) which supplied water for ice lensing during the growth of the frozen annulus. The header tank was connected to the underside of the perspex tank and the inlet was covered in a mesh. The bottom of the tank had a 50 mm layer of 12 mm gravel to ensure that the water table in the soil was at a constant level. Two standpipes were installed at in opposite diagonal corners to monitor the height of the water table.

8.4 Instrumentation.

8.4.1 Thermal Instrumentation.

The pipe and ground temperature regimes were monitored using Copper/Constantan type 'T' thermocouples. These were selected because of their linear voltage/temperature output around 0°C and robustness (Dean Baker *et al.*, 1975) and were constructed and calibrated in the laboratory at Aston University. The thermocouples were installed at the same time as the soil was placed in the tank, the positions are shown in Figure 8.6. Most of the thermocouples were connected to an Orion data logger and readings were taken every hour.

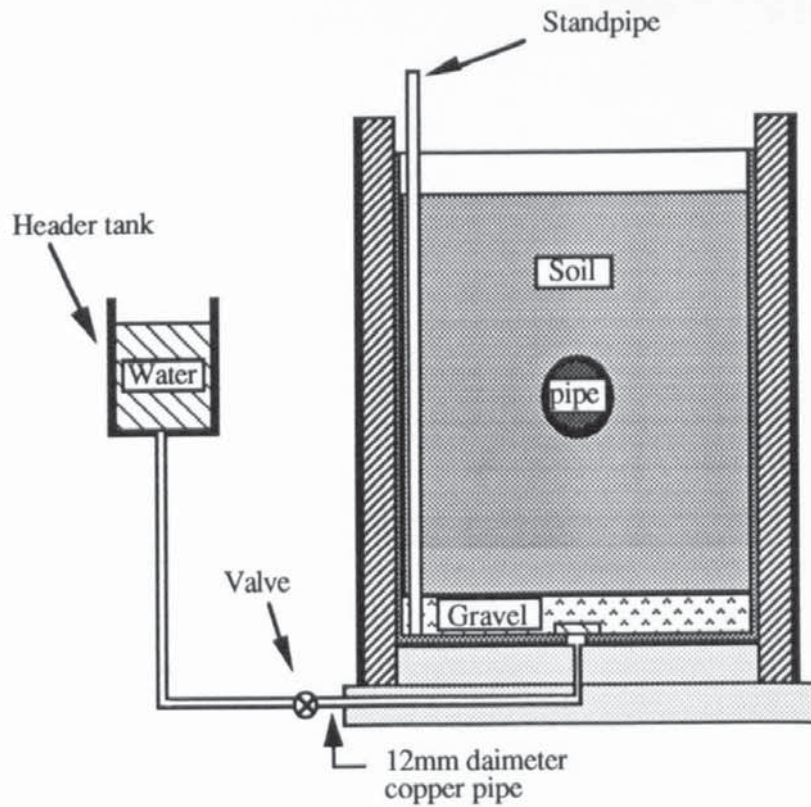


FIGURE 8.5 Diagram Showing the System for Maintaining the 'Artificial' Water Table.

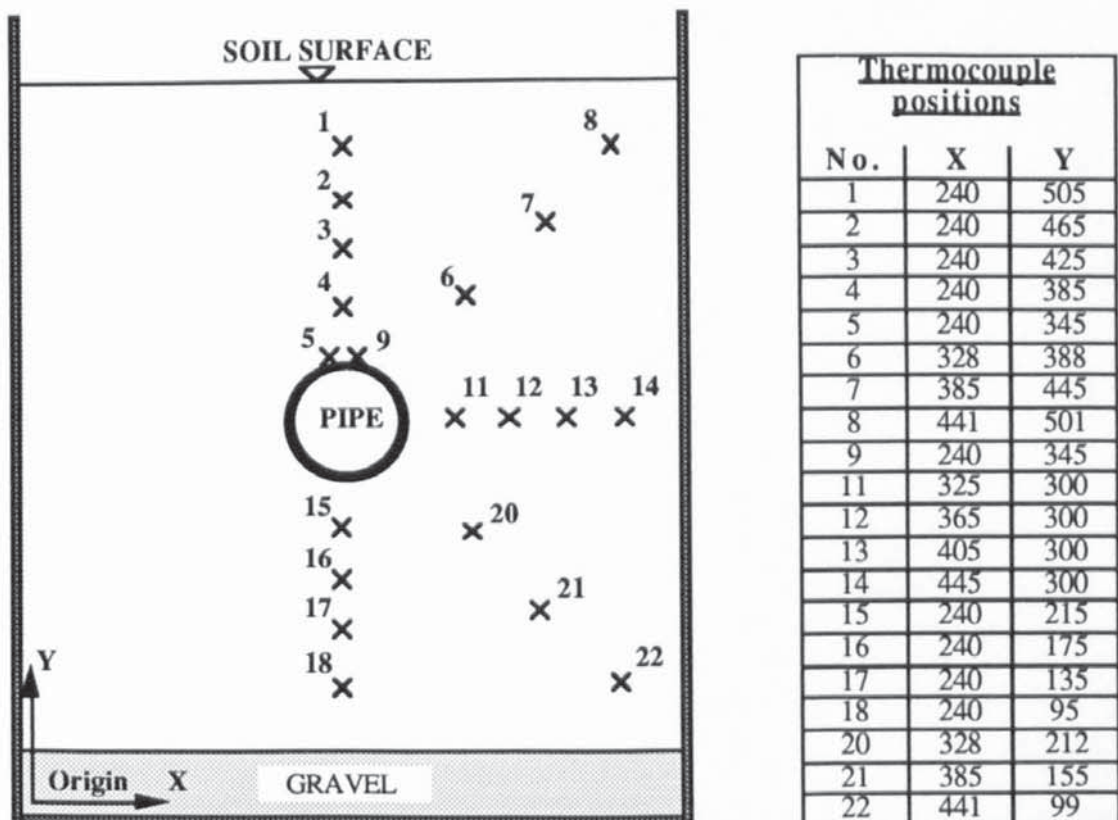


FIGURE 8.6 Diagram Showing the Positions of the Copper/Constantan Thermocouples.

8.4.2 Hydrological Instrumentation.

In order to represent *in situ* field conditions and to provide moisture for the soil freezing process, it was necessary to provide the soil in the tank with an 'artificial' water table. This was simply achieved by using a header tank filled with water, the water level being kept constant during freezing by the addition of water to the header tank.

Thermocouple psychrometers were installed radially above the pipe to monitor the expected soil moisture suctions resulting from the freezing process (Figure 8.7). These instruments were used because they allow the measurement of suctions to -8.0 MN m^{-2} (-80 bar) and have been shown to be reliable under laboratory conditions (Clark, 1989). Their operation and use are further described in Section 7.4.2 and the computer program used to interpret the output is provided in Appendix D.

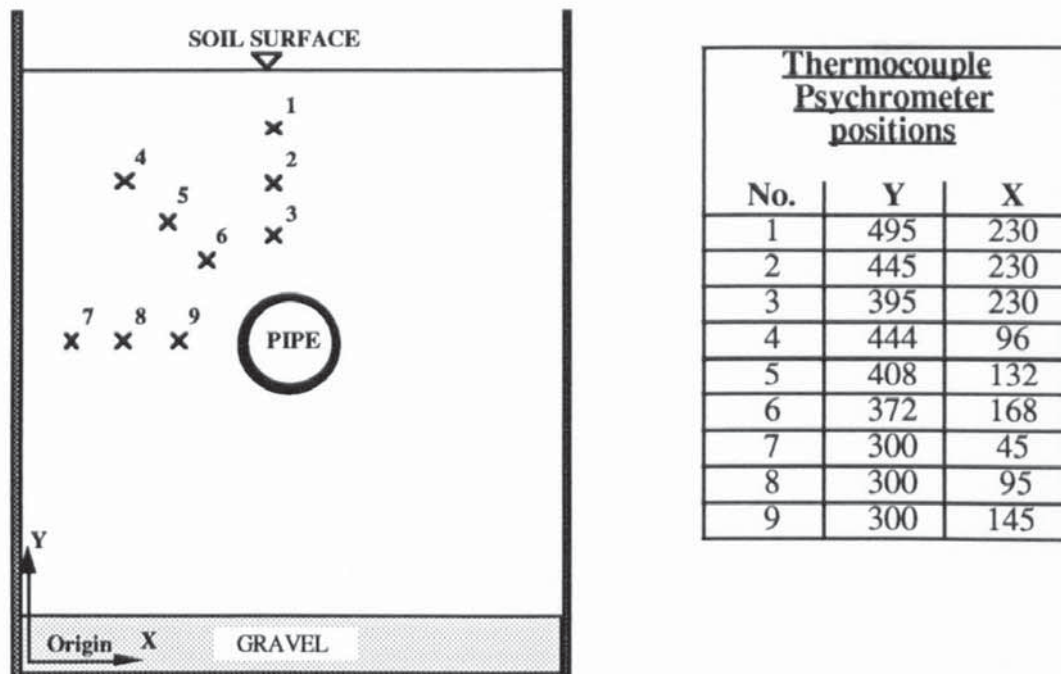


FIGURE 8.7 Diagram Showing the Positions of the Thermocouple-Psychrometers.

8.4.3 Soil Stress Instrumentation.

Soil pressure cells were not installed in the model since ground surface, pipe displacements and ground cracking were being specifically investigated (Section 8.4.4).

8.4.4 Pipe and Ground Movement Instrumentation.

Upward ground movement, perpendicular to the line of the pipe, was monitored automatically by a row of linear voltage displacement transducers (LVDT's) and, manually, by two rows of dial gauges. The position of these instruments is shown in Figure 8.8 and a section through the frost heave box illustrates the layout of the LVDT's (Figure 8.9). The dial gauges and LVDT's were attached to a frame constructed across the tank and bore on

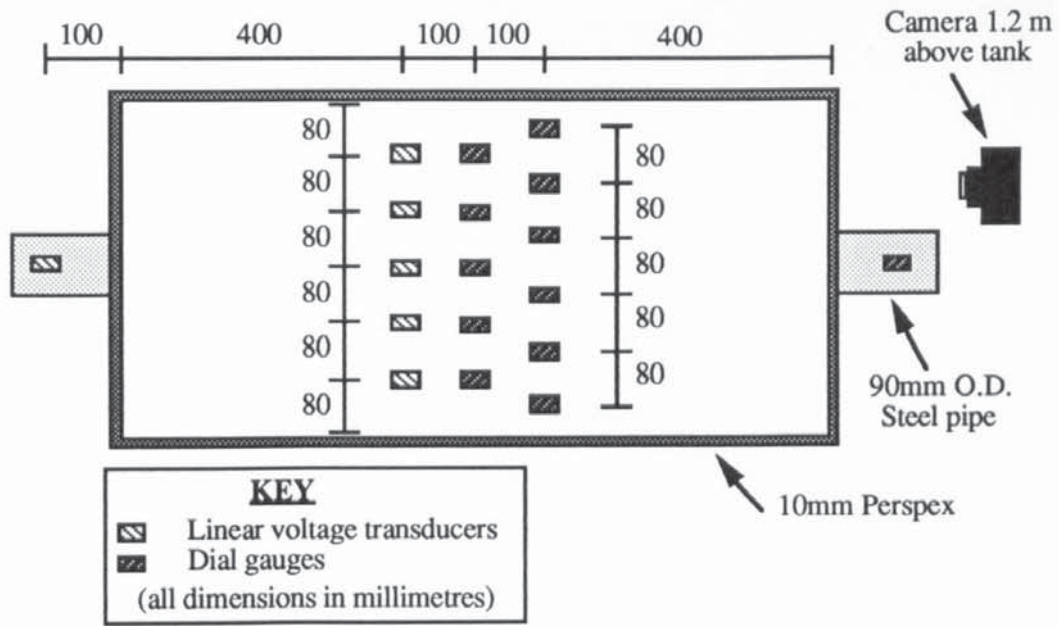


FIGURE 8.8 Plan View of the Ground Heave and Cracking Instrumentation.

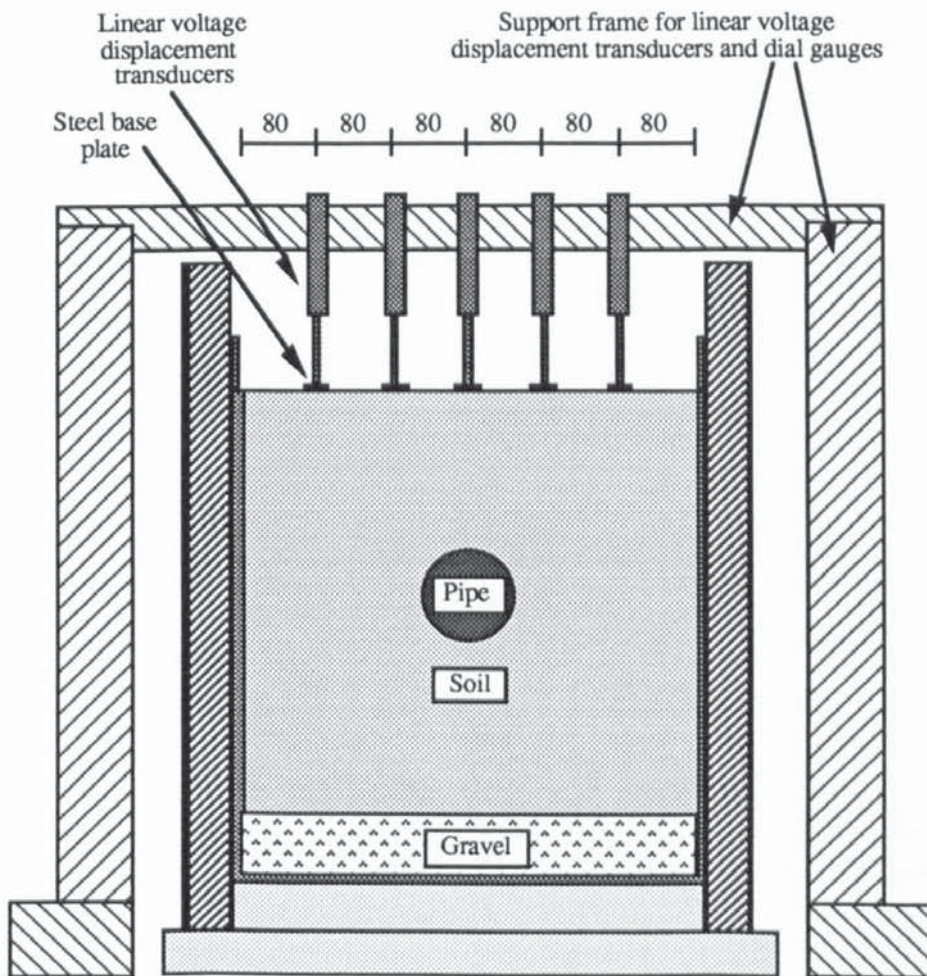


FIGURE 8.9 Diagram Showing the Position of the Linear Voltage Displacement Transducers (dimensions in millimetres).

10 mm square steel plates. These plates allowed the weight/force of the instrument to be spread over a larger area thereby increasing the reliability of monitoring. Pipe heave was also monitored automatically by a linear voltage displacement transducer attached to a pipe heave rod clamped to the pipe outside the tank, a check was provided on the other side of the model using a dial gauge. Since the depth of burial was low the pipe could be regarded as Rigid, in relation to the overlying soil mass, thus pipe heave at either end of the pipe could be reasonably equated to the that within the model.

Detailing of the ground surface of the tank was effected every 6 hours and provided information on the position of the crack and its width at various locations, and was supplemented with a monochrome photograph of the soil surface.

8.4.5 Operation of the Frost Heave Tank.

The soil and instrumentation were installed over 7 days to allow the soil and water to reach an equilibrium state. Aluminium sheeting was placed over the soil surface to prevent moisture losses from evaporation. The frost heave tank was left for a further 7 days to allow for the occurrence of any initial settlement of the ground surface. Once the soil had reached a steady-state, the water/glycol mixture was pumped round the system at a sub-zero temperature. During the test periods, the aluminium sheeting served to prevent both moisture losses and heat gain from the local environment. The pipe was operated for a sufficient period for both significant frost heave and ground cracking to take place. Indeed, it was operated beyond the scaled frost/pipe heave, observed under field conditions in order to exacerbate the ground cracking produced in the model.

The thermocouples and thermocouple-psychrometers were placed on a pre-determined grid around the pipe, but they were not rigidly fixed since this could induce stresses into the soil mass which could impair the analysis of the ground/pipe movement data. Therefore, during each experiment, the position of the thermocouples and thermocouple-psychrometers altered in relation to the pipe.

During the experiments, water was added to the header tank at 6 hour intervals to maintain the water table at a pre-determined constant level. The operating temperature of the pipe was changed in a step-wise manner and this was effected to increase the pipe heave rate after it had slowed to a point where the increase in the width of the ground cracks was minimal.

Monitoring of the instrumentation continued during the freezing phase of the trials, but was continued for a short period after thawing had begun. At the end of the freezing period the insulation around the perspex tank was removed so that any soil failure planes within the soil could be observed and photographed. A small excavation was made across the line of the pipe, again to assess the failure planes within the soil mass.

8.4.6 Monitoring System.

Table 8.1 summarizes the reading intervals for the instrumentation adopted during the tests. Most of thermocouples and all the linear voltage displacement transducers were connected to a 20 channel Orion B data logger and readings were taken hourly. The Orion B data logger stored the data on cassette and a printout was also taken. At the end of the test, the data was transferred directly to an Apple Macintosh micro-computer for analysis.

Thermocouple-psychrometers, dial gauges, crack profile, photographs, water table and some thermocouples were manually monitored every 6 hours during the test. The detailed maps of ground cracking were scanned and the images transferred to a micro-computer. Figure 8.10 shows the data flow from the instrumentation to the micro-computer.

Instrument	No.	Measurement type	Method of reading	Reading interval
Thermocouple copper/constantan	20	Temperature	14 Data logger	1 hour
			6 manually	6 hours
Thermocouple-psychrometers	9	Soil suction	manually	6 hours
Linear voltage displacement transducers	6	Ground movement	5 Data logger	1 hour
		Pipe movement	1 Data logger	1 hour
Dial gauges	11	Ground movement	manually	6 hours
Crack detailing	1	Crack growth	manually	6 hours
Camera	1	Crack growth	manually	6 hours
Standpipes	2	Depth to water table	manually	6 hours
Header	1	Maintain water table	manually	6 hours

TABLE 8.1 Reading Intervals of the Instrumentation during the Small-Scale Models Experiments.

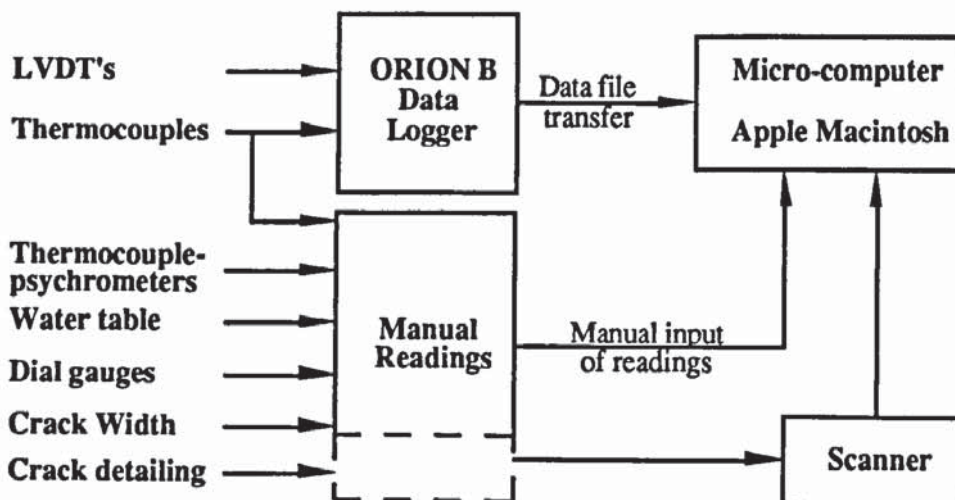


FIGURE 8.10 Data Flow Diagram for the Small-Scale Model Tests.

8.5 Results.

This sections describes the small-scale laboratory validation in brief and further expands on the detailed tests undertaken on soil samples from Blackrod Site C and Tatsfield (Appendix B).

8.5.1 Experimental Validation.

This was specifically undertaken to investigate whether ground cracking could be reproduced under small-scale laboratory model conditions. A local sub-soil material was taken from the University grounds and used in the validation test. The soil was placed in 100 mm layers and compacted over the full surface with two blows of a 5 kg hammer dropped 200 mm. The pipe had a depth of cover of 135 mm which represented a depth of burial ratio of 1.5 from the ground surface to the pipe crown. Subsequently the water table was maintained at 60 mm below the pipe invert level. The water table was maintained at this level during the four day freezing period, with the flow coolers operating between -5 and -10°C during this period.

Monitoring of the ground surface for movement and ground cracking was undertaken on a daily basis and, at the end of the test, both the frozen annulus and the vertical crack above it were exposed to investigate their shape.

8.5.1.1 Ground Surface Cracking.

In this experiment ground cracking, with surface widths up to 5 mm, were observed above and parallel to the pipe after two days of sub-zero operation. After four days a continuous crack had developed with a average crack width of 12-15 mm. A plan view of this ground crack is provided in Figure 8.11 and is supplemented by a photograph of the ground surface (Plate 8.1). From Plate 8.1 it is evident that the ground crack was influenced by the pipe flange plate at the end of the tank, since the crack deviates towards the edge of this plate.

An excavation immediately after the completion freezing cycle showed (Plate 8.2) the frozen annulus to be approximately circular in shape. Plate 8.2 shows the frozen annulus and ground crack at Section B-B and it can be observed that the crack apex is within the frozen annulus. There were no indications of internal soil failure planes as reported by Casson (1984) during pipe uplift tests.

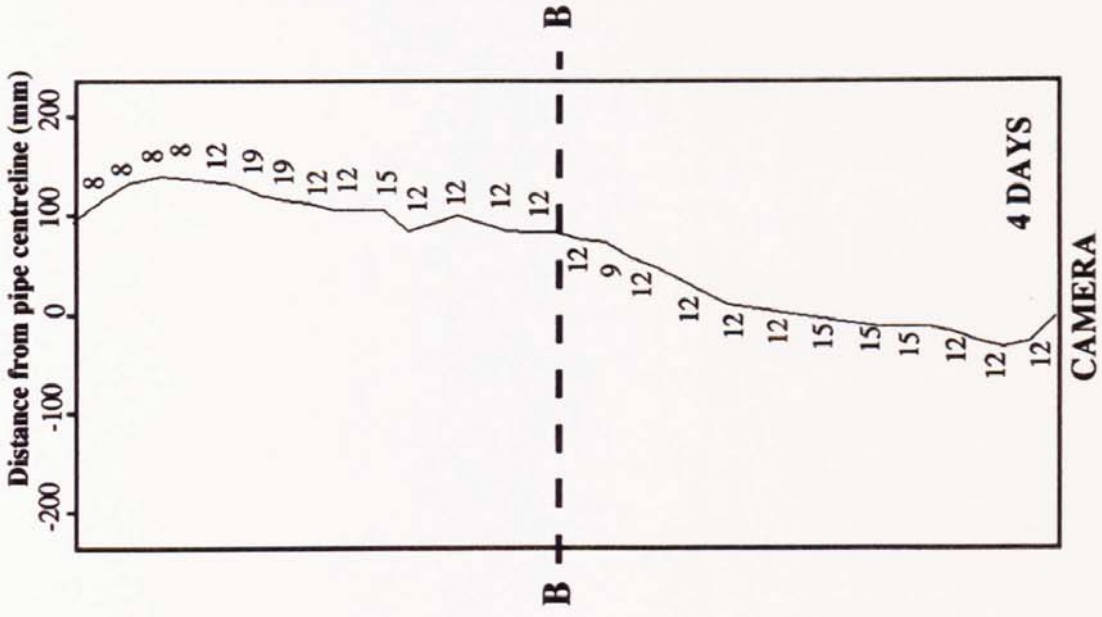


FIGURE 8.11 Plan View of the Soil Surface During the Final Validation Test Showing the Width of Ground Cracking After Four Days (dimensions mm)

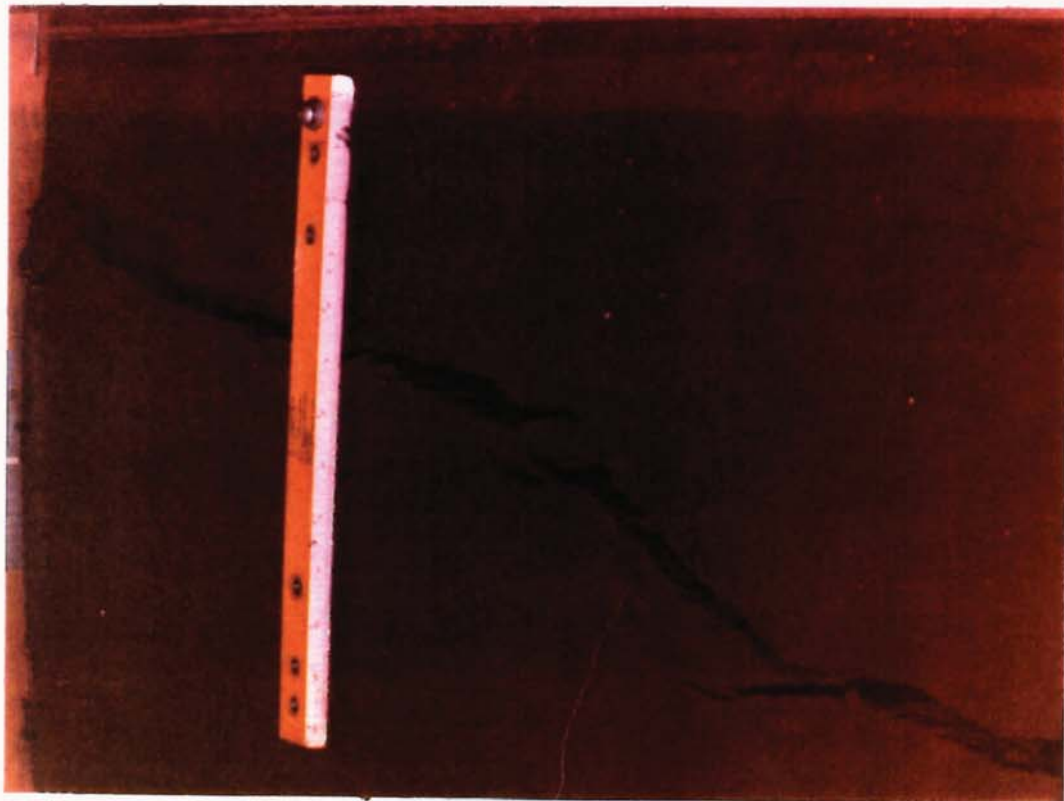


PLATE 8.1 Photograph Showing the Extent of Ground Cracking After Four Days During the Final Validation Test.



PLATE 8.2 Photograph Showing the Shape Frozen Annulus above the Pipe and the Ground Crack Above the Annulus at the end of the Final Validation Test.

8.5.1.2 Ground Surface Movement.

Figure 8.12 shows the vertical ground movement across Section B-B (Figure 8.11) during the final validation test. Ground movement was greatest in the final two days of the test and the maximum ground movement occurred over the pipe centre and decreased with increased distance from the pipe centre. The soil surface profile on day 4 indicates that the whole ground surface was moving upwards (Figure 8.12).

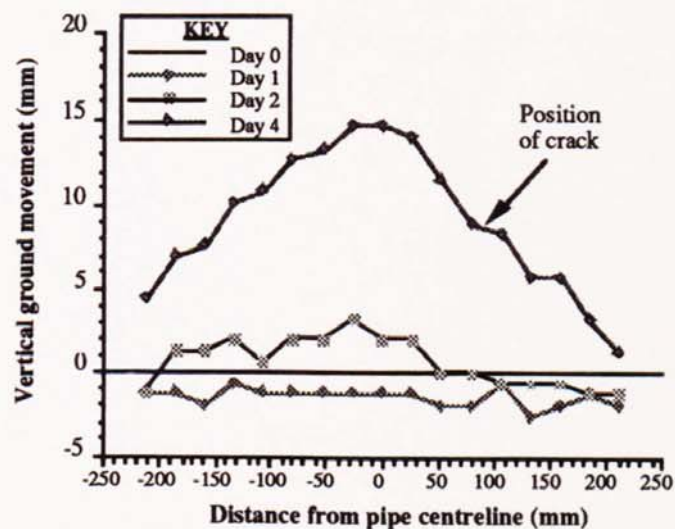


FIGURE 8.12 Ground Surface Profile Perpendicular to the Line of the Pipe at the Centre (Section B-B) of the Small-Scale Model.

8.5.2 Tatsfield Test Run.

8.5.2.1 Introduction.

The soil was collected from an area downstream of Tatsfield PRS (SE GAS) where both ground/pipe heave and ground cracking had been reported (Appendix B). The sample was taken 700 m downstream and from the zone between the ground surface and pipe top.

The pipe centre was 300 mm from the bottom of the tank and had a depth of cover of 160 mm at the start of the test. The water table was maintained at a constant level of 150 mm above the base of the tank which, at the start of the test, was 115 mm below pipe invert level. The test was operated without aluminium foil covering the soil surface in an attempt to induce ground surface movement from pipe heave such as observed in the full-scale test. However, a substantial amount of ground movement was attributed to frost heave in the frozen annulus above the pipe. Consequently, at 312 hours into the test, the foil was placed over the soil surface to increase the rate of growth of the frozen annulus by acting as an insulating layer. The objective of the test was to drop the pipe wall temperature to -2°C until the pipe heave rate had slowed to a limiting rate. Upon reaching this point a sudden temperature drop was applied to investigate the effect of a negative thermal shock on both pipe and ground heave and, consequently, ground cracking.

8.5.2.2 Soil Classification.

	Tatsfield Soil
Gravel	10 %
Sand	43 %
Silt	34 %
Clay	13 %
Plastic limit	19 %
Liquid limit	43 %
Plasticity index	24 %
Shrinkage limit	11 %
Dry density	1780 kg m ⁻³

TABLE 8.2 Soil Properties for Tatsfield Soil.

8.5.2.3 Pipe Operating Characteristics.

The pipe temperature was lowered to -2°C over a period of approximately 100 hours and subsequently maintained at this value until 240 hours had passed (Figure 8.13). At this stage it was initially lowered to -4°C , after which the pipe temperature was lowered progressively to -7°C . Thawing was initiated at 384 hours and monitoring continued until the frozen annulus had completely thawed (Figure 8.13).

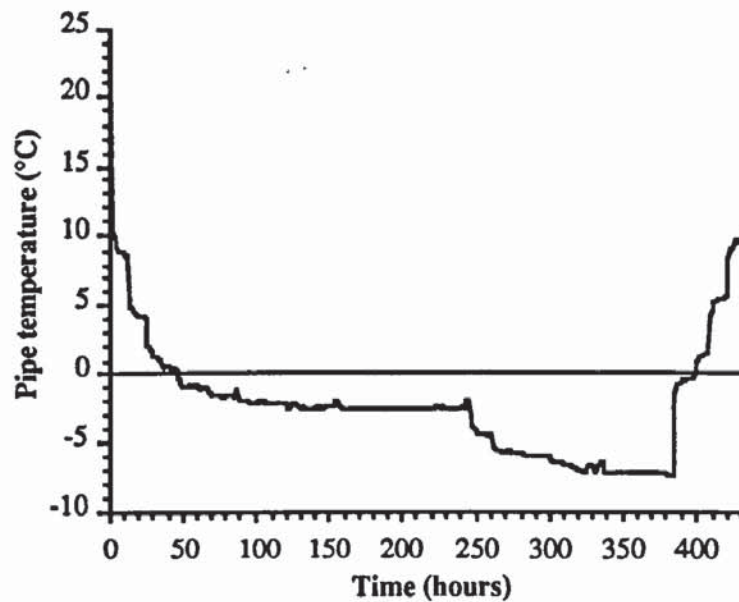


FIGURE 8.13 Pipe Temperature during the Tatsfield Small-Scale Test.

8.5.2.4 Soil Temperatures.

The soil temperatures radiating from the pipe at 0° , 45° , 90° , 145° and 180° to the vertical are shown in Figures 8.14 - 18. The probes were not rigidly fixed around the pipe since this could have altered both ground and pipe movements. Figure 8.14 shows a distinct change in the temperature profile in the thermocouple array vertically above the pipe at 240 hours. It is suggested that this resulted from changes in either the shape of the lower portion of the crack or the thermal regime in the crack, thereby producing a vertical free surface close to the thermocouple probes. At 312 hours there is a drop in the temperature at the locations of the probes closest the ground surface resulting from the application of the aluminium foil to the ground surface (Figures 8.14 and 8.15) but, with depth, this change is less noticeable (Figures 8.16, 8.17 and 8.18).

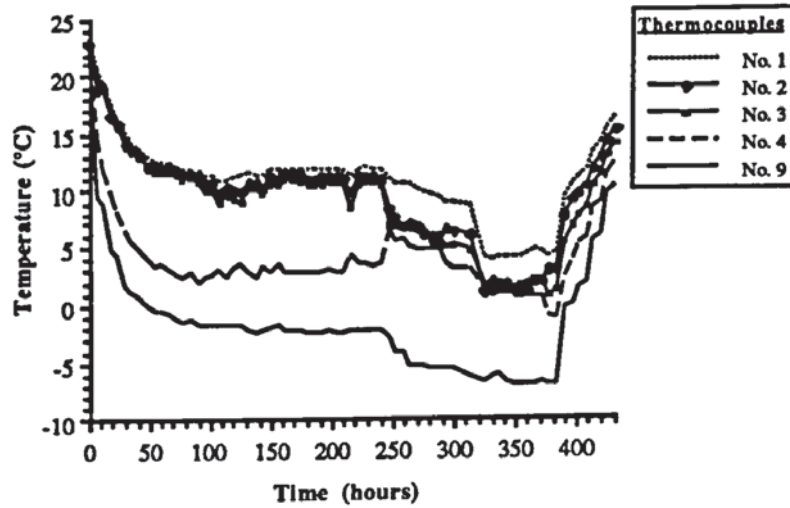


FIGURE 8.14 Vertical Temperature Profile above Pipe Crown (see Figure 8.6).

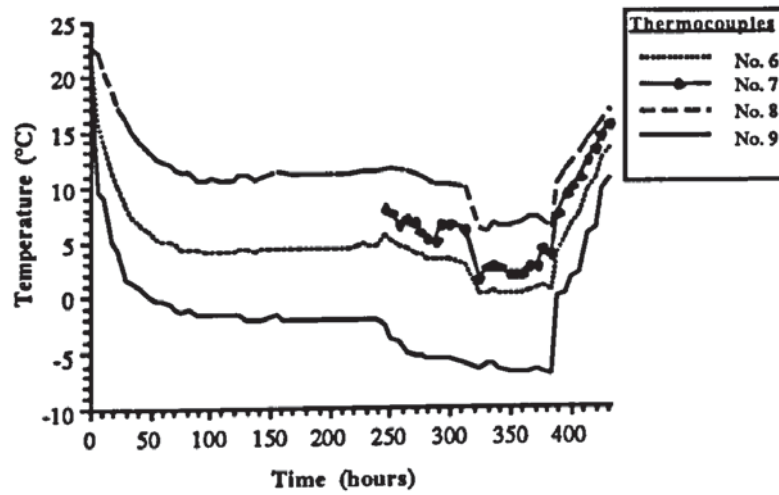


FIGURE 8.15 Temperature Profile at 45° to the Vertical above the Pipe (see Figure 8.6).

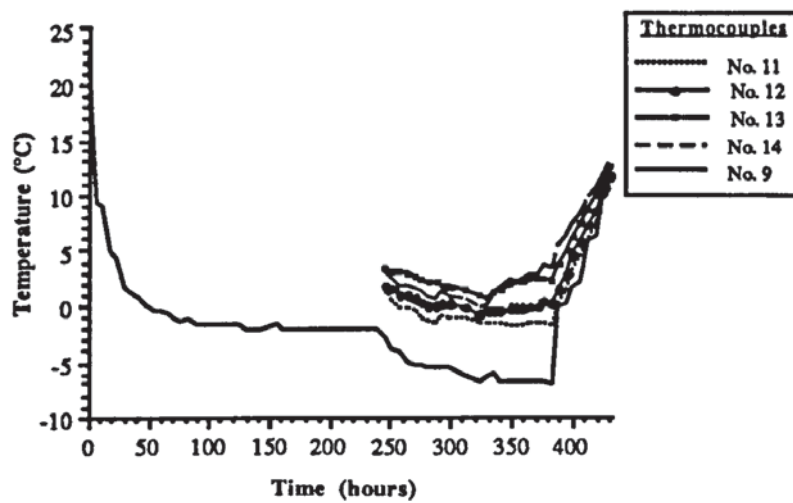


FIGURE 8.16 Horizontal Temperature Profile from the Pipe (see Figure 8.6).

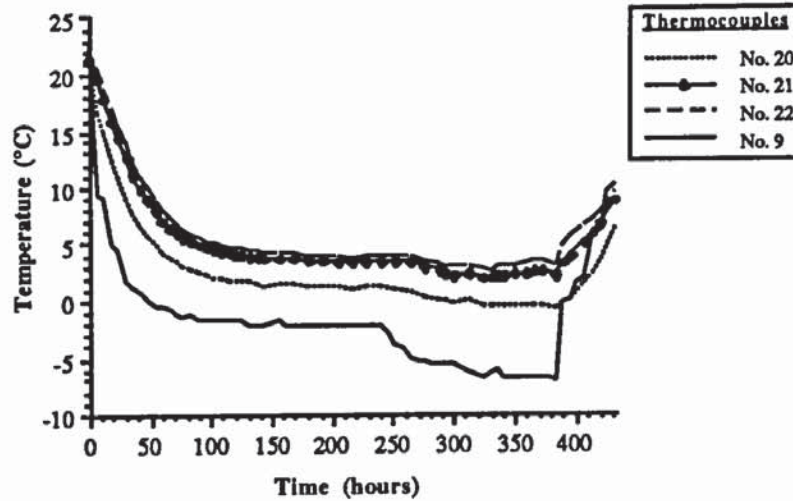


FIGURE 8.17 Temperature Profile at 45° to the Vertical below the Pipe (see Figure 8.6).

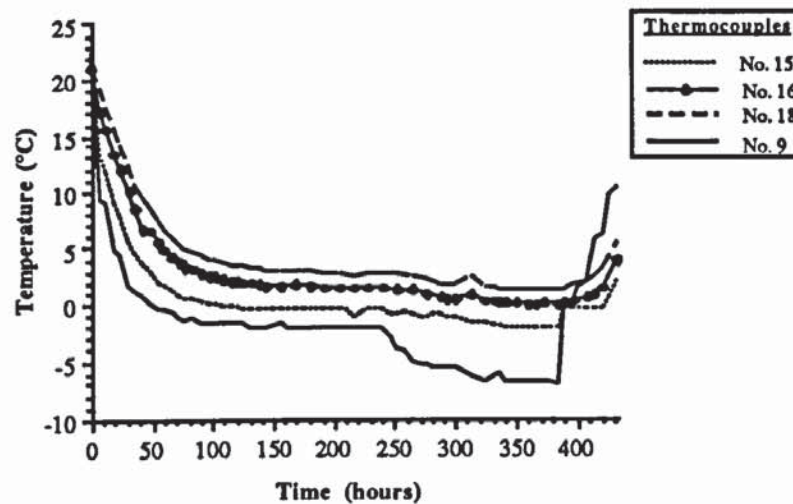


FIGURE 8.18 Vertical Temperature Profile below Pipe (see Figure 8.6).

8.5.2.5 Soil Water Potentials.

The results from thermocouple-psychrometers vertically above, at 45° and horizontally from the pipe centre within the soil mass (Figure 8.7) are provided in Figures 8.19a, 8.20a and 8.21a. Figure 8.19a shows that, in the vertical array of thermocouple-psychrometers above the pipe, the probe closest the ground surface underwent a sudden increase in negative water potential at 240 hours, which coincides with the thermal shock applied to the pipe (Figure 8.13). Low positive outputs from thermocouple-psychrometers have been discussed by Brown and Bartos (1982) under conditions of zero water potential, and it is suggested that positive output from Probe 3 can be interpreted as zero since the probe was found to be satisfactory when re-calibrated after the test. This probe was the closest to the pipe (Figure 8.7), but negative water potentials were not recorded even though its temperature approached 0°C between 312 and 384 hours (Figure 8.19b).

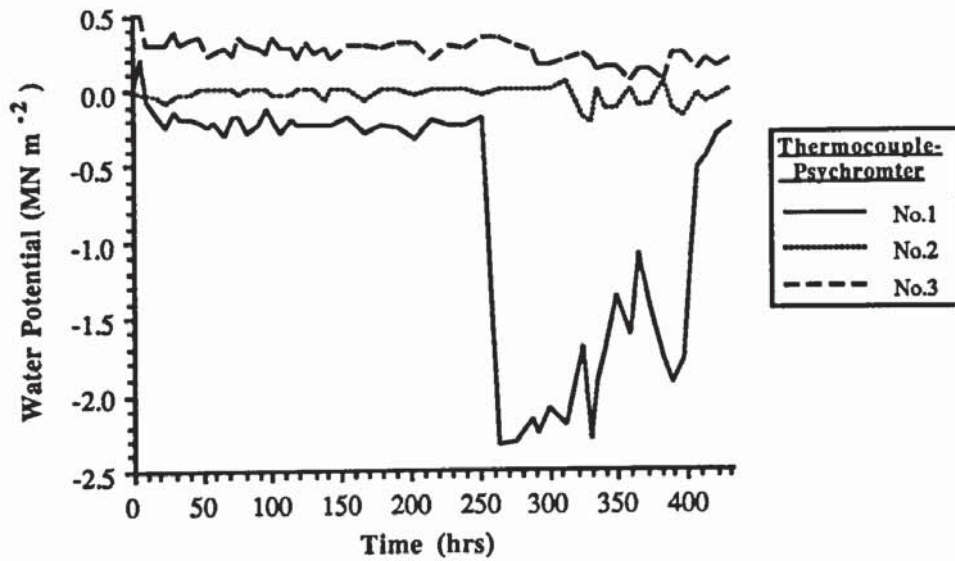


FIGURE 8.19a Soil Water Potential Profile Vertically above Pipe Crown.

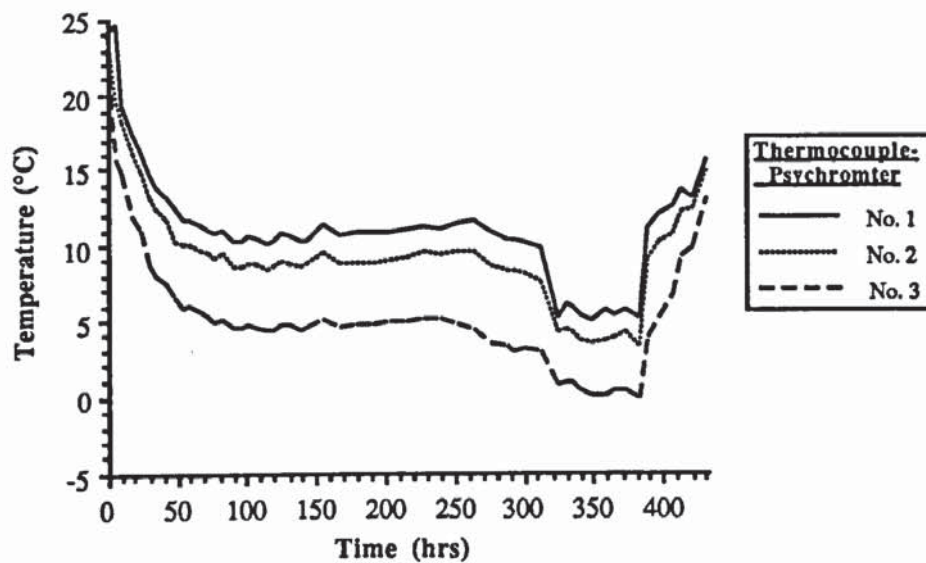


FIGURE 8.19b Soil Temperatures at the Positions where Soil Water Potential was Measured Vertically above Pipe Crown.

The array of thermocouple-psychrometers at 45° to the vertical above the pipe axis (Figure 8.7) indicated negative water potentials at positions 4 and 6 (Figure 8.20a). Probe 6 is closest to the pipe and shows a steady increase in negative potential up to -0.5 MN m^{-2} (-5 bar) from 240 to 384 hours. However probe 4, which is nearest the ground surface, showed similar behaviour to probe 1 (Figure 8.19a) in that at 240 hours, when the pipe

temperature was lowered, there was an increase in negative water potential of -1.2 MN m^{-2} (-12 bar) even though the probe temperature was recorded as $+10^\circ\text{C}$ (Figure 8.20b).

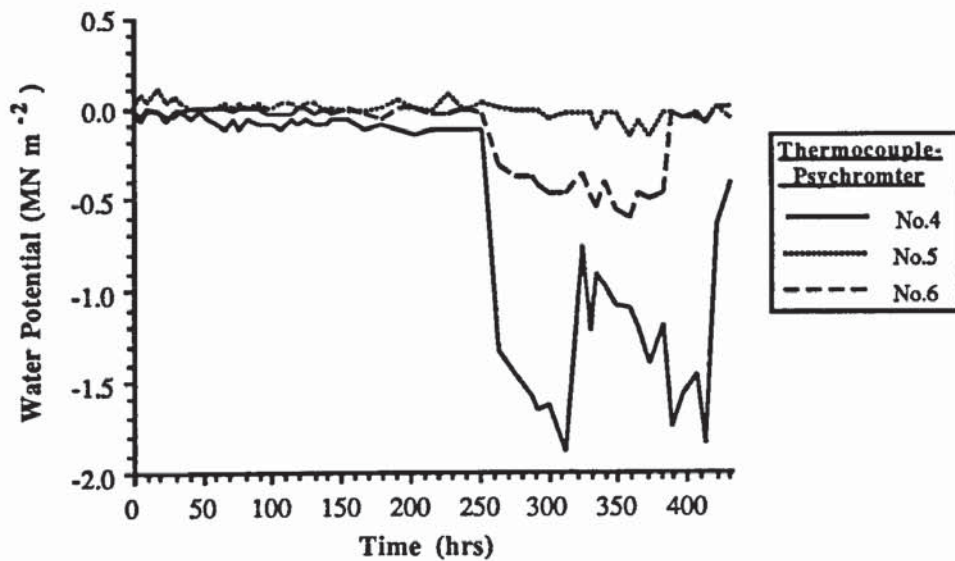


FIGURE 8.20a Soil Water Potential Profile at 45° to the Vertical above the Pipe.

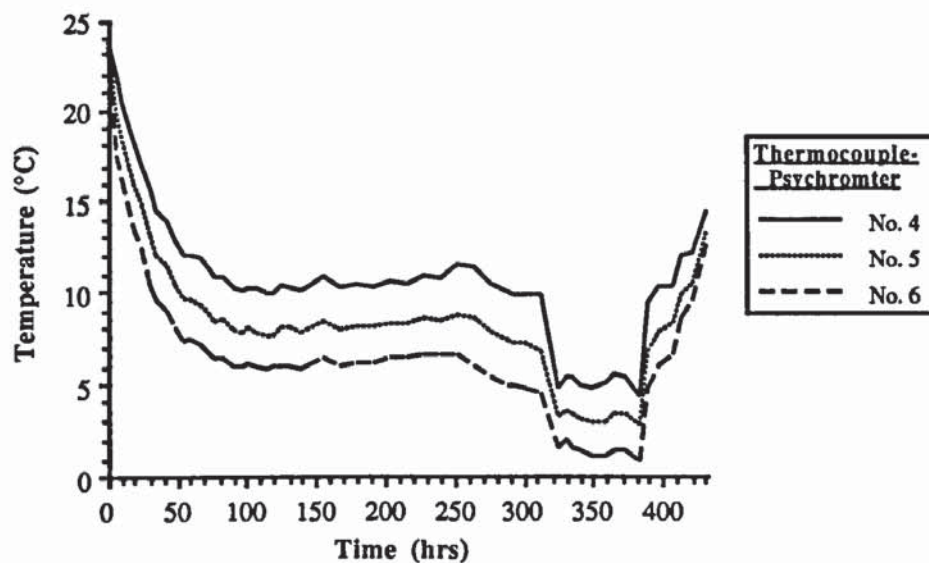


FIGURE 8.20b Soil Temperatures at the Positions where Soil Water Potential was Measured at 45° to the Vertical above the Pipe.

In Figure 8.21a probe 9, which was nearest the pipe (Figure 8.7), showed a rapid increase in negative water potential which coincided with the passage of the zero isotherm at approximately 312 hours (Figure 8.21b). The negative water potential of probe 8 increased steadily to -1.0 MN m^{-2} (-10 bar) between 60 and 324 hours (Figure 8.21a), but then

decreased to zero at 360 hours. This is in contrast to probe 9 which increased to a maximum value of -3.4 MN m^{-2} (-34 bar) at 384 hours and subsequently decreased to zero at 394 hours.

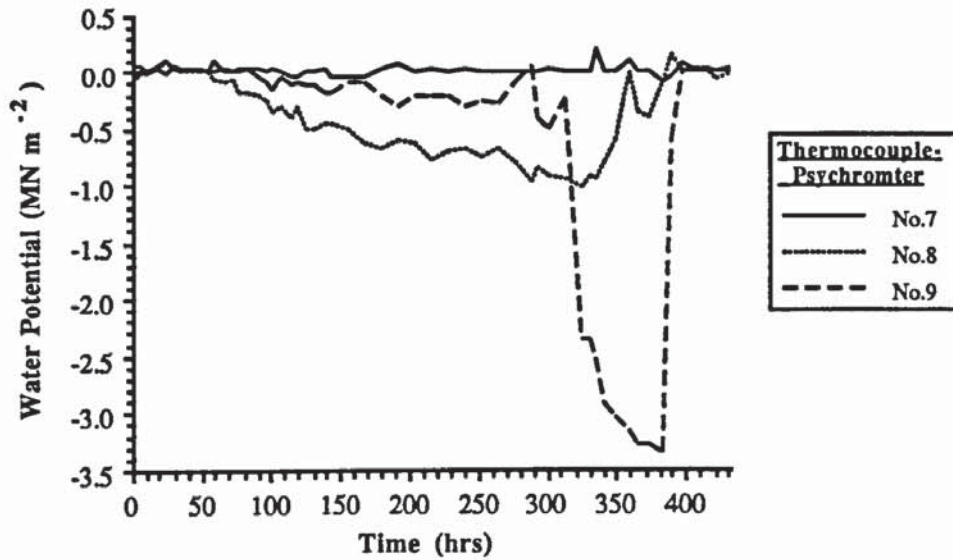


FIGURE 8.21a Soil Water Potential Profile Horizontally from the Pipe.

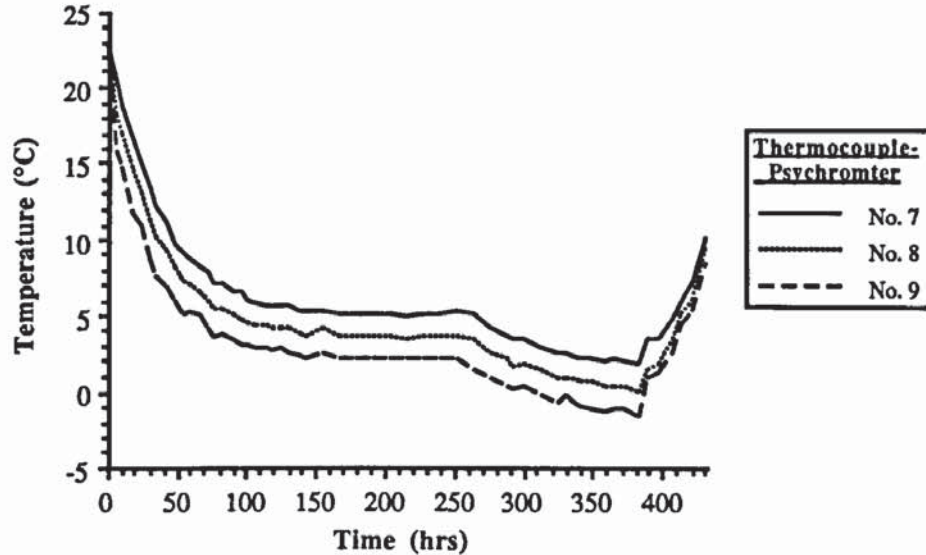


FIGURE 8.21b Soil Temperatures at the Positions where Soil Water Potential was Measured Horizontally from the Pipe.

Probes 6 and 9 both showed increased negative water potential as the frost front moved towards them and upon instigation of thawing these potentials decreased to zero by 390 hours. This suggests that the negative water potentials recorded by these probes were a result of the suction forces developed within the frozen annulus. On thawing, water would

be released from the frozen annulus and, as these probes were in close proximity to the annulus, the measured suctions would be negated very quickly.

Thermocouple-psychrometers 1 and 4 showed increases in negative water potential from zero to -2.3 and -1.3 MN m^{-2} (-23 and -13 bars) respectively between 252 and 264 hours. It is proposed that these increases are the resultant of both their proximity to the walls of the soil failure cracks and to the rapid drop in pipe temperature that subsequently lowered the air temperatures in these cracks. After the pipe temperature was lowered, the air temperature within the cracks could have dropped below $0^{\circ}C$ and so a layer of frozen soil may have formed on the surfaces of the cracks. This would produce in a desiccated zone of soil behind the face of the cracks and thus negative water potentials. Both these probes had very substantial temperature gradients between the sensing junction and the temperature measurement junction indicating that they could have been in close proximity to crack surface. During the thawing of the frozen soil layer the water potential gradient would recede but, unlike probes 6 and 9, there would not be sufficient moisture immediately available to saturate the desiccated zone and return it to zero water potential.

The amount of water added to maintain a constant water table during the test is shown in Figure 8.22 and, up to 240 hours, the average rate of water addition was 0.03 litres/hour. This rate subsequently increased to 0.056 litres/hour suggesting that, after the pipe temperature was lowered at 240 hours, there was an increase in frost heaving for, with the location of the water table remaining constant, the added water must have been drawn to the frozen annulus for freezing.

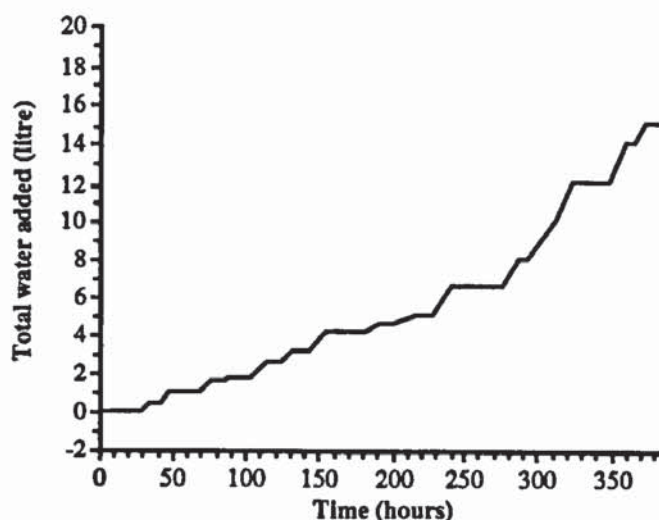


FIGURE 8.22 Water Added to Model during the Tatsfield Test to Maintain a Constant Water Table Level.

8.5.2.6 Ground Cracking.

The total surface crack widths across each of the three sections, where the ground surface profile had been monitored, were summed and the resulting average values are plotted, with pipe wall temperature, against test duration in Figure 8.23. There was rapid crack growth between approximately 42 and 96 hours as the pipe temperature dropped below 0°C. After 96 hours the crack growth rate decreased substantially from 0.18 mm/hour to 0.02 mm/hour until 240 hours. At this time the pipe temperature was further lowered and crack growth recommenced, and increased significantly after the aluminium foil was placed on the ground surface (Figure 8.23). The placing of the aluminium foil induced a rapid decrease in the temperature of the soil above the pipe resulting from its thermal insulation effects, and so the growth of the frozen annulus would have resumed above the pipe. Thus it was hoped by placing aluminium foil to increase the rate of cracking at the end of experiment.

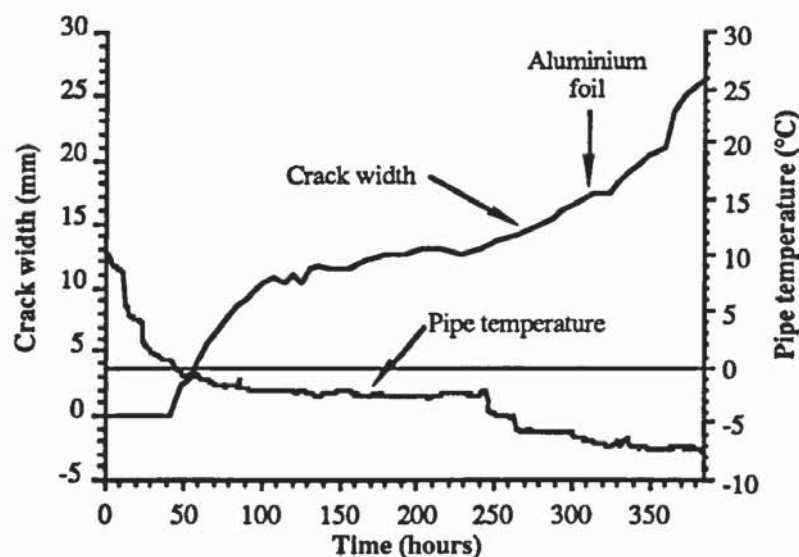


FIGURE 8.23 Average of Width of Cracking Across the Soil Surface at the Locations of the Dial Gauges and LVDT's in Relation to Pipe Temperature.

The data in Figure 8.23 is limited to the period of sub-zero pipe operation since, after thawing was initiated, pipe settlement was hindered by the friction forces generated between the pipe flange plates and the perspex tank wall. Consequently the recorded change in crack width would not necessarily be applicable to *in situ* conditions.

Plates 8.3 to 8.7 show the soil surface during the test and are supplemented by a detailed plan views of the surface showing the positions of the cracks and the their surface widths (Figures 8.24 - 8.28). The selected times of 48, 96, 240, 312 and 384 hours represent the stages at which there were marked changes in the profile of the crack width plot (Figure 8.23).

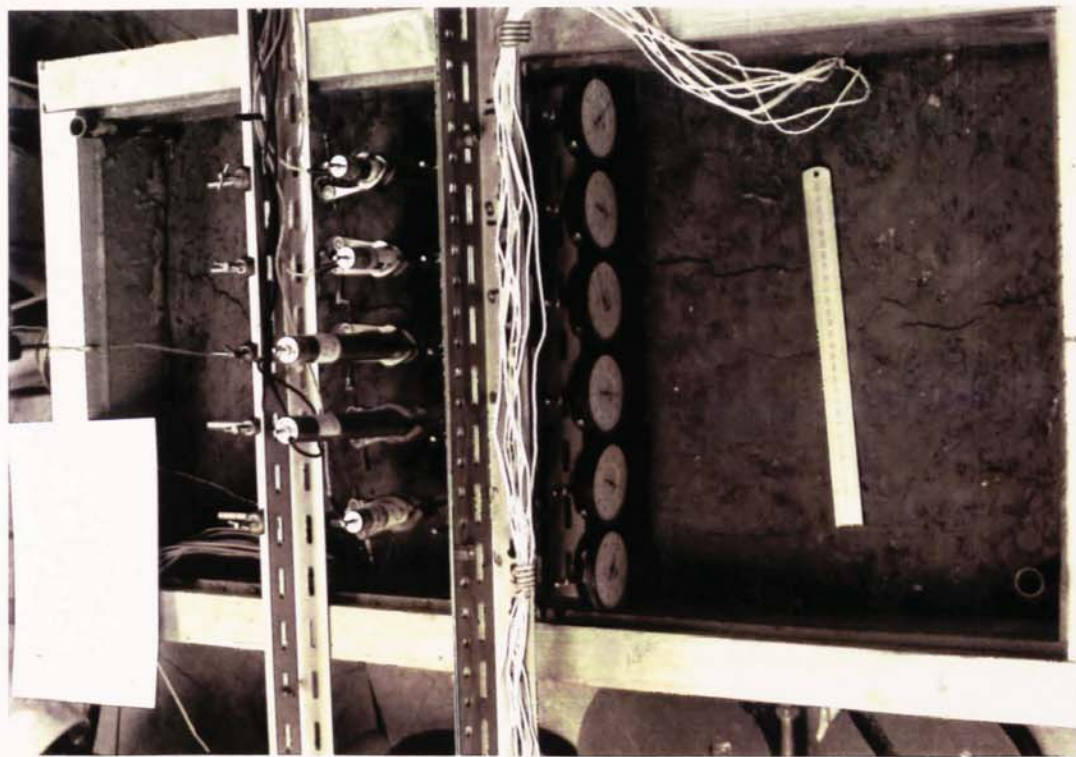


PLATE 8.3 Photograph Showing the Extent of Ground Cracking After 48 hours During the Tatsfield Test.

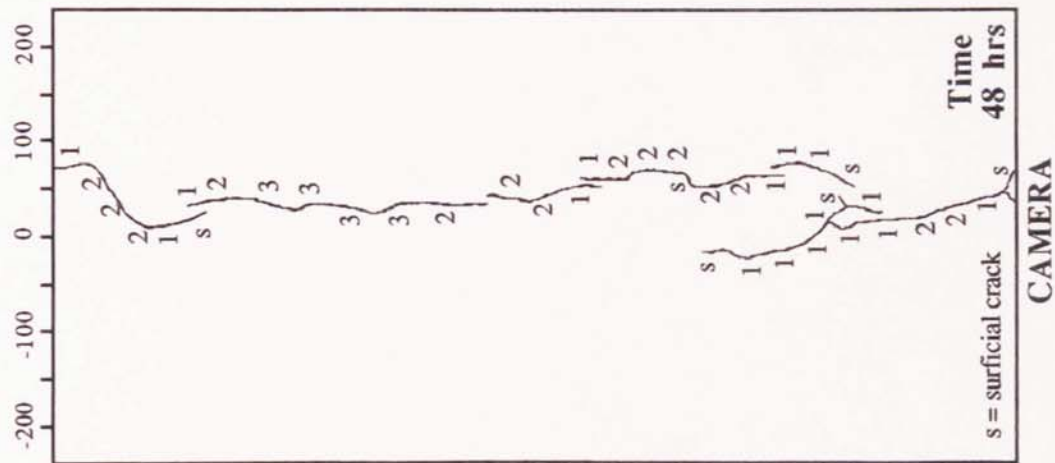


FIGURE 8.24 Plan View of Soil Surface During the Tatsfield Test Showing the Width of Ground Cracking after 48 hours (dimensions mm).

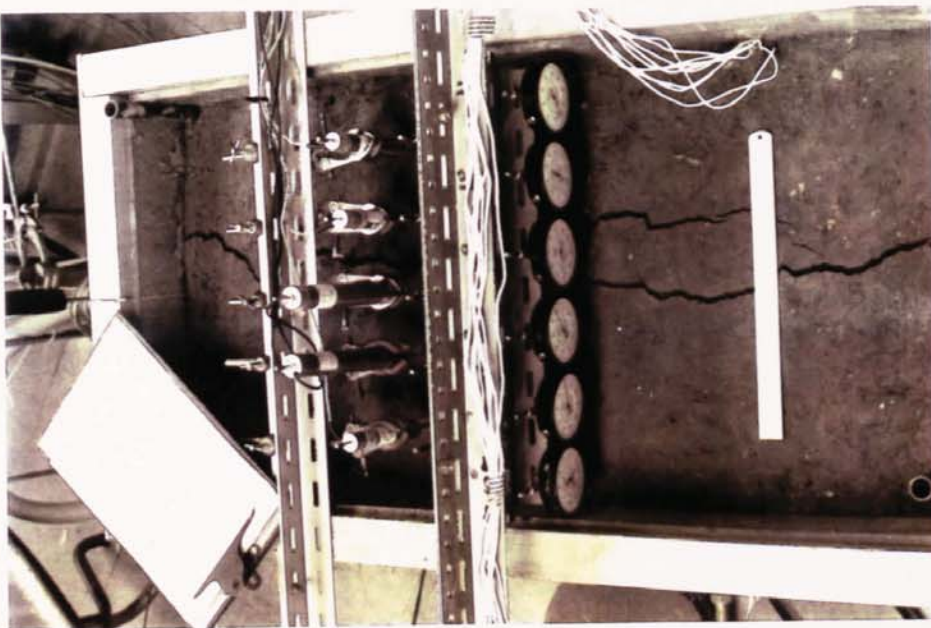


PLATE 8.4 Photograph Showing the Extent of Ground Cracking After 96 hours During the Tatsfield Test.

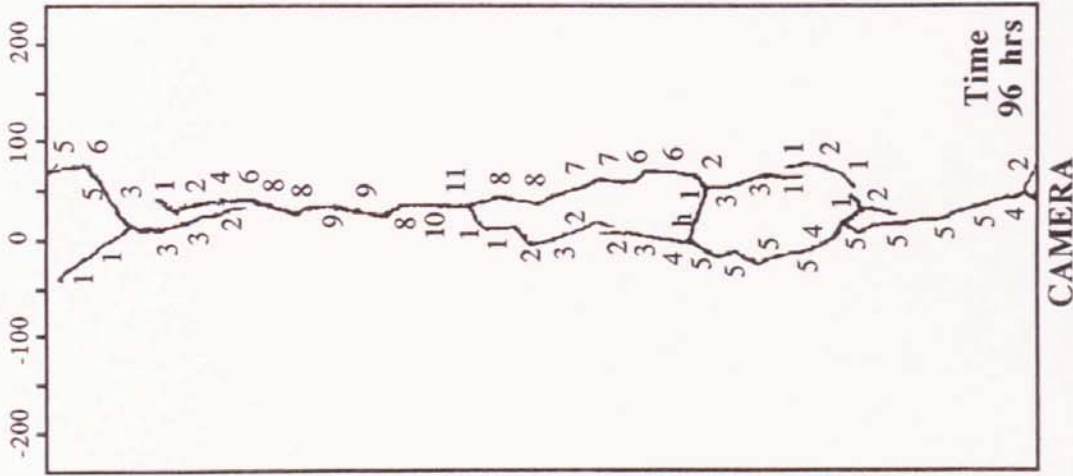


FIGURE 8.25 Plan View of Soil Surface During the Tatsfield Test Showing the Width of Ground Cracking after 96 hours (dimensions mm).

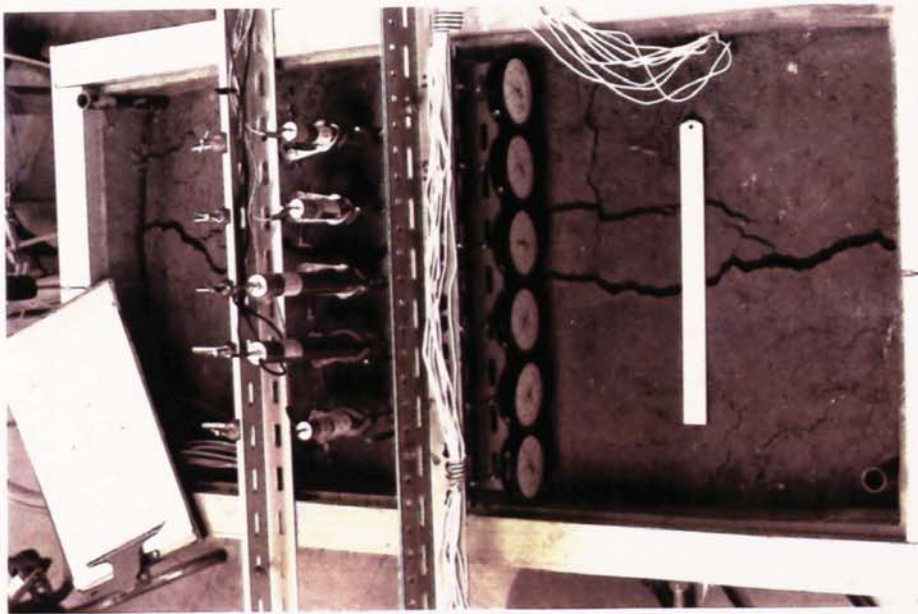


PLATE 8.5 Photograph Showing the Extent of Ground Cracking After 240 hours During the Tatsfield Test.

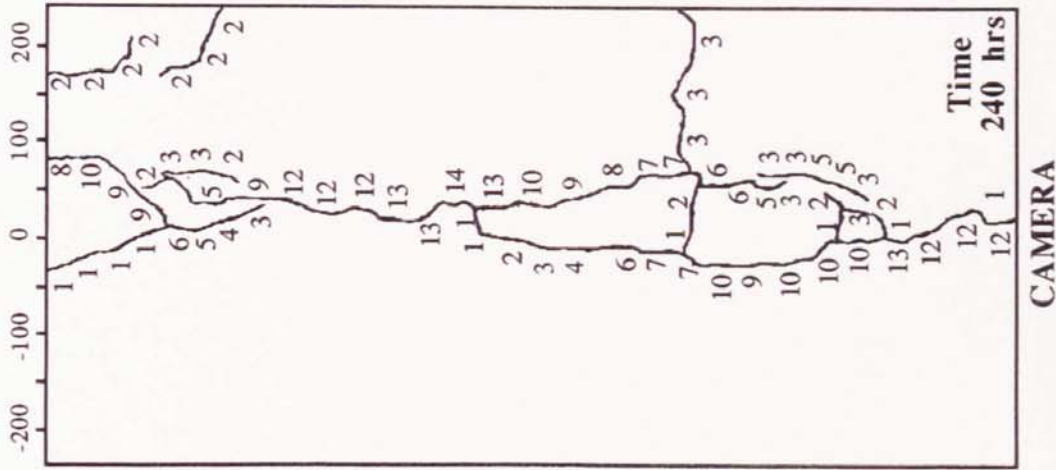


FIGURE 8.26 Plan View of Soil Surface During the Tatsfield Test Showing the Width of Ground Cracking after 240 hours (dimensions mm).

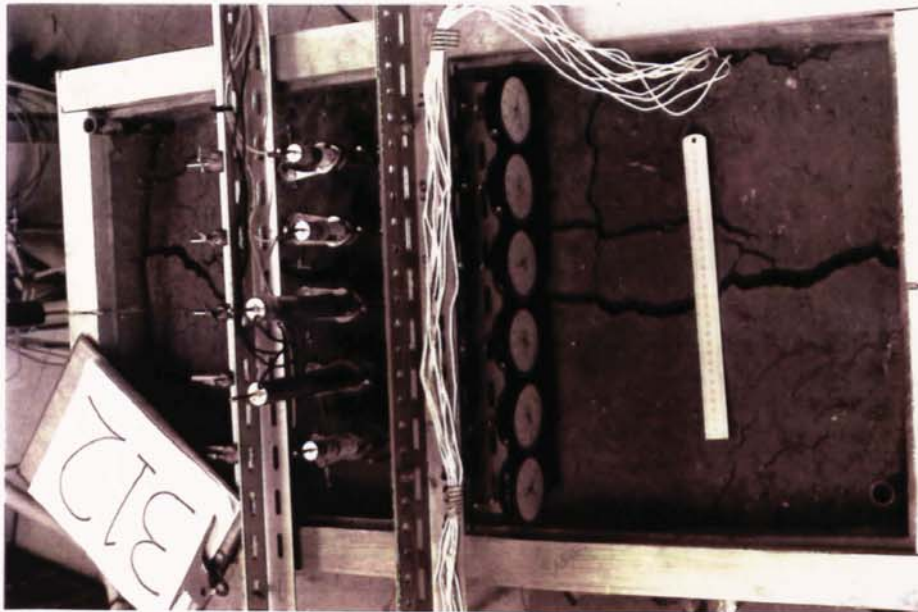


PLATE 8.6 Photograph Showing the Extent of Ground Cracking After 312 hours During the Tatsfield Test.

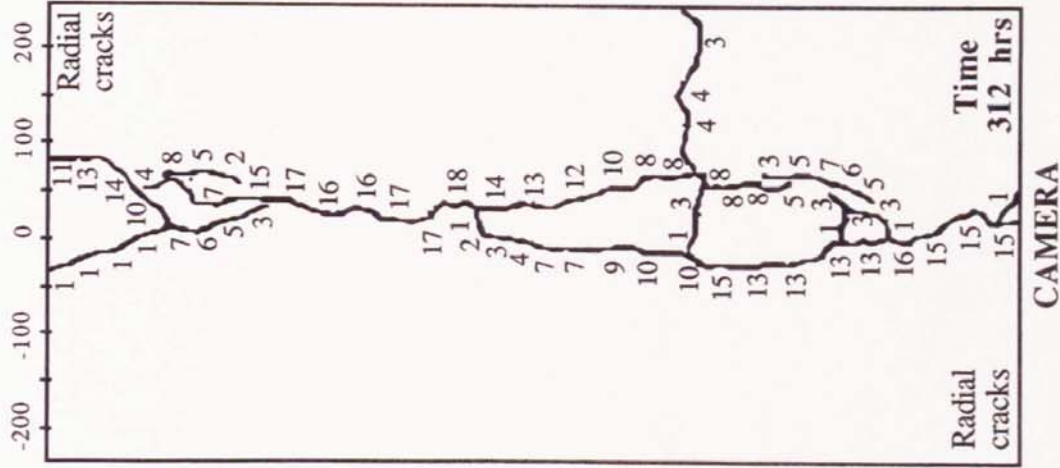


FIGURE 8.27 Plan View of Soil Surface During the Tatsfield Test Showing the Width of Ground Cracking after 312 hours (dimensions mm).



PLATE 8.7 Photograph Showing the Extent of Ground Cracking After 384 hours During the Tatsfield Test.

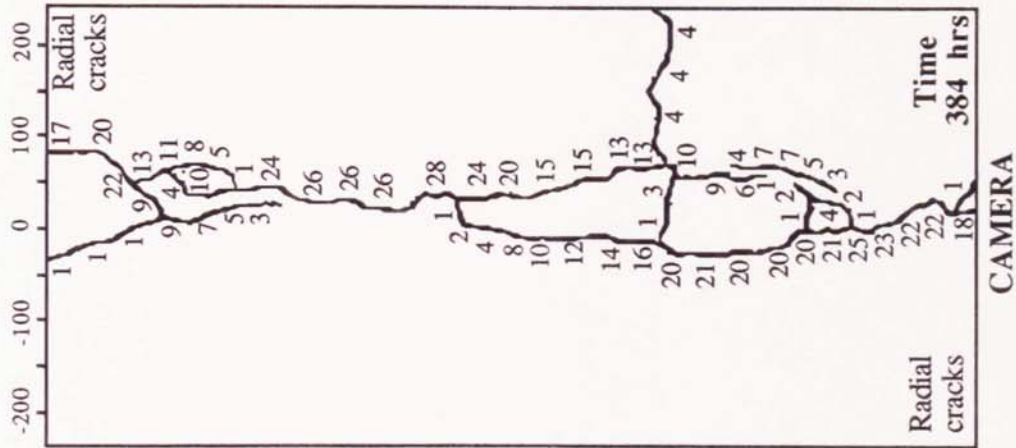


FIGURE 8.28 Plan View of Soil Surface During the Tatsfield Test Showing the Width of Ground Cracking after 384 hours (dimensions mm).

A ground surface crack over the line of the pipe approximately 400 mm in length was initially recorded after 42 hours and, by 48 hours, a number of cracks were observed along the full length of the soil surface over the pipe (Figure 8.24, Plate 8.3). At the centre of the tank two distinct cracks were observed (Figure 8.25, Plate 8.4) indicating that the formation of the initial crack had produced a re-distribution of the tensile stresses in the overlying soil mass leading to a further soil failure plane. Figures 8.26, 8.27 and 8.28 show the increase in cracking as the test continued and it is apparent that the total crack widths, perpendicular to the line of the pipe, were similar whether one or two cracks were observed across the profiles. Radial ground cracks in the corners were recorded in the latter stages of the test (Plates 8.5, 8.6 and 8.7) and it is suggested that they are a resultant of friction forces mobilized between the model tank and the soil mass.

At 396 hours the insulation box around the model tank was temporarily dismantled and an internal soil failure plane was observed through the perspex tank (Plate 8.8). The average measured angle was 65° to the vertical assuming a linear failure plane profile between its apex and the ground surface. This failure plane grew from the edge of the frozen annulus at approximately the level of the pipe centre to approximately 140 mm below the ground surface at the perspex wall. At the perspex wall the average height of the failure plane was 30 mm indicating that it formed at an earlier stage in the experiment since the soil wedge had moved up a similar amount.

Plate 8.9 shows the excavation at 396 hours and after the loose soil debris and hoar ice were cleared from the crack the soil failure planes that penetrated the ground surface are seen to have their apexes within the frozen annulus. This indicated that, after the cracks had penetrated the unfrozen soil mass from the ground surface to the top of the frozen annulus, the annulus grew around these cracks.

8.5.2.7 Pipe Movement.

Significant vertical pipe movement was not recorded until 66 hours into the test (Figure 8.29) indicating that it occurred after the pipe temperature dropped below 0°C at 42 hours. Beyond 66 hours the pipe moved upwards at a steadily decreasing rate but, at 240 hours and again at 312 hours, the rate of pipe movement initially increased in response to changes in the thermal regime of the model. However, the rate of pipe movement in each instance was seen to steadily reduce after these peaks had been noted.

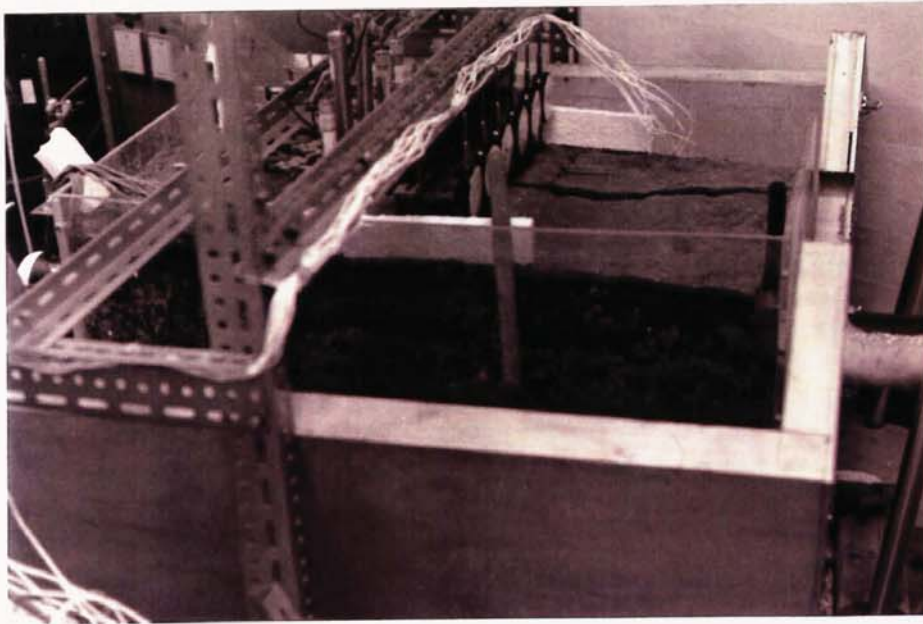


PLATE 8.8 Side View of Perspex Frost Heave Tank showing the Internal Soil Failure Plane during the Tatsfield at 396 hours.

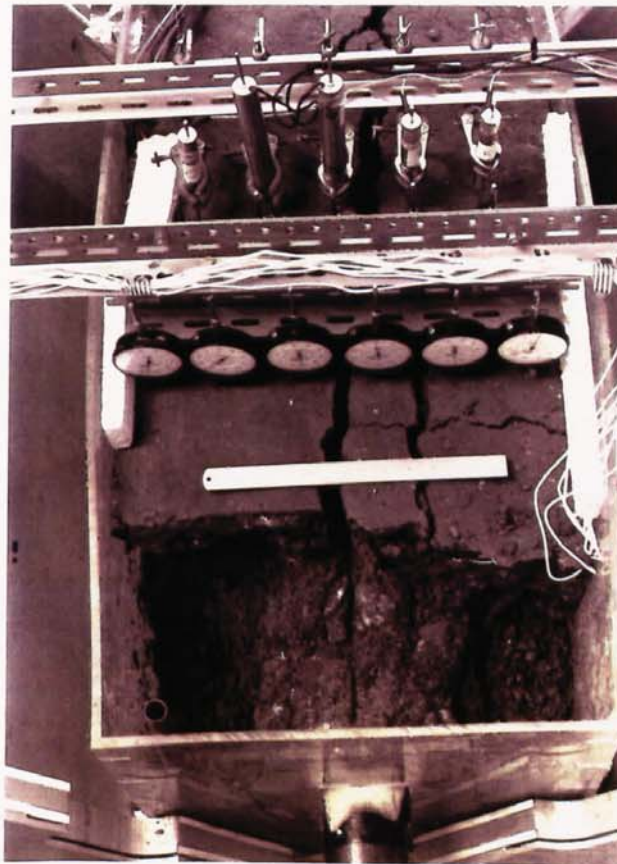


PLATE 8.9 Plan View of the Excavation of the Unfrozen Soil Overlying the Frozen Annulus during the Tatsfield Test at 396 hours.

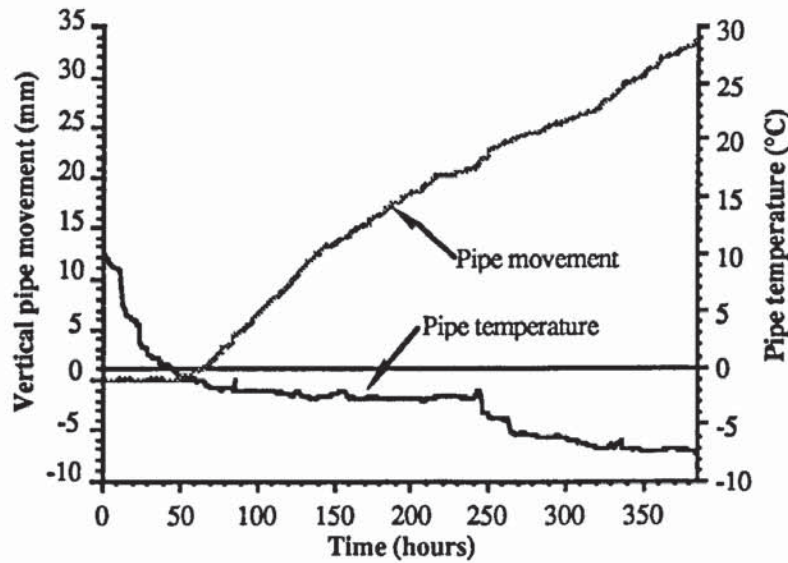


FIGURE 8.29 Vertical Pipe Movement in Relation to Pipe Temperature.

8.5.2.8 Ground Surface Movement.

Ground surface movement was initially recorded by the dial gauges at 42 hours and this was coincidental with the first observation of ground cracking. At this time no pipe movement had taken place, but ground movement over the pipe centre-line was 0.2 mm, so that the ground heave recorded (Figure 8.30) at 42 hours was a result of frost heave above the pipe. The crack recorded at 42 hours was a ground surface crack that extended 400 mm from perspex tank wall through which the pipe inlet passed (*ie.* the face furthest from the camera position).

At 72 hours it was noted from dial gauge measurements that upward displacement was taking place across the full extent of the ground surface profile (Figure 8.31). The wedge of soil bounded by the angle of the internal soil failure plane (Section 8.5.2.6) meant that the entire soil surface would be effected by upward pipe movement. Pipe movement was recorded from 66 hours onwards suggesting that it was frost heave under the pipe that produced the total movement across the soil profiles. Therefore the internal soil failure planes had formed soon after pipe movement had commenced.

The rate of ground surface movement was observed to decrease prior to 240 hours with the heave across the profile increasing on average by 1.13 mm between 216 and 240 hours in contrast to an average increase 2.83 mm between the preceding 24 hours (192 to 216 hours) (Figure 8.31).

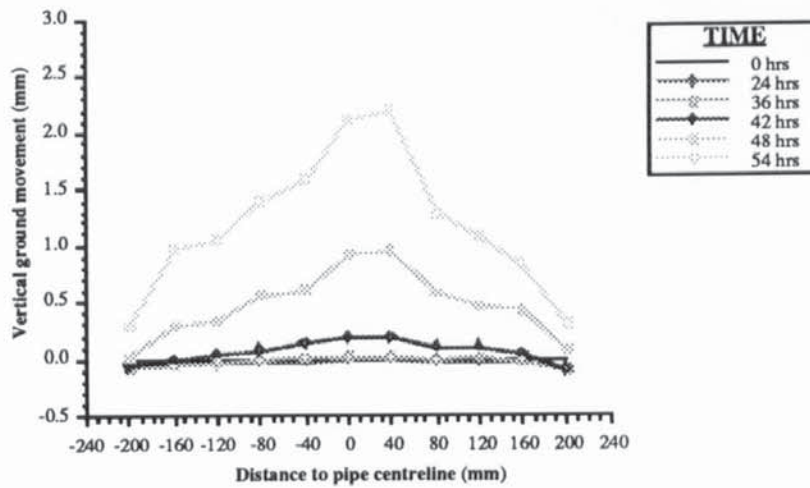


FIGURE 8.30 Mean Ground Surface Profile Across the Line of the Two Sets of Dial Gauges from 0 to 54 hours.

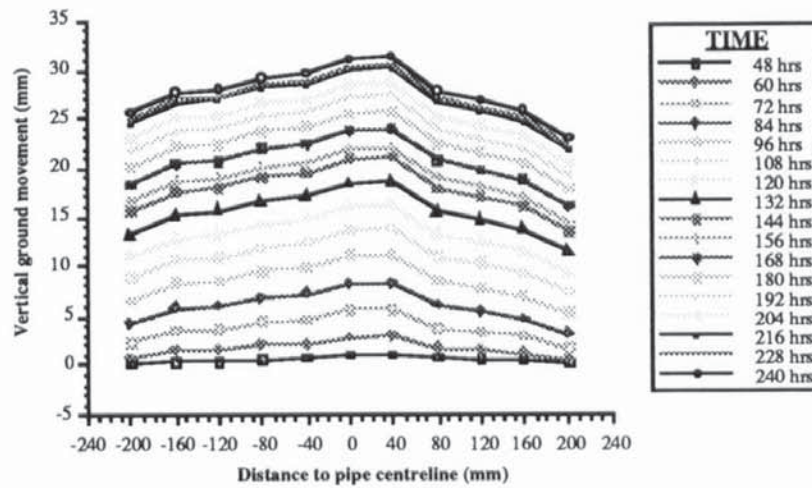


FIGURE 8.31 Mean Ground Surface Profile Across the Line of the Two Sets of Dial Gauges from 54 to 240 hours.

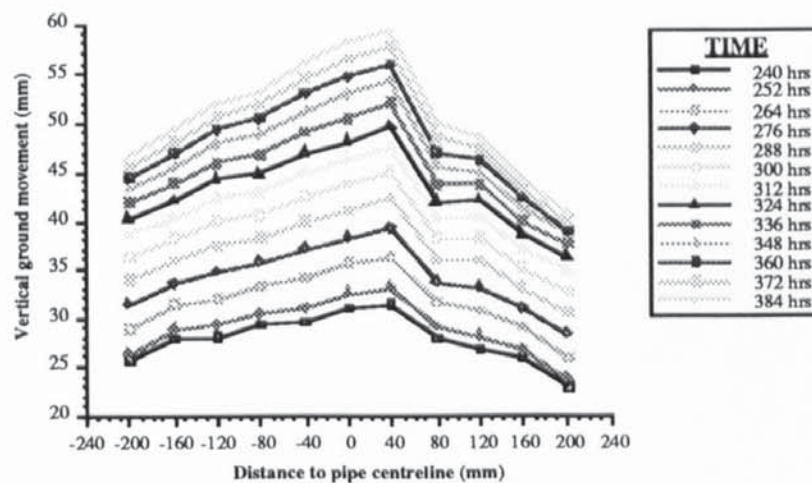


FIGURE 8.32 Mean Ground Surface Profile Across the Line of the Two Sets of Dial Gauges from 240 to 384 hours.

Between +40 and +80 mm in Figure 8.31 there was a distinct drop in the ground surface profile and this position corresponds to the right hand crack in the centre of the model in Figures 8.25 and 8.26. This drop in the ground surface profile became exacerbated after the thermal regimes of the pipe and later of the ground surface were altered at 240 hours and at 312 hours respectively reaching a maximum of 10 mm by 384 hours (Figure 8.32).

Figure 8.33 shows that the ground surface directly above the pipe heaved to a greater extent than the pipe. Both pipe and ground surface heave follow the same profile, but pipe heave is approximately 60% of the ground surface movement. Ground surface movement was noted from 42 hours onwards, but pipe movement was only recorded after 60 hours. This suggests that upward pipe movement was resisted by either overburden pressure and/or friction between the pipe flange plates and the model tank wall. Therefore, either the pipe movement restraining forces were greater than the frost heave pressures or the soil below the frozen annulus was compressible, thereby allowing the frozen annulus to expand into the unfrozen soil. Frost heave in the frozen annulus above the pipe resulted in crack formation and growth to an average width of 4 mm (Figure 8.23) before pipe heave was recorded.

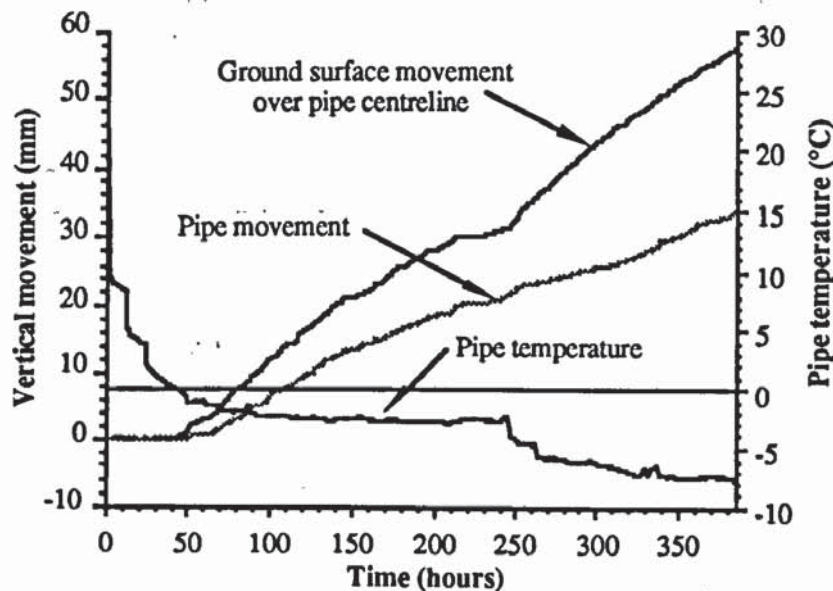


FIGURE 8.33 Pipe and Ground Surface Movement over Pipe Centre against Pipe Temperature

8.5.3 Blackrod Test.

8.5.3.1 Introduction.

The soil used in this test was collected from Site C on the Blackrod to Partington line that had been monitored in the large-scale test. The sample was taken from between the pipe invert and ground level.

The objective was to investigate the effect of negative thermal shocks, induced by rapidly lowering the pipe temperature, on pipe/ground surface movement and, subsequently, the stability of the frozen annulus when the pipe temperature is increased. In effect this matches the actual operating characteristics of the Blackrod system during the trial period (Section 7), and the test was operated with the aluminium foil covering the soil surface throughout the test, to reduce the effect of ambient thermal conditions on the experiment.

8.5.3.2 Soil Classification.

	Blackrod Soil
Gravel	10 %
Sand	15 %
Silt	69 %
Clay	6 %
Organic Content	15 %
Plastic limit	-- %
Liquid limit	68 %
Plasticity index	NP
Shrinkage limit	5 %
Dry density	890 kg m ⁻³

TABLE 8.3 Soil Properties for Blackrod Soil.

8.5.3.3 Operating Characteristics.

The pipe centre was 300 mm from bottom of the tank so that the depth of cover was 190 mm at the start of the test. The water was maintained at a constant level of 195 mm above the base of the tank which, at the start of the test, was 60 mm below the pipe invert level. Figure 8.34 shows the pipe temperature during the test, initially pipe temperature was lowered to -3°C, after which two negative thermal shocks to -5 and -7°C were applied at 72

and 108 hours respectively. The temperature was raised to -2°C at 122 hours and subsequently lowered to -2.75 and -3.5°C at 144 and 179 hours respectively to stabilize and re-initiate frozen annulus growth. Finally, at 217 hours, complete thawing of the frozen annulus was started. Results up to 274 hours are provided for the thermal and hydrological regimes but not for ground movement, pipe movement and crack growth since friction effects, between the pipe flanges and the side wall of the perspex tank, prohibited pipe settlement after 217 hours.

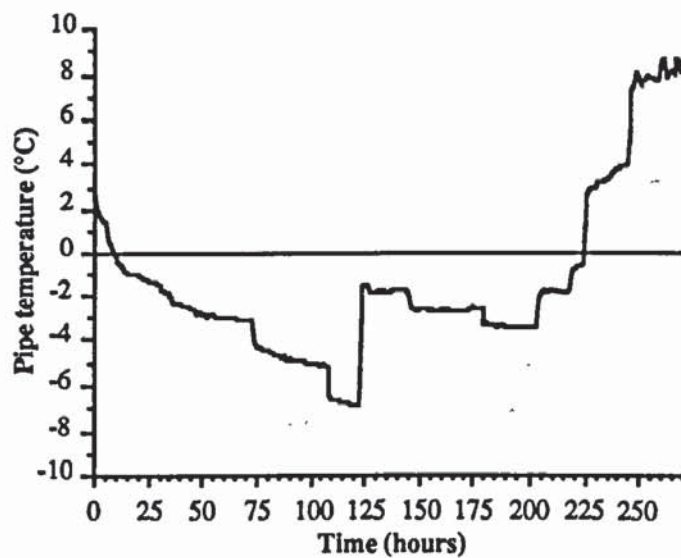


FIGURE 8.34 Pipe Temperature during the Blackrod Small-Scale Test.

8.5.3.4 Soil Temperature.

Figures 8.35 - 8.39 show the soil temperature profiles determined from the thermocouples located around the pipe (Figure 8.6). These probes were not rigidly fixed in relation to the pipe and so, with the growth and recession of the frozen annulus, their relative positions would have altered with respect to the pipe centre.

The curves (Figures 8.35 - 8.39) show a general fall in ground temperature as the pipe temperature (Probe No. 8) was lowered up to 122 hours. Subsequently, during the period of partial thawing and re-freezing, the temperature regimes remained generally constant indicating that significant movements of the freezing front did not take place.

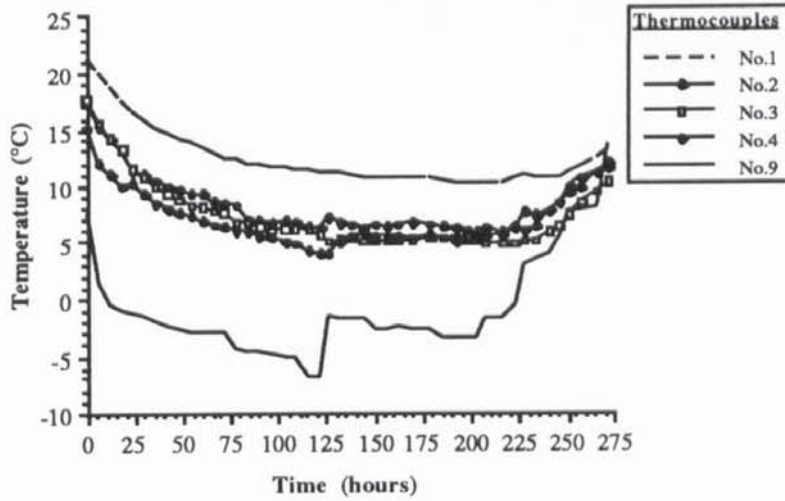


FIGURE 8.35 Vertical Temperature Profile above Pipe Crown (see Figure 8.6).

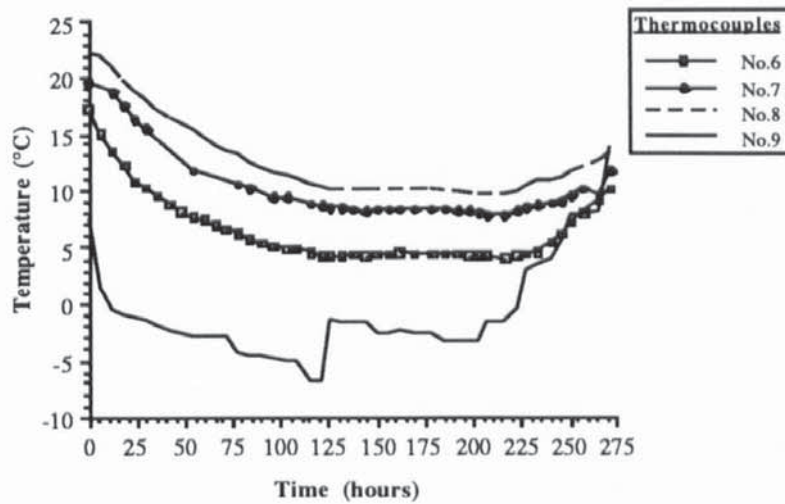


FIGURE 8.36 Temperature Profile at 45° to the Vertical above the Pipe (see Figure 8.6).

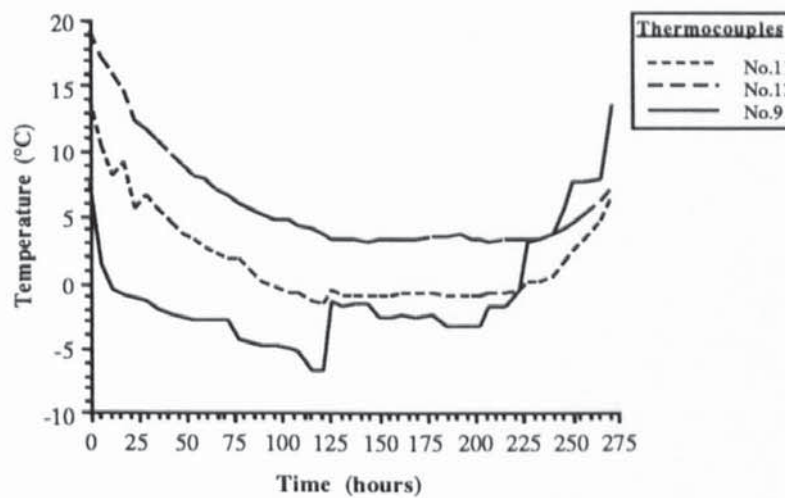


FIGURE 8.37 Horizontal Temperature Profile from the Pipe (see Figure 8.6).

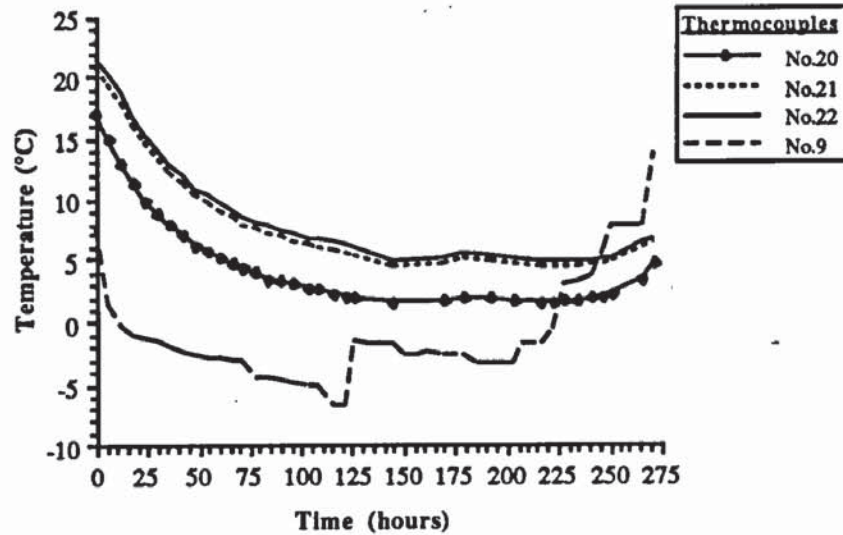


FIGURE 8.38 Temperature Profile at 45° to the Vertical Below the Pipe (see Figure 8.6).

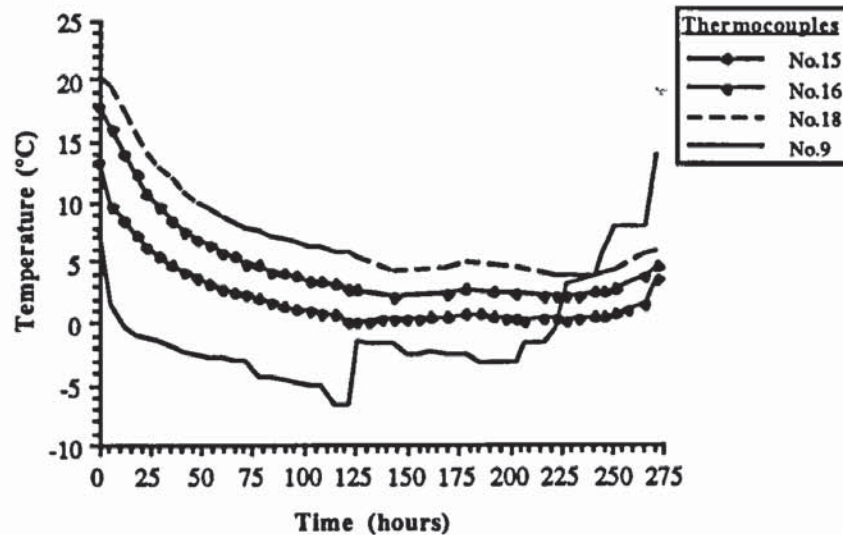


FIGURE 8.39 Vertical Temperature Profile below Pipe (see Figure 8.6).

8.5.3.5 Soil Water Potentials.

The results from the arrays of thermocouple-psychrometers radiating vertically above, at 45° and horizontally from the pipe centre (Figure 8.7) are given in Figures 8.40, 8.41 and 8.42. The water table was maintained at a constant level 60 mm below the initial pipe invert level.

Figure 8.40a shows the soil water potentials vertically above the pipe but, as the test progressed, these values became less negative, especially at probe 3. Further, it is clear from Figure 8.40b that the temperature of these probes did not drop below 5°C and the accompanying negative water potentials decreased. Thus, the formation and growth of the frozen annulus did not seem to produce moisture migration to the frozen front at and beyond

the position of the nearest probe (No. 3), which assuming that if a pure ice lens had formed on the pipe would be a maximum of 50 mm from the frozen annulus.

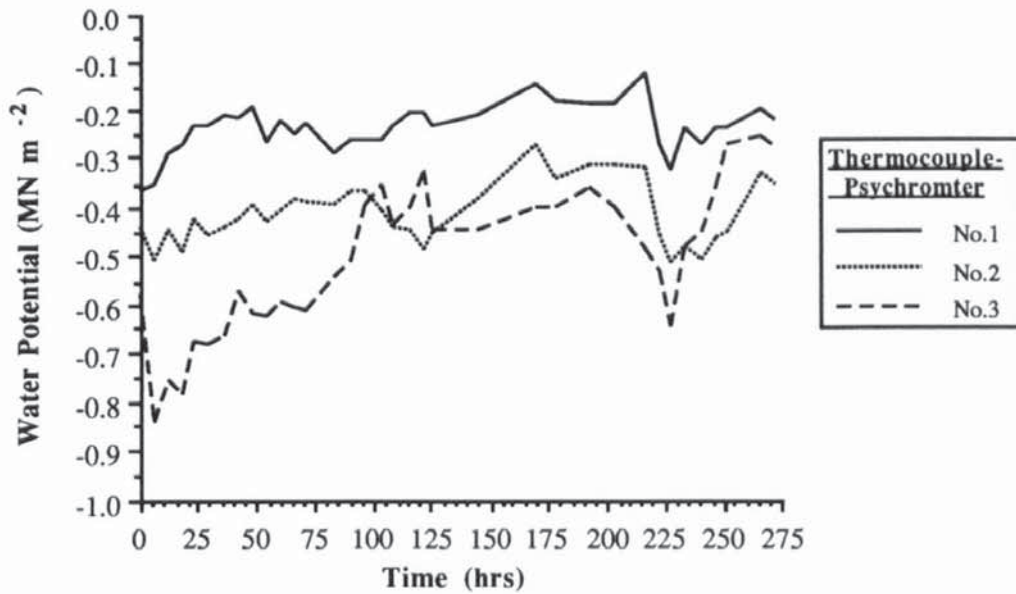


FIGURE 8.40a Soil Water Potentials Vertically above the Pipe Crown (see Figure 8.7).

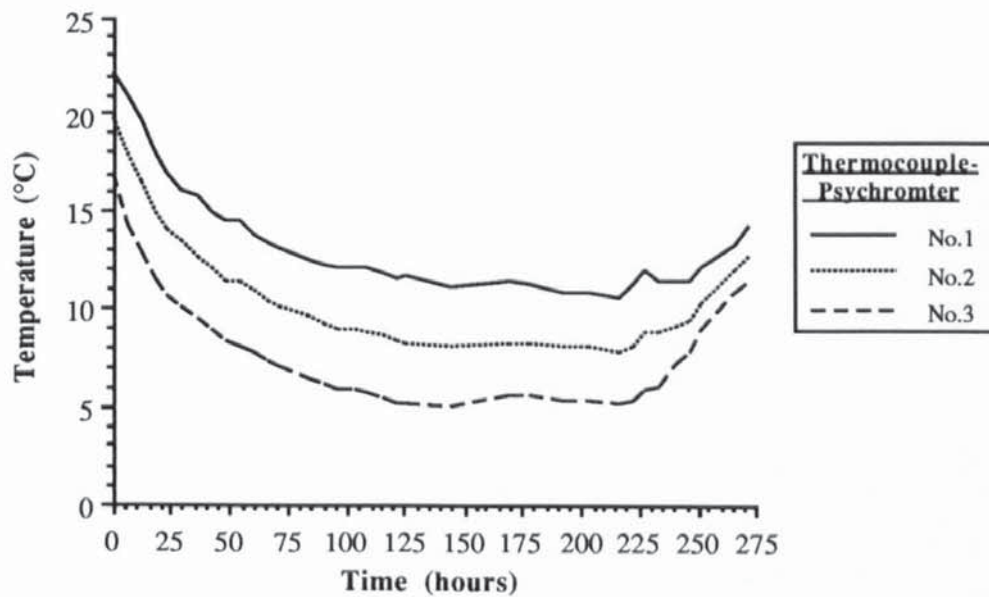


FIGURE 8.40b Soil Temperature at the Positions of Soil Water Potential Measurement Vertically above the Pipe Crown (see Figure 8.7).

The thermocouple-psychrometers at 45° show only small negative soil water potentials at the start of the test and these remained between 0 and -0.3 MN m⁻² (0 and -3 bar) until the end of the test (Figure 8.41b). Again, the temperature profiles of the probes indicated that they were not within the frozen annulus and that, at a maximum distance of 50 mm from the

frost front (if it is assumed that the growth of the frozen annulus was purely by ice lensing), the suctions associated with soil freezing were not detected.

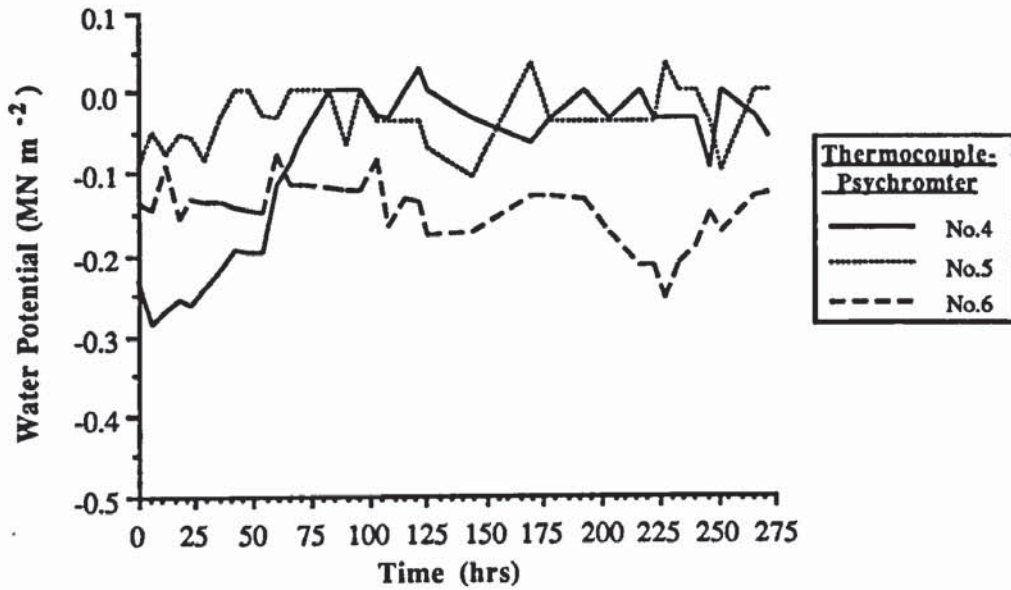


FIGURE 8.41a Soil Water Potentials at 45° to the Vertical above the Pipe (see Figure 8.7).

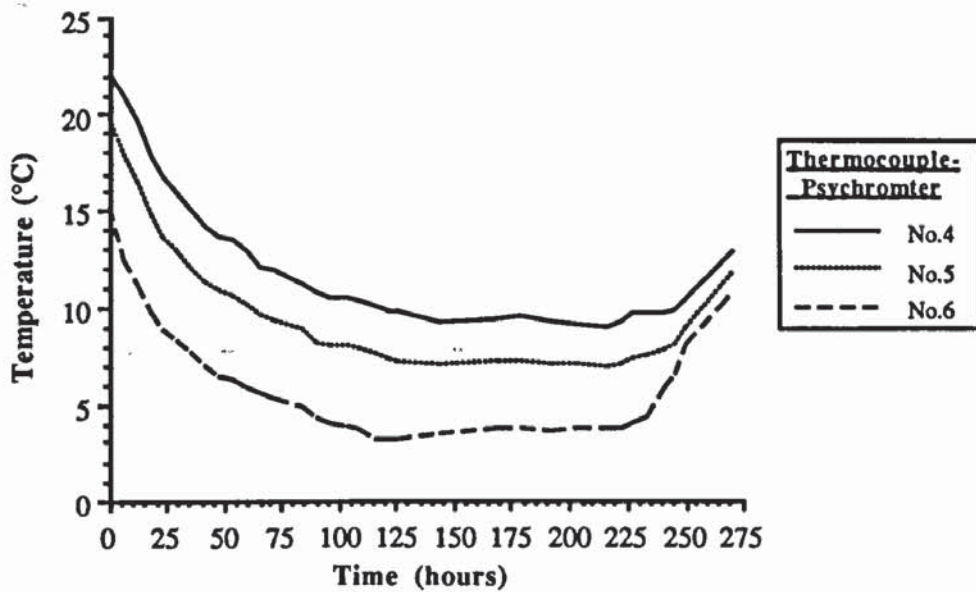


FIGURE 8.41b Soil Temperature at the Positions of Soil Water Potential Measurement at 45° to the Vertical above the Pipe (see Figure 8.7).

In Figure 8.42a, probes 7 and 9 showed negative water potentials of between 0 and -0.1 MN m⁻² (0 and -1 bar), and again the suctions generated, due to soil freezing, did not extend to probe 9 which was at 2°C after 122 hours (Figure 8.42b).

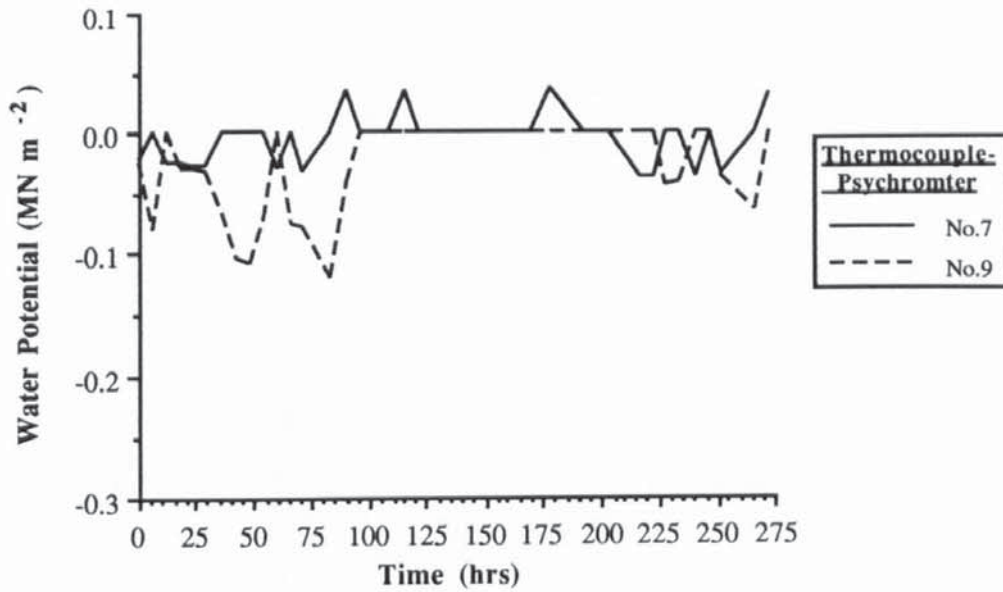


FIGURE 8.42a Soil Water Potentials Horizontal to the Pipe Centre (see Figure 8.7).

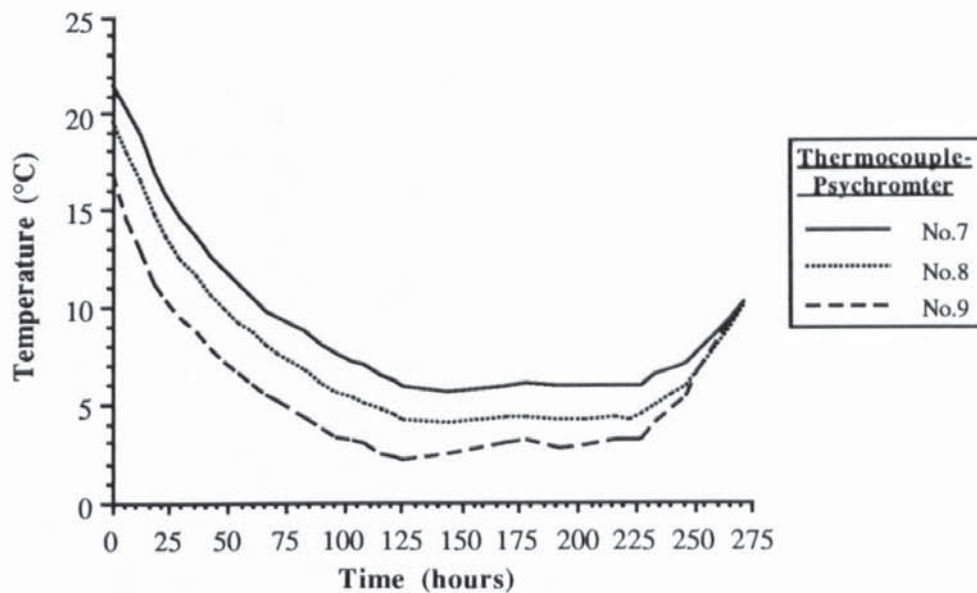


FIGURE 8.42b Soil Temperature at the Positions of Soil Water Potential Measurement Horizontal to the Pipe Centre (see Figure 8.7).

Figures 8.40a, 8.41a and 8.42a illustrate that no increase was recorded in the negative soil water potential ahead of the advancing frost front associated with soil freezing. Thus these negative soil water potentials, if they exist, act over a very short range which on this evidence would seem to be less than 50 mm from the frozen annulus. This suggests that the suction forces developed within the frozen annulus were negated over a very short distance as a result of the soil properties of particle size and hydraulic conductivity.

It was evident from Figure 8.43 that, after 122 hours when the pipe temperature was raised from -7 to -2°C that water was released from the frozen annulus by thawing. After 144 hours when the pipe temperature was lowered to -2.75°C , water intake was again recorded indicating an increase in the size of the frozen annulus.

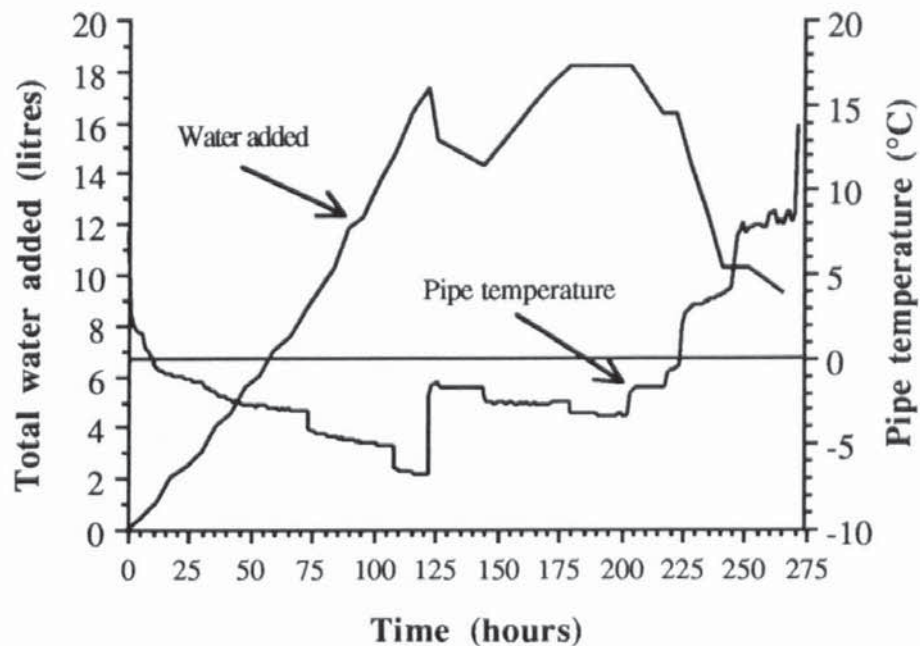


FIGURE 8.43 Water Added to Model during the Blackrod Test to Maintain a Constant Water Table Level.

8.5.3.6 Ground Cracking.

The total width of cracking across the three sections, where ground movement was monitored, was summated and averaged, and these values are shown in Figure 8.44. Rapid crack growth was observed after the pipe temperature dropped below 0°C , with ground surface cracking first recorded after 12 hours and by 18 hours it had opened up to an average value of 3 mm (Figure 8.45).

As a result of partial thawing of the frozen annulus after 122 hours there was an associated reduction in average total crack width. Repeated crack width growth occurred beyond 179 hours when the pipe temperature had dropped to -3.5°C . Results are not provided beyond 217 hours since the pipe was unable to settle during thawing of the frozen annulus due to the friction forces developed between the flange plates and the wall of the perspex tank. In consequence the ground surface had a net upward displacement approximately equal to that of the pipe which was 20.6 mm at the end of the experiment and so the residual ground cracking characteristics would probably have been affected by these displacements.

Plates 8.10, 8.11, 8.12 and 8.13 show the soil surface at 18, 66, 144 and 204 hours and are supplemented with plan views which provide crack width details (Figures 8.45, 8.46,

8.47 and 8.48). The main crack was noted to run parallel and approximately 70 mm to the right of the centre-line of the pipe. The effect of the pipe flange plates was clearly seen at either end of the tank, where small cracks were found to originate from the opposite side of the flange plate to that where the main crack was located (Plate 8.11, Figure 8.46).

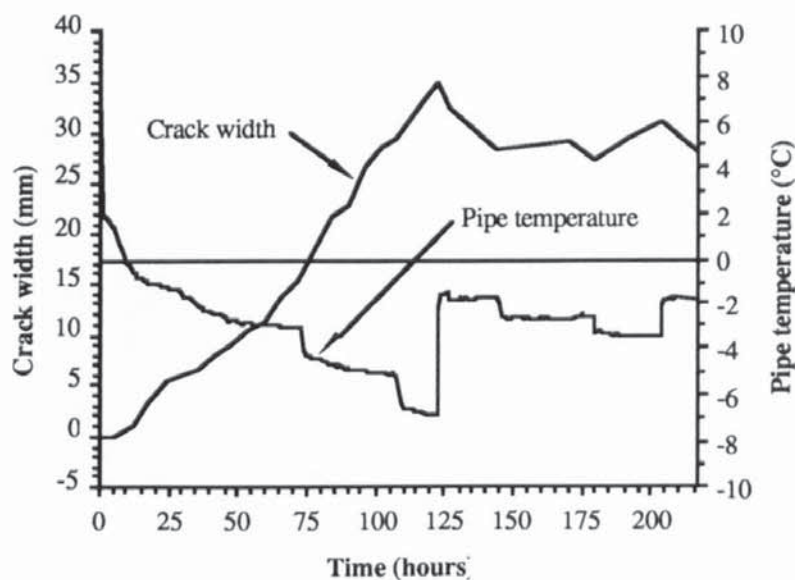


FIGURE 8.44 Average of the Total Width of Cracking Across the Soil Surface at the Locations of the Dial Gauges and LVDT's in Relation to Pipe Temperature.

After 217 hours an excavation was undertaken around both ends of the pipe to identify the soil failure pattern. Plate 8.14 shows the excavation closest to the camera position, as illustrated in Figures 8.8 and 8.45 - 8.48, and it is evident that two soil failure planes formed to produce a wedge of soil with its upper boundary between -240 and +60 mm on the ground surface (Figure 8.49). The vertical crack was observed to slant away from directly over the pipe centre, within the frozen annulus, to reach the ground surface at a location +60 mm from the pipe centreline. The internal soil failure crack was slanted at 35° to the vertical with its lowest, point within the frozen annulus being at a depth of 240 mm below the ground surface and -70 mm the centreline of the pipe (Figure 8.49). This point of contact with the frozen annulus occurred 40 mm above the pipe centre.

The other excavation, shown in Plate 8.15, revealed the expected soil failure pattern for the net upward displacement of a pipe, in relation to the surrounding soil, and involves a vertical crack over the pipe and two internal soil failure planes which were slanted upwards from either side of the frozen annulus. The internal failure planes, which are highlighted on Plate 8.15 with white powder, had angles of 32 and 34° to the vertical to the left and right respectively and the central ground crack was noted to be vertical (Figure 8.50).

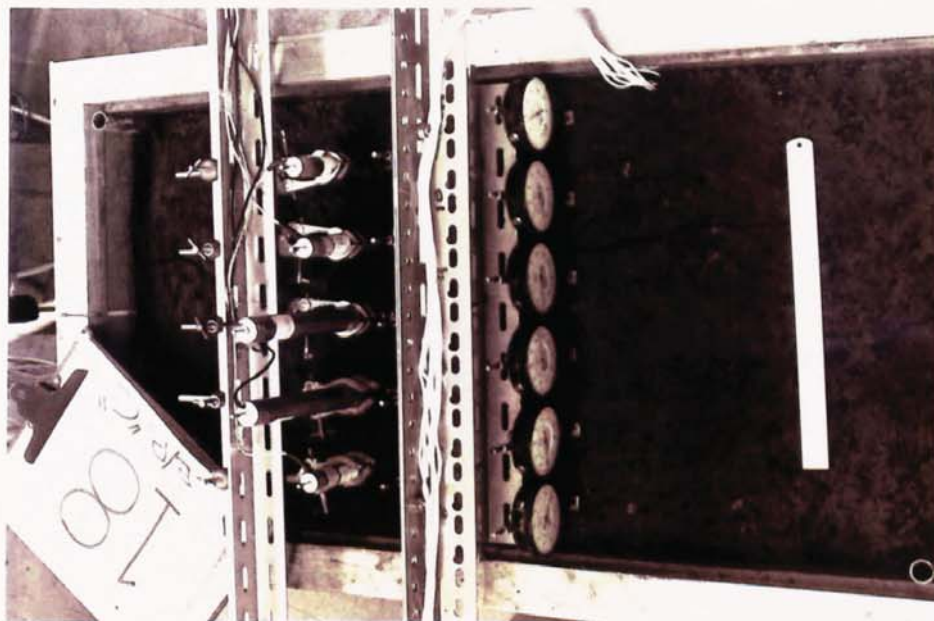


PLATE 8.10 Photograph Showing the Extent of Ground Cracking After 18 hours During the Blackrod Test.

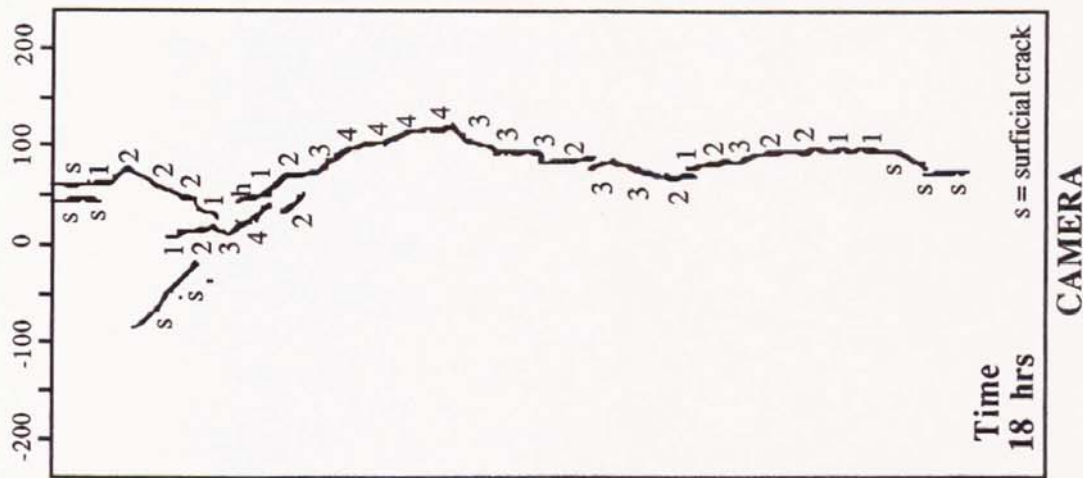


FIGURE 8.45 Plan View of Soil Surface During the Blackrod Test Showing the Width of Ground Cracking after 18 hours (dimensions mm).

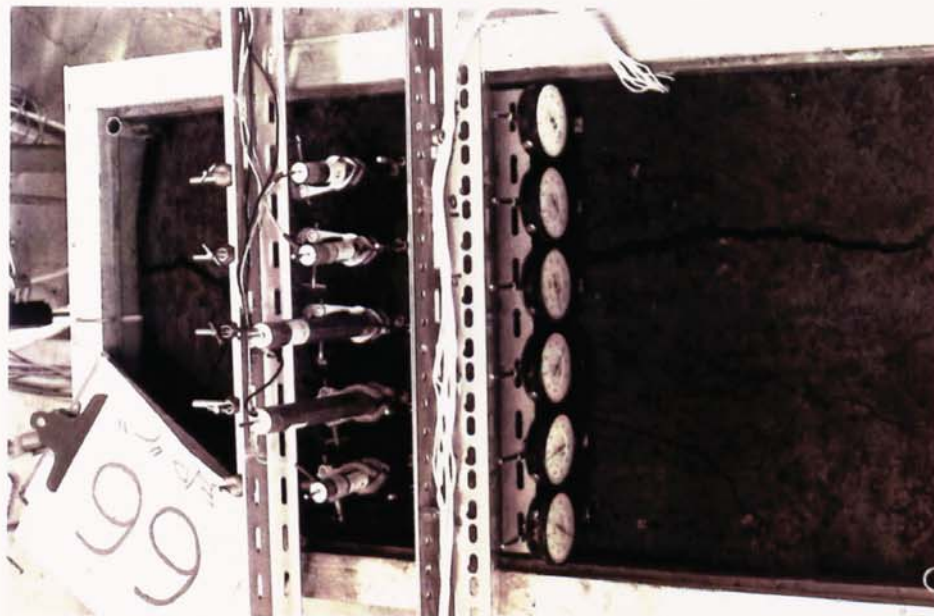


PLATE 8.11 Photograph Showing the Extent of Ground Cracking After 66 hours During the Blackrod Test.

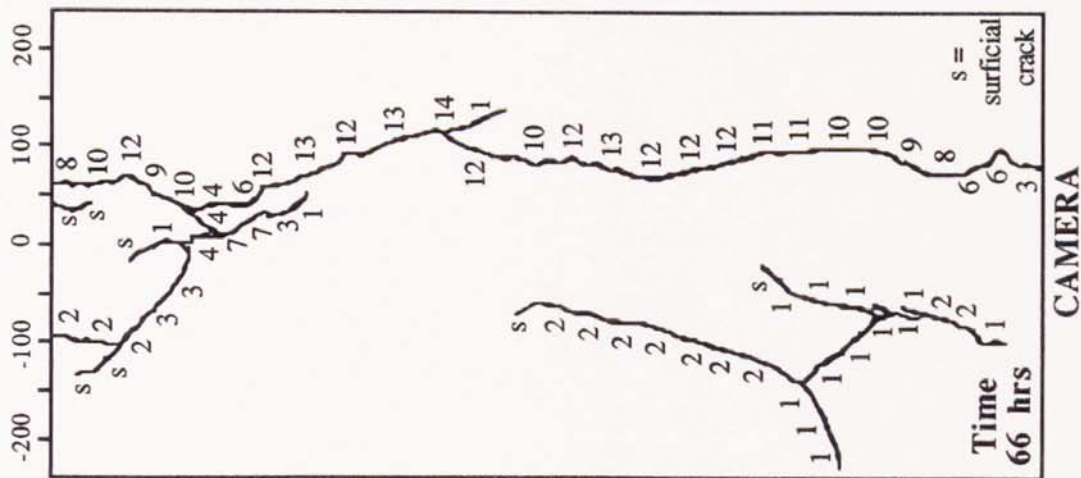


FIGURE 8.46 Plan View of Soil Surface During the Blackrod Test Showing the Width of Ground Cracking after 66 hours (dimensions mm).

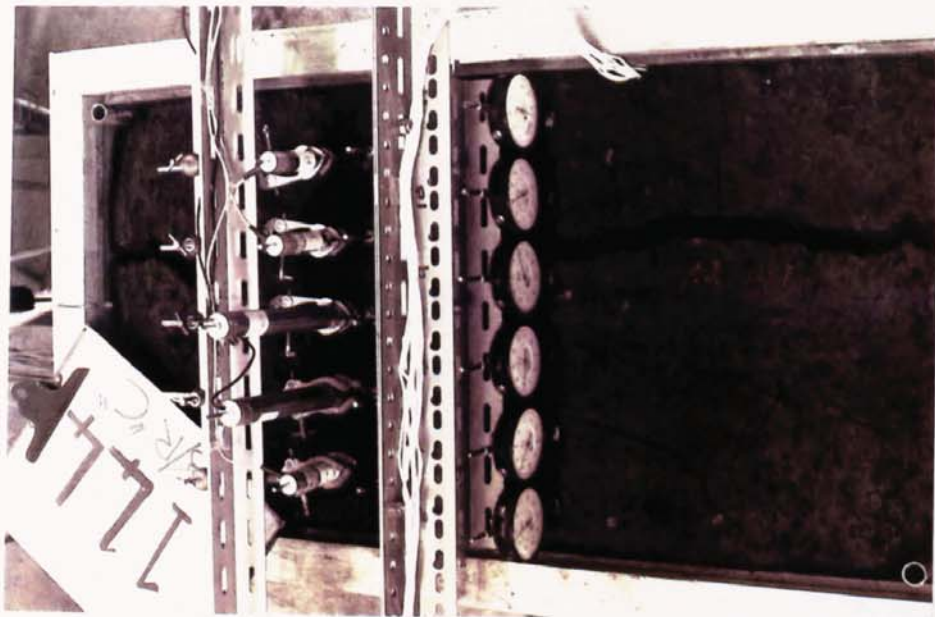


PLATE 8.12 Photograph Showing the Extent of Ground Cracking After 144 hours During the Blackrod Test.

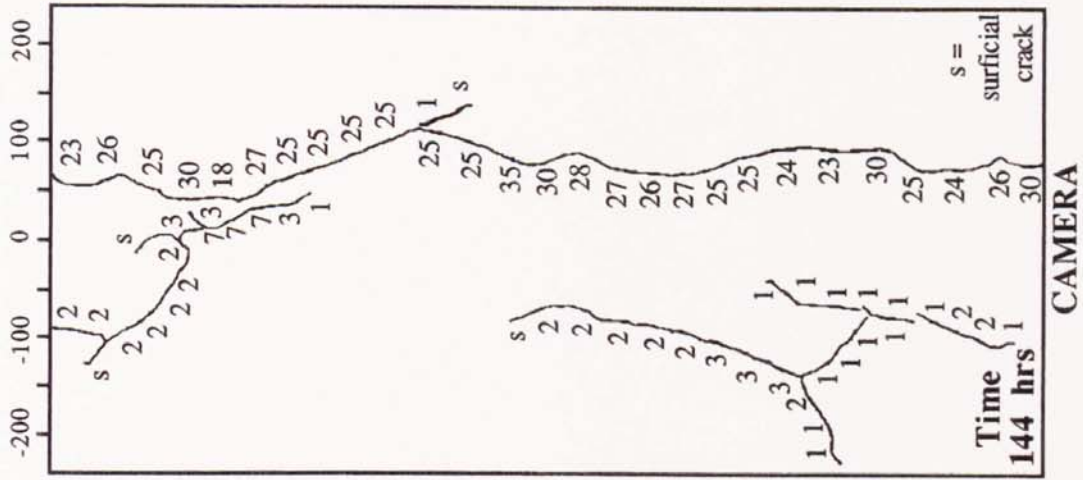


FIGURE 8.47 Plan View of Soil Surface During the Blackrod Test Showing the Width of Ground Cracking after 144 hours (dimensions mm).

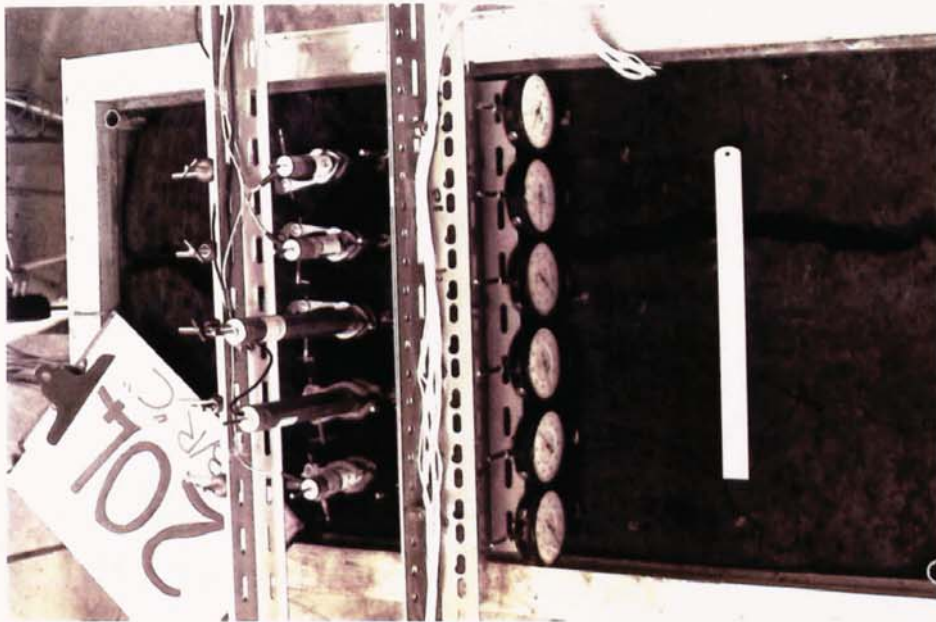


PLATE 8.13 Photograph Showing the Extent of Ground Cracking After 204 hours During the Blackrod Test.

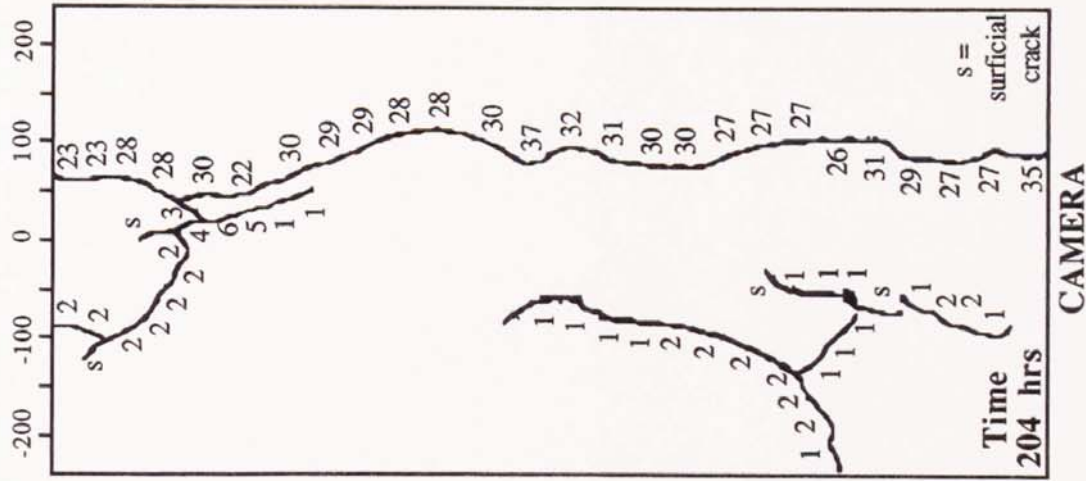


FIGURE 8.48 Plan View of Soil Surface During the Blackrod Test Showing the Width of Ground Cracking after 204 hours (dimensions mm).



PLATE 8.14 Photograph of Soil Failure Pattern 200 mm from the End of the Tank Closest to the Normal Camera Position (Figure 8.8).

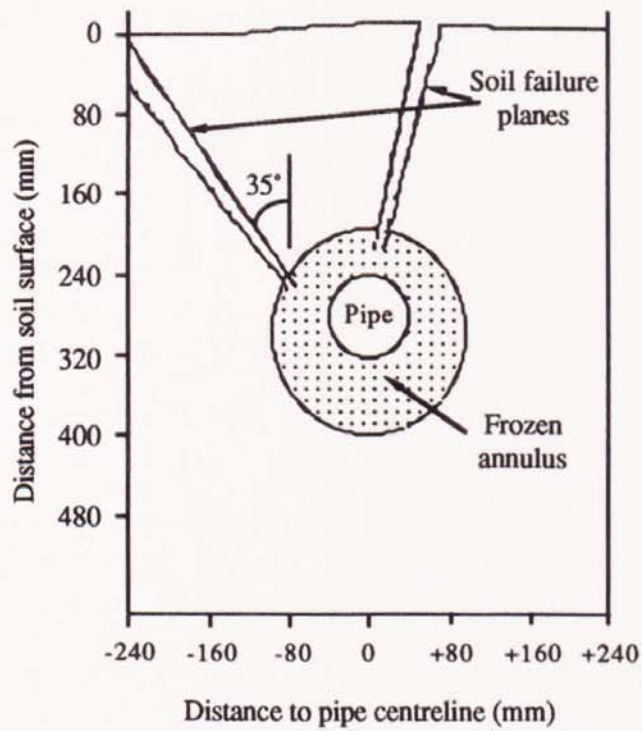


FIGURE 8.49 Illustration of the Soil Failure Planes shown in Plate 8.14.

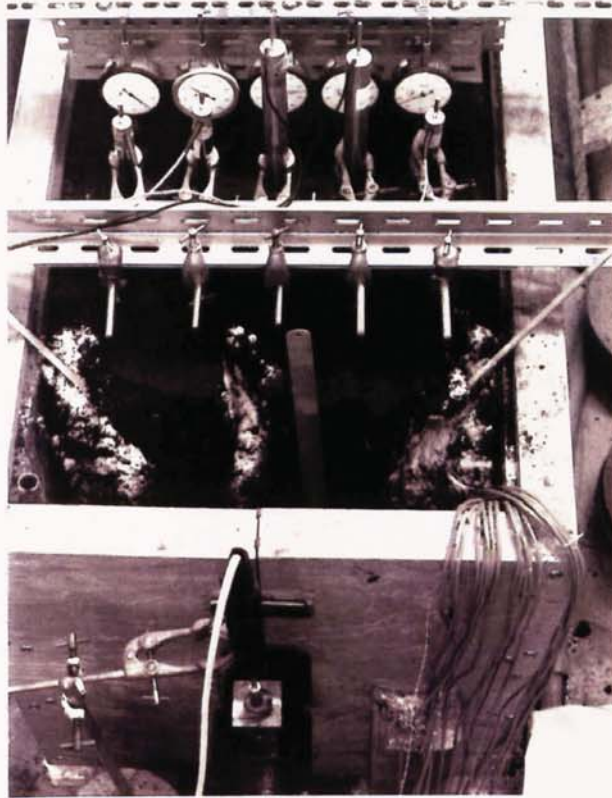


PLATE 8.15 Photograph of Soil Failure Pattern 200 mm from the End of the Tank Furthest from the Normal Camera Position (Figure 8.8).

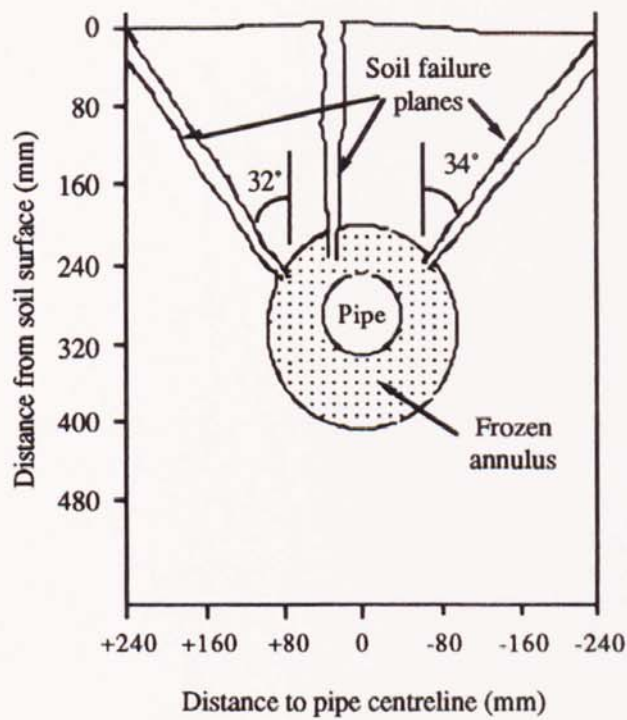


FIGURE 8.50 Illustration of the Soil Failure Planes shown in Plate 8.15.

8.5.3.7 Pipe Movement.

The pipe temperature dropped below 0°C at 10 hours and pipe movement was first recorded at 40 hours (Figure 8.51). Pipe uplift is a function of frost heaving in the frozen annulus below the pipe but, if these heaving pressures were less than the combination of overburden pressures and pipe flange plate friction forces, no movement would take place. However as freezing continued the heaving pressures would increase but, if the subgrade was sufficiently compressible, pipe movement would still not occur for the frozen annulus would have expanded into the subgrade. When sufficient compaction of the subgrade had occurred and the frost heave pressure exceeded the combined overburden pressure and pipe flange plate friction forces, upward pipe movement resulted.

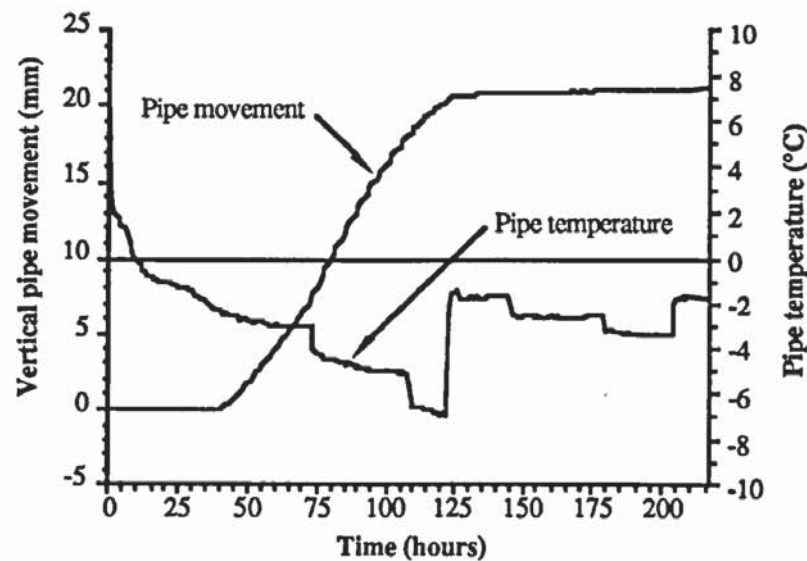


FIGURE 8.51 Vertical Pipe Movement in Relation to Pipe Temperature.

Pipe movement stopped after partial thawing of the frozen annulus was initiated at 122 hours and, presumably, the pipe flange plate friction forces held the pipe in its new position. However, it is uncertain whether the pipe was held in position by the pipe flange friction forces or by the residual frozen annulus below the pipe after 122 hours (Figure 8.51). Upon complete negation of the frozen annulus, the pipe had a residual upward displacement equal to that value recorded at 122 hours of 20.6 mm and this suggests that pipe flange friction forces were indeed present during thawing.

8.5.3.8 Ground Surface Movement.

Upward ground movement over the pipe centre-line was first recorded by the linear voltage displacement transducers at 11 hours (Figure 8.52). This coincides with the pipe temperature dropping below 0°C at 10 hours, but pipe movement was not recorded until 40 hours at which time ground surface movement over the pipe centre was 9 mm.

Consequently ground surface movement was exclusively linked to the growth of the frozen annulus above the pipe between 10 and 40 hours.

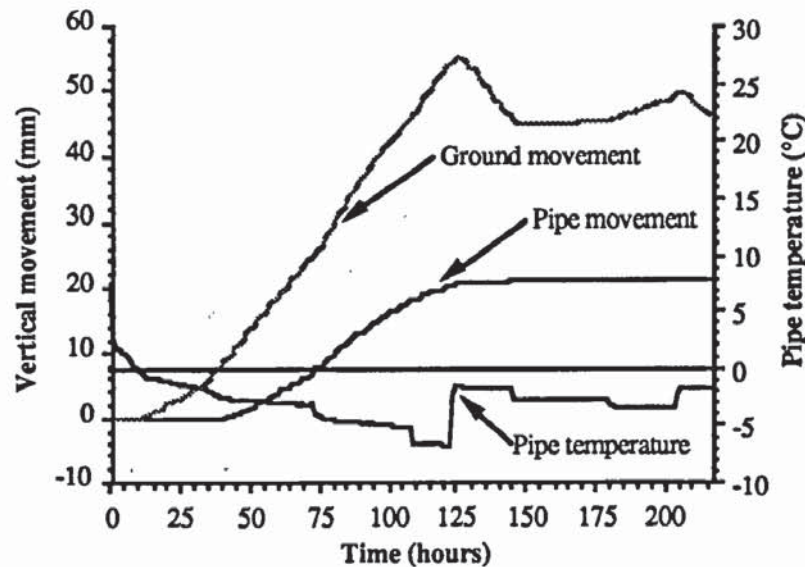


FIGURE 8.52 Pipe and Ground Surface Movement over Pipe Centre against Pipe Temperature.

Figure 8.53 shows that upward ground movement was first recorded by the two arrays of dial gauges at 12 hours and by 30 hours the whole profile was moving upwards. The formation of the main crack (Figure 8.45), at the +90 mm position, can be seen by a distinct drop in the profile between +80 and +120 mm which increased from 0.74 to 3.22 mm between 12 and 36 hours. This suggests that two distinct zones of soil were forming on either side of the crack and moving upwards at different rates. After 30 hours the whole profile was noted to be moving upwards (Figure 8.53), but it was uncertain whether internal soil failure had occurred at this time and produced two soil wedges above the frozen annulus. This is due to the circumferential growth of the frozen annulus imparting a component of vertical movement across the ground surface. As the test proceeded, the shape of the ground profile was noted to be changing slowly which, indicated some expansion of the frozen annulus. However, the whole ground surface was moving upwards (Figure 8.54) and this indicated that internal soil failure had occurred between 36 and 60 hours, since this is the period when the ground surface started to heave at a relatively constant rate and pipe movement was first recorded.

As the crack grew it opened up under the dial gauge at +80 mm and a steel plate was placed across the crack, causing the shape of the ground surface profile to be altered since this dial gauge indicated an average value across the crack (Figure 8.54). After the pipe started to heave at 40 hours the average rate of ground movement over the pipe centre increased from 0.30 to 0.57 mm/hr, but the pipe heave rate in this period, between 40 and 122 hours,

averaged 0.25 mm/hr indicating that the frozen annulus above the pipe was producing an average uplift rate of 0.32 mm/hr.

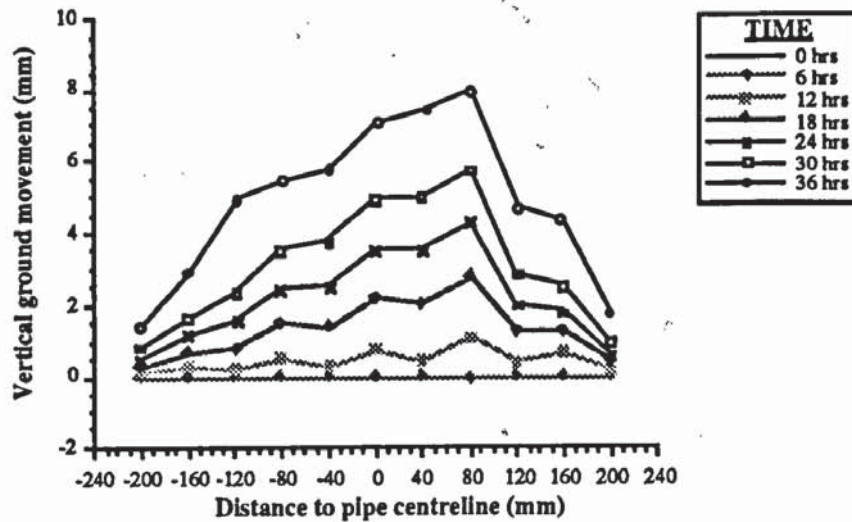


FIGURE 8.53 Mean Ground Surface Profile Across the Line of the Two Sets of Dial Gauges from 0 to 36 hours.

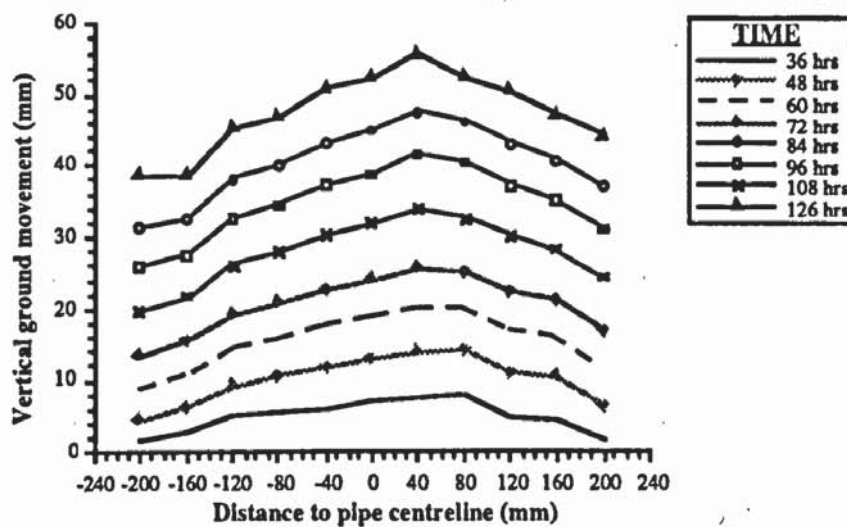


FIGURE 8.54 Mean Ground Surface Profile Across the Line of the Two Sets of Dial Gauges from 36 to 126 hours.

Between 126 and 144 hours there was a average drop in the ground surface across the array of dial gauges of 7.8 mm (Figure 8.55), but after the pipe temperature was lowered at 144 hours from -2 to -2.75°C , surface settlement halted indicating that the frozen annulus was at a steady state thermal condition. At 179 hours the pipe temperature was further lowered to -3.5°C and this produced ground heave. Again after the pipe temperature was subsequently raised to -2°C thaw settlement of the ground surface was recorded.

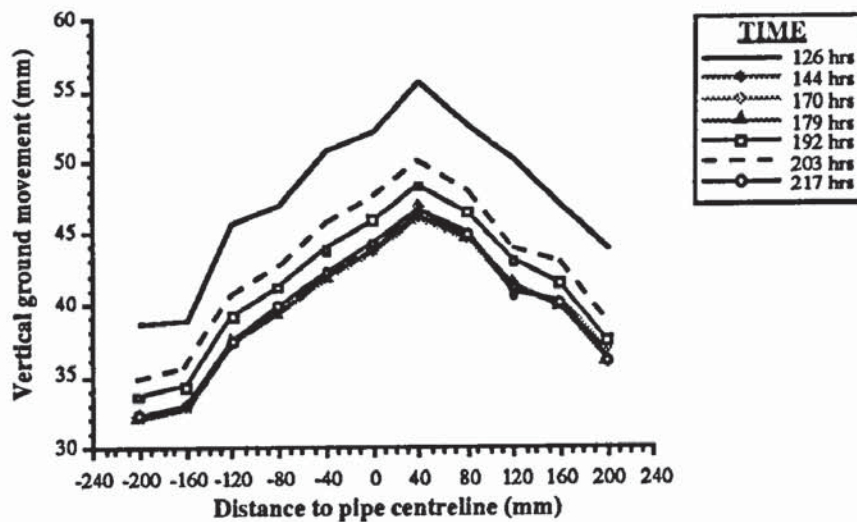


FIGURE 8.55 Mean Ground Surface Profile Across the Line of the Two Sets of Dial Gauges from 126 to 217 hours.

8.6 Summary.

This chapter has described the final phase of the study programme which involved the design and operation of a small-scale laboratory model of a chilled gas pipeline. The model was operated to investigate both the effect of the growth of the frozen annulus on ground cracking and the nature of the soil failure pattern in relation to that observed during pipe uplift tests without the effects of frost action.

Two tests were undertaken using *crack-susceptible* soils from Blackrod and Tatsfield PRSs. After the pipe temperature was reduced below 0°C ground surface fissures were first observed at ground surface displacements of under 1 mm, but no pipe heave was recorded. Pipe heave was however, recorded after the frost heaving pressures in the frozen annulus below the pipe were sufficient to overcome the overburden pressure, pipe weight and flange plate friction. However, initially these frost heaving pressures would have produced compaction of the subgrade. Ground cracking was noted to follow the line of the pipe and increased in width as the tests proceeded. The crack formed from a ground surface fissure which penetrated into the soil to the frozen annulus, and as the test proceeded the frozen annulus grew around its apex. At the end of the tests, excavations indicated that internal soil failure planes similar to those expected during pipe uplift tests had indeed formed. The angles of the failure planes were 65° and 35° to the vertical for the Tatsfield and Blackrod tests. The thermocouple-psychrometers indicated that in the Tatsfield test large suctions were developed within 50 mm of the frozen annulus, but no such suctions were recorded in the Blackrod test. However, these suctions were recorded after cracking had been initiated. These results indicate that ground cracking was produced in response to the expansion of the frozen annulus. Further interpretation and discussion of these findings together with those from the questionnaire and the large-scale study are provided in the next chapter.

CHAPTER 9 DISCUSSION

9.1 Introduction.

In this chapter each phase of the study program is discussed in relation to both ground cracking and frost heave. Subsequently both phenomena are individually elaborated and, finally, a general mechanism for ground cracking is developed in terms of the frost heave process emanating from the frozen soil annulus. As a summary, guide-lines are presented with respect to the soil-pipeline interactions investigated in this study programme, to aid the Engineer in the operation of PRSs at low temperatures.

9.2 Summation of Questionnaire Results.

9.2.1 Introduction.

The questionnaire was basically a medium to gain an engineering perspective of the total scale of chilled gas pipeline operation and whether soil-pipeline interactions were regarded as a potential hazard to the successful maintenance of the National Transmission System within the British Gas Network. More importantly to this investigation, the opportunity was taken to gain useful information on the operating conditions under which ground cracking and frost heave had been observed. These conditions encompassed both the pipeline operating conditions and the local soil conditions, together with observational details on the scale pipe/frost heave and ground cracking. More detailed information was precluded at this stage as the detailed examinations required to successfully define the soil thermal, hydraulic and stress regimes could not be provided by the British Gas pipeline staff. However, they were able to define the PRS operating characteristics with reasonable accuracy. At the end of this section a discussion is given on the extra information provided by the British Gas Regions relating to the troublesome consequences of chilled gas pipeline operation.

9.2.2 Extent of SPIs.

It is important to stress that the soil-pipeline interactions (SPIs) of frost heave and ground cracking were observed but not regularly monitored and, since the questions posed were in hindsight, they relied on the interactions being reported to the local Engineer for his interpretation. The replies from the questionnaire indicated that at least 83 downstream pipelines had been operated in chilled mode and either frost heave and/or ground cracking has been observed along 16 of these pipelines (Figure 6.1). This is similar to the experience of Michigan Consolidated Gas Company whereby nineteen regulator stations and their associated downstream pipelines were operated at sub-zero temperatures with only four showing the effects of ground freezing and frost heaving (Kempner, 1969).

Figure 6.7 provides details on the time periods when the SPIs were observed and it is of interest to note that they invariably started in November and were last reported in June/July, this representing the Pre-heating Season. The peak observation period was from December to March indicating that the phenomenon primarily manifests itself in the Winter under British Gas operating conditions. Frost heave was more predominant early in the Pre-heating Season, with ground cracking being more predominant in the latter part of the season. However these results do not indicate that a single mechanism was responsible for SPI leading to ground cracking.

9.2.3 SPI and Pipe Diameter.

The frequency of both forms of SPI show a general trend whereby both occur more frequently with increasing pipe diameter (Figure 6.5 and, Tables 6.5, 6.6 and 6.7). Generally larger pipelines are utilized for larger flow operations thus the mass flow rate increases with increasing pipe diameter. It can be shown from the Modified Schorre Equation (Archer *et al.*, 1984) that under equal sub-zero PRS outlet temperatures, the temperature recovery distance to 0°C will be greater with larger diameter and mass flow pipeline than for a smaller diameter and lower mass flow pipeline. Therefore, the gas temperature of a small diameter pipeline will recover to 0°C over a very short period, such as described by Kempner (1968), and consequently the SPIs associated with chilled gas pipeline operation will be observed either within the PRS or very close to its outlet. However, it must be noted that smaller diameter pipes fail under lower loads than larger pipes, thus care must be taken in low temperature operation since frost heave can produce very large forces (Section 3.3.4.2).

9.2.4 SPI and Soil Type.

The bar chart illustration in Figure 6.6 shows that SPIs have been observed in the range of sandy to clayey soils and this is in broad agreement with the general criteria (Anderson *et al.*, 1984b) for soils susceptible to frost heave. However, no such definition exists for the relatively novel concept of ground cracking, but clayey soils are regarded as susceptible to shrinkage cracking which develops upon soil desiccation (Reeve *et al.*, 1980). While Figure 6.6 and Tables 6.8, 6.9 and 6.10 provide information on the general soil characteristics they do not take into account the water table level and soil parameters of bulk density, shear strength, plasticity, etc, and therefore cannot be regarded as a definitive descriptions but rather they do provide a general indication of the relationship between the SPIs and broad soil classification.

9.2.5 Ground Cracking and Frost Heave.

When account is taken of each SPI, frost heave was almost exclusively (ie. in 12 of the 14 cases reported) observed within the PRS (Figure 6.3), whereas ground cracking was equally likely (ie. in 6 of the 12 cases reported) to be observed within the PRS and downstream. Both observable frost heave and ground cracking within and downstream of the PRS were only reported along one pipeline, this was the 600 mm pipeline downstream of Tatsfield PRS (SEGas) and the results are given in Appendix B.

These SPIs were primarily observed during the Pre-heating Season and, as expected with frost heave, they were fully negated by June. Unfortunately these results do not indicate whether any residual displacements of the pipe had taken place. Such displacements could include thaw settlement or residual upward movement, such as observed with the *growing stones* phenomenon, this residual movement being reported upon at the Caen facility (Van Vliet-Lanoe *et al.*, 1991). Ground cracking was observed to continue into July and this indicated that the cracks decreased in width in conjunction with a decrease in the observable frost heave. Ground cracking in the soil mass above the pipeline at Caen was observed both during the freeze (Geotechnical Science Laboratories, 1985) and thaw cycles (Geotechnical Science Laboratories, 1986b), cracking in the freeze and thaw cycles were independent of each other. Generally the cracks reported in the questionnaire were noted to develop during the freezing stage and disappear during the thawing stage, and this suggests that these cracks were of a different nature to those observed at Caen.

Tables 6.4 and 9.1 provide information on the estimated width of ground cracking and amount of frost heave both within and downstream of the PRS. The width of the ground cracks in the PRSs was substantially less than that observed downstream, similar trends were also recorded for frost heave. It was uncertain whether the results indicated that generally the magnitudes of ground cracking and frost heave were greater outside the PRS, since the observation of these SPIs within a PRS would probably result in the local Engineer raising the outlet temperature to negate the SPIs. A further uncertainty arises since, these SPIs were more likely to be observed by British Gas personnel within the PRS and for observation downstream, especially in farmland, their magnitudes would have to be greater to be noticed by the Pipeline Inspectors or the local landowner. Thus it was uncertain whether the observed magnitude of the SPIs in the PRS or downstream are a function of the magnitudes necessary for observation.

Table 9.1 summarizes Appendix B by providing details of the all the pipelines where SPIs were observed. Ten of the sixteen downstream pipelines had both ground cracking and frost heave reported along their length (Figure 6.1). However, within this group, seven pipelines

showed both ground cracking and frost heave at the same location and the other three (Pipelines 54, 56 and 62) had frost heave reported in the PRS and ground cracking reported downstream (Figure 6.4). Table 6.3 emphasizes that there was a strong relationship between observed frost heave and ground cracking along the same pipeline irrespective of whether they were recorded at the same location. These observed frequency tables (Table 6.3) illustrate that frost heave was noted along 83.33% of the pipelines where ground cracking was observed, and similarly ground cracking was noted along 71.4% of pipelines where frost heave was observed.

Pipe Number *	Pipe Diameter (mm)	SPI type #	Soil Type	Location	When	Magnitude (mm) +
38	450	GC	Clayey	PRS	Nov-Mar	6
45	450	FH	Clayey	PRS	Jan-Mar	Unknown
46	600	FH	Clayey	PRS	Nov-Mar	Unknown
		GC	Clayey	PRS	Nov-Mar	12
49	450	FH	Clayey	PRS	Nov-Feb	80
		GC	Clayey	PRS	Unknown	Unknown
51	Unknown	FH	Silty	PRS	Unknown	3
		GC	Silty	PRS	Nov-Feb	6
52	600	FH	Sandy	PRS	Most of year	Unknown
54	900	FH	Clayey	PRS	Dec-Apr	15
		GC	Clayey	D/S	May onwards	125
56	300	FH	Made-Up	PRS	Nov-May	80
		GC	Made-Up	D/S	Apr onwards	40
58	750	GC	Unknown	D/S	Dec-May	25
61	300	FH	Clayey	D/S	Feb-Mar	50-70
		GC	Clayey	D/S	Dec-Apr	75
62	600	FH	Clayey	PRS	Apr-Jun	50-70
		GC	Clayey	D/S	May-Jun	50
64	600	FH	Clayey	PRS	Feb-Jun	36
		FH	Clayey	D/S	Feb-Jun	100
		GC	Clayey	PRS	Feb-Jun	100
		GC	Clayey	D/S	Feb-Jun	120
66	900	FH	Clayey	PRS	Nov	26
76	600	FH	Clayey	D/S	Dec-Mar	50
		GC	Clayey	D/S	Dec-Mar	15-20
77	600	FH	Clayey	PRS	Nov-Mar	50
		GC	Clayey	PRS	Nov-Mar	25
81	400	FH	Sandy	PRS	Unknown	Unknown

* See Appendix B for full details of upstream Pressure Reduction Stations.

GC = Ground Cracking & FH = Frost heave.

+ For Frost heave refers to heave, but for Ground Cracking refers to crack width.

TABLE 9.1 Summary of Pipelines Where Frost Heave and Ground Cracking have been Observed.

9.2.6 Problems Associated with Chilled Gas Pipe Operation.

As a result of the low temperature operation a number of problems have been reported, the majority of which are directly attributable to the growth and recession of the frozen annulus. Frost heave and ground cracking has been discussed in the above sections and have similarly been noted by Kempner (1968). Frost heave has led to the surface disruption of roads both within and downstream of the PRS in this study (Appendix B), the W.Midlands Region noted that reconstruction was necessary at one site, and it has been reported in N.America by Kempner (1968) and Ahmad (1978). Pipe uplift within the PRS can lead to significant stresses in the pipe-work if pipe restraint is present, which prompted the N.Thames Region to release all restraints on the pipe work at a number of PRSs. However, at Tatsfield, a comprehensive monitoring program involving strain gauge measurement and pipe levelling was adopted as a methodology for pipe integrity assessment. Large stresses have been noted by Browning (1970) and these were counteracted by the frost heave control measures described in Section 4.5.2.2.

Thaw settlement occurs in thaw susceptible soils and, therefore could be expected to some extent under British conditions. Indeed it was noted by the W.Midlands Region along Pipe No.76 where heave up to 50 mm was recorded during freezing, that during thawing, a depression formed across the line of the pipe, which at its maximum was over 150 mm below the original pre-freeze level. During a visit to Tatsfield PRS to collect soil samples, such depressions were noted both within and downstream of the PRS (Plate 9.1). Thaw settlement, unlike frost heave under the thermal operating procedures of PRSs, is a permanent residual displacement of the ground surface and in the long-term may prove disruptive to overlying structures and activities.

The W.Midlands Region noted that the formation of icings on above-ground pipe-work hampered routine maintenance work. Similarly, damage to buildings/pits from frost heave, has resulted in the reconstruction of a pit at one site.

9.3 Large-Scale Test Site.

9.3.1 Introduction.

The questionnaire replies received by September 1987 (Table 6.2) initially indicated that both ground cracking and frost heave were observed along a majority of chilled gas pipelines, however later replies reduced this number to a small minority of the total pipelines (Section 9.2). After careful examination of the twelve replies received by September 1987 Blackrod, which was the site operated in the earlier study (Archer *et al.*, 1984), was selected for detailed monitoring.

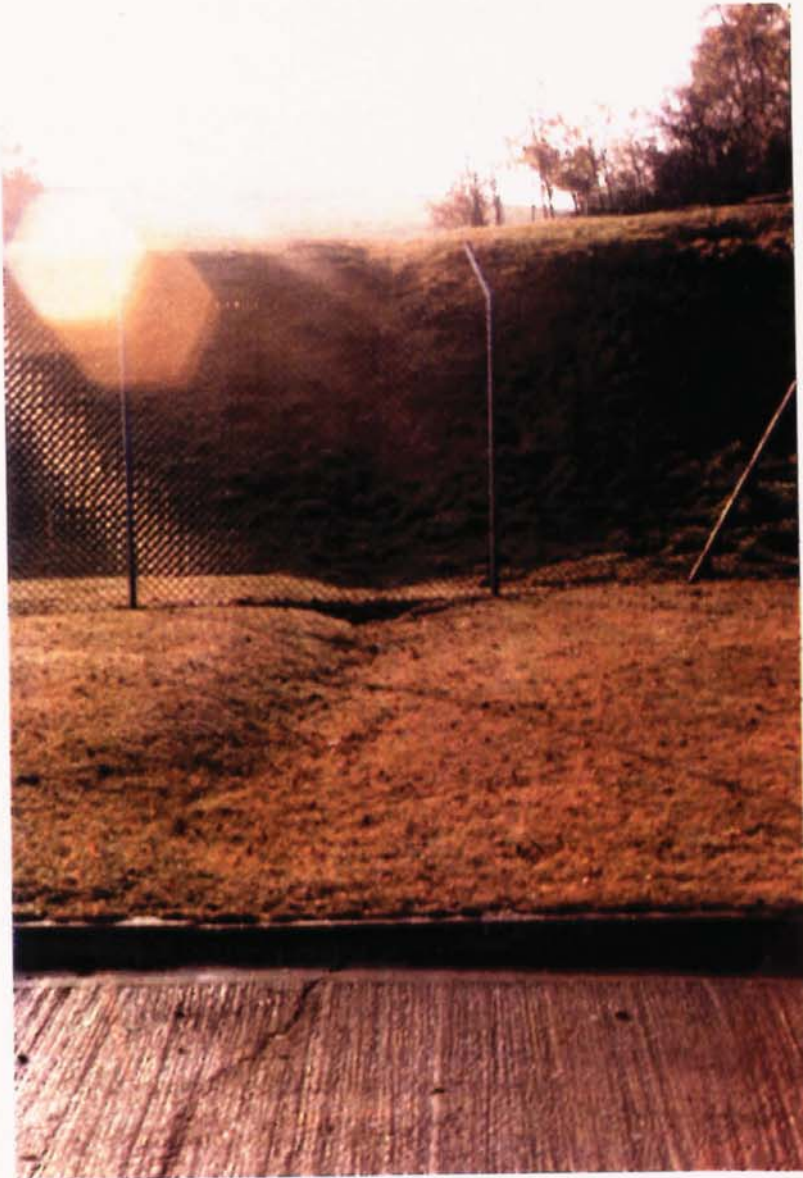


PLATE 9.1 Ground Surface Depression Over the Pipeline on the Exit from Tatsfield PRS.

The study was undertaken in two stages, initially three downstream sites were instrumented to investigate the soil thermal, hydraulic and stress regimes in conjunction with pipe movement and ground crack formation and development. Subsequently the PRS was re-instrumented to provide both a pipe stress monitoring system and an opportunity for the careful study of the ground surface profile above a chilled gas pipeline. The study started on 3/2/88 and continued for 109 weeks until 7/3/90 (Table 7.8), however data logging problems resulted in an almost complete loss of data from the soil thermal and stress instrumentation. The outlet temperature was only lowered to its anticipated level of -5°C for 23 and 11 days respectively during the 1988/89 and 1989/90 Pre-heating Seasons.

9.3.2 Blackrod PRS Operating Conditions and Ambient Conditions.

In comparison with the earlier study (Archer *et al.*, 1984), where the average inlet pressure to Blackrod PRS was 6.9 MN m^{-2} (1000 psi), it was only 5.0 MN m^{-2} (725 psi) (Figure 7.14) throughout this study. This was a result of the installation of extra pipelines within the NorthWestern Region to route natural gas from the Morecambe Bay field into the National Transmission System. This influenced the temperature drop across the station, which was insufficient to achieve both the station setpoint between May and October and the required -5°C during the trial periods (Figure 7.14a). However ground cracking was observed under these operating conditions, but not to the same extent as in the earlier study (Archer *et al.*, 1984).

As expected the inlet temperature approximated to that of the ground at pipe depth (Figure 7.16), and these values indicated that full temperature recovery from upstream PRS (Salisbury), which had an outlet temperature of -2°C , had taken place on arrival at Blackrod PRS. The temperatures of the air and the ground at pipe depth were sinusoidal in shape (Figure 7.15) and were in general agreement with the published literature discussed in Section 3.2.3.1. A simple analysis of rainfall data (Figure 7.17) indicated an average rainfall of 1080 mm/annum and, from an interpolation of a rainfall contour map of Northern England (Jarvis *et al.*, 1984), this was noted to be in agreement with the rainfall statistics for 1941-71.

9.3.3 Sites A, B and C.

This part of the investigation provided the opportunity to both generate ground cracking downstream of a full-scale test facility and monitor the subsequent development of the frozen annulus together with its effects on the surrounding soil mass, including pipe and ground surface movements/distresses.

9.3.3.1 Soil Thermal, Hydraulic and Stress Regimes.

The results from the PRTs indicated that the size of the frozen annulus was inversely related to the distance from the PRS outlet, however it was also very dependent on the thermal conductivity of the surrounding soil. At Sites A and B the width of the frozen annulus was minimal vertically above the pipe centre and increased in size to a horizontal line through the pipe centre (Appendix C) indicating the frozen annulus was elliptical in shape but, at Site C, no inference of this kind could be made (Figures 7.18 - 22). Unfortunately, due to the late installation and lack of reliability of the data loggers, a significant amount of data was lost.

Soil water potential monitoring was primarily aimed at assessing a combination of the suction forces emanating at the frozen front and at the ground surface due to evaporation. It was hoped to further investigate the ground cracking hypothesis put forward by Archer *et al.* (1984), but the low outputs in some cases positive indicate that either limited suction forces were present or the thermocouple-psychrometers were unsuitable for long-term field monitoring. Many of the thermocouple-psychrometers especially at Sites A and B, failed early in the trial period (Appendix C), but those at Site C were noted to consistently produce outputs. The positive outputs, noted especially at Site C (Figure 7.24), could have actually indicated zero water potential since similar findings have been reported by Brown and Bartos (1982). The small-scale model (Chapter 8) showed that, for the soil at Site C, negative water potentials were recorded in close vicinity or behind the frost front and so it is probable that the instruments close to the pipe had correctly recorded the soil water potential. However, the probes closer to the ground surface should show the effect of moisture migration for plant growth and for evaporation at the ground surface, and it is uncertain whether the probes were in error.

Soil stress monitoring was to be undertaken using electrical resistance load transducers connected to a datalogger which had been designed and supplied by British Gas NorthWestern but, late installation and technical problems prohibited sufficient reliable data collection. Shortly after the trial was initiated it was evident that significant pipe movement was occurring, especially at Sites A and C (Figures 7.30 and 7.26), and so the emphasis of the large-scale monitoring moved to the monitoring of pipe and ground movement in conjunction with ground cracking. Consequently the results from the load transducers would have been peripheral, rather than a primary source of evidence, to the tensile failure of the soil mass above the frozen annulus.

9.3.3.2 Pipe Movement.

Figure 7.42 emphasizes that at Site B there was little pipe movement which can be partly attributed to the sand bedding and surround to the pipe at this location. However, it was

uncertain whether the effects of the increased depth of burial and the unknown subgrade reaction of the soil beneath the frozen annulus resulted in lower levels of pipe heave. Basic thermodynamics indicate (Williams *et al.*, 1989) that a consequence of increased overburden pressures would be reduced frost heave. The depth of burial was 2.0 m, which was greater than at Sites A and C (1.2 and 0.9 m) and Carlson (1984) has reported that increased depth of burial, from 0.75 to 1.65 m, resulted in a 10% reduction in the total pipe heave (Section 4.5.3) in a frost susceptible silt. However laying the pipe on a gravel bed produced a further reduction of 55% in pipe heave and so it was probable that the sand, together with the lower water table (Figure 7.23), were the major factors reducing the pipe heave at Site B in comparison to Site A, for the soil classifications were similar at these two sites.

Pipe movement in the first Pre-heating Season (Figure 9.1) of the trial illustrates its temperature dependent nature, since the increase in outlet temperature, coupled with increasing ambient ground temperature, resulted in an immediate lowering of the pipe level presumably in response to the negation of the frozen annulus. Site A showed a more dramatic fall in pipe level than Site C, after the temporary outlet temperature rise at Week 14, and this can be attributed to its closer proximity to the station outlet (Figure 9.1). However at Site A this pipe level quickly stabilized whereas, at Site C, it slowly decreased until Week 20. In contrast, when the pipe temperature was raised to 1°C at 23 weeks, the pipe at Site A had fully settled by Week 24, while the pipe at Site C showed no significant response. Clearly, Site A showed a greater thaw settlement than Site C and this is a result of the outlet temperature dropping below 0°C to -2°C in October 1987, prior to the commencement of this study programme, thereby inducing frozen annulus growth at Site A prior to growth at Site C, some 3 km downstream. Figure 9.3 demonstrates this for the 1989/90 Pre-heating Season, for which the temperature conditions were essentially the same as the 1987/88 Pre-heating Season, and it was noted Site A heaved prior to Site C. If this trend had continued, Site A would have heaved more than Site C however, a temporary rise in the outlet temperature in early November 1989 (Weeks 91-92) prohibited further comparisons. Clearly pipe heave was substantially greater at Site A than Site C and consequently a greater settlement of the pipe would be expected at Site A for the 1987/88 Pre-heating Season.

During the Pre-heating Season 1988/89 the outlet temperature was at 0°C prior to the first trial period (Figure 9.2) and, when the temperature was lowered, Site A again showed pipe movement before Site C. At Sites A and C the pipe uplift was rapid and reached a maximum just before the outlet temperature was raised from -5°C to -2°C, after which both curves remained at a constant plateau until mid May 1989. This plateau, and the subsequent gentle slope of the settlement profile, indicated that careful operation of the upstream PRS could

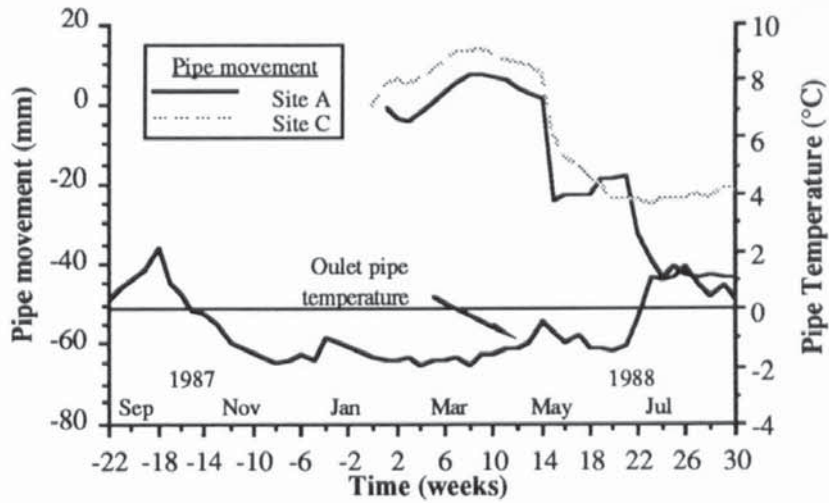


FIGURE 9.1 Average Pipe Movement at Sites A and C, and Outlet Pipe Temperature for the 1987/88 Pre-heating Season.

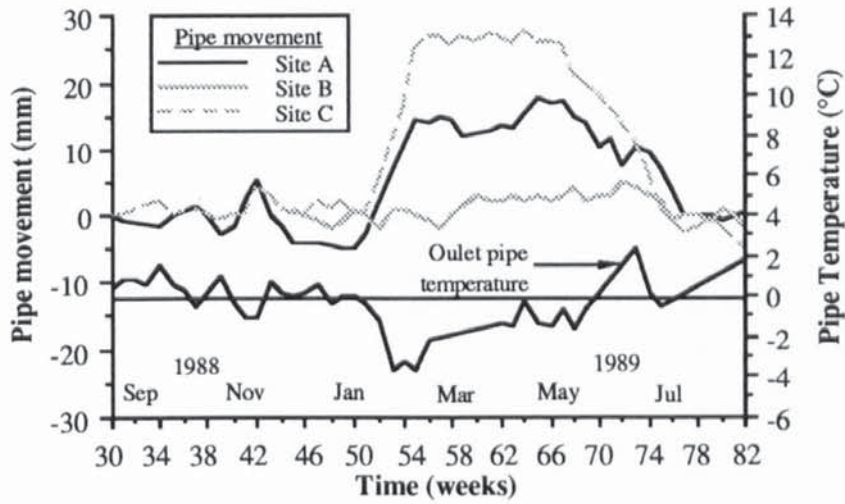


FIGURE 9.2 Average Pipe Movement at Sites A, B and C, and Outlet Pipe Temperature for the 1988/89 Pre-heating Season.

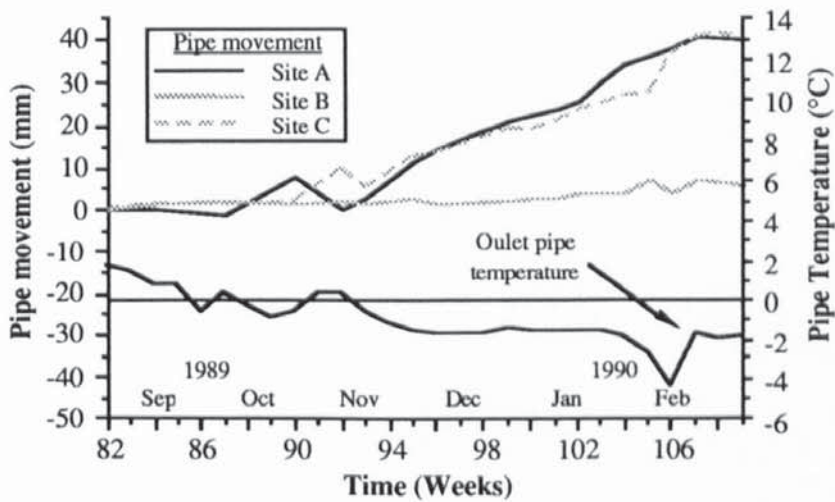


FIGURE 9.3 Average Pipe Movement at Sites A, B and C, and Outlet Pipe Temperature for the 1989/90 Pre-heating Season.

produce slow thawing conditions. This would be especially important in thaw susceptible soils, where soil water saturation would produce ideal conditions for thaw consolidation leading, ultimately, to both the pipe and ground surface settling below their original levels. Pipe thermal conditions indicated that the pipe temperature was higher at Site C (Figure 7.26) than at the outlet suggesting that the soil thermal, hydraulic and stress regimes were more conducive to frost heave than at Site A.

Prior to the second trial period (1989/90 Pre-heating Season), the outlet temperature was lowered below 0°C in Week 89 (mid October) and after a temporary rise in early November 1989 it operated at approximately -2°C until the start of the second trial (5/2/90). At this stage the pipe heaving rates at both Site A and C (Figure 9.3) were steady and low in comparison to the rates observed during the previous trial period (Section 7.7.3.5) but, following the thermal shock produced by lowering the outlet temperature from -2 to -5°C, only Site C showed a significant increase in the rate of pipe heave. This again illustrated that the soil and freezing conditions at Site C were more favourable than those at Site A for pipe heave resulting from the frost heaving process. The outlet temperature was subsequently raised to -2°C as in the first trial period to eliminate the deleterious effects of thaw settlement.

The pipe strain curve (Figure 7.28) shows the expected increase in tensile strains during the Winter since the pipe cannot contract due soil skin friction, a similar concept generates compressive strain in the Summer (Herbert and Leach, 1990). The strains are larger than expected purely from the temperature amplitude of the pipe and so some bending stress must also have been induced during the growth of the frozen annulus.

9.3.3.3 Pipe Floatation.

A point of interest from the pipe heave results obtained from Site C is the anomalous peak registered at Week 92 (Figure 9.3), this occurred when the outlet temperature was above 0°C but, due to previous operating conditions, the pipe temperature at this location was at -0.25°C. This peak is coincidental with a sudden increase in the height of the water table, resulting from both re-routing of land drains and heavy rainfall (Figure 7.17), suggesting that the peak was related to a rise in the water table (Figure 7.27). This is reinforced by the output from strain gauge No.2 (Figure 7.28) where there is also an anomalous peak at Week 92. This peak in compressive strain is indicative of a partial release of tensile strain induced by vertical movement during the lowering of the pipe temperature at this location. It was noted at Site C that the sudden rise in the water table led to flooding and this was accompanied by the greatest pipe movement (Figure 7.25) and this relative upward displacement produced a localised reduction in tensile strain.

9.3.3.4 Ground Cracking.

Over the three Pre-heating Seasons encompassed by the monitoring period ground cracking was annually observed at Site C, however its maximal magnitude was variable and was essentially a function of the frost/pipe heave rate and local soil moisture conditions.

Ground surface fissures, with intermittent ground cracks up to 10 mm wide and 150 mm deep, were recorded at Site C (Figure 7.33) in Week 5 (11/3/88) although the maximum pipe heave was not recorded until Week 9 (Figure 9.1). This primarily indicated that the ground cracks were observed in areas where pipe heave was taking place, and differs from the observations of Archer *et al.* (1984) who reported that ground cracking occurred in the absence of pipe heave at the same location. Thus, at an outlet temperature of -2°C , ground cracking had been initiated in March (Week 5) at this location, while in their earlier study Archer *et al.* (1984), did not observe cracking until May even with an outlet temperature of -5°C . It was observed that by Week 9 (7/4/88) most of the ground cracks had closed and subsequently, in Week 11 (21/4/88), no ground cracking was evident. The period after Week 9 coincides with pipe settlement and consequent thawing of the frozen annulus, and was also coupled with the growth of local vegetation which impaired crack observation.

The first trial period (1988/89 Pre-heating Season) provided, as a consequence of operational decisions, the opportunity to investigate the effect of a thermal shock on crack formation and growth, this was achieved by dropping the outlet temperature from 0 to -5°C . This was investigated because the cracking observed in previous Pre-heating Season had indicated a relationship with the frost heave process and the movement of the soil mass above the frozen annulus. Again ground cracking was observed at Site C but not at Sites A and B. After one week of operation at -5°C ground surface cracking was observed between MP 18 and MP 19+50 m and, in the subsequent week, these had opened up to 5 mm width and 200 mm depth. At the end of the second trial, maximum ground cracks up to 50 mm wide and 600 mm deep were noted (Figure 7.34). This generally indicated that ground cracking was initiated at the ground surface and penetrated into the soil mass with time and upward pipe movement. It is suggested that the ground cracks observed during this trial period were simply a result of tensile failure of the soil mass above the frozen annulus, induced by the upward movement of this soil mass in response to frost heaving. Such tensile failures of the soil mass have been reported by Casson (1984) during pipe uplift tests and Howe (1982), although the pipes were not operating in the chilled mode. After the subsequent 'filling in' of the cracks at Site C using imported topsoil, no further cracking was observed.

In the second trial period (1989/90 Pre-heating Season), ground cracking was again only recorded at Site C but, although the total heave was greater than in the previous Pre-heating Season, the crack width was smaller (Figure 7.35). In the early stage of crack formation, ground surface fissures were observed but this occurred prior to the second trial when the outlet temperature was still at -2°C. After the start of the trial the ground cracks grew and this was co-incidental with an increase in the rate of both pipe heave and upward ground surface movement. This indicates that the crack generation and growth were dependent on rate of frost heave and, thus, on the time dependent stress-strain characteristics of the soil mass above the frozen annulus. These cracks were observed to decrease in size by the Week 107 (23/2/90) and disappeared by Week 109 (7/3/90), but the ground surface was noted to be extremely wet indicating that closure of the cracks could have been partially linked to the changing soil moisture characteristics of the soil mass around the crack.

9.3.4 Blackrod PRS.

Initial results from Site C during the 1987/88 Pre-heating Season indicate that ground cracking occurred during the period of maximum pipe heave, thus it was decided to monitor both pipe and ground surface movement closely during the growth and recession of the frozen annulus. The enclosed nature of a PRS provided an ideal opportunity for monitoring under undisturbed conditions. Secondly this part of the study program was developed to assess the integrity of the pipe network within the PRS resulting when exposed to pipe heave.

9.3.4.1 Pipe Movement.

It is sufficient in the context of this thesis to state that the strains induced at Sites A', B', C', D' and E', by differential movements, were not regarded as serious with respect to the maintenance of pipeline integrity. Discussion will therefore be limited to Sites C' and D' where the ground surface profile was regularly monitored at the same intervals as the pipe movement. During the Pre-heating Seasons of 1988/89 and 1989/90 Site C' had lower maximum pipe heaves of respectively 15 and 21 mm in comparison to those of 32 and 56 mm for Site D' (Figure 7.37). However, following complete thawing of the frozen annulus at the end of each Pre-heating Season, the pipe returned to its original level indicating that neither thaw settlement or residual pipe uplift were problematic with respect to pipeline integrity. This PRS has been operated since 1982 at sub-zero temperatures during the Pre-heating Seasons and so it is probable that the repeated freeze-thaw cycles had affected both the frost heave and thaw settlement characteristics of the surrounding soil, thus the pipe returned to its pre-freezing level after thawing.

9.3.4.2 Ground Movement.

Both Sites C' and D' showed upward ground surface movement during periods of sub-zero operation (Figures 7.39 and 7.41). At both sites the upward ground movement followed a normal probability distribution profile with the maximum uplift directly over the pipe centreline however, as these displacements increased during the trial periods, a depression was observed in ground surface profile over the pipe centre especially at Site C' (Figures 7.39 and 7.41) towards the end of the trial periods. Attewell and Woodman (1982) demonstrated that ground surface settlement above a tunnel can be described by a normal probability distribution curve, this being more applicable to cohesive soils (Section 4.3.2.3). They also concluded that there was considerable variability in the quality between predicted and observed values, but a normal probability curve remains the most appropriate method for describing the transverse settlement profiles above tunnels. The actual shape of the settlement trough is related to the depth of burial and tunnel diameter together with soil type, depth to water table etc.

Given tunnelling effectively involves the loss of a volume of soil at tunnel depth which manifests itself as a settlement trough at the ground surface, it is not unreasonable to regard the increase in volume of the soil around the pipe resulting from the growth of a frozen annulus in the opposite sense. This would produce outward radial soil displacement above the frozen annulus which at the ground surface is observed as an inverted form of the tunnelling settlement trough. However, it is suggested that this shape would be significantly altered upon the formation of internal soil failure planes resulting from the tensile stresses induced in the overlying soil mass. Linear regression analysis was used to test the correlation between the thirty one observed values at the ground surface with expected values which were derived from Equation 4.4. This was achieved by altering the values of the maximum displacement (w_{max}) and the inflection point (i) by a simple iterative process in which the gradient and the intercept of the regression line were adjusted to unity and zero respectively. This allowed the r^2 (sample co-efficient of determination) value to be calculated on the basis of these adjustments and results for Sites C' and D' are provided in Tables 9.2 and 9.3.

The results obtained from Sites C' and D' are given in Appendix E and the datum is 6/1/89 when settlement of both the pipe and ground surface had occurred after the pipe temperature had been raised from -2 to 0°C on the 24/11/88 (Week 42). Both Tables 9.2 and 9.3 show that there was very good agreement between the predicted and observed values during the 1988/89 Pre-heating Season which included the first trial period 31/1/89 to 23/2/89 (Week 52 to 55). Site D' shows the better agreement but both show an increase in agreement

Date	Week	w _{max} (mm)	i (mm)	r ²
19-Jan-89	50	1.5	700	0.30
26-Jan-89	51	2.7	700	0.46
2-Feb-89	52	4.5	330	0.72
9-Feb-89	53	12	490	0.90
16-Feb-89	54	17	790	0.93
23-Feb-89	55	28	965	0.90
2-Mar-89	56	26	940	0.88
10-Mar-89	57	15	760	0.89
16-Mar-89	58	15	690	0.95
25-Mar-89	59	13	670	0.92
31-Mar-89	60	11	660	0.89
7-Apr-89	61	13	700	0.84
15-Apr-89	62	11	710	0.84
22-Apr-89	63	12	650	0.88
28-Apr-89	64	14	620	0.89
4-May-89	65	10	720	0.75
13-May-89	66	9	630	0.77
18-May-89	67	9	640	0.72
27-May-89	68	6	850	0.54
9-Jun-89	70	6	800	0.58

TABLE 9.2 Output Showing Sample Co-efficient of Determination (r^2) for Assumed Maximum Deflection (w_{max}) and Inflection Point (i) at Site C' during Pre-heating Season 1988/89.

Date	Week	w _{max} (mm)	i (mm)	r ²
26-Jan-89	51	0.7	1400	0.07
2-Feb-89	52	7	510	0.75
9-Feb-89	53	18	610	0.95
16-Feb-89	54	26	740	0.96
23-Feb-89	55	47	750	0.98
2-Mar-89	56	40	800	0.97
10-Mar-89	57	30	850	0.97
16-Mar-89	58	32	730	0.97
25-Mar-89	59	31	730	0.97
31-Mar-89	60	29	720	0.97
7-Apr-89	61	33	660	0.97
15-Apr-89	62	29	680	0.96
22-Apr-89	63	31	620	0.97
28-Apr-89	64	30	650	0.96
4-May-89	65	28	680	0.96
13-May-89	66	30	590	0.90
18-May-89	67	28	570	0.96
27-May-89	68	23	540	0.94
2-Jun-89	69	21	520	0.91
9-Jun-89	70	17	540	0.89
15-Jun-89	71	13	520	0.84
23-Jun-89	72	11	480	0.75
30-Jun-89	73	7	650	0.61
6-Jul-89	74	6	610	0.48

TABLE 9.3 Output Showing Sample Co-efficient of Determination (r^2) for Assumed Maximum Deflection (w_{max}) and Inflection Point (i) at Site D' during Pre-heating Season 1988/89.

between the variables soon after sub-zero operation started and a general decrease after May 1989. This coincides with some of the points on the profile dropping below the datum values (Figures 7.39b and 7.41b) indicating that ground surface settlement was irregular with respect to the assumed normal probability distribution curve. Tables 9.2 and 9.3 also demonstrates that the distance to the assumed inflection point increased with increased ground surface uplift and subsequently decreased with ground surface settlement. This can be attributed to the growth and recession of the pipe/frozen annulus composite together with pipe movement. The same analysis was undertaken assuming a linear ground surface profile and the sample co-efficient of determination (r^2) was slightly less than that for the normal probability distribution curve but it was still significant. However, when the best fit line, using the linear ground surface profile, was plotted in comparison to the actual values it was observed that the line deviated at the extreme values (*ie.* the maximum and minimum points of the actual ground surface plot). This suggests that the normal probability distribution curve can be regarded as a more accurate approximation of the shape of the ground surface profile.

Similar results were obtained for the Pre-heating Season 1989/90 during which the second trial from 5/2/90 to 16/2/90 (Week 105 to 106) was undertaken. At Site C' the agreement between the expected and observed values was significantly improved by selecting a further datum of 9/11/89 (Week 92), which corresponded to the lowest ground surface settlement point prior to the 1989/90 Pre-heating Season. Site D' showed very close agreement irrespective of the use of new or existing datum and, again, the normal probability distribution gave better agreement with the observed ground surface than a linear profile.

Ground surface movement over the pipe centre at Site C' was not the point of maximum heave, although the subsequent settlement was maximum at this point and Figure 9.4 illustrates the similar profiles adopted by both the pipe and ground movement at this point. It can also be inferred that ground movement resulted from frost heave in the frozen annulus below and above the pipe (Figure 9.4), since ground movement was greater than pipe movement. Site D' shows (Figure 9.5) that frost heave beneath the pipe accounted for the majority of ground surface movement except during the first and second trial periods, when a significant part of the movement can be attributed to the frost heave in the frozen annulus above the pipe crown.

9.3.4.3 Ground Cracking.

Ground cracking was noted at both Sites C' and D', especially between 31/1/89 and 23/2/89 (Weeks 52 to 55) during the first trial period, after which they closed up so that by 23/3/89 (Week 59) they had been completely negated (Figures 7.40 and 7.42). Even though Site D'

had the larger pipe and ground heave during the first trial period there was significantly less total cracking in comparison to Site C'.

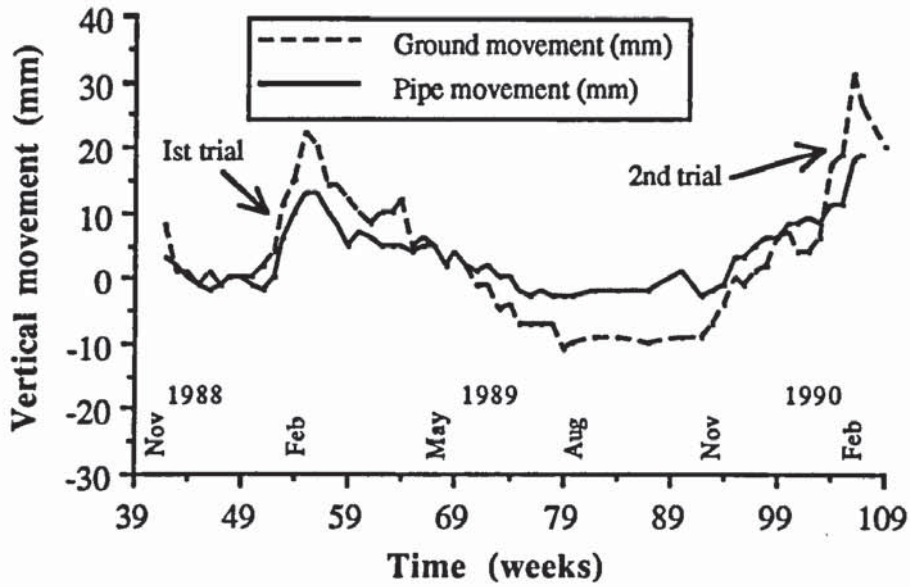


FIGURE 9.4 Pipe Heave and Ground Movement Directly above the Pipe Centreline at Site C' (datum 6/1/89).

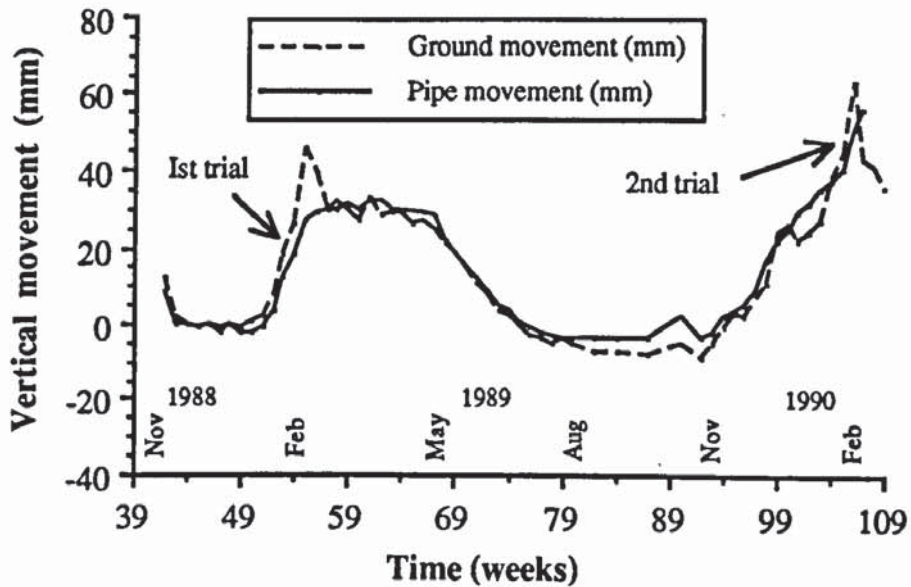


FIGURE 9.5 Pipe Heave and Ground Movement Directly above the Pipe Centreline at Site D' (datum 6/1/89).

On the basis that a normal probability distribution curve models the ground surface profile, the maximum horizontal tensile strains at Site C' are developed directly over the pipe centre and the maximum horizontal compressive strain develops at distance of $\sqrt{3} i$ from the pipe centre. Ground cracking at Site C' took place approximately 0.5 m on either side of the pipe centre (Figure 7.40) and this represented a deviation from the predicted point, but O'Reilly and New (1982) in their derivation of the equations for vertical and horizontal strain over a tunnel noted that they are not applicable to the soil mass within one diameter of the pipe. It is thought that, since the depth of pipe burial was only 500 mm, two vertical shearing planes formed at either side of the pipe/frozen annulus composite and these induced cracking in preference to directly over the pipe centre as predicted by the normal probability distribution curve. These cracks at 0.5 m acted as releases for tensile stresses generated due to the pipe/frozen annulus *expansion* that had occurred and so cracking was not observed directly over the pipe centreline.

At the end of the first trial period the magnitude of the ground surface displacement at Site D' was greater than at Site C', but the visible cracks were only 1 mm in width and located in the zone between 0.2 m either side of the pipe centreline. This is consistent with the prediction, from the normal probability distribution curve, of maximum tensile soil strain directly over the pipe centreline, but in this case three parallel cracks were generated which, if pipe heave had been allowed to continue, would have presumably formed into a single crack.

Ground cracking in the second trial period from 5/2/90 to 16/2/90 (Weeks 105 to 106) was not visible and it was uncertain whether this was due to the heavy rainfall encountered (Figure 7.17) or simply a function of the slow upward ground displacement prior and during the trial period. Both these postulations would produce an attenuation in the magnitude internal stresses developed in the unfrozen soil mass above the pipe since the load displacement characteristics of the soil would be altered.

9.3.5 Ground Cracking and Frost Heave at the Large-Scale Test.

Ground cracks, both directly over and parallel to the pipeline, were observed to form during the Pre-heating Seasons when the outlet temperatures were sub-zero. These cracks were observed to close in the latter months of the Pre-heating Seasons, when both the pipe and ground temperatures rise and this is in disagreement with the earlier study (Archer *et al.*, 1984) where ground cracks were initially observed with no *observable* pipe heave after the end of the Pre-heating Season. Pipe heave was a resultant of frost heave in the frozen annulus beneath the pipe invert and was observed both inside and downstream of the PRS however, at Site B, the sand bedding and surround is thought to have reduced the pipe

heave due to its low frost susceptibility. The ground cracks were observed to initiate during periods when the PRS outlet temperature was -5°C , which coincides with both rapid growth of the frozen annulus and pipe heave. Within the PRS the ground surface profile across the line of the pipe was correlated to the normal probability distribution curve and the ground movement profile directly over the pipe centre was shown to be similar in magnitude and shape to the pipe movement profile (Figures 9.4 and 9.5). A normal probability distribution curve indicated maximum soil strain directly under its point of maximum vertical displacement, which in this case was, directly over the pipe centre, thus cracking would occur preferentially at this point from the ground surface downwards. However at Site C', where the pipe had a very low depth of burial, under 1 diameter, two vertical cracks formed at either side of the pipe/frozen annulus composite.

The above indicates that the formation and growth of ground cracks was a result of ground surface deformation induced by frost heave within the frozen annulus, primarily beneath but also above the pipe. Ground stretching leads to tensile strains within the unfrozen soil mass overlying the pipe, which are maximal at the ground surface and decrease with depth. When these tensile strains cannot be accommodated, a crack develops which is dependent on the soil stress/strain characteristics at the time (Casson, 1984).

9.4 Small-Scale Laboratory Model.

This represented the final stage in the refinement of the mechanism for ground cracking involving a careful assessment of the influence of the soil suction forces, emanating from the frozen annulus, on the overlying unfrozen soil mass. This controlled laboratory study was limited to experiments on soils from the Tatsfield and Blackrod and these are discussed in the following subsections.

9.4.1 Soil Thermal, Hydraulic and Stress Regimes.

The thermal regime was monitored both to provide an estimate of the size of the frozen annulus, and to assist in predicting when to alter the pipe temperature in accordance with the pre-planned operational schedule. In the Tatsfield experiment it was evident that placement of aluminium foil over the soil surface at 312 hours produced a dramatic lowering of the soil temperature in the zone above the pipe (Figures 8.14 and 8.15) but below pipe level, the effect was less noticeable (Figures 8.17 and 8.18). A comparison of the rate frozen annulus growth is prohibited since the operating conditions during the Tatsfield and Blackrod experiments were different.

The thermocouple-psychrometers were successfully used in the experiments and this was demonstrated by the re-calibration curves at the end of each experiment which showed only

insignificant changes in their calibrations. Suctions monitored during the Tatsfield experiment were of a similar magnitude to those produced by frost action (cf. Clark, 1989). These were clearly monitored at probes 6 and 9 (Figures 8.20a and 8.21a), located initially 50 mm from the pipe surface (Figure 8.7) and, upon the imposition of thawing, these suction values dropped to zero within 6 hours (*ie.* the measurement interval). In contrast, during the Blackrod experiment, such behaviour was not observed and it is suggested that this can be attributed to the soil gradation properties (Anderson *et al.*, 1984b). This soil had a much larger grain size than the Tatsfield soil and the water table was below the pipe invert level in both experiments. Consequently the suction forces were negated over a much shorter distance from the Blackrod frost front in relation to the Tatsfield frost front. Tatsfield exhibited large suctions at probes 1 and 4, which were both close to the ground surface and to the soil failure planes, and it is postulated that the cold air in the cracks caused a layer of frozen soil on the crack faces and the negative potentials measured were due to the suction forces within these localised frozen layers. Conversely, these suction could have developed in response to desiccation of the crack surfaces by evaporation, although this is likely to have been a much slower process.

Soil stress was not directly measured, but monitoring of both ground surface and pipe movement provided adequate information which was in a more directly applicable form, since analysis these movements provide information on the points of maximum tensile strains in the soil mass.

9.4.2 Pipe Movement.

In both experiments, initial pipe movement was recorded only after the start of ground surface movement directly above the pipe centre (Figures 8.33 and 8.52), especially in the Blackrod experiment. This indicated that the summation of pipe weight, overburden pressure and the friction developed between the pipe flange plates and tank wall was greater than the soil subgrade reaction below the pipe. As a result the frost heave pressures in the growing frozen annulus initially compressed the soil directly below this annulus. Once pipe heave had started it was noted to be temperature dependent in both experiments although, in the Blackrod experiment, thawing at 122 hours produced a deviation from this general pattern due to pipe flange plate friction. Overall these experiments demonstrated that this small-scale model can successfully reproduce pipe heave, but modifications would be necessary to replicate pipe settlement.

9.4.3 Ground Movement.

In both experiments, ground surface movement quickly followed lowering of the pipe temperature below 0°C, indicating that expansion from either ice lensing or the *in situ*

freezing of pore water produced upward vertical displacement of the ground surface. Initially the displacements were a direct result of frost heaving above the pipe level since ground surface movement was recorded prior to upward pipe movement (Figures 8.33 and 8.52).

A normal probability distribution curve was fitted to the ground surface profile data for both experiments (Appendix F) by the simple iteration process described in Section 9.3.4.2. The results from the Sample Co-efficient of Determination (r^2) for Tatsfield (Table 9.4) indicate that, during the initial stages of ground movement, a reasonable approximation is provided by the normal probability distribution curve (Equation 4.4) but, after some 60 hours when the whole ground surface started to move upwards, this agreement is reduced. Further, the values of the assumed inflection point (i) were close to the tank walls, or even outside the tank, indicating that frozen annulus would have influenced ground movements up to 525 mm from the pipe centre at 240 hours, and such behaviour could only reasonably expected in a pure elastic material. However, since a vertical crack and two internal soil failure planes were recorded, it is unlikely that the frozen annulus would influence the ground surface outside the zone enclosed by the internal soil failure planes. Thus the results provided are for a small range over the pipe centreline and an extrapolation to zero displacement would be inappropriate. The results for the prediction curve from the Blackrod experiment (Table 9.5) are less conclusive, only indicating a tentative relationship between 30 and 42 hours. Blackrod soil is far more granular than Tatsfield and, as reported with tunnelling settlement prediction (O'Reilly and New, 1982), the use of this normal probability distribution curve is less applicable when the particles are likely to undergo some dilation or compaction during deformation. Both experiments indicate that, immediately prior to upward pipe movement, the surface profile was a best fit for the normal probability distribution curve.

Time (hours)	w_{max} (mm)	i (mm)	r^2
48	0.85	100	0.93
54	1.95	111	0.90
60	2.47	121	0.88
66	3.60	131	0.88
72	5.10	144	0.87
240	30.0	302	0.80
312	45.2	297	0.76
384	56.6	267	0.78

TABLE 9.4 Output Showing r^2 for Assumed Maximum Deflection (w_{max}) and Inflection Point (i) At Selected Intervals during the Tatsfield Experiment.

Time (hours)	w_{max} (mm)	i (mm)	r^2
12	0.65	134	0.27
18	2.17	115	0.66
24	3.54	112	0.75
30	5.01	113	0.80
36	7.44	125	0.84
42	10.5	137	0.82
72	24.5	204	0.76
108	45.0	255	0.69
122	52.4	270	0.68
144	43.8	275	0.66
179	43.9	272	0.69

TABLE 9.5 Output Showing r^2 for Assumed Maximum Deflection (w_{max}) and Inflection Point (i) At Selected Intervals during the Blackrod Experiment.

9.4.4 Ground Cracking.

In both the Tatsfield (Figure 9.6) and Blackrod (Figure 9.7) experiments ground cracking occurred prior to pipe movement, indicating that the *expansion* of the pipe/frozen annulus composite above the pipe centre was responsible for the formation of the vertical crack above the pipe (cf. Figures 8.49 and 8.50). Ground cracking was initially observed as ground surface fissures that subsequently grew both in depth and width as the upward ground movement developed. Plates 8.9 and 8.14 show that at the end of the freezing periods for both the Tatsfield and Blackrod experiments, the ground crack had its apex within the frozen annulus indicating that the frozen annulus grew around the apex of the crack. This suggests that cracking did not form in response to a thermal contraction crack developing within the frozen soil mass and subsequently propagating through the overlying unfrozen soil to the ground surface. The apex of cracks were noted to contain soil debris and *hoar ice*. Ground surface movement was allowed to continue beyond the value scaled to the field observations so as to exacerbate the soil failure planes within the soil mass. It was noted that the internal soil failure planes were at angles of 65° to the vertical for the Tatsfield experiment, the corresponding value for Blackrod being 35° . However, many more experiments under a wide range of parameters are necessary to permit correlations between properties such the internal angle of the soil failure planes and shear strength.

The plan view of the soil surface during both experiments illustrates that more than one longitudinal crack may develop over the line of the pipe (Figures 9.6 and 9.7). This can be explained in terms of the spatial variability in the soil properties in both the unfrozen and frozen soil, since these variabilities will alter the local response to the tensile stresses generated in the overlying unfrozen soil mass. Indeed, in some cases, the formation of the

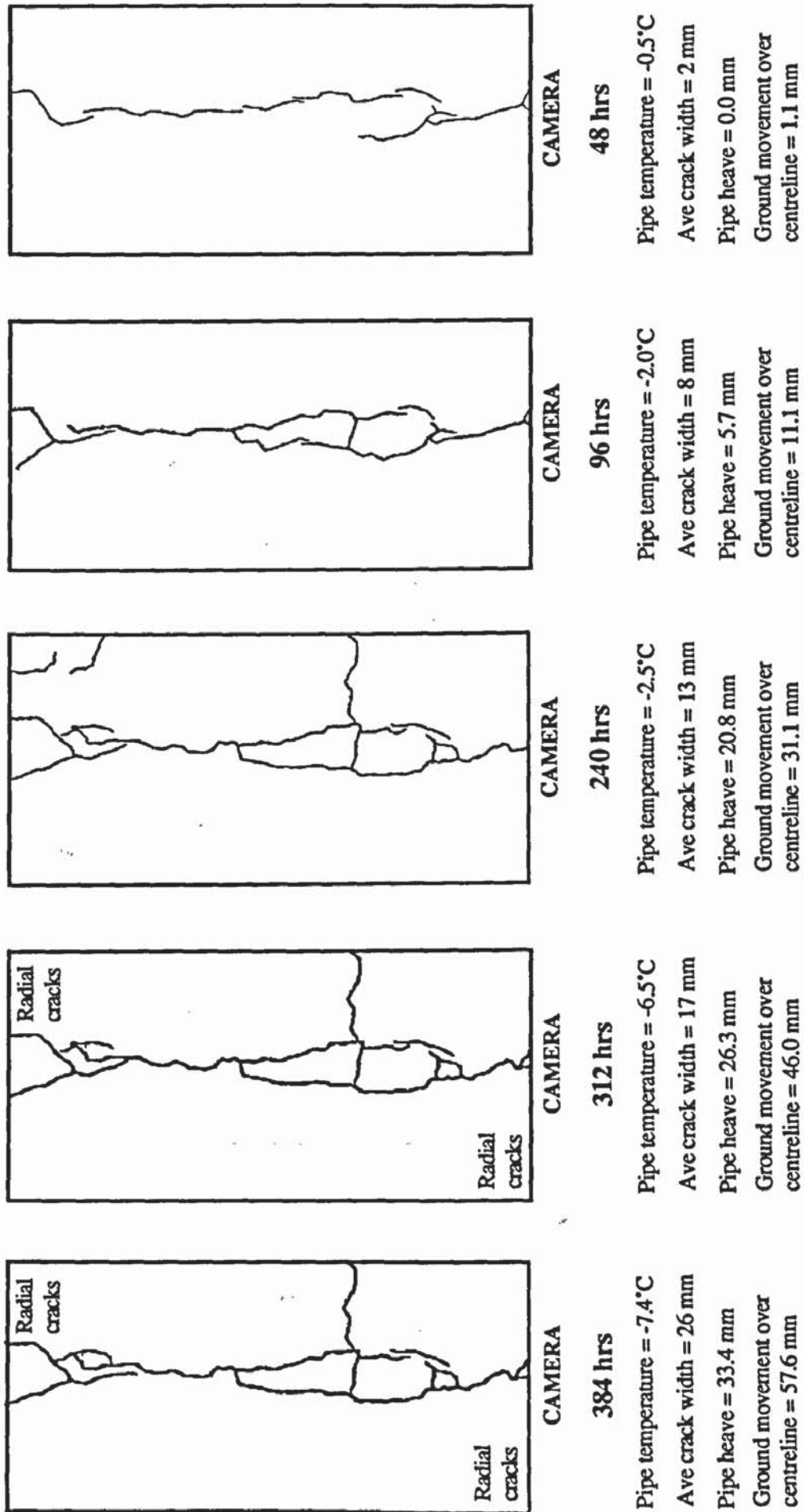


FIGURE 9.6 Plan View of Cracking During the Tatsfield Experiment Showing Crack Growth with Time.

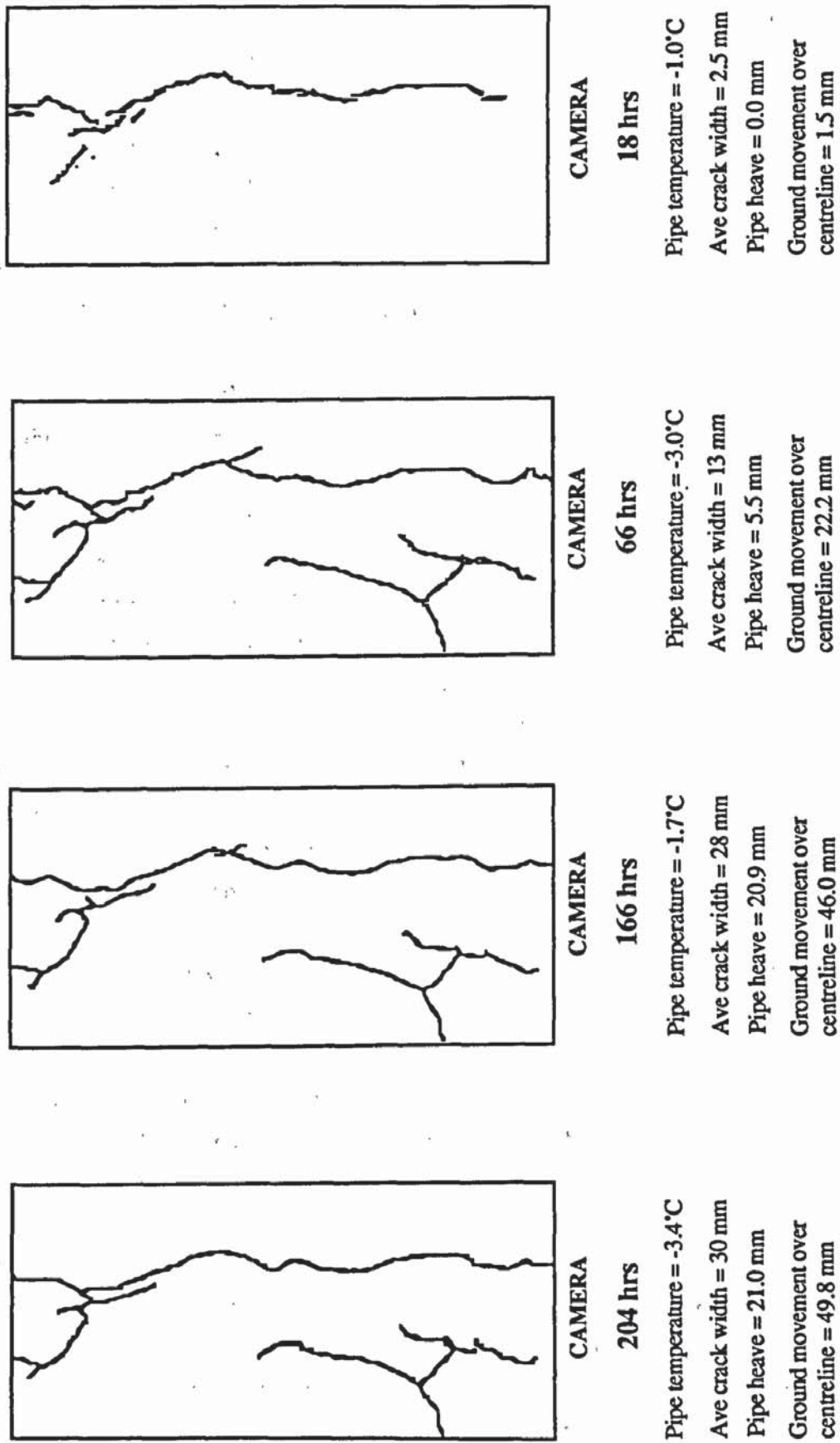


FIGURE 9.7 Plan View of Cracking During the Blackrod Experiment Showing Crack Growth with Time.

first crack may produce a redistribution of stresses which causes a second parallel crack over or close to the line of the pipe.

As upward ground surface continued, edge effects, especially in the corners of the model, were producing radial cracking which is unrealistic and a function of the size of the small-scale model. This is due to the friction mobilized between the soil and the perspex wall in the direction parallel to the pipe which, under full-scale conditions, would not occur as the adjacent soil would also be moving upwards.

9.4.5 The Influence of the Pipe Flange Plates on Ground Cracking.

While the effect of the friction, mobilized at the perspex walls, was obvious a further effect, that of the movement at the pipe flange plates, had also to be taken into account during the design phase. The flange plates are attached to the pipe and this caused the soil close to the plate to be restrained since the soil above the pipe moved upwards to a greater extent than the pipe (Figures 8.33 and 8.52). To compensate for this localised effect at the flange plates, the perspex tank was made 1000 mm long, to provide a sufficient area for the occurrence of ground cracking due to pipe/ground heave. The pipe fluid flowed from the end furthest from the camera position towards the camera and so it was expected that crack growth would initially be observed at the fluid entry end and, additionally, the flange plate at the fluid exit point would have only limited initial impact on the cracking since the crack was propagating towards this point (Figures 9.6 and 9.7). This localised impact of the flange plate on soil movement induced a triangular surface failure pattern at the furthest from the camera both in the Tatsfield (Figure 9.6) and Blackrod experiments (Figure 9.7). The failure pattern indicates that the zone of influence of the flange plate only extended some 150 mm from the flange plate and so the central portion of the soil surface (700 mm in length) was only acted upon by the frost heave process. In support of this, the ground surface profiles at the centre of the tank (Figures 8.30 - 8.32 and 8.53 - 8.55) showed no evidence of the plateau over the pipe centre that would have been produced by flange plate interaction.

9.4.6 Ground Cracking and Frost Heave.

Ground cracking in both tests was observed at very small vertical ground surface displacements. Surficial ground cracking was first noted in the six hourly interval readings taken at 42 and 12 hours respectively in the Tatsfield and Blackrod experiments, the respective vertical ground surface displacements over the pipe centre being 0.18 and 0.77 mm. The cracking was observed prior to pipe heave (Figures 9.6 and 9.7) indicating that the expansion of the pipe/frozen annulus composite above the pipe was primarily responsible for ground cracking in these experiments. Such expansion is equivalent to an

upward movement of the pipe and the zone of influence of this composite on the overlying unfrozen soil increased as the annulus grew. Within sensible engineering limits this zone of influence will stabilise after the development of internal failure planes in the soil mass around the pipe.

In the Tatsfield experiment the soil suctions that were directly attributable to the growth of the frozen annulus extended into the unfrozen soil for a maximum 50 mm. However these suctions cannot be scaled since the frost susceptibility and soil properties are the same in the model as at the full-scale site, thus these values are directly applicable without any scaling factor, in this case ten. The Blackrod experiment indicated that the suctions produced were negated a short distance from the frozen front and this brings into question the hypothesis put forward by Archer *et al.* (1984), since this soil was taken from an area where cracking was observed in their study programme. Their hypothesis (Archer *et al.*, 1984) was dependent on the development of suctions due to soil moisture movement to both the frost front and ground surface, however the suctions developed at the frost front would have not influenced the majority of the soil mass above the frozen annulus.

9.5 Relationship Between Ground Cracking and Frost/Pipe Heave.

The questionnaire provided basic background information on the occurrences of both frost heave and ground cracking. Basically it was noted that along pipelines where ground cracking was observed frost/pipe heave was also likely to be present. This tendency increased with increased pipe diameter and they were more likely to be observed during the Pre-heating Season. These results suggest a relationship exists between ground cracking and frost/pipe heave since they were observed under similar circumstances.

Results from the Blackrod full-scale test showed that pipe heave occurred after the outlet temperature was lowered below 0°C during Pre-heating Season and was dependent on the interrelationship between both the pipe and the ambient ground temperatures. Monitoring of the soil thermal, stress and hydraulic regimes at the three downstream Sites was effected with varying degrees of success and subsequent results indicated that their definition was not necessary, however results from the temperature and hydraulic regimes proved useful. Ground cracking was observed downstream at Site C at times of rapid pipe heave which followed large negative thermal shocks, such as lowering the outlet temperature from 0 to -5°C. Monitoring of both the ground surface and pipe heave in the Blackrod PRS showed that ground surface movement occurred at the same time as pipe heave. The ground surface profile was shown to approximate a normal probability distribution curve (Equation 4.4), which has been used to predict the ground surface settlement produced by tunnel driving in

cohesive soils (O'Reilly and New, 1982). The vertical displacement of the ground surface indicates that tensile stresses are developed in the soil mass above the pipe/frozen annulus composite and, if displacement is sufficient, these tensile stresses are released by cracking downwards from the ground surface. Differentiation of the normal probability distribution curve indicates that the maximum tensile forces are generated above the pipe centre with the maximum compressive strain at 1.73i. Thus a ground crack is predicted directly above the pipe centre. However, at Site C' within Blackrod, cracking was observed 0.5 m to either side of the pipe centre and this has been attributed to the low depth of burial. The results from the full-scale test indicated that a ground crack formed in response to tensile strains generated in the overlying unfrozen soil mass by the expansion of the pipe/frozen annulus composite. The conditions during the trial also indicated that ground cracking was dependent on the rate of pipe/ground heave and it is suggested that this is a function of the time dependent nature of the stress/strain characteristics of the overlying unfrozen soil mass.

A small-scale model was designed to specifically investigate the actual nature of the soil failure pattern and to compare it to that observed during pipe uplift tests, such as reported by Casson (1984). Ground cracking was successfully re-produced however, edge effects were noted at the points closest to the entry and exit of the pipe. The results indicated that ground cracking occurred before pipe movement but after ground movement had started, and this initial movement has been attributed to frost heaving in the frozen annulus above the pipe. Pipe movement was initially inhibited as the subgrade reaction was insufficient to overcome that summation of the overburden pressure and pipe flange plate friction force with the perspex tank wall. The ground surface profile was not satisfactorily described by a normal probability distribution curve, but there was a definite peak in the profile over the pipe centre indicating that this was the point of maximum tensile strain at the ground surface. Continued operation produced increased pipe and ground movement together with increasing crack growth. At the end of the freezing period, excavations revealed that internal soil failure planes had formed from the side of the pipe/frozen annulus composite and these internal soil failure planes slanted upwards towards the ground surface. Such failure patterns are indicative of the relative upward displacement of the pipe in relation to the surrounding soil mass. The angles of the soil failure plane to the vertical were respectively 35° and 65° for the Blackrod and Tatsfield experiments, and it is suggested that this difference is a function of the shear strength of the individual soils. The measured suctions, which were due directly to the growth of the frozen annulus, were negated over distances of about 50 mm in the case of Tatsfield and were not detected in the Blackrod experiment. Ground cracking was, therefore, again attributed to the tensile stresses developed in the overlying unfrozen soil mass due the upward motion of the pipe/frozen annulus composite.

The results from each of the three stages of the study program put forward the following general concepts:-

- Stage 1. Ground cracking and frost heave occurred under the same conditions,
- Stage 2. Ground cracking occurred after pipe heave had started especially at periods of rapid pipe heave, and that frost heaving above and below the pipe produced upward ground movement which could be modelled by a normal probability distribution curve,
- Stage 3 Under excessive frost heaving conditions, the soil failure pattern was similar to that found when a pipe moves upward in relation to the surrounding soil mass.

The progression of these results has led to the conclusion that ground cracking is initiated, under chilled operation, by the tensile strains developed in the overlying soil mass by the upward expansion of the pipe/frozen annulus composite. Thus ground cracking takes place when the overlying unfrozen soil mass can no longer accommodate the tensile strains induced, and is dependent on the stress-strain characteristics of the soil which, in turn, are dependent on factors such as time, displacement, soil type and geotechnical classifications.

9.6 Summary.

This section has linked together the three stages of the study programme which were questionnaire, large-scale test and small-scale laboratory modelling. The results initially indicated that frost heave and ground cracking occurred under similar soil conditions, and along larger diameter pipelines. The large-scale test indicated that cracking formed from tensile stresses generated above the expanding pipe/frozen annulus composite and was inferred from pipe and ground surface movements. Finally the small-scale laboratory model investigated whether this cracking was related to the classical soil failure around a pipe undergoing relative upward movement. The soil failure plots from experiments indicated that ground cracking above a chilled gas pipeline was similar to that of pipe uplift. Soil suctions in front of the frost front were negated over very short distances, indicating cracking was not a resultant of soil shrinkage.

CHAPTER 10 CONCLUSIONS

10.1 Introduction.

Ground cracking was first reported under British Gas operating conditions by Archer *et al.* (1984) in a trial to assess the minimum acceptable outlet temperature at a Pressure Reduction Station (PRS). They provided a general mechanism for ground cracking (Section 4.5.2.1) involving soil moisture migrations to the frozen annulus and the ground surface and, as a consequence, suggested that a soil shrinkage crack formed parallel and directly over the pipeline from May onwards. Importantly this hypothesis did not involve pipe heave for they had reported (Archer *et al.*, 1984) that no pipe heave was observed at the intermittent, downstream locations of ground cracking. Similar ground cracks have also been recorded in Canada (Williams, 1987) above large-diameter transmission gas pipelines, but little information was available.

Two soil-pipeline interactions are known, these are ground cracking and frost/pipe heave, and both are regarded as problematic, with frost/pipe heave considered to have a more direct impact on the integrity of the pipeline system. Frost/pipe heave produces upward pipe displacement that, at points of restraint (Archer *et al.*, 1984) or sites of differential pipe movement, induces strain into the pipeline network (Nyman and Lara, 1986). Ground cracking affects the ground surface by disrupting overlying structures, thereby necessitating expensive remedial work. In open areas, such as farmland, cracking can pose a number of problems presenting a hazard to people and livestock and its aesthetic impact can suggest, to an untrained observer, a problem with pipeline integrity. The net result of this is again to facilitate expensive remedial actions, such as the annual reinstatement of the ground cracks.

This chapter provides a summary of the important results of this study programme together with a mechanism for ground cracking under British operating conditions. Subsequently ground cracking is discussed in relation to methodologies for limiting its magnitude both at the design stage and during in-service pipeline operations.

10.2 Aims of the Thesis.

Before any mitigative procedure for ground cracking can be developed it was necessary to define its mechanism, therefore this represented the primary objective of the study. The starting point for this investigation was the hypothesis developed by British Gas (Archer *et al.*, 1984) involving soil suctions (Section 4.5.2.1). As a consequence of investigating this phenomena, information was collected to provide input data for the development of possible

predictive/mitigative procedures for ground cracking. A subsidiary aim was to investigate mitigative solutions for frost/pipe heave, but limits on time and resources made this prohibitive.

10.3 Summary of Study Programme.

10.3.1 Introduction.

The soil-pipeline interaction system under investigation, in this instance the operation of a chilled gas pipeline, necessitated three regimes to be defined:- pipeline, frozen soil annulus and surrounding unfrozen soil. The study methodology was designed to assess the extent of ground cracking in terms of these three regimes, subsequently to generate and monitor it at a large-scale test site and, finally, to investigate ground cracking under laboratory controlled conditions by designing a small-scale model from information gathered in the previous stages. The logical order of the stages of the study programme enabled an increased definition to be made of the variables producing ground cracking as each stage progressed. The opportunity was also taken to gather information of value for the development any subsequent predictive/mitigative tools.

10.3.2 Previous Studies.

Previous research in chilled gas pipeline operation has taken place for either Northern Arctic Gas pipelines (Williams, 1986, Geotechnical Science Laboratories, 1984b) or in temperate climates involving gas transmission and distribution systems (Kempner, 1968, Yie, 1969b, Browning, 1970, Ahmad, 1978 and Archer *et al.*, 1984). These have investigated the effects of frost/pipe heave in terms of magnitude and mitigation, but ground cracking was only reported by Archer *et al.* (1984) and Williams (1987) and limited information was available. More recently a thoroughly instrumented full-scale indoor test facility at Caen (Section 4.5.4) has been operating since 1982 under chilled air and pipe conditions (Geotechnical Science Laboratories, 1991) and has provided information on the frost heave process together with the deformation of a pipe across an interface between soils of varying frost susceptibility. Prior to developing an understanding of the behaviour of the pipe-frozen annulus system, it is essential to understand the complexities of frost action and these are discussed in Chapter 3.

10.3.3 Questionnaire.

This was designed to provide background information on both frost/pipe heave and ground cracking (Chapter 6). Eighty three replies were received from the twelve British Gas Regions and these indicated that along only ten pipelines were both frost/pipe heave and ground cracking observed, and along six of these pipelines their occurrence was noted at the

same location. Along two pipelines ground cracking was observed in the absence of frost/pipe heave and frost/pipe heave was noted without ground cracking along only four pipelines. Overall the magnitudes of frost/pipe heave and ground cracking were greater downstream of the PRS and the likelihood of observation increased with increasing pipe diameter. Both these soil-pipeline interactions were observed during the Pre-heating Season (November to May), generally frost/pipe heave was more predominant earlier than ground cracking, but ground cracking persisted longer. The similarity in the conditions necessary for frost/pipe heave and ground cracking suggested a link between these phenomena.

10.3.4 Large-Scale Study Programme.

Blackrod PRS (NorthWest Gas) was selected for a large-scale test site and instrumentation was effected in two stages, downstream and within the PRS. Monitoring took place over three Pre-heating Seasons (1987/88, 1988/89 and 1989/90), but there were only two trial periods (31/1/89 - 23/2/89 and 5/2/90 - 16/2/90) during the first the outlet temperature was lowered from 0°C to -5°C and in the second from -2°C to -5°C.

Three downstream sites (Section 7.4) were selected, based on their observed susceptibilities to ground cracking, and instrumented to define the soil thermal, hydraulic and stress regimes around the pipe, pipe movement and strain were also monitored. Problems with data logging prevented sufficient information on soil temperature and stress, however soil suctions were monitored with thermocouple-psychrometers which in many cases failed or consistently gave zero readings. More importantly ground cracking was observed during each Pre-heating Season and its magnitude was a maximal when pipe uplift peaked especially during the trial periods. Ground cracking was generated at Site C which was regarded as the most crack susceptible location soon after the imposition of a negative thermal shock at the start of the trial periods, but its magnitude was dependent on the previous pipeline operating conditions. Ground cracking was observed intermittently along the pipeline up to 3 km downstream and had a maximum width of 50 mm and a depth of 600 mm at the end of the first trial period when pipe heave was 27 mm in 23 days. Ground cracking was first observed as ground surface fissures directly over the pipeline, and subsequently these developed both in width and depth, indicating that cracking was not due to the formation of a thermal contraction crack in top of the frozen annulus which would have propagated vertically upwards to the ground surface.

Initial results from the downstream sites during the first Pre-heating Season indicated that a relationship existed between pipe uplift and ground cracking, consequently ground and pipe movements were monitored within the PRS at two sites (C' and D') during the second and third Pre-heating Seasons. Results indicated that frost heave occurred both below and above

the pipe during the growth of the frozen annulus, and this was responsible for upward movement of the ground surface across the line of the pipeline. The ground surface profiles during the trial periods at both sites were fitted to a normal probability distribution curve (Equation 10.1) which effectively is an inverted form of that used in the prediction of ground surface settlements resulting from tunnelling activities in cohesive soils. A normal probability distribution curve (O'Reilly and New, 1982) indicates that the maximum tensile strains at the ground surface are generated directly over the pipe centreline and maximum compressive strains at 1.73 i from the pipe axis. Ground cracking at Site C in the first trial period was noted at 0.5 m either side of the pipe axis and was probably a function of the low depth of burial of the pipe (O'Reilly and New, 1982).

$$w_h = w_{h \max} \exp \left(\frac{-y^2}{2(i^2)} \right) \quad 10.1$$

- w_h = vertical ground heave (mm),
- $w_{h \max}$ = maximum vertical ground heave (mm),
- y = perpendicular distance from the pipe centre-line (mm),
- i = point of inflection of the curve, occurs at $w_h = 0.606 w_{h \max}$ (mm).

Each trial was terminated due to overriding engineering considerations, but the outlet temperature of the station was raised to -2°C and not to above 0°C as originally specified by the local Engineers. This could have produced conditions favourable for the thaw settlement of both the pipe and overlying soil mass since a rapid thawing would have been induced. Raising the temperature to -2°C at the end of the first trial period proved successful for, although pipe heave was arrested, pipe settlement did not commence until towards the end of the Pre-heating Season, from early May to late July (Figure 9.2), indicating slow thawing.

10.3.5 Small-Scale Laboratory Model.

The model was specifically designed to investigate the effect of the growth of the frozen annulus on ground movements, pipe movements and ground cracking. Additionally it offered the opportunity to define the influence of the soil water suction forces, emanating from the frozen annulus, on the surrounding unfrozen soil mass. Two soils were selected from locations downstream of Tatsfield and Blackrod PRS, as they were known to be crack susceptible, and these were examined, under pipe temperature conditions which were known to produce cracking, but over a shorter time period.

In both experiments ground surface movement took place after the pipe temperature was lowered below 0°C and prior to pipe movement. Pipe movement occurred later and it is

suggested that initially the subgrade reaction below the pipe/frozen annulus composite was insufficient to resist the pipe weight, overburden pressure and, friction between the soil and the perspex tank and thus, frost heaving compressed the soil below the frozen annulus. While a direct comparison with the vertical load-displacement response curves for pipe uplift tests (Section 4.3.2.1), as reported (Trautmann *et al.*, 1985), was impractical it was noted that soil failure occurred at very small displacements both in this study and in the study programme of Trautmann *et al.* (1985).

Ground cracking was initiated at ground surface displacements over the pipe centre of under 1 mm and prior to pipe movement. This cracking was first observed as fissures on the ground surface, and these increased in depth and width with increasing ground movement (Figures 9.6 and 9.7). At the end of each of the freezing periods in these experiments, the vertical crack directly over the pipe was noted to have its apex within the frozen annulus and this resulted from the expansion/growth of the frozen annulus around the apex. That part of the apex within the frozen annulus was noted at the end of each test to contain soil debris and hoar ice. Generally two internal soil failure planes were observed, slanted away from the side of the pipe/frozen annulus composite to the ground surface (cf. 8.49 and 8.50). This soil failure pattern is indicative of soil failure due to the relative uplift of a pipe in relation to the surrounding soil as described by Casson (1984) for unfrozen soils. The normal probability distribution curve was fitted to the ground surface movement but less agreement was noted than at the large-scale test site and this is probably a result of the scaling factors. Soil suctions, as defined by thermodynamic equilibrium within the frozen annulus (Section 3.3), were noted in the Tatsfield soil up to 50 mm beyond the frost front but, for Blackrod, they were not recorded, this suggests that any suctions were negated over a very short distance. As a result of the limitations of a small-scale model, edge effects between the soil, pipe wall and pipe flange plates were noted to produce local soil failure patterns especially in corners and at the flange plates (Figures 9.6 and 9.7). However the model was sufficiently long to allow cracking to develop under the influence of the expansion of the pipe/frozen annulus composite without the edge factors affecting the results. Two parallel ground cracks were observed at locations above the pipe (Figures 9.6 and 9.7) and it is suggested that growth of the second crack resulted from the redistribution of tensile strain after the formation of the initial crack.

10.4 Ground Cracking Above Chilled Large Diameter Gas Pipelines.

The summary of the results has shown that ground cracking is dependent on frost/pipe heave and takes place during the Pre-heating Season.

Generally ground cracking and frost/pipe heave take place along large diameter pipelines which by virtue of their size carry large amounts of gas at high pressures. During the Pre-heating Season demand for natural gas is maximal and the inlet gas temperature is at its lowest level, therefore pressure reduction can produce minimum outlet gas temperatures that can be substantially below 0°C. If the mass flow rate is large then a substantial length of the downstream pipeline will be sub-zero and a frozen soil annulus will form around the pipe producing a pipe/frozen annulus composite.

If the soil in the frozen annulus is frost susceptible and favourable conditions exist for frost heave the net result is an expansion of the pipe/frozen annulus composite. This produces deformation of the unfrozen soil mass especially above the pipe centre causing ground surface movement (uplift) and it has been shown that this transverse soil profile can be approximately fitted to a normal probability distribution curve (Section 9.3.4.2). The turning points of this curve indicate that the maximum tensile strain occurs at the ground surface directly over the pipe centre and maximum compressive strain at 1.73i. This leads to the conclusion that, if the ground surface movement is sufficient, the unfrozen soil mass above the pipe/frozen annulus composite becomes unable to accommodate the associated tensile strains leading to the development of a tensile crack at the ground surface directly over the pipe centre. The continued expansion of the pipe/frozen annulus composite induces greater ground surface heave with the inflection point moving further away from the pipe centre and leads to the continuing re-orientation of the tensile strains resulting in increased crack depth and width. When the crack meets the pipe/frozen annulus composite its growth is subsequently limited to increases in width. In the small-scale laboratory tests, excessive expansion of the pipe/frozen annulus composite, in relation to actual field conditions, has shown the development of internal soil failure planes that slope away from the centre of the pipe/frozen annulus composite towards the ground surface (cf. Figure 8.50). This indicates that the failure of the soil mass above the pipe/frozen annulus composite is equivalent to pipe uplift relative to its surrounding soil mass. The depth of burial in these experiments was low so that the internal soil failure planes were observed to be linear unlike the log spiral shape reported by Casson (1984) for uplift of pipes in unfrozen soil.

On the basis of the foregoing studies it is clear that ground cracking is simply initiated by the expansion of the pipe/frozen annulus composite, induced by the frost heave process. This produced upward vertical ground surface movement, thereby inducing tensile strains in the overlying unfrozen soil mass that are relieved by the formation and growth of a vertical ground crack and, if the subsequent expansion is excessive, internal soil failure planes will develop. Both the large-scale test (Chapter 7) and the small-scale laboratory experiments (Chapter 8) have indicated that ground cracking is very dependent on pipe temperature,

previous pipeline operating conditions, frost susceptibility of the surrounding soil and, since it is a tensile crack in the unfrozen soil, the stress-strain properties of the overlying soil mass. Typically the rate of frost heave within the frozen annulus will have influence on the time dependent nature of the stress-strain properties of the overlying unfrozen soil mass. This leads the basic conclusion that the prediction of ground cracking is based on three very complex parameters:-

1. The pipeline operating conditions and its downstream temperature profile,
2. Frost heave characteristics of the surrounding soil, and
3. Stress-strain characteristics of the surrounding soil.

The results from the small-scale model indicate that the hypothesis advocated by Archer *et al.* (1984) is unlikely since the suctions measured during the Blackrod small-scale experiment were very small and ground cracking at Site C (Blackrod large-scale test) took place during the Pre-heating Season rather than after it. Similarly pipe heave and ground cracking were noted in the Pre-heating Season, which was in opposition to the findings of Archer *et al.* (1984) and indicated that it was a tensile crack rather than an shrinkage crack.

10.5 Engineering Considerations.

10.5.1 In-Service Pipelines.

The prediction of the magnitude of both frost/pipe heave and ground cracking is very complex due to the spatial variability of soil properties and hydraulic conditions along any pipeline. Therefore a detailed investigation of these properties would be expensive and may provide little useful information. The dependency of frost/pipe heave and ground cracking on the pipeline operating conditions and its downstream temperature profile add to the uncertainty of prediction. Previous experience along the Blackrod to Partington pipeline has shown that certain areas are more prone to ground cracking than others and that cracking tends to re-occur at *crack susceptible zones*. Further experience indicated that the imposition of large negative thermal shocks induced considerable frost/pipe heave which provided ideal conditions for ground cracking, due to the accelerated movement of the ground surface.

A preferable Engineering Operational Procedure would involve careful control of the outlet temperature of the upstream PRS together with monitoring of the downstream pipeline by Pipeline Inspectors. This would involve lowering the outlet temperature by increments each Pre-heating Season until the magnitude of ground cracking or frost/pipe heave is deemed to be problematic and, at this stage, two options can be selected. The first would involve the continued operation of the pipeline at this temperature with careful monitoring of the soil-

pipeline interactions until the heave or ground cracking reached a limiting value at which time the outlet temperature would be carefully raised to arrest these problems without instigating rapid thaw settlement for this could produce a settlement trough over the pipeline. Therefore the soil-pipeline interactions are constantly monitored and any problems are countered by control of the outlet temperature, the criteria for these decisions being modified with continued experience. Such a procedure could involve a 'real time' application of a computer linked to linear displacement transducers monitoring the ground and/or pipe movement at selected sites and using this information to control the outlet temperature. The second option would involve remedial actions being taken at zones of soil-pipeline interactions to limit their magnitude through the application of the following procedures:-

1. Grouting,
2. Water table reduction by drainage,
3. Soil replacement with non-frost susceptible materials.

Applications of the above techniques have been discussed in Chapter 4, and the use soil reinforcement geotextiles could be considered for the overlying unfrozen soil mass so as to act to resist the tensile strains induced by ground movement. The application of these remedial measures would allow the operation of the pipeline with confidence at the desired outlet temperature. However the use of these techniques would have to be analysed in terms of the total cost of providing an effective pressure reduction operation.

10.5.2 Planned Pipelines.

This represents the most direct method of controlling these soil-pipeline interactions when allowance is made in the design stage. The most effective method would involve surrounding the pipe in a non frost susceptible material to a diameter equivalent to that of the predicted pipe/frozen annulus composite. The size of the non frost susceptible surround would be governed by its thermal conductivity and the depth to the water table. Whilst insulating the pipe seems a practical solution by limiting the size and growth of the frozen annulus it would necessitate an increased amount of pre-heating at downstream PRSs prior to the entry of natural gas into the local medium and low pressure pipeline networks. Other methods include installing land drains and placement of soil reinforcement.

10.6 Recommendations for Future Work.

This study programme has demonstrated that ground cracking occurs as a result of tensile strain in the overlying soil mass. However, from fundamental and practical viewpoints, a

number of factors need further investigation to assess their effect on ground cracking. In particular the effect of the rate of frost heave on the stress-strain characteristics of the overlying unfrozen soil mass together with the influence on this relationship of soil classification, depth of pipe burial and depth to water table. Similarly the stress-strain properties of the overlying unfrozen soil could be compared with a wide range of soil properties such as shear strength, plasticity etc. so that future consideration can be given to the development of a simple predictive tool for ground cracking. Further validation of the normal probability distribution curve is necessary for its incorporation into such a predictive procedure for ground cracking.

Ground cracking is dependent on frost heave, which is a complex temperature and pressure dependent process, and it is important to precisely assess its role in ground cracking. Firstly a knowledge of the rate of frost heave, in relation to pipe temperature and mass flow rates, together with the stress-strain response for a variety of soil conditions should be sufficient to allow the frost heave rate to be controlled by adjustment of the PRS outlet temperature. Secondly, freeze-thaw cycles are known (Chamberlain, 1981, Van Vliet-Lanoe and Dupas, 1991) to alter the frost susceptibility of the soil and it is important to define the freeze-thaw response of a number soils over a number of cycles so that pipe heave and ground movement can be estimated from one Pre-heating Season to the next.

The small-scale model has demonstrated that laboratory modelling of physical geotechnical interactions is possible when the parameters under investigation are carefully considered and the model correctly designed. Further testing of the effects discussed above could be investigated under laboratory controlled conditions, however it is suggested these be undertaken in a perspex tank with a greater width and that the pipe flange plates be replaced with sealed rubber membrane. The small-scale model is particularly useful for the investigation of frost heave characteristics, unfrozen soil stress-strain characteristics, mitigative procedures for frost heave and ground cracking and, with modifications, thaw settlement characteristics. It also enables data to be obtained more quickly than by full-scale tests.

The mechanism of ground cracking has been defined and related to frost heave, therefore it is logical to extend the knowledge base to mitigative geotechnical procedures including grouting, ground water lowering, soil replacement with non-frost susceptible materials and geotextile reinforcements. The performance of these solutions could be assessed using the small-scale laboratory model. Real-time applications of computers, linked to instrumentation monitoring pipe strain, pipe and ground movements and pipeline operating characteristics, could be developed by linking local knowledge of the previous operating methodologies

with a fuller knowledge of the mechanism from the above recommended work. This would allow the pipeline operating conditions to be altered to limit the soil-pipeline interaction and could be achieved locally at the upstream PRS or on a much larger scale by involving a number of PRSs. A similar approach would be to prepare a schedule for the outlet temperature so that it would be altered on a weekly basis, using previous operational knowledge, to limit frost heave and ground cracking. A further option to control the soil-pipeline interactions could involve oscillating the outlet temperature on a regular basis between sub and above-zero temperatures. Therefore partial thawing of the frozen annulus would take place at regular intervals and a period of oscillation could be selected to reduce the effects of both frost/pipe heave and thaw settlement.

Finally thawing could produce settlement of both the pipe and the ground surface and was not the subject of this thesis, but further research is necessary since it can result in settlement of structures and, if severe, could affect pipe integrity. It is also uncertain as to whether settlements have a positive or negative effect on the magnitude of frost heave and ground cracking and, for a long term strategy for low temperature operation, this is a particularly important aspect for future investigation.

REFERENCES

- Ahmad, H. 1978. Soil Treatment Controls Frost Heave Conditions. Pipeline Industry, December. pp 51-54.
- Ahmed, S. McMickle, R.W. and Brassow, C.L. 1981. Soil-Pipe Interaction and Pipeline Design. Transportation Engineering Journal of the ASCE, Vol 107, No TE1. pp 45-58.
- Andersland, O.B. and Al-Moussawi, H.M. 1985. Thermal Contraction and Crack Formation Potential in Soil Landfill Covers. Proceedings of an International Conference on New Frontiers for Hazardous Waste Management, Spon. USA Environmental Protection Agency. pp 247-281.
- Andersland, O.B., Sayles, F.H. and Ladanyi, B. 1978. Chapter 5. Mechanical Properties of Frozen Ground. In. Geotechnical Engineering for Cold Regions. Eds. Andersland, O.B. and Anderson, D.M., Published McGraw-Hill Book Company. pp 216-275.
- Anderson, D.L., Chamberlain, E.J. and Co-workers. 1984a. Ice Segregation and Frost Heaving. Ad Hoc Study Group on Ice Segregation and Frost Heaving, Published National Academy Press, Washington, D.C. 72pp.
- Anderson, D.M. and Morgenstern, N.R. 1973. Physics, Chemistry and Mechanics of Frozen Ground : A Review. Proceedings of the Second International Conference on Permafrost, Yakutsh, USSR. pp 257-288.
- Anderson, D.M., Pusch, R. and Penner, E. 1978. Chapter 2. Physical and Thermal Properties of Frozen Ground. In. Geotechnical Engineering for Cold Regions. Eds. Andersland, O.B. and Anderson, D.M., Published McGraw-Hill Book Company. pp 37-102.
- Anderson, D.M. and Tice, A.R. 1989. Unfrozen Water Contents of Six Antarctic Soils. Proceedings of the Fifth International Conference on Cold Regions Engineering, St. Pauls, Minnesota, USA. Ed. Michalowski, R.L., Published ASCE. pp 353-366.
- Anderson, D.M., Williams, P.J., Guymon, G.L. and Kane, D.L. 1984b. Principles of Soil Freezing and Frost Heaving. In. Frost Action and its Control. Technical Council on Cold Regions Engineering Monograph. Eds. Berg, R.L. and Wright, E.A., Published ASCE. pp 1-21.

- Archer, G.L., Makinson, A. and Middleton, E . 1984. Pre-Heating at Pressure Reduction Stations - How much do we Really Need?. Institute of Gas Engineers, Communication No 1243. Presented 50th Autumn Meeting of the Institution of Gas Engineers, Eastbourne, England. 40pp.
- ASME. 1986. American Society of Mechanical Engineers Code for Pressure Piping, Gas Transmission and Distribution Piping Systems, ANSI/ASME B31.8. Published ASME, New York, USA. 154pp.
- Attewell, P.B. and Woodman, J.P. 1982. Predicting the Dynamics of Ground Settlement and its Derivatives Caused by Tunnelling in Soil. *Ground Engineering*, Vol 15. pp 13-22.
- Audibert, J.M.E. and Nyman, K.J. 1975. Coefficients of Subgrade Reaction for the Design of Buried Piping. Proceedings of the Second ASCE Speciality Conference on Structural Design of Nuclear Plant Facilities, New Orleans. Published ASCE, Vol 1A . pp 109-141.
- Audibert, J.M.E. and Nyman, K.J. 1977. Soil Restraint against Horizontal Motion of Pipes. *Journal of Geotechnical Engineering*, ASCE, Vol 111, No 103. pp 1119-1143.
- Bahmanyar, G.H. 1982. A Study of Buried-Pipe Failures in Cold Climates. PhD Thesis, Department of Civil Engineering, University of Wisconsin, Madison, USA.
- Berdie, D.R. and Anderson, J.F. 1974. Questionnaires: Design and Use. Published Scarecrow Press, Inc, N.J., U.S. 225pp.
- Bishop, A.W. and Blight, G.E. 1963. Some Aspects of Effective Stress in Saturated and Unsaturated Soils. *Geotechnique*, Vol 13. pp 177-197.
- Blanchard, D. and Fremond, M. 1985. Soils Frost Heaving and Thaw Settlement. Proceedings of the Fourth International Symposium on Ground Freezing, Sapporo, Japan. Published Balkema, Rotterdam. Eds. Kinosita, S. and Fukuda, M. Vol 1. pp 209-216.
- Bonar, A.J. and Ghazzaly, O.I. 1973. Research on Pipeline Flootation. *Journal Of Transportation Engineering*, ASCE, Vol 99, No TE2. pp 211-233.
- Bowes, W.H. 1984. Bending Stresses in a Pipe due to Frost Heave. Proceedings of a Seminar on Pipelines and Frost Heave, Caen, France. Published Carleton University, Ottawa, Canada, 1985. pp 31-33.

- Briscoe, R.D. 1984. Thermocouple Psychrometers for Water Potential Measurements. Proceedings of the NATO Advanced Study Institute on Advanced Agricultural Instrumentation, Pisa, Italy. 14pp.
- British Gas Corporation. 1988. Unpublished Data, British Gas NorthWestern.
- British Standards Institution. 1975. BS 1337 Methods for Testing Soils for Civil Engineering Purposes.
- British Standards Institution. 1989. BS 812 Testing Aggregates, Part 124: Methods for Determining Frost Heave.
- Brown, R.W. and Bartos, D.L. 1982. A Calibration Model for Screen-Caged Peltier Thermocouple Psychrometers. United States Department of Agriculture, Forest Service, Research Paper INT-293. 31pp.
- Brown, R.W. and Johnston, R.S. 1976. Extended Field Use of Screen-Covered Thermocouple Psychrometers. Agronomy Journal, Vol 68. pp 995-996.
- Browning, E.W. 1970. Pipe Stresses due to Frost Heave. Gas, August. pp 74-77.
- Burgess, M.M. 1985. Permafrost: Large-Scale Research at Calgary and Caen. Geos, Energy Mines and Resources, Canada. Vol 14, No 2. pp 19-22.
- Burgess, M.M., Lemaire, G., Smith, M.W. and Williams, P.J. 1982. Investigation of Soil Freezing in Association with a Buried Chilled Pipeline. Published Geotechnical Science Laboratories, Carleton University, Ottawa, Canada. 73pp.
- Burt, T.P. and Williams, P.J. 1976. Hydraulic Conductivity in Frozen Soils. Earth Surface Processes, Vol 1. pp 349-360.
- Carlson, L.E. 1984. Frost Heave and Thaw Settlement Test Facilities. Proceedings of a Seminar on Pipelines and Frost Heave, Caen, France. Published Carleton University, Ottawa, Canada, 1985. pp 43-48.
- Carlson, L.E. and Butterwick, D.E. 1983. Testing Pipelining Techniques in Warm Permafrost. Proceedings of the Fourth International Conference on Permafrost, Fairbanks, Alaska. Published National Academy Press, Washington D.C., 1984. pp 97-102.

- Carlson, L.E., Ellwood, J.R., Nixon, J.F. and Slusarchuk, W.A. 1981. Field Test Results of Operating a Chilled Buried Pipeline in Unfrozen Ground. Proceedings of the Fourth Canadian Permafrost Conference, Calgary, Alta. Published National Research Council of Canada, Ottawa, 1982. pp 475-480.
- Carlson, L.E. and Nixon, J.F. 1988. Subsoil Investigation of Ice Lensing at the Calgary, Canada, Frost Heave Test Facility. Canadian Geotechnical Journal, Vol 25, No 2. pp 307-319.
- Casagrande, A. 1931. A Discussion of Frost Heaving. Highway Research Board Proceedings, Vol 11. pp 168-173.
- Casson, D.R. 1984. Settlement Loading on Buried Pipelines. Proceedings of the Third International Conference on Ground Movements and Structures, UWIST, Cardiff, Wales. Published Pentech Press, London, 1985. pp 80-96.
- Chamberlain, E.J. 1981. Frost Susceptibility of Soil: A Review of Index Tests. Cold Regions Research and Engineering Laboratory, Monograph 81-2. Published CRREL, Hanover, N.H., USA. 121pp.
- Chamberlain, E.J. 1988. A New Freezing Test for Determining Frost Susceptibility. Proceedings of the Fifth International Conference on Permafrost, Trondheim, Norway. Published Tapir Publishers, Trondheim, Norway, 1988. Vol 2. pp 1045-1050.
- Chamberlain, E.J., Gaskin, P.N., Esch, D. and Berg, R.L. 1984. Survey of Methods for Classifying Frost Susceptibility. In. Frost Action and its Control. Technical Council on Cold Regions Engineering Monograph. Eds. Berg, R.L. and Wright, E.A., Published ASCE. pp 104-141.
- Chamberlain, E.J. and Gow, A.J. 1979. Effect of Freezing and Thawing on the Permeability and the Structure of Soils. Engineering Geology, Vol 13. pp 73-92.
- Chapuis, R.P. 1988. Two Case Histories of Major Frost Heaving in Refrigerated Buildings: Thermal Analyses, Repairs and Prevention. Canadian Geotechnical Journal, Vol 25, No 3. pp 535-540.
- Clark, B.D. 1988. The Role of Environmental Impact Assessment in the Context of the EEC Directive. Proceedings of a Conference on Pipelines and the Environment, Bournemouth, Dorset, England. Published by Scientific Surveys Ltd, Bucks., England. 16pp.

- Clark, M.A. 1989. Application of Thermal Neutron Radiography for the Mass Transport of Moisture through Freezing Soil. Ph.D Thesis, Aston University, Birmingham, England. 239pp.
- Cooper, L.S. 1976. Dewpoint Control and Prevention of Hydrate Formation in the British Gas High Pressure System. In. The Institution of Chemical Engineering Symposium Series No. 44. Natural Gas Processing and Utilization. Published I.Ch.E., London. pp 1.1-1.9.
- Copp, D.L. 1967. Gas Transmission and Distribution. Published Walter King Ltd, England. 347pp.
- Dallimore, S.R. 1985. Observations and Predictions of Frost Heave Around a Chilled Pipeline. M.A. Thesis. Dept. of Geography, Carleton University. Published Geotechnical Science Laboratories, Carleton University, Ottawa, Canada. 110pp.
- Dallimore, S.R. and Crawford, H. 1984. Experimental Observations of Differential Heaving and Thaw Settlement Around a Chilled Pipeline. Proceedings of a Seminar on Pipelines and Frost Heave, Caen, France. Published Carleton University, Ottawa, Canada, 1985. pp 5-17.
- Daniel, D.E., Hamilton, J.M. and Olson, R.E. 1981. Suitability of Thermocouple Psychrometers for Studying Moisture Movement in Unsaturated Soils. In. Permeability and Groundwater Contaminant Transport, ASTM STP 746, Eds. Zimmie, T.F. and Riggs, C.O. pp 84-100.
- Davison, B.E., Nottingham, D., Rooney, J.W. and Charles, L.V. 1979. Chilled Pipeline Frost Heave Mitigation Concepts. Proceedings, Speciality Conference on Pipelines in Adverse Environments, New Orleans, Published by the ASCE, Vol 2. pp 294-306.
- Dean Baker, H., Ryder, E.A. and Baker, N.H. 1975. Temperature Measurement in Engineering, Vol 1. Published Omega Press, Stamford, Conn., US. 179pp.
- Domaschuk, L. 1981. Frost Heave Forces on Embedded Structural Units. Proceedings of the Fourth Canadian Permafrost Conference. Published National Research Council of Canada, Ottawa, 1982. pp 487-496.
- Edil, T.B. and Bahmanyar, G.H. 1983. Stresses in Buried Conduits Caused by Freezing Front. Cold Regions Science and Technology, Vol 8, No 2. pp 129-137.
- Everett, D.H. 1961. The Thermodynamics of Frost Damage to Porous Solids. Transactions of the Faraday Society, Vol 57. pp 1541-1551.

- Farouki, O.T. 1982. Thermal Properties of Soils Relevant to Ground Freezing. Proceedings of the Third International Symposium on Ground Freezing, Hanover, N.H., CRREL Special Report 82-16. Published CRREL, N.H. pp 139-146.
- Farouki, O.T. 1986. Thermal Properties of Soils. Series on Rock and Soil Mechanics, Volume 11, Published Trans Tech Publications, Germany. 151pp.
- Firoozabadi, A. 1977. Effect of Gas Cooling on IGAT Performance. American Gas Association, Operating Section, Distribution Conference, New Orleans, Paper 77-T-49. Published AGA. pp 87-89.
- Francis, R.F. 1981. The Efficient Management of the Bulk Transmission of Gas. Institute of Gas Engineers, Communication 1144. Presented 118th Annual General Meeting of the Institution of Gas Engineers, Birmingham. 25pp
- Francis, R.F. 1984. Opportunities for Skill- The Management of the National Transmission System. Gas Engineering and Management, May. pp 206-216.
- Geotechnical Science Laboratories. 1982. Feasibility Study for Stresses in a Pipeline in Freezing Soil, IR32. Published Geotechnical Science Laboratories, Carleton University, Ottawa, Canada. 36pp.
- Geotechnical Science Laboratories. 1983. Investigation of Soil Freezing in Association With a Buried Chilled Pipeline in a Large-Scale Test Facility. Phase 2 and Interim Report - Analysis of Stresses Developed in Pipeline Buried in Freezing Ground. IR33. Published Geotechnical Science Laboratories, Carleton University, Ottawa, Canada. 41pp.
- Geotechnical Science Laboratories. 1984a. Analysis of Stresses Developed in Pipelines Buried in Freezing Ground. IR36. Published Geotechnical Science Laboratories, Carleton University, Ottawa, Canada. 64pp.
- Geotechnical Science Laboratories. 1984b. Pipelines and Frost Heave. Proceedings of a Seminar, Caen, France, 1984. Published Geotechnical Science Laboratories, Carleton University, Ottawa, Canada. 1985. 75pp.
- Geotechnical Science Laboratories. 1985. Analysis of Stresses Developed in Pipelines Buried in Freezing Ground. IR43. Published Geotechnical Science Laboratories, Carleton University, Ottawa, Canada. 44pp.

- Geotechnical Science Laboratories. 1986a. Investigation of Frost Heave as a Cause of Pipeline Deformation. IR50. Published Geotechnical Science Laboratories, Carleton University, Ottawa, Canada. 71pp.
- Geotechnical Science Laboratories. 1986b. Thermodynamics and Mechanics of Freezing Soil Around a Pipeline. IR51. Published Geotechnical Science Laboratories, Carleton University, Ottawa, Canada. 111pp.
- Geotechnical Science Laboratories. 1988a. The Third Freeze Cycle of the Canada-France Ground Freezing Experiment. IR54. Published Geotechnical Science Laboratories, Carleton University, Ottawa, Canada. 78pp.
- Geotechnical Science Laboratories. 1988b. Spatial Variability of Heave Around a Pipeline and the Effects of Repeated Freezing and Thawing. IR55. Published Geotechnical Science Laboratories, Carleton University, Ottawa, Canada. 35pp.
- Geotechnical Science Laboratories. 1989. Canada-France Ground Freezing Experiment: Phase VIII. Fourth Freeze Cycle. IR58. Published Geotechnical Science Laboratories, Carleton University, Ottawa, Canada. 76pp.
- Geotechnical Science Laboratories. 1991. Gas Pipelines, Oil Pipelines, Civil Engineering in Arctic Climates. Proceedings of a Seminar, Caen, France, October, 1991. To be Published Geotechnical Science Laboratories, Carleton University, Ottawa, Canada.
- Goodrich, L.E. 1986. Field Measurements of Soil Thermal Conductivity. Canadian Geotechnical Journal, Vol 23. pp 51-59.
- Goto, S., Minegishi, K. and Tanaka, M. 1988. Direct Shear Test at a Frozen/Unfrozen Interface. Proceedings of the Fifth International Symposium on Ground Freezing, Nottingham, England. Published Balkema, Rotterdam, 1988. Eds. Jones, R.H. and Holden, J.T. Vol 1. pp 181-185.
- Grechischev, S.Y. 1973. Basic Laws of Thermorheology and Temperature Cracking of Frozen Ground. Proceedings of the Second International Conference on Permafrost, Yakutsh, USSR. Published National Academy of Sciences, Washington, D.C., USA. pp 228-234.
- Hale, D. 1979. Frost Heave Tests Underway for Alaska Gas Pipeline. Pipeline and Gas Journal, Vol 206, No 11. pp 24-26.

- Hanna, A.J., Saunders, R.J., Lem, G.N. and Carlson, L.E. 1983. Alaskan Highway Gas Pipeline Project (Yukon) Section Thaw Settlement Design Approach. Proceedings of the Fourth International Conference on Permafrost, Fairbanks, Alaska. Published National Academy Press, Washington D.C., 1984. pp 439-444.
- Harlan, R.L. 1973. Analysis of Coupled Heat-Fluid Transport in Partially Frozen Soil. Water Resources Research, Vol 9. pp 1314-1323.
- Harlan, R.L. and Nixon, J.F. 1978. Chapter 3. Ground Thermal Regime. In. Geotechnical Engineering for Cold Regions. Eds. Andersland, O.B. and Anderson, D.M., Published McGraw-Hill Book Company. pp 103-163.
- Harris, S.A. 1986. The Permafrost Environment. Published Croom Helm Ltd, London, England. 276pp.
- Haynes, C.D. 1974. Calculating Temperature Profile along a Buried Pipeline. Pipeline and Gas Journal, Vol 201, No 6. pp 48-56.
- Herbert, R. and Leach, G. 1990. Damage Control Procedures for Distribution Mains. Institute of Gas Engineers, Communication No. 1347. Presented 56th Autumn Meeting of the Institution of Gas Engineers, London. 64pp.
- Hillel, D. 1971. Soil and Water:- Physical Principles and Processes. Published Academic Press, New York, USA. 288pp.
- Hoekstra, P. 1969. The Physics and Chemistry of Frozen Soils. Highway Research Record, Special Report 103 . pp 78-90.
- Horton, R., Wierenga, P.J. and Nielson, D.R. 1983. Evaluation of Methods for Determining the Apparent Thermal Diffusivity of Soil Near the Surface. Soil Science Society of America Journal, Vol 47. pp 25-32.
- Howe, M. 1982. Damage Control for Distribution Systems. Gas Engineering and Management, Vol 22. pp 377-401.
- Hunter, P. 1983. The Effect of the Environment on Buried Distribution Mains- A Review of the ERS Experimental Work to September 1983. ERS Report R.2823, British Gas Corporation. 20pp.
- Hunter, P. 1985. Effect of Surface Cooling on the Strains Induced in Buried Pipe, Second Thermal Cycle. ERS Report R.3152, British Gas Corporation. 17pp.

- Huskens, L. and Rick, H. 1980. Indirect Heating of Natural Gas Prior to Pressure Reduction. *Warne Gas International*, Feb/Mar. pp 85-91.
- IGE. 1977. *Recommendations on Transmission and Distribution Practice, IGE/TD/1 Edition 2*. Published Institute of Gas Engineers, London.
- Ingersoll, J. and Berg, R.L. 1985. Hydraulic Properties of Selected Soils. In. *Freezing and Thawing of Soil Water Systems*. Technical Council on Cold Regions Engineering Monograph. Eds. Anderson, D.M. and Williams, P.J., Published ASCE. pp 26-35.
- Institute of Gas Engineers. 1970. *Steel Pipelines for High Pressure Gas Transmission, Recommendations on Transmission and Distribution Practice, IGE/TD/1*. Published Institute of Gas Engineers, London.
- Irwin, G.R. 1958. The Crack Extension-Force for a Crack at a Free Surface Boundary. Naval Research Laboratory Report 5120, Washington DC. 10pp.
- Jahns, H.O. and Heuer, C.E. 1983. Frost Heave Mitigation and Permafrost Protection for a Buried Chilled Pipeline. *Proceedings of the Fourth International Conference on Permafrost, Fairbanks, Alaska*. Published National Academy Press, Washington D.C., 1984. pp 531-536.
- Jarvis, R.A., Bendelow, V.C. and Co-workers. 1984. *Soil Survey of England and Wales, Bulletin No.10, Soils and their Use in Northern England*. Published Soil Survey of England and Wales, Harpenden, England. 411pp.
- Jesseberger, H.L. 1980. Theory and Application of Ground Freezing in Civil Engineering. *Cold Regions Science and Technology, Vol 3*. pp 3-27.
- Johansen, O. and Frivik, P.E. 1980. Thermal Properties of Soils and Rock Materials. *Pre-Prints of the Second International Symposium on Ground Freezing, Trondheim, Norway*. Published Norwegian Institute of Technology, Trondheim. pp 427-453.
- Johnson, T.C., McRoberts, E.C. and Nixon, J.F. 1984. Design Implications of Subsoil Thawing. In. *Frost Action and its Control, Technical Council on Cold Regions Engineering Monograph*, Eds. Berg, R.L. and Wright, E.A. Published ASCE. pp 45-103.
- Johnston, G.H. 1981. *Permafrost, Engineering Design and Construction*. Published John Wiley and Sons, Toronto, Canada. 540pp.

- Katz, D.L., Cornell, D., Kobayashi, R., Poettmann, F.H., Vary, J.A., Elenbaas, J.R. and Weinaug, C.F. 1959. Handbook of Natural Gas Engineering. Published McGraw-Hill Book Company. 802pp
- Katz, D.L. and King, G. 1973. Dense Phase Transmission of Natural Gas. Energy Processing/Canada, Nov-Dec. pp 36-47.
- Kay, B.D. and Perfect, E. 1988. State of the Art: Heat and Mass Transfer in Freezing Soils. Proceedings of the Fifth International Symposium on Ground Freezing, Nottingham, England. Published Balkema, Rotterdam, 1988. Eds. Jones, R.H. and Holden, J.T. Vol 1. pp 3-22.
- Kempner, R.D. 1968. Ground Heave Control at Pressure Reducing Stations. American Gas Association District Conference, Houston. Paper GSTS-68-A. pp 53-59.
- Kettle, R.J. 1984. Experience with a Chilled Gas Pipeline. Symposium on Relating Theory to Practice in Artificial Ground Freezing, Nottingham, England. Published Dept. Civ. Eng., Uni. Nottingham. Ed. Jones, R.H. pp 43-48.
- King, G.G. 1977. Cooling of Arctic Natural Gas Pipelines. American Gas Association, Operating Section, Distribution Conference, New Orleans, Paper 77-T-21. Published AGA. pp 79-86.
- Kinosita, S., Fukuda, M., Ishizaki, T. and Yamamoto, H. 1982. Frost Action of Freezing Ground Surrounding Underground Storage of a Cold Liquid. Proceedings of the Third International Symposium on Ground Freezing, Hanover, N.H. , CRREL Special Report 82-16. Published CRREL, N.H. pp 305-309.
- Knowles, A.E., Tweedle, F. and van der Post, J.L. 1977. The Background and Implications of IGE/TD/1. Edition 2. Institute of Gas Engineers Communication 1044. Presented 43rd Autumn Meeting of the Institution of Gas Engineers, London. 38pp.
- Konrad, J.M. 1987a. The Influence of Heat Extraction Rate in Freezing Soils . Cold Regions Science and Technology, Vol 14. pp 129-137.
- Konrad, J.M. 1987b. Procedure for Determining the Segregation Potential of Freezing Soils. Geotechnical Testing Journal, Vol 10. pp 51-58.
- Konrad, J.M. and Morgenstern, N.R. 1980. A Mechanistic Theory of Ice Lens Formation in Fine Grained Soils. Canadian Geotechnical Journal, Vol 17. pp 473-486.

- Konrad, J.M. and Morgenstern, N.R. 1981. The Segregation Potential of a Freezing Soil. *Canadian Geotechnical Journal*, Vol 18. pp 482-491.
- Konrad, J.M. and Morgenstern, N.R. 1982a. Prediction of Frost Heave in the Laboratory during Transient Freezing. *Canadian Geotechnical Journal*, Vol 19. pp 250-259.
- Konrad, J.M. and Morgenstern, N.R. 1982b. Effects of Applied Pressure on Freezing Soils. *Canadian Geotechnical Journal*, Vol 19. pp 494-505.
- Konrad, J.M. and Morgenstern, N.R. 1984. Frost Heave Prediction of Chilled Pipelines Buried in Unfrozen Soils. *Canadian Geotechnical Journal*, Vol 21. pp 100-115.
- Lachenbruch, A.H. 1961. Depth and Spacing of Tension Cracks. *Journal of Geophysical Research*, Vol 66. pp 4273-4292.
- Lachenbruch, A.H. 1962. Mechanics of Thermal Contraction Cracks and Ice Wedge Polygons in Permafrost. *Geological Society of America, Special Paper 70*. 69pp.
- Lachenbruch, A.H. 1970. Some Estimates of the Thermal Effects of a Heated Pipeline in Permafrost. *US Geological Survey Circular 632*. 23pp.
- Ladanyi, B. 1981. Mechanical Behaviour of Frozen Soils. *Proceedings of an International Symposium, Mechanics of Structured Media, Ottawa, Published Elsevier Publishing Company*. Part B. pp 205-245.
- Leonoff, C.E. and Lo, R.C. 1981. Solution to Frost Heave of Ice Arenas. *Proceedings of the Fourth Canadian Permafrost Conference, Calgary, Alta. Published National Research Council of Canada, Ottawa, 1982*. pp 481-486.
- Loch, J.P.G. 1979. Influence of Heat Extraction Rate on the Ice Segregation Rate of Soils. *Frost i Jord*, Vol 20. pp 19-30.
- Lunardini, V.J. 1981. *Heat Transfer in Cold Climates*. Published Van Nostrand Reinhold Company. 731pp.
- Luscher, U., Thomas, H.P. and Marple, J.A. 1979. Pipe-Soil Interaction Trans-Alaskan Pipeline. *Proceedings, Speciality Conference on Pipelines in Adverse Environments, New Orleans, Published by the ASCE, Vol 2*. pp 486-502.
- Mackay, J.R. 1974. Ice-Wedge Cracks, Garry Island, Northwest Territories. *Canadian Journal of Earth Sciences*, Vol 11. pp 1366-1383.

- Marshall, T.J. and Holmes, J.W. 1988. Soil Physics. Published Cambridge University Press, Cambridge, England. 374pp.
- Matyas, E.L. and Davis, J.B. 1983a. Prediction of Vertical Earth Loads on Rigid Pipes. *Journal of Geotechnical Engineering, ASCE*, Vol 109, No 2. pp 190-201.
- Matyas, E.L. and Davis, J.B. 1983b. Experimental Study of Earth Loads on Rigid Pipes. *Journal of Geotechnical Engineering, ASCE*, Vol 109, No 2. pp 202-209.
- Merrill, S.D. and Rawlins, S.L. 1972. Field Measurements of Soil Water Potential with Thermocouple Psychrometers. *Soil Science*, Vol 113, No 2. pp 102-109.
- Miller, R.D. 1972. Freezing and Thawing of Saturated and Unsaturated Soils. *Highway Research Board, Record*, Vol 393. pp 1-11.
- Miller, R.D. 1978. Frost Heaving in Non-Colloidal Soils. *Proceedings of the Third International Conference on Permafrost, Edmonton, Canada*. Published National Research Council of Canada, Ottawa, Canada, 1978. Vol 1. pp 708-717.
- Miller, R.D. 1980. Chapter 11. Freezing Phenomena in Soils. In. *Applications of Soil Physics*. Ed. Hillel, D. Published Academic Press, New York, USA. pp 254-299.
- Monie, W.D. and Clark, C.M. 1974. Loads on Underground Pipe due to Frost Penetration. *American Water Works Association Journal*, Vol 66, No 6. pp 353-358.
- Morgenstern, N.R. and Nixon, J.F. 1971. One-Dimensional Consolidation of Thawing Soils. *Canadian Geotechnical Journal*, Vol 8. pp 558-565.
- Morgenstern, N.R. and Smith, L.B. 1973. Thaw-Consolidation Tests on Remoulded Clays. *Canadian Geotechnical Journal*, Vol 10. pp 25-40.
- Nixon, J.F. 1982. Field Frost Heave Prediction Using the Segregation Potential Concept. *Canadian Geotechnical Journal*, Vol 19. pp 526-529.
- Nixon, J.F. 1986. Pipeline Frost Heave Predictions Using a 2-D Thermal Model. *Proceedings of Research on Transportation Facilities in Cold Regions, ASCE Convention, Boston, Massachusetts, USA*. Published ASCE. pp 67-82.
- Nixon, J.F. 1987. Ground Freezing and Frost Heave - A Review. *Proceedings of the 1987 International Symposium on Cold Regions Heat Transfer, University of Alberta, Edmonton, Canada*. Eds. Cheng, K.C., Lunardini, V.J. and Seki, N. Published ASME, New York, USA. pp 1-10.

- Nixon, J.F., Ellwood, J. and Slusarchuk, W. 1981. In Situ Frost Heaving Testing using Cold Plates. Proceedings of the Fourth Canadian Permafrost Conference, Calgary, Alta. Published National Research Council of Canada, Ottawa, 1982. pp 466-474.
- Nixon, J.F. and Ladanyi, B. 1978. Chapter 4. Thaw Consolidation. In. Geotechnical Engineering for Cold Regions. Eds. Andersland, O.B. and Anderson, D.M., Published McGraw-Hill Book Company. pp 164-215.
- Nixon, J.F. and Morgenstern, N.R. 1973. The Residual Stress in Thawing Soils. Canadian Geotechnical Journal, Vol 10. pp 571-580.
- Nixon, J.F., Stuchly, J. and Pick, A.R. 1984. Design of Norman Wells Pipeline for Frost Heave and Thaw Settlement. Proceedings of the Third International Symposium on Offshore Mechanics and Arctic Engineering, New Orleans. Published ASME. ASME Paper No 83 OMA 303 . pp 69-76.
- Nyman, K.J. and Lara, P. 1986. Structural Monitoring Concepts for Arctic Pipelines. In. Research on Transportation Facilities in Cold Regions. Published A.S.C.E., New York, USA. pp 47-66.
- O'Neill, K. and Miller, R.D. 1985. Exploration of a Rigid Ice Model of Frost Heave. Water Resources Research, Vol 21, No 3. pp 281-296.
- O'Reilly, M.P. and New, B.M. 1982. Settlements Above Tunnels in the United Kingdom - Their Magnitude and Prediction. Proceedings of the Third International Symposium on Tunnelling, London, England. Ed. Jones, M.J. Published Institute of Mining and Metallurgy. pp 173-181.
- Ogata, N., Masayuki, Y. and Kataoka, T. 1983. Effects of Salt Concentration on Strength and Creep Behaviour of Artificially Frozen Soils. Cold Regions Science and Technology, Vol 8. pp 139-153.
- Ohari, T. and Yamamoto, H. 1985. Growth and Migration of Ice Lenses in Partially Frozen Soil. Proceedings of the Fourth International Symposium on Ground Freezing, Sapporo, Japan. Published Balkema, Rotterdam. Eds. Kinoshita, S. and Fukuda, M. Vol 1. pp 79-84.
- Oppenheim, A.N. 1970. Questionnaire Design and Attitude Measurement.
- Osborne, G. 1985. The Use of Vibrating Wire Strain Gauges for Long-Term Measurements on Buried Gas Mains. Strain, Feb. pp 23-27.

- Parmuzin, S.Yu., Perelmiter, A.D. and Naidenok, I.Ye. 1988. Studies of Pipeline Interaction with Heaving Soils. Proceedings of the Fifth International Conference on Permafrost, Trondheim, Norway. Published Tapir Publishers, Trondheim, Norway, 1988. Vol 2. pp 1307-1311.
- Peng, L.C. 1978a. Stress Analysis Methods for Underground PipeLines- Part 1- Basic Calculations. Pipeline Industry, Vol 47, No 5. pp 65-74.
- Peng, L.C. 1978b. Stress Analysis Methods for Underground PipeLines- Part 2- Soil-Pipe Interaction. Pipeline Industry, Vol 48, No 4. pp 67-72.
- Perfect, E., Groenevelt, P.H. and Kay, B.D. 1989. Transport Phenomena in Frozen Porous Media. Presented at NATO Advanced Study Institute on Transport Processes in Porous Media, Washington State University, Pullman, Washington, USA. Ed. M.Y. Corapcioglu. 26pp.
- Piper, D., Holden, J.T. and Jones, R.H. 1988. A Mathematical Model of Frost Heave in Granular Materials. Proceedings of the Fifth International Symposium on Ground Freezing, Nottingham, England. Published Balkema, Rotterdam, 1988. Eds. Jones, R.H. and Holden, J.T. Vol 2. pp 569-570.
- Reeve, M.J, Hall, D.G.M. and Bullock, P. 1980. The Effect of Soil Composition and Environmental Factors on the Shrinkage of some Clayey British Soils. Journal of Soil Science, Vol 31. pp 429-442.
- Riseborough, D.W., Smith, M.W. and Halliwell, D.H. 1983. Determination of the Thermal Properties of Frozen Soils. Proceedings of the Fourth International Conference on Permafrost, Fairbanks, Alaska. Published National Academy Press, Washington D.C., 1984. pp 1070-1077.
- Roe, P.G. and Webster, D.C. 1984. Specification for the TRRL Frost-Heave Test. Department of Transport, TRRL Supplementary Report 829.
- Sanger, F.J. 1968. Ground Freezing in Construction. Journal of the Soil Mechanics and Foundation Engineering Division, ASCE, Vol 94, No SM1. pp 131-158.
- Sayles, F.H. 1988. State of the Art: Mechanical Properties of Frozen Soil. Proceedings of the Fifth International Symposium on Ground Freezing, Nottingham, England. Published Balkema, Rotterdam, 1988. Eds. Jones, R.H. and Holden, J.T. Vol 1. pp 143-166.

- Schorre, C.E. 1954. Flow Temperature in a Gas Pipeline. *Oil and Gas Journal*, Vol 53, No 21. pp 66-68.
- Sellers, W.D. 1965. *Physical Climatology* . Published the University of Chicago Press, USA. 272pp.
- Slusarchuk, W.A., Clark, J.I., Nixon, J.F., Morgenstern, N.R. and Gaskin, P.N. 1978. Field Test Results of a Chilled Pipeline Buried in Unfrozen Ground. *Proceedings of the Third International Conference on Permafrost*, Edmonton, Canada. Published National Research Council of Canada, Ottawa, Canada, 1978. Vol 1. pp 878-890.
- Slusarchuk, W.A. and Watson, G.H. 1975. Thermal Conductivity of some Ice-Rich Permafrost. *Canadian Geotechnical Journal*, Vol 12. pp 413-424.
- Smith, M.W. 1985a. Observations of Soil Freezing and Frost Heave at Inuvik, NorthWest Territories, Canada. *Canadian Journal of Earth Sciences*, Vol 22. pp 283-290.
- Smith, M.W. 1985b. Chapter 6. Models of Soil Freezing. In. *Field and Theory: Lectures in Geocryology*. Eds. Church, M. and Slaymaker, O. Published University of Columbia Press, Vancouver, Canada. pp 96-120.
- Smith, M.W., Dallimore, S.R. and Kettle, R.J. 1985. Observations and Prediction of Frost Heave of an Experimental Pipeline. *Proceedings of the Fourth International Symposium on Ground Freezing*, Sapporo, Japan. Published Balkema, Rotterdam. Eds. Kinoshita, S. and Fukuda, M. Vol 1. pp 297-304.
- Smith, M.W. and Patterson, D.E. 1989. Detailed Observations on the Nature of Frost Heaving at a Field Scale. *Canadian Geotechnical Journal*, Vol 26. pp 306-312.
- Smith, M.W. and Riseborough, D.W. 1985. The Sensitivity of Thermal Predictions to Assumptions in Soil Properties. *Proceedings of the Fourth International Symposium on Ground Freezing*, Sapporo, Japan. Published Balkema, Rotterdam. Eds. Kinoshita, S. and Fukuda, M. pp 17-23.
- Smith, W.H. 1976. Frost Loadings on Underground Pipe. *American Water Works Association Journal*, Vol 68, No 12. pp 673-674.
- Svec, O.J. 1981. Chilled Gas Pipeline:- Frost Heave Design . *Proceedings of an ASCE Speciality Conference, The Northern Community*, Published ASCE. pp 705-718.
- Taber, S. 1918. Ice Forming in Clay Soils will lift Surface Weights. *Engineering News-Record*, Vol 80, Part 6. pp 262-263.

- Taber, S. 1929. Frost Heaving. *Journal of Geology*, Vol 37. pp 428-461.
- Taber, S. 1930. The Mechanics of Frost Heaving. *Journal of Geology*, Vol 38. pp 303-317.
- Takagi, S. and Tanaka, M. 1980. A Model Tank Test to Estimate the Additional Earth Pressure due to Freezing of the Soil. Pre-Prints of the Second International Symposium on Ground Freezing, Trondheim, Norway. Published Norwegian Institute of Technology, Trondheim. pp 1037-1048
- Trautmann, C.H. and O'Rourke, T.D. 1985. Lateral Force-Displacement Response of Buried Pipe. *Journal of Geotechnical Engineering, ASCE*, Vol 111, No 9. pp 1077-1092.
- Trautmann, C.H., O'Rourke, T.D. and Kulhawy, F.H. 1985. Uplift Force-Displacement Response of Buried Pipe. *Journal of Geotechnical Engineering, ASCE*, Vol 111, No 9. pp 1061-1076.
- VanGasson, W. and Sego, D.C. 1989. Problems with the Segregation Potential Theory. *Cold Regions Science and Technology*, Vol 17. pp 95-97.
- VanLoon, W.K.P., VanHaneghem, I.A. and Boshoven, H.P.A. 1988. Thermal and Hydraulic Conductivity of Unsaturated Frozen Sands. Proceedings of the Fifth International Symposium on Ground Freezing, Nottingham, England. Published Balkema, Rotterdam, 1988. Eds. Jones, R.H. and Holden, J.T. Vol 1. pp 81-90.
- Van Haveren, B.P. and Brown, R.W. 1972. The Properties and Behaviour of Water in the Soil-Plant-Atmosphere Continuum. In *Psychrometry in Water Relations, Proceedings of the Symposium on Thermocouple Psychrometers*, Eds. Brown, R.W. and Van Haveren, B.P. Published Utah Agricultural Experimental Station, Utah State University, U.S. pp 1-28.
- Van Vliet-Lanoe, B. and Dupas, A. 1991. Development of Soil Fabric by Freeze/Thaw Cycles- Its Effect on Frost Heave. Proceedings of the Sixth International Symposium on Ground Freezing, Beijing, China. Published Balkema, Rotterdam. Eds. Xiang, Y. and Changsheng, W. Vol 1. pp 189-195.
- Vermeulen, F.E., Chute, F.S. and Cervenak, M.R. 1981. Physical Scale Modelling of Electrothermic Thawing of Permafrost for the Alleviation of Frost Heave Problems in Chilled Gas Pipelines. *Journal Of Canadian Petroleum Technology*, Vol 20, No 3. pp 102-111.

- Vinson, D.J. and Burgar, J.F. 1964. Natural Gas Temperatures in a Buried Pipeline. Petroleum Mechanical Engineering Conference, Los Angeles, California. Paper No 64-PET-30. 4pp.
- Vinson, T.S. and Palmer, A.C. 1988. Physical Model Study of Arctic Pipeline Settlement. Proceedings of the Fifth International Conference on Permafrost, Trondheim, Norway. Published Tapir Publishers, Trondheim, Norway, 1988. Vol 2. pp 1324-1329.
- Watson, G.H., Slusarchuk, W.A. and Rowley, R.K. 1973. Determination of Some Frozen and Thawed Properties of Permafrost Soils. Canadian Geotechnical Journal, Vol 10. pp 592-606.
- Wheeler, J.A. 1978. Permafrost Thermal Design for the Trans-Alaska Pipeline. In. Moving Boundary Problems, Eds. Wilson, D.G., Solomon, A.D. and Boggs, P.T. Published Academic Press. pp 267-284.
- Wilbur, W.E. 1963. Analyzing Pipe Line Stresses. Pipeline Industry, Vol 18. No 2. pp 25-31.
- Wilkins, S.O. 1988. Agricultural Aspects of Gas Pipeline Construction and Reinstatement. Proceedings of a Conference on Pipelines and the Environment, Bournemouth, Dorset, England. Published by Scientific Surveys Ltd, Bucks., England. 10pp.
- Williams, P.J. 1982. The Surface of the Earth (An Introduction to Geotechnical Engineering). Published Longman, London. 212pp.
- Williams, P.J. 1986. Pipelines and Permafrost, Science in a Cold Region. Published Carleton University Press, Ottawa, Canada. 129pp.
- Williams, P.J. 1987. Personnel Communication to Dr.R.J.Kettle, Dept. Civil Engineering, Aston University, Birmingham, England.
- Williams, P.J. 1988. Thermodynamic and Mechanical Conditions within Frozen Soils and their Effects. Proceedings of the Fifth International Conference on Permafrost, Trondheim, Norway. Published Tapir Publishers, Trondheim, Norway, 1988. Vol 1. pp 493-498.
- Williams, P.J. and Smith, M.W. 1989. The Frozen Earth. Fundamentals of Geocryology. Published Cambridge University Press, England. 306pp.

- Williams, P.J. and Wood, J.A. 1984. Internal Stresses in Soils during Frost Heaving. IR41. Published Geotechnical Science Laboratories, Carleton University, Ottawa, Canada. 53pp.
- Williams, P.J. and Wood, J.A. 1985a. Internal Stresses in Frozen Ground. Canadian Geotechnical Journal, Vol 22. pp 413-416.
- Williams, P.J. and Wood, J.A. 1985b. Investigation of the Internal Stresses in Freezing Soils and their Effects on Long-Term Migration of Moisture. IR43. Published Geotechnical Science Laboratories, Carleton University, Ottawa, Canada. 38pp.
- Wilun, Z. and Starzweski, K. 1975. Soil Mechanics in Foundation Engineering. Vol. 1, Properties of Soils and Site Investigations. Published Surrey University Press, London. 252pp.
- Wood, J.A. and Williams, P.J. 1985a. Further Experimental Investigation of Regelation Flow with an Ice Sandwich Permeameter. In. Freezing and Thawing of Soil Water Systems. Technical Council on Cold Regions Engineering Monograph. Eds. Anderson, D.M. and Williams, P.J., Published ASCE. pp 85-94.
- Wood, J.A. and Williams, P.J. 1985b. Stress Distribution in Frost Heaving Soils. Proceedings of the Fourth International Symposium on Ground Freezing, Sapporo, Japan. Published Balkema, Rotterdam. Eds. Kinoshita, S. and Fukuda, M. Vol 1. pp 165-171.
- Xiaozu, X., Oliphant, J.L. and Tice, A.R. 1987. Factors Affecting Water Migration in Frozen Soils. Cold Regions Research and Engineering Laboratory, Report 87-9. Published CRREL, Hanover, N.H., USA. 25pp.
- Yen, Y.C. 1990. Natural Convection Heat Transfer in Water near its' Density Maximum. Cold Regions Research and Engineering Laboratory, Monograph 90-4. Published CRREL, Hanover, N.H., USA. 104pp.
- Yie, G.G. 1968a. Summary of Soil Grouting Materials for Prevention of Cast Iron Main Breakage. American Gas Association Special Report on Project ID-4-7. 17pp.
- Yie, G.G. 1968b. Frost Heaving in Soils and the Breakage of Cast Iron Mains. American Gas Association Special Report on Project ID-4-7. 67pp.
- Yie, G.G. 1969a. Analysis of Frost Action at Gas Regulator Stations. American Gas Association Special Report on Project ID-4-7. 46pp.

Yie, G.G. 1969b. Soil Stabilization Field Test Results. American Gas Association Special Report on Project ID-4-7. 47pp.

Zhaojun, X. 1985. A Study of Thermal Cracks in Frozen Ground No 3. Proceedings of the Fourth International Symposium on Ground Freezing, Sapporo, Japan. Published Balkema, Rotterdam. Eds. Kinosita, S. and Fukuda, M. Vol 1. pp 3-8.

APPENDIX A PROBLEMS EXPERIENCED WITH LARGE-SCALE TEST

A.1 Introduction.

The large-scale test was undertaken at Blackrod PRS and along its associated downstream pipelines in the North West Region of the British Gas Corporation and, the author is extremely grateful for efforts made by the Region to support this work. A number of adverse conditions combined leading to a lack of data and, as a consequence the experimental programme was continued into a fourth year. Subsequent data reduction and analysis together with extra laboratory testing produced severe delays in the submission of this thesis. The problems were with the control of the outlet temperature at Blackrod and the reliability of the downstream data-loggers at Sites A, B and C.

The earlier study (Archer *et al.*, 1984) was undertaken by the Pipelines Division of the Research and Development Department at the Engineering Research Station in Newcastle-upon-Tyne in conjunction with North West Gas, Regional Transmission Department. However in this study Aston University and the above two mentioned British Gas Departments collaborated to undertake a low temperature trial.

A.2 Outlet Temperature.

In the earlier study (Archer *et al.*, 1984) the outlet temperature was -5°C and it was expected to operate this large-scale trial at a similar outlet temperature. Consequently the positions of the instruments (thermocouples, thermocouple-psychrometers and soil stress transducers), in relation to the pipe, were determined from data collected during the earlier study which had indicated that the frozen annulus could extend up to 600 mm from the pipe wall, even at distances 3 km downstream of Blackrod Pressure Reduction Station (PRS). Thus it was envisaged that, during this large-scale trial, the Blackrod PRS outlet temperature would be operating at -5°C , but this was only achieved for 34 days out of 763. Table A.1 summarizes the outlet temperature of Blackrod PRS during this study.

At the start of the trial British Gas North Western (BGNW) were confident of ground cracking at -2°C , consequently the outlet temperature for the 1987-88 Pre-heating Season was set to this temperature, but only surficial ground cracking was noted at Site C. It was, therefore suggested that for the 1988-89 Pre-heating Season, the outlet temperature should be set at -5°C , however a new Engineering Director was appointed to the Region and a directive was issued stating that the trial could continue only if the integrity of the pipe system could be guaranteed by the Engineering Research Station. As a result a monitoring

Preheating Season	Outlet Temperature	Start Date	Finish Date	Remarks
1987 to 1988 -----	-2°C	pre Dec 1987	24/11/88	British Gas North Western (BGNW) expected cracking to occur at this temperature. The only reported instances of cracking involved surficial cracking.
	0°C	24/11/88	31/1/89	New Engineering Director appointed to BGNW and asked for the installation of further equipment to monitor pipe integrity within Blackrod PRS prior to re-commencement of large-scale trial.
1988 to 1989 -----	-5°C	31/1/89	23/2/89	The author designed and installed an monitoring system within Blackrod PRS that provided the Engineer with pipe movements at various locations, from which an estimation of pipeline stresses could be made. After installation BGNW agreed to lower the outlet temperature.
	-2°C	23/2/89	5/2/90	Cracking had appeared at Site C within 10 days at -5°C, however BGNW decided to raise the outlet temperature since it was envisaged that further operation could produce serious ground surface disruptions due to ground cracking and frost heave.
1989 to 1990	-5°C	5/2/90	16/2/90	More results were needed because most of the data loggers had not been installed and/or were unreliable last year in the period 31/1/89 to 23/2/89. Also further validation was deemed necessary of the results recorded 31/1/89 to 23/2/89 when the outlet temperature was at -5°C.
	-2°C	16/2/90	to date	A cold spell was forecast and BGNW raised the outlet temperature as they were concerned about icing around the valves in Blackrod PRS. Since there was no likelihood of lowering the outlet temperature back to -5°C, the site visits stopped on the 7/3/90.

TABLE A.1 Outlet Temperature of Blackrod PRS with Accompanying Remarks.

system was designed and installed prior to the re-commencement of the trial and this resulted in the trial starting much later in the Pre-heating Season than had been originally envisaged. Subsequently this trial was halted at an early stage as BGNW regarded the magnitudes of ground cracking and frost heave as problematic. A further trial during the 1989-90 Pre-heating Season was considered necessary for validation of the results collected previously and -5°C operation started on 5/2/90 but was stopped on 16/2/90 as a result of maintenance considerations.

In the early study by Archer *et al.* (1984), flows were much higher and the pressure drop across the station was greater. Typically the pressure drop was from 69 to 32 bar which gave a maximum temperature drop of approximately 18°C , but in this trial the pressure drop especially in the periods of -5°C operation was insufficient to achieve a temperature drop down to the required setpoint. However BGNW were able to supply a maximum amount gas, as dictated by Regional supply considerations, through the Blackrod pipeline system and so the operating conditions which were expected during the design phase of the monitoring programme were rarely achieved.

These two problems combined to allow a very short period of 34 days in which useful measurements of ground crack growth could be monitored. It must be stressed that the trial was undertaken on an *in-use* pipeline system which has the primary function to supply natural gas at periods of demand and under strict safety considerations. Therefore, disruption of the trial was to be expected at various times since operational constraints and the security of the gas supply were paramount. The author acknowledges that while much potential data was unavailable, BGNW made every possible effort to provide the pipeline operating conditions necessary for this trial.

A.3 Data Loggers.

The data loggers were designed by Ketron Ltd and constructed under licence by British Gas North Western and are powered by re-chargeable batteries. They supply an excitation voltage to the instrument such as a transducer or platinum resistance thermometer and measure the reading as a number between 0 and 255. Readings can be taken at specified intervals and are stored in a 6k ram. The loggers are down-loaded to an Epson Px-8 lap held computer which can transfer the data to a Vax mainframe for analysis.

Problems were encountered with the downstream data-loggers (DL 40 to 45), these data loggers were installed to monitor the soil thermal regime around the pipe and the change in soil stress vertically above the pipe crown. Table 7.8 shows that the 24 channel

thermocouple data loggers were installed prior to the start of the first operation at -5°C (Week 52 to 55) however their reliability was poor. This was a result of many considerations, including environmental factors and the availability of technical personnel for servicing and repairing the loggers. The data loggers for the soil pressure cells were designed to monitor the change in soil stress but, unfortunately, there were problems with the design, reliability and late installation. These problems resulted in the total loss of soil stress information and partial loss of temperature data. However the author is grateful to BGNW for their concerted efforts in supplying and repairing data loggers which was a considerable task considering the conditions under which the loggers had to function.

A.4 Summary.

Problems with the operating conditions at Blackrod PRS and the downstream data-loggers resulted in the continuation of the study programme beyond its three year specification and necessitated extending the trial period and additional laboratory work. Whilst severe delays were encountered, the author stresses that British Gas North Western made every possible effort to ensure that the project ran smoothly.

A.5 Acknowledgements.

The author expresses his gratitude to the British Gas Corporation for funding this project, for the use of their facilities and for the helpful assistance provided by both the Engineering Research Station, Newcastle-upon-Tyne and British Gas North West, Transmission Department. Special thanks are given to Eric Middleton (Senior Engineer) and Grahame Archer (Principal Engineer) at the Engineering Research Station, who acted as External Supervisors to this project, for their continual support, guidance and friendship during this investigation. The author is indebted to Alan Makinson (Assistant Regional Gas Transmission Engineer, North West Gas) for permission to allow a large-scale test to be undertaken within the North West Region, and supporting the project with engineering and technical staff:- Peter Tipping, Mark Williams and Ken Hinkson of Northern Unit, Mike O'Hare and Neil Hitchmough of Southern Unit, Nigel Basquill and Jim McDonald of C&I, John Blackburn of Scientific Services. The large-scale test was co-ordinated at regular Pre-heating meetings under the chairmanship of Alan Makinson with many of the above mentioned present and their input allowed the project to run smoothly.

APPENDIX B QUESTIONNAIRE AND SUMMARY OF REPLIES

This section contains :-

1. A copy of the questionnaire issued to each British Gas Region.
2. Tables containing the full results of the questionnaire, however full details on the operating conditions have not been included due to constraints on space. The details of these conditions are highly variable but pipeline diameter gives an indication of expected flows, pressures etc, as this is determined from design considerations.

Table B.1. is a summary of the pipelines where soil-pipeline interactions were observed, the pipeline number refers to Table B.2.

Pipeline number	Frost heave	Ground cracking
38	No	Yes
45	Yes	No
46	Yes	No
49	Yes	Yes
51	Yes	Yes
52	Yes	No
54	Yes	Yes
56	Yes	Yes
58	No	Yes
61	Yes	Yes
62	Yes	Yes
64	Yes	Yes
66	Yes	No
76	Yes	Yes
77	Yes	Yes
81	Yes	No

TABLE B.1. Summary of Pipelines along which Frost Heave or Ground Cracking Occurred.

British Gas

Memorandum

From G L Archer

To REGIONAL
TRANSMISSION
ENGINEERS

British Gas plc
Engineering Research Station
PO Box
Newcastle upon Tyne NE99 1LH

Telephone 091-268 4828

Extension

Date 19 January 1987

Subject GROUND FREEZING PROBLEMS
ASSOCIATED WITH SUB-ZERO
OPERATION OF PIPELINES

Reference GLA/KLB/

A number of Regions have been experiencing problems resulting from ground freezing around pipelines operating at sub-zero temperatures. There have been occasional incidences of frost heave resulting in pipe lift and these have usually been associated with cracking in the ground above. It seems, however, that ground cracking, often over considerable lengths with no apparent lift, is a more common problem.

ERS have been concerned with sub-zero operation of pipelines for a number of years and have carried out some work on the effects of ground freezing. It was decided that the most economic and effective way to continue this work was through a University contract. Consequently, a 3 year CASE Award was recently negotiated with Aston University who have considerable experience and expertise in the effects of ground freezing. This work will be closely supervised by ERS.

Preliminary meetings have been held and several visits to British Gas sites with ground freezing problems have been made. A programme, involving theoretical, laboratory and site work is currently being drawn up. It is hoped that this work will give us a better understanding of the problems leading to better ways of predicting and even preventing future problems.

Before finalising the programme, we need to obtain as much background information as we can, so that our approach is as realistic as possible. Consequently, we have drawn up a questionnaire attached and we would be very grateful if you could spare some time to complete it. Since we are hoping to start our programme by the end of February. We realise that the questionnaire may not be suitable for every situation and that all the details required may not always be available. If you would like to discuss any aspects of the information required, please do not hesitate to contact me.

G L ARCHER

Questionnaire On Operation Of Pipelines At Sub-Zero Temperatures.

Name of Region

Has the Region operated pipelines at sub-zero temperatures ? YES / NO

If YES, please complete sections, A, B and C where appropriate.

A) DETAILS OF PIPELINE AND SUB-ZERO OPERATIONS.

1. Pipeline Reference No.
2. Name and Location of Upstream P.R.Station
.....
.....
3. Pipeline diameter (mm)
4. Pipeline depth of burial (m)
5. Total length of time pipeline has been operating at sub-zero temperatures.
(years, months)
6. Complete Table I as far as possible (reasonable estimates would be better than no information).
7. Complete the following table concerning soil composition (if possible)

CONSTITUENTS OF SOILS (%)			
CLAY	SILT	SAND	GRAVEL

or describe the general type of soil
(eg. Clayey)

8. Have there been any incidents of frost heave or ground cracking ? YES / NO
9. If YES complete section B and / or C as appropriate.

B) FROST HEAVE

Please complete one form for each incident.

1. Pipeline Reference No.
2. Distance from P.R. station (m)
3. Indicate general location
(eg. Road, Field etc.)
4. Duration of visible frost heave
(give the actual months eg. Dec - Apr)
5. Estimate maximum pipe lift (mm)
6. Depth of water table (m)
7. Was there any associated ground cracking ? YES / NO

B) GROUND CRACKING.

Please complete one form for each incident.

1. Pipeline Reference No.
2. Distance from P.R. station (m)
3. Indicate general location (eg. Road, Field etc.)
4. Duration of visible ground cracking
(give the actual months eg. June-Oct)
5. Length of cracking (m)
6. Maximum width of cracks (mm)
7. Depth of water table (m)

	JAN	FEB	MAR	APR	MAY	JUN	JUL	AUG	SEP	OCT	NOV	DEC
Average gas temperature after pressure reduction (°C)												
Average flow (mscf/hr)												
Average ground temperature at pipeline depth (°C)												
Average air temperature (°C)												
Rainfall (mm)												

E = Estimate

TABLE I

SHTOF.....SHTS

Pipeline No.	1	2	3	4	5	6	7	8
SECTION A	East Midlands Annesley 450 1	East Midlands Ashleghag 100 1	East Midlands Barton 450 1	East Midlands Birley 600 1	East Midlands Blyborough 600 1	East Midlands Bellock Lane 400 1	East Midlands Caenby Corner 300 1	East Midlands Coddington 300 1
Upstream PRS	1	1	1	1	1	1	1	1
Pipe diameter (mm)	450	100	450	600	600	400	300	300
Depth of Burial (m)	1	1	1	1	1	1	1	1
Duration of freezing period (months)	6	6	6	6	0	6	6	6
Soil type	sandy	clayey	unknown	limestone	limestone	clayey	limestone	clayey
SECTION B	No heave	No heave	No heave	No heave	No heave	No heave	No heave	No heave
Frost heave								
Location								
Distance from PRS (m)								
When visible								
Estimated pipe lift (mm)								
Depth to WT (m)								
SECTION C	No cracking	No cracking	No cracking	No cracking	No cracking	No cracking	No cracking	No cracking
Ground cracking								
Location								
Distance from PRS (m)								
Length of cracking (m)								
When visible								
Crack width (mm)								
Depth to WT (m)								
TABLE I								
Was information available on :-	No	No	No	No	No	No	No	No
Gas Temperature	No	No	No	No	No	No	No	No
Gas flow	No	No	No	No	No	No	No	No
Ground Temperatures	No	No	No	No	No	No	No	No
Air Temperatures	No	No	No	No	No	No	No	No
Rainfall	No	No	No	No	No	No	No	No

TABLE B.2. Summary of the questionnaire replies

Pipeline No.	9	10	11	12	13	14	15	16
SECTION A								
Region	East Midlands							
Upstream PRS	Guilthwaite	Hellaby	Hellaby	Hilton Garage	Melton Spiney	Milton Ross	Pinchbeck	Silk Willoughby
Pipe diameter (mm)	600	300	200	0	200	150	250	150
Depth of Burial (m)	1	1	1	1	1	1	1	1
Duration of freezing period (months)	6	6	6	6	6	6	6	6
Soil type	limestone	limestone	limestone	unknown	unknown	limestone	silty	clayey
SECTION B								
Frost heave	No heave	No heave	No heave	No heave	No heave	No heave	No heave	No heave
Location								
Distance from PRS (m)								
When visible								
Estimated pipe lift (mm)								
Depth to WT (m)								
SECTION C								
Ground cracking	No cracking	No cracking	No cracking	No cracking	No cracking	No cracking	No cracking	No cracking
Location								
Distance from PRS (m)								
Length of cracking (m)								
When visible								
Crack width (mm)								
Depth to WT (m)								
TABLE 1								
Was information available on :--	No							
Gas Temperature	No							
Gas flow	No							
Ground Temperatures	No							
Air Temperatures	No							
Rainfall	No							

TABLE B.2. Summary of the questionnaire replies (continued)

Pipeline No.	17	18	19	20	21	22	23	24
SECTION A								
Region	East Midlands	East Midlands	Eastern	Eastern	Eastern	Eastern	Eastern	Eastern
Upstream PRS	Sinfin	Stainton	Bourne End	Cow Lane	Cow Lane	Eye Green	Huntington	Huntington
Pipe diameter (mm)	150	450	200	150	200	300	300	375
Depth of Burial (m)	1	1	1	1	1	1	1	1
Duration of freezing period (months)	6	6	12	0	0	7	6	6
Soil type	unknown	limestone	clayey	silty	silty	silty	clayey	clayey
SECTION B								
Frost heave	No heave	No heave	No heave	No heave	No heave	No heave	No heave	No heave
SECTION C								
Location								
Distance from PRS (m)								
When visible								
Estimated pipe lift (mm)								
Depth to WT (m)								
Ground cracking	No cracking	No cracking	No cracking	No cracking	No cracking	No cracking	No cracking	No cracking
Location								
Distance from PRS (m)								
Length of cracking (m)								
When visible								
Crack width (mm)								
Depth to WT (m)								
TABLE 1								
Was information available on :-								
Gas Temperature	No	No	Yes	No	No	Yes	Yes	Yes
Gas flow	No	No	Yes	No	No	Yes	Yes	Yes
Ground Temperatures	No	No	No	No	No	No	Yes	Yes
Air Temperatures	No	No	Yes	No	No	No	Yes	Yes
Rainfall	No	No	No	No	No	No	No	No

TABLE B.2. Summary of the questionnaire replies (continued)

Pipeline No.	25	26	27	28	29	30	31	32
SECTION A								
Region	Eastern	Eastern	Eastern	Eastern	Eastern	Eastern	Eastern	Eastern
Upstream PRS	Matching Green	Peters Green	Snakeley	West Winch	West Winch	West Winch	Whitwell	Whitwell
Pipe diameter (mm)	200	750	450	200	300	0	300	450
Depth of Burial (m)	1	1	1	1	1	1	1	1
Duration of freezing period (months)	6	4	0	12	12	12	6	6
Soil type	gravelly	chalk	clayey	clayey	clayey	clayey	chalk	chalk
SECTION B								
Frost heave	No heave	No heave	No heave	No heave	No heave	No heave	No heave	No heave
SECTION C								
Ground cracking	No cracking	No cracking	No cracking	No cracking	No cracking	No cracking	No cracking	No cracking
TABLE 1								
Location								
Distance from PRS (m)								
Length of cracking (m)								
When visible	Yes	Yes	No	Yes	Yes	Yes	Yes	Yes
Crack width (mm)	Yes	No	No	Yes	Yes	Yes	Yes	Yes
Depth to WT (m)	No	No	No	No	No	No	No	No
TABLE 1								
Was information available on :-	Yes	Yes	No	Yes	Yes	Yes	Yes	Yes
Gas Temperature	Yes	No	No	Yes	Yes	Yes	Yes	Yes
Gas flow	No	No	No	No	No	No	No	No
Ground Temperatures	Yes	Yes	No	No	No	No	Yes	Yes
Air Temperatures	No	No	No	No	No	No	No	No
Rainfall								

TABLE B.2. Summary of the questionnaire replies (continued)

Pipeline No.	33	34	35	36	37	38	39	40
SECTION A								
Region	Eastern Whitwell	North Thames Chigwell	North Thames Cookham	North Thames Denham				
Upstream PRS	750	0	0	0	0	450	300	300
Pipe diameter (mm)	1	1	1	1	1	1	1	1
Depth of Burial (m)	6	6	6	6	6	12	7	6
Duration of freezing period (months)	chalk	chalk	chalk	chalk	chalk	clayey	clayey	clayey
Soil type								
SECTION B								
Frost heave	No heave	No heave	No heave	No heave	No heave	No heave	No heave	No heave
Location								
Distance from PRS (m)								
When visible								
Estimated pipe lift (mm)								
Depth to WT (m)								
SECTION C								
Ground cracking	No cracking	No cracking	No cracking	No cracking	No cracking	Cracking PRS	No cracking	No cracking
Location						0		
Distance from PRS (m)						60		
Length of cracking (m)						Nov - Mar		
When visible						6		
Crack width (mm)						Unknown		
Depth to WT (m)								
TABLE 1								
Was information available on :-								
Gas Temperature	Yes	Yes	Yes	Yes	Yes	Yes	Yes	Yes
Gas flow	Yes	Yes	Yes	Yes	Yes	No	Yes	Yes
Ground Temperatures	No	No	No	No	No	No	No	No
Air Temperatures	Yes	Yes	Yes	Yes	Yes	No	No	No
Rainfall	No	No	No	No	No	No	No	No

TABLE B.2. Summary of the questionnaire replies (continued)

Pipeline No.	41	42	43	44	45	46	47	48
SECTION A								
Region	North Thames Glory Hill	North Thames Hedgerley	North Thames Hedgerley	North Thames Hedgerley	North Thames Holloway lane	North Thames Ilford Holder	North Thames Marlow Road	North Thames NorthWood
Upstream PRS	300	450	750	600	450	600	450	450
Pipe diameter (mm)	1	1	1	1	1	1	1	1
Depth of Burial (m)	6	9	9	9	5	4	6	6
Duration of freezing period (months)	clayey	clayey	clayey	clayey	clayey	clayey	silty	clayey
Soil type								
SECTION B								
Frost heave	No heave	No heave	No heave	No heave	Heave	Heave	No heave	No heave
Location					PRS	PRS		
Distance from PRS (m)					10	0		
When visible					Jan - Mar*	Nov - Mar		
Estimated pipe lift (mm)					Unknown	Unknown		
Depth to WT (m)					0.5	Unknown		
SECTION C								
Ground cracking	No cracking	No cracking	No cracking	No cracking	No cracking	Cracking	No cracking	No cracking
Location						PRS		
Distance from PRS (m)						0		
Length of cracking (m)						60		
When visible						Nov - Mar		
Crack width (mm)						12		
Depth to WT (m)						Unknown		
TABLE 1								
Was information available on :--								
Gas Temperature	Yes	Yes	Yes	Yes	Yes	Yes	Yes	Yes
Gas flow	Yes	Yes	Yes	Yes	Yes	No	Yes	Yes
Ground Temperatures	No	No	No	No	No	No	No	No
Air Temperatures	No	No	No	No	No	No	No	No
Rainfall	No	No	No	No	No	No	No	No

TABLE B.2. Summary of the questionnaire replies (continued)

Pipeline No.	49	50	51	52	53	54	55	56
SECTION A								
Region	North Thames Redbridge Lane	North Thames Staines Moor	North Thames Stanford-le-Hope	North Thames Tailing End	North Thames Woodfield	North West Blackrod	North West Blackrod	North West Orrell
Upstream PRS	450	600	0	600	0	900	600	300
Pipe diameter (mm)	1	1	1	1	1	1	1	1
Depth of Burial (m)	10	6	2	8	2	6	6	6
Duration of freezing period (months)	clayey	sandy	silty	sandy	clayey	clayey	clayey	made-up ground
SECTION B								
Frost heave	Heave	No heave	Heave	Heave	No heave	Heave	No heave	Heave
Location	PRS		PRS	PRS		PRS - gravel		PRS
Distance from PRS (m)	0		0	5		0		0
When visible	Nov - Feb		Unknown	Most of year		Dec - Apr		Nov - May
Estimated pipe lift (mm)	80		3	Unknown		15		80
Depth to WT (m)	Unknown		Unknown	0.75		Various		4.5
SECTION C								
Ground cracking	Cracking	No cracking	Cracking	No cracking	No cracking	Cracking	No cracking	Cracking
Location	PRS - Road		PRS - Road			Fields		Gravelled path
Distance from PRS (m)	0		0			Upto 3 Km d/s		30
Length of cracking (m)	Unknown		6			Various		300
When visible	Unknown		Nov - Feb			May onwards		Apr onwards
Crack width (mm)	Unknown		6			125		40
Depth to WT (m)	Unknown		Unknown			Various		Unknown
TABLE 1								
Was information available on :-								
Gas Temperature	Yes	Yes	No	Yes	Yes	Yes	Yes	Yes
Gas flow	No	Yes	No	Yes	No	Yes	Yes	Yes
Ground Temperatures	No	No	No	No	No	Yes	Yes	Yes
Air Temperatures	No	No	No	No	No	Yes	Yes	Yes
Rainfall	No	No	No	No	No	Yes	Yes	Yes

TABLE B.2. Summary of the questionnaire replies (continued)

Pipeline No.	57	58	59	60	61	62	63	64
SECTION A								
Region	North West Salmsbury	North West Salmsbury	North West Salmsbury	Northern Elton	Northern Plawsworth	Northern Saltwick	Northern Wetheral	South East Taisfield
Upstream PRS	400	750	450	450	300	600	450	600
Pipe diameter (mm)	1	1	1	1	1	1	1	1
Depth of Burial (m)	6	6	6	2	5	3	4	6
Duration of freezing period (months)	unknown	unknown	unknown	clayey	clayey	clayey	clayey	clayey
Soil type								
SECTION B								
Frost heave	No heave	No heave	No heave	No heave	Heave road	Heave PRS	No heave	Heave PRS
Location					250	0		Fields
Distance from PRS (m)					Feb - Mar	Apr - Jun		100 - 800
When visible					50 - 70	50 - 70		Feb - June
Estimated pipe lift (mm)					Unknown	Unknown		100
Depth to WT (m)					Unknown	Unknown		Unknown
SECTION C								
Ground cracking	No cracking	Cracking Fields	No cracking	No cracking	Cracking Field	Cracking Field	No cracking	Cracking Field
Location		100			200	1500		100 - 800
Distance from PRS (m)		Unknown			200	Unknown		700
Length of cracking (m)		Dec-May			Dec - Apr	May - Jun		Feb - June
When visible		25			75	50		120
Crack width (mm)		Unknown			Unknown	Unknown		Unknown
Depth to WT (m)								
TABLE 1								
Was information available on :-	Yes	Yes	Yes	Yes	Yes	Yes	Yes	Yes
Gas Temperature	Yes	Yes	Yes	Yes	Yes	Yes	Yes	Yes
Gas flow	Yes	Yes	Yes	Yes	Yes	Yes	Yes	Yes
Ground Temperatures	Yes	Yes	Yes	Yes	Yes	Yes	Yes	Yes
Air Temperatures	Yes	Yes	Yes	Yes	Yes	Yes	Yes	Yes
Rainfall	No	No	No	Yes	Yes	Yes	Yes	No

TABLE B.2. Summary of the questionnaire replies (continued)

Pipeline No.	65	66	67	68	69	70	71	72
SECTION A								
Region	South Western	Southern	Wales/Cymru	Wales/Cymru	Wales/Cymru	West Midlands	West Midlands	West Midlands
Upstream PRS	Kenn	Braishfield	Maelor	Maelor	Maelor	Abrewas	Austrey	Coleshill Hp
Pipe diameter (mm)	350	900	200	300	350	600	900	300
Depth of Burial (m)	1	1	1	1	1	1	1	1
Duration of freezing period (months)	6	12	4	4	4	6	6	2
Soil type	clayey	clayey	clayey	clayey	clayey	sandy	clayey	clayey
SECTION B								
Frost heave	No heave	Heave	No heave	No heave	No heave	No heave	No heave	No heave
Location		PRS - Road						
Distance from PRS (m)		0						
When visible		Nov						
Estimated pipe lift (mm)		26						
Depth to WT (m)		200						
SECTION C								
Ground cracking	No cracking	No cracking	No cracking	No cracking	No cracking	No cracking	No cracking	No cracking
Location								
Distance from PRS (m)								
Length of cracking (m)								
When visible								
Crack width (mm)								
Depth to WT (m)								
TABLE 1								
Was information available on :-								
Gas Temperature	Yes	Yes	No	No	No	Yes	Yes	Yes
Gas flow	Yes	No	No	No	No	No	No	No
Ground Temperatures	No	Yes	No	No	No	Yes	Yes	No
Air Temperatures	No	No	No	No	No	Yes	Yes	No
Rainfall	No	No	No	No	No	No	No	No

TABLE B.2. Summary of the questionnaire replies (continued)

Pipeline No.	73	74	75	76	77	78	79	80
SECTION A								
Region	West Midlands	West Midlands	West Midlands	West Midlands				
Upstream PRS	Coleshill Hp	Coleshill Hp	Coleshill Hp	Coseley No2	Essington	Hinckley	Hinckley	Kenilworth
Pipe diameter (mm)	400	400	450	600	600	200	300	300
Depth of Burial (m)	1	1	1	1	1	1	1	1
Duration of freezing period (months)	2	2	2	3	5	0	0	2
Soil type	clayey	clayey	clayey	clayey	clayey	unknown	unknown	clayey
SECTION B								
Frost heave	No heave	No heave	No heave	Heave	Heave	No heave	No heave	No heave
Location				Path & grass	PRS-Roads etc			
Distance from PRS (m)				Upto 400	30			
When visible				Dec - Mar	Nov - Mar			
Estimated pipe lift (mm)				50	50			
Depth to WT (m)				Below pipe	1.5			
SECTION C								
Ground cracking	No cracking	No cracking	No cracking	Cracking	Cracking	No cracking	No cracking	No cracking
Location				Path & grass	PRS- Roads etc			
Distance from PRS (m)				400	30			
Length of cracking (m)				400	Hard surfaces			
When visible				Dec - Mar	Nov - Mar			
Crack width (mm)				15 - 20	25			
Depth to WT (m)				Below pipe	1.5			
TABLE 1								
Was information available on :-								
Gas Temperature	Yes	Yes	Yes	Yes	Yes	No	No	Yes
Gas flow	No	No	No	Yes	Yes	No	No	No
Ground Temperatures	No	No	No	Yes	No	No	No	No
Air Temperatures	No	No	No	Yes	No	No	No	No
Rainfall	No	No	No	No	No	No	No	No

TABLE B.2. Summary of the questionnaire replies (continued)

Pipeline No.	81	82	83				
SECTION A							
Region	West Midlands	West Midlands	West Midlands				
Upstream PRS	Maxstoke	Nechells	Shustoke				
Pipe diameter (mm)	400	150	350				
Depth of Burial (m)	1	1	1				
Duration of freezing period (months)	9	2	2				
Soil type	sandy	made-up ground	clayey				
SECTION B							
Frost heave	Heave	No heave	No heave				
Location	PRS						
Distance from PRS (m)	0						
When visible	Unknown						
Estimated pipe lift (mm)	Unknown						
Depth to WT (m)	Unknown						
SECTION C							
Ground cracking	No cracking	No cracking	No cracking				
Location							
Distance from PRS (m)							
Length of cracking (m)							
When visible							
Crack width (mm)							
Depth to WT (m)							
TABLE 1							
Was information available on :-							
Gas Temperature	Yes	No	Yes				
Gas flow	No	No	Yes				
Ground Temperatures	Yes	No	No				
Air Temperatures	No	No	No				
Rainfall	No	No	No				

TABLE B.2. Summary of the questionnaire replies (continued)

**APPENDIX C TEMPERATURE AND SOIL WATER POTENTIAL
RESULTS FOR SITES A AND B**

C.1 SITE A.

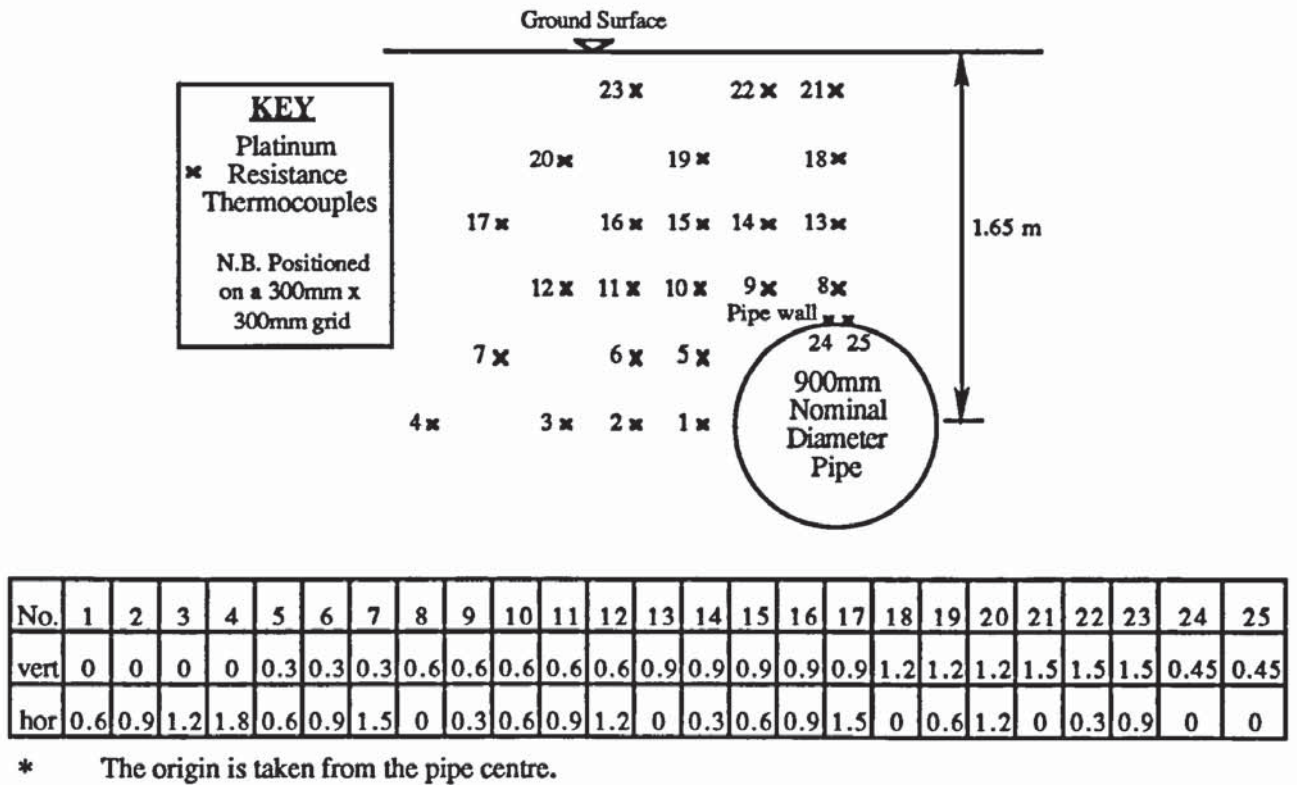


FIGURE C.1 Layout of Platinum Resistance Thermocouples at Site A.

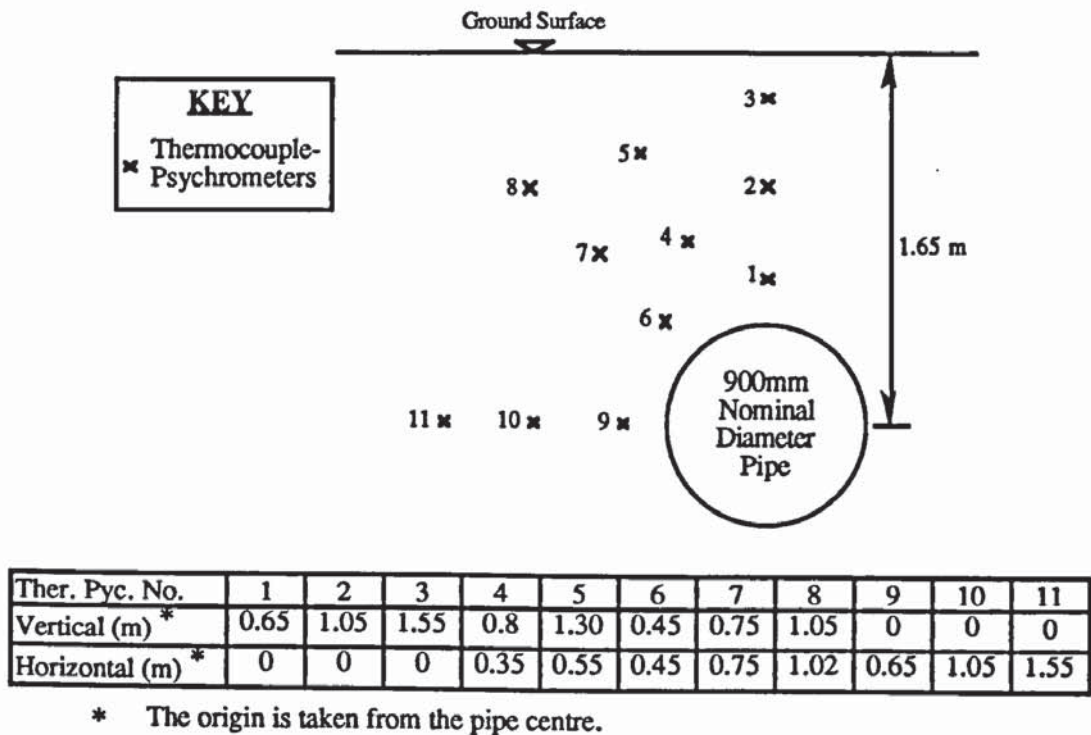


FIGURE C.2 Layout of the Thermocouple-Psychrometers at Site A.

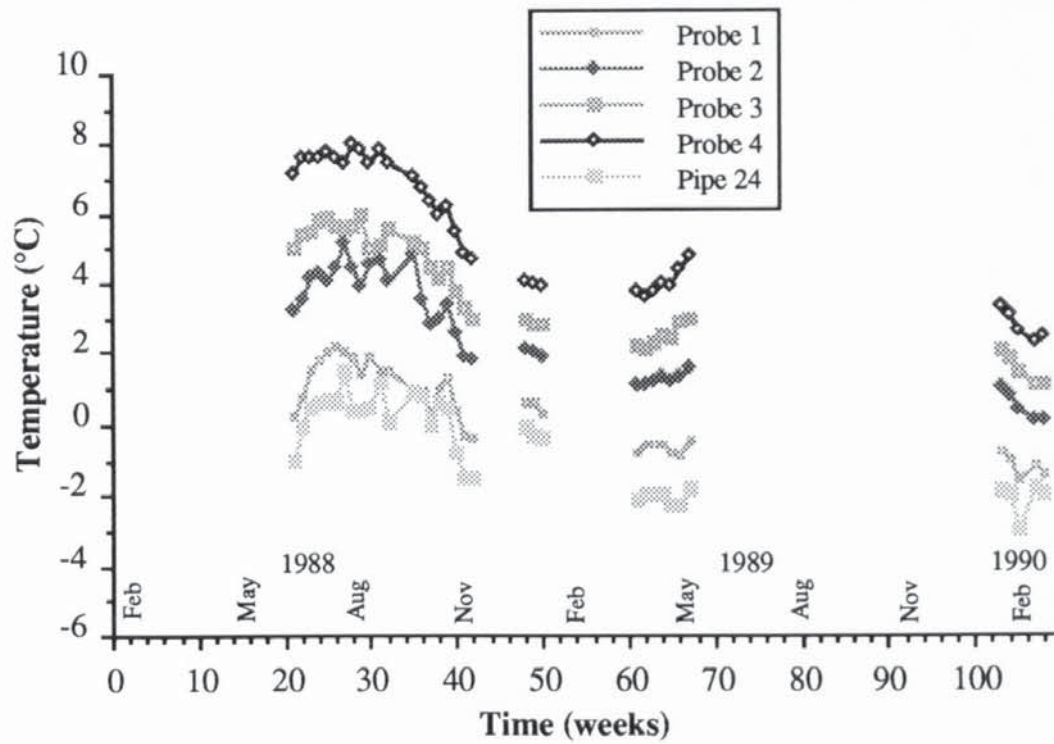


FIGURE C.3 Average Weekly Temperature Profile at 90° to the Vertical at Site A.

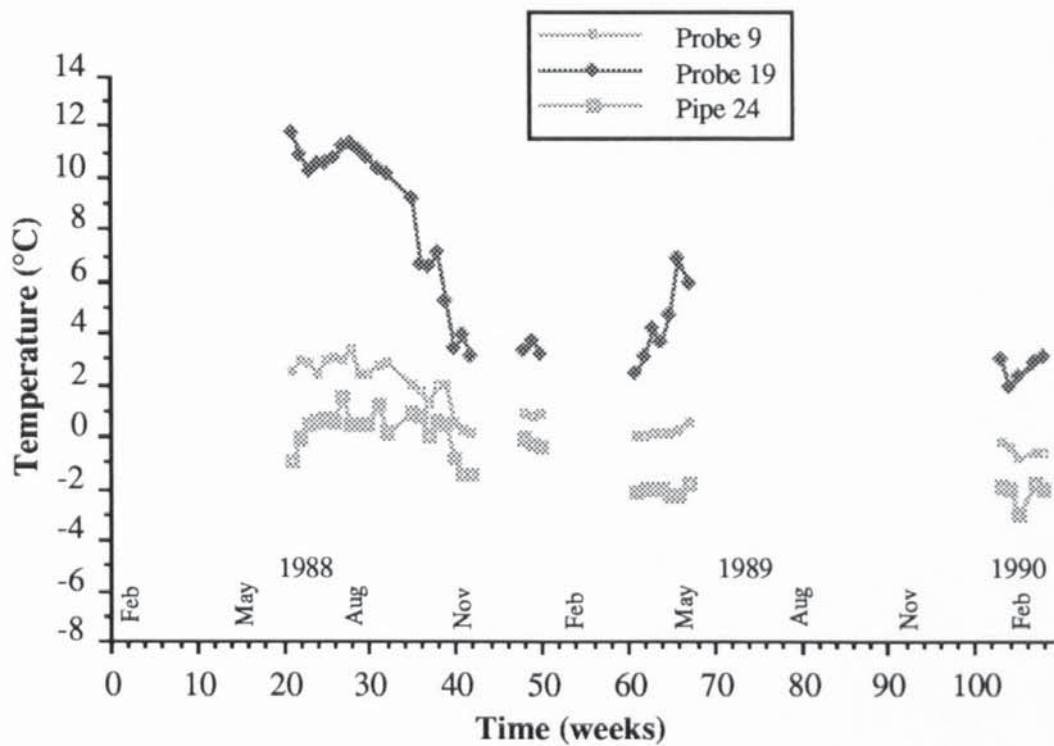


FIGURE C.4 Average Weekly Temperature Profile at 60° to the Vertical at Site A.

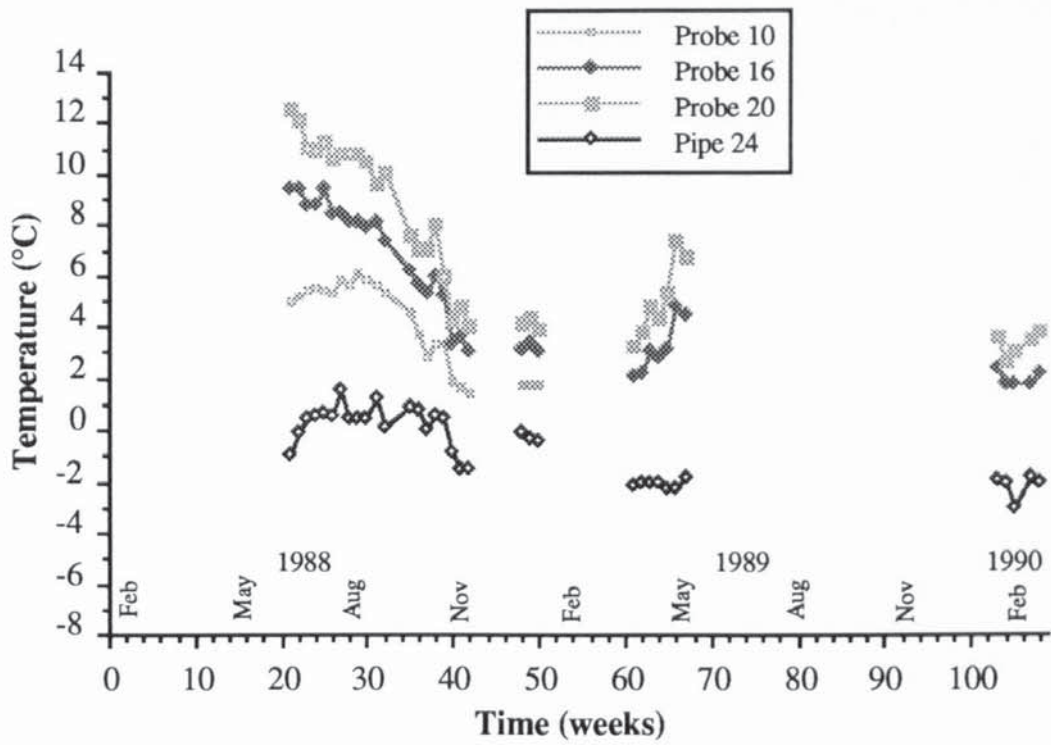


FIGURE C.5 Average Weekly Temperature Profile at 45° to the Vertical at Site A.

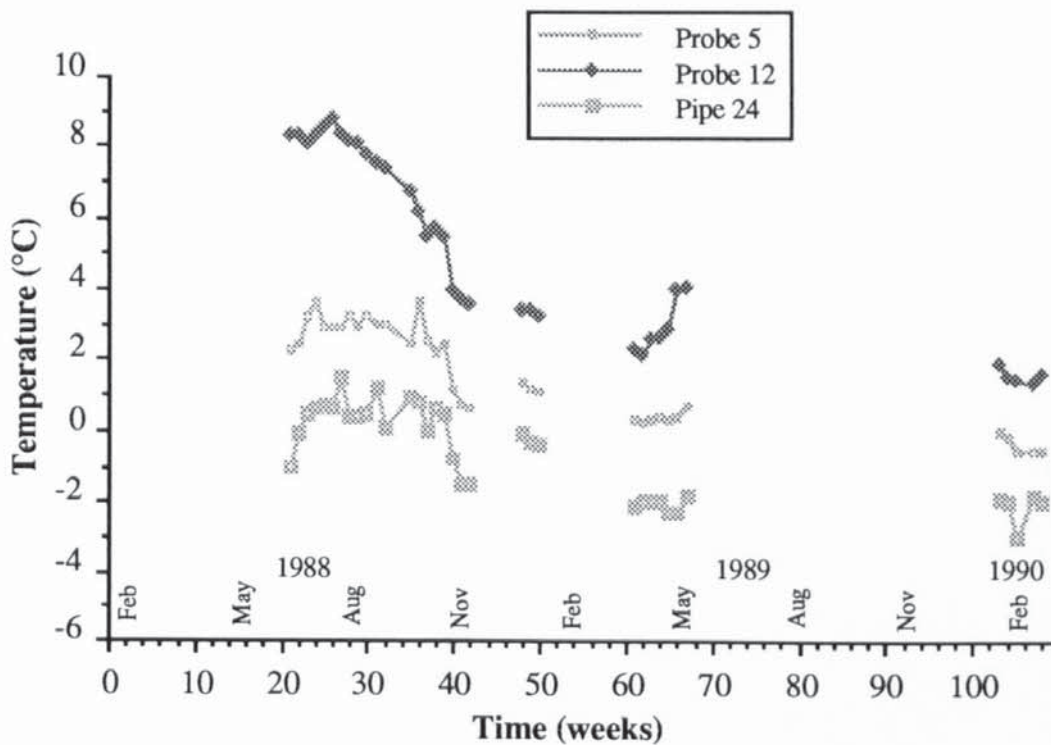


FIGURE C.6 Average Weekly Temperature Profile at 30° to the Vertical at Site A.

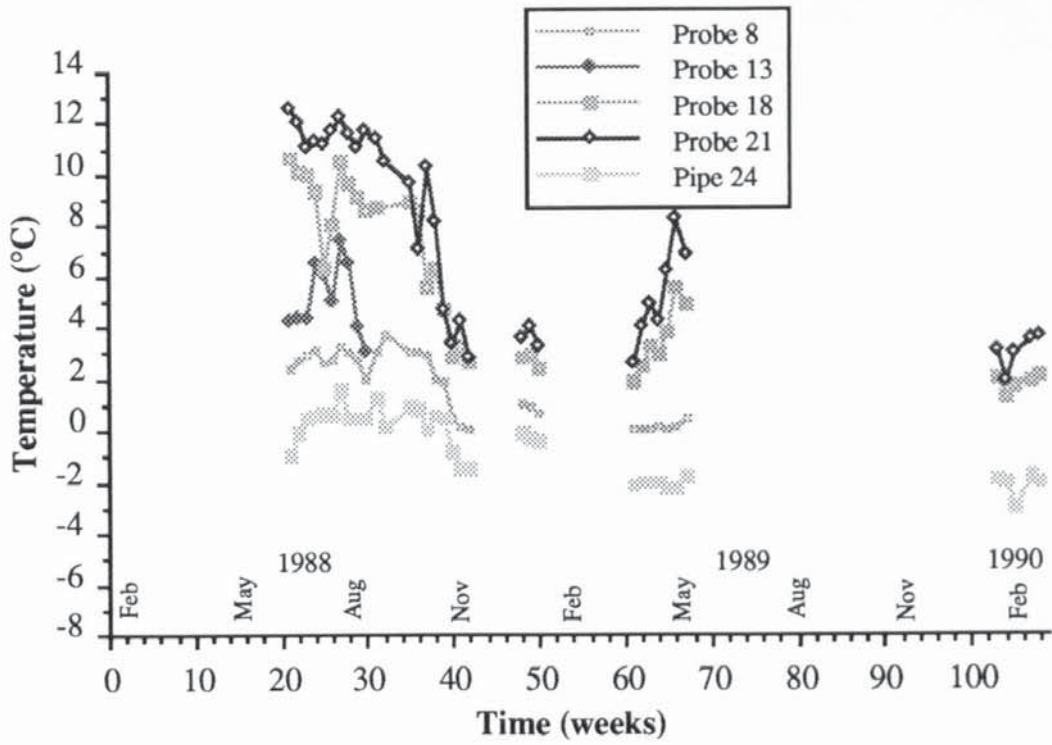


FIGURE C.7 Average Weekly Temperature Profile at 0° to the Vertical at Site A.

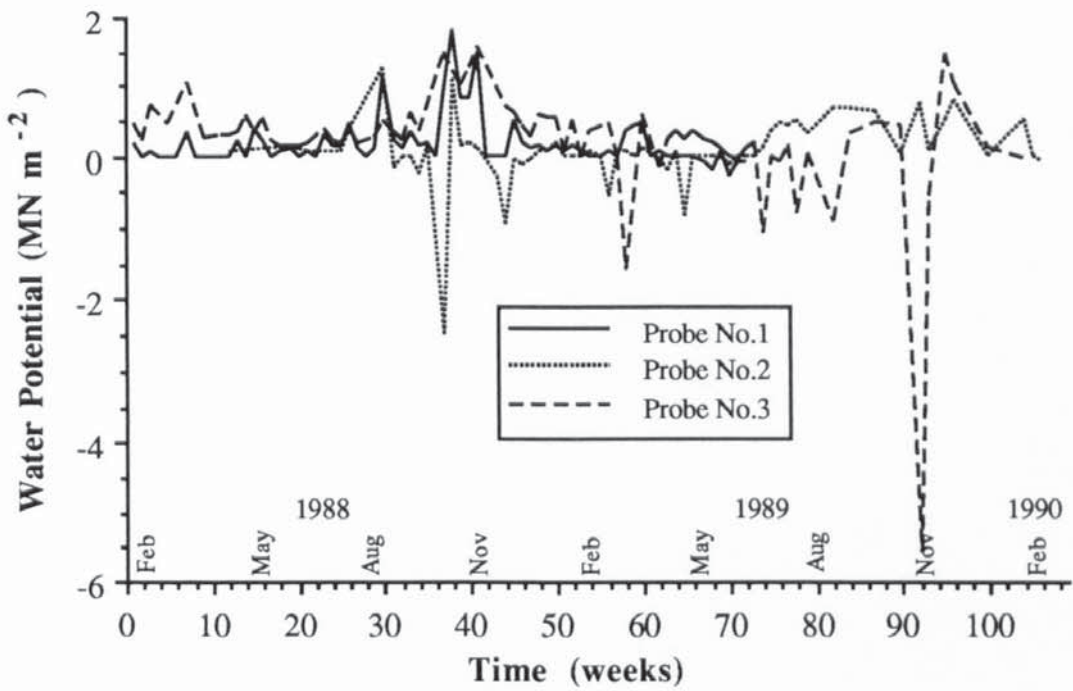


FIGURE C.8 Output from Thermocouple-Psychrometers at Site A, Profile at 0° to the Vertical.

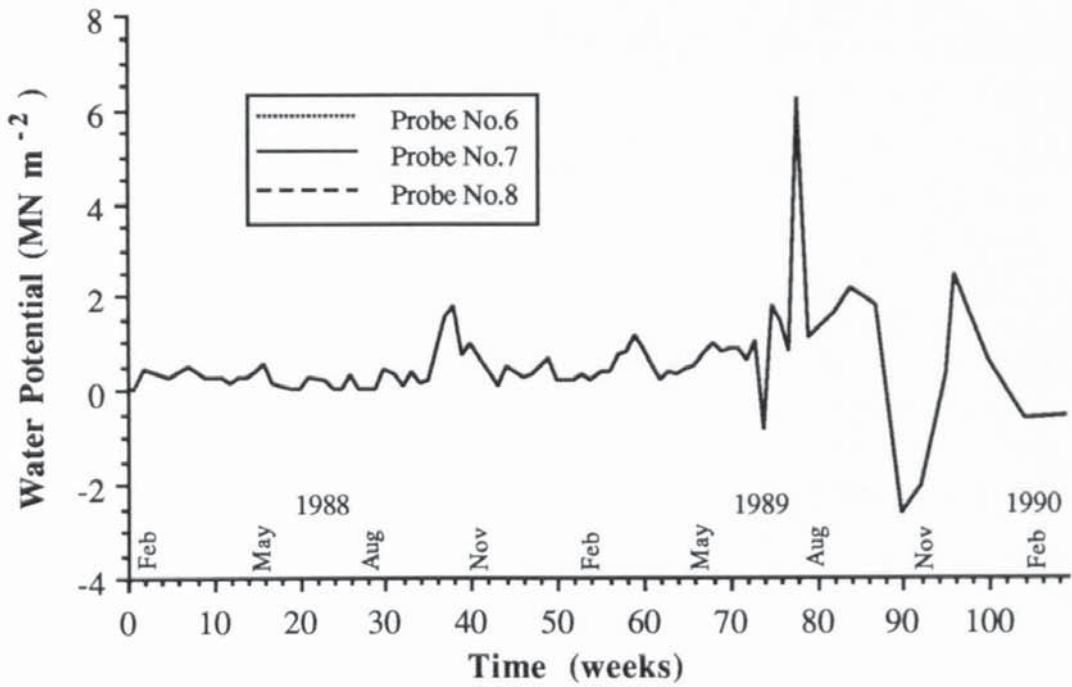


FIGURE C.9 Output from Thermocouple-Psychrometers at Site A, Profile at 45° to the Vertical.

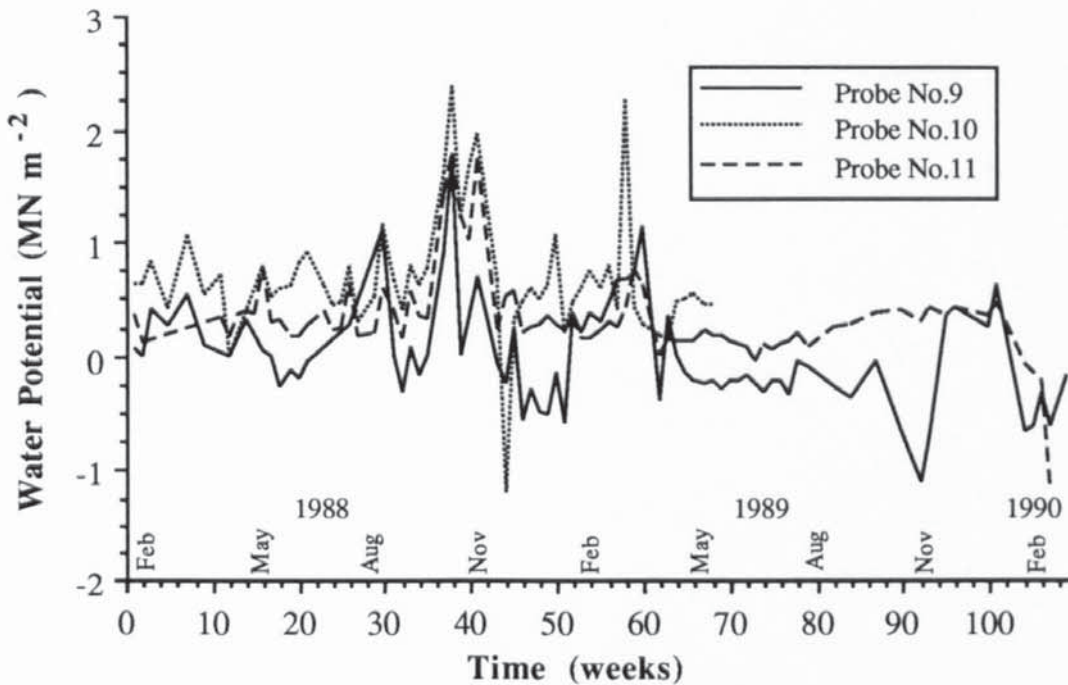


FIGURE C.10 Output from Thermocouple-Psychrometers at Site A, Profile at 90° to the Vertical.

C.2 SITE B.

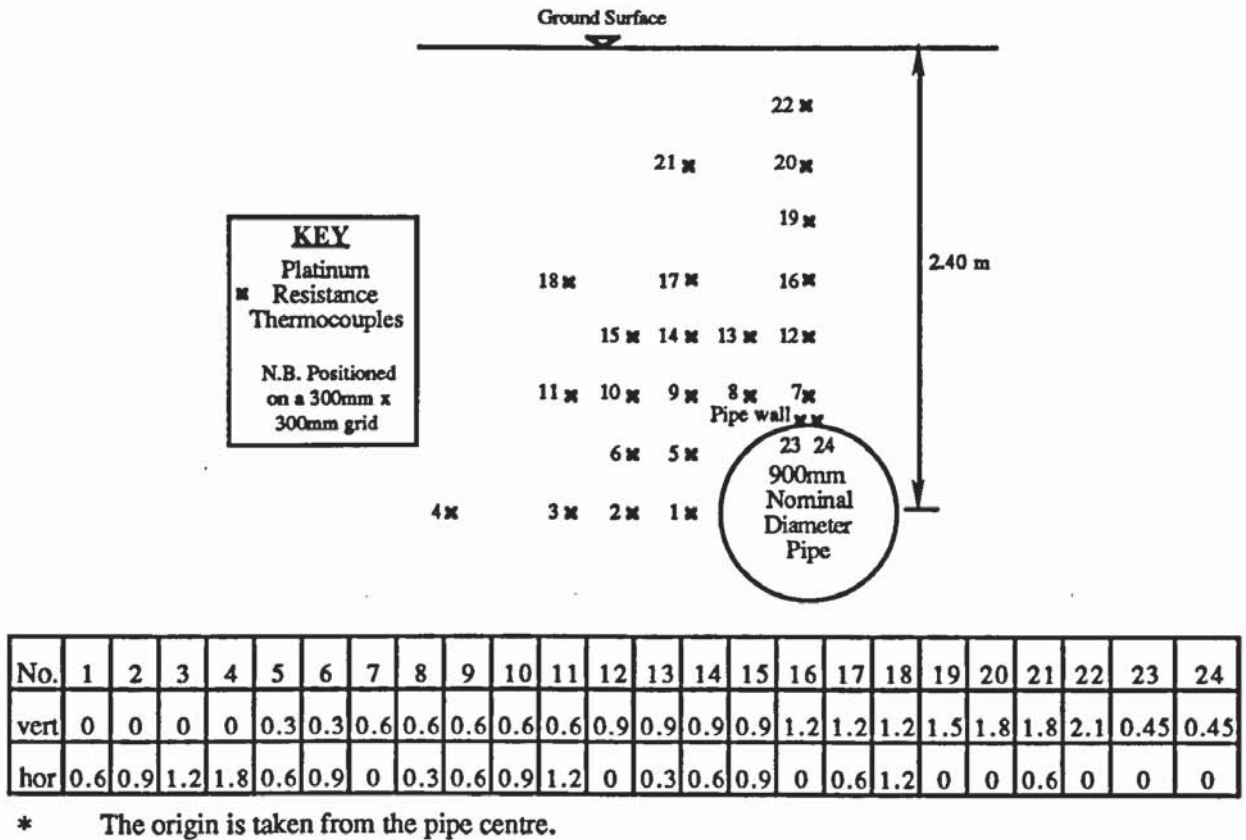


FIGURE C.10 Layout of Platinum Resistance Thermocouples at Site B.

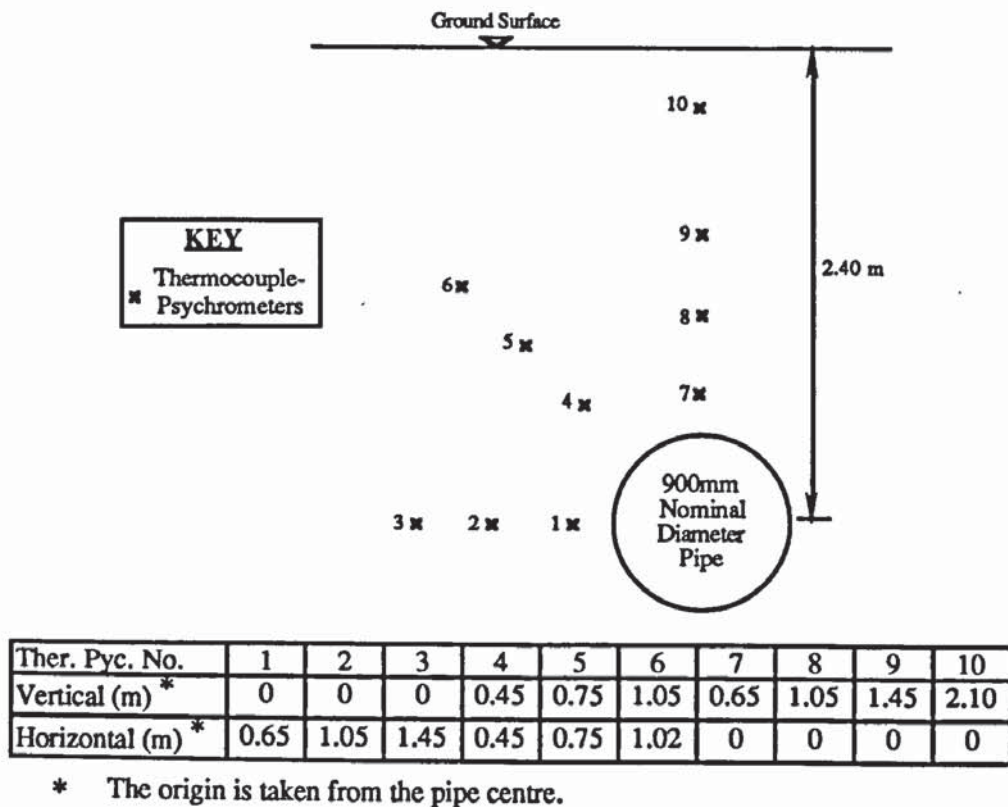


FIGURE C.12 Layout of the Thermocouple-Psychrometers at Site B.

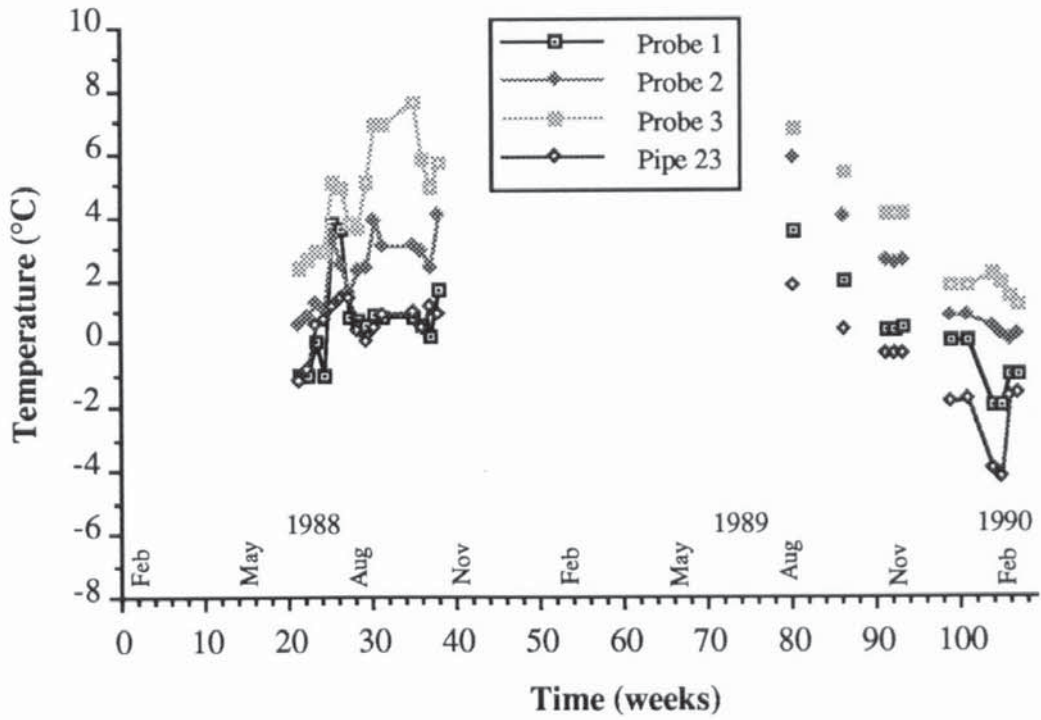


FIGURE C.13 Average Weekly Temperature Profile at 90° to the Vertical at Site B.

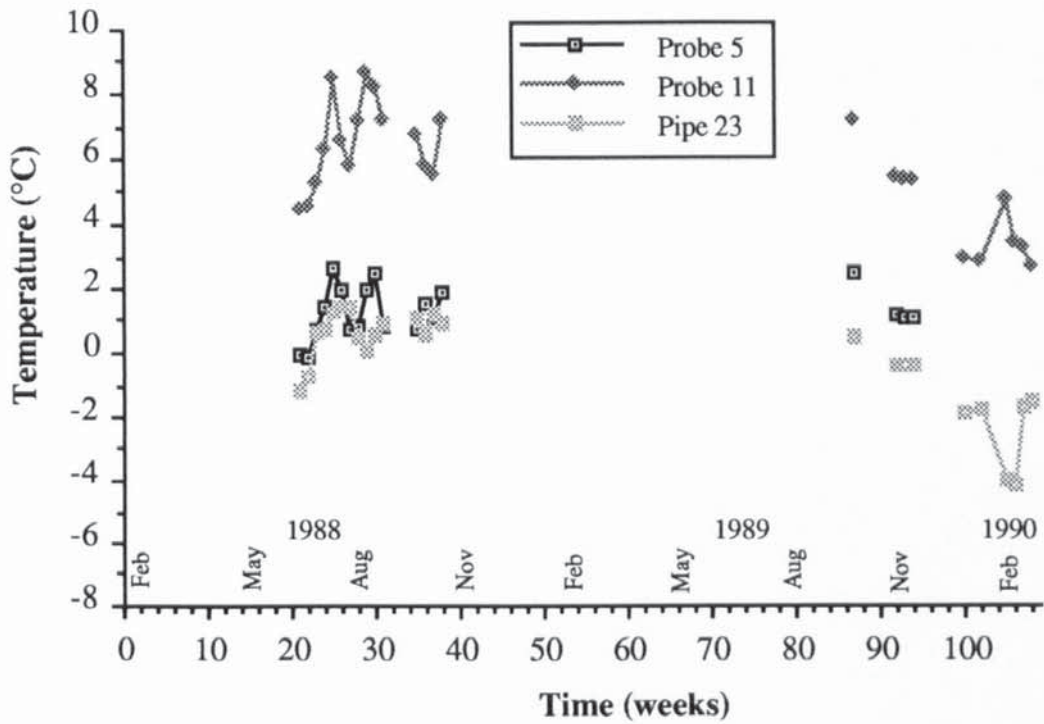


FIGURE C.14 Average Weekly Temperature Profile at 60° to the Vertical at Site B.

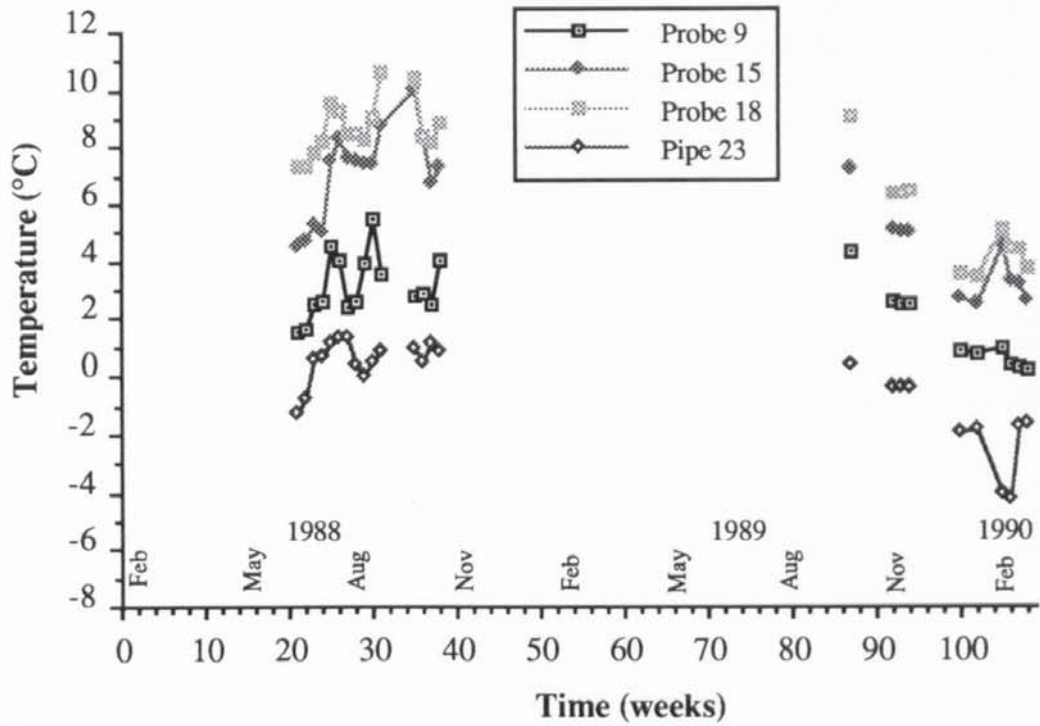


FIGURE C.15 Average Weekly Temperature Profile at 45° to the Vertical at Site B.

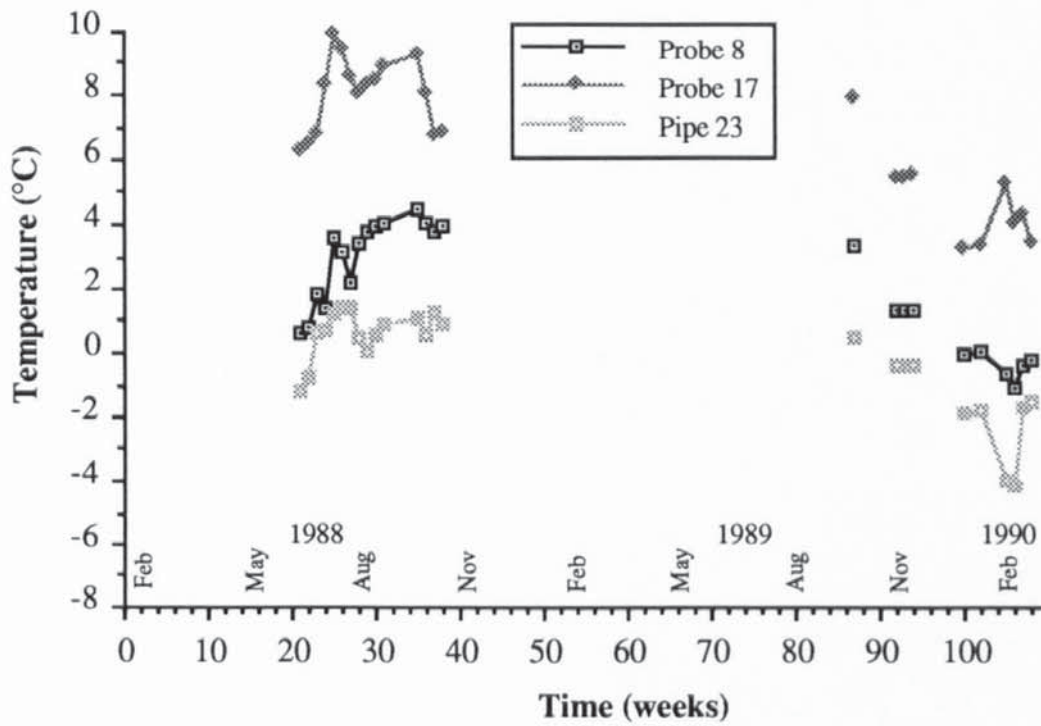


FIGURE C.16 Average Weekly Temperature Profile at 30° to the Vertical at Site B.

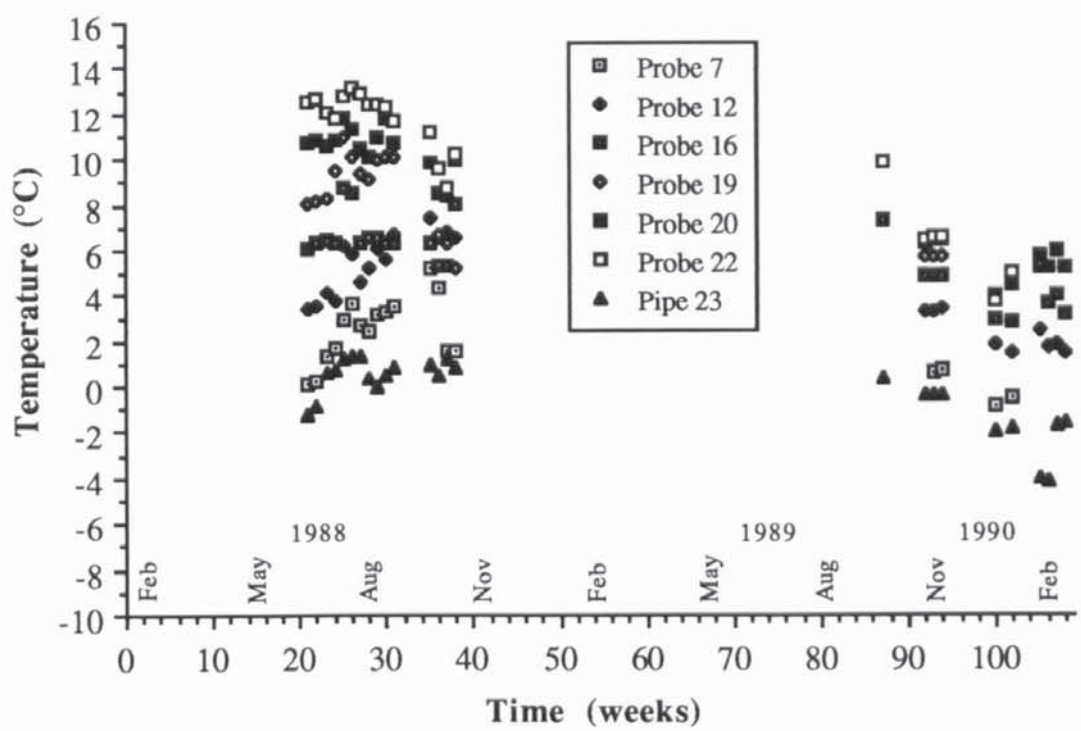


FIGURE C.17 Average Weekly Temperature Profile at 0° to the Vertical at Site B.

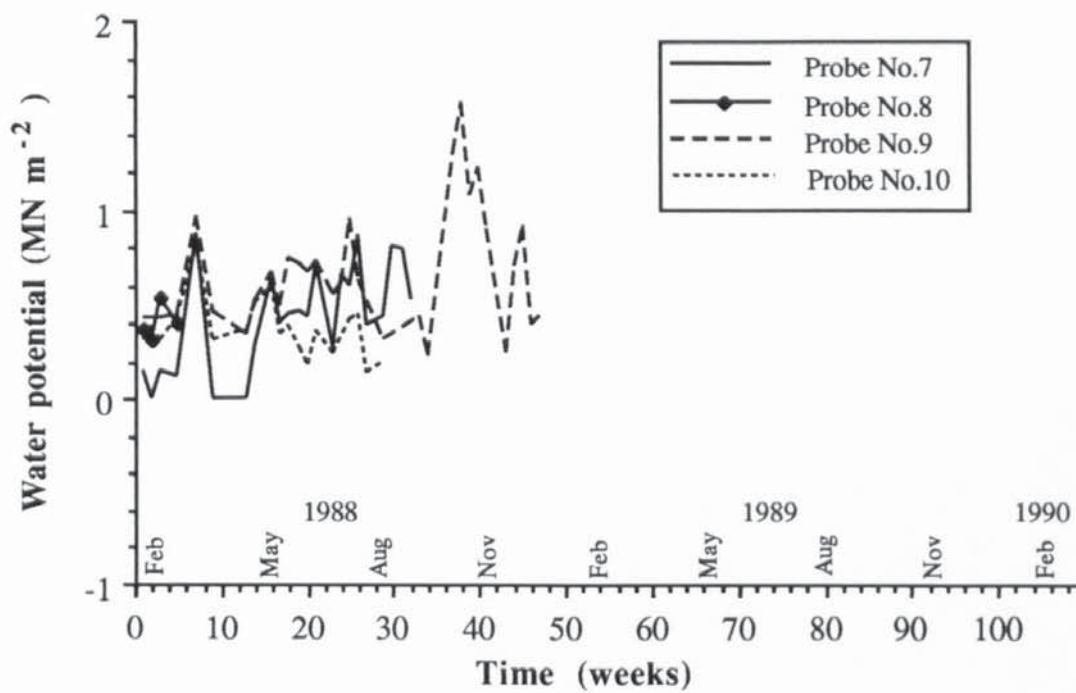


FIGURE C.18 Output from Thermocouple-Psychrometers at Site B, Profile at 0° to the Vertical.

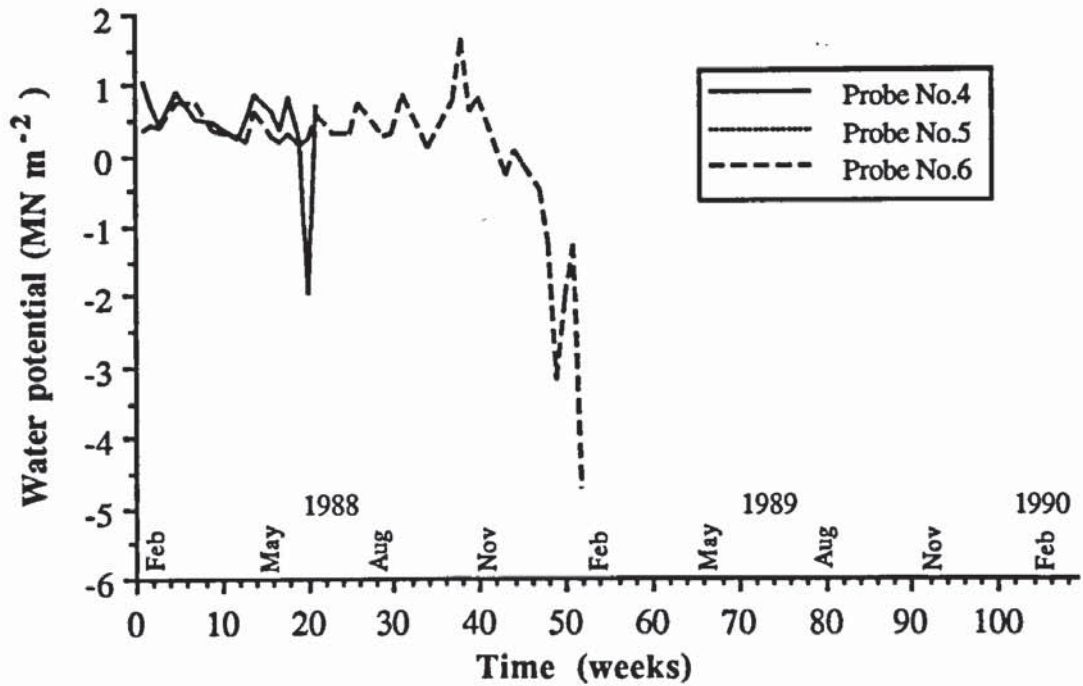


FIGURE C.19 Output from Thermocouple-Psychrometers at Site B, Profile at 45° to the Vertical.

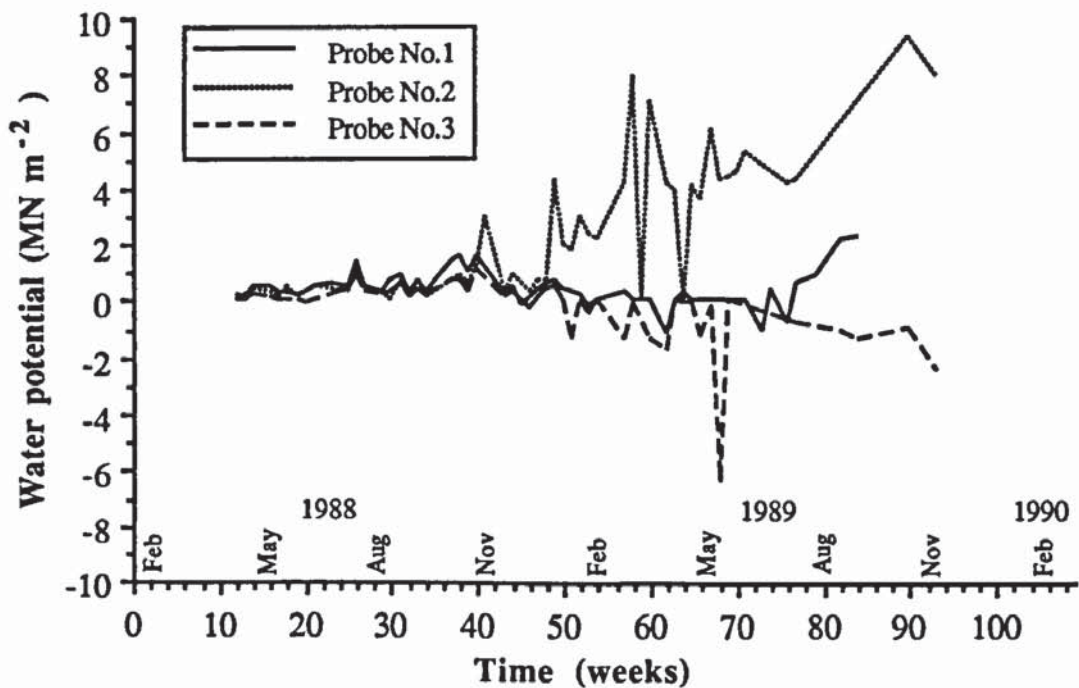


FIGURE C.20 Output from Thermocouple-Psychrometers at Site B, Profile at 90° to the Vertical.

APPENDIX D THERMOCOUPLE-PSYCHROMETER PROGRAM

A modified version of Brown and Bartos's (1982) computer program is given below, this can be either run on a BBC or an Apple Macintosh microcomputer using BBC Basic.

```
10 CLS
20 REM *****
30 REM Ray Brown's water potential equation coded by Denis
40 REM Greene in BBC Basic on 17/5/88. This is an
50 REM enhanced version of Mike Clarke's program written
60 REM in Microsoft Basic 3.0 18/5/87.
70 REM This program should be read in conjunction with a
80 REM research paper by R.W.Brown and D.L.Bartos;
90 REM A calibration model for screen-caged Peltier
100 REM Thermocouple Psychrometers, United States Department
110 REM of Agriculture, Forest Service, Research Paper
120 REM INT-293, July 1982.
130 REM The equations used for this method are shown on pages
140 REM 12 to 20. The program is written using the same
150 REM symbols as appear in the paper.
160 REM *****
170 REM ***** CALCULATES THE NUMBER OF OBSERVATIONS *****
180 REM ***** TO BE CALCULATED *****
190 INPUT "Number of sets of observations = ";Z
200 PRINT
210 INPUT "Correction co-efficient = ";B
220 PRINT
230 INPUT "Site = ";A$
240 PRINT
250 PRINT
260 REM ***** INPUT DIMENSIONAL ARRAY *****
270 REM Loop to allow for the number of observations
280 LET Z1=Z-1
290 DIM Potential(Z1,3)
300 FOR Q=0 TO Z1
310 PRINT
320 PRINT
330 INPUT "PSYCHROMETER NUMBER =" Potential(Q,0)
340 INPUT "MICROVOLT READING =" Potential(Q,1)
350 INPUT "ZERO ERROR =" Potential(Q,2)
360 INPUT "TEMPERATURE =" Potential(Q,3)
370 NEXT Q
380 REM ***** OUTPUT SHEET *****
390 PRINT
400 PRINT TAB(30);"===== "
410 PRINT TAB(30);"* SITE= "A$ " *
420 PRINT TAB(30);"===== "
430 PRINT
440 PRINT
450 PRINT TAB(10);"Psyr No.", "Volts", "Offset", "Temp", "Cool Time", " Potential"
460 PRINT TAB(10);"===== "
470 REM ***** START OF CALCULATION *****
480 REM ***** INPUT LOOP FROM DIMENSIONAL ARRAY *****
490 FOR Q2=0 TO Z1
500 CS=Potential(Q2,0)
510 MV=Potential(Q2,1)
520 OMV=Potential(Q2,2)
530 T=Potential(Q2,3)
540 SEC= 15
550 REM ***** CALCULATE UI FOR THE COOL TIME OF *****
```

```

560 REM ***** VARIABLE LENGTH(1) AND OF 15 SECONDS (A) *****
570 YP1 = 39.2 - 0.0004346*(60-SEC)^2.45
580 YPA = 39.2 - 0.0004346*(60-15)^2.45
590 IN1 = 12.1 - 0.003475*(60-SEC)^1.63
600 INA = 12.1 - 0.003475*(60-15)^1.63
610 IF T > 0 THEN 650
620 UI1=IN1
630 UIA=INA
640 GOTO 670
650 UI1 = IN1 + 0.017288*YP1*(T^1.1)
660 UIA = INA + 0.017288*YPA*(T^1.1)
670 REM ***** CALCULATE SP FOR THE COOL TIME OF *****
680 REM ***** VARIABLE LENGTH(1) AND OF 15 SECONDS (A) *****
690 YP21 = 8.4 + 2.734E-7*(60-SEC)^3.97
700 YP2A = 8.4 + 2.734E-7*(60-15)^3.97
710 IN21 = 88 - 0.0002579*(60-SEC)^2.7
720 IN2A = 88 - 0.0002579*(60-15)^2.7
730 SP1 = -(IN21-YP21*0.00017185*(40-T)^2.35)
740 SPA = -(IN2A-YP2A*0.00017185*(40-T)^2.35)
750 REM ***** CALCULATING N, CALCULATE I FOR COOL *****
760 REM ***** TIME OF VARIABLE LENGTH (1) AND OF *****
770 REM ***** 15 SECONDS (A) *****
780 I1 = 0.45+0.000333*(SEC)+1.9846E-19*SEC^10
790 IA = 0.45+0.000333*(15)+1.9846E-19*15^10
800 REM ***** CALCULATE M FOR COOL TIME OF VARIABLE *****
810 REM ***** LENGTH(1) AND OF 15 SECONDS(A) *****
820 M1 = 2.5 +EXP(-(ABS((60-SEC)/60-1)/0.405)^3.0)
830 MA = 2.5 +EXP(-(ABS((60-15)/60-1)/0.405)^3.0)
840 REM ***** CALCULATING N, BUT SPLIT EXPRESSION INTO *****
850 REM ***** N = 1.18 + 0.185*((EX1-EX2)/(1-EX2)) *****
860 EX11 = EXP(-(ABS(((40-T)/40-1)/(1-I1))^M1))
870 EX1A = EXP(-(ABS(((40-T)/40-1)/(1-IA))^MA))
880 EX21 = EXP(-(1/(1-I1))^M1)
890 EX2A = EXP(-(1/(1-IA))^MA)
900 REM ***** CALCULATE N *****
910 N1 = 1.18+0.185*((EX11-EX21)/(1-EX21))
920 NA = 1.18+0.185*((EX1A-EX2A)/(1-EX2A))
930 REM ***** CALCULATING CORRECTION FACTORS *****
940 C1 = UI1-UI1/ABS(SP1)^N1*ABS(SP1-(-22.5))^N1
950 C2 = UIA-UIA/ABS(SPA)^NA*ABS(SPA-(-22.5))^NA
960 C3 = C1/C2*(0.015*OMV+0.00147*T*OMV)
970 C = (C3+C1)/C1
980 REM ***** CALCULATING WATER POTENTIAL *****
990 WP=(ABS(SP1)^N1*(UI1*C*B-MV)/(UI1*C*B))^(1/N1)+SP1
1000 PRINT
1010 PRINT TAB(10);CS;TAB(20);MV;TAB(30);OMV;TAB(40);T;TAB(50);SEC;TAB(60);WP
1020 NEXT Q2
1030 PRINT
1040 PRINT
1050 CLEAR
1060 INPUT "Do you wish to continue(Y or N)"Y$
1070 IF Y$="Y" THEN 10
1080 PRINT
1090 PRINT
1100 PRINT TAB(30) "*****"
1110 PRINT TAB(30) "** THIS RUN IS CONCLUDED **"
1120 PRINT TAB(30) "*****"

```

**APPENDIX E GROUND SURFACE MOVEMENTS WITHIN
BLACKROD PRS**

Date	Week	Distance from pipe centreline (m)																				Pipe move ment (mm)											
		-2.0	-1.8	-1.6	-1.4	-1.2	-1.0	-0.9	-0.8	-0.7	-0.6	-0.5	-0.4	-0.3	-0.2	-0.1	0.0	0.1	0.2	0.3	0.4		0.5	0.6	0.7	0.8	0.9	1.0	1.2	1.4	1.6	1.8	2.0
24/1/88	42	-1	1	-1	3	3	1	2	2	4	7	7	7	8	10	8	11	11	11	11	5	5	5	2	6	1	-1	2	1	-1	2	0	
1/12/88	43	-1	1	0	3	3	4	1	1	2	0	3	2	1	1	4	1	3	4	5	7	1	2	2	-1	5	3	-1	3	3	0	1	-1
9/12/88	44	0	1	-1	5	3	3	1	1	1	3	1	1	2	3	1	2	4	3	4	1	1	0	-1	2	1	-1	2	2	0	1	-3	
15/12/88	45	-2	0	-1	2	0	2	1	0	0	0	0	1	2	3	-1	1	3	3	2	1	1	0	-1	0	-1	0	-1	-2	1	-1	0	-4
21/12/88	46	0	-1	-1	3	0	2	1	0	0	1	1	1	2	3	1	1	2	2	2	0	0	-1	-1	2	0	-2	0	1	1	0	-5	
29/12/88	47	0	1	0	-1	-2	1	1	-1	0	0	1	1	1	2	-1	1	4	2	2	1	0	0	0	3	0	-1	1	1	0	1	-4	
6/1/89	48	0	0	0	0	0	0	0	0	0	0	0	0	0	0	0	0	0	0	0	0	0	0	0	0	0	0	0	0	0	0	-3	
13/1/89	49	-1	-1	0	2	0	-1	0	0	1	0	0	1	1	-1	0	0	1	0	0	2	1	0	-1	1	0	-2	0	0	-2	0	-3	
19/1/89	50	-1	-1	-1	1	0	0	-1	1	0	1	1	0	1	2	0	1	2	2	1	1	1	-1	-1	1	-2	-2	0	0	-1	1	-4	
26/1/89	51	-1	-2	-1	0	0	-2	1	0	0	1	2	1	0	2	2	3	2	3	3	2	2	0	0	1	-3	-1	0	0	0	1	-5	
2/2/89	52	-2	-1	-1	0	-1	1	1	1	2	3	3	2	4	4	4	5	3	4	4	0	2	0	1	1	-2	-1	0	0	0	1	-3	
9/2/89	53	-1	0	-1	2	2	2	5	4	4	7	10	11	9	12	11	12	12	13	12	10	8	5	5	6	1	2	2	0	2	3		
16/2/89	54	1	0	2	4	5	7	6	9	10	9	13	16	17	14	16	15	16	16	18	16	14	11	10	9	6	5	4	2	2	7		
23/2/89	55	3	5	7	11	12	17	20	22	22	27	30	29	23	25	22	24	24	29	31	31	27	23	20	18	13	11	8	6	5	10		
2/3/89	56	2	2	4	7	10	13	15	19	21	19	25	27	27	20	22	20	22	23	27	30	26	22	19	17	13	10	8	6	4	5	10	
10/3/89	57	1	0	2	3	4	5	6	8	9	6	11	14	14	12	18	14	15	14	13	14	17	12	9	8	7	4	4	3	0	7		
16/3/89	58	1	1	1	3	4	5	6	8	9	7	11	13	14	13	14	14	15	13	14	14	15	11	8	7	6	3	3	2	1	-1	2	
25/3/89	59	1	-1	0	3	3	4	4	7	7	5	10	12	13	10	11	12	13	13	12	12	10	7	6	5	2	2	2	1	-1	2	2	
31/3/89	60	0	-1	-1	2	4	4	3	5	5	4	8	10	10	8	9	10	11	10	11	11	8	5	4	4	2	1	1	1	0	2	4	
7/4/89	61	0	-1	0	2	3	4	4	6	7	5	9	12	14	11	10	8	14	15	14	15	13	11	7	6	6	3	2	2	0	3	3	
15/4/89	62	0	-1	0	2	3	3	3	6	6	3	6	11	11	8	10	10	11	11	11	12	10	6	6	6	2	2	1	2	0	3	2	
22/4/89	63	0	-1	-1	2	3	3	3	5	6	3	8	11	11	9	11	10	11	12	12	12	9	6	5	6	1	2	1	1	-1	2	2	
28/4/89	64	0	-1	-1	2	2	3	3	6	6	4	9	12	13	11	13	12	14	12	15	14	11	8	7	7	2	2	2	1	-1	2	2	
4/5/89	65	0	-1	0	2	2	3	3	5	5	3	7	9	9	6	8	5	9	11	13	12	11	9	6	5	4	2	2	1	0	2	1	
13/5/89	66	0	-1	-1	2	2	3	3	4	4	2	7	9	10	7	10	6	10	12	14	11	12	10	7	6	4	1	3	1	-1	1	2	
18/5/89	67	0	-1	-1	2	1	2	1	4	4	1	6	8	8	5	10	5	7	10	11	9	11	9	6	5	3	1	3	1	1	-1	1	2

TABLE E.1a Ground Surface Movement (mm) and Pipe Movement (mm) at Site C' Within Blackrod PRS from Week 42 to 109.

Date	Week	Distance from pipe centreline (m)																			Pipe movement (mm)												
		-2.0	-1.8	-1.6	-1.4	-1.2	-1.0	-0.9	-0.8	-0.7	-0.6	-0.5	-0.4	-0.3	-0.2	-0.1	0.0	0.1	0.2	0.3		0.4	0.5	0.6	0.7	0.8	0.9	1.0	1.2	1.4	1.6	1.8	2.0
27/5/89	68	0	-1	1	2	2	2	2	3	2	1	5	7	6	3	7	2	6	9	9	6	9	7	5	4	3	1	2	1	2	0	3	-1
2/6/89	69	0	-2	-2	1	1	1	3	3	0	5	7	8	5	8	4	6	8	8	10	11	7	6	5	4	0	3	1	0	-2	2	1	
9/6/89	70	0	-1	1	2	2	2	3	2	1	5	7	6	3	7	2	6	9	9	6	9	7	5	4	5	1	2	1	2	0	1	-1	
15/6/89	71	-1	-2	0	2	2	1	2	2	2	1	3	5	5	2	3	-1	4	5	7	7	8	5	4	4	4	0	2	1	1	-1	2	-2
23/6/89	72	-1	-1	-2	2	2	1	2	2	2	0	3	5	5	2	3	-1	2	5	7	7	8	5	4	4	5	0	2	0	0	-1	1	-1
30/6/89	73	-2	-1	-2	3	1	1	1	1	1	-2	1	2	2	-1	0	-5	0	2	3	4	6	3	2	3	4	0	1	0	0	-1	1	-3
6/7/89	74	-1	-1	-1	3	2	0	1	2	1	-1	1	3	2	-1	0	-4	1	2	4	5	6	5	2	3	4	-1	2	0	1	-1	2	-3
12/7/89	75	-1	-1	-1	3	1	0	1	1	0	-2	1	2	1	-2	-1	-7	0	1	1	3	6	1	1	3	4	0	2	0	1	-1	1	-5
20/7/89	76	-1	-1	-1	3	2	1	0	1	0	-2	0	2	1	-2	-2	-7	-1	0	0	2	5	2	2	2	4	0	2	1	0	-1	1	-6
28/7/89	77	-1	-1	-1	2	1	0	0	1	0	-2	0	1	1	-3	-2	-7	-1	0	0	3	4	2	1	2	3	-1	1	0	0	-1	1	-5
6/8/89	78	0	-1	0	2	2	0	0	1	0	-2	-1	1	0	-4	-3	-7	-3	-1	-1	3	4	0	1	2	3	-2	1	0	0	-1	1	-6
12/8/89	79	-1	-2	-2	2	0	0	1	-1	-3	-2	1	0	-4	-3	-11	-2	-1	-1	2	4	-1	1	2	2	-1	1	0	0	-2	1	-6	
19/8/89	80	-2	-3	-2	2	0	0	0	-1	-2	-2	1	0	-4	-4	-10	-2	-1	-1	2	4	-1	1	1	3	-2	1	0	0	-1	1	-6	
26/8/89	81																																
1/9/89	82	-2	-4	-3	1	0	-1	-2	-1	-2	-3	0	-1	-4	-3	-9	-3	-2	-1	2	3	-1	0	1	2	-3	0	0	-1	-2	0	-5	
8/9/89	83																																
14/9/89	84	-2	-4	-4	0	0	-1	-2	-1	-2	-4	-2	0	-1	-4	-3	-9	-4	-3	-2	1	3	-1	0	1	2	-2	0	-1	0	-3	0	-5
21/9/89	85																																
28/9/89	86																																
5/10/89	87	-2	-4	-3	1	0	-1	-1	0	-1	-4	-2	0	0	-4	-3	-10	-3	-2	-1	0	3	-1	1	1	3	-2	1	0	1	-2	1	-5
12/10/89	88																																
19/10/89	89																																
26/10/89	90	-1	-4	-3	1	0	0	-2	0	-1	-5	-3	0	-1	-4	-3	-9	-3	-2	-2	1	3	-1	0	0	3	-2	1	-1	0	-2	1	-2
2/11/89	91																																
9/11/89	92	-1	-4	-4	1	1	-1	-2	0	-1	-5	-3	0	-1	-3	-4	-9	-3	-3	-1	0	3	-2	0	1	2	-3	1	-1	0	-3	1	-6
16/11/89	93	-1	-4	-3	1	1	-1	-1	0	-1	-4	-2	1	1	-2	-1	-7	-1	-1	1	2	5	1	1	1	3	-2	1	-1	0	-3	1	-5

TABLE E.1b Ground Surface Movement (mm) and Pipe Movement (mm) at Site C' Within Blackrod PRS from Week 42 to 109.

Date	Week	Distance from pipe centreline (m)																				Pipe movement (mm)											
		-2.0	-1.8	-1.6	-1.4	-1.2	-1.0	-0.9	-0.8	-0.7	-0.6	-0.5	-0.4	-0.3	-0.2	-0.1	0.0	0.1	0.2	0.3	0.4		0.5	0.6	0.7	0.8	0.9	1.0	1.2	1.4	1.6	1.8	2.0
24/11/88	42	-3	1	1	5	6	4	5	8	7	10	11	15	11	12	16	12	13	12	11	12	15	10	9	7	8	11	4	5	6	4	2	0
1/12/88	43	0	4	-2	1	1	0	1	2	0	2	3	6	2	0	7	2	0	0	0	2	5	1	2	1	0	5	-1	4	2	1	0	-9
9/12/88	44	0	3	-2	1	1	0	1	1	-1	1	4	-4	1	6	0	-1	0	-2	-2	3	0	1	0	-1	3	-1	3	1	-1	-1	-9	
15/12/88	45	0	3	-1	1	2	-1	1	0	-3	0	2	-2	-3	3	-1	-2	1	-2	-2	3	-3	-1	-1	-2	1	-2	1	-3	-1	0	-10	
21/12/88	46	-1	3	-1	1	-1	0	1	-1	-4	0	4	-1	-2	0	0	-2	0	-1	-1	3	-2	-1	-2	0	0	0	-4	-2	-1	-3	-1	-9
29/12/88	47	0	4	-1	2	0	0	1	-1	-2	-1	3	1	-2	0	0	-1	0	-1	-4	1	-2	-2	0	0	0	0	0	2	0	-1	0	-11
6/1/89	48	0	0	0	0	0	0	0	0	0	0	0	0	0	0	0	0	0	0	0	0	0	0	0	0	0	0	0	0	0	0	0	-9
13/1/89	49	0	-3	-2	-2	0	0	-1	1	0	2	2	-1	0	0	-1	-2	0	-1	-3	1	-1	-1	0	0	0	0	-4	0	-1	-2	0	-11
19/1/89	50	0	-1	-1	2	3	1	2	1	-1	2	1	2	1	1	2	1	1	2	1	0	5	1	1	1	0	3	-1	2	2	-1	2	-11
26/1/89	51	0	-2	-1	3	3	0	3	-1	-2	1	2	3	1	1	-2	2	0	3	2	-1	2	-1	0	0	1	0	-3	0	-1	-1	-10	
2/2/89	52	1	-3	-2	0	1	-1	4	3	2	4	6	4	4	5	9	8	6	7	5	4	7	4	4	3	2	4	-2	0	-1	-1	-5	
9/2/89	53	0	-2	0	2	2	4	8	6	6	10	13	15	16	16	20	18	17	19	14	12	13	9	9	7	7	8	0	3	1	-1	3	
16/2/89	54	1	-1	1	4	8	10	13	13	13	17	22	24	24	25	28	26	25	28	24	19	19	16	16	13	12	15	5	6	3	1	2	9
23/2/89	55	2	2	3	8	13	17	22	25	28	32	41	44	46	45	49	46	45	50	45	40	40	33	29	25	22	21	14	13	8	1	2	18
2/3/89	56	2	2	5	11	14	15	23	23	24	28	35	40	39	39	41	39	37	44	36	31	34	28	26	25	23	19	12	11	7	1	2	20
10/3/89	57	2	0	4	9	12	13	19	20	20	22	26	29	28	30	31	30	29	32	28	24	25	21	21	19	18	18	9	6	1	3	21	
16/3/89	58	2	2	3	6	11	10	16	16	17	21	26	31	31	32	35	32	31	34	31	25	24	20	19	17	16	14	7	5	1	1	21	
25/3/89	59	2	3	2	8	10	10	15	17	16	19	26	30	30	30	31	30	28	34	30	26	24	20	17	15	15	14	8	7	4	-1	0	22
31/3/89	60	1	2	2	5	8	9	14	16	15	18	24	28	28	27	29	27	25	32	27	22	23	19	16	14	14	12	6	7	4	-1	1	21
7/4/89	61	2	2	2	4	9	9	15	16	16	20	26	28	28	29	32	34	33	31	36	31	25	26	18	15	15	11	3	6	3	-1	1	23
15/4/89	62	1	2	1	4	9	8	13	16	14	18	24	28	26	28	30	28	26	32	27	23	15	15	14	13	11	5	6	3	-2	1	23	
22/4/89	63	0	0	-1	3	7	6	13	15	14	17	24	28	27	29	32	29	27	33	29	24	23	15	15	13	12	10	3	5	3	-2	1	21
28/4/89	64	0	1	0	4	9	7	13	14	14	17	25	29	27	29	31	29	27	32	29	24	23	15	15	13	12	11	4	5	3	-2	1	
4/5/89	65	0	1	0	5	8	7	12	14	15	16	24	27	26	27	29	26	24	27	27	22	23	14	14	13	12	11	4	5	3	-2	1	
13/5/89	66	-1	-1	-2	2	7	5	11	13	14	16	24	27	27	30	27	26	29	28	23	24	13	13	12	11	10	2	4	2	-4	0	20	
18/5/89	67	-1	-1	-2	2	5	4	10	12	12	15	21	26	24	25	29	25	23	28	24	21	22	12	12	11	10	9	1	3	0	-4	0	19

TABLE E.2a Ground Surface Movement (mm) and Pipe Movement (mm) at Site D' Within Blackrod PRS from Week 42 to 109.

Date	Week	Distance from pipe centreline (m)																				Pipe movement (mm)												
		-2.0	-1.8	-1.6	-1.4	-1.2	-1.0	-0.9	-0.8	-0.7	-0.6	-0.5	-0.4	-0.3	-0.2	-0.1	0.0	0.1	0.2	0.3	0.4		0.5	0.6	0.7	0.8	0.9	1.0	1.2	1.4	1.6	1.8	2.0	
27/5/89	68	-2	-1	-3	2	3	3	8	9	8	12	17	21	18	21	23	21	18	23	20	17	18	11	9	8	7	6	0	3	1	-5	0	13	
2/6/89	69	-3	-1	-3	-2	3	1	8	8	4	12	16	20	17	19	21	19	16	21	18	16	17	9	8	7	7	6	0	3	2	-4	0	10	
9/6/89	70	-3	-1	-3	-1	3	1	7	7	6	9	12	18	14	16	17	15	13	17	15	14	15	8	7	8	7	6	0	3	1	-5	0	6	
15/6/89	71	-4	-1	-3	-1	2	1	5	6	3	7	9	13	10	12	14	11	9	13	11	11	13	6	5	5	5	0	2	1	-5	0	3		
23/6/89	72	-5	-2	-3	-2	1	-1	4	5	2	5	8	11	8	9	11	8	6	11	9	9	10	5	4	5	5	-1	1	0	-5	-1	0		
30/6/89	73	-4	-2	-2	0	4	0	4	5	3	4	6	9	4	6	8	4	2	8	6	6	8	4	5	4	4	0	3	1	-5	0	-4		
6/7/89	74	-4	-1	-2	1	2	1	3	5	0	2	3	9	4	5	6	2	1	6	6	4	9	4	4	4	4	4	-1	1	0	-5	0	-5	
12/7/89	75	-4	-1	-2	0	2	1	3	3	0	2	3	6	2	3	5	0	-1	5	5	4	5	4	3	3	3	4	0	1	0	-5	0	-8	
20/7/89	76	-4	-2	-4	-1	1	-1	2	2	-2	1	2	4	0	1	2	-3	-5	3	2	3	4	3	3	2	3	4	-1	1	-1	-5	0	-10	
28/7/89	77	-5	-2	-3	-2	0	-1	2	2	-2	-1	0	3	-1	0	1	-4	-6	1	1	1	3	3	2	2	2	4	-1	0	-2	-6	-1	-11	
6/8/89	78	-4	-2	-3	-2	0	-1	2	2	-2	-1	0	3	-1	0	0	-5	-5	1	2	1	3	2	2	1	2	3	-1	1	-1	-5	0	-12	
12/8/89	79	-4	-1	-3	-1	1	-3	3	2	-2	-1	0	3	-1	0	0	-4	-6	1	3	1	1	1	1	2	1	3	3	-2	1	0	-5	0	-13
19/8/89	80	-4	-2	-3	-2	2	-2	2	0	-3	-1	0	2	-2	0	-1	-5	-7	0	2	1	1	1	1	3	-1	2	3	0	-2	-5	-1	-13	
26/8/89	81																																	
1/9/89	82	-5	-3	-3	-1	1	-3	1	1	-3	0	-1	1	-2	-1	-1	-7	-7	-1	0	1	1	0	3	0	2	3	0	2	0	-6	-1	-13	
8/9/89	83																																	
14/9/89	84	-5	-5	-4	-2	0	-4	1	0	-2	-1	-1	2	-3	-2	-1	-7	-8	-1	1	-1	0	0	4	1	1	2	-1	1	0	-6	-1	-13	
21/9/89	85																																	
28/9/89	86																																	
5/10/89	87	-5	-6	-5	-3	0	-5	0	0	-6	-1	-1	1	-4	-3	-3	-8	-9	-2	-1	0	0	0	3	1	1	2	-1	1	-1	-6	-1	-13	
12/10/89	88																																	
19/10/89	89																																	
26/10/89	90	-5	-4	-3	-2	1	-3	1	1	-4	1	-1	2	-2	0	0	-5	-7	1	1	6	1	0	1	0	1	1	-1	2	0	-6	-1	-7	
2/11/89	91																																	
9/11/89	92	-5	-3	-3	-3	0	-3	1	0	-4	-1	0	-1	-5	-3	-4	-9	-7	-2	-1	3	3	-2	-1	-1	1	2	-2	0	0	-6	-1	-13	
16/11/89	93	-5	-3	-4	-2	0	-4	1	0	-2	1	2	1	-1	0	-1	-5	-4	1	1	6	3	0	2	0	1	3	-1	0	-1	-6	-1	-11	

TABLE E.2b Ground Surface Movement (mm) and Pipe Movement (mm) at Site D' Within Blackrod PRS from Week 42 to 109.

**APPENDIX F GROUND SURFACE MOVEMENTS IN SMALL-SCALE
LABORATORY TESTS**

Time (hrs)	Distance from pipe centreline (mm)											Pipe movement (mm)
	-200	-160	-120	-80	-40	0	40	80	120	160	200	
0	0.00	0.00	0.00	0.00	0.00	0.00	0.00	0.00	0.00	0.00	0.00	0.00
6	0.00	0.00	-0.03	0.00	-0.02	0.03	-0.01	0.03	0.00	0.03	0.02	-0.06
12	0.00	0.03	0.01	0.05	0.01	0.05	0.00	0.05	0.02	0.03	0.03	0.23
18	0.00	0.00	0.00	0.00	0.00	0.03	-0.01	0.03	0.00	0.03	0.00	0.05
24	-0.10	-0.03	-0.02	-0.03	-0.01	0.00	-0.02	-0.03	-0.03	-0.03	-0.04	-0.01
30	-0.09	-0.05	-0.04	-0.05	-0.05	0.00	-0.05	-0.03	-0.07	-0.08	-0.08	0.03
36	-0.09	-0.03	0.01	0.00	0.03	0.03	0.01	0.00	-0.03	-0.05	-0.08	0.08
42	-0.09	0.05	0.09	0.10	0.18	0.18	0.13	0.08	0.05	0.00	-0.06	-0.01
48	0.08	0.43	0.46	0.58	0.95	0.91	0.61	0.56	0.33	0.28	0.01	0.01
54	0.31	0.84	1.07	1.27	2.20	2.11	1.59	1.40	1.05	0.97	0.29	0.48
60	0.50	1.14	1.40	1.70	2.75	2.67	2.03	1.93	1.42	1.45	0.59	0.72
66	0.83	1.80	2.15	2.54	3.98	3.89	3.03	2.95	2.26	2.26	1.20	1.28
72	1.56	2.74	3.17	3.68	5.52	5.44	4.52	4.29	3.51	3.48	2.16	2.08
78	2.23	3.78	4.34	4.93	6.97	6.93	5.95	5.64	4.78	4.70	3.25	3.18
84	3.03	4.62	5.31	5.84	8.16	8.08	7.09	6.65	5.83	5.66	4.15	3.71
90	4.15	5.87	6.62	7.19	9.69	9.60	8.53	8.10	7.19	6.99	5.34	4.92
96	5.16	6.96	7.78	8.38	11.07	10.97	9.83	9.40	8.40	8.20	6.47	5.69
102	6.32	8.15	9.13	9.65	12.49	12.37	11.28	10.72	9.75	9.45	7.81	6.77
108	7.32	9.22	10.15	10.77	13.65	13.51	12.36	11.84	10.87	10.54	8.83	7.69
114	8.29	10.36	11.28	11.91	14.87	14.66	13.55	13.03	12.04	11.71	9.93	8.43
120	9.34	11.38	12.36	13.03	16.06	15.93	14.70	14.20	13.16	12.85	11.02	9.22
126	10.42	12.55	14.12	14.25	17.37	17.22	16.00	15.47	14.44	14.05	12.23	10.20
132	11.33	13.61	14.58	15.29	18.45	18.31	17.04	16.56	15.47	15.11	13.21	11.24
138	12.50	14.83	15.83	16.64	19.90	19.74	18.45	17.91	16.85	16.38	14.48	12.24
144	13.39	15.80	16.81	17.63	20.95	20.78	19.46	18.97	17.85	17.50	15.49	13.18
156	14.39	16.89	17.84	18.75	21.94	21.82	20.44	20.04	18.85	18.54	16.53	14.03
168	15.96	18.59	19.59	20.55	23.93	23.77	22.32	21.89	20.65	20.32	18.21	15.03
180	17.56	20.27	21.25	22.33	25.69	25.53	24.04	23.67	22.41	22.15	19.95	16.45
192	18.96	21.79	22.80	23.83	27.30	27.13	25.65	25.25	24.03	23.75	21.57	17.74
204	20.22	23.09	24.08	25.12	28.58	28.37	26.89	26.54	25.30	25.10	22.89	18.76
216	21.66	24.56	25.57	26.64	30.14	29.95	28.41	28.09	27.06	26.64	24.47	20.00
228	22.10	25.04	25.95	27.05	30.44	30.20	28.71	28.40	27.22	27.03	24.83	20.33
240	22.91	25.88	26.71	27.86	31.26	30.96	29.47	29.18	27.97	27.84	25.59	20.82
244	22.94	25.60	26.67	27.51	31.05	30.51	29.26	28.78	27.80	27.46	25.47	21.19
252	23.73	26.70	28.08	28.96	33.16	32.54	31.00	30.38	29.10	28.75	26.31	22.76
264	25.86	28.98	30.69	31.60	36.24	35.64	34.01	33.25	31.90	31.27	28.83	23.69
276	28.10	30.96	33.17	33.71	39.21	38.23	36.94	35.61	34.62	33.45	31.35	24.22
288	30.58	33.02	35.82	35.86	42.24	40.92	39.90	38.10	37.42	35.74	33.87	24.87
300	32.69	35.03	38.07	38.07	44.93	43.56	42.49	40.54	39.93	38.05	36.22	25.63
312	34.74	37.03	40.26	40.11	47.55	46.08	45.00	42.85	42.27	40.18	38.47	26.28
324	36.28	38.58	41.98	41.81	49.71	48.16	46.98	44.75	44.12	41.96	40.19	27.26
330	36.82	39.22	42.66	42.65	50.70	49.15	47.88	45.69	44.95	42.80	40.91	27.94
336	37.51	39.90	43.59	43.61	51.97	50.42	49.13	46.79	46.04	43.76	41.83	28.57
342	38.00	40.61	44.26	44.63	52.97	51.64	50.05	47.83	46.82	44.68	42.41	29.55
348	38.56	41.30	45.07	45.54	54.28	52.88	51.24	48.90	47.84	45.59	43.26	30.15
360	38.99	42.42	46.20	47.02	55.94	54.71	52.92	50.52	49.31	46.99	44.46	31.51
366	39.59	42.80	46.73	47.78	57.00	55.68	53.90	51.16	50.10	47.55	45.12	32.12
372	39.88	43.28	47.31	48.41	57.73	56.49	54.62	51.77	50.69	48.08	45.58	32.62
384	40.69	44.30	48.49	49.81	59.31	58.17	56.15	53.19	52.00	49.33	46.60	33.69

TABLE F.1 Average Vertical Ground Movement (mm) Across the Two Rows of Dial Gauges for the Tatsfield Small-Scale Laboratory Experiment.

Time (hrs)	Distance from pipe centreline (mm)											Pipe movement (mm)
	-200	-160	-120	-80	-40	0	40	80	120	160	200	
0	0.00	0.00	0.00	0.00	0.00	0.00	0.00	0.00	0.00	0.00	0.00	0.00
6	-0.01	-0.03	-0.01	-0.05	-0.02	-0.03	-0.01	-0.03	0.00	0.00	0.00	0.00
12	0.14	0.69	0.39	1.13	0.46	0.77	0.30	0.51	0.20	0.28	0.08	0.00
18	0.39	1.28	1.27	2.79	2.04	2.20	1.39	1.54	0.83	0.72	0.28	0.00
24	0.65	1.79	1.98	4.25	3.49	3.48	2.48	2.46	1.50	1.15	0.50	0.00
30	0.92	2.51	2.87	5.73	4.98	4.89	3.71	3.56	2.32	1.64	0.76	0.00
36	1.76	4.33	4.74	7.96	7.38	7.07	5.75	5.43	4.87	2.92	1.39	0.00
42	3.32	7.27	7.65	11.14	10.59	10.04	8.71	7.96	6.34	4.79	2.71	0.22
48	6.06	10.29	10.82	14.13	13.76	12.95	11.72	10.60	8.99	6.17	4.36	1.32
54	8.93	13.16	13.88	17.18	16.91	15.87	14.71	13.26	11.72	8.29	6.41	2.61
60	11.64	15.95	16.79	19.94	19.87	18.69	17.43	15.87	14.31	10.68	8.66	4.03
66	14.26	18.61	18.60	22.58	22.85	21.50	20.17	18.51	16.89	13.24	11.19	5.46
72	16.59	21.04	22.15	24.91	25.50	24.04	22.66	20.86	19.21	15.46	13.40	6.88
78	19.91	24.50	25.60	28.49	29.18	27.57	25.98	23.99	22.13	18.33	16.13	9.29
84	23.91	28.24	29.75	32.33	33.63	31.64	30.09	27.67	25.91	21.66	19.65	11.46
90	27.70	31.87	33.58	35.30	37.78	35.53	33.95	31.23	29.47	24.86	22.94	13.35
96	30.79	34.84	36.74	40.04	41.19	38.73	37.11	34.12	32.43	27.52	25.75	15.15
103	34.34	38.37	40.45	43.93	45.17	42.57	40.80	37.96	35.85	30.52	29.15	16.98
108	36.55	40.29	42.69	46.05	47.51	44.88	43.06	40.04	37.99	32.44	31.19	18.07
116	41.23	44.52	47.57	50.25	52.80	49.59	48.08	44.36	42.75	36.33	35.77	19.55
122	43.66	46.75	50.16	52.43	55.63	52.02	50.75	46.64	45.24	38.37	38.18	20.36
126	43.97	47.03	50.32	52.48	55.73	52.25	50.87	46.92	45.48	38.76	38.58	20.66
144	36.55	40.17	41.01	44.65	46.88	43.60	41.71	39.40	37.39	32.84	32.17	20.94
170	35.89	39.76	41.36	44.54	45.95	43.62	41.70	39.32	37.20	32.74	31.99	20.97
179	35.93	39.83	41.41	44.62	46.07	43.75	41.79	39.42	37.27	32.82	32.07	20.98
192	37.38	41.37	43.07	46.41	48.23	45.77	43.78	41.19	39.01	34.28	33.50	21.01
203	38.69	42.85	43.92	48.05	50.10	47.49	45.48	42.70	40.47	35.43	34.67	21.01
217	36.05	40.14	40.73	44.95	46.55	44.24	42.08	39.76	37.38	32.97	32.26	21.17

TABLE F.2 Average Vertical Ground Movement (mm) Across the Two Rows of Dial Gauges for the Blackrod Small-Scale Laboratory Experiment.